CROP RESPONSE TO WATERLOGGING

EDITED BY: Iduna Arduini, Makie Kokubun, Guangcheng Shao and Francesco Licausi

PUBLISHED IN: Frontiers in Plant Science

frontiers Research Topics

frontiers

ISSN 1664-8714
ISBN 978-2-88963-366-1
DOI 10.3389/978-2-88963-366-1

About Frontiers

Frontiers is more than just an open-access publisher of scholarly articles: it is a pioneering approach to the world of academia, radically improving the way scholarly research is managed. The grand vision of Frontiers is a world where all people have an equal opportunity to seek, share and generate knowledge. Frontiers provides immediate and permanent online open access to all its publications, but this alone is not enough to realize our grand goals.

Frontiers Journal Series

The Frontiers Journal Series is a multi-tier and interdisciplinary set of open-access, online journals, promising a paradigm shift from the current review, selection and dissemination processes in academic publishing. All Frontiers journals are driven by researchers for researchers; therefore, they constitute a service to the scholarly community. At the same time, the Frontiers Journal Series operates on a revolutionary invention, the tiered publishing system, initially addressing specific communities of scholars, and gradually climbing up to broader public understanding, thus serving the interests of the lay society, too.

Dedication to Quality

Each Frontiers article is a landmark of the highest quality, thanks to genuinely collaborative interactions between authors and review editors, who include some of the world's best academicians. Research must be certified by peers before entering a stream of knowledge that may eventually reach the public - and shape society; therefore, Frontiers only applies the most rigorous and unbiased reviews.
Frontiers revolutionizes research publishing by freely delivering the most outstanding research, evaluated with no bias from both the academic and social point of view. By applying the most advanced information technologies, Frontiers is catapulting scholarly publishing into a new generation.

What are Frontiers Research Topics?

Frontiers Research Topics are very popular trademarks of the Frontiers Journals Series: they are collections of at least ten articles, all centered on a particular subject. With their unique mix of varied contributions from Original Research to Review Articles, Frontiers Research Topics unify the most influential researchers, the latest key findings and historical advances in a hot research area! Find out more on how to host your own Frontiers Research Topic or contribute to one as an author by contacting the Frontiers Editorial Office: researchtopics@frontiersin.org

CROP RESPONSE TO WATERLOGGING

Topic Editors:
Iduna Arduini, University of Pisa, Italy
Makie Kokubun, Tohoku University, Japan
Guangcheng Shao, Hohai University, China
Francesco Licausi, University of Pisa, Italy

Citation: Arduini, I., Kokubun, M., Shao, G., Licausi, F., eds. (2020). Crop Response to Waterlogging. Lausanne: Frontiers Media SA. doi: 10.3389/978-2-88963-366-1

Table of Contents

frontiers in Plant Science

EDITORIAL
published: 11 December 2019
doi: 10.3389/fpls.2019.01578

Editorial: Crop Response to Waterlogging

Iduna Arduini[1]*, *Makie Kokubun*[2] *and Francesco Licausi*[3]

[1] Department of Agriculture, Food and Environment, University of Pisa, Pisa, Italy, [2] Tohoku University, Sendai, Japan, [3] Department of Biology, University of Pisa, Pisa, Italy

Keywords: climate change, crop species, flooding, multidisciplinary approach, waterlogging

Editorial on the Research Topic

Crop Response to Waterlogging

Soil waterlogging occurs when excess water saturates the soil pores with either no layer of water or a very fine one on the soil surface. Since gas diffusion in water is several folds slower than in air, the oxygen concentration decreases rapidly in waterlogged soils, thereby triggering a cascade of conditions that are detrimental to the growth of most plant species (Colmer and Greenway, 2011).

Flooding is the primary cause of yield losses in Asia and Latin America while, worldwide, between 10 and 16% of the arable soils are estimated to be affected by waterlogging (Yaduvanshi et al., 2014; FAO, 2015). Moreover, the frequency and intensity of flooding events is expected to increase in all world regions in consequence of climate change (Westra et al., 2014; IPCC, 2018). Thus, the purpose of the research topic "Crop Response to Waterlogging" is to gather knowledge from different geographic regions and research fields in order to help the scientific and social community to elaborate an integrated approach to face its adverse effects.

The articles published in this research topic deal with a wide range of crop species, including cereals (Arduini et al.; Panozzo et al.; Yamauchi et al.), forage and grain legumes (Pucciariello et al.; Zhang et al.), and tree crops (Ruperti et al.; Iacona et al.), thus demonstrating the widespread interest in plant sciences for this soils condition. The researches published in this e-book describe different investigation approaches and propose alternative solutions, which range from the reduction of waterlogging risk by improving agronomic and engineering solutions (Manik et al.; Zhang et al.), to the better understanding of crop response to waterlogging (Arduini et al.; Ejiri and Shiono; Lin and Sauter; Pucciariello et al.; Ruperti et al.; Yamauchi et al.), and the selection of crops and genotypes that are more tolerant to waterlogging conditions (Iacona et al.; Panozzo et al.; Pompeiano et al.).

Waterlogging generally induces changes in gene expressions, which result in physiological and morphological changes in plants. Flooding responses on grapevine are reviewed by Ruperti et al., and their findings enable us to draft a first comprehensive view of the metabolic pathways involved in grapevine's root responses and to highlight a transcriptional and metabolic reprograming during and after exposure to waterlogging. The gene expressions of *AOX1A*, *CYP81D8*, and putative *PFP* genes were analyzed in a large set of commercial maize hybrids under extreme waterlogging conditions and their involvement in the morphological changes are discussed (Panozzo et al.).

Roots are the first target of waterlogging stress in plants, and it is well documented that aerenchyma formation plays a crucial role in internal long-distance oxygen transport from shoot to root under waterlogged soil. A comparison of the cross-sectional area of root tissues among three crop species (wheat, maize, and rice), subjected to aerated or deoxygenated conditions, revealed that

Edited and reviewed by:
Vicent Arbona,
University of Jaume I, Spain

****Correspondence:***
Iduna Arduini
iduna.arduini@unipi.it

Specialty section:
This article was submitted to Plant Abiotic Stress, a section of the journal Frontiers in Plant Science

Received: *24 October 2019*
Accepted: *12 November 2019*
Published: *11 December 2019*

Citation:
Arduini I, Kokubun M and Licausi F (2019) Editorial: Crop Response to Waterlogging. Front. Plant Sci. 10:1578. doi: 10.3389/fpls.2019.01578

high cortex to stele ratio in combination with large root diameter is a feature which promotes oxygen transport from shoot to root tips (Yamauchi et al.). Previous studies indicate that a structural barrier is formed in wetland plant root, which might help impede radial oxygen loss in the course of oxygen transport. Three species of *Echinochloa*, well adapted to various soil water conditions, were found to constitutively develop the barrier under aerated conditions, and suberin was an important component of the barrier (Ejiri and Shiono). These studies provided new findings on the morphological features of waterlogging-adapted plant species. Moreover, Lin and Sauter found that auxin signaling is likely to contribute to the coordinated processes of adventitious roots formation, which might support or replace the main root system in flooded rice plants.

Flooding-induced physiological dysfunctions include the impairment of water and nutrients uptake, of hormonal balance and photosynthesis, which consequently result in poor growth under flooding. In legume crops, flooding conditions can harm N assimilation through weakened capacity for symbiotic N_2 fixation. The mechanisms underlying symbiotic processes and functioning under waterlogging are reviewed, with a focus on the mechanisms of oxygen sensing of the host plant and the symbiotic partner (Pucciariello et al.). The findings presented in this review would help in understanding the mechanisms regulating flooding tolerance in legume species, which may lead to isolate tolerant crop species and varieties in the field. The severity of yield reduction by waterlogging varies with crop species, partly because of the specific phenology of each of them. In the Mediterranean environment, winter cereals can experience waterlogging at their early growth stage. Late sown oats subjected to waterlogging at tillering failed to produce acceptable yield, primarily because of insufficient capacity for tiller and panicle formation after the release from waterlogging (Arduini et al.).

Under severe waterlogging, in addition to genetic improvement, agronomic and engineering measures are required to minimize the impact of waterlogging. Hence, management practices to alleviate the damage by waterlogging are reviewed (Manik et al.). Based on their comprehensive analyses of literature on crop management practices, the authors suggest that the strategies to withstand waterlogging should be adopted in a manner where genetic, agronomic, and engineering measures are complementarily integrated depending on the respective environments. They suggest further research aspects such as the comparison of cost/benefit analyses of different drainage strategies, understanding the mechanisms of nutrient loss during waterlogging and quantifying the benefits of nutrient application. Among strategies to adopt, Zhang et al. showed evidence that melatonin improves waterlogging tolerance in alfalfa by reprogramming polyamine and ethylene metabolism. In addition, photosynthetic performance and growth response of giant cane, which spontaneously grows in different kinds of harsh environments, are characterized, with the aim to replace sensitive crops in waterlogging prone soils (Pompeiano et al.).

The research published in this topic clearly demonstrate that a multidisciplinary approach is crucial to reduce waterlogging risk and ameliorate its adverse effects on crops. The first step should be the adoption of soil management practices that reduce soil compaction and improve drainage (Manik et al.), followed by the use of crop management techniques that increase plant resistance (Zhang et al.), or the choice of crops and genotypes that are more adaptable to soil hypoxia (Pompeiano et al.; Iacona et al.; Panozzo et al.). The published articles also highlight that crop species respond differently to waterlogging stress, so that basic research is still needed.

To conclude, we are deeply grateful to all scientists who answered to the call and allowed us to publish their researches in this collection on "Crop Response to Waterlogging," which provides the unique opportunity to integrate the knowledge from many research fields for facing waterlogging and reduce crop loss worldwide.

AUTHOR CONTRIBUTIONS

Authors contributed equally to writing and revising the editorial.

ACKNOWLEDGMENTS

Authors wish to thank Prof. Guangsheng Shao for his competent and precious collaboration as handling co-editor of the research topic "Crop Response to Waterlogging."

REFERENCES

Colmer, T. D., and Greenway, H. (2011). Ion transport in seminal and adventitious roots of cereals during O2 deficiency. *J. Exp. Bot.* 62, 39–57. doi: 10.1093/jxb/erq271

FAO. (2015). *The Impact of Disasters on Agriculture and Food Security* (Rome: FAO). Available at http://www.fao.org/3/a-i5128e.pdf.

IPCC. (2018). "Global warming of 1.5_C. An IPCC Special Report on the Impacts of Global Warming of 1.5_C Above Pre-Industrial Levels and Related Global Greenhouse Gas Emission Pathways," in *Context Of Strengthening the Global Response to the Threat of Climate Change, Sustainable Development, and Efforts to Eradicate Poverty*. Eds. V. Masson-Delmotte, P. Zhai, H. O. Pörtner, D. Roberts, J. Skea, and P. R. Shukla , et al (Cambridge: Cambridge University Press).

Westra, S., Fowler, H. J., Evans, J. P., Alexander, L. V., Berg, P., Johnson, F., et al. (2014). Future changes to the intensity and frequency of shortduration extreme rainfall. *Rev. Geophys.* 52, 522–555. doi: 10.1002/2014RG000464

Yaduvanshi, N., Setter, T., Sharma, S., Singh, K., and Kulshreshtha, N. (2014). Influence of waterlogging on yield of wheat (*Triticum aestivum*), redox potentials, and concentrations of microelements in different soils in India and Australia. *Soil Res.* 50, 489–499. doi: 10.1071/SR11266FAO2015

Conflict of Interest: The authors declare that the research was conducted in the absence of any commercial or financial relationships that could be construed as a potential conflict of interest.

frontiers in Plant Science

ORIGINAL RESEARCH
published: 01 February 2019
doi: 10.3389/fpls.2019.00044

Melatonin Improved Waterlogging Tolerance in Alfalfa (*Medicago sativa*) by Reprogramming Polyamine and Ethylene Metabolism

*Qiang Zhang†, Xiaofei Liu†, Zhifei Zhang, Ningfang Liu, Danzhu Li and Longxing Hu**

Department of Pratacultural Sciences, College of Agriculture, Hunan Agricultural University, Changsha, China

OPEN ACCESS

Edited by:
Francesco Licausi, University of Pisa, Italy

Reviewed by:
Liang Chen, University of Chinese Academy of Sciences (UCAS), China
María Serrano, Universidad Miguel Hernández de Elche, Spain

***Correspondence:**
Longxing Hu
grass@hunau.edu.cn

† These authors have contributed equally to this work

Specialty section:
This article was submitted to Plant Abiotic Stress, a section of the journal Frontiers in Plant Science

Received: *24 August 2018*
Accepted: *11 January 2019*
Published: *01 February 2019*

Citation:
Zhang Q, Liu X, Zhang Z, Liu N, Li D and Hu L (2019) Melatonin Improved Waterlogging Tolerance in Alfalfa (Medicago sativa) by Reprogramming Polyamine and Ethylene Metabolism. Front. Plant Sci. 10:44. doi: 10.3389/fpls.2019.00044

Melatonin (MT), polyamines (PAs), and ethylene have been suggested to play key roles in plant growth and development in response to environmental abiotic stresses. However, the effect of melatonin on polyamine and ethylene metabolism under waterlogging stress has rarely been elucidated. The main purpose of this study was to investigate the effect of melatonin pretreatment on waterlogging stress in alfalfa. The experiment was arranged into four treatment groups control with water pretreatment (CK-MT), control with melatonin pretreatment (CK+MT), waterlogging pretreated with water (WL-MT) and waterlogging pretreated with melatonin (WL+MT), with three replications. Six-week-old alfalfa seedlings were pretreated with 100 μM melatonin and exposed to waterlogging stress for 10 days. Plant growth rate, different physiological characteristics, and gene expression level were measured. Results showed that waterlogging induced melatonin accumulation, and melatonin pretreatment increased endogenous MT levels for the control and water-logged plants. Waterlogging stress caused a significant reduction in plant growth, chlorophyll content, photochemical efficiency (Fv/Fm) and net photosynthetic rate (P_n), while also causing increased leaf electrolyte leakage (EL) and malondialdehyde (MDA) content. Pretreatment with melatonin alleviated the waterlogging-induced damage and reduction in plant growth, chlorophyll content, Fv/Fm and P_n. Waterlogging stress significantly increased leaf polyamines (Put, Spd, Spm) and ethylene levels, and the increased PAs and ethylene levels are coupled with higher metabolic enzymes and gene expressions. While pretreatment with melatonin further increased Put, Spd and Spm levels, it also decreased ethylene levels under waterlogging, and those increased PAs levels or decreased ethylene levels are regulated by the metabolic enzymes and gene expressions. The results in this study provide more comprehensive insight into the physiological and molecular mechanisms of melatonin-improved waterlogging tolerance in alfalfa. Furthermore, they suggested that melatonin

improved waterlogging tolerance in alfalfa at least partially by reprogramming ethylene and PA biosynthesis, attributable to the increased PAs and decreased ethylene levels, which leads to more enhanced membrane stability and photosynthesis as well as less leaf senescence caused by ethylene.

Keywords: alfalfa, ethylene, melatonin, polyamine, waterlogging

INTRODUCTION

Waterlogging has been suggested as a major environmental stress that affects crop survival, growth, and productivity in those areas prone to heavy rainfall, poor soil drainage as well as high water table fluctuations (Jackson and Colmer, 2005). The availability of molecular oxygen is required to support metabolism and growth of higher plants. However, excess water in the soil often results in inadequate provision of oxygen to the plant cells, causing several phenotypic, physiological and metabolic disturbances, including growth inhibition of shoots and roots, reduction in water and nutrient uptake, leaf photosynthesis and photochemical efficiency as well as root respiratory disturbances and leaf senescence (Boru et al., 2003). In addition, waterlogging often results in a significant increase in ethylene levels in plants. The high ethylene level under waterlogging stress often causes a significant decrease in shoot and root growth, inducing leaf senescence and abscission (Najeeb et al., 2018) as well as a reduction in photosynthesis (Rajala and Peltonen-Sainio, 2001; Pierik et al., 2007). Ethylene biosynthesis begins with the formation of *S*-adenosyl-L-methionine (SAM) from methionine by SAM synthetase. The 1-aminocyclopropane-1-carboxylic acid (ACC) synthase (ACS) then catalyzes the production of ACC from SAM followed by its oxidation to ethylene by ACC oxidase (ACO) (Najeeb et al., 2018).

Polyamines (PAs) are low molecular weight and aliphatic nitrogenous compounds (Groppa and Benavides, 2008), which include spermidine (Spd), spermine (Spm), and putrescine (Put). They have been regarded as a class of plant growth regulators and suggested to be involved in plant growth and development (Tavladoraki et al., 2012). In addition, numerous studies have implied the associations of PA metabolism with plant responses to environmental stress conditions, including drought, high temperature, salinity, nutrient deficiency, and others (Zhao et al., 2017), because of their roles in membrane stability, scavenging free radicals and preserving nucleic acids and proteins structures (Alcázar et al., 2010). PA synthesis and catabolism have been well-illustrated in plants. Ornithine decarboxylase (ODC), ADC, Spd synthase (SPDS), Spm synthase (SPMS), and SAM decarboxylase (SAMDC) are involved in PA synthesis, and DAO and polyamine oxidase (PAO) are involved in the catabolism of PAs in plant tissues (Alcázar et al., 2010). Generally, the biosynthesis and catabolism of PAs are interconnected with other metabolic pathways that function in plant stress tolerance (Alcázar et al., 2010). For example, the interconnection between the stress-induced PA and ethylene metabolism reflect the fact that their biosynthethic pathways share SAM as a substrate, and the functions of PAs and ethylene differ diametrically (Apelbaum et al., 1981).

Melatonin (*N*-acetyl-5-methoxytryptamine) is a low molecular-weight indole amine synthesized from the essential amino acid L-tryptophan (Koyama et al., 2013) and has been reported as a universal signaling molecule in mammals and plant species (Hardeland et al., 2011; Tan et al., 2012). Numerous studies have implied the essential role of melatonin in plant growth and development and in protecting plants from environmental stressors, including heat and cold temperatures, water stress, osmotic and ionic stress, ultraviolet radiation and heavy metal stress (Tan et al., 2012; Shi and Chan, 2014; Shi et al., 2015; Gong et al., 2017; Zhao et al., 2017).

Alfalfa (*Medicago sativa*) is an important perennial forage grass worldwide because of its high yield and high quality. Introduction of alfalfa into south China has the potential for alleviating shortages of good forage that limit the development of herbivorous animal husbandry. However, the growth range of alfalfa is limited due to its sensitivity to waterlogging or flooding in Southern China (Smethurst et al., 2005).

It has been suggested that melatonin can regulate PA levels in rat brains and human skin (Lee et al., 2000, 2003). However, few studies have been conducted to elucidate how melatonin modulates PA metabolism in response to abiotic stress in plants, such as waterlogging. Melatonin may exert its protective effects through PAs and ethylene metabolism under waterlogging stress in plants. In this study, the effects of melatonin pretreatment on polyamine and ethylene metabolism were investigated in alfalfa leaves under waterlogging stress. Polyamines and ethylene levels, key metabolic enzymatic activities and their respective gene expression levels were determined after 10 days of waterlogging stress was imposed.

MATERIALS AND METHODS

Plant Materials and Growth Conditions

Alfalfa '55v48' cultivars, supplied by Beijing RYTWAY, were used in our study. Twenty-five seeds were planted in each pot (10 cm × 10 cm in diameter and height) with 16 pots in total, which were filled with a mixture of loamy topsoil and sand (1:2, v/v). Seedlings were cultured in the greenhouse with the following environmental conditions: 18/25°C temperature (day/night), 14 h/10 h photoperiod, 500–550 μmol m^{-2} s^{-1}

Abbreviations: ACC, 1-aminocyclopropane-1-carboxylic acid'CO, ACC oxidase; ACS, ACC synthase; ADC, arginine decarboxylase; DAO, diamine oxidase; MDA, malondialdehyde; ODC, ornithine decarboxylase; PA, polyamine; PAO, polyamine oxidase; Put, putrescine; SAM, *S*-adenosylmethionine; SAMDC, *S*-adenosylmethionine decarboxylase; Spd, spermidine; Spm, spermine; SPDS, spermidine synthase; SPMS, spermine synthase.

light intensity, and 60–85% relative humidity. The plants were fertilized weekly with Hoagland's liquid solution.

Treatments and Experimental Design

Plants at six- to seven-leaf stages (about 6 weeks after sowing) were exposed to soil waterlogging. A preliminary study showed that 100 μM melatonin was the most effective concentration to improve waterlogging tolerance. At 1 day prior to waterlogging, 100 μM of melatonin were foliar sprayed for 15 ml per pot and the non-melatonin treatment were pretreated with water. Plants were subjected to waterlogging by immersing the plastic pots into water-filled plastic tubs by maintaining 1 cm water layer above the soil surface and last for 10 days, whereas the control pots were watered regularly to field capacity. There are four treatments in this experiment: control with water pretreatment (CK-MT), control with melatonin pretreatment (CK+MT), waterlogging pretreated with water (WL-MT) and waterlogging pretreated with melatonin (WL+MT). All pots with four treatments were divided into three groups and maintained in three growth chambers (three replicates), with a temperature of 20/25°C (day/night), 14 h/10 h photoperiod, 60–85% relative humidity and a light intensity of 500 μmol m^{-2} s^{-1}. Plants were sampled at 10 days of waterlogging stress for physiological and PA analysis and harvested at 0, 4, 24 h and 5, 10 days after waterlogging stress was imposed for molecular analysis.

Determination of Plant Growth Rate

Plant growth rate was determined by measuring the shoot height with three seedlings per pot and calculating the difference before and after waterlogging stress was imposed.

Determination of Leaf Chlorophyll Content

Leaf chlorophyll content was measured on the fourth leaves from the top by using a hand-held chlorophyll meter (SPAD-502, Minolta, Corp., Spectrum Technologies).

Determination of Leaf Photochemical Efficiency

Leaf photochemical efficiency (Fv/Fm) was evaluated by using a chlorophyll fluorometer (OS1-FL, Opti-Sciences, Hudson, NH, United States). Plants were adapted in darkness for 30 min and the then the measurements were made on intact leaves with the fluorometer.

Determination of Leaf Net Photosynthetic Rate (P_n)

Net photosynthetic rate (P_n) was measured in the third leaves by using a gas analyzer (Li-6400, LICOR, Inc., Lincoln, NE, United States) with controlled conditions (400 μmol mol^{-1} CO_2, 500 μmol s^{-1} flow rate) and a Licor 6400 LED external light source providing a photosynthetic photon flux density of 500 μmol m^{-2} s^{-1}. Net photosynthetic rate was measured for three subsamples in each pot.

Determination of Leaf Electrolyte Leakage (EL)

Leaf electrolyte leakage (EL) was measured using ≈0.1 g fresh samples. Leaf segments were immersed in a 50 ml tube filled with 15 ml of deionized water and then shaken for 24 h at room temperature. The initial conductance (Ci) was recorded using a conductance meter (YSI-3100; Guangzhou, China). Leaf segments in the 50 ml tube were then autoclaved at 120°C for 30 min. The maximum conductance (Cmax) of the incubation solution with killed tissues was recorded after the solution cooled to room temperature. Relative EL was calculated as (Ci/Cmax) × 100.

Determination of Leaf Malondialdehyde (MDA)

For leaf malondialdehyde (MDA) measurement, leaf samples were homogenized with ice-cold extraction buffer (100 mM PBS, pH 8.0). After that, the extraction was then centrifuged at 14,000 *g* for 20 min at 4°C. The supernatant was transferred to a new tube and used for the determination of MDA content according to the method of Heath and Packer (1968).

Determination of Leaf Endogenous Melatonin Levels

Endogenous melatonin levels of alfalfa leaves were determined according to the method described by Shi and Chan (2014). Briefly, 1 g of alfalfa tissues was homogenized thoroughly in 5 ml of extraction solution (acetone: methanol: water = 89: 10: 1). The supernatant was transferred to a new tube containing 0.5 ml of 1% trichloric acid for protein precipitation after being centrifuged at 1000 *g* for 10 min at 4°C. Then, the centrifuged extract was used for quantification of melatonin using the Melatonin ELISA Kit (EK-DSM; Buhlmann Laboratories AG, Schönenbuch, Switzerland) according to the user manuals.

Determination of Leaf Free PA Levels

Leaf free PAs were extracted as the approaches described by Duan et al. (2008) with modifications. Briefly, 0.4 g fresh tissues were homogenized in 4 ml of 5% (v/v) cold perchloric acid and incubated at 4°C for 1 h. 1,6-hexanediamine was added as an internal standard prior to centrifugation at 12,000 × *g* for 30 min at 4°C. An aliquot of the supernatant was reacted with 2 ml of 2N NaOH and 15 μl of benzoyl chloride and then vortexed and incubated for 30 min at 37°C, and then 4 ml saturated NaCl was added to terminate the reaction. The diethyl ether extracted benzoyl PAs were evaporated to dryness and re-dissolved in 1 ml methanol. The benzoyl derivatives were separated and analyzed by an HPLC system (Waters Series HPLC, Milford, MA, United States). Samples were injected with a volume of 20 μl into a 20-μl loop on a C18 reverse-phase column (250 mm × 2.1 mm, 5 μm; Supelco Analytical, Bellefonte, PA, United States) at room temperature. The samples were then eluted from the C18 column in a gradient program at a flow rate of 0.2 ml/min and detected at 254 nm with a UV detector. The three PA standards (Aladdin, Co.) of Put, Spd, and Spm were prepared at various

concentrations for the production of the appropriate standard curves.

Determination of PA Metabolism Key Enzyme Activities

The activities of ADC, ODC, and SAMDC were tested according to the approaches described by Zhao et al. (1996) and Hu et al. (2012). Briefly, Fresh tissues were homogenized in 100 mM PBS (pH 8.0) containing 0.1 mM PMSF, 1 mM PLP, 5 mM DTT, 5 mM EDTA, 25 mM ASA and 0.1% PVP. The supernatant was then dialyzed after centrifugation at 12,000 × *g* for 40 min at 4°C. The dialysis was started with the addition of 3 ml 100 mM PBS (pH 8.0) containing 0.05 mM PLP, 1 mM DTT, and 0.1 mM EDTA for 24 h in darkness at 4°C. The dialyzed samples were then used for enzyme determination. 0.3 ml of the dialyzed enzyme extract was mixed with 1 ml of the reaction mixtures containing 100 mM Tris-HCl buffer (pH 7.5), 5 mM EDTA, 50 mM pyridoxal phosphate and 5 mM DTT. After which, 0.2 ml of 25 mM L-arginine, L-ornithine, or *S*-adenosyl methionine was added respectively. The mixtures were incubated at 37°C for 1 h. After that, PCA was added until the final concentration of PCA was 5%. After centrifuging at 3000 × *g* for 10 min, 0.5 ml of the supernatant was mixed with 1 ml of 2 mM NaOH and 10 μl benzoyl chloride and then stirred for 20 s. After incubation for another 30 min at 37°C, 4 ml saturated NaCl solution and 3 ml ether were added to the mixture. 2 ml of the ether phase was evaporated to dryness and re-dissolved in 1 ml 60% methyl alcohol. The absorbance of this solution was measured at 254 nm using a Shimadzu UV1800 spectrophotometer (Shimadzu, Co., Ltd., Japan). Enzyme activities were expressed in nmol Arg g^{-1} FW h^{-1}, nmol Put g^{-1} FW h^{-1}, and nmol SAM g^{-1} FW h^{-1}.

TABLE 1 | Details of primers used for analyzing the expression of genes involved in the biosynthesis of polyamines in alfalfa by quantitative real-time PCR.

Gene	Primer	Nucleotide sequence	Accession
SAMDC	SAMDC-F	5′-CAA CGG TGG CGT AGA AAA AT-3′	CB891404*
	SAMDC-R	5′-GCC TTC AAA ACC GAT AGC TG-3′	
SPDS	SPDS-F	5′-AAG GGA TGA GTG TGC GTA CC-3′	TA22135_3880*
	SPDS-R	5′-TTT GGA GAC ATC GAC AAC CA-3′	
SPMS	SPMS-F	5′-GCC AGT GAA GAA AAG GGT CA-3′	TA27030_3880*
	SPMS-R	5′-AGA ACC ACC CAG AAA CAA CG-3′	
ADC	ADC-F	5′-CTG GCC ATT TTG GTT CAA CT-3′	TA20893_3880*
	ADC-R	5′-ACC CAA ACG AAG CAA TTC AC-3′	
PAO	PAO-F	5′-TTT TGG CAG CAC ATG GAT AA-3′	BQ122766*
	PAO-R	5′-TTA TTC CAC CAG CAG GGA AC-3′	
DAO	DAO-F	5′-TGC AAT CCC AGA TGA AGT GA-3′	AJ500329*
	DAO-R	5′-CAG CTA GCA ATG TGC CAT GT-3′	
MtACS3	ACS-F	5′-GTCTACCAGGTTTCAGAGTTG-3′	MTR 8g101820##
	ACS-R	5′-CTCTTCTTCAATCTTTCCCTAT-3′	
MtACO1	ACO-F	5′-CCAAAGGGCTAGAGGCTGTTC-3′	MTR3g083370##
	ACO-R	5′-GGTAGGTGACGCAAATGGAAA-3′	
MsETR8	ETR -F	5′-GTGACAACATCTCTGACCCGT-3′	JF965422##
	ETR -R	5′-ACCCTGCTTCCTTCCCTTGAT-3′	
MtActin	Actin -F	5′-ACGAGCGTTTCA GATG-3′	MTR 7g026230##
	Actin -R	5′-ACCTCCGATCCAGACA-3′	

##**Medicago EST sequence Accession no.*

The activities of DAO and PAO were measured according to the method described by Hu et al. (2012). Briefly, 0.4 g fresh leaves were homogenized using pre-chilled mortar and pestle at 4°C in 100 mM sodium phosphate buffer (pH 6.5). The homogenates were then centrifuged at 10,000 *g* for 20 min at 4°C and the supernatants were used for the determination of DAO and PAO activities. The reactions were started by adding 15 μl of Put (for DAO measurement) and 15 μl of Spd + Spm (for PAO measurement) to the mixture of the supernatant with 4-aminoantipyrine/*N*, *N*-dimethylaniline reaction solution and 0.1 ml horseradish peroxidase (250 U ml^{-1}). A unit of enzyme activity was defined as one giving a change in optical density of 0.001 absorbance units at 254 nm (Zhao et al., 2017).

Determination of Leaf Ethylene Production Rate and Key Enzyme Gene Expressions

The ethylene production rate was assayed as the method described by Wilkinson and Davies (2009) with modification.

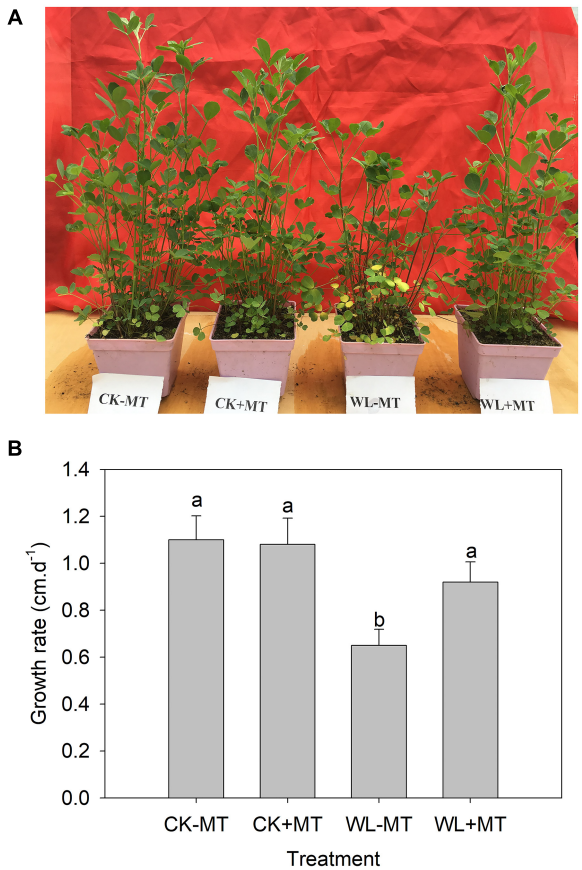

FIGURE 1 | Effect of melatonin (MT) pretreatment on alfalfa plants under control and waterlogging stress. The representative picture **(A)** and shoot growth rate **(B)** of 45-day-old plants of the alfalfa cultivars '55v48' pretreated with 100 μM MT and then subjected to waterlogging stress for 10 days. Vertical bars on the top indicate the means ± SD (n = 4). Letters marked by the same letters are not significant at $P < 0.05$ (Ducan's multiple range test).

Briefly, 0.5 g of the third expanded leaves (from top) were collected at 0, 4, 24 h and 5, 10 days of waterlogging stress, and put into 25 ml sealed glass vials. Samples were held for 5 h at 25°C under illumination with 5000 Lx. Gas samples (1 ml) were withdrawn from the vial head space with a disposable plastic syringe and manually injected into a gas chromatograph (5890 C, Agilent Technologies UK, Ltd., Wokingham, United Kingdom). The temperature was maintained at 100°C for 5 min to resolve ethylene, increased at 15°C min^{-1} to 150°C and held for 1.5 min to remove any water vapor introduced into the column in the sample injection. The helium carrier gas was set at a flow rate of 5.7 ml min^{-1} and detection was performed by flame ionization. Ethylene concentration was calculated with reference to peak areas of known ethylene standards (BOC Special Gases, Manchester, United Kingdom) and the ethylene emission rate was calculated for tissue fresh weight and the duration of incubation (Wilkinson and Davies, 2009). The amount of released ethylene was expressed in μl per g plant tissue per hour. The measurement was conducted in three biological replicates.

Total RNA extraction, cDNA synthesis, and qRT-PCRs were performed as Hu et al. (2016) described. Briefly, 0.1 g fresh tissues were used for total RNA extraction by using Trizol reagent (Invitrogen, Carlsbad, CA, United States). RNA quality and integrity were checked by Nanodrop 2000 and 0.8% agarose gel. Then, the first strand cDNA were synthesized from 2 μg of total RNA using oligo(dT)12-18 primer with the cDNA synthesis kit (Fermentas, Burlington, ON, Canada). Gene-specific primers were designed based on the target gene sequences using Primer 5 software (**Table 1**). The real-time RT-PCR was conducted in ABI7500 with a final volume of 20 μl. The real-time PCR analysis contained three independent biological replicates and two technical replicates for each sample. The PCR conditions were as follows: 40 cycles of 95°C denaturation for 5 s, and 52∼55°C annealing and extension for 20 s. The relative expression level of genes for each sample was calculated relative to a calibrator using the DDCT method as described by Livak and Schmittgen (2001).

Statistical Analysis

Data statistical analysis was conducted following the ANOVA analysis of variance using SAS for Windows (SAS Institute, Cary, NC, United States). Means and standard errors were calculated for three replicates. Comparisons between means were carried out using Duncan's multiple range tests at a significance level of $p < 0.05$.

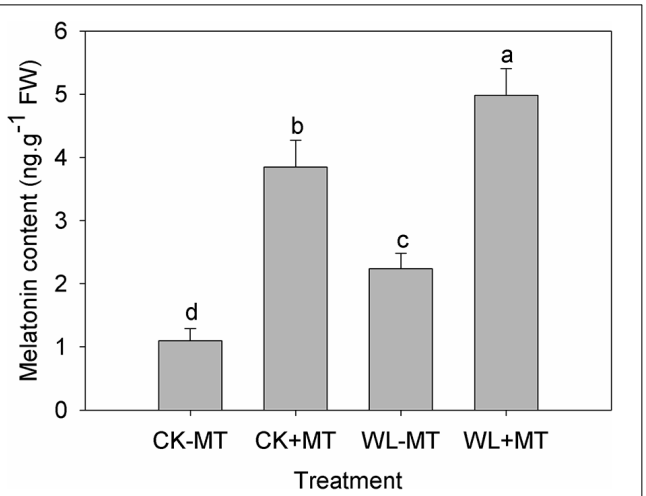

FIGURE 2 | Effects of waterlogging (WL) and exogenous melatonin (MT) pretreatment on the endogenous melatonin content in the leaves of alfalfa. 45-day-old alfalfa plants pretreated with 100 μM melatonin and then exposed to 10 days of waterlogging stress. CK-MT, control without melatonin pretreatment; CK+MT, control with melatonin pretreatment; WL-MT, waterlogging without melatonin pretreatment; WL+MT, waterlogging with melatonin pretreatment. Data are expressed as mean ± SE of four replications. Letters marked by the same letters are not significant at $P < 0.05$ (Ducan's multiple range test).

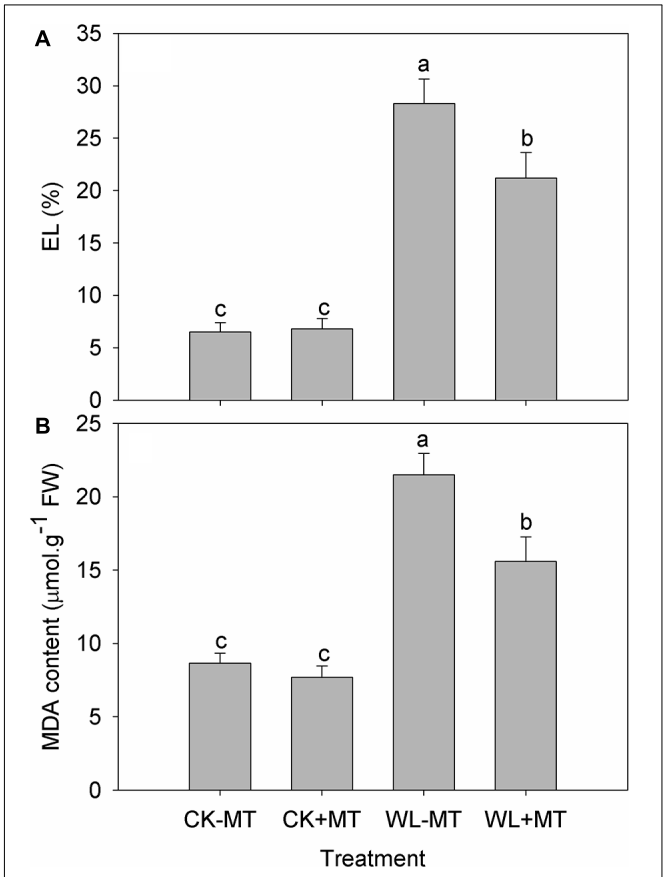

FIGURE 3 | Effects of waterlogging (WL) and exogenous melatonin (MT) pretreatment on the leaf electrolyte leakage (EL, **A**) and MDA **(B)** content in alfalfa. 45-day-old alfalfa plants pretreated with 100 μM melatonin and then exposed to 10 days of waterlogging stress. CK-MT, control without melatonin pretreatment; CK+MT, control with melatonin pretreatment; WL-MT, waterlogging without melatonin pretreatment; WL+MT, waterlogging with melatonin pretreatment. Data are expressed as mean ± SE of four replications. Letters marked by the same letters are not significant at $P < 0.05$ (Ducan's multiple range test).

RESULTS

Exogenous Melatonin Alleviates Waterlogging-Induced Growth Inhibition in Alfalfa Plants

Prolonged waterlogging stress (10 days) caused significant growth inhibition and leaf necrosis as demonstrated by **Figures 1A,B**. The growth rate of the alfalfa plants decreased from about 1.1 cm per day under control conditions to about 0.65 cm per day under waterlogging stress (**Figures 1A,B**). However, a remarkable alleviating effect was observed in melatonin pretreated plants subjected to waterlogging stress for 10 days. The plants pretreated with melatonin grown in control conditions displayed similar phenotypes with the control plants and showed no signs of damage symptoms.

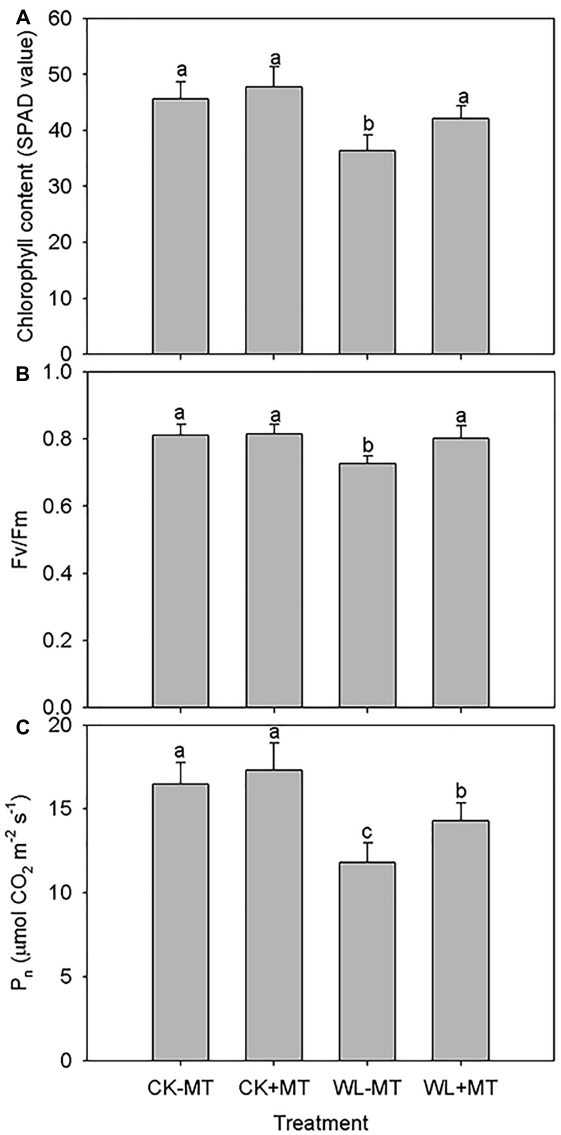

FIGURE 4 | Effects of waterlogging (WL) and exogenous melatonin (MT) pretreatment on the leaf chlorophyll content **(A)**, leaf maximum photochemical efficiency (Fv/Fm, **B**) and net photosynthetic rate (P_n, **C**) in alfalfa. 45-day-old alfalfa plants pretreated with 100 μM melatonin and then exposed to 10 days of waterlogging stress. CK-MT, control without melatonin pretreatment; CK+MT, control with melatonin pretreatment; WL-MT, waterlogging without melatonin pretreatment; WL+MT, waterlogging with melatonin pretreatment. Data are expressed as mean ± SE of four replications. Letters marked by the same letters are not significant at $P < 0.05$ (Ducan's multiple range test).

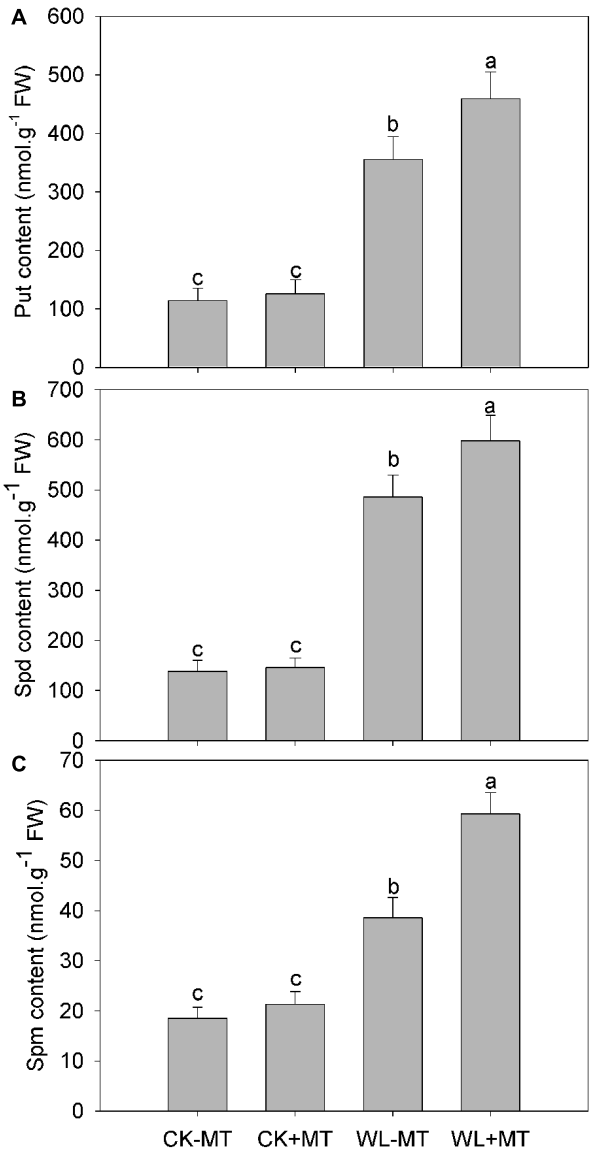

FIGURE 5 | Effects of waterlogging (WL) and exogenous melatonin (MT) pretreatment on leaf putrescine (Put, **A**), spermidine (Spd, **B**) and spermine (Spm, **C**) content in alfalfa plants. 45-day-old alfalfa plants pretreated with 100 μM melatonin and then exposed to 10 days of waterlogging stress. CK-MT, control without melatonin pretreatment; CK+MT, control with melatonin pretreatment; WL-MT, waterlogging without melatonin pretreatment; WL+MT, waterlogging with melatonin pretreatment. Data are expressed as mean ± SE of four replications. Letters marked by the same letters are not significant at $P < 0.05$ (Ducan's multiple range test).

Waterlogging Stress and Exogenous Melatonin Increased Endogenous Melatonin Content in Alfalfa

To determine whether the waterlogging stress and exogenous melatonin influence the endogenous melatonin levels, the endogenous melatonin concentration of alfalfa leaves was quantified after 10 days of waterlogging treatment. The melatonin concentration was about 1.1 ng g^{-1} fresh weight for the plants grown at control conditions (CK-MT) (**Figure 2**). Waterlogging (WL-MT) stress substantially increased the endogenous melatonin content in leaves of alfalfa, which increased 2.0-fold when compared to the control levels (CK-MT). However, pretreatment with exogenous melatonin resulted in a significant increase in melatonin content for the control plants (CK+MT) and water-logged plants (WL+MT), which enhanced 3.5- and 4.5-fold as compared to the control plants (CK-MT).

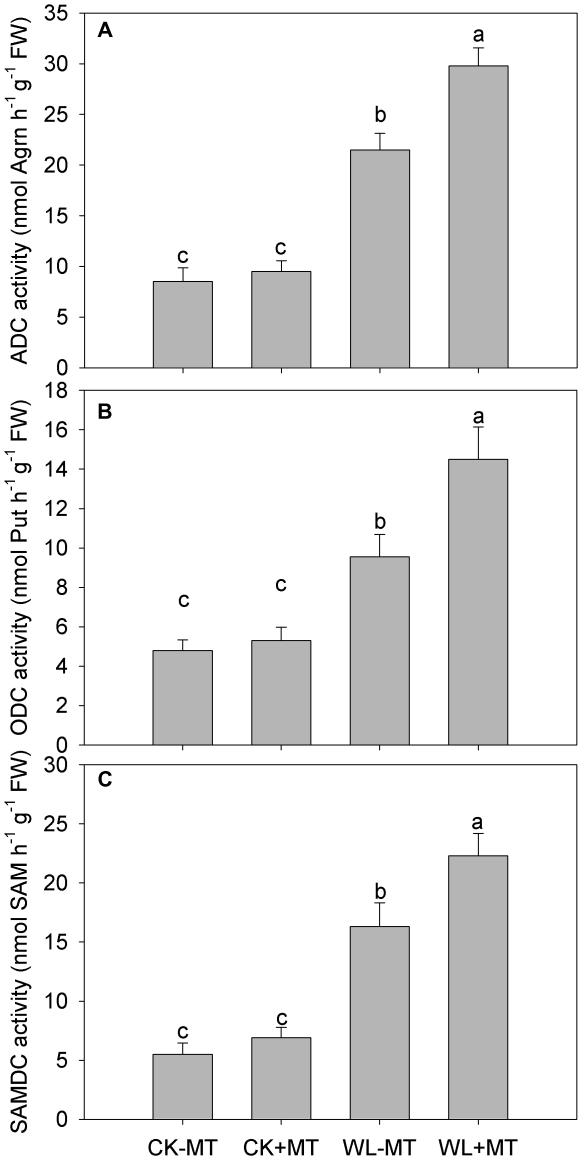

FIGURE 6 | Effect of waterlogging (WL) and exogenous melatonin (MT) pretreatment on ADC **(A)**, ornithine decarboxylase (ODC, **B**) and *S*-adenosylmethionine decarboxylase (SAMDC, **C**) activity in leaves of alfalfa plants. 45-day-old alfalfa plants pretreated with 100 μM melatonin and then exposed to 10 days of waterlogging stress. CK-MT, control without melatonin pretreatment; CK+MT, control with melatonin pretreatment; WL-MT, waterlogging without melatonin pretreatment; WL+MT, waterlogging with melatonin pretreatment. Data are expressed as mean ± SE of four replications. Letters marked by the same letters are not significant at $P < 0.05$ (Ducan's multiple range test).

Exogenous Melatonin Improved Waterlogging Stress-Induced Membrane Damage

Waterlogging stress caused a significant increase in leaf EL (**Figure 3A**) and malonaldehyde (MDA) content (**Figure 3B**), which increased to 4.4- and 2.5-fold of the control level for

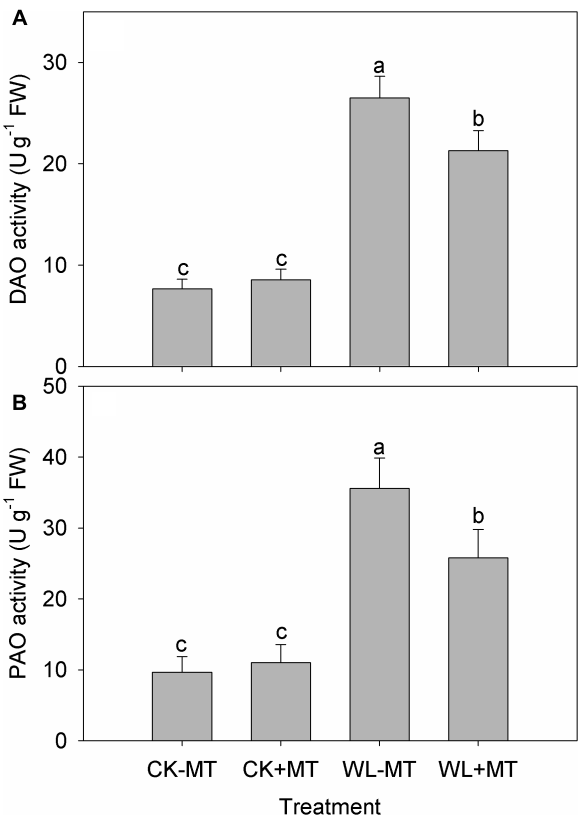

FIGURE 7 | Effects of waterlogging (WL) and exogenous melatonin (MT) pretreatment on leaf DAO **(A)** polyamine oxidase (PAO, **B**) activity in alfalfa plants. 45-day-old alfalfa plants pretreated with 100 μM melatonin and then exposed to 10 days of waterlogging stress. CK-MT, control without melatonin pretreatment; CK+MT, control with melatonin pretreatment; WL-MT, waterlogging without melatonin pretreatment; WL+MT, waterlogging with melatonin pretreatment. Data are expressed as mean ± SE of four replications. Letters marked by the same letters are not significant at $P < 0.05$ (Ducan's multiple range test).

EL and MDA content after 10 days of exposure, respectively. Instead, the leaf EL and MDA content significantly reduced in the waterlogging-stressed plants after melatonin pretreatment, which decreased by 25% for EL and 27% for MDA after 10 days of exposure when compared to the waterlogging stress alone (**Figures 3A,B**). Pretreatment with melatonin had no effect on leaf EL and MDA content in alfalfa under control conditions.

Effect of Exogenous Melatonin Improved Waterlogging Stress-Induced Leaf Senescence and Photosynthesis Reduction

Waterlogging stress caused significant leaf necrosis and senescence as indicated by the reduction of leaf chlorophyll content. Leaf chlorophyll content in water-logged plants was 80% of the water pretreated control level, while chlorophyll content in plants pretreated with melatonin was similar to the water pretreated control level (CK-MT) for both under waterlogged and non-waterlogged conditions (**Figure 4A**).

The leaf maximum photochemical efficiency (Fv/Fm) and net photosynthetic rate (P_n) under waterlogging were 11 and 28% lower than in the nation water-logged controls, respectively (**Figures 4B,C**). Pretreatment with melatonin improved Fv/Fm and P_n by 10 and 18% under waterlogging when compared with non-melatonin pretreatment. Melatonin pretreatment had no effect on the Fv/Fm and P_n under non-water-logged conditions as compared to the water pretreated plants.

Exogenous Melatonin Application Improved Free Polyamine Levels

The levels of the three soluble Pas—Put, Spd, and Spm—ncreased substantially under waterlogging, which increased to 3.1-, 3.5-, and 2.1-fold higher than the control levels, respectively (**Figures 5A–C**). However, pretreatment with melatonin further increased leaf Put, Spd, and Spm levels under waterlogging, whereas pretreatment with melatonin has no effect on Put, Spd, and Spm levels under control conditions.

Exogenous Melatonin Application Regulated Key Enzymes Involved in Polyamine Metabolism

Waterlogging stress dramatically increased ADC, ODC, and SAMDC activities in leaves of alfalfa, which increased to 2.5-, 2.0-, and 3.0-fold of the control levels, respectively (**Figures 6A–C**). Pretreatment with melatonin accelerated the increase and significantly increased ADC, ODC, and SAMDC activities in water-logged plants, while plants pretreated with melatonin had

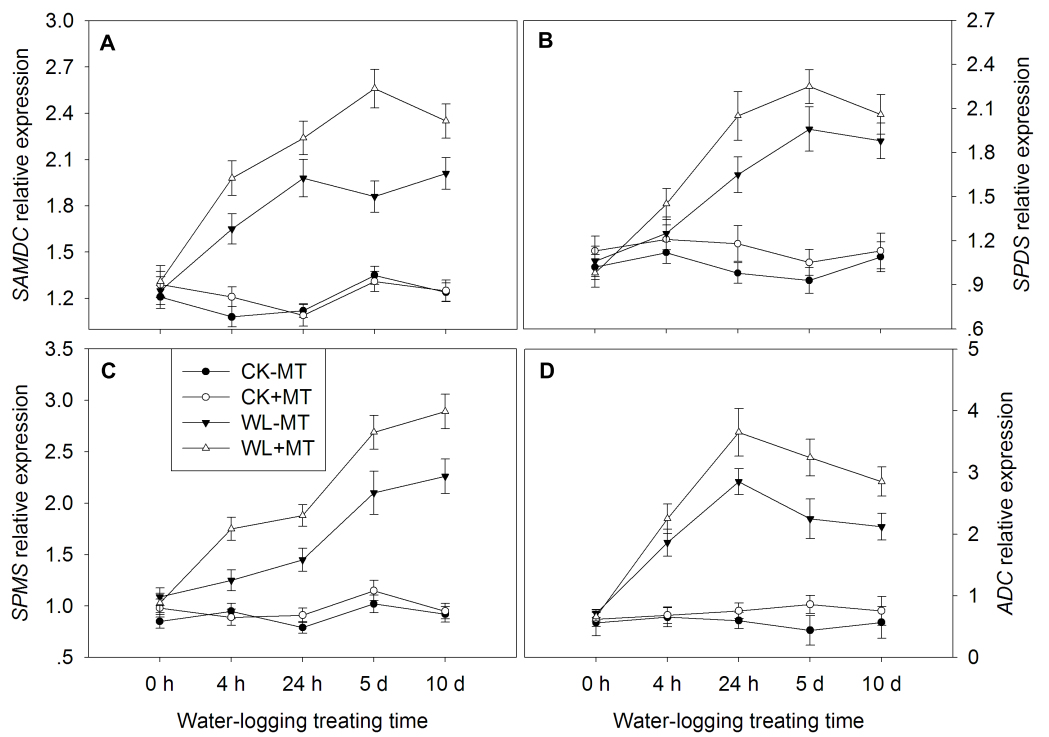

FIGURE 8 | Effects of waterlogging (WL) and exogenous melatonin (MT) pretreatment on SAM decarboxylase (SAMDC, **A**), spermidine synthase (SPDS, **B**), spermine synthase (SPMS, **C**) and ADC **(D)** gene expression in alfalfa plants. 45-day-old alfalfa plants pretreated with 100 μM melatonin and then exposed to 10 days of waterlogging stress. CK-MT, control without melatonin pretreatment; CK+MT, control with melatonin pretreatment; WL-MT, waterlogging without melatonin pretreatment; WL+MT, waterlogging with melatonin pretreatment. Data are expressed as mean ± SE of four replications.

no obvious effect on the ADC, ODC, and SAMDC activities under non-water-logged conditions.

Waterlogging increased leaf DAO and PAO activity in alfalfa plants, which increased 3.5- and 3.7-fold when compared to the control levels (**Figures 7A,B**), respectively. However, the DAO and PAO activity was reduced by 24 and 38% in the melatonin pretreated plants under waterlogged conditions as compared to the waterlogged alone.

Exogenous Melatonin Application Regulated the Expression of Key Genes Involved in Polyamine Metabolism

The key enzyme genes involved in the polyamine biosynthetic and catabolic pathways, i.e., *SAMDC, SPDS, SPMS*, *ADC*, *DAO,* and *PAO* were analyzed by qRT-PCR (**Figure 8**). The expression levels of *SAMDC* start to rise 4 h after waterlogging and generally remained high till day 10 (**Figure 9A**). The expression level of *SAMDC* in waterlogging stress was upregulated by 1.5-fold at 4 h, 1.8-fold at 24 h, 1.4-fold at day 5, and 1.6-fold at day 10 as compared with the control levels. Pretreatment with melatonin caused further upregulation of *SAMDC* during waterlogging treatment, which upregulated 1.8-fold at 4 h, 2.0-fold at 24 h, and 1.9-fold at days 5 and 10 when compared to the control levels. The expression levels of *SPDS* started to rise 24 h after waterlogging and peaked at 5 days (**Figure 9B**). The expression level of *SPDS* in waterlogging stress was upregulated by 1.7-fold at 24 h, 2.1-fold at day 5, and 1.7-fold at day 10 as compared with the control levels. Pretreatment with melatonin caused further upregulation of *SPDS* during waterlogging treatment, which upregulated 1.3-fold at 4 h, 2.1-fold at 24 h, 2.4-fold at day 5, and 1.9-fold at day 10 when compared to the control levels. Waterlogging induced significant upregulation of *SPMS* in leaves of alfalfa, which upregulated by 1.3-fold at 4 h, 1.8-fold at 24 h, 2.1-fold at day 5, and 2.5-fold at day 10 when compared to the control levels (**Figure 8C**). However, those upregulated folds rose to 1.8-fold at 4 h, 2.4-fold at 24 h, 2.6-fold at day 5, and 3.1-fold at day 10 by melatonin pretreatment, respectively. The expression level of *ADC* significantly increased with the progress of waterlogging and peaked at 24 h, when compared to the control level (**Figure 8D**). Melatonin pretreatment substantially upregulated the expression level of *ADC* under waterlogging treatment.

Pretreatment with melatonin alone had no significant effect on the expression levels of *PAO* and *DAO* under control condition (**Figure 9**). Waterlogging did not significantly affect the expression level of *PAO* during the first 4 h but began to rise 24 h after waterlogging, and the expression levels peaked at 5 days of waterlogging (**Figure 9A**). Melatonin pretreatment dramatically downregulated the expression levels of *PAO* from 24 h to 10 days when compared with waterlogging alone. Waterlogging stress induced a higher expression level of *DAO* as compared to the control plants (**Figure 9B**). Evidently, foliar pretreatment with melatonin remarkably depressed the expression levels of *DAO* as compared to waterlogging alone.

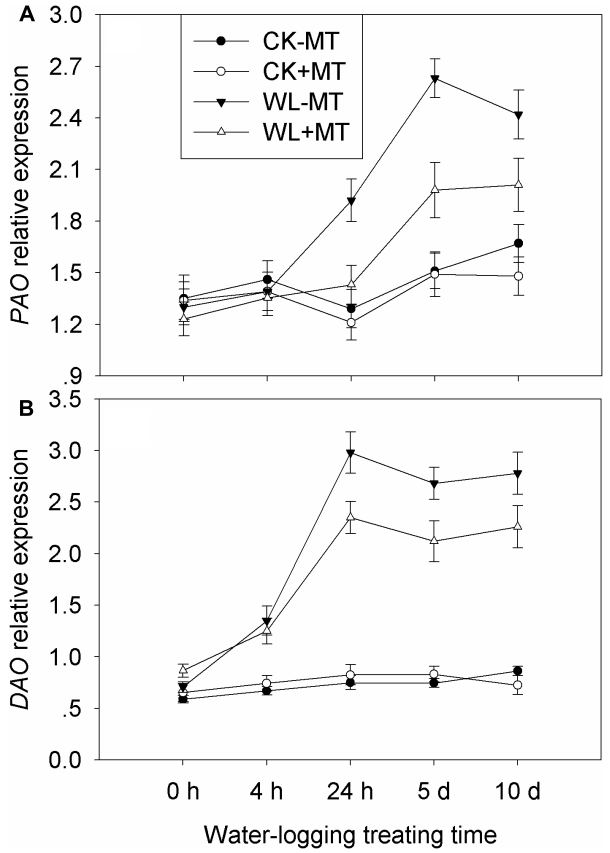

FIGURE 9 | Effects of waterlogging (WL) and exogenous melatonin (MT) pretreatment on DAO **(A)** polyamine oxidase (PAO, **B**) gene expression in alfalfa plants. 45-day-old alfalfa plants pretreated with 100 μM melatonin and then exposed to 10 days of waterlogging stress. CK-MT, control without melatonin pretreatment; CK+MT, control with melatonin pretreatment; WL-MT, waterlogging without melatonin pretreatment; WL+MT, waterlogging with melatonin pretreatment. Data are expressed as mean ± SE of four replications.

Exogenous Melatonin Application Downregulates Ethylene Synthesis and Signaling

The leaf ethylene production rate started to rise 4 h after waterlogging and continually increased over the l0 days of treatment (**Figure 10A**). The amount of ethylene increased to 1.6-, 1.7-, and 2.0-fold of the control levels at 24 h, 5 and 10 days under waterlogging, respectively. However, pretreatment with melatonin dramatically repressed the leaf ethylene production rate under waterlogging. Under water-logged conditions, the leaf ethylene production rate in melatonin pretreated plants decreased by 39, 23, and 22% when compared to the waterlogging alone at 24 h, 5 and 10 days of treatment, respectively.

The genes possibly involved in ethylene biosynthesis (*ACS, ACO*) and signaling (*ERF*) were determined in alfalfa plants. Plants pretreated with melatonin have no obvious effect

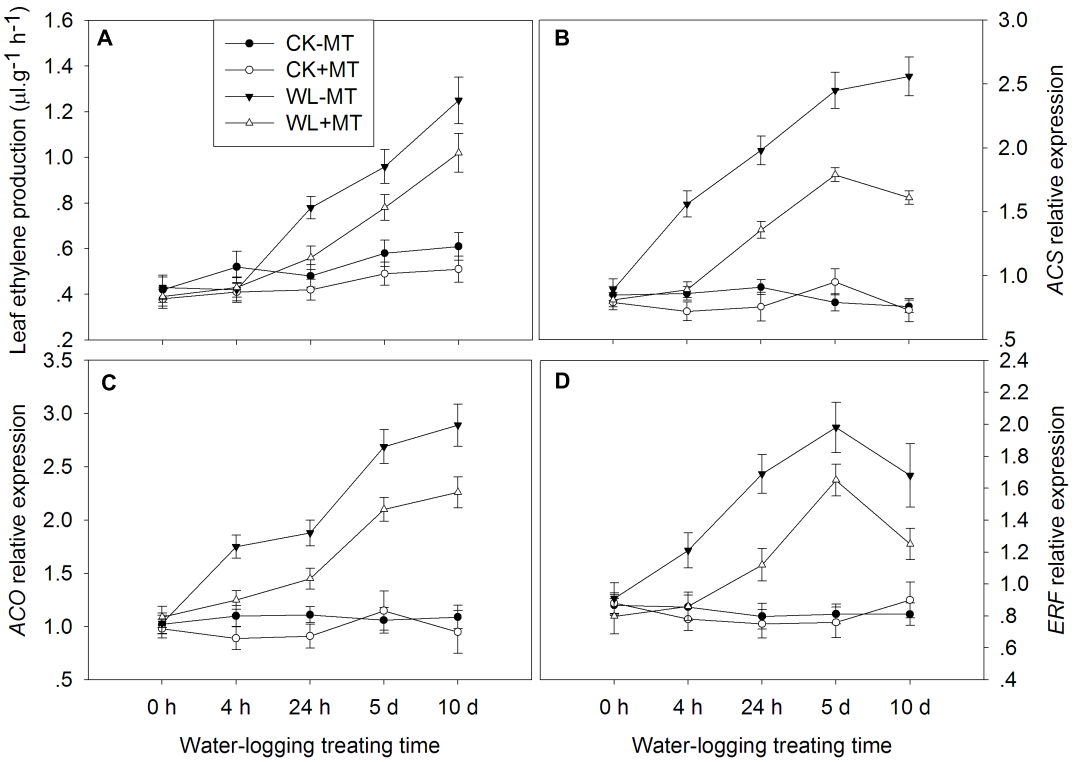

FIGURE 10 | Effect of waterlogging (WL) and exogenous melatonin (MT) pretreatment on ethylene production **(A)**, and key genes involved in ethylene synthesis **(B,C)** and signaling **(D)** in leaves of alfalfa plants. 45-day-old alfalfa plants pretreated with 100 μM melatonin and then exposed to 10 days of waterlogging stress. CK-MT, control without melatonin pretreatment; CK+MT, control with melatonin pretreatment; WL-MT, waterlogging without melatonin pretreatment; WL+MT, waterlogging with melatonin pretreatment. Data are expressed as mean ± SE of four replications.

on the *ACS, ACO,* and *ERF* expression under non-waterlogged conditions (**Figure 10**). Waterlogging dramatically increased the expression levels of *ACS* in leaves of alfalfa, which increased to 1.8-, 2.2-, 3.1-, and 3.4-fold of the control levels at 4 h, 24 h, 5 and 10 days, respectively (**Figure 10B**). However, pretreatment with melatonin significantly decreased *ACS* expression in water-logged plants as compared to the waterlogging alone. Waterlogging induced a significantly higher expression level of *ACO* and *ERF* over the 10 days of treatment when compared to the control plants (**Figures 10C,D**). Pretreatment with melatonin remarkably decreased the expression level of *ACO* and *ERF* over the 10 days of treatment when compared to the waterlogging alone.

DISCUSSION

The excessive water content in soil (waterlogging) is a major environmental stress that limits crop production and causes yield losses worldwide (Jackson and Colmer, 2005). Crops can endure soil waterlogging from some hours to some days or months, depending on the tolerance to flooding for the crop species or cultivars (Voesenek and Bailey-Serres, 2015). However, excess water in soil often exerts detrimental effects to these crops which are intolerant to waterlogging stress. Alfalfa is the most widely used forage legume, but it is susceptible to waterlogging stress, and this is a serious constraint in areas with shallow water tables and heavy rainfalls (Striker and Colmer, 2016).

Waterlogging induces several phenotypic and physiological disturbances, including growth inhibition of roots and shoots, impairs water and nutrient uptake, and eventually results in plants chlorosis and even death (Arbona et al., 2008). Here, waterlogging caused a dramatic increase in EL and MDA content and a remarkable decrease in chlorophyll content in alfalfa plants, but this response was greatly suppressed by melatonin pretreatment. These results implied that melatonin pretreatment can alleviate the detrimental effect of waterlogging in alfalfa. To confirm this finding, we also measured variations in the plant growth rate and leaf P_n and found that plant growth rate and leaf P_n also reduced dramatically under waterlogging. However, this response is remarkably suppressed in alfalfa plants with melatonin pretreatment. Such growth and photosynthesis-preserving effects of melatonin have already been shown for numerous plant species under various stress conditions (Mukherjee et al., 2014; Zhao et al., 2017; Zheng et al., 2017).

It has been reported that various environmental abiotic stresses such as temperature stress, salt and water stress, heavy

metal stress that stimulated melatonin accumulation in plant species, and this stimulation have been regarded as a self-defense response to external stimuli through the regulation of leaf senescence, antioxidant systems, carbon and nitrogen metabolism in plants (Li et al., 2012; Bajwa et al., 2014; Byeon and Back, 2014; Tan, 2015). In the present study, both waterlogging stress and melatonin pretreatment remarkably increased melatonin levels in alfalfa plants, indicating that waterlogging stress can induce the accumulation of endogenous melatonin in plants as a protective response (Paredes et al., 2009). A greater increase in the melatonin pretreated plants than the untreated ones suggests that melatonin absorbed from outside mainly resulted in melatonin increase in addition to a post-transcriptional regulation of melatonin synthesis (Zheng et al., 2017). The chlorosis is a regular indicator unavoidably happening after severe waterlogging stress, because waterlogging results in over-production of $O_2^{\cdot-}$ and H_2O_2, which destroys chlorophyll and leads to the breakdown of chloroplasts (Smethurst and Shabala, 2003). The protective effects of melatonin on Chl degradation and photosynthetic capacity have been investigated previously in other abiotic stresses, such as water deficit and high temperature (Wang et al., 2013; Zhang et al., 2017). The chloroplast has been proved to be the major site for melatonin production, but it was one of the organelles that suffered most from ROS. Plenty of melatonin is required to sustain its structure and function. Therefore, the absorbed and *in vivo*-synthesized melatonin can function together to mitigate waterlogging-induced membrane damage and help alfalfa plants to survive the stress.

Waterlogging decreases photosynthesis in many plant species and develops leaf injury symptoms, such as wilting and chlorosis (Shao et al., 2013), which were also observed in this study. These symptoms developed under waterlogging have been attributed to ethylene production in addition to other restricting factors (Loreti et al., 2016). In our study, ethylene production significantly increased along with the prolonged waterlogging stress treatment in alfalfa, which was inconsistent with previous reports that enhanced ethylene production in perennial pepperweed (*Lepidium latifolium*) (Chen et al., 2002), avocado (*Persea americana*) (Gil et al., 2009), and cotton (*Gossypium hirsutum*) (Najeeb et al., 2018) caused leaf senescence and abscission of leaves and fruits. Ethylene aggravates the effects of abiotic stresses, whereas the detrimental effect of waterlogging on plants can be alleviated by reducing the levels of endogenous ethylene in plants (Najeeb et al., 2015). In this study, alfalfa plants pretreated with melatonin dramatically decreased ethylene production during waterlogging stress, suggesting that the mitigation of melatonin on waterlogging stress in alfalfa are at least partially attributed to reduced ethylene production.

During the ethylene biosynthesis process, both *ACS* and *ACO* are regulated by various external and internal cues to control ethylene production. In addition, the transcription factor

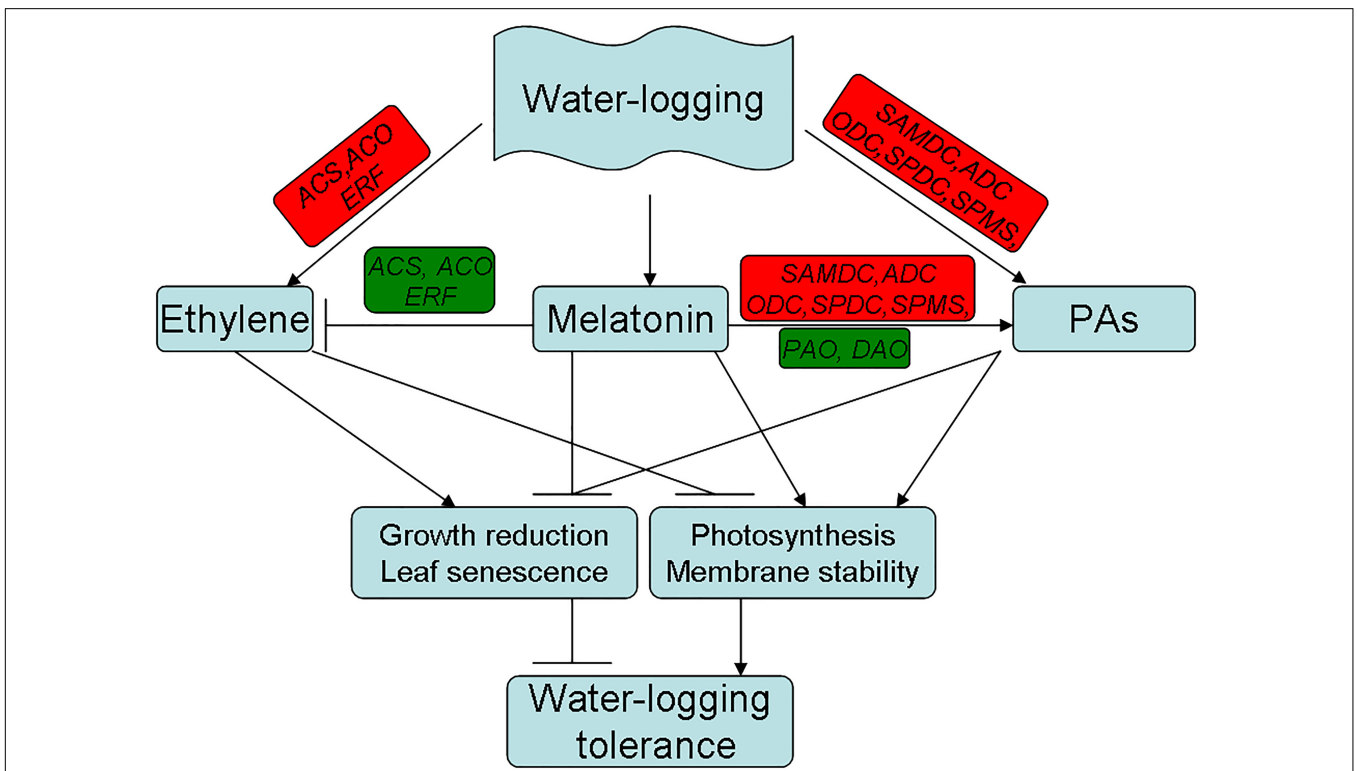

FIGURE 11 | Proposed pathways for the melatonin mediated waterlogging stress response in alfalfa derived from results involving ethylene and PAs metabolism. (Red color indicates induced and green color indicates suppressed for the expression of the gene.)

ethylene response factor (*ERF*) has also been associated with waterlogging and modulates ethylene response under flooding (Yang et al., 2011). Under waterlogged conditions, more ACC is synthesized in roots and transported to plant shoots, where it is converted to ethylene by *ACO* (Sasidharan and Voesenek, 2015). In the current study, a remarkable upregulation of *ACS* and *ACO* in alfalfa plants under waterlogging stress occurred, along with significantly enhanced ethylene production. Meanwhile pretreatment with melatonin significantly suppressed the *ACS* and *ACO* expression and was accompanied by depressed ethylene production in alfalfa plants under waterlogging. These results suggested that waterlogging stress mitigation by the exogenous melatonin in alfalfa was associated with the ethylene biosynthesis at transcription levels.

Polyamines are polybasic amines that interact with polycationic macromolecules such as DNA, RNA, and proteins (Bouchereau et al., 1999), processes which are positively associated with the endogenous PA levels. In the current study, melatonin pretreatment downregulated ethylene biosynthesis-related gene expression, leading to depressed ethylene production. This process may suppress SAM for ethylene production and moved to PAs biosynthesis. To confirm this hypothesis, free PA content was determined in alfalfa plants after pretreatment with melatonin under waterlogging and it was found that Put, Spd, and Spm contents significantly increased in melatonin pretreated plants. These results indicate that melatonin may strengthen the SAM to PA metabolism, thus increasing waterlogging tolerance in alfalfa plants.

Previous studies indicated that melatonin induces the activity of the PA metabolism enzymes, thus affecting endogenous PA levels under chilling (Zhao et al., 2017). To reveal how melatonin regulates PA levels under waterlogging, the activity of related enzymes and gene expressions related to PA metabolism were determined. The results showed that the gene expression levels and activities of the PA synthesis enzymes, ADC, ODC, SAMDC and also those of the PA catabolism enzymes, DAO, PAO, were dramatically increased under waterlogging, suggesting that PA metabolism was promoted by waterlogging. Furthermore, melatonin pretreatment further increased the activities and gene expression levels of the ADC, ODC and SAMDC enzymes, while it suppressed the activities and gene expression levels of the DAO and PAO enzyme in alfalfa plants under waterlogging. These results indicated that melatonin improved waterlogging tolerance through the regulation of PA metabolism controlled at transcriptional and translational levels in alfalfa plants. It has been well-documented that PAs are involved in the acquisition of plant tolerance to diverse environmental stresses (Groppa and Benavides, 2008; Gupta et al., 2013). *SPMS* and *SPDS* gene expressions are up-regulated by melatonin pretreatment under waterlogging with concomitant suppression of PAO and DAO activity, possibly helping to maintain Spm and Spd content at a high level, which implies that melatonin mitigates waterlogging stress by activating enzymes involved in the PA metabolism to increase the PA levels.

CONCLUSION

Based on the above observations, a model for melatonin-mediated waterlogging stress response in alfalfa was proposed in the current study (**Figure 11**). In this study, we demonstrated that melatonin has significant involvement in mitigating waterlogging stress in alfalfa. The mechanisms through which melatonin alleviates waterlogging injury may be presented as follows. First, melatonin suppressed ethylene production through downregulating the ethylene biosynthesis-related genes and mitigating waterlogging-induced growth reduction, chlorosis and premature senescence in plants. Second, melatonin increases PA content by enhancing the activity and gene expressions of the PA metabolism enzymes. The positive result in this study indicated that melatonin suppressed ethylene production in alfalfa under waterlogging at least partially by reprogramming ethylene and PA biosynthesis. This study provides new evidence that melatonin mitigates waterlogging stress through cross-talk with or directly modulating the metabolic pathways of PAs and ethylene in alfalfa.

AUTHOR CONTRIBUTIONS

QZ and XL performed the experiments. NL, DL, and LH conceived, designed, executed, and evaluated of the experiments. ZZ, NL, and LH analyzed the data of the experiments. QZ and LH helped to draft the manuscript. All authors read and approved the final manuscript.

FUNDING

This work was financially supported by the Science Foundation for The Excellent Youth of the Hunan Provincial Education Department (Grant No. 17B120), the Natural Science Foundation of Hunan Province (Grant No. 2018JJ3223), and the Changsha Municipal Key Research & Development Program (Grant No. kq1801019).

REFERENCES

Alcázar, R., Altabella, T., Marco, F., Bortolotti, C., Reymond, M., Koncz, C., et al. (2010). Polyamines: molecules with regulatory functions in plant abiotic stress tolerance. *Planta* 231, 1237–1249. doi: 10.1007/s00425-010-1130-0

Apelbaum, A., Burgoon, A. C., Anderson, J. D., Lieberman, M., Ben-Arie, R., and Matto, A. K. (1981). Polyamines inhibit biosynthesis of ethylene in higher plant tissue and fruit protoplasts. *Plant Physiol.* 68, 453–456. doi: 10.1104/pp.68.2.453

Arbona, V., Hossain, Z., López-Climent, M. F., Pérez-Clemente, R. M., and Gómez-Cadenas, A. (2008). Antioxidant enzymatic activity is linked to waterlogging stress tolerance in citrus. *Physiol. Plant.* 132, 452–466. doi: 10.1111/j.1399-3054.2007.01029.x

Bajwa, V. S., Shukla, M. R., Sherif, S. M., Murch, S. J., and Saxena, P. K. (2014). Role of melatonin in alleviating cold stress in *Arabidopsis thaliana*. *J. Pineal Res.* 56, 238–245. doi: 10.1111/jpi.12115

Boru, G., Vantoai, T. T., Alves, J., Hua, D., and Knee, M. (2003). The response of soybean to oxygen deficiency and elevated root-zone

carbon dioxide concentration. *Ann. Bot.* 91, 447–453. doi: 10.1093/aob/mcg040

Bouchereau, A., Aziz, A., Larher, F., and Martin-Tanguy, J. (1999). Polyamines and environmental challenges: recent development. *Plant Sci.* 140, 103–125. doi: 10.1104/pp.68.2.453

Byeon, Y., and Back, K. (2014). An increase in melatonin in transgenic rice causes pleiotropic phenotypes, including enhanced seedling growth, delayed flowering, and low grain yield. *J. Pineal Res.* 56, 408–414. doi: 10.1111/jpi.12129

Chen, H. J., Qualls, R. G., and Miller, G. C. (2002). Adaptive responses of Lepidium latifolium to soil flooding: biomass allocation adventitious rooting aerenchyma formation and ethylene production. *Environ. Exp. Bot.* 48, 119–128. doi: 10.1016/S0098-8472(02)00018-7

Duan, J. J., Li, J., Guo, S. R., and Kang, Y. Y. (2008). Exogenous spermidine affects polyamine metabolism in salinity-stressed Cucumis sativus roots and enhances short-term salinity tolerance. *J. Plant Physiol.* 165, 1620–1635. doi: 10.1016/j.jplph.2007.11.006

Gil, P. M., Gurovich, L., Schaffer, B., García, N., and Iturriaga, R. (2009). Electrical signaling, stomatal conductance, ABA and an ethylene content in avocado trees in response to root hypoxia. *Plant Signal. Behav.* 4, 100–108. doi: 10.4161/psb.4.2.7872

Gong, X., Shi, S., Dou, F., Song, Y., and Ma, F. (2017). Exogenous melatonin alleviates alkaline stress in *Malus hupehensis* Rehd. by regulating the biosynthesis of polyamines. *Molecules* 22:E1542. doi: 10.3390/molecules22091542

Groppa, M., and Benavides, M. (2008). Polyamines and abiotic stress: recent advances. *Amino Acids* 34, 35–45. doi: 10.1007/s00726-007-0501-8

Gupta, K., Dey, A., and Gupta, B. (2013). Plant polyamines in abiotic stress responses. *Acta Physiol. Plant.* 35, 2015–2036. doi: 10.1007/s11738-013-1239-4

Hardeland, R., Cardinall, D. P., Srinivasan, V., Spencee, D. W., Brownf, G. M., and Pandi-Perumalg, S. R. (2011). Melatonin – a pleiotropic, orchestrating regulator molecule. *Prog. Neurobiol.* 93, 350–384. doi: 10.1016/j.pneurobio.2010.12.004

Heath, R. L., and Packer, L. (1968). Photoperoxidation in isolated chloroplasts. I. Kinetics and stoichiometry of fatty acid peroxidation. *Arch. Biochem. Biophys.* 125, 189–198. doi: 10.1016/0003-9861(68)90654-1

Hu, L. X., Zhang, Z. F., Xiang, Z. X., and Yang, Z. J. (2016). Exogenous application of citric acid ameliorates the adverse effect of heat stress in tall fescue (Lolium arundinaceum). *Front. Plant Sci.* 7:179. doi: 10.3389/fpls.2016.00179

Hu, X., Zhang, Y., Shi, Y., Zhang, Z., Zou, Z., Zhang, H., et al. (2012). Effect of exogenous spermidine on polyamine content and metabolism in tomato exposed to salinity-alkalinity mixed stress. *Plant Physiol. Biochem.* 57, 200–209. doi: 10.1016/j.plaphy.2012.05.015

Jackson, M. B., and Colmer, T. D. (2005). Response and adaptation by plants to flooding stress. *Ann. Bot.* 96, 501–505. doi: 10.1093/aob/mci205

Koyama, F. C., Carvalho, T. L. G., Alves, E., da Silva, H. B., de Azevedo, M. F., Hemerly, A. S., et al. (2013). The structurally related auxin and melatonin tryptophan-derivatives and their roles in *Arabidopsis thaliana* and in the human malaria parasite *Plasmodium falciparum*. *J. Eukaryotic Microbiol.* 60, 646–651. doi: 10.1111/jeu.12080

Lee, K. S., Lee, W. S., Suh, S. I., Kim, S. P., Lee, S. R., Ryoo, Y. W., et al. (2003). Melatonin reduces ultraviolet-B induced cell damages and polyamine levels in human skin fibroblasts in culture. *Exp. Mol. Med.* 35, 263–268. doi: 10.1038/emm.2003.35

Lee, Y. K., Lee, S. R., and Kim, C. Y. (2000). Melatonin attenuates the changes in polyamine levels induced by systemic kainate administration in rat brains. *J. Neurol. Sci.* 178, 124–131. doi: 10.1016/S0022-510X(00)00393-2

Li, C., Wang, P., Wei, Z., Liang, D., Liu, C., Yin, L., et al. (2012). The mitigation effects of exogenous melatonin on salinity induced stress in *Malus hupehensis*. *J. Pineal Res.* 53, 298–306. doi: 10.1111/j.1600-079X.2012.00999.x

Livak, K. J., and Schmittgen, T. D. (2001). Analysis of relative gene expression data using real-time quantitative PCR and the 2-ddCT method. *Methods* 25, 402–408. doi: 10.1006/meth.2001.1262

Loreti, E., van Veen, H., and Perata, P. (2016). Plant responses to flooding stress. *Cur. Opin. Plant Biol.* 33, 64–71. doi: 10.1016/j.pbi.2016.06.005

Mukherjee, S., David, A., Yadav, S., Baluška, F., and Bhatla, S. C. (2014). Salt stress-induced seedling growth inhibition coincides with the differential distribution of serotonin and melatonin in sunflower seedling roots and cotyledons. *Physiol. Plant* 152, 714–728. doi: 10.1111/ppl.12218

Najeeb, U., Atwell, B. J., Bange, M. P., and Tan, D. K. Y. (2015). Aminoethoxyvinylglycine (AVG) ameliorates waterlogging-induced damage in cotton by inhibiting ethylene synthesis and sustaining photosynthetic capacity. *Plant Growth Regul.* 76, 83–98. doi: 10.1007/s10725-015-0037-y

Najeeb, U., Tan, D. K. Y., Bange, M. P., and Atwell, B. J. (2018). Protecting cotton crops under elevated CO2 from waterlogging by managing ethylene. *Fun. Plant Biol.* 45:340. doi: 10.1071/FP17184

Paredes, S. D., Korkmaz, A., Manchester, L. C., Tan, D. X., and Reiter, R. J. (2009). Phytomelatonin: a review. *J. Exp. Bot.* 60, 57–69. doi: 10.1093/jxb/ern284

Pierik, R., Sasidharan, R., and Voesenek, L. A. C. J. (2007). Growth control by ethylene: adjusting phenotypes to the environment. *J. Plant Growth Regul.* 26, 188–200. doi: 10.1007/s00344-006-0124-4

Rajala, A., and Peltonen-Sainio, P. (2001). Plant growth regulator effects on spring cereal root and shoot growth. *Agron. J.* 93, 936–943. doi: 10.2134/agronj2001.934936x

Sasidharan, R., and Voesenek, L. A. C. J. (2015). Ethylene-mediated acclimations to flooding stress. *Plant Physiol.* 169, 3–12. doi: 10.1104/pp.15.00387

Shao, G. C., Lan, J. J., Yu, S. E., Liu, N., Guo, R. Q., and She, D. L. (2013). Photosynthesis and growth of winter wheat in response to waterlogging at different growth stages. *Photosynthetica* 51, 429–437. doi: 10.1007/s11099-013-0039-9

Shi, H. T., and Chan, Z. L. (2014). The Cysteine2/Histidine2-type transcription factor zinc finger of *Arabidopsis thaliana* 6-activated C-repeat-binding factor pathway is essential for melatonin-mediated freezing stress resistance in Arabidopsis. *J. Pineal Res.* 57, 185–191. doi: 10.1111/jpi.12155

Shi, H. T., Wang, X., Tan, D., Reiter, R. J., and Chan, Z. L. (2015). Comparative physiological and proteomic analyses reveal the actions of melatonin in the reduction of oxidative stress in Bermuda grass (*Cynodon dactylon* (L). *Pers. J. Pineal Res.* 59, 120–131. doi: 10.1111/jpi.12246

Smethurst, C. F., Garnett, T., and Shabala, S. (2005). Nutritional and chlorophyll fluorescence responses of lucerne (Medicago sativa) to waterlogging and subsequent recovery. *Plant Soil* 270, 31–45. doi: 10.1007/s11104-004-1082-x

Smethurst, C. F., and Shabala, S. (2003). Screening methods for waterlogging tolerance in Lucerne: a comparative analysis of waterlogging effects on chlorophyll fluorescence, photosynthesis, biomass, and chlorophyll content. *Fun. Plant Biol.* 30, 335–343. doi: 10.1071/FP02192

Striker, G. G., and Colmer, T. D. (2016). Flooding tolerance of forage legumes. *J. Exp. Bot.* 68, 1851–1872. doi: 10.1093/jxb/erw239

Tan, D. X. (2015). Melatonin and plants. *J. Exp. Bot.* 66, 625–626. doi: 10.1093/jxb/eru523

Tan, D. X., Hardeland, R., Manchester, L. C., Korkmaz, A., Ma, S., Rosales-Corral, S., et al. (2012). Functional roles of melatonin in plants, and perspectives in nutritional and agricultural science. *J. Exp. Bot.* 63, 577–597. doi: 10.1093/jxb/err256

Tavladoraki, P., Cona, A., Federico, R., Tempera, G., Viceconte, N., Saccoccio, S., et al. (2012). Polyamine catabolism: a target for antiproliferative therapies in animals and stress tolerance strategies in plants. *Amino Acids* 42, 411–426. doi: 10.1007/s00726-011-1012-1

Voesenek, L. A., and Bailey-Serres, J. (2015). Flood adaptive traits and processes: an overview. *New Phytol.* 206, 57–73. doi: 10.1111/nph.13209

Wang, P., Sun, X., Li, C., Wei, Z., Liang, D., and Ma, F. (2013). Long-term exogenous application of melatonin delays drought-induced leaf senescence in apple. *J. Pineal Res.* 54, 292–302. doi: 10.1111/jpi.12017

Wilkinson, S., and Davies, W. J. (2009). Ozone suppresses soil drying- and abscisic acid (ABA)-induced stomatal closure via an ethylene-dependent mechanism. *Plant Cell Environ.* 32, 949–959. doi: 10.1111/j.1365-3040.2009.01970.x

Yang, C. Y., Hsu, F. C., Li, J. P., Wang, N. N., and Shih, M. C. (2011). The AP2/ERF transcription factor AtERF73/HRE1 modulates ethylene responses during hypoxia in Arabidopsis. *Plant Physiol.* 156, 202–212. doi: 10.1104/pp.111.172486

Zhang, J., Shi, Y., Zhang, X., Du, H., Xu, B., and Huang, B. R. (2017). Melatonin suppression of heat-induced leaf senescence involves crosstalk with abscisic acid and cytokinin biosynthesis and signaling pathways in perennial ryegrass (*Lolium perenne* L.). *Environ. Exp. Bot.* 138, 36–45. doi: 10.1016/j.envexpbot.2017.02.012

Zhao, F. G., Zhang, G. Z., Zhang, Z. F., and Wang, X. Y. (1996). Changes of free polyamines levels and activities of some enzymes during senescence stage of peanut leaves. *Plant Physiol. Commun.* 32, 351–353.

Zhao, H. L., Zhang, K., Zhou, X. T., Xi, L. J., Wang, Y. P., Xu, H. J., et al. (2017). Melatonin alleviates chilling stress in cucumber seedlings by up-regulation of CsZat12 and modulation of polyamine and abscisic acid metabolism. *Scient. Rep.* 7:4998. doi: 10.1038/s41598-017-05267-3

Zheng, X., Zhou, J., Tan, D. X., Wang, N., Wang, L., Shan, D., et al. (2017). Melatonin improves waterlogging tolerance of *Malus baccata* (Linn.) Borkh. seedlings by maintaining aerobic respiration, photosynthesis and ROS migration. *Front. Plant Sci.* 8:483. doi: 10.3389/fpls.2017.00483

Conflict of Interest Statement: The authors declare that the research was conducted in the absence of any commercial or financial relationships that could be construed as a potential conflict of interest.

frontiers in Plant Science

ORIGINAL RESEARCH
published: 04 February 2019
doi: 10.3389/fpls.2019.00062

Morphological Changes and Expressions of *AOX1A*, *CYP81D8*, and Putative *PFP* Genes in a Large Set of Commercial Maize Hybrids Under Extreme Waterlogging

Anna Panozzo, Cristian Dal Cortivo, Manuel Ferrari, Bianca Vicelli, Serena Varotto and Teofilo Vamerali*

Department of Agronomy, Food, Natural Resources, Animals and the Environment, University of Padua, Padua, Italy

OPEN ACCESS

Edited by:
Iduna Arduini,
University of Pisa, Italy

Reviewed by:
Katsuhiro Shiono,
Fukui Prefectural University, Japan
Lorenzo Guglielminetti,
University of Pisa, Italy

***Correspondence:**
Anna Panozzo
anna.panozzo.1@phd.unipd.it;
nn.panozzo@gmail.com

Specialty section:
This article was submitted to Plant Abiotic Stress, a section of the journal Frontiers in Plant Science

Received: *31 October 2018*
Accepted: *16 January 2019*
Published: *04 February 2019*

Citation:
Panozzo A, Dal Cortivo C, Ferrari M, Vicelli B, Varotto S and Vamerali T (2019) Morphological Changes and Expressions of AOX1A, CYP81D8, and Putative PFP Genes in a Large Set of Commercial Maize Hybrids Under Extreme Waterlogging. Front. Plant Sci. 10:62. doi: 10.3389/fpls.2019.00062

Waterlogging is a severe abiotic stressor causing significant growth impairment and yield losses in many crops. Maize is highly sensitive to the excess of water, and against the background of climate change there is an urgent need for deeper insights into the mechanisms of crop adaptation to waterlogging. In the present study, changes in maize morphology at the 4–5 leaf stage and the expression of three candidate genes for flooding tolerance in plants subjected to six continuous days of waterlogging were recorded in 19 commercial hybrids and in the inbred line B73, with the aim of investigating the current variability in cultivated hybrids and identifying useful morphological and molecular markers for screening tolerant genotypes. Here it was demonstrated that root parameters (length, area, biomass) were more impaired by waterlogging than shoot parameters (shoot height and biomass). Culm height generally increased in stressed plants (by up to +24% vs. controls), while shoot biomass was significantly reduced in only two hybrids. Root biomass was reduced in all the hybrids, by an average of 30%, and significantly in 7 hybrids, while root length and area were even more severely reduced, by 30–55% vs. controls, depending on the hybrid. The earlier appearance of aerial roots seemed to be associated with greater root injuries. In leaves, the transcript of the PFP enzyme (phosphofructokinase), which is involved in glycolytic reactions, was markedly up-regulated (up to double the values) in half the waterlogged hybrids, but down-regulated in the others. The transcript of *CYP81D8* (ROS-related proteins) in waterlogged plants exhibited relevant increases or strong decreases in level, depending on the hybrid. The transcript of the *AOX1A* gene, coding for a mitochondrial respiratory electron transport chain-related protein, was markedly down-regulated in all the treated hybrids. Expression analysis of these genes under extreme waterlogging only partially correlate with the shoot and root growth impairments observed, and *AOX1A* seems to be the most informative of them.

Keywords: hypoxia, gene expression, maize hybrids, root length, shoot biomass, SPAD

INTRODUCTION

Both hypoxia and anoxia are severe abiotic stresses that severely limit growth and development in many crops worldwide. Maize is very sensitive to excessive soil moisture resulting from abundant rainfall, a shallow water table or heavy soils (Zaidi et al., 2004; Lone and Warsi, 2009). In South Asia, more than 15% of total maize production is affected by floods. In India, excessive soil moisture is estimated to cause an average 25–30% loss of national maize production almost every year, while in United States waterlogging accounted for 70% of yield losses in 2011 (Zaidi et al., 2004; Lone and Warsi, 2009; Bailey-Serres et al., 2012). As climate change is expected to further exacerbate the frequency and intensity of flooding events, there is a need for greater knowledge of the plant's mechanisms of adaptation to waterlogging.

Gas diffusivity is 10^4-fold slower in water than in air, and oxygen dissolved in water is quickly depleted by plant root respiration and soil microorganisms resulting in hypoxic conditions. Oxygen deficiency in soils has several negative effects: it alters the nitrogen pathways, reduces nutrient availability and pH (Zaidi et al., 2004; Abiko et al., 2012; Bailey-Serres et al., 2012), and increases the solubility of toxic metals (Setter et al., 2008; Herzog et al., 2016). Respiration is the plant physiological process most sensitive to flooding. Molecular oxygen is a terminal electron acceptor in the mitochondrial electron transport chain (ETC) and in the oxidative phosphorylation process; it enables plants to generate sufficient chemical energy stored as adenosine triphosphate (ATP), which is needed for intracellular physiological and biochemical reactions. An effect of both hypoxia and anoxia is a lack of the electron acceptors that promote anaerobic respiration patterns through the activity of alcohol dehydrogenase (ADHase), the most widely studied enzyme involved in fermentation processes (Liao and Lin, 2001; Ren et al., 2014). This is the process by which flooding impairs plant growth, reduces yields and can even cause plant death.

Plant responses to flooding vary according to the duration of root submergence, soil and air temperature, plant growth stage and specific genotype tolerance. Several studies have observed that plant growth impairments and grain yield losses are greatest when flooding occurs at early growth stages (Kanwar et al., 1988; Ren et al., 2014; McDaniel et al., 2016; Yamauchi et al., 2018). However, cereals have developed morpho-physiological adaptations in response to flooding, like increased amylolytic activities in rice seedling to sustain coleoptile elongation, as well as increased production of α-amylase in maize caryopses to avoid sugar starvation, and formation of aerenchyma in maize and barley roots (Guglielminetti et al., 2000; Pompeiano et al., 2013; Yamauchi et al., 2018). A better understanding of the changes in plant morphology that take place when extreme waterlogging events occur will help identify useful morphological markers for screening tolerant genotypes. Morphological responses are driven by adjustments of gene expressions responsible for adaptation to low-oxygen regimes. The molecular mechanisms of flooding tolerance have been more extensively investigated in tolerant species, like *Oryza sativa* L., with the ethylene-response-factor-like genes SUBMERGE1 (*Sub1*) (Xu et al., 2006), SNORKEL (*SK*) (Hattori et al., 2009), and qAG-9-2 (Angaji et al., 2010; Kretzschmar et al., 2015). Only in recent years has molecular characterization of the tolerance to flooding mechanism been more widely extended to other relevant species, like *Hordeum vulgare* L. (Mendiondo et al., 2016), *Brachypodium distachyon* L. Beauv. (Rivera-Contreras et al., 2016), and *Zea mays* L. (Campbell et al., 2015). A flooding tolerance QTL named Submerge Tolerance 6 (*Subtol6*) has been recently mapped to chromosome 6 of maize (Campbell et al., 2015). *Subtol6* seems to include six genes involved in abiotic stress responses, hypoxia and senescence/oxidative stress. Two of them, RELATED TO ABA-INSENSITIVE3 (*ABI3*)/VIVIPARUS1 (*RAV1*) and HEMOGLOBIN2 (*HB2*) show differential expressions between sensitive and tolerant maize lines, suggesting their possible role as marker genes for tolerance. Besides Subtol6, other genes show differential expression after short-term submergence stress (Campbell et al., 2015): ALTERNATIVE OXIDASE 1A (*AOX1A*; Zm00001d002436), *WRKY6* maize ortholog (Zm00001d039245), *CYP81D8* (Zm00001d012322), a putative PYROPHOSPHATE-DEPENDENT FRUCTOSE-6-PHOSPHATE 1-PHOSPHOTRANSFERASE (*PFP*; JQ522972.1), PYRUVATE DECARBOXYLASE3 gene (*PDC3*; Zm00001d028759) and a gene encoding ALCOHOL DEHYDROGENASE1 (*ADH1*; Zm00001d033931).

Three out of the genes identified in the study of Campbell et al. (2015), *AOX1A*, *CYP818D8*, and *PFP*, are related to respiration and energy-production processes, that are compromised under anoxia conditions and are expected to be informative of plant tolerance to waterlogging as well. *CYP81D8* is a gene codifying for cytochrome P450, whose expression profile various studies have found to be stress-related, while its involvement in waterlogging stress tolerance has been reported by a few authors (Xu et al., 2001; Glombitza et al., 2004; Narusaka et al., 2004; Campbell et al., 2015). The genes *PFP* and *AOX1A* have received greater attention than *CYP81D8* only in recent years, and various studies (Campbell et al., 2015; Dwivedi, 2015; Gupta et al., 2015) have ascertained their involvement in flooding tolerance. The PFP enzyme can operate alternatively as a non-ATP-requiring enzyme and an ATP-dependent phosphofructokinase to catalyze the interconversion between fructose-6-phosphate and fructose-1,6-biphosphate in glycolysis reactions. *AOX1A*, the only form of alternative oxidase in monocot species (Considine et al., 2002), contributes to the maintenance of the ETC and the tricarboxylic acid cycle (TCA), pathways that are slowed down as a consequence of the increased NADH/NAD^+ and ATP/ADP ratios (Gupta et al., 2015). *AOX1A* is also known to prevent the over-reduction in respiratory chain components that might occur after the production of harmful reactive oxygen species (ROS), thus playing an important role in avoiding cell damage by ROS (Dwivedi, 2015).

In this study, 19 commercial maize hybrids and the inbred line B73 were cultivated under extreme waterlogging conditions (6 continuous days) during early growth stages and compared with untreated controls. The aim of this study was (i) to measure the effects on shoot and root growth in order to assess the extent of tolerance to extreme waterlogging conditions in this large set of hybrids; (ii) to assess the expression analysis of

the three candidate marker genes for anoxia tolerance *AOX1A*, *CYP818D8* and *PFP*, and verify if they are informative also for the hypoxic conditions of extreme waterlogging; and (iii) to identify useful morphological markers in screening tolerant genotypes. Compared with the experiment of Campbell et al. (2015) on maize submergence, in this study waterlogging was also functional to avoid interactions with other stressors (e.g., plant/water overheating), which may mask gene expression and morphological responses.

MATERIALS AND METHODS

Experimental Set-Up

The experiment was carried out in June 2016 at the "Lucio Toniolo" experimental farm of the University of Padua, Italy (45°21′ N, 11°58′ E, 6 m a.s.l.). Seeds of 19 commercial maize (*Z. mays* L.; **Supplementary Table S1**) hybrids and the inbred line B73, used as reference for evaluating the efficiency of primer amplification, were sown in 4-L black PVC pots (18 cm high, 17 cm superior diameter) (4 seeds/pot) filled with 4 kg of a 1:1 (w/w) mixture of silty loam soil and sand, and fertilized with an N-P-K granular fertilizer at a rate which mimicked pre-sowing fertilization of maize (150 kg ha^{-1} K_2O, 75 kg ha^{-1} P_2O_5, and 50 kg ha^{-1} N). Sowing occurred on 28 June and complete germination and emergence were recorded within 5–6 days.

Following a randomized experimental design, pots were placed in a greenhouse with 16/8 h and 24/18°C day/night conditions, and 70% RH. They were irrigated with 300 mL of water every 2 days until 11 days after sowing (DAS). In order to apply waterlogging, the pots were transferred to a tank filled with water to impose flooding for 6 days, from 11 DAS (stage BBCH 13) to 17 DAS (BBCH 15), and flooded pots were cut on the top edge (2–3 cm^2) to allow a thin layer of water of only ∼5 mm to remain above the soil surface. To prevent water overheating during the daytime, the pots were protected with a shading net which kept the water temperature below 20°C. The experiment consisted of three pots/replicates per genotype/treatment (120 pots in total).

Morphological Parameters

Shoot morphological parameters were recorded on three plants per pot, and three pots per hybrid-treatment ($n = 3$). At the end of the experiment (17 DAS), chlorophyll content was estimated on the last fully expanded leaf, i.e., the 5th, using a SPAD-502 chlorophyll meter (Konica-Minolta, Hong Kong). Two measures were taken from each plant, one at 1/3 and one at 2/3 the leaf length, then averaged with those from the other plants in the same pot to obtain one value per replicate.

At the end of the experiment (17 DAS), the maize plants were collected and the shoots separated from the roots. Shoot height was obtained by analyzing digital images at 300 DPI resolution with the Gimp 2.8 software, according to the leaf collar method (Abendroth et al., 2011). Shoot dry weight was recorded after oven drying at 105°C for 24 h.

Roots from the three plants in each pot were washed and separated from soil particles with a hydraulic centrifugation device and collected in a 500-μm mesh sieve. Morphological parameters were recorded through image analysis. Roots were digitized with an EPSON Expression 11000KL PRO scanner (Epson, Suwa, Japan) in binary format (1-bit) at 400 DPI resolution. Root images were then analyzed with the KS 300 ver. 3.0 software (Carl Zeiss Vision GmbH, Munich, Germany) to obtain root length, area and diameter, according to Vamerali et al.'s (2003) method.

Leaf Sampling and cDNA Synthesis

Following phenotypic characterization of the 19 hybrids, 10 with contrasting responses to flooding stress (on a scale of shoot and root injury severity) were selected for gene expression analysis: P1733, P1570, P1547, LOLITA, P1535, P1028, P1134, SY HYDRO, DKC6752, and DKC6664, together with the inbred line B73.

Gene expression analysis was performed on leaf tissues, as non-destructive and timeliness procedure compared to root sampling. This also allowed to relate expression analysis to morphological traits of intact shoots.

RNA extraction was performed at the end of the 6-day period of waterlogging, with the aim of identifying molecular markers with stable expression over a prolonged/extreme hypoxic condition. Two-cm^2 tissue samples from the third leaf of the three plants of each replicate were collected, immediately frozen in liquid nitrogen and stored at −80°C until further processing. Total leaf RNA was extracted from submerged and control plants with the TRIzol® Reagent (Thermo Fisher Scientific), according to the manufacturer's protocol. RNA concentration was verified with NANODROP 2000c (Thermo Fisher Scientific). One microgram of total RNA from each sample was reverse-transcribed to cDNA in a 20 μL reaction volume using SuperScript III™ Reverse Transcriptase (Thermo Fisher Scientific), according to the manufacturer's instructions.

Real-Time Quantitative PCR (qRT-PCR) Analysis

Expression analysis was performed on three genes, among others from Campbell et al.'s (2015) studies, having the highest efficiency of primer amplification (without problems linked to the sequence diversity) according to a preliminary test: *AOX1A* (Zm00001d002436), *CYP81D8* (Zm00001d012322), and a putative *PFP* (JQ522972.1). The three marker genes were tested by qRT-PCR. Specific primers were selected from Campbell et al. (2015, **Supplementary Table S2**) and first evaluated in the inbred line B73 to assess their amplification efficiency.

For each gene, 3 biological replicates (each derived from the 3 plants of each pot) and 2 technical replicates were analyzed using 4 μL of cDNA samples diluted 1:5 (*AOX1A* and *CYP81D8*) or 1:20 (*PFP*) in 20 μL reaction mixture containing 2× Power SYBR™ Green PCR Master Mix (Applied Biosystems). The analyses were performed with the StepOne™ and StepOnePlus™ Systems (Applied Biosystems). Real-time conditions were: 20 s at 95°C, 40 cycles of 3 s at 95°C, and 30 s at 60°C. For each reaction, the product melting curve was generated by heating from 60 to 95°C in increments of 0.2/s°C. The

constitutively expressed *EF1-α* gene was used as the housekeeping internal control of the cDNA quantity. Relative quantification of gene expressions [normalized to EF1-α transcript quantities, selected from Lin et al. (2014, **Supplementary Table S2**)] was performed with the Applied Biosystems 7500 ver. 2.0.5 software and the $\Delta\Delta$CT method.

Statistical Analysis

The data from the morphological parameters examined in waterlogged plants and untreated controls were subjected to an ANOVA using the Statgraphics Centurion XVII software (Adalta, Arezzo, Italy). Separation of means was set at $P \leq 0.05$ with the Newman–Keuls test. Significant differences between treatments are indicated with asterisks in the figures below.

Factorial discriminant analysis [Multigroup Discriminant Analysis (MDA) with Wilks' lambda and Pillai's trace tests], and principal component analysis (PCA) were also carried out. MDA allowed us to describe the changes in morphological traits in response to hypoxia, and PCA to describe the relationship between the morphological changes and the expressions of the three genes examined. Before analysis, multivariate data normality was verified by the Shapiro test, and data were standardized by subtracting the mean and dividing the result by the standard deviation for each variable. All analyses were performed in MS Excel XLSTAT (Addinsoft, Paris, France).

RESULTS

Shoot Growth Parameters

SPAD Readings

SPAD values, which represent the leaf chlorophyll content, were generally lower in the plants subjected to 6 days of waterlogging than in untreated controls, with almost 50% of the hybrids showing a significant decrease (**Figure 1**). Considerable phenotypic variability in response to waterlogging was observed among hybrids (CV = 180%), with the largest decreases in SPAD recorded in the DKC5530 and P1535 hybrids (both −16% vs. respective controls), while some others, i.e., P1028, P1134, DKC6664, and DKC6752, as well as the inbred line B73 exhibited only slight increases, up to a maximum of 5%.

Culm Height

Culm height generally increased in plants affected by waterlogging compared to controls (**Figure 2**), but the increase was significant ($P \leq 0.05$) in only two hybrids, P1570 (+24%) and LOLITA (+11%). The inbred line B73 also exhibited a 9% increase in culm height under waterlogging, whereas SY SENKO, SY HELIUM, and SY HYDRO exhibited a decrease, albeit slight (−4, −3, and −3%, respectively, vs. respective controls).

Shoot Biomass

Shoot biomass was weakly affected by the waterlogging stress imposed. A slight decrease in shoot fresh weight was observed in 12 hybrids, but was significant only for P1547 (−14% vs. controls, $P \leq 0.05$) (**Figure 3**). Shoot dry weight followed the same trend as fresh weight, their variations in control vs. waterlogged conditions correlating positively ($R^2 = 0.60$; $P \leq 0.05$) and involving the same hybrids. Waterlogging significantly decreased the shoot DW of only two hybrids, P1547 and PR31Y43 (−22 and −21%, respectively, vs. controls, $P \leq 0.05$) (**Figure 3**). There were increases in shoot DW in the other hybrids, with the maximum variation (+24%) found in P1570 (like culm height), but none was significant. The variations in shoot DW in response to waterlogging were higher than in FW and culm height (CV = 414% vs. 28 and 120%, respectively).

Root Growth Parameters

Root growth was more impaired by waterlogging than shoot growth. Length was the root parameter most affected, and was reduced in all the hybrids except P1028, which exhibited slightly higher values in waterlogged than in control plants (**Figure 4**). The reduction in root length across the whole set of hybrids was on average 31%, and was significant in 13 of them. The greatest effect was observed in P1570, which was also greatly affected above ground, followed by PR31Y43 and DK6650 (−53, −44, −43% vs. controls, respectively). Less damage was observed in P1134 and DKC5830 (−16 and −24%, respectively).

Similarly, root area was also greatly reduced by waterlogging, although to a lesser extent than root length, the decrease being 24% on average, and significant in 7 hybrids ($P \leq 0.05$). Only one hybrid, P1028, slightly increased in root area as a consequence of hypoxia stress (**Figure 4**), as it did in root length. P1570, SY HELIUM, and PR31Y43 suffered the most severe decreases (−51, −37, and −36%, respectively), while P1134 and DKC5830 again exhibited the smallest reductions, as they did for root length.

Regarding root biomass (DW), this was again reduced by waterlogging in all hybrids, by an average of 18%, and significantly in 7 of them ($P \leq 0.05$) (**Figure 4**). The greatest decreases were recorded in hybrids P1535, P1733, and P1114 (−38, −35, and −34%, respectively), while DKC6752, P1028, and SY ZOAN were only slightly impaired. P1134 was the only hybrid that increased its root biomass under waterlogging, although not by much (+6% vs. control).

Root diameter exhibited an opposite trend to the other root parameters under hypoxic conditions in that it generally increased, by an average of 12%, and by maximum of 21% in SY ZOAN and 25% in DKC6650, while P1570 and LOLITA remained very stable (+1% and +2%, respectively) (data not shown).

As a consequence of the plants' responses to waterlogging, the root-to-shoot ratio was always reduced, by between 6% (hybrid P1134) and 29% (P1733 and DKC 5530), with a 58% variability (data not shown).

Of the various root parameters, root length varied the least across hybrids (CV = 48%), followed by root area and biomass (CV = 61 and 70%, respectively).

Adventitious aerial roots were observed to start growing on the 4th day of waterlogging treatment (15 DAS). On that day, aerial roots were visible in all waterlogged replicates of only one hybrid, i.e., DKC5530, in 2 of the 3 replicates of SY

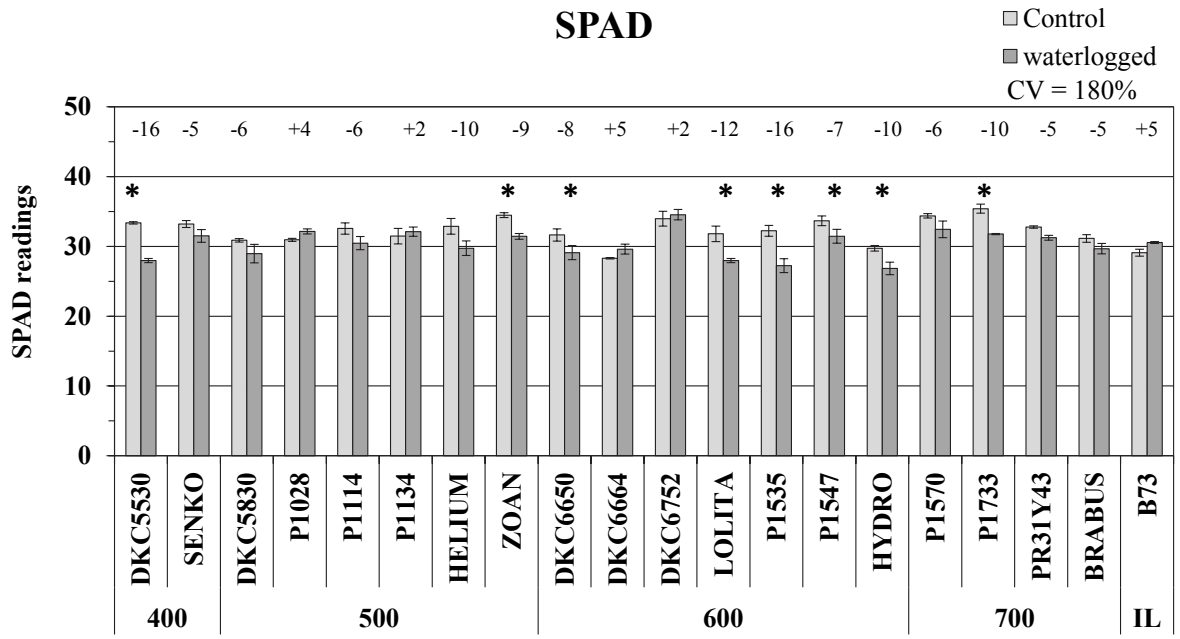

FIGURE 1 | SPAD readings (average ± SE; $n = 3$) from control and waterlogged plants of commercial hybrids and the inbred line B73 at 17 days after sowing (DAS), grouped according to FAO class of maturity (from 400 to 700). Numbers above histograms indicate the percentage variation between waterlogged plants and controls for each hybrid, with asterisks indicating significance ($P \leq 0.05$).

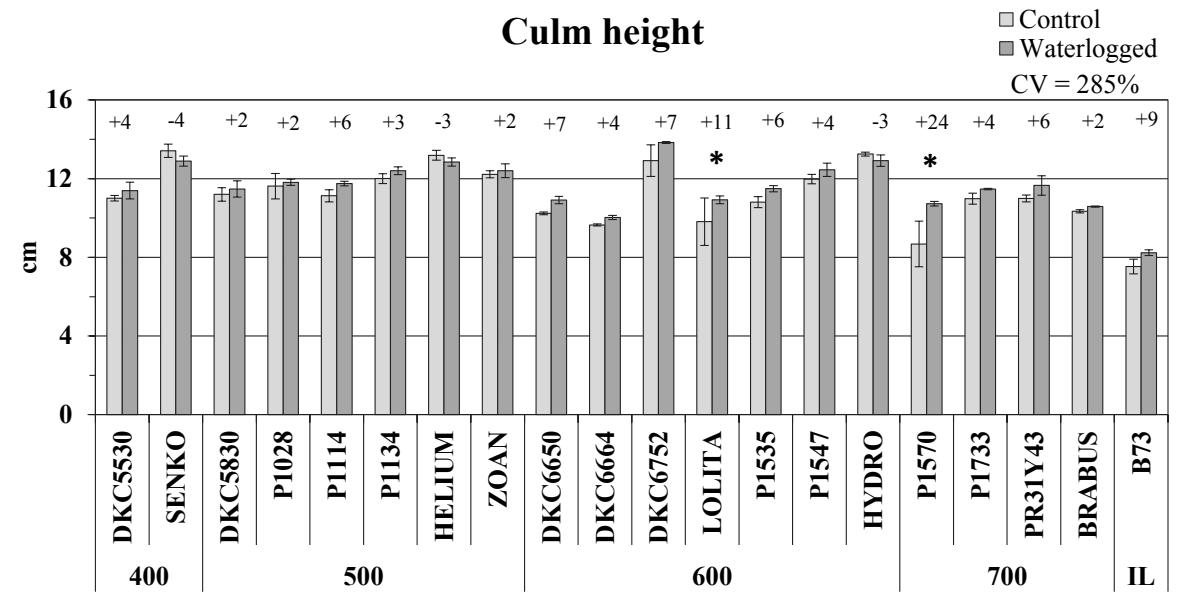

FIGURE 2 | Culm height (average ± SE; $n = 3$) of control and waterlogged plants of commercial hybrids and the inbred line B73 at 17 DAS, grouped according to FAO class of maturity (from 400 to 700). Numbers above histograms indicate the percentage variation between waterlogged plants and controls for each hybrid, with asterisks indicating significance ($P \leq 0.05$).

HELIUM and SY ZOAN, and in only 1 of the 3 replicates of SY BRABUS, DKC5830, DKC6664, PR31Y43, and P1547. Aerial roots were visible in a few other hybrids at 16 DAS (5th day of waterlogging), and in the whole set of hybrids at 17 DAS (6th day of waterlogging). The inbred line B73 was recorded as having aerial roots in 2 of the 3 replicates at 16 DAS and still only 2 at 17 DAS.

The hybrids that formed aerial roots earlier (4th day of waterlogging stress) were among the highest impaired in terms of root length, area, and biomass.

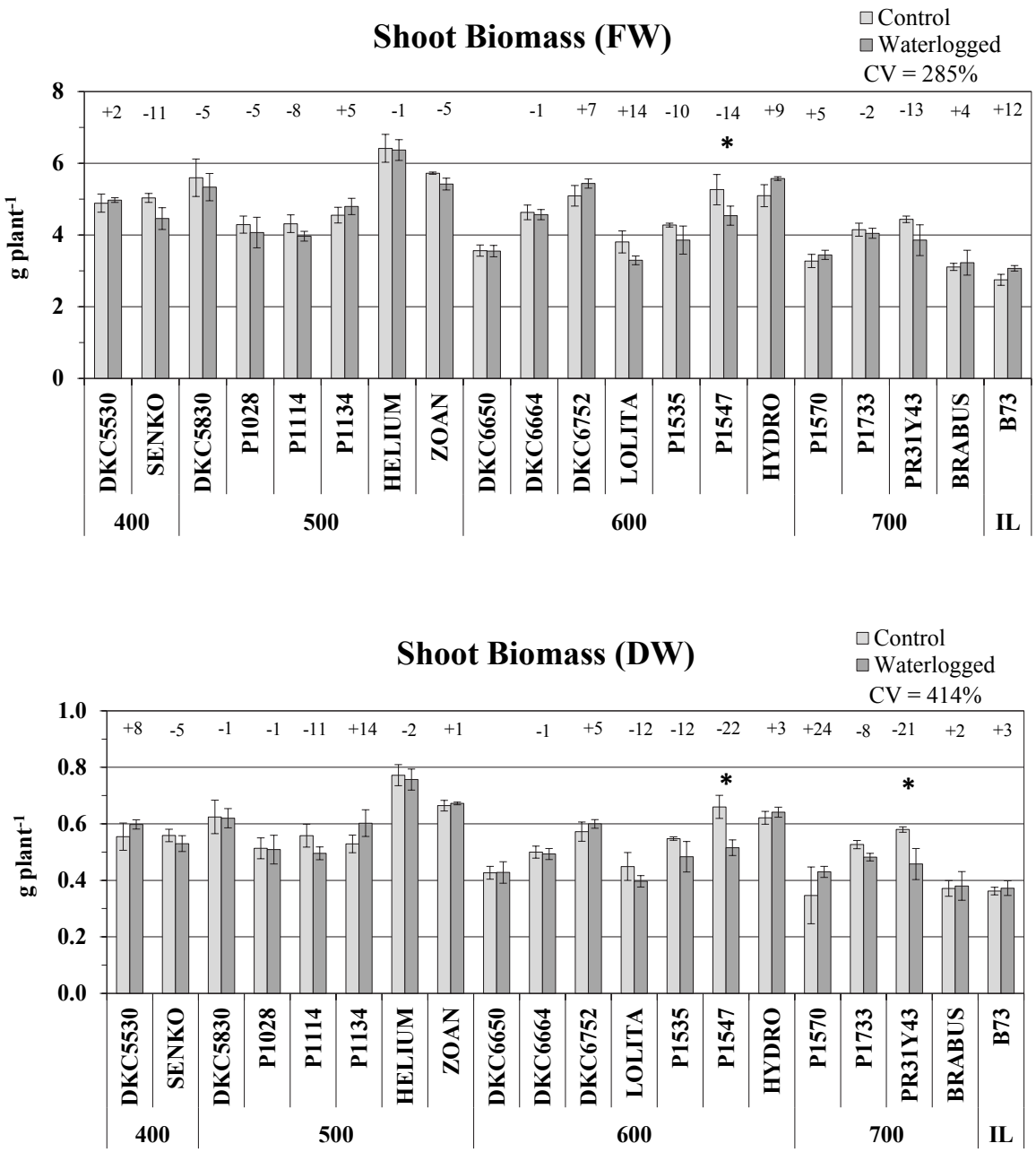

FIGURE 3 | Shoot fresh weight (FW) and dry weight (DW) (average ± SE; $n = 3$) of control and waterlogged plants of commercial hybrids and the inbred line B73 at 17 DAS, grouped according to FAO class of maturity (from 400 to 700). Numbers above histograms indicate the percentage variation between waterlogged plants and controls for each hybrid, with asterisks indicating significance ($P \leq 0.05$).

PCA and MDA on Morphological Parameters

Principal component analysis conducted on the data for shoot and root morphological parameters allowed us to identify two synthetic variables, which explained an overall variability of 89.36% (**Figure 5**). The most informative variables (loadings > |0.4|) were root length, followed by root area and biomass, suggesting that the root system is more involved in adaption to a waterlogged environment than the aboveground compartment. According to the vector direction of each variable, good correlations among variables are indicated by vectors plotted very close together in the same quadrant, as occurs between root length and SPAD, and between root length and root area.

Centroid position and cluster separation in the DA summarize the phenotypic variability in the response of maize hybrids to waterlogging stress, and show that under hypoxic conditions all

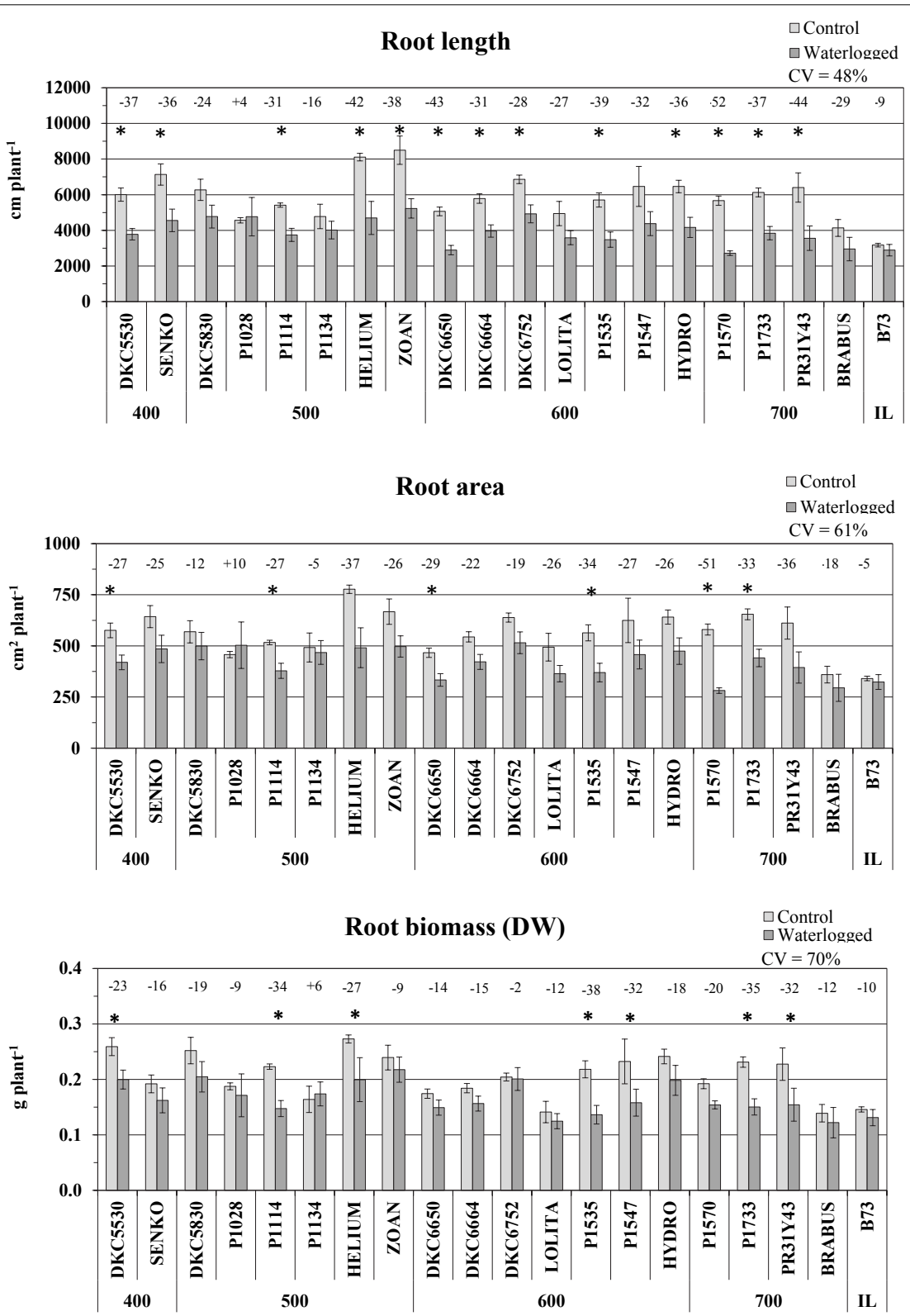

FIGURE 4 | Root length (average ± SE; $n = 3$), area (average ± SE; $n = 3$), and biomass (average ± SE; $n = 3$) of control and waterlogged plants of commercial hybrids and the inbred line B73 at 17 DAS, grouped according to FAO class of maturity (from 400 to 700). Numbers above histograms indicate the percentage variation between waterlogged plants and controls for each hybrid, with asterisks indicating significance ($P \leq 0.05$).

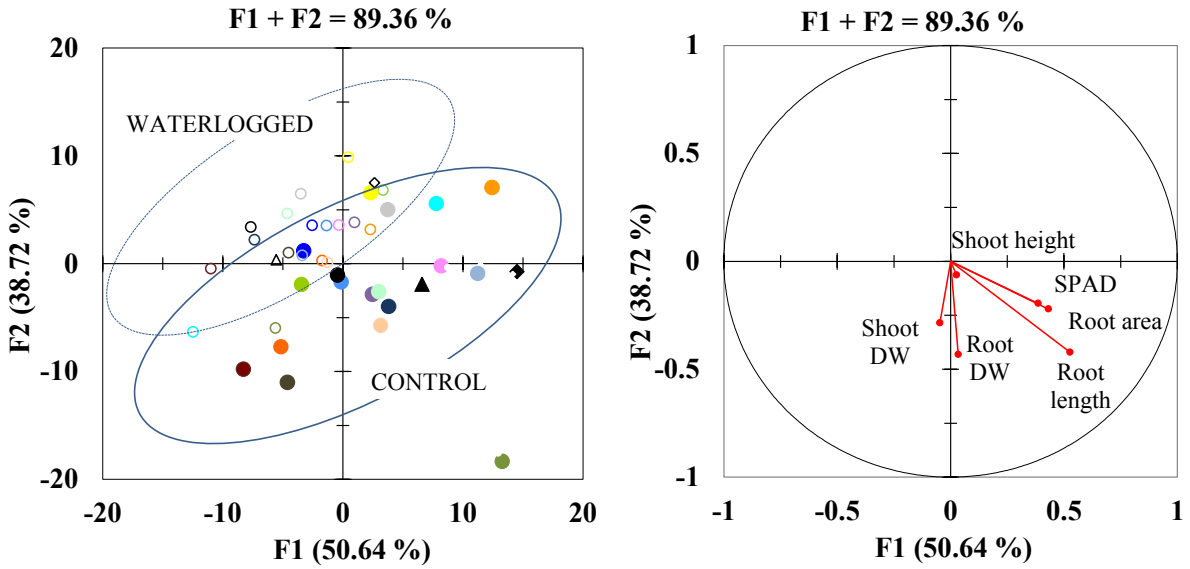

Legend:

B73-C	B73-W	DKC5530-C	DKC5530-W
DKC5830-C	DKC5830-W	DKC6650-C	DKC6650-W
DKC6664-C	DKC6664-W	DKC6752-C	DKC6752-W
LOLITA-C	LOLITA-W	P1028-C	P1028-W
P1114-C	P1114-W	P1134-C	P1134-W
P1535-C	P1535-W	P1547-C	P1547-W
P1570-C	P1570-W	P1733-C	P1733-W
PR31Y43-C	PR31Y43-W	BRABUS-C	BRABUS-W
HELIUM-C	HELIUM-W	HYDRO-C	HYDRO-W
SENKO-C	SENKO-W	ZOAN-C	ZOAN-W

Variables	F1	F2
SPAD	0.387	-0.195
Shoot DW	-0.047	-0.285
Shoot height	0.027	-0.063
Root DW	0.034	**-0.432**
Root area	**0.432**	-0.221
Root length	**0.528**	**-0.422**

Hybrid	FAO Class (precocity)	Distance between centroids
B73	-	**2.5**
P1733	**700**	**3.3**
P1535	**600**	**5.6**
P1547	**600**	**7.2**
BRABUS	700	7.7
P1114	500	7.9
P1134	**500**	**8.6**
DKC6664	**600**	**9.4**
DKC5530	**400**	**9.9**
LOLITA	**600**	**9.9**
P1028	**500**	**10.0**
PR31Y43	700	10.0
HYDRO	**600**	**10.4**
HELIUM	500	12.5
DKC5830	500	12.7
DKC6650	600	13.7
SENKO	400	15.4
DKC6752	**600**	**15.4**
P1570	**700**	**22.5**
ZOAN	500	24.0

FIGURE 5 | Principal component analysis (PCA; top right) for morphological shoot and root parameters with highly informative variables (loadings > | 0.4|) in bold within synthetic variables F1 and F2 (bottom left Table); and multigroup discriminant analysis (MDA; top left) of waterlogged (W) and control (C) plants of commercial hybrids and the inbred line B73 at 17 DAS. Distances between centroids for each hybrid (waterlogged vs. control) in MDA (bottom right Table) are reported in ascending order, with highlighted hybrids (bold) considered for the subsequent molecular analysis.

the parameters studied generally decreased, but to varying extents across hybrids.

The overall variability between waterlogged and control conditions in each hybrid is summarized as the distance between the two centroids (waterlogged and control) for each hybrid (**Figure 5**). The decreasing values of this centroid inter-distance across the hybrids show that the morphological changes from the control to the waterlogged environment ranged from large in hybrids DKC6752 and P1570, to intermediate in SY HYDRO, P1028, LOLITA, DKC6664, and P1134, and few in the inbred line B73, followed by hybrids P1733, P1535, P1547. These 10 hybrids and the inbred line B73 were considered in the following step of this research, which was to identify gene expressions in response to waterlogging within a wide range of phenotypic variability.

Gene Expression Analysis

In light of the results of the DA of the morphological parameters, gene expression focused on 10 maize hybrids as representative of a wide variability in phenotypic response to waterlogging treatment (**Figure 6**).

In leaves, after 6 days of submergence treatment, transcript qPCR analysis of *AOX1A* revealed marked down-regulation, from −10 to −80%, in all the flooded hybrids compared with untreated controls, except for the P1028 hybrid in which a slight increase occurred (+10%). There was also very large (and significant) down-regulation of the *AOX1A* gene transcript in the reference inbred line B73 (−87%). The variability among hybrids for changes in transcript expression (control vs. waterlogged conditions) was relatively high (CV = 58%).

Expression of the *PFP* transcript was up-regulated in half the waterlogged genotypes compared with respective controls, from +5% in P1733 to values >100%, with the greatest increases in those hybrids that were less impaired in the root, i.e., P1028, DK6664, and P1134. *PFP* expression was down-regulated in the other hybrids, but with smaller decreases compared with *AOX1A* gene expression (from −9% in P1570 and DKC6752 to −44% in LOLITA). The variability among hybrids in the changes in transcript expression (control vs. waterlogged conditions) was high (CV = 259%).

Lastly, the *CYP81D8* transcript of waterlogged plants showed relevant increases or strong decreases in level according to the hybrid considered. In P1547, P1733, P1535, and P1028, expression doubled under waterlogging stress (significantly except for P1028), in SY HYDRO it only slightly increased, and in all other hybrids a marked down-regulation was observed (from −46 to −77% compared with untreated controls). The variability among hybrids in changes in transcript expression (control vs. waterlogged conditions) was also very high in this case (CV = 927%).

PCA and MDA of Morphological and Molecular Responses

Principal component analysis carried out on the whole dataset, including morphological traits and gene expression data, identified two synthetic variables, which explained a large part of the overall variability (F1 + F2 = 81.99%) (**Figure 7**). Root parameters again explained more variability than shoot parameters, root length being the most representative (loadings: F1 = 0.43; F2 = 0.37). Of the three genes studied, *AOX1A* was the most relevant (loadings: F1 = 0.25; F2 = 0.33). *PFP* and *CYP81D8* seemed to be positively correlated with root and shoot growth, as they are plotted closer together in the quadrants according to their vector direction, but they had very low loadings.

Correlation analysis of all the parameters, calculated as the differences between control and waterlogged plants for the 10 representative hybrids, revealed generally high positive and significant correlations among the variations in shoot (biomass) and root (biomass, area and length) caused by waterlogging (**Table 1**). However, morphological changes were poorly correlated with gene regulation. Root length correlated with up-regulation of *AOX1A* (R^2 = 2.4%; $P > 0.05$) and *CYP81D1* (R^2 = 0.7%; $P > 0.05$), and with down-regulation of *PFP* (R^2 = 14%, $P \leq 0.05$), although none explained much variability. The down-regulation of PFP was also significantly correlated with root area (R^2 = 16.6%) and SPAD (R^2 = 21.6%), while the up-regulation of *CYP81D1* significantly correlated with shoot and root biomass (R^2 = 19.9 and 24.5%, respectively). In general, up-regulation of *CYP81D8* correlated better with root biomass, whereas down-regulation of *PFP* correlated better with root area and length ($P \leq 0.05$; **Table 1**).

DISCUSSION

Waterlogging is a severe abiotic stressor causing significant growth impairment and yield losses in maize, with different intensities according to the severity and duration of the anoxic/hypoxic conditions, the phenological stage of the plant and the sensitivity of the genotype. In the present study, an extreme flooding condition imposed on maize plants at early growth stage severely impaired all the shoot and root morphological parameters examined, although root growth was more impaired than shoot growth. Root length, area and biomass were significantly reduced after 6 days of waterlogging in almost all the hybrids, with one exception, but to different extents according to genotype-specific sensitivity. The reduction in length ranged from −16% to as much as −52% compared with controls over this short stress period. Aboveground plant parameters were less sensitive to waterlogging, but variability was very high due to either positive or negative variations in shoot biomass associated with a general increase in plant height, probably because oxygen was better diffused in the shoot tissues of some hybrids than in others (Armstrong et al., 1994). As a consequence, leaf chlorophyll content was also generally compromised in the waterlogging treatment (on average −6%) as a consequence of reduced synthesis and increased oxidation of pigments (Yan et al., 1996; Zheng et al., 2009). According to the effect on shoot and root growth, the inbred line B73 showed appreciable tolerance to waterlogging, similarly to the studies of Mano et al. (2002, 2006).

Early vegetative stages are the most susceptible to excessive soil moisture, whereas well-developed maize plants suffer less damaged from similar stress conditions (Kanwar et al., 1988; Zaidi et al., 2004). McDaniel et al. (2016) observed that during the V4 stage, a 3-day period of flooding led to the immature nodal roots and most of the small, less active primary roots dying – an effect that would explain the substantial root injuries to our plants after 6 days of flooding – whereas non-significant root mortality was recorded between the V12 and R1 stages. Flooding stress imposed at early vegetative growth is known to translate into severe reductions in plant height, dry matter production and yield at maturity, with plants exhibiting a dwarfing effect, which varies according to the duration of the waterlogging (Zaidi et al., 2004; Ren et al., 2014). As in our study shoot height did not decrease, but even increased in a couple of hybrids, we suspect this is a transient effect, which will reverse in later stages as a result of permanent plant damage. Indeed, culm elongation has been reported to be a common strategy for withstanding stress

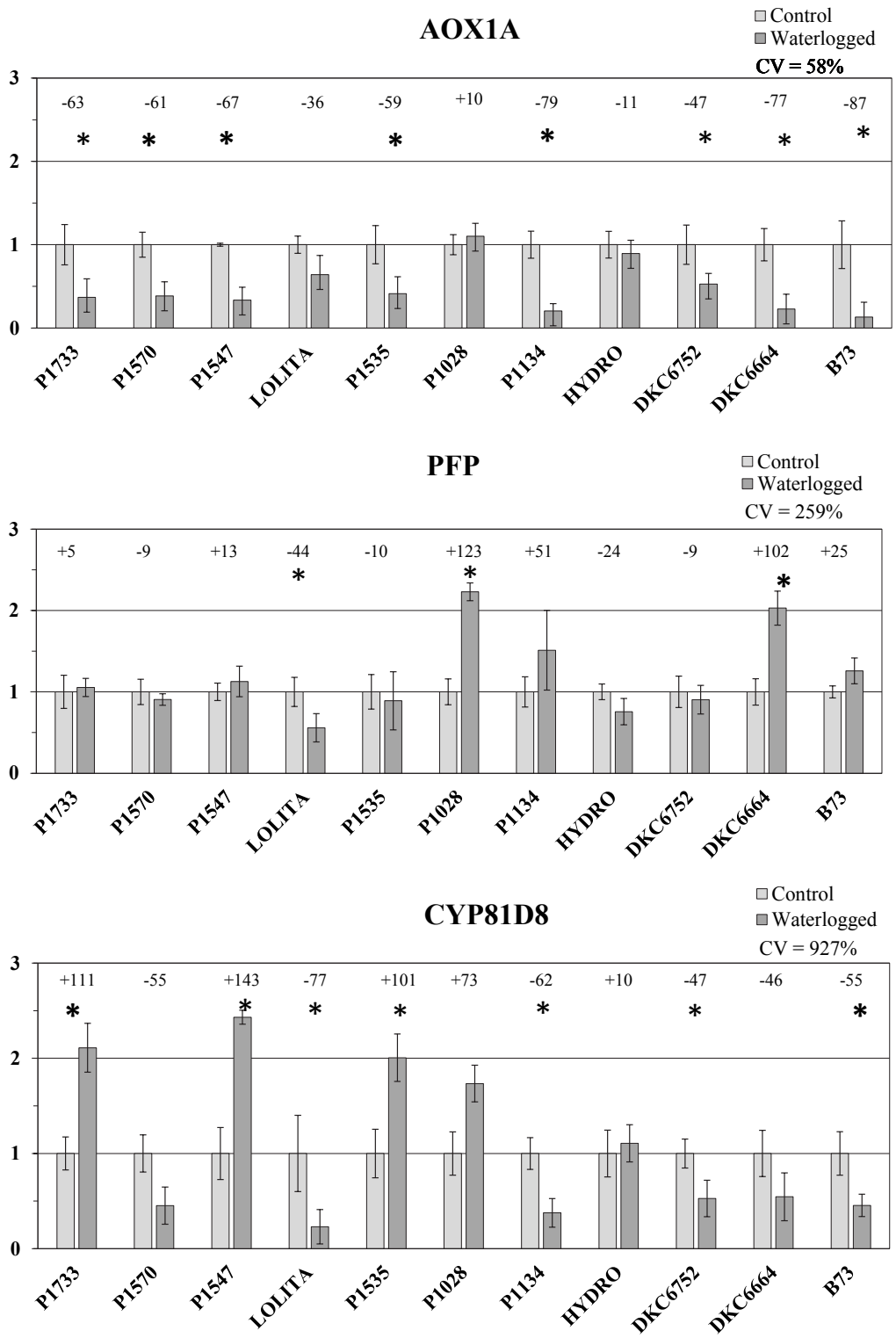

FIGURE 6 | Standardized (on controls) transcript levels of genes CYP81D8, PFP, and AOX1A in waterlogged conditions (average ± SE; $n = 3$) in 10 representative hybrids and the inbred line B73. Numbers above histograms indicate the percentage variation between waterlogged plants and controls for each hybrid, with asterisks indicating significance ($P \leq 0.05$).

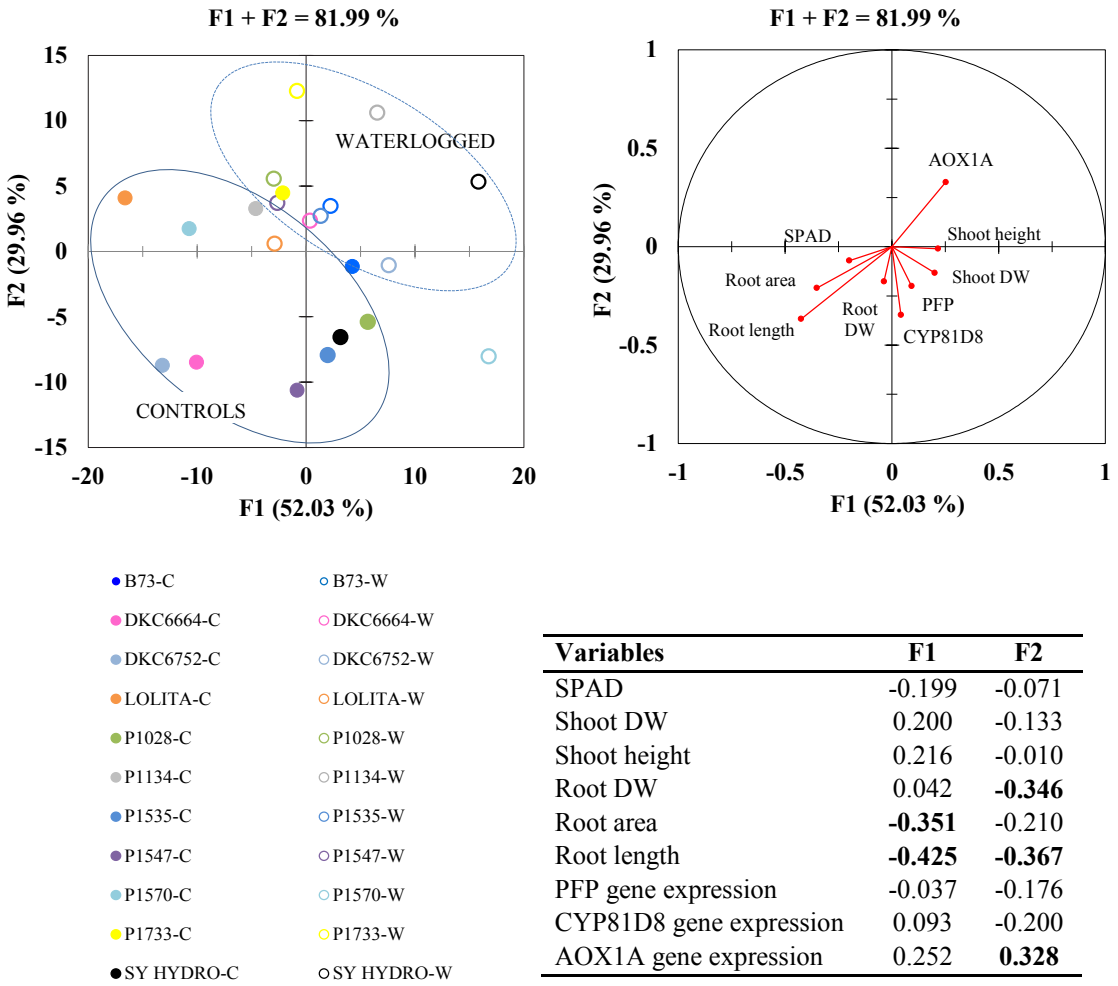

Variables	F1	F2
SPAD	-0.199	-0.071
Shoot DW	0.200	-0.133
Shoot height	0.216	-0.010
Root DW	0.042	**-0.346**
Root area	**-0.351**	-0.210
Root length	**-0.425**	**-0.367**
PFP gene expression	-0.037	-0.176
CYP81D8 gene expression	0.093	-0.200
AOX1A gene expression	0.252	**0.328**

FIGURE 7 | Principal component analysis (PCA; top right) with highly informative variables (loadings > | 0.3|) in bold within synthetic variables F1 and F2 (bottom right Table); and multigroup discriminant analysis (MDA; top left) in waterlogged (W) and control (C) plants of 10 representative hybrids and the inbred line B73 at 17 DAS.

TABLE 1 | Correlation coefficients (r) among the differences (control – waterlogged) for morphological and gene expression variables, with significant correlations in bold ($P \leq 0.05$).

Variables	SPAD	Shoot biomass	Shoot height	Root biomass	Root area	Root length	PFP gene	CYP81D8 gene	AOX1A gene
SPAD	–	0.323	0.029	**0.543**	**0.532**	**0.475**	**−0.465**	0.288	0.138
Shoot biomass		–	0.165	**0.583**	0.269	0.267	−0.037	**0.446**	0.021
Shoot height			–	0.267	0.039	0.110	0.163	0.233	0.278
Root biomass				–	**0.768**	**0.746**	−0.164	**0.495**	0.172
Root area					–	**0.979**	**−0.407**	0.069	0.137
Root length						–	**−0.376**	0.084	0.155
PFP gene							–	0.305	−0.195
CYP81D8 gene								–	0.154
AOX1A gene									–

conditions (Bailey-Serres et al., 2012). According to these authors, when hypoxia is imposed on maize roots, ethylene concentration increases in root tissues, thereby altering the phytohormonal balance and leading to the onset of the "low oxygen escape strategy," which consists in extending the culm to compensate for the alterations caused by flooding.

As oxygen is rapidly depleted in water of saturated soil (within 24–36 h), the prolonged period of flooding in this study caused

substantial root damage and probably reduced the variability among hybrids compared with shoot response, in agreement with the results of Mano et al. (2005), Mano and Omori (2007), and Abiko et al. (2012). The general increase in root diameter (up to +25%) observed after 6 days of waterlogging might also be a morphological change linked to the formation of aerenchyma, commonly reported in maize and barley (Rajhi et al., 2011; Herzog et al., 2016; Yamauchi et al., 2018), as a key adaptation to flooding. Although less efficient than schizogenous aerenchyma in rice, the formation of lysigenous aerenchyma, with its poorly specialized intercellular spaces, enables the internal movement of gasses in plant roots, petioles and stems. This aerenchyma has been found to start forming between 18 and 24 h after waterlogging treatment, and to be ethylene mediated (Rajhi et al., 2011; Bailey-Serres et al., 2012; Yamauchi et al., 2018).

Similarly, adventitious root formation is reported to be an adaptive strategy to compensate for growth inhibition or even death of distal portions of roots during waterlogging (Sauter, 2013; Yamauchi et al., 2018). Having applied waterlogging stress for an uninterrupted 10-day period at various maize growth stages, Zaidi et al. (2004) found the number of newly developed adventitious roots to be the most notable morphological change they observed: the number of adventitious roots increased in all the genotypes investigated, but to a greater extent in the more tolerant ones. They also observed that early increased adventitious rooting during waterlogging was closely related to final grain yield, allowing them to conclude that this morphological trait can be profitably used as a selection criterion for flooding tolerance in maize. In our study, the earlier appearance of aerial roots seemed to be associated with greater plant injuries, although we did not count the number of aerial roots, nor were the plants grown to maturity, so we cannot directly compare our results with those of Zaidi et al. (2004).

As an overall evaluation of the morphological responses of hybrids, it was not possible to establish a relationship between growth impairment under waterlogging and the FAO class of maturity, although growth was generally slightly earlier/higher in non-waterlogged plants of early-season hybrids compared with late-season hybrids.

The set of hybrids investigated in this study was sufficiently large to evidence considerable variability in their morphological responses to waterlogging, and suitable for relating to gene expression. Some useful indications to better identify waterlogging-tolerant hybrids were obtained. However, molecular characterization for mechanisms of tolerance to anoxia/hypoxia has only recently been broadened to include maize (Voesenek and Bailey-Serres, 2015), but investigations have concerned only inbred reference lines. On the basis of a transcriptome analysis in roots of a tolerant inbred line, Arora et al. (2017) has recently demonstrated existing 21,364 differentially expressed genes (DEGs) under waterlogging stress conditions, which regulate relevant pathways for energy-production, programmed cell-death (PDC), aerenchyma formation and ethylene responsiveness. In this study we aimed at identifying useful morphological and molecular markers for screening rapidly large sets of genotypes. In this view, we investigated whether there was a correlation between the morphological changes observed and expression of the three putative marker genes reported in recent studies (Campbell et al., 2015). In the research of Campbell et al. (2015), as in other recent studies (Guo et al., 2011; Gupta et al., 2015), *CYP81D8*, *PFP*, and *AOX1A* are proposed as marker genes to identify submergence tolerance lines.

Under submergence, *CYP81D8*, a stress-related gene codifying for cytochrome P450, was significantly down-regulated in tolerant lines compared with sensitive ones (Xu et al., 2001; Glombitza et al., 2004; Narusaka et al., 2004; Campbell et al., 2015). The expression of *PFP*, involved in glycolytic reactions (Dwivedi, 2015), was strongly reduced by submergence in all the maize lines studied by Campbell et al. (2015), although in our study *PFP* transcript abundance was higher in the hybrids more tolerant to extreme waterlogging. *AOX1A*, known for its contribution to the maintenance of the ETC and the tricarboxylic acid cycle (TCA), was down-regulated in maize hybrids with higher tolerance to submergence (Dwivedi, 2015; Gupta et al., 2015).

In our study, waterlogged plants showed contrasting variations in *CYP81D8* transcript levels, both relevant increases and strong decreases, depending on the hybrid considered. The expression level of the PFP enzyme was also up-regulated in half the waterlogged hybrids and down-regulated in the others. In contrast, qPCR analysis of *AOX1A* revealed important down-regulation of this transcript in all waterlogged hybrids, except P1028, compared to controls (from −10 to −80%). The expression of this gene was also significantly down-regulated in the inbred line B73, suggesting that this trait can be incorporated into commercial hybrids. Discriminant analysis confirmed *AOX1A* as the most informative of the three genes investigated under waterlogging conditions.

Morphological parameters (damage to shoot and root growth) did not correlate highly with the expression levels of the putative marker genes *CYP81D8*, *PFP*, and *AOX1A*, and it was not possible to discriminate clearly between the more tolerant and susceptible hybrids. We may argue that these genes, codifying for proteins related to physiological processes, like the respiratory chain, glycolytic reaction, and ROS production, do not completely explain the morphological changes observed. As these genes were instead well correlated with the changes in plant morphology observed by Campbell et al. (2015) under submergence, we may conclude that they are less informative under waterlogging. However, the good level of tolerance of some hybrids, like P1028, which was associated with significant up-regulation of PFP, also suggests that there probably is large genetic variability among hybrids for this trait, which hampered identification of a general rule/relationship between phenotypic response and gene transcript level.

CONCLUSION

When a period of extreme flooding is imposed at the early growth stage of maize, greater growth impairment is detectable in the root than in the shoot. As we found large variability in the responses of shoot traits, and of root traits, although to

a lesser extent, in the set of commercial hybrids we studied, there is reasonable scope for screening for waterlogging stress tolerance, although the growth and yield of mature plants should be verified in further studies. The expressions of *CYP81D8*, *PFP*, and *AOX1A* genes, codifying for proteins related to essential physiological processes, explained only partially the shoot and root damage observed, suggesting that genetic variability in waterlogging tolerance in current commercial hybrids is probably small, and/or other candidate genes should be investigated under hypoxic stress conditions. Meanwhile, *AOX1A*, codifying for an alternate oxidase involved in the respiratory chain, which was clearly down-regulated in almost all the hybrids under extreme waterlogging, can be used for screening currently available genotypes. Although *AOX1A* turned out to be the most informative gene in explaining morphological responses across hybrids (by discriminant analysis), up-regulation of *CYP81D1* and down-regulation of PFP should also be considered for preserving root growth, which showed the greatest impairment by waterlogging.

AUTHOR CONTRIBUTIONS

TV and SV conceived the research. CDC and MF recorded the morphological parameters. BV performed the qRT-PCR analysis. CDC, AP, and BV analyzed the data. AP, CDC, SV, and TV wrote the manuscript. All authors read and approved the final manuscript.

FUNDING

This research was supported by the University of Padua (PRAT project CPDA157779) in 2015.

ACKNOWLEDGMENTS

The authors wish to thank Alberto di Stefano and Alessandro Ghiraldini for help with root data collection; Cristian Forestan for preparing the samples for PCR analysis; and Tessa Say for revising the English text.

SUPPLEMENTARY MATERIAL

The Supplementary Material for this article can be found online at: https://www.frontiersin.org/articles/10.3389/fpls.2019.00062/full#supplementary-material

REFERENCES

Abendroth, L. J., Elmore, R. W., Boyer, M. J., and Marlay, S. K. (2011). *Corn Growth and Development. Iowa State Univ. Extension Publication. PMR-1009*. https://store.extension.iastate.edu/Product/Corn-Growth-andDevelopment

Abiko, T., Kotula, L., Shiono, K., Colmer, T. D., and Nakazono, M. (2012). Enhanced formation of aerenchyma and induction of a barrier to radial oxygen loss in adventitious roots of *Zea nicaraguensis* contribute to its waterlogging tolerance as compared with maize (*Zea mays* ssp. *mays*). *Plant Cell Environ.* 35, 1618–1630. doi: 10.1111/j.1365-3040.2012.02513.x

Angaji, S. A., Septiningsih, E. M., Mackill, D. J., and Ismail, A. M. (2010). QTLs associated with tolerance of flooding during germination in rice (*Oryza sativa* L.). *Euphytica.* 172, 159–168. doi: 10.1007/s10681-009-0014-5

Armstrong, W., Brändle, R., and Jackson, M. B. (1994). Mechanisms of flood tolerance in plants. *Acta Bot. Neerl.* 43, 307–358. doi: 10.1111/j.1438-8677.1994.tb00756.x

Arora, K., Panda, K. K., Mittal, S., Mallikarjuna, M. G., Rao, A. R., Dash, P. K., et al. (2017). RNAseq revealed the important gene pathways controlling adaptive mechanisms under waterlogged stress in maize. *Sci. Rep.* 7:10950. doi: 10.1038/s41598-017-10561-1

Bailey-Serres, J., Lee, S. C., and Brinton, E. (2012). Waterproofing crops: effective flooding survival strategies. *Plant Physiol.* 160, 1698–1709. doi: 10.1104/pp.112.208173

Campbell, M. T., Proctor, C. A., Dou, Y., Schmitz, A. J., Phansak, P., Kruger, G. R., et al. (2015). Genetic and molecular characterization of submergence response identifies Subtol6 as a major submergence tolerance locus in maize. *PLoS One* 10:e120385. doi: 10.1371/journal.pone.0120385

Considine, M. J., Holtzapffel, R. C., Day, D. A., Whelan, J., and Millar, A. H. (2002). Molecular distinction between alternative oxidase from monocots and dicots. *Plant Physiol.* 129, 949–953. doi: 10.1104/pp.004150

Dwivedi, P. (2015). "Regulation of cytochrome and alternative pathways under light and osmotic stress," in *Alternative Respiratory Pathways in Higher Plants*, eds K. J. Gupta, L. A. J. Mur, and B. Neelwarne (Hoboken, NJ: John Wiley & Sons, Ltd), 185–199.

Glombitza, S., Dubuis, P. H., Thulke, O., Welzl, G., Bovet, L., Götz, M., et al. (2004). Crosstalk and differential response to abiotic and biotic stressors reflected at the transcriptional level of effector genes from secondary metabolism. *Plant Mol. Biol.* 5, 817–835. doi: 10.1007/s11103-004-0274-3

Guglielminetti, L., Busilacchi, H. A., and Alpi, A. (2000). Effect of anoxia on α-amylase induction in maize caryopsis. *J. Plant Res.* 113, 185–192. doi: 10.1007/PL00013929

Guo, X., Ronhovde, K. J., Yuan, L., Yao, B., Soundararajan, M. P., Elthon, T. E., et al. (2011). Pyrophosphate dependent fructose-6-phosphate 1-phosphotransferase induction and attenuation of Hsp gene expression during endosperm modification in quality protein maize. *Plant Physiol.* 158, 917–929. doi: 10.1104/pp.111.191163

Gupta, K. J., Neelwarne, B., and Mur, L. A. (2015). "Integrating classical and alternative respiratory pathways," in *Alternative Respiratory Pathways in Higher Plants*, eds K. J. Gupta, L. A. J. Mur, and B. Neelwarne (Hoboken, NJ: John Wiley & Sons, Ltd), 3–19.

Hattori, Y., Nagai, K., Furukawa, S., Song, X. J., Kawano, R., Sakakibara, H., et al. (2009). The ethylene response factors SNORKEL1 and SNORKEL2 allow rice to adapt to deep water. *Nature* 460, 1026–1031. doi: 10.1038/nature08258

Herzog, M., Striker, G. G., Colmer, T. D., and Pedersen, O. (2016). Mechanisms of waterlogging tolerance in wheat–a review of root and shoot physiology. *Plant Cell Environ.* 39, 1068–1086. doi: 10.1111/pce.12676

Kanwar, R. S., Baker, J. L., and Mukhtar, S. (1988). Excessive soil water effects at various stages of development on the growth and yield of corn. *Trans. ASAE* 31, 133–141. doi: 10.13031/2013.30678

Kretzschmar, T., Pelayo, M. A. F., Trijatmiko, K. R., Gabunada, L. F. M., Alam, R., Jimenez, R., et al. (2015). A trehalose-6-phosphate phosphatase enhances anaerobic germination tolerance in rice. *Nat. Plants* 1:15124. doi: 10.1038/NPLANT.2015.124

Liao, C. T., and Lin, C. H. (2001). Physiological adaptation of crop plants to flooding stress. *Proc. Natl. Sci. Counc. Repub. China B* 25, 148–157.

Lin, Y., Zhang, C., Lan, H., Gao, S., Liu, H., Liu, J., et al. (2014). Validation of potential reference genes for qPCR in maize across abiotic stresses, hormone treatments, and tissue types. *PloS One* 9:e95445. doi: 10.1371/journal.pone.0095445

Lone, A. A., and Warsi, M. Z. K. (2009). Response of maize (*Zea mays* L.) to excess soil moisture (ESM) tolerance at different stages of life cycle. *Bot. Res. Intl.* 2, 211–217.

Mano, Y., Muraki, M., Komatsu, T., Fujimori, M., Akiyama, F., and Takamizo, T. (2002). Varietal difference in pre-germination flooding tolerance and waterlogging tolerance at the seedling stage in maize inbred lines. *Jpn. J. Crop Sci.* 71, 361–367. doi: 10.1626/jcs.71.361

Mano, Y., and Omori, F. (2007). Breeding for flooding tolerant maize using "teosinte" as a germplasm resource. *Plant Root* 1, 17–21. doi: 10.3117/plantroot.1.17

Mano, Y., Omori, F., Muraki, M., and Takamizo, T. (2005). QTL mapping of adventitious root formation under flooding conditions in tropical maize (*Zea mays* L.) seedlings. *Breed. Sci.* 55, 343–347. doi: 10.1270/jsbbs.55.343

Mano, Y., Omori, F., Takamizo, T., Kindiger, B., Bird, R. M., and Loaisiga, C. H. (2006). Variation for root aerenchyma formation in flooded and non-flooded maize and teosinte seedlings. *Plant Soil* 281, 269–279. doi: 10.1007/s11104-005-4268-y

McDaniel, V., Skaggs, R. W., and Negm, L. M. (2016). Injury and recovery of maize roots affected by flooding. *Appl. Eng. Agric.* 32, 627–638. doi: 10.13031/aea.32.11633

Mendiondo, G. M., Gibbs, D. J., Szurman-Zubrzycka, M., Korn, A., Marquez, J., Szarejko, I., et al. (2016). Enhanced waterlogging tolerance in barley by manipulation of expression of the N-end rule pathway E3 ligase *PROTEOLYSIS6*. *Plant Biotechnol. J.* 14, 40–50. doi: 10.1111/pbi.12334

Narusaka, Y., Narusaka, M., Seki, M., Umezawa, T., Ishida, J., Nakajima, M., et al. (2004). Crosstalk in the responses to abiotic and biotic stresses in *Arabidopsis*: analysis of gene expression in *cytochrome P450* gene superfamily by cDNA microarray. *Plant Mol. Biol.* 55, 327–342. doi: 10.1007/s11103-004-0685-1

Pompeiano, A., Fanucchi, F., and Guglielminetti, L. (2013). Amylolytic activity and carbohydrate levels in relation to coleoptile anoxic elongation in *Oryza sativa* genotypes. *J. Plant Res.* 126, 787–794. doi: 10.1007/s10265-013-0567-1

Rajhi, I., Yamauchi, T., Takahashi, H., Nishiuchi, S., Shiono, K., Watanabe, R., et al. (2011). Identification of genes expressed in maize root cortical cells during lysigenous aerenchyma formation using laser microdissection and microarray analyses. *New Phytol.* 190, 351–368. doi: 10.1111/j.1469-8137.2010.03535.x

Ren, B., Zhang, J., Li, X., Fan, X., Dong, S., Liu, P., et al. (2014). Effects of waterlogging on the yield and growth of summer maize under field conditions. *Can. J. Plant Sci.* 94, 23–31. doi: 10.4141/cjps2013-175

Rivera-Contreras, I. K., Zamora-Hernández, T., Huerta-Heredia, A. A., Capataz-Tafur, J., Barrera-Figueroa, B. E., Juntawong, P., et al. (2016). Transcriptomic analysis of submergence-tolerant and sensitive *Brachypodium distachyon* ecotypes reveals oxidative stress as a major tolerance factor. *Sci. Rep.* 6:27686. doi: 10.1038/srep27686

Sauter, M. (2013). Root responses to flooding. *Curr. Opin. Plant Biol.* 16, 282–286. doi: 10.1016/j.pbi.2013.03.013

Setter, T. L., Waters, I., Sharma, S. K., Singh, K. N., Kulshreshtha, N., Yaduvanshi, N. P. S., et al. (2008). Review of wheat improvement for waterlogging tolerance in Australia and India: the importance of anaerobiosis and element toxicities associated with different soils. *Ann. Bot.* 103, 221–235. doi: 10.1093/aob/mcn137

Vamerali, T., Guarise, M., Ganis, A., Bona, S., and Mosca, G. (2003). Analysis of root images from auger sampling with a fast procedure: a case of application to sugar beet. *Plant Soil* 255, 387–397. doi: 10.1023/A:1026147607879

Voesenek, L. A., and Bailey-Serres, J. (2015). Flood adaptive traits and processes: an overview. *New Phytol.* 206, 57–73. doi: 10.1111/nph.13209

Xu, K., Xu, X., Fukao, T., Canlas, P., Maghirang-Rodriguez, R., Heuer, S., et al. (2006). Sub1A is an ethylene-response-factor-like gene that confers submergence tolerance to rice. *Nature.* 442, 705–708. doi: 10.1038/nature04920

Xu, W., Bak, S., Decker, A., Paquette, S. M., Feyereisen, R., and Galbraith, D. W. (2001). Microarray-based analysis of gene expression in very large gene families: the cytochrome P450 gene superfamily of *Arabidopsis thaliana*. *Gene* 272, 61–74. doi: 10.1016/S0378-1119(01)00516-9

Yamauchi, T., Colmer, T. D., Pedersen, O., and Nakazono, M. (2018). Regulation of root traits for internal aeration and tolerance to soil waterlogging-flooding stress. *Plant Physiol.* 176, 1118–1130. doi: 10.1104/pp.17.01157

Yan, B., Dai, Q., Liu, X., Huang, S., and Wang, Z. (1996). Flooding-induced membrane damage, lipid oxidation and activated oxygen generation in corn leaves. *Plant Soil* 179, 261–268. doi: 10.1007/BF00009336

Zaidi, P. H., Rafique, S., Rai, P. K., Singh, N. N., and Srinivasan, G. (2004). Tolerance to excess moisture in maize (*Zea mays* L.): susceptible crop stages and identification of tolerant genotypes. *Field Crops Res.* 90, 189–202. doi: 10.1016/j.fcr.2004.03.002

Zheng, C., Jiang, D., Liu, F., Dai, T., Jing, Q., and Cao, W. (2009). Effects of salt and waterlogging stresses and their combination on leaf photosynthesis, chloroplast ATP synthesis, and antioxidant capacity in wheat. *Plant Sci.* 176, 575–582. doi: 10.1016/j.plantsci.2009.01.015

Conflict of Interest Statement: The authors declare that the research was conducted in the absence of any commercial or financial relationships that could be construed as a potential conflict of interest.

frontiers in Plant Science

REVIEW
published: 12 February 2019
doi: 10.3389/fpls.2019.00140

Soil and Crop Management Practices to Minimize the Impact of Waterlogging on Crop Productivity

*S. M. Nuruzzaman Manik[1], Georgina Pengilley[1], Geoffrey Dean[1], Brian Field[1], Sergey Shabala[1] and Meixue Zhou[1,2]**

[1] Tasmanian Institute of Agriculture, University of Tasmania, Prospect, TAS, Australia, [2] Hubei Collaborative Innovation Center for Grain Industry/School of Agriculture, Yangtze University, Jingzhou, China

Waterlogging remains a significant constraint to cereal production across the globe in areas with high rainfall and/or poor drainage. Improving tolerance of plants to waterlogging is the most economical way of tackling the problem. However, under severe waterlogging combined agronomic, engineering and genetic solutions will be more effective. A wide range of agronomic and engineering solutions are currently being used by grain growers to reduce losses from waterlogging. In this scoping study, we reviewed the effects of waterlogging on plant growth, and advantages and disadvantages of various agronomic and engineering solutions which are used to mitigate waterlogging damage. Further research should be focused on: cost/benefit analyses of different drainage strategies; understanding the mechanisms of nutrient loss during waterlogging and quantifying the benefits of nutrient application; increasing soil profile de-watering through soil improvement and agronomic strategies; revealing specificity of the interaction between different management practices and environment as well as among management practices; and more importantly, combined genetic, agronomic and engineering strategies for varying environments.

Keywords: agronomic practices, soil engineering, drainage, genetic solutions, waterlogging tolerance

OPEN ACCESS

Edited by:
Iduna Arduini,
University of Pisa, Italy

Reviewed by:
Baizhao Ren,
Shandong Agricultural University, China
Ümit Barış Kutman,
Gebze Technical University, Turkey
Giacomo Tosti,
University of Perugia, Italy

***Correspondence:**
Meixue Zhou
mzhou@utas.edu.au

Specialty section:
This article was submitted to Plant Abiotic Stress, a section of the journal Frontiers in Plant Science

Received: *28 October 2018*
Accepted: *28 January 2019*
Published: *12 February 2019*

Citation:
Manik SMN, Pengilley G, Dean G, Field B, Shabala S and Zhou M (2019) Soil and Crop Management Practices to Minimize the Impact of Waterlogging on Crop Productivity. Front. Plant Sci. 10:140. doi: 10.3389/fpls.2019.00140

INTRODUCTION

Waterlogging is one of the focal abiotic stresses, which affects crop growth (Linkemer et al., 1998; Setter and Waters, 2003; Lone et al., 2018). It has become the key constraint to crop production in the temperate high rainfall zone (HRZ) of Australia (Acuña et al., 2011), particularly in regions with duplex soils (Yaduvanshi et al., 2012). Global climate change causes waterlogging events to be more frequent, severe, and unpredictable (Jackson and Colmer, 2005; Intergovernmental Panel on Climate Change [IPCC], 2014). Some currently wet areas will become wetter and prolonged waterlogging will also become more prevalent (Dore, 2005; Intergovernmental Panel on Climate Change [IPCC], 2014). The value of this loss is also signficiant to the Australian grains industry where waterlogging causes an estimated annual production loss of AU$180 M (Pang et al., 2004) with a greater proportion of this being incurred in Western Australia (Zhang et al., 2006). Waterlogging caused 40–50% wheat yield reduction in a wet year (Zhou, 2010) resulting in AU$100 M in crop losses (Zhang et al., 2004).

Waterlogging is also a matter of worldwide concern affecting 16% of the soils in the United States, 10% of the agricultural lands of Russia and irrigated crop production areas of India,

Pakistan, Bangladesh, and China (Yaduvanshi et al., 2014; Food and Agriculture Organization [FAO], 2015). Globally, between 10 and 15 million ha of wheat are affected by waterlogging annually causing yield losses of between 20 and 50% (Hossain and Uddin, 2011). Waterlogging also causes yield losses in other grain crops such as barley, canola, lupins, field peas (Bakker et al., 2007; Romina et al., 2018), lentils and chickpeas (Solaiman et al., 2007).

Appropriate soil and crop management practices improve soil quality and crop productivity, through improved ecological and economical flexibility by reducing the need for additional agricultural land (Setter and Belford, 1990; Tilman et al., 2002; Shaxson and Barber, 2003). Improved soil management can increase infiltration, reduce surface runoff, and additionally improve availability of water and nutrients to plants (Amare et al., 2013; Negusse et al., 2013; Schmidt and Zemadim, 2015; Masunaga and Marques Fong, 2018). Crop management can contribute to higher yields (Soomro et al., 2009; Amare et al., 2013). This review focuses on the impact of waterlogging on soil properties, plant growth and agricultural management practices to mitigate waterlogging. The gaps in current knowledge, technology and farm practices are identified, and recommendations are made for future opportunities to ensure sustainable soil and crop management under waterlogged conditions.

WATERLOGGING EFFECT ON SOIL AND PLANT GROWTH

Waterlogging impedes the ability of soil to provide an optimum medium for plant growth and alters its physical, chemical, electro-chemical and biological characteristics as summarized in **Figure 1** (Pulford and Tabatabai, 1988; Glinski, 2018; Ferronato et al., 2019). This has a significant impact on the development of the root biomass and subsequently on plant overall development (**Figure 2**) (Ernst, 1990; Pierret et al., 2007; de San Celedonio et al., 2016). Fundamentally, the soil should have optimal water and air content for the proper physiological performance of the all phases of plant growth (Crawford, 1982).

Waterlogging hinders the growth of plants by reducing the dispersal of oxygen through the pore spaces in the soil around the root zone (Drew and Sisworo, 1977; Lee T.G. et al., 2007; Christianson et al., 2010) with the dispersal of oxygen being 320K times lower than that in non-submerged soils (Armstrong, 1980; Barrett-Lennard, 2003; Lee T. et al., 2007; Colmer and Greenway, 2011). The plant root needs an adequate supply of oxygen so as to fulfill the water and nutrient requirements of the shoots, and the soil oxygen concentration should be above 10% where atmospheric molecular oxygen concentration is 21% (Sojka and Scott, 2002; Brady and Weil, 2008; Colmer and Greenway, 2011; Morales-Olmedo et al., 2015; da Ponte et al., 2019). Under waterlogging conditions, oxygen demand to the root tip and to the rhizosphere is supplied by forming aerenchyma through removal of some cells of the cortex and these remove excess gases from the root and soil (Armstrong, 1980; Colmer and Greenway, 2011). The gas exchange between soil and atmosphere in a well aerated soil is amply rapid to decelerate O_2 deficiency and toxicity caused by excess CO_2 or other gases such as ethylene and methane (Sojka and Scott, 2002). A number of hydroponic or inert substrate experiments assessed the effect of hypoxia and anoxia on plants in waterlogged conditions, and determined the soil is a vital factor (Morard and Silvestre, 1996; Striker, 2008; Arbona et al., 2009; Bai et al., 2013; Morales-Olmedo et al., 2015). Excessive water content in the soil upon waterlogging decreases O_2 diffusion capacity, leading to hypoxic or even anoxic environments that inhibit the activity of nitrifying communities, resulting in depleted soil N availability that will negatively affect N-dependent crop productivity (Jaiswal and Srivastava, 2018; Nguyen L.T. et al., 2018). Thus, the rate of nitrification is estimated to decrease in response to waterlogging conditions (Reddy and Patrick, 1975; Laanbroek, 1990).

Moreover, decreasing molecular oxygen prompts a sequence of changes in the physico-chemical properties of the soil (Ponnamperuma, 1984). Many of these also change soil chemical and electro chemicals by decreasing redox potential and excess electron changes, such as Fe^{3+} and Mn^{4+} to Fe^{2+} and Mn^{2+}, correspondingly (Ponnamperuma, 1984; Jackson and Colmer, 2005; Singh and Setter, 2017). Thus, solubility of iron and manganese rises to toxic levels, which are potentially damaging to plant roots (Jones and Etherington, 1970; Aldana et al., 2014; Marashi, 2018; Sharma et al., 2018). Apart from the elemental toxicities to the sensitive root tips, increased concentration of secondary metabolites such as phenolics and volatile fatty acids may become injurious in the low-pH rhizosphere (Pang et al., 2007a; Shabala, 2011; Coutinho et al., 2018). pH values of waterlogged soil can be further reduced by the accumulation of volatile organic acids as well as the high concentration of CO_2 (Greenway et al., 2006) which reduces root growth (Boru et al., 2003). As mentioned, another potential toxic metabolite found in waterlogged soil is ethylene, which suppresses root expansion growth (Drew and Lynch, 1980; Shabala, 2011). In addition, with the re-introduction of oxygen at the recovery phase, the remaining ethanol in anoxic cells will be transformed into acetaldehyde which may cause cell injuries (Bailey-Serres and Voesenek, 2008). Under abiotic stress conditions, reactive oxygen species (ROS) levels are always elevated compared to pre-stress levels (Miller et al., 2008). Excessive production of various ROS such as superoxide radicals, hydroxyl radicals, hydrogen peroxide, and singlet oxygen found in hypoxia-stressed leaf and root tissues (Blokhina et al., 2003; Sairam et al., 2009; Petrov et al., 2015; Shabala et al., 2016) can also cause severe damage to plants. All of these lead to restricted root growth, reduced tiller number, premature leaf senescence and production of sterile florets thus affecting the grain yield (Collaku and Harrison, 2005; Hossain and Uddin, 2011; Cannarozzi et al., 2018).

Even though the accumulation of phytotoxic compounds requires time, the absence of oxygen alone is enough to change the plant metabolic activities to critical levels (Geigenberger, 2003; Perata et al., 2011). O_2 deficiency during waterlogging leads to reduced availability of energy in the roots (Armstrong et al., 1991) and, as a result, energy-dependent processes such as nutrient uptake are inhibited (Setter and Belford, 1990). N deficiency is believed to be the other cause of the suppression of growth under waterlogging (Cannell et al., 1980;

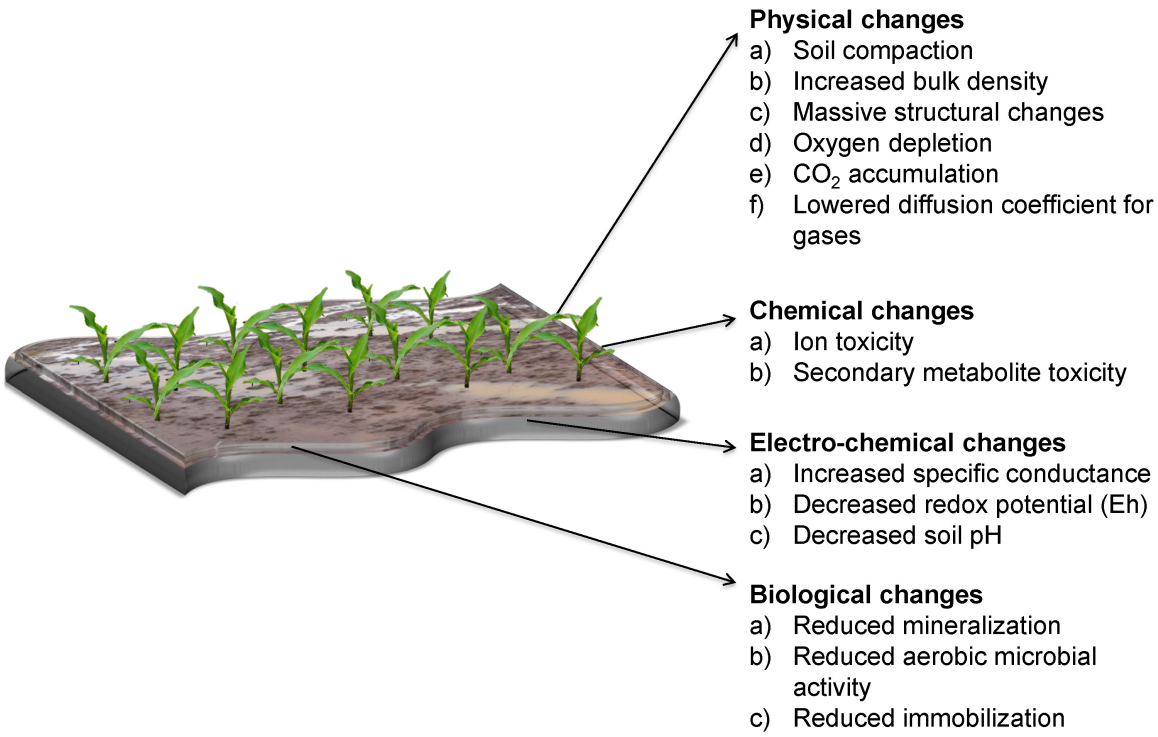

FIGURE 1 | Effects of waterlogging on soil properties.

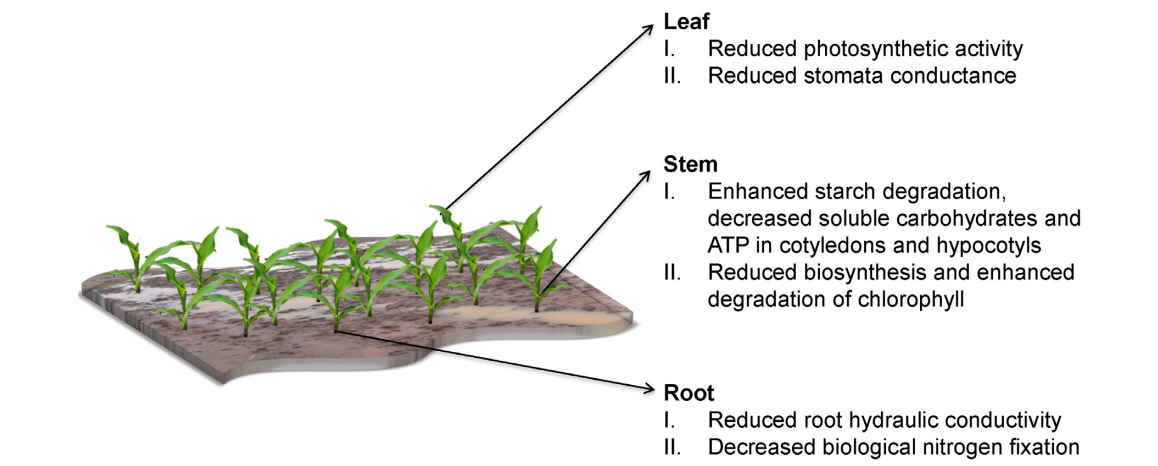

FIGURE 2 | Effects of waterlogging on plant growth.

Robertson et al., 2009; Wollmer et al., 2018). Carbohydrate (the energy reserve) production reduced dramatically during complete submergence or subsequent de-submergence due to reduced photosynthetic rate (Sarkar et al., 2006; Pérez-Jiménez et al., 2018), reduced stomatal conductance, declined root hydraulic conductivity and reduced translocation of photo assimilates (Parent et al., 2008). One of the first plant responses to waterlogging is the reduction in stomata conductance (Folzer et al., 2006), for example, fast stomata closure in barley (Yordanova et al., 2005) and pea (Zhang and Zhang, 1994). The stomata closure was attributed to abscisic acid (ABA) transport from older to younger leaves or *de novo* synthesis of this hormone (Zhang and Zhang, 1994). Waterlogging also decreases the leaf chlorophyll content (Malik et al., 2001; Ashraf et al., 2011; Li et al., 2018; Ma et al., 2018). This decrease in chlorophyll directly or indirectly affects the photosynthetic capacity of plants (Azhar et al., 2018; Rasheed et al., 2018; Yu et al., 2019). This decrease in transpiration and photosynthesis is attributed to stomata closure (Ashraf and Arfan, 2005; Tian et al., 2018) which restricts CO_2 movement (Jackson and Hall, 1987;

Malik et al., 2001; Chu et al., 2018). To summarize, waterlogging affects overall plant growth, which leads to a substantial yield loss (Kumar, 2018; Romina et al., 2018; Wollmer et al., 2018).

SOIL MANAGEMENT

Soil management practices such as drainage, tillage and traffic control can alter soil structure directly or indirectly (Pagliai et al., 2004; Unger et al., 2018). Many of these changes are relatively short term and reversible. Management-induced changes in the quantity and characteristics of soil can also lead to changes in soil structure that are much more persistent. Management practices which are sustainable must maintain the structure of soil, over the long term, in a state that is optimum for a range of processes related to crop production and environmental quality (Bogunovic et al., 2017; Belmonte et al., 2018).

Soil surface biological communities provide critical functions in many ecosystems by controlling infiltration and thus ensure suitable water availability for crop, soil biota, nutrient cycles and vascular vegetation (Chamizo et al., 2016). They increase biodiversity, accelerate soil formation rates, and contribute to the biogeochemical cycling of nutrients by fixing atmospheric carbon (C) and nitrogen (N) (Elbert et al., 2012; Weber and Hill, 2016). Therefore, a key consideration in designing management practices must be targeting the soil surface.

Various soil management practices can mitigate adverse effects of waterlogging stresses. Here, we review some soil management practices emphasizing the system used for waterlogging-prone areas.

Controlled Traffic Farming (CTF)

Controlled traffic farming (CTF) is a management system to control extensive unsystematic trafficking by farm machinery/vehicles and protect soil structure from indiscriminate change (Hamza and Anderson, 2005). CTF (**Figure 3**) is a crop production system where the crop region and traffic-lanes are markedly divided (Taylor, 1983; Raper, 2005; Bochtis and Vougioukas, 2008). It creates two distinct zones, the crop region which is non-trafficked and traffic region or non-cropped. Consequently, CTF systems always maintain the crop region unaffected by wheel tracks, whereas the traffic zone develops into a compacted zone for machinery draught efficacy (Taylor, 1992). CTF is differentiated from conventional traffic practices, known as random traffic farming (RTF) by reducing the trafficked area.

Random traffic farming or disorganized traffic causes increases in the soil bulk density resulting in increases in strength limiting soil porosity further leading to soil compaction (Tullberg, 2000; Chen et al., 2010; Rasaily et al., 2012). RTF has an adverse effect on a wide range of soil physical characteristics, including the infiltration and drainage of water, amenability for crop sowing, establishment and nurture, and soil gaseous exchange medium and soil-living organism (Gasso et al., 2013; Gasso et al., 2014). Due to random traffic a large amount of soil is adversely affected resulting in soil degradation issues in Australia (4 million ha), Europe (33 million ha), Asia (10 million ha), Africa (18 million ha) (Flowers and Lal, 1998; Hamza and Anderson, 2003; Shahrayini et al., 2018).

The advantages of CTF have been well documented. These include reduced incidence of waterlogging, soil compaction, erosion, tillage, water and nutrient losses and thus increased crop yield (Morling, 1982; Raper, 2005; Tullberg et al., 2007; Chamen, 2015). Adoption of CTF by Australian grain growers was 3% in 2003 (Price, 2004), 15% in 2006 and 36% in 2008 (Robertson, 2008). In Australia a minimum of 10% yield improvement in barley, wheat, and canola across diverse soil types has been noted along with decreases in fuel consumption of machinery due to improved draught on the traffic area (Webb et al., 2004; Li et al., 2007; Robertson et al., 2007; Lorimer, 2008; Davies et al., 2012). In Europe yield of cereal crops (i.e., wheat and barley) increased from 9 to 21% with CTF compared with RTF (Gasso et al., 2013). Similarly, wheat yield with CTF increased by 6.9% compared to traditional tillage in China (Qingjie et al., 2009).

Strategic Deep Tillage and Subsoil Manuring

Strategic deep tillage (SDT) is a single or occasional practice with a deep ripper, rotary, spader, mouldboard plow or disk plow to help sustain the long-standing productivity of the no-till system (Renton and Flower, 2015; Roper et al., 2015; Rincon-Florez et al., 2016; Kuhwald et al., 2017; Scanlan and Davies, 2019). Deep tillage or soil cultivation to loosen compact soil layers, particularly the clay subsoil, has been suggested to improve drainage in the subsoil, thus reducing waterlogging (Gardner et al., 1992). The technique may also incorporate slotting of gypsum to reduce sodicity and improve soil structure, which also reduces waterlogging (Crabtree, 1989; McFarlane and Cox, 1992).

Deep ripping loosens hard layers of soil by using sturdy tines to 35–50 cm depth. It is not suitable for all soils and crops, therefore season, timing, soil type, tine spacing, shallow leading tines, soil moisture content, and working depth are all factors that need to be taken into consideration. The benefit of combined CTF and SDT may last for three seasons but can be as long as ten seasons with average wheat yield increase in Western Australia being 0.6 t/ha and 0.5 t/ha at 12 sites and 16 sites, respectively (Davies et al., 2012; Roper et al., 2015). Schneider et al. (2017) conducted a meta-analysis of 1530 yield comparison at 67 experimental sites across Germany, United States, Canada, and India and showed increased yield of greater than 6% between deep and ordinary tillage systems.

There are, however, several disadvantages of deep ripping including its short-term nature (especially if traffic is not managed to reduce re-compaction), effectiveness in hostile sub-soils, such as acidity, sodicity or subsoil salinity, and its implementation on a large scale (Bakker et al., 2007). In this case, amelioration with gypsum or lime may be helpful to stabilize the soil (Henry et al., 2018; Matosic et al., 2018). Although yield benefit from SDT has been demonstrated, organic matter, texture and soil nutrients distribution within the root zone need appropriate long term agronomic management to maximize the benefit (Roper et al., 2015).

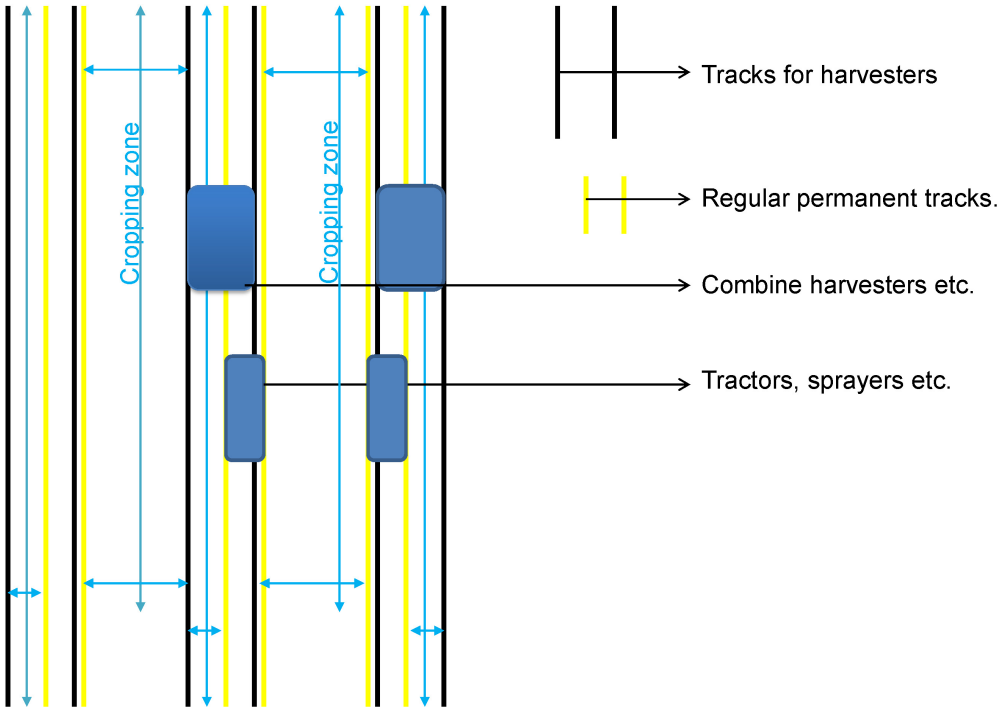

FIGURE 3 | Controlled traffic farming.

Another way of reducing waterlogging is through a similar practice where large volume of organic matter with high N levels are placed within and above the heavy clay layers. This practice is referred to as sub-soil manuring (Gill et al., 2009; Peries, 2013; Celestina et al., 2018). In south eastern Australia approximately 80% of the cropping zone of medium annual rainfall (375–500 mm) and high rainfall (>500 mm) are affected by subsoil constraints (Grains Research, and Development Corporation [GRDC], 2016). Amelioration of subsoil constraints may be possible by slotting large quantities (>10 t/ha) of organic matter and other amendments (Sale, 2014; Armstrong et al., 2015). Experiments carried out in Victoria, Australia demonstrated that lucerne pellets and commercial poultry manure can significantly improve soil properties and crop growth as well as yield by improving subsoil structure and supplying N (Gill et al., 2009, 2012).

The increase in water extraction by roots also provides a greater buffer for subsequent waterlogging events. However, adoption on a commercial scale has remained low due to a combination of high upfront costs (up to $1200/ha) to implement, variable yield responses and logistical constraints such as the limited availability of suitable organic matter sources and access to appropriate machinery (Nicholson, 2016; Armstrong et al., 2017).

Drainage Systems

Land drainage is one of the main approaches to improve yields per unit of accessible agricultural area (Bos and Boers, 1994; Malano and van Hofwegen, 2006; Singh, 2018b). Reducing soil submergence, salinity control, and making new land accessible for agriculture are the three main objectives of agricultural drainage (Singh and Panda, 2012; Singh, 2018b). However, drainage, an efficient agriculture engineering system to combat waterlogging, has not been given equal importance when compared to irrigation by individual farmers and governmental agencies.

Drainage is used to alleviate waterlogging not only in some parts of Australia (Cox et al., 1994; Milroy et al., 2009), but also world-wide. Various studies, conducted in England, Europe, and North America indicate that drainage can effectively lower the water table and improve crop yields (Cannell and Jackson, 1981; Evans and Fausey, 1999; Bullock and Acreman, 2003; Blann et al., 2009; Smedema et al., 2014; Gramlich et al., 2018). It was also reported to greatly reduce wheat yield losses due to waterlogging in south-western Victoria (Gardner and Flood, 1993; Christy et al., 2015; Feng et al., 2018). Despite the yield losses associated with waterlogging on prone Australian texture-contrast soils, large scale adoption of drainage is still limited in the HRZ (Cox et al., 2005; Rengasamy, 2006; Christy et al., 2015). Various methods have been recommended to mitigate the waterlogging problems, such as surface drainage, subsurface drainage, and mole drains (Muirhead et al., 1996; Misak et al., 1997; Konukcu et al., 2006; Ram et al., 2007; Ritzema et al., 2008; Kazmi et al., 2012; Singh, 2012, 2016; Singh and Panda, 2012).

Surface Drainage

Surface drainage is defined as the safe removal of excess water through constructed channels from the land surface

(Ritzema et al., 2008; Ayars and Evans, 2015). Surface drains such as 'spoon-drains,' 'W-drains' and reverse seepage interceptor banks and interceptor drains have been used to alleviate the conditions of waterlogging in south-western Australia (Cox et al., 1994). Surface drainage systems have been shown to be cost effective with cost-benefit ratios being in the range from 1.2 to 3.2, internal return rates from 20 to 58%, and payback periods from 3 to 9 years (Ritzema et al., 2008). The simplest and cheapest option is to maintain existing surface drains and install extra drains along fence lines or through depressions considering adequate size and proper position. Preventing water flow from upper to lower paddocks with cut-off drains should also be implemented (Palla et al., 2018). However, the success of surface drainage is often limited due to the poor lateral water movement or internal soil drainage properties, which results in poor drainage in the vicinity of the drains (McFarlane and Cox, 1992; Cox and McFarlane, 1995; Saadat et al., 2018). Both surface and subsurface drainage may thus be required to solve these problems.

Raised Bed System

The use of raised beds (**Figure 4**) is an important soil management option to improve crop yield, soil structure, and productivity under waterlogged conditions (Hamilton et al., 2000; Bakker et al., 2005b; Hussain et al., 2018). The beds reduce waterlogging and improve the overall soil structure through installing shallow drains or furrows approximately 15–20 cm wide at regular intervals. These are then used for tractors, and sprayers to control traffic movement over the paddock (control traffic farming) (Collis, 2015). The 2–3 m wide and 10–30 cm height bed is formed using soil creating a raised bed allowing water to drain away from the plant root zone and reducing the likelihood of waterlogging damage (Riffkin et al., 2003; Bakker et al., 2007; Gibson, 2014; Ghazouani et al., 2015). Planting on beds also diminishes pesticide applications due to a reduction in fungal and other diseases with improved radiation interception, acquisitive temperature and reduced humidity in the canopy (Alwang et al., 2018).

When seasonal conditions are appropriate, raised beds can significantly increase grain yield under waterlogged conditions compared with crops grown conventionally on flat ground (Bakker et al., 2007; Acuña et al., 2011). In Australia, raised beds are used in irrigated agriculture in New South Wales and north-west Victoria, as well as in cotton growing areas in New South Wales to minimize the impacts of waterlogging (Bakker et al., 2005a; Bakker et al., 2007). The use of raised beds is also prominent in high rainfall areas across Victoria and experiments demonstrated that wheat and barley yield increased by 50% and 30%, respectively (Collis, 2015), and were proposed for the waterlogged duplex soils of Western Australia (Bakker et al., 2005a; Bakker et al., 2005b), and for the frequently waterlogged arable land across the south-eastern wheat belt of Western Australia (Bakker et al., 2007). Permanent raised beds and furrow systems are also used to manage waterlogging in Mexico (Roth et al., 2005) and coastal lowlands in humid tropical regions in some South Asian countries (Velmurugan et al., 2016), consistently delivering higher returns based on cost–benefit analyses.

While raised beds have had a positive impact on alleviating the effects of waterlogging they also have a number of disadvantages. These include the cost of adapting and modifying machinery, greater difficulty in controlling sowing depth and seed placement on beds, management of drainage water, limited use where the water table is too high, stubble handling and fodder conservation, firefighting and mustering livestock, the possibility of pesticide contamination into waterways and leaching into the water table and inefficiencies of machinery and weed control in furrows (Bakker et al., 2005b; Gibson, 2014). When raised beds were compared with hump and hollow surface drainage in waterlogged pastures at Derrinallum, Victoria it was concluded that the use of raised beds for the growing of pastures for grazing had little to offer the sheep industry (Ward et al., 2007). This poses a significant research question around suitability of raised beds in the many mixed farming systems that operate across the HRZ of Australia.

Subsurface Drainage

Poor subsurface water movement occurs due to the inability of water to move through soil as a result of heavy soil

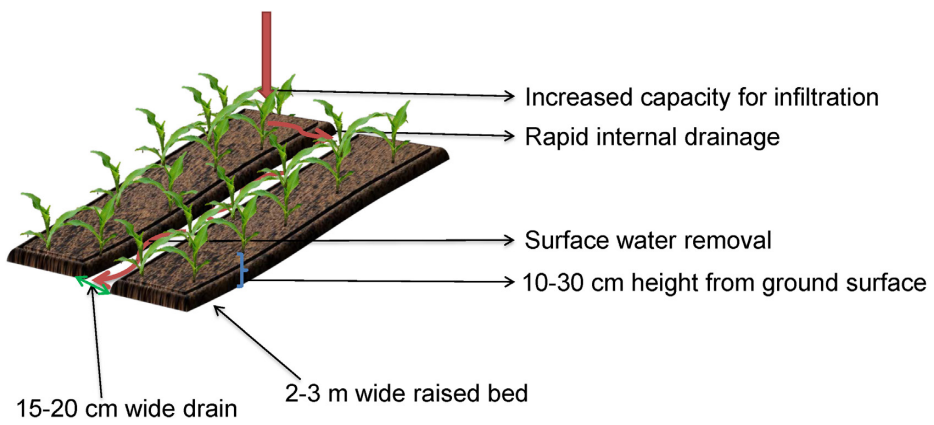

FIGURE 4 | Raised bed cropping system.

texture, compacted layers and naturally created or induced hard pans as well as water moving downhill from upper slopes or from springs, raising the water table (Ward et al., 2018). Subsurface drainage lowers the water table or perched water and ensures a suitable environment in the root region where waterlogging occurs (Christen et al., 2001; Xian et al., 2017). About 50% of waterlogged areas in western Europe, 20–35% of total cultivated land in Europe and North America, 5–10% in Asia, Australia, and South America, and 0–3% in Africa have used subsurface drainage measures (Food and Agriculture Organization [FAO], 2002). Subsurface drainage systems consist of open and pipe drains with variable drain depth and spacing (Ritzema et al., 2008). The systems are more effective in areas where the subsoils are sufficiently stable (Gardner et al., 1992) and not exhibiting characteristics of hostile sub-soils such as sodicity.

Subsurface pipe drains are the main forms of subsurface drainage found in the HRZ of Australia (Christen et al., 2001). Usually, the type of drain to be installed depends on topography, soil characteristics and rate of drainage required. There has been successful use of sub-surface drainage in areas of Tasmania, Australia and grain growers are willing to invest in drainage as a long-term solution to waterlogging (Gibson, 2014). This is also supported by a study into the economics of drainage, which indicated that subsurface drainage provided crop growers with the confidence to target high potential yields where the cost benefit was positive (Bastick and Walker, 2000).

Although, subsurface deep drains (depth > 1.75 m) are recommended in India (Gupta, 2002), these deep drains can be economically installed only by mechanical construction practices, and the deeper the drain the higher the installation cost (Gupta, 1997). In some parts of Australia, several types of subsurface drainage were found to be unsuccessful because they were expensive and failed to control surface water (McFarlane and Cox, 1992). Managing waterlogging with horizontal tile drainage systems (using a combined drainage system with tube wells plus horizontal drainage systems) is more beneficial in maintaining the water table within the desirable depths (Chandio et al., 2013). In Australia, subsurface drainage such as tile and mole drainage are shown to be particularly useful for irrigated high-value crops such as perennial horticulture, cotton, pasture, sugarcane and perennial pastures for dairying (MacEwan et al., 1992; Christen et al., 2001).

Subsurface Pipe Drains

Horizontal subsurface (**Figure 5**) drainage removes excess water from the crop root zone (Tanji, 1990; Teixeira et al., 2018). Below the ground surface, the drainage structure comprises a grid of perforated pipes connected to control the water table. Tile drainage is a form of horizontal subsurface drainage consisting of small pipes of concrete or burnt clay installed at a certain depth below the ground surface (King et al., 2014). Tile drainage is used widely in agricultural areas where subsoil surplus water is a common problem (Williams et al., 2015). To improve the system gravel is usually used above the tile drains as a backfill material in the areas where there is shallow groundwater and heavy soil conditions (Filipović et al., 2014).

Besides water table control, horizontal drainage controls soil salinity in the root zone of the soil by leaching out the concentrated and harmful salt solutions (Christen and Skehan, 2001). This is an established and significantly relevant system for saline land reclamation in Australia and India in irrigation areas where excess soil salinity is the prime limitation in agricultural production (Christen and Skehan, 2001; Prathapar et al., 2018). However, this method may not be suitable for agricultural lands where the top soils are prone to seasonal waterlogging due to poor hydraulic conductivity and the need to find appropriate outfall for drained water (Christen and Skehan, 2001; Food and Agriculture Organization [FAO], 2002; Prathapar et al., 2018; Singh, 2018a).

Vertical Subsurface Drainage

Vertical drainage (VD) (**Figure 6**) is used for controlling rising groundwater levels in some parts of Australia such as Burdekin, Kerang, and Shepparton (Christen et al., 2001; Kijne, 2006). Recent results showed that installing VD can reduce the duration of seasonal waterlogging in Bihar, India (Prathapar et al., 2018). Various types of vertical drains have been used to consolidate the soil, such as prefabricated vertical drains (PVDs), sand compaction piles, sand drains, gravel piles and stone columns (Indraratna et al., 2005; Indraratna, 2017). Recently, PVDs have been installed in Brisbane and Ballina in Australia (Indraratna, 2017). The VD system has some advantages over other subsurface drainage systems. For example, VDs are often preferred because of relative low capital cost and the length of open surface drains is less with VD when compared with other types of drainage (Christen et al., 2001). VDs also allow the groundwater level to be lowered to a greater depth than other drainage systems (Kruseman and Ridder, 1990). However, the maintenance and operational costs are higher than horizontal drainage systems as it involves high energy to operate a network of tube wells (Christen et al., 2001; Food and Agriculture Organization [FAO], 2002; Prathapar et al., 2018). The effectiveness of the VD system is demonstrated by the drop in the groundwater level, therefore, the system is more suitable for an area with fluctuating high levels of groundwater.

Mole Drains

Mole drainage (**Figure 7**) is another form of subsurface drainage. Its effects on reducing waterlogging have been shown in Victoria, Australia (Frank, 2010; Gibson, 2014). Mole drain systems were found to improve performance in terms of growth parameters, yield attributes and economic parameters of soybean (*Glycine max*) and wheat (*Triticum aestivum*) in Madhya Pradesh, India (Dhakad et al., 2018).

Mole drains are a semi-permanent system from a layout and operational point of view and are similar to tile drainage. Although costing less than tile drainage, they do require more maintenance (Tuohy et al., 2016, 2018; Dhakad et al., 2018). This drainage system is generally installed to manage rising groundwater levels and land salinization problems (Robinson et al., 1987; Castanheira and Serralheiro, 2010; Kolekar et al., 2014). Mole drainage relies on closely spaced channels and subsoil cracks to quickly send surplus soil water to the tile or

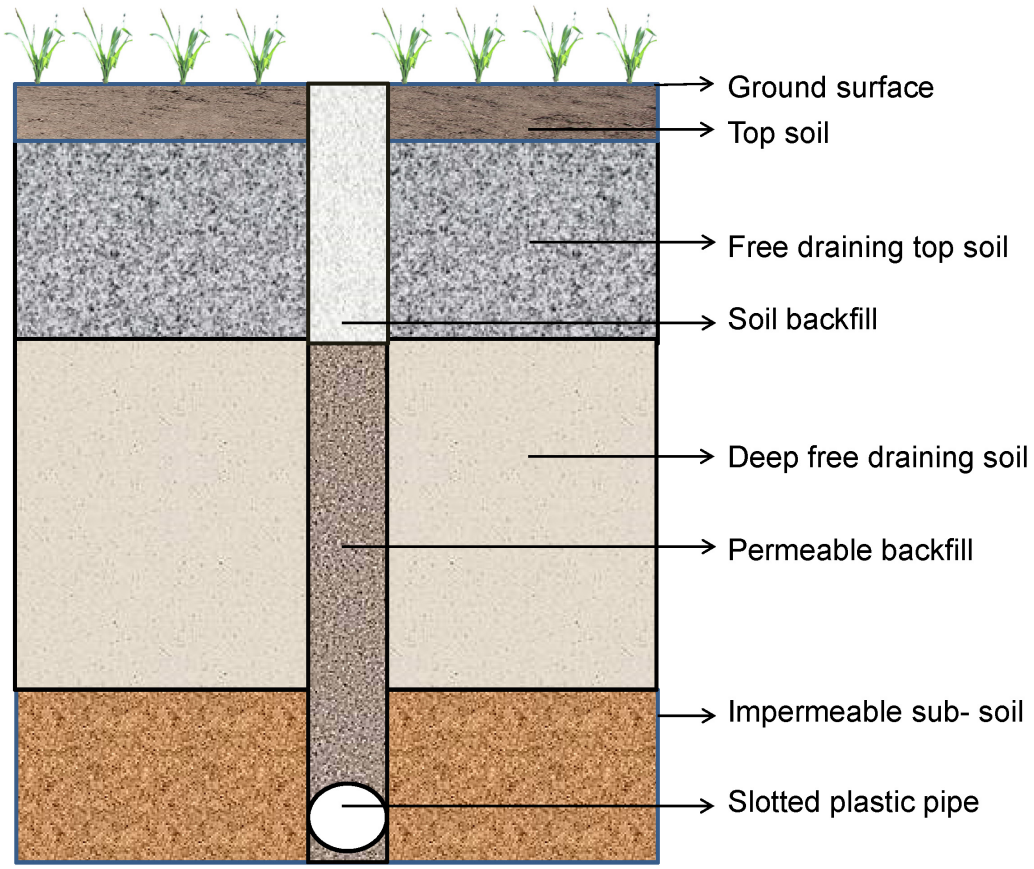

FIGURE 5 | Horizontal drainage system.

agricultural (ag) pipe drainage system throughout the season (Childs, 1943; Hallard and Armstrong, 1992; Tuohy et al., 2015, 2016). Mole drains are installed in close proximity to tile drains and are most suitable for low-permeability heavy soils such as clay (Monaghan et al., 2002; Monaghan and Smith, 2004). These drains should be installed at less than 600 mm from the ground surface and form 40–50 mm diameter circle of drainage (Gibson, 2014). A mole drain can be formed by dragging a metal object (viz. a blade like bullet with cylindrical foot, or mole plow) through the soil which creates an open channel. The installation cost of mole drainage is low but the moles should be re-formed at approximately 2- to 5-year intervals to uphold the channel integrity and optimize overall performance of the system (Tuohy et al., 2016, 2018). Combined drainage systems (mole and tile drainage) can be used efficiently to simulate water balance and drainage network system over a watershed, and to aid drainage management in a floodplain landscape (Tuohy et al., 2018).

CROP MANAGEMENT

There are a large and diverse number of crop management practices used by grain growers to alleviate the effects of waterlogging. These include: crop choice, waterlogging tolerant crop varieties, bio-drainage, and different agronomic practices such as sowing time, nutrient application and plant growth regulators (PGRs).

Early Sowing and Vigorous Crops

Crop management options to increase crop water use and decrease the incidence of waterlogging include early sowing and higher sowing rates (Gardner et al., 1992). Early sowing of wheat varieties showed better performance (Setter and Waters, 2003; Bassu et al., 2009; Ali et al., 2018) due to reduced risk of waterlogging damage through de-watering of the soil profile and avoiding waterlogging at vulnerable early growth stages (Gardner and Flood, 1993). Wheat, barley and rapeseed plants were less affected by early waterlogging (vegetative stages) than late (reproductive stages) (Ploschuk et al., 2018; Wollmer et al., 2018). Early sowing can also avoid late season terminal waterlogging events (Stapper and Harris, 1989). In addition, higher sowing rates can compensate for reduced tiller numbers and fertile heads (Watson et al., 1976; Belford et al., 1992).

Early crop vigor can be another important trait for waterlogging tolerance in the field (Sundgren et al., 2018). Tillering and reproductive stages are crucial for waterlogging tolerance in crops such as wheat and barley (Setter and Waters, 2003). Reduced nitrogen uptake is one of the main effects of

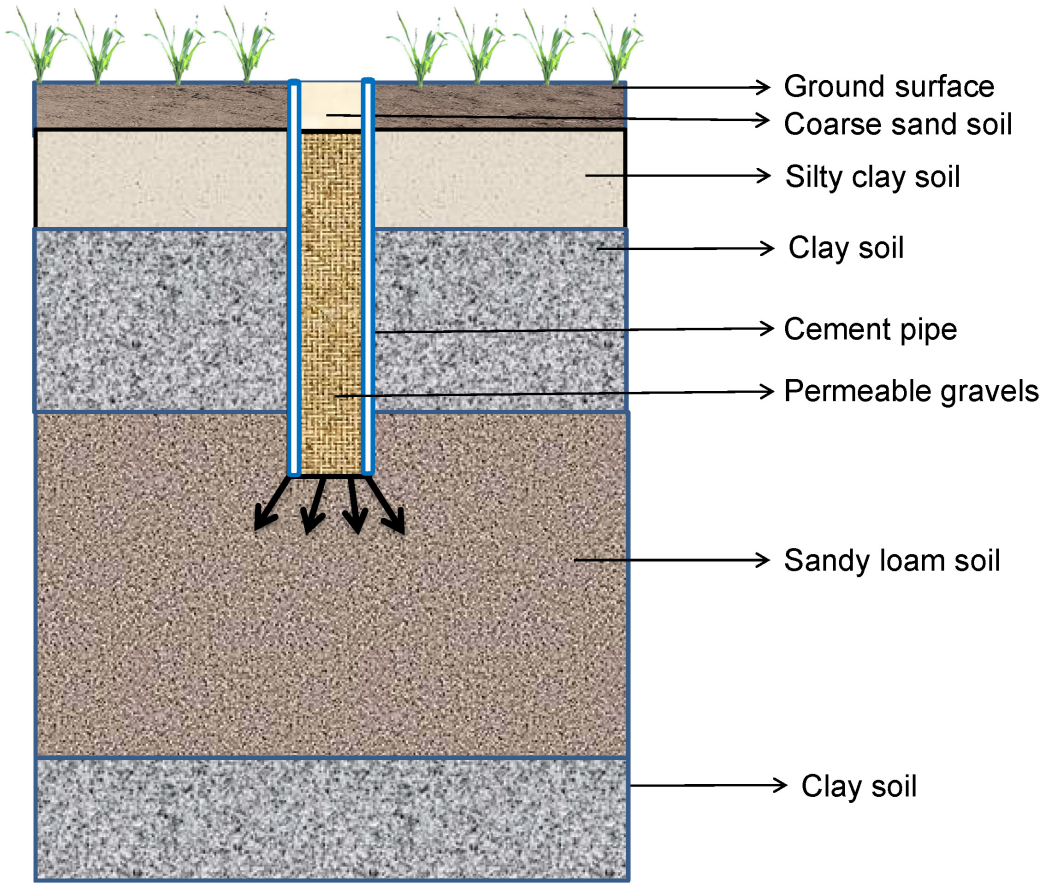

FIGURE 6 | Vertical drainage system.

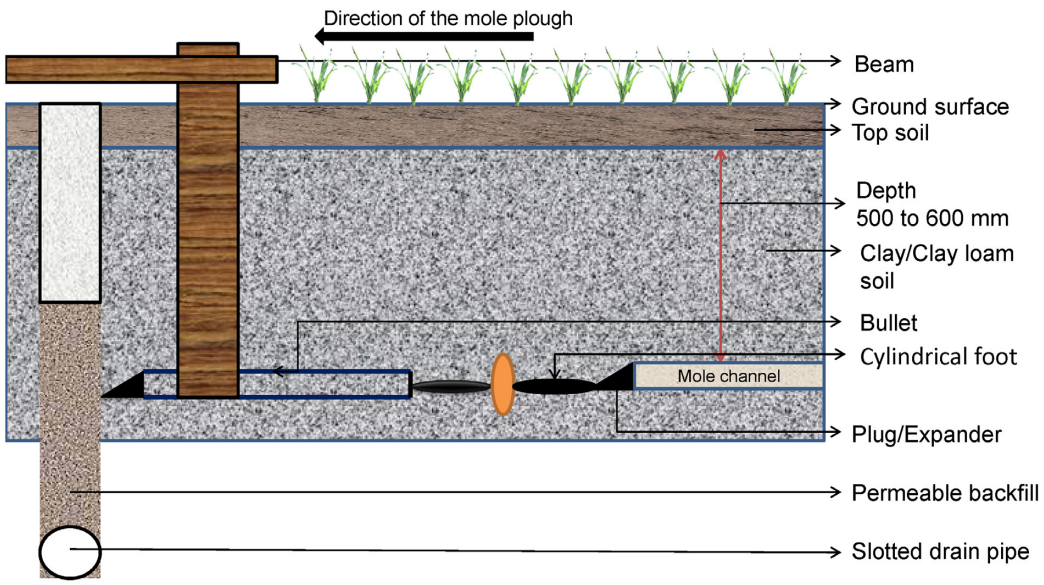

FIGURE 7 | Mole drainage system.

waterlogging stress in crops (Jaiswal and Srivastava, 2018; Nguyen L.T. et al., 2018). Early vigor may be linked with increased uptake of nitrogen (Liao et al., 2004; Sundgren et al., 2018). However, under normal conditions seedling growth rates can also vary with genotypic differences (Rebetzke et al., 2004). Further research may provide more insight into the interactions and possible use of early vigor to mitigate the effects of waterlogging.

Bio-Drainage

The incorporation of herbaceous perennial legumes such as lucerne, clovers and Messina (*Melilotus siculus*) adapted to waterlogging and inundation into cropping systems has been suggested to reduce waterlogging (Cocks, 2001; Nichols, 2018). Usually these deep rooted pasture plants can extract water and dry the soil to greater depths than most annual crops (McCaskill and Kearney, 2016). However, there is significant variation in tolerance to waterlogging between different pasture species (Cocks, 2001), and their suitability for grain production systems and how they would be integrated to provide maximum benefit has been identified as a gap in knowledge and warrants further investigation.

Bio-drainage or bio-pumping is the VD of soil water using specific types of fast growing tree vegetation with high evapotranspiration demand and is considered an economically viable option in dealing with the drainage congestion and environment hazards (Kapoor, 2000; Heuperman and Kapoor, 2003; Dash et al., 2005; Sarkar et al., 2018; Singh and Lal, 2018). Bio-drainage vegetation has been demonstrated to lower the rising water table around the root zone of adjacent cultivated crops in waterlogged areas through drainage (Roy Chowdhury et al., 2011; Sarkar et al., 2018; Singh and Lal, 2018).

Lowering of the rising water table is apparent within 5–10 years of growing vegetation and trees (Silberstein et al., 1999; Singh and Lal, 2018). If trees tolerant to waterlogging are introduced into the prone areas, these can easily assist in controlling water stagnation and rising water table (Banik et al., 2018; Sarkar et al., 2018). The right choice of plant species with optimum plant population and suitable plant geometry will help to control the elevated groundwater table in waterlogged areas and thus maintain the desired soil moisture regime for timely cultivation (Sarkar et al., 2018; Singh and Lal, 2018).

Prevention and remediation are the two stages of bio-drainage where the trees planted could provide a benefit to agriculture as well as resolving other issues such as waterlogging, salinity and shelter. Therefore, incorporation of a bio-drainage system with a conventional agriculture farming system could improve land and water productivity as well as the environment (Roy Chowdhury et al., 2011). Integration of bio-drainage with conventional drainage measures is an option to consider with the possibility of integration of silviculture and aquaculture with conventional agriculture to improve land and water productivity (Roy Chowdhury et al., 2011).

Bio-drainage systems may be established under both rainfed and irrigated conditions (Heuperman, 2000). When established under rainfed conditions, the plant roots reduce the soil bulk density and enhance groundwater recharge capacity. The roots also draw subsurface flow to reduce the water load. It is particularly useful when there is a perched water table and the water cannot easily move down the soil profile due to the presence of an impermeable layer. Recharge planting and slope break planting (**Figure 8**) may be adopted in the above situations. In irrigated and low lands, which are prone to waterlogging, the discharge planting method (**Figures 8**, **9**) is useful (Donnan, 1947; Dash et al., 2005). In HRZs, application of vegetative buffer strips is also effective for controlling runoff quantity and quality (Borin et al., 2010; Kavian et al., 2018; Saleh et al., 2018). Vegetative buffer strips have also been proposed as one of the best management or conservation practices to protect water bodies from nutrients, antibiotics, bacteria and pesticides applied on adjacent agricultural fields (Muñoz-Carpena et al., 2010; Lin et al., 2011; Lerch et al., 2017; Muñoz-Carpena et al., 2018). Tree species with high transpiration rates are selected to mitigate waterlogging from canal seepage in irrigated areas. Water quality in supply canals is suitable and can be effectively intercepted and used by the trees planted along the canals (Dash et al., 2005; Singh and Lal, 2018). However, the efficiency of bio-drainage plantations needs to be verified in HRZs where permanent stagnant water is a real problem. Lack of proper knowledge, plantation techniques, expertise, motivation as well as maintenance are issues that need to be addressed to derive the real benefit of this system. In addition, the land under bio-drainage cannot be utilized for growing other crops, as in the case of conventional drainage (Dash et al., 2005; Sarkar et al., 2018; Singh and Lal, 2018). Therefore, an economic analysis of the bio-drainage endeavor is required on a case by case basis.

Nutrient Application

Nutrient deficiency is one of the major effects of waterlogging on plants, resulting in reduced photosynthesis and net carbon fixation ultimately leading to a reduction in growth and therefore yield (Bange et al., 2004). Application of essential nutrients will assist in mitigating the negative effects of abiotic stresses like waterlogging leading to increased productivity (Noreen et al., 2018). The use of enhanced-efficiency N fertilizers such as slow-release or controlled-release (SR/CR) fertilizers (Shaviv, 2001; Varadachari and Goertz, 2010) play an important role in improving plant growth and development under waterlogged conditions (Dinnes et al., 2002). Slow-release fertilizer can release nitrogen over a prolonged period during crop growth, thus maximize nitrogen-use efficiency (NUE) by synchronizing nitrogen release according to the crop demand (Lubkowski and Grzmil, 2007; Trenkel, 2010). Several studies (Ashraf et al., 2011; Habibzadeh et al., 2012; Najeeb et al., 2015) suggested that exogenously applied fertilizers could be effective if the nutrient ions enter into the root architecture, consequently, plants are able to recover from the injury caused by waterlogging. Application of fertilizer diminishes the effects of waterlogging of barley (Pang et al., 2007b), wheat (Kaur et al., 2017; Pereira et al., 2017; Zheng et al., 2017), maize (Rao et al., 2002), corn (Kaur et al., 2018), cotton (Guo et al., 2010; Wu et al., 2012; Li et al., 2013) and canola (Habibzadeh et al., 2012). In Australia, studies under both controlled-environments and field conditions have shown that additional CR urea application can mitigate waterlogging effects (Allen et al., 2010; Najeeb

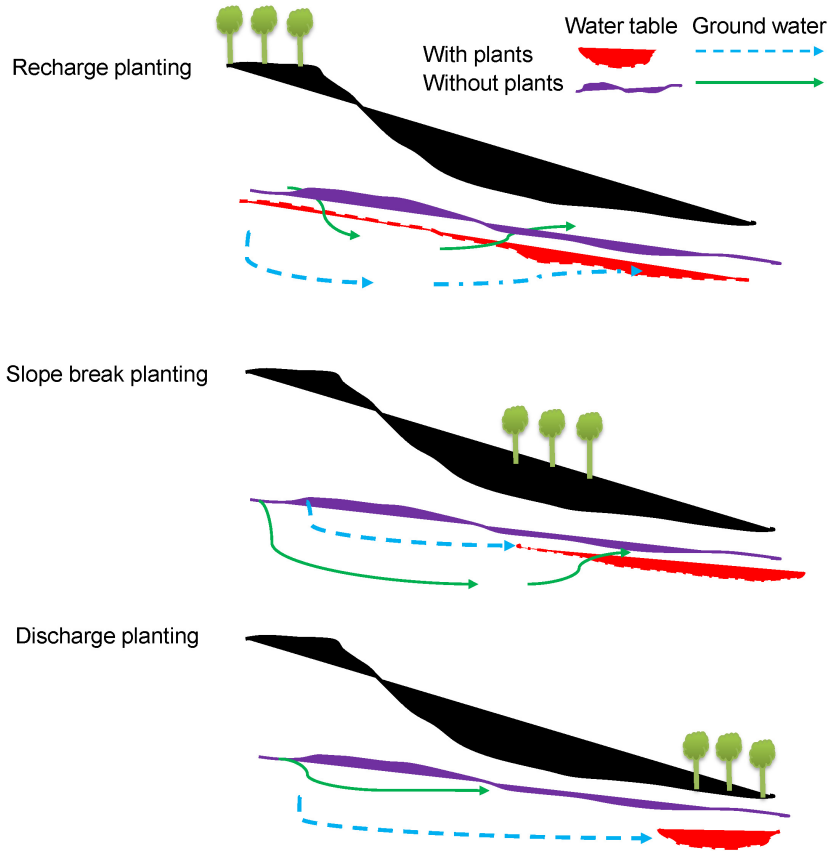

FIGURE 8 | Bio-drainage system.

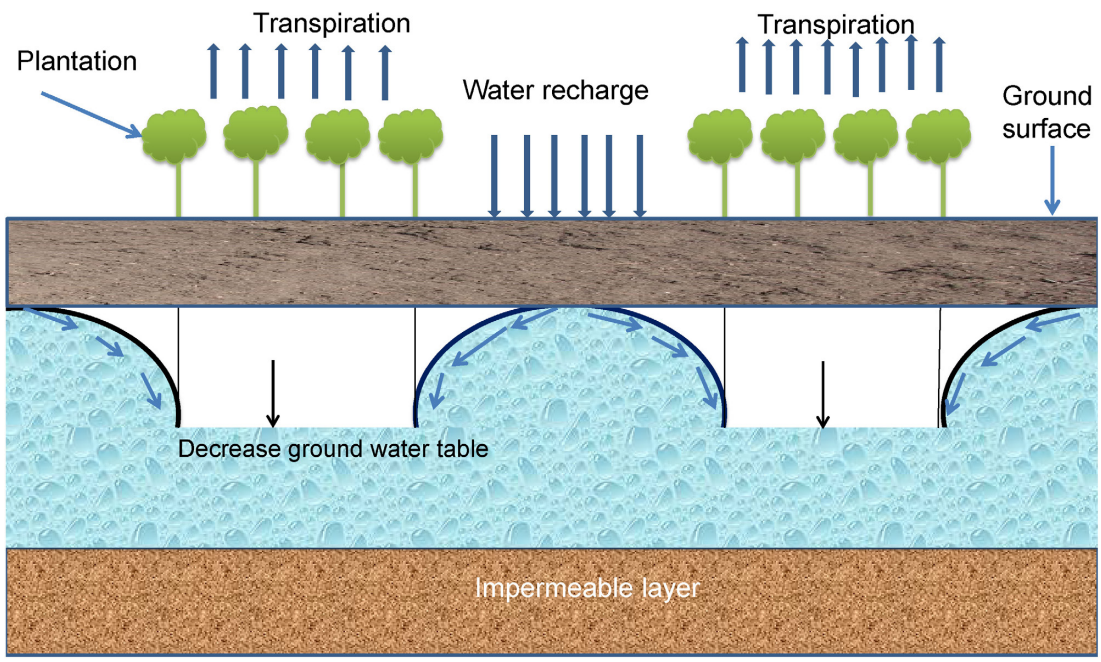

FIGURE 9 | Bio-drainage planting system (modified from Donnan, 1947).

et al., 2015) of wheat and increase growth (Kisaakye et al., 2017) and grain yield by approximately 20% (Robertson et al., 2009). Similar findings reported by Mondal et al. (2018) and Swarup and Sharma (1993) showed that increased rates of top-dressed urea significantly increased wheat grain yield on flooded sodic soils in India. Likewise, the use of polyolefin-coated urea (a controlled-release fertilizer) resulted in a total N recovery of 66% in flood irrigated barley grown in north eastern Colorado, United States (Shoji et al., 2001). Fertilizer application also increases canopy duration and accelerates the production of photo-assimilates translocated to the grain compared with the straw thus increasing the harvest index (Kisaakye et al., 2015, 2017).

Potassium fertilizer has also been reported to ameliorate the detrimental effects of waterlogging in several crops including sugarcane (Sudama et al., 1998), rapeseed (Cong et al., 2009) and cotton (Ashraf et al., 2011). Exogenous application of various phosphorus (P) sources such as dairy cow manure (DCM) and meat and bone meal (MBM) is effective for producing optimum yields in P-deficient conditions during a wet growing season (Ylivainio et al., 2008, 2018). Application of farmyard manure also significantly increased grain Fe, Zn, Cu concentration of paddy under flooded conditions (Masunaga and Marques Fong, 2018). Similarly, foliar application of boron has been reported to increase overall plant growth and alleviate deleterious effect of waterlogging of maize (Sayed, 1998).

The use of fertilizers to alleviate waterlogging damage in broadacre cropping, even with high value crops, has been limited by lack of research and availability of information on their potential use in improving crop performance under waterlogged conditions (Lubkowski and Grzmil, 2007; Trenkel, 2010). Appropriate application methods, nutrient types, timing and rate should be considered to avoid the negative effect of tissue toxicities (e.g., manganese) (Silva et al., 2017; Huang et al., 2018) and nutrient imbalance on soil ecology (Rochester et al., 2001; Jackson and Ricard, 2003). The ability to predict waterlogging events (variable seasons) and therefore the crops' nitrogen demand also limits the effectiveness of SR/CR fertilizers and therefore raises the question of whether highly available N applications would be preferable when waterlogging limits growth (Lubkowski and Grzmil, 2007; Trenkel, 2010). Robertson et al. (2007) suggested that pre-waterlogging application of N fertilizer might not be effective on wheat at the tillering stage. Application of nitrogen fertilizer during or immediately following waterlogging was less effective than pre-waterlogging due to inefficient nutrient ion absorption capacity of impaired roots, high leaching risks in the wet soils and at the late growth phase additional fertilizer applied could cause excessive vegetative growth and harvesting problems of cotton plant (Najeeb et al., 2015). Therefore, this strategy has limitations on a large-scale as the damaging effects of waterlogging can only be partially alleviated by the addition of fertilizers because of the reduced capability of roots to absorb nutrients (Trought and Drew, 1980; Kisaakye et al., 2015, 2017). For example, a drop in root membrane potential by 60 mV, often observed under hypoxic conditions (Gill et al., 2018) will require a 10-fold increase in cation (e.g., K^+ or NH_4^+) concentration in the rhizosphere, to enable thermodynamically passive uptake (Gill et al., 2018). This approach is difficult to justify based on cost efficiency.

Plant Growth Regulators

Plant growth regulators may mitigate waterlogging damage of plants by applying at the appropriate growth stage (Nguyen H.C. et al., 2018; Ren et al., 2018; Wu H. et al., 2018). The application of PGRs such as auxins and cytokinins has been reported to improve plant growth under waterlogged conditions (Pang et al., 2007b; Ren et al., 2016). The two hormones act in concert to promote stomatal conductance and photosynthetic capacity of waterlogged plants (Drew et al., 1979). Synthetic auxin 1-naphthaleneacetic acid (1-NAA), was reported to promote the growth of adventitious roots in waterlogged barley plants (Pang et al., 2007b) and; exogenous application of a cytokinin, 6-benzyladenine (6-BA) can alleviate waterlogging injuries and increase yield of maize (Ren et al., 2016, 2018). Pre-waterlogging foliar application of ABA increased tolerance to successive waterlogging-induced injury in cotton plant by improving photosynthesis of leaf (Pandey et al., 2002; Kim et al., 2018). Triazoles are known as fungitoxic and also have plant-growth regulatory effects and protect plants against various stresses (Leul and Zhou, 1998; Rademacher, 2015). For example, paclobutrazol mitigates waterlogging induced damage in canola and sweet potato plants (Lin et al., 2006). Uniconazole can also increase the chlorophyll content and the activity of antioxidant enzymes in canola (Leul and Zhou, 1999). Under waterlogging condition, the application of tricyclazole [5-methyl-1,2,4-triazole(3,4-b) benzothiazole] also mitigates the damage in plants (Habibzadeh et al., 2013). However, due to inconsistent results there has been little commercial use of PGRs to alleviate waterlogging damage.

Combined Application of Fertilizer and Growth Regulators

Combined application of fertilizers and growth regulators can provide another option for ameliorating detrimental effects of waterlogging in crops, with the fertilizers acting as a nutrient supplier, while the PGRs assist with recovery from physiological injury (Li et al., 2013). 1% urea + 0.5% potassium chloride and growth regulators [brassin (0.02 mg/L) + diethyl aminoethyl hexanoate (10 mg/L)] improved growth and yield of waterlogged cotton (Li et al., 2013). Both foliar nutrient and PGRs application provide opportunities for future research.

Use of Anti-ethylene Agents

Plant hypoxia-induced growth and yield losses could be the consequence of increased accumulation of ethylene (Shabala, 2011; Najeeb et al., 2018). Use of anti-ethylene agents such as 1-methylcyclopropene (1-MCP), amino ethoxyvinyl glycine (AVG), 1-aminocyclopropane-1-carboxylic acid (ACC), amino ethoxyacetic acid (AOA), silver and cobalt ions have been reported to inhibit the synthesis or accumulation of ethylene through blocking the biosynthetic pathway (Najeeb et al., 2017; Vwioko et al., 2017) of ethylene (McDaniel and Binder, 2012).

TABLE 1 | Summary of advantages and disadvantages of different soil and crop management practices.

Soil and crop management practices	Advantages (in addition to reducing waterlogging)	Disadvantages	Reference
Surface drainage	Both installation and maintenance are simplest and cheapest	Open drains with less cropping area; needs periodic maintenance	Food and Agriculture Organization [FAO], 2002; Ritzema et al., 2008; Ayars and Evans, 2015; Palla et al., 2018
Raised bed system	Improvements in soil structure	Efficiency depends on height of water table; poorer weed control in furrows; cost of modifying machinery; less cropping area	Bakker et al., 2005b, 2007; Roth et al., 2005; Zhang, 2005; Acuña et al., 2011; Gibson, 2014
Pipe drains	Well tested method for severe waterlogging	Needs outfall and periodic maintenance; cost of installation is high	Tanji, 1990; Food and Agriculture Organization [FAO], 2002; Filipović et al., 2014; Teixeira et al., 2018
Vertical drainage	Well tested method for severe waterlogging	Maintenance and operational costs are higher than for horizontal pipe drainage systems	Christen et al., 2001; Food and Agriculture Organization [FAO], 2002; Kijne, 2006; Prathapar et al., 2018
Mole drains	Well tested method; cheaper than other underground drainage	Needs periodic maintenance; will not maintain integrity in dispersive soils	Tuohy et al., 2016, 2018; Dhakad et al., 2018
Controlled traffic farming (CTF)	Reduced soil compaction, erosion, tillage costs, water and nutrient losses	Variable results with different conditions, such as different crops, soil types and tillage	Zhang, 2005; Chamen et al., 2006; Guenette and Hernandez-Ramirez, 2018; Thomsen et al., 2018; Bennett et al., 2019
Strategic deep tillage and subsoil manuring	Decreases soil strength resulting in deeper and denser rooting	SDT with no added amendment is often short-term nature, less effective in hostile sub-soils, such as acidity, sodicity or subsoil salinity	Gajri et al., 1994; Bakker et al., 2007; Roper et al., 2015
Early sowing and vigorous crop	Use of existing soil water provides a buffer; avoids terminal waterlogging events	Minor benefit with severe waterlogging	Stapper and Harris, 1989; Setter and Waters, 2003; Bassu et al., 2009; Ploschuk et al., 2018; Sundgren et al., 2018; Wollmer et al., 2018
Bio-drainage	Tried and tested at many locations with success	Needs proper plantation techniques, expertise, thinning, pruning, and harvesting	Kapoor, 2000; Food and Agriculture Organization [FAO], 2002; Heuperman and Kapoor, 2003; Dash et al., 2005; Lin et al., 2011; Lerch et al., 2017; Muñoz-Carpena et al., 2018; Sarkar et al., 2018; Singh and Lal, 2018;
Nutrient application, in particular, N	Improving plant growth and development	Appropriate methods, nutrient types, timing and rate should be considered for large-scale application	Rao et al., 2002; Pang et al., 2007b; Guo et al., 2010; Ashraf et al., 2011; Habibzadeh et al., 2012; Wu et al., 2012; Li et al., 2013; Najeeb et al., 2015; Kaur et al., 2017, 2018; Pereira et al., 2017; Zheng et al., 2017
Plant growth regulators	Promote stomatal conductance and photosynthetic capacity of waterlogged plants	Appropriate methods, timing and rate should be considered for large-scale application; unproven in broad scale agriculture	Drew et al., 1979; Lin et al., 2006; Habibzadeh et al., 2013; Ren et al., 2016, 2018
Use of anti-ethylene agents	Increase both photosynthesis and fruit retention; diminish crop loss induced by ethylene accumulation	Untested in broad scale agriculture	Kawakami et al., 2010; Shabala, 2011; Najeeb et al., 2018
Pretreatment with hydrogen peroxide	Protect crops from oxidative damage caused by waterlogging	Untested in broad scale agriculture	Gechev et al., 2002; Ishibashi et al., 2011; Rajaeian and Ehsanpour, 2015; Savvides et al., 2016; Andrade et al., 2018
Tolerant species and varieties	Cost effective for farmers	The introduction of waterlogging tolerance into existing plant varieties is time consuming and complex	Davies and Hillman, 1988; Gardner and Flood, 1993; Zhou et al., 2007; Gill et al., 2018; Huang et al., 2018

Application of 1-MCP and AVG has been shown to diminish crop loss induced by ethylene accumulation (Kawakami et al., 2010; Najeeb et al., 2018). Brito et al. (2013) reported a positive effect of 1-MCP and AVG on cotton seed and lint yield. They determined that the initial reproductive phase is the best time for AVG application for improving cotton yield under waterlogging condition. In cotton, waterlogging prompts ethylene accumulation leading to young fruit abscission (Najeeb

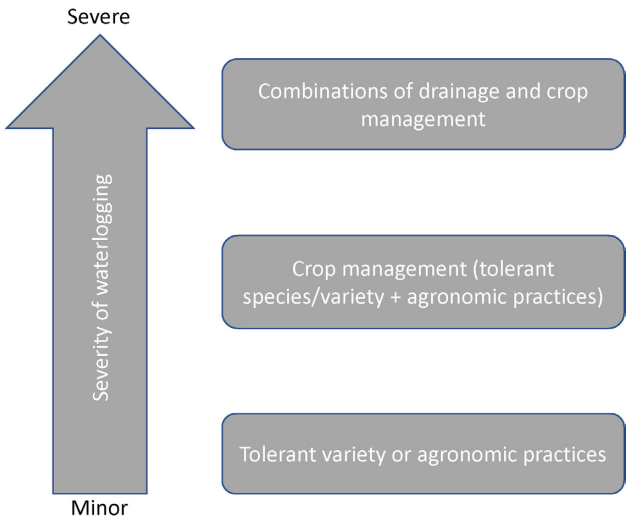

FIGURE 10 | Recommendation of soil and crop management based on different waterlogging severity.

et al., 2017, 2018). During waterlogging conditions, an inverse link between ethylene production and cotton yield has also been found, therefore the application of AVG can regulate ethylene production and increase both photosynthesis and fruit retention of cotton (Bange et al., 2010; Najeeb et al., 2017). Likewise, the positive effect of 1-MCP has been studied on hypoxia cotton plants, where it also blocked ethylene action and enhanced physiological processes, such as antioxidant enzyme activity and stomatal resistance (Kawakami et al., 2010). Utilizing an ethylene-insensitive cotton mutant (eliminating ethylene sensitivity) may be another option for waterlogged areas, where the mutant plant showed a remarkably improved yield of cotton (Najeeb et al., 2017). There is further research required to fully understand the ethylene mediated pathways in other crops such as grains.

Pretreatment With Hydrogen Peroxide

Pretreatment of crops with an agent may be an effective way to increase tolerance to different stresses (Jisha et al., 2013). For example, pretreatment with H_2O_2 can protect crops from oxidative damage caused by waterlogging, high light intensity, low temperature, salt stress, drought and exposure to heavy metals (Gechev et al., 2002; Ishibashi et al., 2011; Rajaeian and Ehsanpour, 2015; Savvides et al., 2016; Andrade et al., 2018). Priming seeds with H_2O_2 generated seedlings exhibiting elevated activity of antioxidant enzymes, low H_2O_2 and $O_2^{-\cdot}$ content, and low cell membrane damage under waterlogged conditions (Andrade et al., 2018). H_2O_2 pre-treatment also resulted in increases in net photosynthetic rate and photosynthetic pigments, root volume, high biomass accumulation, and stem diameter (Andrade et al., 2018). Despite much research being conducted on priming with agents against biotic and abiotic stresses (Mustafa et al., 2017; Ashraf et al., 2018; Lal et al., 2018), pre-treatment with H_2O_2 tolerant to waterlogging still in its infancy.

Use of Tolerant Species and Varieties

One of the key economical approaches for reducing the loss caused by waterlogging is to introduce waterlogging tolerance into existing plant varieties (Zhou, 2010; Tewari and Mishra, 2018; Wani et al., 2018). Genetic differences exist for tolerance to waterlogging in different crops (Setter and Waters, 2003) which include barley (Takeda and Fukuyama, 1986; Qiu, 1991; Pang et al., 2004; Xiao et al., 2007; Zhou et al., 2007; Huang et al., 2015; Zhang et al., 2015; Romina et al., 2018) and wheat (Davies and Hillman, 1988; Gardner and Flood, 1993; Huang et al., 1994; Herzog et al., 2016; Nguyen T.N. et al., 2018; Wu X. et al., 2018). However, waterlogging tolerance is a complex trait which is controlled by many different mechanisms, such as aerenchyma formation in roots (Zhang et al., 2015; Luan et al., 2018; Pujol and Wissuwa, 2018) under waterlogging stress, tolerance to secondary metabolites (Pang et al., 2006), ion toxicities (Huang et al., 2018), the maintenance of membrane potential (Gill et al., 2018) and control of ROS production under stress, with many QTL being reported to control these traits (Li et al., 2008; Zhou, 2011; Zhang et al., 2017; Huang et al., 2018; Gill et al., 2018). The success of a breeding program relies on the discovery of genes and linked markers to various tolerance mechanisms, which enable breeders to pyramid tolerance genes.

SUMMARY AND RECOMMENDATIONS

Many soil and crop management practices have been employed to alleviate waterlogging in crop production systems as summarized in **Table 1**. For severe waterlogging, combinations of drainage and crop management will be the foremost step (**Figure 10**). For minor waterlogging, choosing tolerant varieties or applying appropriate agronomic practices can be effective.

There are still significant knowledge gaps in our understanding of the advantages or disadvantages of relevant management measures under different soil types or different crops, management of other macro- and micronutrients; and the genetic basis of plants' adaptation to hypoxia and elemental toxicities in waterlogged soils. While many tolerance mechanisms and related quantitative trait loci (QTL) have been reported, most of them are focused around oxygen availability and largely ignore other constraints imposed by waterlogged soils.

For improved mitigation strategies, further research should be focused on the following aspects:

- Comparison of the cost/benefit analyses of different drainage strategies;
- Understanding the mechanisms of nutrient loss during waterlogging and quantifying the benefits of nutrient application;
- Increasing soil profile de-watering through soil improvement and agronomic strategies;

- Increased specificity of the interaction between different management practices and environment (soil types, severity of waterlogging, etc.) as well as among management practices.
- Discovering new (non-oxygen-associated) QTLs; the effectiveness of these mechanisms/QTL (and combined) on improving waterlogging tolerance in paddocks with soils with multiple constraints; the effect of these QTL on other agronomic, yield and quality traits, as well as management packages for varieties with diverse waterlogging tolerance genes.

AUTHOR CONTRIBUTIONS

SM and GP prepared the draft. GD supervised the project. GP, GD, BF, SS, and MZ reviewed and revised the manuscript.

FUNDING

This project was supported by the Grains Research and Development Corporation (GRDC) grant to GD, MZ, GP, and BF.

REFERENCES

Acuña, T. B., Dean, G., and Riffkin, P. (2011). Constraints to achieving high potential yield of wheat in a temperate, high-rainfall environment in south-eastern Australia. *Crop Pasture Sci.* 62, 125–136. doi: 10.1071/CP10271

Aldana, F., García, P. N., and Fischer, G. (2014). Effect of waterlogging stress on the growth, development and symptomatology of cape gooseberry (*Physalis peruviana* L.) plants. *Rev. Acad. Colomb. Cienc. Exactas Fís. Nat.* 38, 393–400. doi: 10.18257/raccefyn.114

Ali, N., Dayal, A., Thomas, N., Lal, G., and Gupta, J. (2018). Effect of different sowing time on seed vigour parameters of wheat (*Triticum aestivum* L.) varieties. *Int. J. Pure Appl. Biosci.* 6, 1532–1538. doi: 10.18782/2320-7051.6627

Allen, D. E., Kingston, G., Rennenberg, H., Dalal, R. C., and Schmidt, S. (2010). Effect of nitrogen fertilizer management and waterlogging on nitrous oxide emission from subtropical sugarcane soils. *Agric. Ecosyst. Environ.* 136, 209–217. doi: 10.1016/j.agee.2009.11.002

Alwang, J., Sabry, S., Shideed, K., Swelam, A., and Halila, H. (2018). Economic and food security benefits associated with raised-bed wheat production in Egypt. *Food Sec.* 10, 589–601. doi: 10.1007/s12571-018-0794-3

Amare, T., Terefe, A., Selassie, Y. G., Yitaferu, B., Wolfgramm, B., and Hurni, H. (2013). Soil properties and crop yields along the terraces and toposequece of Anjeni Watershed, Central Highlands of Ethiopia. *J. Agric. Sci.* 5:134.

Andrade, C. A., de Souza, K. R. D., de Oliveira Santos, M., da Silva, D. M., and Alves, J. D. (2018). Hydrogen peroxide promotes the tolerance of soybeans to waterlogging. *Sci. Hortic.* 232, 40–45. doi: 10.1016/j.scienta.2017.12.048

Arbona, V., López-Climent, M. F., Pérez-Clemente, R. M., and Gómez-Cadenas, A. (2009). Maintenance of a high photosynthetic performance is linked to flooding tolerance in citrus. *Environ. Exp. Bot.* 66, 135–142. doi: 10.1016/j.envexpbot.2008.12.011

Armstrong, R., Eagle, C., and Flood, R. (2015). Improving grain yields on a sodic clay soil in a temperate, medium-rainfall cropping environment. *Crop Pasture Sci.* 66, 492–505. doi: 10.1071/CP14210

Armstrong, R., Sale, P., Tavakkoli, E., Wilhelm, N., Davenport, D., Dean, G., et al. (2017). "Can subsoil amelioration improve the productivity of grain production in medium-high rainfall environments?," in *Proceedings of the 18th Australian Agronomy Conference 2017*, (Ballarat: Australian Society of Agronomy Inc), 24–28.

Armstrong, W. (1980). *Aeration in Higher Plants Advances in Botanical Research*. New York, NY: Elsevier, 225–332.

Armstrong, W., Justin, S., Beckett, P., and Lythe, S. (1991). Root adaptation to soil waterlogging. *Aquat. Bot.* 39, 57–73. doi: 10.1016/0304-3770(91)90022-W

Ashraf, M., and Arfan, M. (2005). Gas exchange characteristics and water relations in two cultivars of Hibiscus esculentus under waterlogging. *Biol. Plant.* 49, 459–462. doi: 10.1007/s10535-005-0029-2

Ashraf, M. A., Ahmad, M. S. A., Ashraf, M., Al-Qurainy, F., and Ashraf, M. Y. (2011). Alleviation of waterlogging stress in upland cotton (*Gossypium hirsutum* L.) by exogenous application of potassium in soil and as a foliar spray. *Crop Pasture Sci.* 62, 25–38. doi: 10.1071/CP09225

Ashraf, M. A., Akbar, A., Askari, S. H., Iqbal, M., Rasheed, R., and Hussain, I. (2018). "Recent advances in abiotic stress tolerance of plants through chemical priming: An overview," in *Advances in Seed Priming*, eds A. Rakshit and H. Bahadur Singh (Singapore: Springer), 51–79. doi: 10.1007/978-981-13-0032-5_4

Ayars, J. E., and Evans, R. G. (2015). Subsurface drainage—What's next? *Irrigation Drainage* 64, 378–392. doi: 10.1002/ird.1893

Azhar, A., Makihara, D., Naito, H., and Ehara, H. (2018). Evaluating sago palm (Metroxylon sagu Rottb.) photosynthetic performance in waterlogged conditions: utilizing pulse-amplitude-modulated (PAM) fluorometry as a waterlogging stress indicator. *J. Saudi Soc. Agric. Sci.* (in press). doi: 10.1016/j.jssas.2018.05.004

Bai, T., Li, C., Li, C., Liang, D., and Ma, F. (2013). Contrasting hypoxia tolerance and adaptation in Malus species is linked to differences in stomatal behavior and photosynthesis. *Physiol. Plant.* 147, 514–523. doi: 10.1111/j.1399-3054.2012.01683.x

Bailey-Serres, J., and Voesenek, L. (2008). Flooding stress: acclimations and genetic diversity. *Annu. Rev. Plant Biol.* 59, 313–339. doi: 10.1146/annurev.arplant.59.032607.092752

Bakker, D., Hamilton, G., Houlbrooke, D., and Spann, C. (2005a). The effect of raised beds on soil structure, waterlogging, and productivity on duplex soils in Western Australia. *Soil Res.* 43, 575–585. doi: 10.1071/SR03118

Bakker, D., Houlbrooke, D., Hamilton, G., and Spann, C. (2005b). *A Manual for Raised Bed Farming in Western Australia*. Perth: Department of Agriculture and Food.

Bakker, D., Hamilton, G., Houlbrooke, D., Spann, C., and Van Burgel, A. (2007). Productivity of crops grown on raised beds on duplex soils prone to waterlogging in Western Australia. *Aust. J. Exp. Agric.* 47, 1368–1376. doi: 10.1071/EA06273

Bange, M., Milroy, S., Ellis, M., and Thongbai, P. (2010). "Opportunities to reduce the impact of water-logging on cotton," in *Proceedings of the 15 Agronomy Conference*, Lincoln.

Bange, M., Milroy, S., and Thongbai, P. (2004). Growth and yield of cotton in response to waterlogging. *Field Crops Res.* 88, 129–142. doi: 10.1093/pcp/pcp163

Banik, M., Sarkar, A., Ghatak, P., Ray, R., and Patra, S. (2018). Reclamation of waterlogged lowland in indo-gangetic alluvial plains using some biodrainage species. *Int. J. Curr. Microbiol. Appl. Sci.* 7, 1028–1038. doi: 10.20546/ijcmas.2018.702.127

Barrett-Lennard, E. (2003). The interaction between waterlogging and salinity in higher plants: causes, consequences and implications. *Plant Soil* 253, 35–54. doi: 10.1023/A:1024574622669

Bassu, S., Asseng, S., Motzo, R., and Giunta, F. (2009). Optimising sowing date of durum wheat in a variable mediterranean environment. *Field Crops Res.* 111, 109–118. doi: 10.1016/j.fcr.2008.11.002

Bastick, C., and Walker, M. (2000). *Extent and Impacts of Dryland Salinity in Tasmania*. Canberra: National Land and Water Resources Audit Dryland Salinity Project Report.

Belford, R., Dracup, M., and Tennant, D. (1992). Limitations to growth and yield of cereal and lupin crops on duplex soils. *Aust. J. Exp. Agric.* 32, 929–945. doi: 10.1071/EA9920929

Belmonte, S. A., Luisella, C., Stahel, R. J., Bonifacio, E., Novello, V., Zanini, E., et al. (2018). Effect of long-term soil management on the mutual interaction among soil organic matter, microbial activity and aggregate stability in a vineyard. *Pedosphere* 28, 288–298. doi: 10.1016/S1002-0160(18)60015-3

Bennett, J. M., Roberton, S. D., Marchuk, S., Woodhouse, N. P., Antille, D. L., Jensen, T. A., et al. (2019). The soil structural cost of traffic from heavy machinery in Vertisols. *Soil Till. Res.* 185, 85-93. doi: 10.1016/j.still.2018.09.007

Blann, K. L., Anderson, J. L., Sands, G. R., and Vondracek, B. (2009). Effects of agricultural drainage on aquatic ecosystems: a review. *Crit. Rev. Environ. Sci. Technol.* 39, 909–1001. doi: 10.1080/10643380801977966

Blokhina, O., Virolainen, E., and Fagerstedt, K. V. (2003). Antioxidants, oxidative damage and oxygen deprivation stress: a review. *Ann. Bot.* 91, 179–194. doi: 10.1093/aob/mcf118

Bochtis, D., and Vougioukas, S. (2008). Minimising the non-working distance travelled by machines operating in a headland field pattern. *Biosyst. Eng.* 101, 1–12. doi: 10.1016/j.biosystemseng.2008.06.008

Bogunovic, I., Bilandzija, D., Andabaka, Z., Stupic, D., Comino, J. R., Cacic, M., et al. (2017). Soil compaction under different management practices in a Croatian vineyard. *Arab. J. Geosci.* 10:340. doi: 10.1007/s12517-017-3105-y

Borin, M., Passoni, M., Thiene, M., and Tempesta, T. (2010). Multiple functions of buffer strips in farming areas. *Eur. J. Agron.* 32, 103–111. doi: 10.1007/s00267-011-9696-2

Boru, G., Vantoai, T., Alves, J., Hua, D., and Knee, M. (2003). Responses of soybean to oxygen deficiency and elevated root-zone carbon dioxide concentration. *Ann. Bot.* 91, 447–453. doi: 10.1093/aob/mcg040

Bos, M. G. and Boers, T. M. (1994). "Land drainage: why and how?" In *Drainage Principles and Applications*, ed. H.P. Ritzema (Wageningen: International Institute for Land Reclamation & Improvement), 23–32.

Brady, N., and Weil, R. (2008). *Soil Colloids: Seat of Soil Chemical And Physical Acidity*. Upper Saddle River, NJ: Pearson Education Inc.

Brito, G. G. D., Ferreira, A. C. D. B., Borin, A. L. D. C., and Morello, C. D. L. (2013). 1-Methylcyclopropene and Aminoethoxyvinylglycine effects on yield components of field-grown cotton. *Ciênc. Agrotecnol.* 37, 9–16. doi: 10.1590/S1413-70542013000100001

Bullock, A., and Acreman, M. (2003). The role of wetlands in the hydrological cycle. *Hydrol. Earth Syst. Sci. Discuss.* 7, 358–389. doi: 10.5194/hess-7-358-2003

Cannarozzi, G., Weichert, A., Schnell, M., Ruiz, C., Bossard, S., Blösch, R., et al. (2018). Waterlogging affects plant morphology and the expression of key genes in tef (Eragrostis tef). *Plant Direct* 2:e00056. doi: 10.1002/pld3.56

Cannell, R., and Jackson, M. B. (1981). *Alleviating Aeration Stresses [Soil, Plant Growth and Crop Production]. Modifying the Root Environment to Reduce Crop Stress*, eds G. F. Arkin and H. M. Taylor (St. Joseph, MI: American Society of Agricultural Engineers).

Cannell, R. Q., Belford, R. K., Gales, K., Dennis, C. W., and Prew, R. D. (1980). Effects of waterlogging at different stages of development on the growth and yield of winter wheat. *J. Sci. Food Agric.* 31, 117–132. doi: 10.1002/jsfa.2740310203

Castanheira, P. J., and Serralheiro, R. P. (2010). Impact of mole drains on salinity of a vertisoil under irrigation. *Biosyst. Eng.* 105, 25–33. doi: 10.1016/j.biosystemseng.2009.08.010

Celestina, C., Midwood, J., Sherriff, S., Trengove, S., Hunt, J., Tang, C., et al. (2018). Crop yield responses to surface and subsoil applications of poultry litter and inorganic fertiliser in south-eastern Australia. *Crop Pasture Sci.* 69, 303–316. doi: 10.1071/CP17439

Chamen, T. (2015). Controlled traffic farming–from worldwide research to adoption in Europe and its future prospects. *Acta Technol. Agric.* 18, 64–73. doi: 10.1515/ata-2015-0014

Chamen, T., Cottage, C. C., and Maulden, B. (2006). *'Controlled Traffic' Farming: Literature Review and Appraisal of Potential Use in the UK, HGCA Research Review No. 59*. Maulden: The Home-Grown Cereals Authority.

Chamizo, S., Cantón, Y., Rodríguez-Caballero, E., and Domingo, F. (2016). Biocrusts positively affect the soil water balance in semiarid ecosystems. *Ecohydrology* 9, 1208–1221. doi: 10.1002/eco.1719

Chandio, A. S., Lee, T. S., and Mirjat, M. S. (2013). Simulation of horizontal and vertical drainage systems to combat waterlogging problems along the Rohri Canal in Khairpur District, Pakistan. *J. Irrigation Drainage Eng.* 139, 710–717. doi: 10.1061/(ASCE)IR.1943-4774.0000590

Chen, H., Wu, W., Liu, X., and Li, H. (2010). Effect of wheel traffic on working resistance of agricultural machinery in field operation. *Trans. Chin. Soc. Agric. Machinery* 41, 52–98.

Childs, E. (1943). Studies in mole-draining Interim report on an experimental drainage field. *J. Agric. Sci.* 33, 136–146. doi: 10.1017/S002185960000650X

Christen, E., and Skehan, D. (2001). Design and management of subsurface horizontal drainage to reduce salt loads. *J. Irrigation Drainage Eng.* 127, 148–155. doi: 10.1061/(ASCE)0733-9437(2001)127:3(148)

Christen, E. W., Ayars, J. E., and Hornbuckle, J. W. (2001). Subsurface drainage design and management in irrigated areas of Australia. *Irrigation Sci.* 21, 35–43.

Christianson, J. A., Llewellyn, D. J., Dennis, E. S., and Wilson, I. W. (2010). Comparisons of early transcriptome responses to low-oxygen environments in three dicotyledonous plant species. *Plant Signal. Behav.* 5, 1006–1009. doi: 10.1093/pcp/pcp163

Christy, B., Clough, A., Riffkin, P., Norton, R., Midwood, J., and O'Leary, G. (2015). *Managing Crop Inputs in a High Yield Potential Environment-Hrz of Southern Australia*. Melbourne: Department of Economic Development, Jobs, Transport & Resources (DEDJTR).

Chu, X., Han, G., Xing, Q., Xia, J., Sun, B., Yu, J., et al. (2018). Dual effect of precipitation redistribution on net ecosystem CO2 exchange of a coastal wetland in the Yellow River Delta. *Agric. For. Meteorol.* 249, 286–296. doi: 10.1016/j.agrformet.2017.11.002

Cocks, P. (2001). Ecology of herbaceous perennial legumes: a review of characteristics that may provide management options for the control of salinity and waterlogging in dryland cropping systems. *Aust. J. Agricu. Res.* 52, 137–151. doi: 10.1071/AR99170

Collaku, A., and Harrison, S. (2005). Heritability of waterlogging tolerance in wheat. *Crop Sci.* 45, 722–727. doi: 10.2135/cropsci2005.0722

Collis, C. (2015). *Raised Beds Exemplify on-Farm Adaptation. GRDC GroundCover™* . Available at: https://grdc.com.au/resources-and-publications/groundcover/ground-cover-issue-117-july-august-2015/raised-beds-exemplify-on-farm-adaptation

Colmer, T. D., and Greenway, H. (2011). Ion transport in seminal and adventitious roots of cereals during O2 deficiency. *J. Exp. Bot.* 62, 39–57. doi: 10.1093/jxb/erq271

Cong, Y., Li, Y. J., Zhou, C. J., Zou, C. S., Zhang, X. K., Liao, X., et al. (2009). Effect of application of nitrogen, phosphorus and potassium fertilizers on yield in rapeseed (*Brassica napus* L.) under the waterlogging stress. *Plant Nutr. Fertilizer Sci.* 15, 1122–1129.

Coutinho, I. D., Henning, L. M. M., Döpp, S. A., Nepomuceno, A., Moraes, L. A. C., Marcolino-Gomes, J., et al. (2018). Flooded soybean metabolomic analysis reveals important primary and secondary metabolites involved in the hypoxia stress response and tolerance. *Environ. Exp. Bot.* 153, 176–187. doi: 10.1016/j.envexpbot.2018.05.018

Cox, J., and McFarlane, D. (1995). The causes of waterlogging in shallow soils and their drainage in southwestern Australia. *J. Hydrol.* 167, 175–194. doi: 10.1016/0022-1694(94)02614-H

Cox, J., McFarlane, D., and Skaggs, R. (1994). Field-evaluation of DRAINMOD for predicting waterlogging intensity and drain performance in south-western Australia. *Soil Res.* 32, 653–671. doi: 10.1071/SR9940653

Cox, S. A., Sutton, R. P., Stoltz, R. P., and Knobloch, T. S. (2005). "Determination of effective drainage area for tight gas wells," in *Paper Presented at the SPE Eastern Regional Meeting*, (Houston,TX: Society of Petroleum Engineers). doi: 10.2118/98035-MS

Crabtree, W. L. (1989). Cereal grain yield responses to deep ripping on duplex soils. *Aust. J. Exp. Agric.* 29, 691–694. doi: 10.1071/EA9890691

Crawford, R. (1982). "Physiological responses to flooding," in *Physiological Plant Ecology II*, eds O. L. Lange, P. S. Nobel, C. B. Osmond, and H. Ziegler (Berlin: Springer), 453–477.

da Ponte, N. H. T., Nunes Santos, R. I., Lima Lopes, Filho, W. R., Lisboa Cunha, R., Murad Magalhães, M., et al. (2019). Morphological assessments evidence that higher number of pneumatophores improves tolerance to long-term waterlogging in oil palm (*Elaeis guineensis*) seedlings. *Flora* 250, 52–58. doi: 10.1016/j.flora.2018.11.017

Dash, C., Sarangi, A., Singh, A., and Dahiya, S. (2005). Bio-drainage: an alternate drainage technique to control waterlogging and salinity. *J. Soil Water Conserv. India* 4, 149–155.

Davies, M., and Hillman, G. (1988). Effects of soil flooding on growth and grain yield of populations of tetraploid and hexaploid species of wheat. *Ann. Bot.* 62, 597–604. doi: 10.1093/oxfordjournals.aob.a087699

Davies, S., Blackwell, P., Bakker, D., Scanlon, C., Roper, M., and Ward, P. (2012). "Developing and assessing agronomic strategies for water repellent soils," in *Crop Updates*, (Perth: GRDC/DAFWA), 71–77.

de San Celedonio, R. P., Abeledo, L. G., Brihet, J., and Miralles, D. J. (2016). Waterlogging affects leaf and tillering dynamics in wheat and barley. *J. Agron. Crop Sci.* 202, 409–420. doi: 10.1111/jac.12151

Dhakad, S., Ambawatia, G., Verma, G., Patel, S., Rao, K. R., and Verma, S. (2018). Performance of Mole drain system for soybean (glycine max)-wheat (*Triticum aestivum*) cropping system of madhya pradesh. *Int. J. Curr. Microbiol. Appl. Sci.* 7, 2107–2112. doi: 10.20546/ijcmas.2018.702.251

Dinnes, D. L., Karlen, D. L., Jaynes, D. B., Kaspar, T. C., Hatfield, J. L., Colvin, T. S., et al. (2002). Nitrogen management strategies to reduce nitrate leaching in tile-drained Midwestern soils. *Agron. J.* 94, 153–171. doi: 10.2134/agronj2002.1530

Donnan, W. W. (1947). Model tests of a tile-spacing formula 1. *Soil Sci. Soc. Am. J.* 11, 131–136. doi: 10.2136/sssaj1947.036159950011000C0025x

Dore, M. H. (2005). Climate change and changes in global precipitation patterns: what do we know? *Environ. Int.* 31, 1167–1181. doi: 10.1016/j.envint.2005.03.004

Drew, M., and Lynch, J. M. (1980). Soil anaerobiosis, microorganisms, and root function. *Ann. Rev. Phytopathol.* 18, 37–66. doi: 10.1146/annurev.py.18.090180.000345

Drew, M., and Sisworo, E. (1977). Early effects of flooding on nitrogen deficiency and leaf chlorosis in barley. *New Phytol.* 79, 567–571. doi: 10.1111/j.1469-8137.1977.tb02241.x

Drew, M., Sisworo, E., and Saker, L. (1979). Alleviation of waterlogging damage to young barley plants by application of nitrate and a synthetic cytokinin, and comparison between the effects of waterlogging, nitrogen deficiency and root excision. *New Phytol.* 82, 315–329. doi: 10.1111/j.1469-8137.1979.tb02657.x

Elbert, W., Weber, B., Burrows, S., Steinkamp, J., Büdel, B., Andreae, M. O., et al. (2012). Contribution of cryptogamic covers to the global cycles of carbon and nitrogen. *Nat. Geosci.* 5:459. doi: 10.1038/ngeo1486

Ernst, W. (1990). Ecophysiology of plants in waterlogged and flooded environments. *Aquat. Bot.* 38, 73–90. doi: 10.1016/0304-3770(90)90099-7

Evans, R. O., and Fausey, N. R. (1999). Effects of inadequate drainage on crop growth and yield. *Agric. Drainage* 38, 13–54.

Feng, P., Wang, B., Liu, D. L., Xing, H., Ji, F., Macadam, I., et al. (2018). Impacts of rainfall extremes on wheat yield in semi-arid cropping systems in eastern Australia. *Clim. Change* 147, 555–569. doi: 10.1007/s10584-018-2170-x

Ferronato, C., Marinari, S., Francioso, O., Bello, D., Trasar-Cepeda, C., and Antisari, L. V. (2019). Effect of waterlogging on soil biochemical properties and organic matter quality in different salt marsh systems. *Geoderma* 338, 302–312. doi: 10.1016/j.geoderma.2018.12.019

Filipović, V., Mallmann, F. J. K., Coquet, Y., and Šimùnek, J. (2014). Numerical simulation of water flow in tile and mole drainage systems. *Agric. Water Manag.* 146, 105–114. doi: 10.1016/j.agwat.2014.07.020

Flowers, M., and Lal, R. (1998). Axle load and tillage effects on soil physical properties and soybean grain yield on a mollic ochraqualf in northwest Ohio. *Soil Tillage Res.* 48, 21–35. doi: 10.1016/S0167-1987(98)00095-6

Folzer, H., Dat, J. F., Capelli, N., Rieffel, D., and Badot, P.-M. (2006). Response of sessile oak seedlings (*Quercus petraea*) to flooding: an integrated study. *Tree Physiol.* 26, 759–766. doi: 10.1093/treephys/26.6.759

Food and Agriculture Organization [FAO] (2002). *Food and Agriculture Organization of the United Nations*. Available at: http://www.fao.org/3/a-bc600e.pdf

Food and Agriculture Organization [FAO] (2015). *Food and Agriculture Organization of the United Nations*. Available at: http://www.fao.org/3/a-bc600e.pdf

Frank, M. (2010). *Managing wet Soils – Mole Drainage (AG0949)*. Orange: Department of Primary Industries.

Gajri, P. R., Arora, V. K., and Chaudhary, M. R. (1994). Maize growth responses to deep tillage, straw mulching and farmyard manure in coarse textured soils of N.W. India. *Soil Use Manage.* 10, 15–19. doi: 10.1111/j.1475-2743.1994.tb00451.x

Gardner, B., Nielsen, D., and Shock, C. (1992). Infrared thermometry and the crop water stress index. I. History, theory, and baselines. *J. Prod. Agric.* 5, 462–466. doi: 10.2134/jpa1992.0462

Gardner, W., and Flood, R. (1993). Less waterlogging damage with long season wheats. *Cereal Res. Commun.* 21, 337–343.

Gasso, V., Oudshoorn, F. W., Sørensen, C. A., and Pedersen, H. H. (2014). An environmental life cycle assessment of controlled traffic farming. *J. Cleaner Prod.* 73, 175–182. doi: 10.1016/j.jclepro.2013.10.044

Gasso, V., Sørensen, C. A., Oudshoorn, F. W., and Green, O. (2013). Controlled traffic farming: A review of the environmental impacts. *Eur. J. Agron.* 48, 66–73. doi: 10.1111/j.1467-789X.2007.00432.x

Gechev, T., Gadjev, I., Van Breusegem, F., Inzé, D., Dukiandjiev, S., Toneva, V., et al. (2002). Hydrogen peroxide protects tobacco from oxidative stress by inducing a set of antioxidant enzymes. *Cell. Mol. Life Sci.* 59, 708–714. doi: 10.1007/s00018-002-8459-x

Geigenberger, P. (2003). Response of plant metabolism to too little oxygen. *Curr. Opin. Plant Biol.* 6, 247–256. doi: 10.1016/S1369-5266(03)00038-4

Ghazouani, W., Molle, F., Swelam, A., Rap, E., and Abdo, A. (2015). *Understanding Farmers' Adaptation to Water Scarcity: A Case Study from the Western Nile Delta*. Pelawatte: IWMI.

Gibson, G. (2014). *Utilising Innovative Management Techniques to Reduce Waterlogging*. Moama, NSW: Nuffield Australia Farming Scholars.

Gill, J., Clark, G., Sale, P., Peries, R., and Tang, C. (2012). Deep placement of organic amendments in dense sodic subsoil increases summer fallow efficiency and the use of deep soil water by crops. *Plant Soil* 359, 57–69. doi: 10.1007/s11104-012-1126-6

Gill, J., Sale, P., Peries, R., and Tang, C. (2009). Changes in soil physical properties and crop root growth in dense sodic subsoil following incorporation of organic amendments. *Field Crops Res.* 114, 137–146. doi: 10.1016/j.fcr.2009.07.018

Gill, M. B., Zeng, F., Shabala, L., Böhm, J., Zhang, G., Zhou, M., et al. (2018). The ability to regulate voltage-gated K+-permeable channels in the mature root epidermis is essential for waterlogging tolerance in barley. *J. Exp. Bot.* 69, 667–680. doi: 10.1093/jxb/erx429

Glinski, J. (2018). *Soil Physical Conditions and Plant Roots*. Boca Raton, FL: CRC press. doi: 10.1201/9781351076708

Grains Research, and Development Corporation [GRDC] (2016). *Understanding the Amelioration Processes of the Subsoil Application of Amendments in the Southern Region. Scoping Review for Project dav*00149. Sri Lanka: GRDC.

Gramlich, A., Stoll, S., Stamm, C., Walter, T., and Prasuhn, V. (2018). Effects of artificial land drainage on hydrology, nutrient and pesticide fluxes from agricultural fields–A review. *Agric. Ecosyst. Environ.* 266, 84–99. doi: 10.1016/j.agee.2018.04.005

Greenway, H., Armstrong, W., and Colmer, T. D. (2006). Conditions leading to high CO2 (> 5 kPa) in waterlogged–flooded soils and possible effects on root growth and metabolism. *Ann. Bot.* 98, 9–32. doi: 10.1093/aob/mcl076

Guenette, K. G., and Hernandez-Ramirez, G. (2018). Tracking the influence of controlled traffic regimes on field scale soil variability and geospatial modeling techniques. *Geoderma* 328, 66–78. doi: 10.1016/j.geoderma.2018.04.026

Guo, W. Q., Chen, B. L., Liu, R. X., and Zhou, Z. G. (2010). Effects of nitrogen application rate on cotton leaf antioxidant enzyme activities and endogenous hormone contents under short-term waterlogging at flowering and boll-forming stage. *Yingyong Shengtai Xuebao* 21, 53–60.

Gupta, S. (1997). Himalayan drainage patterns and the origin of fluvial megafans in the Ganges foreland basin. *Geology* 25, 11–14. doi: 10.1130/0091-7613(1997)025<0011:HDPATO>2.3.CO;2

Gupta, S. (2002). A century of subsurface drainage research in India. *Irrigation Drainage Syst.* 16, 69–84. doi: 10.1023/A:1015525405522

Habibzadeh, F., Sorooshzadeh, A., Pirdashti, H., and Modarres-Sanavy, S. A. M. (2013). Alleviation of waterlogging damage by foliar application of nitrogen compounds and tricyclazole in canola. *Aust. J. Crop Sci.* 7, 401–406.

Habibzadeh, F., Sorooshzadeh, A., Pirdashti, H., and Sanavy, S. (2012). Effect of nitrogen compounds and tricyclazole on some biochemical and morphological characteristics of waterlogged-canola. *Int. Res. J. Appl. Basic Sci.* 3, 77–84.

Hallard, M., and Armstrong, A. (1992). Observations of water movement to and within mole drainage channels. *J. Agric. Eng. Res.* 52, 309–315. doi: 10.1016/0021-8634(92)80069-5

Hamilton, G., Bakker, D., Houlebrook, D., and Spann, C. (2000). Raised beds prevent waterlogging and increase productivity. *J. Dep. Agric. West. Aust. Ser.* 4, 3–9.

Hamza, M., and Anderson, W. (2003). Responses of soil properties and grain yields to deep ripping and gypsum application in a compacted loamy sand soil

contrasted with a sandy clay loam soil in Western Australia. *Aust. J. Agric. Res.* 54, 273–282. doi: 10.1071/AR02102

Hamza, M., and Anderson, W. (2005). Soil compaction in cropping systems: a review of the nature, causes and possible solutions. *Soil Tillage Res.* 82, 121–145. doi: 10.1016/j.still.2004.08.009

Henry, C. G., Sarzi Sartori, G. M., Gaspar, J. P., Marchesan, E., Hirsh, S. M., Horton, A. P., et al. (2018). Deep tillage and gypsum amendments on fully, deficit irrigated, and dryland soybean. *Agron. J.* 110, 737–748. doi: 10.2134/agronj2015.11.0567

Herzog, M., Striker, G. G., Colmer, T. D., and Pedersen, O. (2016). Mechanisms of waterlogging tolerance in wheat–a review of root and shoot physiology. *Plant Cell Environ.* 39, 1068–1086. doi: 10.1111/pce.12676

Heuperman, A. (2000). "Bio-drainage - an australian overview and two victorian case studies," in. *Proceedings of the Eighth ICID International Drainage Workshop Role of Drainage and Challenges in 21st century*, New Delhi, 1–16.

Heuperman, A., and Kapoor, A. (2003). *Biodrainage Status in India and Other countries*. New Delhi: Indian National Committee on Irrigation and Drainage, 147.

Hossain, M. A., and Uddin, S. N. (2011). Mechanisms of waterlogging tolerance in wheat: morphological and metabolic adaptations under hypoxia or anoxia. *Aust. J. Crop Sci.* 5, 1094–1101.

Huang, B., Johnson, J. W., Nesmith, S., and Bridges, D. C. (1994). Growth, physiological and anatomical responses of two wheat genotypes to waterlogging and nutrient supply. *J. Exp. Bot.* 45, 193–202. doi: 10.1093/jxb/45.2.193

Huang, X., Fan, Y., Shabala, L., Rengel, Z., Shabala, S., and Zhou, M. (2018). A major QTL controlling the tolerance to manganese toxicity in barley (*Hordeum vulgare* L.). *Mol. Breed.* 38:16.

Huang, X., Shabala, S., Shabala, L., Rengel, Z., Wu, X., Zhang, G., et al. (2015). Linking waterlogging tolerance with Mn2+ toxicity: a case study for barley. *Plant Biol.* 17, 26–33. doi: 10.1111/plb.12188

Hussain, I., Sohail, M., Tanveer, S. K., and Muneer, M. (2018). Impact of planting density and growth habit of genotypes on wheat yield under raised bed planting method. *Science* 37, 158–162.

Indraratna, B. (2017). "Recent advances in vertical drains and vacuum preloading for soft ground stabilisation," in, *Proceedings of 19th International Conference on Soil Mechanics and Geotechnical Engineering, Seou*, (London: International Society for Soil Mechanics and Geotechnical Engineering), 145–170.

Indraratna, B., Rujikiatkamjorn, C., and Sathananthan, I. (2005). Analytical and numerical solutions for a single vertical drain including the effects of vacuum preloading. *Can. Geotech. J.* 42, 994–1014. doi: 10.1139/t05-029

Intergovernmental Panel on Climate Change [IPCC] (2014). *Climate Change 2014: Synthesis Report. Contribution of working groups I, II and III to the Fifth Assessment Report of the Intergovernmental Panel on Climate Change*. Geneva: IPCC. doi: 10.1017/CBO9781107415416

Ishibashi, Y., Yamaguchi, H., Yuasa, T., Iwaya-Inoue, M., Arima, S., and Zheng, S.-H. (2011). Hydrogen peroxide spraying alleviates drought stress in soybean plants. *J. Plant Physiol.* 168, 1562–1567. doi: 10.1016/j.jplph.2011.02.003

Jackson, M., and Colmer, T. (2005). Response and adaptation by plants to flooding stress. *Ann. Bot.* 96, 501–505. doi: 10.1093/aob/mci205

Jackson, M., and Hall, K. (1987). Early stomatal closure in waterlogged pea plants is mediated by abscisic acid in the absence of foliar water deficits. *Plant Cell Environ.* 10, 121–130.

Jackson, M., and Ricard, B. (2003). *Physiology, Biochemistry and Molecular Biology of Plant Root Systems Subjected to Flooding of the Soil, in Root Ecology*. Berlin: Springer, 193–213. doi: 10.1007/978-3-662-09784-7_8

Jaiswal, A., and Srivastava, J. (2018). Changes in reactive oxygen scavenging systems and protein profiles in maize roots in response to nitric oxide under waterlogging stress. *Indian J. Biochem. Biophys.* 55, 26–33.

Jisha, K., Vijayakumari, K., and Puthur, J. T. (2013). Seed priming for abiotic stress tolerance: an overview. *Acta Physiol. Plant.* 35, 1381–1396. doi: 10.1007/s11738-012-1186-5

Jones, H. E., and Etherington, J. (1970). Comparative studies of plant growth and distribution in relation to waterlogging: I. The survival of Erica cinerea L. and E. tetralix L. and its apparent relationship to iron and manganese uptake in waterlogged soil. *J. Ecol.* 58, 487–496. doi: 10.2307/2258285

Kapoor, A. (2000). "Bio-drainage feasibility and principles of planning and design," in *Proceedings of the Eighth ICID International Drainage Workshop*, (New Delhi: International Commission on Irrigation and Drainage), 17–32.

Kaur, G., Nelson, K., and Motavalli, P. (2018). Early-season soil waterlogging and N fertilizer sources impacts on corn N uptake and apparent N recovery efficiency. *Agronomy* 8:102. doi: 10.3390/agronomy8070102

Kaur, G., Zurweller, B. A., Nelson, K. A., Motavalli, P. P., and Dudenhoeffer, C. J. (2017). Soil waterlogging and nitrogen fertilizer management effects on corn and soybean yields. *Agron. J.* 109, 97–106. doi: 10.2134/agronj2016.07.0411

Kavian, A., Saleh, I., Habibnejad, M., and Jafarian, Z. (2018). Application of vegetative buffer strips under natural rainfall to conserve soil and water. *Agriculture* 64, 17–27.

Kawakami, E. M., Oosterhuis, D. M., and Snider, J. L. (2010). Physiological effects of 1-methylcyclopropene on well-watered and water-stressed cotton plants. *J. Plant Growth Regul.* 29, 280–288. doi: 10.1007/s00344-009-9134-3

Kazmi, S. I., Ertsen, M. W., and Asi, M. R. (2012). The impact of conjunctive use of canal and tube well water in Lagar irrigated area, Pakistan. *Phys. Chem. Earth Parts A B C* 47–48, 86–98. doi: 10.1016/j.pce.2012.01.001

Kijne, J. W. (2006). Abiotic stress and water scarcity: identifying and resolving conflicts from plant level to global level. *Field Crops Res.* 97, 3–18. doi: 10.1016/j.fcr.2005.08.011

Kim, Y., Seo, C.-W., Khan, A. L., Mun, B.-G., Shahzad, R., Ko, J.-W., et al. (2018). Ethylene mitigates waterlogging stress by regulating glutathione biosynthesis-related transcripts in soybeans. *bioRxiv* [Preprint]. doi: 10.1101/252312

King, K., Fausey, N., and Williams, M. (2014). Effect of subsurface drainage on streamflow in an agricultural headwater watershed. *J. Hydrol.* 519, 438–445. doi: 10.1016/j.jhydrol.2014.07.035

Kisaakye, E., Acuña, T. B., Johnson, P., and Shabala, S. (2017). "Improving wheat growth and nitrogen-use efficiency under waterlogged conditions," in *Proceedings of the 18th Australian Agronomy Conference*, Ballarat, 1–4.

Kisaakye, E., Botwright Acuna, T., Johnson, P., and Shabala, S. (2015). "Effect of water availability and nitrogen source on wheat growth and nitrogen-use efficiency," in *Proceedings of the 17th Australian Society of Agronomy Conference*, Hobart, 20–24.

Kolekar, O., Patil, S., and Rathod, S. (2014). Effects of different mole drain spacings on the yield of summer groundnut. *Int. J. Res. Eng. Technol.* 3, 2321–7308.

Konukcu, F., Gowing, J., and Rose, D. (2006). Dry drainage: a sustainable solution to waterlogging and salinity problems in irrigation areas? *Agric. Water Manag.* 83, 1–12. doi: 10.1016/j.agwat.2005.09.003

Kruseman, G. P., and Ridder, N. A. (1990). Analysis and evaluation of pumping test data. *Anal. Eval. Pumping Test Data.* 47:377.

Kuhwald, M., Blaschek, M., Brunotte, J., and Duttmann, R. (2017). Comparing soil physical properties from continuous conventional tillage with long-term reduced tillage affected by one-time inversion. *Soil Use Manag.* 33, 611–619. doi: 10.1111/sum.12372

Kumar, N. (2018). Effect of planting method on productivity and economics of sugarcane (Saccharum spp. hybrid complex) varieties under waterlogged condition. *Indian Soc. Agron.* 63, 95–99.

Laanbroek, H. (1990). Bacterial cycling of minerals that affect plant growth in waterlogged soils: a review. *Aquat. Bot.* 38, 109–125. doi: 10.1016/0304-3770(90)90101-P

Lal, S. K., Kumar, S., Sheri, V., Mehta, S., Varakumar, P., Ram, B., et al. (2018). "Seed priming: An emerging technology to impart abiotic stress tolerance in crop plants," in *Advances in Seed Priming*, eds A. Rakshit and H. Bahadur Singh (Singapore: Springer), 41–50. doi: 10.1007/978-981-13-0032-5_3

Lee, T., Jang, C., Kim, J., Seong, R., Kim, I., Kim, D., et al. (2007). Expressed sequence tags from wheat roots under hypoxia. *Russ. J. Plant Physiol.* 54, 659–668. doi: 10.1134/S1021443707050147

Lee, T. G., Jang, C. S., Kim, J. Y., Kim, D. S., Park, J. H., Kim, D. Y., et al. (2007). A Myb transcription factor (TaMyb1) from wheat roots is expressed during hypoxia: roles in response to the oxygen concentration in root environment and abiotic stresses. *Physiol. Plant.* 129, 375–385. doi: 10.1111/j.1399-3054.2006.00828.x

Lerch, R. N., Lin, C. H., Goyne, K. W., Kremer, R. J., and Anderson, S. H. (2017). Vegetative buffer strips for reducing herbicide transport in runoff: effects of buffer width, vegetation, and season. *J. Am. Water Resour. Assoc.* 53, 667–683. doi: 10.1111/1752-1688.12526

Leul, M., and Zhou, W. (1998). Alleviation of waterlogging damage in winter rape by application of uniconazole: effects on morphological characteristics, hormones and photosynthesis. *Field Crops Res.* 59, 121–127. doi: 10.1016/S0378-4290(98)00112-9

Leul, M., and Zhou, W. (1999). Alleviation of waterlogging damage in winter rape by uniconazole application: effects on enzyme activity, lipid peroxidation, and membrane integrity. *J. Plant Growth Regulation* 18, 9–14. doi: 10.1007/PL00007046

Li, H. B., Vaillancourt, R., Mendham, N., and Zhou, M. X. (2008). Comparative mapping of quantitative trait loci associated with waterlogging tolerance in barley (*Hordeum vulgare* L.). *BMC Genomics* 9:401. doi: 10.1186/1471-2164-9-401

Li, M.-F., Zhu, J.-Q., and Jiang, Z.-H. (2013). "Plant growth regulators and nutrition applied to cotton after waterlogging," in *Proceedings of the Intelligent System Design and Engineering Applications (ISDEA), Third International Conference on*, (Piscataway, NJ: IEEE), 1045–1048. doi: 10.1109/ISDEA.2012.246

Li, W., Mo, W., Ashraf, U., Li, G., Wen, T., Abrar, M., et al. (2018). Evaluation of physiological indices of waterlogging tolerance of different maize varieties in South China. *Appl. Ecol. Environ. Res.* 16, 2059–2072. doi: 10.15666/aeer/1602_20592072

Li, Y., Tullberg, J., and Freebairn, D. (2007). Wheel traffic and tillage effects on runoff and crop yield. *Soil Tillage Res.* 97, 282–292. doi: 10.1016/j.still.2005.10.001

Liao, M., Fillery, I. R., and Palta, J. A. (2004). Early vigorous growth is a major factor influencing nitrogen uptake in wheat. *Funct. Plant Biol.* 31, 121–129. doi: 10.1071/FP03060

Lin, C. H., Lerch, R. N., Goyne, K. W., and Garrett, H. E. (2011). Reducing herbicides and veterinary antibiotics losses from agroecoystems using vegetative buffers. *J. Environ. Qual.* 40, 791–799. doi: 10.2134/jeq2010.0141

Lin, K.-H. R., Tsou, C.-C., Hwang, S.-Y., Chen, L.-F. O., and Lo, H.-F. (2006). Paclobutrazol pre-treatment enhanced flooding tolerance of sweet potato. *J. Plant Physiol.* 163, 750–760. doi: 10.1016/j.jplph.2005.07.008

Linkemer, G., Board, J. E., and Musgrave, M. E. (1998). Waterlogging effects on growth and yield components in late-planted soybean. *Crop Sci.* 38, 1576–1584. doi: 10.2135/cropsci1998.0011183X003800060028x

Lone, A. A., Khan, M. H., Dar, Z. A., and Wani, S. H. (2018). Breeding strategies for improving growth and yield under waterlogging conditions in maize: a review. *Maydica* 61:11.

Lorimer, R. (2008). *The Adoption of GPS in Cropping Agriculture*. Cleveland, OH: GPS.

Luan, H., Guo, B., Pan, Y., Lv, C., Shen, H., and Xu, R. (2018). Morpho-anatomical and physiological responses to waterlogging stress in different barley (*Hordeum vulgare* L.) *genotypes*. *Plant Growth Regulation* 85, 399–409. doi: 10.1007/s10725-018-0401-9

Lubkowski, K., and Grzmil, B. (2007). Controlled release fertilizers. *Pol. J. Chem. Technol.* 9, 83–84. doi: 10.2478/v10026-007-0096-6

Ma, Y. L., Wang, H. F., Wang, P., Yu, C. G., Luo, S. Q., Zhang, Y. F., et al. (2018). Effects of cadmium stress on the antioxidant system and chlorophyll fluorescence characteristics of two Taxodium clones. *Plant Cell Rep.* 37, 1547–1555. doi: 10.1007/s00299-018-2327-0

MacEwan, R., Gardner, W., Ellington, A., Hopkins, D., and Bakker, A. (1992). Tile and mole drainage for control of waterlogging in duplex soils of south-eastern Australia. *Aust. J. Exp. Agric.* 32, 865–878. doi: 10.1071/EA9920865

Malano, H. M., and van Hofwegen, P. (2006). *Management of Irrigation and Drainage Systems*. London: CRC Press.

Malik, A. I., Colmer, T. D., Lambers, H., and Schortemeyer, M. (2001). Changes in physiological and morphological traits of roots and shoots of wheat in response to different depths of waterlogging. *Funct. Plant Biol.* 28, 1121–1131. doi: 10.1071/PP01089

Marashi, S. K. (2018). Evaluation of uptake rate and distribution of nutrient ions in wheat (*Triticum aestivum* L.) under waterlogging condition. *Plant Physiol.* 8, 2539–2547.

Masunaga, T., and Marques Fong, J. D. (2018). "Chapter 11 - strategies for increasing micronutrient availability in soil for plant uptake," in *Plant Micronutrient Use Efficiency*, eds M. A. Hossain, T. Kamiya, D. J. Burritt, L.-S. Phan Tran, and T. Fujiwara (Cambridge, MA: Academic Press), 195–208.

Matosic, S., Birkás, M., Vukadinovic, V., Kisic, I., and Bogunovic, I. (2018). Tillage, manure and gypsum use in reclamation of saline-sodic soils. *Agric. Conspectus Sci.* 83, 131–138.

McCaskill, M., and Kearney, G. (2016). Control of water leakage from below the root zone by summer-active pastures is associated with persistence, density and deep rootedness. *Crop Pasture Sci.* 67, 679–693. doi: 10.1071/CP15337

McDaniel, B. K., and Binder, B. M. (2012). Ethylene receptor1 (ETR1) is sufficient and has the predominant role in mediating inhibition of ethylene responses by silver in *Arabidopsis thaliana*. *J. Biol. Chem.* 112:383034.

McFarlane, D., and Cox, J. (1992). Management of excess water in duplex soils. *Aust. J. Exp. Agric.* 32, 857–864. doi: 10.1071/EA9920857

Miller, G., Shulaev, V., and Mittler, R. (2008). Reactive oxygen signaling and abiotic stress. *Physiol. Plant.* 133, 481–489. doi: 10.1111/j.1399-3054.2008.01090.x

Milroy, S. P., Bange, M. P., and Thongbai, P. (2009). Cotton leaf nutrient concentrations in response to waterlogging under field conditions. *Field Crops Res.* 113, 246–255. doi: 10.1016/j.fcr.2009.05.012

Misak, R., Baki, A. A., and El-Hakim, M. (1997). On the causes and control of the waterlogging phenomenon, Siwa Oasis, northern Western Desert, Egypt. *J. Arid Environ.* 37, 23–32. doi: 10.1006/jare.1997.0252

Monaghan, R., Paton, R., and Drewry, J. (2002). Nitrogen and phosphorus losses in mole and tile drainage from a cattle-grazed pasture in eastern Southland. *N. Zealand J. Agric. Res.* 45, 197–205. doi: 10.1080/00288233.2002.9513510

Monaghan, R., and Smith, L. (2004). Minimising surface water pollution resulting from farm-dairy effluent application to mole-pipe drained soils. II. The contribution of preferential flow of effluent to whole-farm pollutant losses in subsurface drainage from a West Otago dairy farm. *N. Zealand J. Agric. Res.* 47, 417–428. doi: 10.1080/00288233.2004.9513610

Mondal, T., Mitra, B., and Das, S. (2018). Precision nutrient management in wheat (*Triticum aestivum*) using Nutrient Expert®: Growth phenology, yield, nitrogen-use efficiency and profitability under eastern sub-Himalayan plains. *Indian J. Agron.* 63, 174–180.

Morales-Olmedo, M., Ortiz, M., and Sellés, G. (2015). Effects of transient soil waterlogging and its importance for rootstock selection. *Chilean J. Agric. Res.* 75, 45–56. doi: 10.4067/S0718-58392015000300006

Morard, P., and Silvestre, J. (1996). Plant injury due to oxygen deficiency in the root environment of soilless culture: a review. *Plant Soil* 184, 243–254. doi: 10.1007/BF00010453

Morling, R. (1982). *Pros and Cons of Controlled Traffic Farming. ASAE Paper 82-1043*. Washington, DC: ASAE.

Muirhead, W., Humphreys, E., Jayawardane, N., and Moll, J. (1996). Shallow subsurface drainage in an irrigated vertisol with a perched water table. *Agric. Water Manag.* 30, 261–282. doi: 10.1016/0378-3774(95)01225-7

Muñoz-Carpena, R., Fox, G. A., Ritter, A., Perez-Ovilla, O., and Rodea-Palomares, I. (2018). Effect of vegetative filter strip pesticide residue degradation assumptions for environmental exposure assessments. *Sci. Total Environ.* 619, 977–987. doi: 10.1016/j.scitotenv.2017.11.093

Muñoz-Carpena, R., Fox, G. A., and Sabbagh, G. J. (2010). Parameter importance and uncertainty in predicting runoff pesticide reduction with filter strips. *J. Environ. Qual.* 39, 630–641. doi: 10.2134/jeq2009.0300

Mustafa, H. S. B., Mahmood, T., Ullah, A., Sharif, A., Bhatti, A. N., Muhammad Nadeem, M., et al. (2017). Role of seed priming to enhance growth and development of crop plants against biotic and abiotic stresses. *Bull. Biol. Allied Sci. Res.* 2, 1–11.

Najeeb, U., Bange, M. P., Tan, D. K., and Atwell, B. J. (2015). Consequences of waterlogging in cotton and opportunities for mitigation of yield losses. *AoB Plants* 7:lv080. doi: 10.1093/aobpla/plv080

Najeeb, U., Tan, D., Bange, M., and Atwell, B. (2017). "Stress-induced fruit abscission in cotton and role of ethylene," in *Proceedings of the 18th Australian Agronomy Conference*, (Ballarat VIC: Australian Society of Agronomy), 1–4.

Najeeb, U., Tan, D. K., Bange, M. P., and Atwell, B. J. (2018). Protecting cotton crops under elevated CO2 from waterlogging by managing ethylene. *Funct. Plant Biol.* 45, 340–349. doi: 10.1071/FP17184

Negusse, T., Yazew, E., and Tadesse, N. (2013). Quantification of the impact of integrated soil and water conservation measures on groundwater availability in Mendae Catchment, Abraha We-Atsebaha, eastern Tigray, Ethiopia. *Momona Ethiopian J. Sci.* 5, 117–136.

Nguyen, H. C., Lin, K. H., Ho, S. L., Chiang, C. M., and Yang, C. M. (2018). Enhancing the abiotic stress tolerance of plants: From chemical treatment to

biotechnological approaches. *Physiol. plant.* 164, 452–466. doi: 10.1111/ppl.12812

Nguyen, L. T., Osanai, Y., Anderson, I. C., Bange, M. P., Tissue, D. T., and Singh, B. K. (2018). Flooding and prolonged drought have differential legacy impacts on soil nitrogen cycling, microbial communities and plant productivity. *Plant Soil* 431, 371–387. doi: 10.1007/s11104-018-3774-7

Nguyen, T. N., Tuan, P. A., Mukherjee, S., Son, S., and Ayele, B. T. (2018). Hormonal regulation in adventitious roots and during their emergence under waterlogged conditions in wheat. *J. Exp. Bot.* 69, 4065–4082. doi: 10.1093/jxb/ery190

Nichols, P. (2018). *Yanco Subterranean Clover*. Orange: Department of Primary Industries and Regional Development (DPIRD).

Nicholson, C. (2016). "Business case for investment in subsoil modification with organic material," in *Prepared for Southern Farming Systems, As Part of the National Landcare project, INNOV*-108, (St, Inverleigh VIC: Southern Farming Systems (SFS)).

Noreen, S., Fatima, Z., Ahmad, S., and Ashraf, M. (2018). *Foliar Application of Micronutrients in Mitigating Abiotic Stress in Crop Plants Plant Nutrients and Abiotic Stress Tolerance*. Singapore: Springer, 95–117. doi: 10.1007/978-981-10-9044-8_3

Pagliai, M., Vignozzi, N., and Pellegrini, S. (2004). Soil structure and the effect of management practices. *Soil Tillage Res.* 79, 131–143. doi: 10.1016/j.still.2004.07.002

Palla, A., Colli, M., Candela, A., Aronica, G., and Lanza, L. (2018). Pluvial flooding in urban areas: the role of surface drainage efficiency. *J. Flood Risk Manag.* 11, S663–S676. doi: 10.1111/jfr3.12246

Pandey, D., Goswami, C., Kumar, B., and Jain, S. (2002). Effect of growth regulators on photosynthetic metabolites in cotton under water stress. *Biol. Plant.* 45, 445–448. doi: 10.1023/A:1016286121451

Pang, J., Cuin, T., Shabala, L., Zhou, M., Mendham, N., and Shabala, S. (2007a). Effect of secondary metabolites associated with anaerobic soil conditions on ion fluxes and electrophysiology in barley roots. *Plant Physiol.* 145, 266–276.

Pang, J., Ross, J., Zhou, M., Mendham, N., and Shabala, S. (2007b). Amelioration of detrimental effects of waterlogging by foliar nutrient sprays in barley. *Funct. Plant Biol.* 34, 221–227. doi: 10.1071/FP06158

Pang, J., Zhou, M., Mendham, N., and Shabala, S. (2004). Growth and physiological responses of six barley genotypes to waterlogging and subsequent recovery. *Aust. J. Agric. Res.* 55, 895–906. doi: 10.1071/AR03097

Pang, J. Y., Newman, I., Mendham, N., Zhou, M., and Shabala, S. (2006). Microelectrode ion and O2 fluxes measurements reveal differential sensitivity of barley root tissues to hypoxia. *Plant Cell Environ.* 29, 1107–1121. doi: 10.1111/j.1365-3040.2005.01486.x

Parent, C., Capelli, N., Berger, A., Crèvecoeur, M., and Dat, J. F. (2008). An overview of plant responses to soil waterlogging. *Plant Stress* 2, 20–27.

Perata, P., Armstrong, W., and Voesenek, L. A. (2011). Plants and flooding stress. *N. Phytol.* 190, 269–273. doi: 10.1111/j.1469-8137.2011.03702.x

Pereira, E. I, Nogueira, A. A. R., Cruz, C. C., Guimaraþes, G. G., Foschini, M. M., Bernardi, A. C., et al. (2017). Controlled urea release employing nanocomposites increases the efficiency of nitrogen use by forage. *ACS Sustain. Chem. Eng.* 5, 9993–10001. doi: 10.1021/acssuschemeng.7b01919

Pérez-Jiménez, M., Hernández-Munuera, M., Piñero, M. C., López-Ortega, G., and del Amor, F. M. (2018). Are commercial sweet cherry rootstocks adapted to climate change? Short-term waterlogging and CO2 effects on sweet cherry cv.'Burlat'. *Plant Cell Environ.* 41, 908–918. doi: 10.1111/pce.12920

Peries, R. (2013). *Subsoil Manuring: An Innovative Approach To Addressing Subsoil Problems Targeting Higher Water Use Efficiency In Southern Australia*. St, Inverleigh VIC: Southern Farming Systems.

Petrov, V., Hille, J., Mueller-Roeber, B., and Gechev, T. S. (2015). ROS-mediated abiotic stress-induced programmed cell death in plants. *Front. Plant Sci.* 6:69. doi: 10.3389/fpls.2015.00069

Pierret, A., Doussan, C., Capowiez, Y., and Bastardie, F. (2007). Root functional architecture: a framework for modeling the interplay between roots and soil. *Vadose Zone J.* 6, 269–281. doi: 10.2136/vzj2006.0067

Ploschuk, R. A., Miralles, D. J., Colmer, T. D., Ploschuk, E. L., and Striker, G. G. (2018). Waterlogging of winter crops at early and late stages: impacts on leaf physiology, growth and yield. *Front. Plant Sci.* 9:1863. doi: 10.3389/fpls.2018.01863

Ponnamperuma, F. (1984). "Effects of flooding on soils," in *Flooding and Plant Growth*, ed. T. T. Kozlowski (Cambridge, MA: Academic Press), 9–45. doi: 10.1016/B978-0-12-424120-6.50007-9

Prathapar, S., Rajmohan, N., Sharma, B., and Aggarwal, P. (2018). Vertical drains to minimize duration of seasonal waterlogging in Eastern Ganges Basin flood plains: a field experiment. *Nat. Hazards* 92, 1–17. doi: 10.1007/s11069-018-3188-0

Price, P. (2004). *Spreading the PA Message*. Canberra, ACT: Grains Research and Development Corporation.

Pujol, V., and Wissuwa, M. (2018). Contrasting development of lysigenous aerenchyma in two rice genotypes under phosphorus deficiency. *BMC Res. Notes* 11:60. doi: 10.1186/s13104-018-3179-y

Pulford, I., and Tabatabai, M. (1988). Effect of waterlogging on enzyme activities in soils. *Soil Biol. Biochem.* 20, 215–219. doi: 10.1016/0038-0717(88)90039-9

Qingjie, W., Hao, C., Hongwen, L., Wenying, L., Xiaoyan, W., McHugh, A. D., et al. (2009). Controlled traffic farming with no tillage for improved fallow water storage and crop yield on the Chinese Loess Plateau. *Soil Tillage Res.* 104, 192–197. doi: 10.1016/j.still.2008.10.012

Qiu, J. (1991). Study on determination of wet tolerance of 4572 barley germplasm resources. *Acta Agric. Shanghai* 7, 27–32.

Rademacher, W. (2015). Plant growth regulators: backgrounds and uses in plant production. *J. Plant Growth Regulation* 34, 845–872. doi: 10.1007/s00344-015-9541-6

Rajaeian, S., and Ehsanpour, A. (2015). Physiological responses of tobacco plants (*Nicotiana rustica*) pretreated with ethanolamine to salt stress. *Russ. J. Plant Physiol.* 62, 246–252. doi: 10.1134/S1021443715020156

Ram, J., Garg, V., Toky, O., Minhas, P., Tomar, O., Dagar, J., et al. (2007). Biodrainage potential of Eucalyptus tereticornis for reclamation of shallow water table areas in north-west India. *Agrofor. Syst.* 69, 147–165. doi: 10.1007/s10457-006-9026-5

Rao, R., Li, Y., Bryan, H. H., Reed, S. T., and D'AMBROSIO, F. (2002). "Assessment of foliar sprays to alleviate flooding injury in corn (*Zea mays* L.)," in *Proceedings of the Florida State Horticultural Society*, (Lake Alfred: Florida State Horticultural Society), 208–211.

Raper, R. (2005). Agricultural traffic impacts on soil. *J. Terramech.* 42, 259–280. doi: 10.1016/j.jterra.2004.10.010

Rasaily, R. G., Li, H., He, J., Wang, Q., and Lu, C. (2012). Influence of no tillage controlled traffic system on soil physical properties in double cropping area of North China plain. *Afr. J. Biotechnol.* 11, 856–864.

Rasheed, R., Iqbal, M., Ashraf, M. A., Hussain, I., Shafiq, F., Yousaf, A., et al. (2018). Glycine betaine counteracts the inhibitory effects of waterlogging on growth, photosynthetic pigments, oxidative defence system, nutrient composition, and fruit quality in tomato. *J. Hortic. Sc. Biotechnol.* 93, 385–391. doi: 10.1080/14620316.2017.1373037

Rebetzke, G., Botwright, T., Moore, C., Richards, R., and Condon, A. (2004). Genotypic variation in specific leaf area for genetic improvement of early vigour in wheat. *Field Crops Res.* 88, 179–189. doi: 10.1016/j.fcr.2004.01.007

Reddy, K., and Patrick, W. H. Jr. (1975). Effect of alternate aerobic and anaerobic conditions on redox potential, organic matter decomposition and nitrogen loss in a flooded soil. *Soil Biol. Biochem.* 7, 87–94. doi: 10.1016/0038-0717(75)90004-8

Ren, B., Zhang, J., Dong, S., Liu, P., and Zhao, B. (2018). Exogenous 6-benzyladenine improves antioxidative system and carbon metabolism of summer maize waterlogged in the field. *J. Agron. Crop Sci.* 204, 175–184. doi: 10.1111/jac.12253

Ren, B., Zhu, Y., Zhang, J., Dong, S., Liu, P., and Zhao, B. (2016). Effects of spraying exogenous hormone 6-benzyladenine (6-BA) after waterlogging on grain yield and growth of summer maize. *Field Crops Res.* 188, 96–104. doi: 10.1016/j.fcr.2015.10.016

Rengasamy, P. (2006). World salinization with emphasis on Australia. *J. Exp. Bot.* 57, 1017–1023. doi: 10.1093/jxb/erj108

Renton, M., and Flower, K. C. (2015). Occasional mouldboard ploughing slows evolution of resistance and reduces long-term weed populations in no-till systems. *Agric. Syst.* 139, 66–75. doi: 10.1016/j.agsy.2015.06.005

Riffkin, P., Evans, P., Chin, J., and Kearney, G. (2003). Early-maturing spring wheat outperforms late-maturing winter wheat in the high rainfall environment of south-western Victoria. *Aust. J. Agric. Res.* 54, 193–202. doi: 10.1071/AR02081

Rincon-Florez, V. A., Dang, Y. P., Crawford, M. H., Schenk, P. M., and Carvalhais, L. C. (2016). Occasional tillage has no effect on soil microbial biomass, activity and composition in Vertisols under long-term no-till. *Biol. Fertil. Soils* 52, 191–202. doi: 10.1007/s00374-015-1066-4

Ritzema, H., Satyanarayana, T., Raman, S., and Boonstra, J. (2008). Subsurface drainage to combat waterlogging and salinity in irrigated lands in India: lessons learned in farmers' fields. *Agric. Water Manag.* 95, 179–189. doi: 10.1016/j.agwat.2007.09.012

Robertson, D., Zhang, H., Palta, J. A., Colmer, T., and Turner, N. C. (2009). Waterlogging affects the growth, development of tillers, and yield of wheat through a severe, but transient, N deficiency. *Crop Pasture Sci.* 60, 578–586. doi: 10.1071/CP08440

Robertson, M. (2008). *The Economics of Precision. Grains Research Update: Northern Region*. New South Wales: Grains Research and Development Corporation.

Robertson, M., Carberry, P., and Brennan, L. (2007). *The Economic Benefits of Precision Agriculture: Case Studies From Australian Grain Farms*. Available at: https://grdc.com.au/resources-and-publications/grdc-update-papers/tab-content/grdc-update-papers/2008/02/economic-benefits-of-precision-agriculture-case-studies-from-australian-grain-farms

Robinson, M., Mulqueen, J., and Burke, W. (1987). On flows from a clay soil—seasonal changes and the effect of mole drainage. *J. Hydrol.* 91, 339–350. doi: 10.1016/0022-1694(87)90210-1

Rochester, I., Peoples, M., Hulugalle, N., Gault, R., and Constable, G. (2001). Using legumes to enhance nitrogen fertility and improve soil condition in cotton cropping systems. *Field Crops Res.* 70, 27–41. doi: 10.1016/S0378-4290(00)00151-9

Romina, P., Abeledo, L. G., and Miralles, D. J. (2018). Physiological traits associated with reductions in grain number in wheat and barley under waterlogging. *Plant Soil* 429, 1–13.

Roper, M. M., Davies, S. L., Blackwell, P. S., Hall, D. J. M., Bakker, D. M., Jongepier, R., et al. (2015). Management options for water-repellent soils in Australian dryland agriculture. *Soil Res.* 53, 786–806. doi: 10.1071/SR14330

Roth, C. H., Fischer, R. A., Piggin, C., and Meyer, W. (2005). *Evaluation and Performance of Permanent Raised Bed Systems in Asia, Mexico and Australia: A Synopsis* Griffith, NSW: Australia and Mexico: 200–208.

Roy Chowdhury, S., Kumar, A., Brahmanand, P., Ghosh, S., Mohanty, R., Jena, S., et al. (2011). *Application of Bio-Drainage for Reclamation of Waterlogged Situations in Deltaic Orissa. Research Bulletin 53*. Bhubaneswar: Directorate of Water Management.

Saadat, S., Bowling, L., Frankenberger, J., and Kladivko, E. (2018). Nitrate and phosphorus transport through subsurface drains under free and controlled drainage. *Water Res.* 142, 196–207. doi: 10.1016/j.watres.2018.05.040

Sairam, R., Kumutha, D., Ezhilmathi, K., Chinnusamy, V., and Meena, R. (2009). Waterlogging induced oxidative stress and antioxidant enzyme activities in pigeon pea. *Biol. Plant.* 53, 493–504. doi: 10.1007/s10535-009-0090-3

Sale, P. (2014). *Final report for ULA00008 Validating subsoil manuring in the High Rainfall Zone in Victoria (VIC)*. Barton ACT: GRDC.

Saleh, I., Kavian, A., Roushan, M. H., and Jafarian, Z. (2018). The efficiency of vegetative buffer strips in runoff quality and quantity control. *Int. J. Environ. Sci. Technol.* 15, 811–820. doi: 10.1007/s13762-017-1411-2

Sarkar, A., Banik, M., Ray, R., and Patra, S. (2018). Soil moisture and groundwater dynamics under biodrainage vegetation in a waterlogged land. *Int. J. Pure Appl. Biosci.* 6, 1225–1233. doi: 10.18782/2320-7051.6052

Sarkar, R., Reddy, J., Sharma, S., and Ismail, A. M. (2006). Physiological basis of submergence tolerance in rice and implications for crop improvement. *Curr. Sci.* 91, 899–906.

Savvides, A., Ali, S., Tester, M., and Fotopoulos, V. (2016). Chemical priming of plants against multiple abiotic stresses: mission possible? *Trends Plant Sci.* 21, 329–340. doi: 10.1016/j.tplants.2015.11.003

Sayed, S. A. (1998). Impacts of boron application on maize plants growing under flooded and unflooded conditions. *Biol. Plant.* 41, 101–109. doi: 10.1023/A:1001720702268

Scanlan, C. A., and Davies, S. L. (2019). Soil mixing and redistribution by strategic deep tillage in a sandy soil. *Soil Tillage Res.* 185, 139–145. doi: 10.1016/j.still.2018.09.008

Schmidt, E., and Zemadim, B. (2015). Expanding sustainable land management in Ethiopia: scenarios for improved agricultural water management in the Blue Nile. *Agric. Water Manag.* 158, 166–178. doi: 10.1016/j.agwat.2015.05.001

Schneider, F., Don, A., Hennings, I., Schmittmann, O., and Seidel, S. J. (2017). The effect of deep tillage on crop yield–What do we really know? *Soil Tillage Res.* 174, 193–204. doi: 10.1016/j.still.2017.07.005

Setter, T., and Belford, B. (1990). Waterlogging: how it reduces plant growth and how plants can overcome its effects. *J. Dep. Agric. West. Aust. Ser.* 4, 51–55.

Setter, T., and Waters, I. (2003). Review of prospects for germplasm improvement for waterlogging tolerance in wheat, barley and oats. *Plant Soil* 253, 1–34. doi: 10.1023/A:1024573305997

Shabala, S. (2011). Physiological and cellular aspects of phytotoxicity tolerance in plants: the role of membrane transporters and implications for crop breeding for waterlogging tolerance. *N. Phytol.* 190, 289–298. doi: 10.1111/j.1469-8137.2010.03575.x

Shabala, S., White, R. G., Djordjevic, M. A., Ruan, Y.-L., and Mathesius, U. (2016). Root-to-shoot signalling: integration of diverse molecules, pathways and functions. *Funct. Plant Biol.* 43, 87–104. doi: 10.1071/FP15252

Shahrayini, E., Fallah, M., Shabanpour, M., Ebrahimi, E., and Saadat, S. (2018). Investigation of soil compaction on yield and agronomic traits of wheat under saline and non-saline soils. *Arch. Agron. Soil Sci.* 64:10. doi: 10.1080/03650340.2018.1431832

Sharma, S. K., Kulshreshtha, N., Kumar, A., Yaduvanshi, N. P. S., Singh, M., Prasad, K. R. K., et al. (2018). Waterlogging effects on elemental composition of wheat genotypes in sodic soils. *J. Plant Nutr.* 41, 1252–1262. doi: 10.1080/01904167.2018.1434541

Shaviv, A. (2001). Advances in controlled-release fertilizers. *Adv. Agron.* 71, 1–49. doi: 10.1016/S0065-2113(01)71011-5

Shaxson, F., and Barber, R. (2003). *Optimizing Soil Moisture For Plant Production: The Significance Of Soil Porosity*. Rome: UN-FAO.

Shoji, S., Delgado, J., Mosier, A., and Miura, Y. (2001). Use of controlled release fertilizers and nitrification inhibitors to increase nitrogen use efficiency and to conserve air andwater quality. *Commun. Soil Sci. Plant Anal.* 32, 1051–1070. doi: 10.1081/CSS-100104103

Silberstein, R., Vertessy, R., Morris, J., and Feikema, P. (1999). Modelling the effects of soil moisture and solute conditions on long-term tree growth and water use: a case study from the Shepparton irrigation area, Australia. *Agric. Water Manag.* 39, 283–315. doi: 10.1016/S0378-3774(98)00083-3

Silva, D. M. D., Fonte, N. D. S. D., Souza, K. R. D. D., Rodrigues-Brandão, I., Alves, I. T. L., and Donizeti, J. (2017). Relationship between manganese toxicity and waterlogging tolerance in *Zea mays* L. *cv*. Saracura. *Acta Sci. Agron.* 39, 75–82. doi: 10.4025/actasciagron.v39i1.30997

Singh, A. (2012). Development and application of a watertable model for the assessment of waterlogging in irrigated semi-arid regions. *Water Resour. Manag.* 26, 4435–4448. doi: 10.1007/s11269-012-0154-6

Singh, A. (2016). Hydrological problems of water resources in irrigated agriculture: A management perspective. *J. Hydrol.* 541, 1430–1440. doi: 10.1016/j.jhydrol.2016.08.044

Singh, A. (2018a). Managing the salinization and drainage problems of irrigated areas through remote sensing and GIS techniques. *Ecol. Indic.* 89, 584–589. doi: 10.1016/j.ecolind.2018.02.041

Singh, A. (2018b). Salinization of agricultural lands due to poor drainage: A viewpoint. *Ecol. Indic.* 95, 127–130. doi: 10.1016/j.ecolind.2018.07.037

Singh, A., and Panda, S. N. (2012). Integrated salt and water balance modeling for the management of waterlogging and salinization. I: validation of SAHYSMOD. *J. Irrigation Drainage Eng.* 138, 955–963. doi: 10.1061/(ASCE)IR.1943-4774.0000511

Singh, G., and Lal, K. (2018). Review and case studies on biodrainage: An alternative drainage system to manage waterlogging and salinity. *Irrigation Drainage* 67, 51–64. doi: 10.1002/ird.2252

Singh, S. P., and Setter, T. L. (2017). Effect of waterlogging on element concentrations, growth and yield of wheat varieties under farmer's sodic field conditions. *Proc. Natl. Acad. Sci. India Section B Biol. Sci.* 87, 513–520. doi: 10.1007/s40011-015-0607-9

Smedema, L. K., Vlotman, W. F., and Rycroft, D. (2014). *Modern Land Drainage: Planning, Design and Management of Agricultural Drainage Systems*. Boca Raton, FL: CRC Press.

Sojka, R., and Scott, H. (2002). *Aeration Measurement Encyclopedia of Soil Science*, 1st Edn. New York, NY: Marcel Dekker, Inc, 27–29.

Solaiman, Z., Colmer, T., Loss, S., Thomson, B., and Siddique, K. (2007). Growth responses of cool-season grain legumes to transient waterlogging. *Aust. J. Agric. Res.* 58, 406–412. doi: 10.1071/AR06330

Soomro, U. A., Rahman, M. U., Odhano, E. A., Gul, S., and Tareen, A. Q. (2009). Effects of sowing method and seed rate on growth and yield of wheat (*Triticum aestivum*). *World J. Agric. Sci.* 5, 159–162.

Stapper, M., and Harris, H. (1989). Assessing the productivity of wheat genotypes in a Mediterranean climate, using a crop-simulation model. *Field Crops Res.* 20, 129–152. doi: 10.1016/0378-4290(89)90057-9

Striker, G. (2008). Visiting the methodological aspects of flooding experiments: Quantitative evidence from agricultural and ecophysiological studies. *J. Agron. Crop Sci.* 194, 249–255. doi: 10.1111/j.1439-037X.2008.00317.x

Sudama, S., Tiwari, T. N., Srivastava, R. P., Singh, G. P., and Singh, S. (1998). Effect of potassium on stomatal behaviour, yield and juice quality of sugarcane under moisture stress condition. *Indian J. Plant Physiol.* 3, 303–305.

Sundgren, T. K., Uhlen, A. K., Lillemo, M., Briese, C., and Wojciechowski, T. (2018). Rapid seedling establishment and a narrow root stele promotes waterlogging tolerance in spring wheat. *J. Plant Physiol.* 227, 45–55. doi: 10.1016/j.jplph.2018.04.010

Swarup, A., and Sharma, D. (1993). Influence of top-dressed nitrogen in alleviating adverse effects of flooding on growth and yield of wheat in a sodic soil. *Field Crops Res.* 35, 93–100. doi: 10.1016/0378-4290(93)90142-A

Takeda, K., and Fukuyama, T. (1986). *Variation and Geographical Distribution Of Varieties For Flooding Tolerance In Barley Seeds*. Okayama: Barley Genetics Newsletter.

Tanji, K. K. (1990). "Nature and extent of agricultural salinity. agricultural salinity assessment and management," in *ASCE Manuals and Reports on Engineering Practice No. 671*, ed. K. K. Tanji (New York, NY: American Society of Civil Engineers), 619.

Taylor, J. (1992). Reduction of traffic-induced soil compaction. *Soil Tillage Res.* 24, 301–302. doi: 10.1016/0167-1987(92)90115-R

Taylor, J. H. (1983). Benefits of permanent traffic lanes in a controlled traffic crop production system. *Soil Tillage Res.* 3, 385–395. doi: 10.1016/0167-1987(83)90040-5

Teixeira, D. L., de Matos, A. T., de Matos, M. P., Miranda, S. T., and Vieira, D. P. (2018). Evaluation of the effects of drainage and different rest periods as techniques for unclogging the porous medium in horizontal subsurface flow constructed wetlands. *Ecol. Eng.* 120, 104–108. doi: 10.1016/j.ecoleng.2018.05.042

Tewari, S., and Mishra, A. (2018). *Flooding Stress in Plants and Approaches to Overcome Plant Metabolites and Regulation Under Environmental Stress*. New York,NY: Elsevier, 355–366. doi: 10.1016/B978-0-12-812689-9.00018-2

Thomsen, M. N., Tamirat, T. W., Pedersen, S. M., Lind, K. M., Pedersen, H. H., de Bruin, S., et al. (2018). "Farmers' perception of Controlled Traffic Farming (CTF) and associated technologies (No. 2018/12)," in *IFRO Working Paper* (Copenhagen: University of Copenhagen).

Tian, S., Fischer, M., Chescheir, G. M., Youssef, M. A., Cacho, J. F., and King, J. S. (2018). Microtopography-induced transient waterlogging affects switchgrass (Alamo) growth in the lower coastal plain of North Carolina, USA. *GCB Bioenergy* 10, 577–591. doi: 10.1111/gcbb.12510

Tilman, D., Cassman, K. G., Matson, P. A., Naylor, R., and Polasky, S. (2002). Agricultural sustainability and intensive production practices. *Nature* 418, 671–677. doi: 10.1038/nature01014

Trenkel, M. E. (2010). *Slow-and Controlled-Release and Stabilized Fertilizers: An Option for Enhancing Nutrient Use Efficiency in Agriculture*. Paris: International fertilizer industry association.

Trought, M., and Drew, M. (1980). The development of waterlogging in wheat seedlings. I. Shoot and root growth in relation to changes in the concentration of dissolved gases and solutes in the soil solution. *Plant Soil* 54, 77–94. doi: 10.1007/BF02182001

Tullberg, J. (2000). Wheel traffic effects on tillage draught. *J. Agric. Eng. Res.* 75, 375–382. doi: 10.1006/jaer.1999.0516

Tullberg, J., Yule, D., and McGarry, D. (2007). Controlled traffic farming—from research to adoption in Australia. *Soil Tillage Res.* 97, 272–281. doi: 10.1016/j.still.2007.09.007

Tuohy, P., Humphreys, J., Holden, N., and Fenton, O. (2015). "Mole drainage performance in a clay loam soil," in *NJF Congress: Nordic view to sustainable rural development*, (Riga: NJF).

Tuohy, P., Humphreys, J., Holden, N., and Fenton, O. (2016). Runoff and subsurface drain response from mole and gravel mole drainage across episodic rainfall events. *Agric. Water Manag.* 169, 129–139. doi: 10.1016/j.agwat.2016.02.020

Tuohy, P., O'Loughlin, J., and Fenton, O. (2018). Modeling performance of a tile drainage system incorporating mole drainage. *Trans. ASABE* 61, 169–178. doi: 10.13031/trans.12203

Unger, P. W., Sharpley, A. N., Steiner, J. L., Papendick, R. I., and Edwards, W. M. (2018). *Soil Management Research for Water Conservation and Quality, Advances in Soil and Water Conservation*. Abingdon: Routledge, 69–98. doi: 10.1201/9781315136912-5

Varadachari, C., and Goertz, H. M. (2010). "Slow-release and controlled-release nitrogen fertilizers," in *ING Bulletins on Regional Assessment of Reactive Nitrogen*. ed. S. Bijay (New Delhi: SCON-ING).

Velmurugan, A., Swarnam, T., Ambast, S., and Kumar, N. (2016). Managing waterlogging and soil salinity with a permanent raised bed and furrow system in coastal lowlands of humid tropics. *Agric. Water Manag.* 168, 56–67. doi: 10.1016/j.agwat.2016.01.020

Vwioko, E., Adinkwu, O., and El-Esawi, M. A. (2017). Comparative physiological, biochemical, and genetic responses to prolonged waterlogging stress in okra and maize given exogenous ethylene priming. *Front. Physiol.* 8:632. doi: 10.3389/fphys.2017.00632

Wani, S. H., Choudhary, M., Kumar, P., Akram, N. A., Surekha, C., Ahmad, P., et al. (2018). "Marker-assisted breeding for abiotic stress tolerance in crop plants," in *Biotechnologies of Crop Improvement*, eds S. Gosal and S. Wani (Cham: Springer), 3.

Ward, A., Johnston, T., Watson, D., and Jenkin, T. (2007). .

Ward, A., Sharpley, A., Miller, K., Dick, W., Hoorman, J., Fulton, J., et al. (2018). An assessment of in-field nutrient best management practices for agricultural crop systems with subsurface drainage. *J. Soil Water Conser.* 73, 5A–10A. doi: 10.2489/jswc.73.1.5A

Watson, E., Lapins, P., and Barron, R. (1976). Effect of waterlogging on the growth, grain and straw yield of wheat, barley and oats. *Aust. J. Exp. Agric.* 16, 114–122. doi: 10.1071/EA9760114

Webb, B., Blackwell, P., Riethmuller, G., and Lemon, J. (2004). *Tramline Farming Systems: Technical Manual*. State of Western: DAFWA.

Weber, B., and Hill, J. (2016). *Remote Sensing of Biological Soil Crusts at Different Scales Biological Soil Crusts: An Organizing Principle in Drylands*. Berlin: Springer, 215–234. doi: 10.1007/978-3-319-30214-0_12

Williams, M., King, K., and Fausey, N. (2015). Drainage water management effects on tile discharge and water quality. *Agric. Water Manag.* 148, 43–51. doi: 10.1016/j.agwat.2014.09.017

Wollmer, A. C., Pitann, B., and Mühling, K. H. (2018). Nutrient deficiencies do not contribute to yield loss after waterlogging events in winter wheat (Triticum aestivum). *Ann. Appl. Biol.* 173, 141–153. doi: 10.1111/aab.12449

Wu, H., Xiang, J., Chen, H., Zhang, Y., Zhang, Y., and Zhu, F. (2018). Effects of exogenous growth regulators on plant elongation and carbohydrate consumption of rice seedlings under submergence. *J. Appl. Ecol.* 29, 149–157. doi: 10.13287/j.1001-9332.201801.021

Wu, X., Tang, Y., Li, C., McHugh, A., Li, Z., and Wu, C. (2018). Individual and combined effects of soil waterlogging and compaction on physiological characteristics of wheat in southwestern China. *Field Crops Res.* 215, 163–172. doi: 10.1016/j.fcr.2017.10.016

Wu, Q.-X., Zhu, J.-Q., Liu, K.-W., and Chen, L.-G. (2012). Effects of fertilization on growth and yield of cotton after surface waterlogging elimination. *Adv. J. Food Sci. Technol.* 4, 398–403.

Xian, C., Qi, Z., Tan, C. S., and Zhang, T.-Q. (2017). Modeling hourly subsurface drainage using steady-state and transient methods. *J. Hydrol.* 550, 516–526. doi: 10.1016/j.jhydrol.2017.05.016

Xiao, Y.-P., Wei, K., Chen, J.-X., Zhou, M.-X., and Zhang, G.-P. (2007). Genotypic difference in growth inhibition and yield loss of barley under waterlogging stress. *Agric. Life Sci.* 33, 525–532.

Yaduvanshi, N., Setter, T., Sharma, S., Singh, K., and Kulshreshtha, N. (2012). Influence of waterlogging on yield of wheat (*Triticum aestivum*), redox

potentials, and concentrations of microelements in different soils in India and Australia. *Soil Res.* 50, 489–499. doi: 10.1071/SR11266

Yaduvanshi, N., Setter, T., Sharma, S., Singh, K., and Kulshreshtha, N. (2014). Influence of waterlogging on yield of wheat (*Triticum aestivum*), redox potentials, and concentrations of microelements in different soils in India and Australia. *Soil Res.* 50, 489–499. doi: 10.1071/SR11266

Ylivainio, K., Jauhiainen, L., Uusitalo, R., and Turtola, E. (2018). Waterlogging severely retards P use efficiency of spring barley (*Hordeum vulgare*). *J. Agron. Crop Sci.* 204, 74–85. doi: 10.1111/jac.12241

Ylivainio, K., Uusitalo, R., and Turtola, E. (2008). Meat bone meal and fox manure as P sources for ryegrass (Lolium multiflorum) grown on a limed soil. *Nutr. Cycling Agroecosyst.* 81, 267–278. doi: 10.1007/s10705-007-9162-y

Yordanova, R., Uzunova, A., and Popova, L. (2005). Effects of short-term soil flooding on stomata behaviour and leaf gas exchange in barley plants. *Biol. Plant.* 49, 317–319. doi: 10.1007/s10535-005-7319-6

Yu, Q., Shen, Y., Wang, Q., Wang, X., Fan, L., Wang, Y., et al. (2019). Light deficiency and waterlogging affect chlorophyll metabolism and photosynthesis in *Magnolia sinostellata*. *Trees* 33, 11–22. doi: 10.1007/s00468-018-1753-5

Zhang, H., Turner, N., Poole, M., and Simpson, N. (2006). Crop production in the high rainfall zones of southern Australia—potential, constraints and opportunities. *Aust. J. Exp. Agric.* 46, 1035–1049. doi: 10.1071/EA05150

Zhang, H., Turner, N. C., and Poole, M. L. (2004). Yield of wheat and canola in the high rainfall zone of south-western Australia in years with and without a transient perched water table. *Aust. J. Agric. Res.* 55, 461–470. doi: 10.1071/AR03122

Zhang, J., and Zhang, X. (1994). Can early wilting of old leaves account for much of the ABA accumulation in flooded pea plants? *J. Exp. Bot.* 45, 1335–1342. doi: 10.1093/jxb/45.9.1335

Zhang, S. (2005). *Soil Hydraulic Properties and Water Balance Under Various Soil Management Regimes on the Loess Plateau, China*. Ph.D. thesis, Swedish University of Agricultural Sciences, Umeå.

Zhang, X., Shabala, S., Koutoulis, A., Shabala, L., Johnson, P., Hayes, D., et al. (2015). Waterlogging tolerance in barley is associated with faster aerenchyma formation in adventitious roots. *Plant Soil* 394, 355–372. doi: 10.1007/s11104-015-2536-z

Zhang, X. C., Fan, Y., Shabala, S., Koutoulis, A., Shabala, L., Johnson, P., et al. (2017). A new major-effect QTL for waterlogging tolerance in wild barley (H. *spontaneum*). *Theor. Appl. Genet.* 130, 1559–1568. doi: 10.1007/s00122-017-2910-8

Zheng, W., Liu, Z., Zhang, M., Shi, Y., Zhu, Q., Sun, Y., et al. (2017). Improving crop yields, nitrogen use efficiencies, and profits by using mixtures of coated controlled-released and uncoated urea in a wheat-maize system. *Field Crops Res.* 205, 106–115. doi: 10.1016/j.fcr.2017.02.009

Zhou, M. (2010). "Improvement of plant waterlogging tolerance," in *Waterlogging Signalling and Tolerance In Plants*, eds S. Shabala and S. Mancuso (Berlin: Springer), 267–285.

Zhou, M., Li, H., and Mendham, N. (2007). Combining ability of waterlogging tolerance in barley. *Crop Sci.* 47, 278–284. doi: 10.2135/cropsci2006.02.0065

Zhou, M. X. (2011). Accurate phenotyping reveals better QTL for waterlogging tolerance in barley. *Plant Breed.* 130, 203–208. doi: 10.1111/j.1439-0523.2010.01792.x

Conflict of Interest Statement: The authors declare that the research was conducted in the absence of any commercial or financial relationships that could be construed as a potential conflict of interest.

frontiers in Plant Science

ORIGINAL RESEARCH
published: 11 March 2019
doi: 10.3389/fpls.2019.00254

Prevention of Radial Oxygen Loss Is Associated With Exodermal Suberin Along Adventitious Roots of Annual Wild Species of *Echinochloa*

*Masato Ejiri and Katsuhiro Shiono**

Laboratory of Plant Ecophysiology, Graduate School of Bioscience and Biotechnology, Fukui Prefectural University, Eiheiji, Japan

Internal aeration is crucial for root growth under waterlogged conditions. Some wetland plants have a structural barrier that impedes oxygen leakage from the basal part of roots called a radial oxygen loss (ROL) barrier. The ROL barrier reduces loss of oxygen transported via the aerenchyma to the root tips, enabling root growth into anoxic soil. The roots of some plants develop an ROL barrier under waterlogged conditions, while they remain leaky to oxygen under well-drained or aerated conditions. The main components of the inducible ROL barrier are thought to be suberin and lignin deposited at the outer cellular space (apoplast) in the outer part of roots. On the other hand, a few wetland plants including a species of *Echinochloa* form a constitutive ROL barrier, i.e., it is formed even in the absence of waterlogging. However, little is known about the components of constitutive ROL barriers. An ROL barrier is considered to be a characteristic of wetland species because it has not been found in any non-wetland species so far. Here, we examined whether *Echinochloa* species from non-waterlogged fields also form an inducible or constitutive ROL barrier. We found that three species of *Echinochloa* from non-waterlogged fields constitutively developed an ROL barrier under aerated conditions. Over 85% of their root exodermis cells were covered with suberin lamellae and had well-developed Casparian strips. These substances inhibited the infiltration of an apoplastic tracer (periodic acid), suggesting that the ROL barrier can also prevent the entry of phytotoxic compounds from the soil. Unlike the other *Echinochloa* species, *E. oryzicola*, which mainly inhabits rice paddies, was found to lack a constitutive ROL barrier under aerated conditions. Although close to 90% of its sclerenchyma was well lignified, it leaked oxygen from the basal part of roots. A high percentage (55%) of the root exodermis cells were not fortified with suberin lamellae. These results suggest that suberin is an important component of constitutive ROL barriers.

Keywords: barrier to radial oxygen loss, Casparian strip, exodermis, hypoxia, lignin, suberin, waterlogging

OPEN ACCESS

Edited by:
Makie Kokubun,
Tohoku University, Japan

Reviewed by:
Mikio Nakazono,
Nagoya University, Japan
Yoshiro Mano,
Institute of Livestock and Grassland Science (NARO), Japan

***Correspondence:**
Katsuhiro Shiono
shionok@fpu.ac.jp

Specialty section:
This article was submitted to Plant Abiotic Stress, a section of the journal Frontiers in Plant Science

Received: *31 October 2018*
Accepted: *18 February 2019*
Published: *11 March 2019*

Citation:
Ejiri M and Shiono K (2019) Prevention of Radial Oxygen Loss Is Associated With Exodermal Suberin Along Adventitious Roots of Annual Wild Species of Echinochloa. Front. Plant Sci. 10:254. doi: 10.3389/fpls.2019.00254

INTRODUCTION

Echinochloa is a grass with both annual and perennial species. The annual species are highly pernicious weeds in rice paddies (Rao et al., 2007; Kraehmer et al., 2016). Three such species are known: *Echinochloa crus-galli*, *E. colona*, and *E. oryzicola* (**Table 1**). They are well adapted to various soil water situations and their habitats range from waterlogged paddy fields to

well-drained crop fields (Yamasue, 2001; Rao et al., 2007; Tanesaka et al., 2010). Their life cycles and morphological characters closely resemble those of rice (Barrett, 1983), which makes it difficult to remove them. Although most weeds cannot grow and survive in the waterlogged soil in rice paddies, some *Echinochloa* species have well adapted to and become dominant in these habitats (Kraehmer et al., 2016). A better understanding of how these species acclimate to waterlogging will help to develop more effective herbicides or crop cultivation methods for controlling them.

Under waterlogged conditions, plants can suffer from hypoxia or anoxia because the ability of oxygen do diffuse through the water to the soil is extremely low (Jackson et al., 1985). Other problems associated with waterlogging are the accumulation of phytotoxic compounds in the soil (Ponnamperuma, 1984; Ernst, 1990; Lamers et al., 1998; Kreuzwieser et al., 2004) and a decline in the availability of some nutrients (Laanbroek, 1990). The roots of wetland plants contain a large volume of aerenchyma, which provides a low-resistance pathway for diffusion of oxygen from the shoot to the root (Armstrong, 1979; Kawai et al., 1998; Mano et al., 2006; Shiono et al., 2011; Nishiuchi et al., 2012). Some wetland species also form a barrier to radial oxygen loss (ROL) (Colmer, 2003b). The ROL barrier forms at the basal part of roots, and reduces the loss of oxygen transported via the aerenchyma to the root tips. In the roots with an ROL barrier, oxygen at the root tips and short lateral roots can be maintained at a higher level to allow root elongation into hypoxic/anoxic soil (Armstrong and Armstrong, 2005). In some wetland plants including rice, an ROL barrier is induced by stagnant or waterlogged conditions, while a weak barrier or no barrier forms in well-drained or aerated conditions (Colmer et al., 1998, 2006; Visser et al., 2000; Colmer, 2003a; Garthwaite et al., 2003; Abiko et al., 2012). However, a few wetland plants including *Echinochloa* form a constitutive ROL barrier, i.e., it is formed even in the absence of waterlogging (Visser et al., 2000; McDonald et al., 2001, 2002; Manzur et al., 2015).

Suberin and lignin deposits in the apoplast (the outer cellular space) prevent movement of water, ions and mycorrhizal fungi through the apoplast and thus act as an apoplastc barrier (Aloni et al., 1998; Enstone et al., 2003). Suberin is a hydrophobic macromolecule built from long-chain fatty acids and glycerol (Enstone et al., 2003; Graca, 2015). Lignin is a complex of polyphenolic polymers (Barros et al., 2015). Casparian strips, which are present in radial and transverse cell walls in the early developmental stage (State I), are comprised of lignin and suberin (Zeier et al., 1999; Schreiber and Franke, 2011; Naseer et al., 2012). Suberin lamellae, which are deposited on the inner surface of cell walls and surround the symplast in the subsequent developmental stage (State II), are comprised of suberin (Zeier et al., 1999; Schreiber and Franke, 2011). Because suberin was observed to accumulate at the exodermis and lignin was observed to accumulate at the sclerenchyma when plants formed an ROL barrier, the barrier is thought to be formed by deposits of suberin and lignin in the outer part of the roots (Watanabe et al., 2013). Thus, the ROL barrier is also thought to act as an apoplastic barrier, not only to impede oxygen loss but also to block the entry of phytotoxins (e.g., reduced metal ions) from waterlogged soil (Armstrong, 1979; Colmer, 2003b; Cheng et al., 2012). In wetland species that have an inducible ROL barrier, suberin has been suggested to be a major component of the barrier (Kulichikhin et al., 2014; Shiono et al., 2014b; Watanabe et al., 2017). However, little is known about which compound is the main constituent in constitutive ROL barriers. In *Cyperus eragrostis*, which has a constitutive ROL barrier, blue autofluorescence, a sign of both suberin and lignin, was stronger at the outer part of roots than in other species that do not have an ROL barrier (Manzur et al., 2015). It remains unclear which compound is the main constituent in constitutive ROL barriers.

An ROL barrier is considered to be a characteristic of wetland species because it has not been found in any non-wetland species so far. An annual wild *Echinochloa* species (*E. crus-galli* var. *mitis*) forms a constitutive ROL barrier (McDonald et al., 2001, 2002). However, it is not known whether the other annual wild *Echinochloa* species, which are distributed in both waterlogged and well-drained fields, form a constitutive barrier, and if they do, what it consists of. Here, we examined each of the three known wild annual *Echinochloa* species for constitutive ROL barriers. In the species that formed an ROL barrier, we also examined their chemical composition.

MATERIALS AND METHODS

Plant Materials

This study was conducted with seeds of annual *Echinochloa* species collected from wild habitats (well-drained or waterlogged fields) in Japan and Bolivia (**Table 1**). The species included *Echinochloa crus-galli* (var. *crus-galli*, var. *formosensis* and var. *praticola*), *E. colona* and *E. oryzicola* and ecotypes of *E. crus-galli* var. *crus-galli* (**Table 1**). The Japanese and Bolivian seeds were kindly provided by Prof. Toshihito Yoshioka (Fukui Prefectural University) and Dr. Yuichiro Nakayama (Osaka Prefecture University), respectively.

Growth Conditions

Seeds were sterilized for 30 min in 0.6% (w/v) sodium hypochlorite, washed thoroughly with deionized water, and for imbibition, placed in Petri dishes (8.5 cm diameter) containing about 6 ml of deionized water (about 1 mm water-depth) at 28°C under light to stimulate germination. The plants were grown in a controlled-environment chamber under constant light to avoid effects of circadian rhythm on gene expression (24-h light, 28°C, relative humidity over 50%, photosynthetic photon flux density at 248.8 μmol m^{-2} s^{-1}). For the next phase, a soft sponge was floated on a container (380 mm × 260 mm × 160 mm high) of aerated quarter-strength nutrient solution (Colmer, 2003a; Shiono et al., 2011). Vertical slits were cut into the edges of the sponge. Four days after imbibition, each plant was slid into the slit so that the roots were submerged and the shoot protruded through the sponge into the light. Eight days after imbibition, the solution was replaced with aerated full-strength nutrient solution. To evaluate the constitutive ROL barrier under aerated conditions, 10 days after imbibition, plants were transplanted into aerated nutrient solution in 5-L pots

TABLE 1 | Accessions of annual wild *Echinochloa* used in the present study.

Species	Conditions of seed collection site	Region of origin	Chromosome number[1–3]	Accession
Echinochloa crus-galli var. *crus-galli*	Waterlogged field	Kyoto, Japan*	2n = 6X = 54	ECC-WL
E. crus-galli var. *crus-galli*	Well-drained field	Sendai, Japan*	2n = 6X = 54	ECC-D
E. crus-galli var. *formosensis*	Waterlogged field	Kyoto, Japan*	2n = 6X = 54	ECF-WL
E. crus-galli var. *praticola*	Well-drained field	Sendai, Japan*	2n = 6X = 54	ECP-D
E. colona	Well-drained field	Santa Cruz, Bolivia**	2n = 6X = 54	EC-D
E. oryzicola	Waterlogged field	Kyoto, Japan*	2n = 4X = 36	EO-WL

*Sources of seeds: *Prof. T. Yoshioka, Fukui Prefectural University; **Dr. Y. Nakayama, Osaka Prefecture University. [1,2]Yabuno (1962, 1984); [3]Aoki and Yamaguchi (2009).*

(120 mm × 180 mm × 250 mm high, four plants per pot) for an additional 13–15 days. In each pot, a rectangular 2-cm-thick piece of foam was placed on the solution and aluminum foil was placed on the top of the foam to keep the solution dark. Vertical cuts were made on the four sides of the foam to accommodate stems. Then four plants were transferred to each pot, sliding the stems into the cuts. In this way, the roots were kept in the dark. The nutrient solutions were renewed every 7 days.

To evaluate the inducible ROL barrier under stagnant conditions, 10 days after imbibition, plants were transplanted into stagnant deoxygenated nutrient solution in 5-L pots for 13–15 days. The stagnant solution was prepared by adding 0.1% (w/v) agar to the nutrient solution and boiling the solution to dissolve the agar. The low concentration of agar produced a viscous liquid rather than a gel. By preventing convective movements, the solution mimics the changes in gas composition found in waterlogged soils (e.g., decreased oxygen and increased ethylene) (Wiengweera et al., 1997). The solution was poured into the pots and deoxygenated by bubbling N_2 gas through two air stones at a flow rate of about 2.2 L min^{-1} for 15 min per pot. The dissolved oxygen (DO) level was confirmed to be less than 1.0 mg L^{-1} by DO meter (SG6-ELK, Mettler Toledo, Greifensee, Switzerland).

ROL Barrier Formation

Methylene blue, which turns blue when exposed to oxygen, was used to evaluate oxygen leakage from roots. A solution containing 0.1% (w/v) agar was prepared, and after cooling, methylene blue (Sigma-Aldrich, St. Louis, MO, United States) was added to a final concentration of 13 mg l^{-1}. The blue solution containing oxidized dye was reduced by addition of 130 mg l^{-1} sodium dithionite ($Na_2S_2O_4$) to make it colorless. The test solution was placed in a clear plastic box (220 mm × 35 mm × 300 mm high) and the plant was held with tape so that the root–shoot junction was 50 mm below the surface, and the remainder of the shoot was in the air. The roots were stained for 30–60 min at room temperature. When the roots formed an ROL barrier, their basal parts were colorless (Shiono et al., 2011). We also measured the lengths of roots with an ROL barrier. The percentage of roots that formed an ROL barrier in a plant was calculated as: [(number of roots that formed a barrier to ROL)/(total root number)] × 100.

Radial oxygen loss from adventitious roots range from 100 mm to 120 mm length without lateral roots (i.e., it seems to be relatively young and active roots) was measured with Pt cylindrical root-sleeving O_2 electrodes (Armstrong and Wright, 1975; Armstrong, 1994). The plant was placed in clear plastic boxes (55 mm × 55 mm × 300 mm high) fitted with rubber lids. The boxes were filled with an O_2-free medium containing 0.1% (w/v) agar, 0.5 mM $CaSO_4$ and 5 mM KCl. The shoot base was fixed to the rubber lids, so that the shoot was in the air and the root was in the O_2-free medium. An adventitious root was inserted through the cylindrical root-sleeving O_2 electrode (internal diameter, 2.25 mm; height, 5.0 mm). For calculation of ROL, root diameters of the position were measured with a micrometer caliper. ROL was measured in a lighted room kept at a constant 23°C.

Histochemical Staining

Adventitious roots (100–120 mm length) without lateral roots were cut at the root–shoot junction. Their basal parts (15–25 mm below root–shoot junction) were embedded in 5% (w/v) agar. Root cross-sections of ca. 100 μm thickness were made using a vibrating microtome (Leica VT1200S, Leica Biosystems, Wetzlar, Germany). The cross-sections were made transparent by incubating them in lactic acid saturated with chloral hydrate at 70°C for 60 min (Lux et al., 2005). To detect suberin lamellae in the basal parts, we used 0.01% (w/v) Fluorol Yellow 088 in polyethylene glycol 400 as described by Brundrett et al. (1991). Suberin lamellae were visualized as a yellowish-green fluorescence excited by UV light. The cross-sections were viewed with an 02 UV filter set, an Axio Imager.A2 and an AxioCam MRc CCD camera (all Carl Zeiss, Oberkochen, Germany). To visualize lignin, transparent cross-sections of the basal parts were stained for 3 min with saturated phloroglucinol in 20% (w/w) hydrochloric acid at room temperature (Jensen, 1962). The reagent reacts with cinnamyl aldehyde groups in the lignin to produce an orange/red color under white light. The cross-sections were viewed with the Axio Imager.A2 microscope and AxioCam MRc CCD camera. Casparian strips in the basal parts were stained with 0.1% (w/v) berberine hemisulfate and 0.5% (w/v) aniline blue (Brundrett et al., 1988), which appears as bright white fluorescence under UV light. The cross-sections were viewed with the 02 UV filter set, Axio Imager.A2 and AxioCam MRc CCD camera. The ratio of cells with suberin lamellae, lignin or Casparian strips was determined by manually counting the numbers of cells in each photograph. To reduce bias, we randomly selected 30 cells in a cross-section derived from four independent roots.

Permeability Test

Adventitious roots (100–120 mm length) without lateral roots were cut at the root–shoot junction. The permeability of the exodermal layers at the basal parts (15–25 mm below root–shoot junction) was assessed with an apoplastic tracer, periodic acid (Soukup et al., 2002; Shiono et al., 2014a; Pecková et al., 2016). The cut ends were covered with lanolin (Sigma-Aldrich) to prevent penetration of tracer. The roots were incubated in 0.1% (w/v) periodic acid (H_5IO_6) (Sigma-Aldrich) for 1 h, washed thoroughly with deionized water, incubated in reducing solution [1 g of potassium iodide (Wako) and 1 g of sodium thiosulfate (Wako) dissolved in 50 ml of water and acidified with 0.2 ml of 5 M hydrochloric acid (Wako)] for 1 h at room temperature, washed thoroughly with deionized water and incubated overnight at 4°C in the dark. The basal parts (17.5–22.5 mm below root–shoot junction) of adventitious roots were embedded in 5% (w/v) agar and cut in ca. 100-μm-thick cross-sections with a vibrating microtome (Leica VT1200S, Leica Biosystems). The sections were stained with Schiff's reagent (Sigma-Aldrich) for 2 min and washed twice with 75% (v/v) glycerol (Wako). Periodic acid that penetrated into root tissue was visualized as a purple color under white light with the above microscope and camera.

Root Porosity

Root porosity is the ratio of the gas volume to the volume of roots:

$$P = \frac{V_g}{V_r} \times 100,$$

where V_g is the gas volume in the roots (including aerenchyma and intercellular space) and V_r is the volume of the root tissue. It is measured by determining root buoyancy before and after vacuum infiltration of water into the gas spaces in the roots (Katayama, 1961; Raskin, 1983; Thomson et al., 1990).

Adventitious roots were separated from the shoot and cut into 50 mm segments. All of the segments from one plant were combined, gently blotted to remove excess water and weighed (*w1*). Three paper clips were used to hold the segments together and act as a sinker. Using an underhook balance (PA213CJP, Ohaus Corporation, Parsippany, NJ, United States), which weighs objects suspended below the balance, we measured the weight of just the paper clips hanging from a metal hook below the balance in a 2-L beaker of water (*w2*) and the weight of the roots held with the same paper clips in the water (*w3*). A smaller beaker containing the roots and paper clips in the water was placed in a vacuum desiccator and subjected to two 15-min periods of light vacuum (pressure, −50 kPa) to release the gas in the roots and infiltrate the roots with water. Finally, the paper clips and infiltrated roots were weighed in water (*w4*). Following Thomson et al. (1990), the above equation can then be expressed as

$$P = \frac{w4 - w3}{w1 + w2 - w3} \times 100$$

Growth Parameters

Plants were harvested after 14 days treatment in aerated or stagnant deoxygenated nutrient solutions. Leaf age, shoot length, the numbers of roots and the longest root length were recorded per plant. Shoots and roots were dried in an oven at 60°C for 3 days and weighed. For each growth parameter, percent control was calculated as: [(value under stagnant conditions)/(average value under aerated conditions)] × 100.

Statistical Analysis

Means of root porosity and growth parameters among *Echinochloa* accessions were compared with one-way ANOVA and Tukey HSD for multiple comparisons at the 5% probability level. Means of root porosity and growth parameters between aerated and stagnant conditions were compared with a two-sample *t*-test. The data were analyzed with SPSS 16.0 for Windows (SPSS Inc., Chicago, IL, United States). The percentage of roots that formed an ROL barrier in a plant and the ratios of cells with suberin lamellae, lignin or Casparian strips were compared with Fisher's exact test at the 5% probability level. The data were analyzed with R version 3.5.0 (R Core Team, 2018) (R packages: pwr).

RESULTS

All but One Species of *Echinochloa* Formed a Constitutive Barrier to ROL

In *E. colona* and all three varieties of *E. crus-galli*, 52–75% of the roots formed an ROL barrier under aerated conditions (**Figure 1**). However, in *E. oryzicola*, only 9% of the roots had an ROL barrier under aerated conditions. When these *Echinochloa* accessions including *E. oryzicola* were grown in stagnant solutions for 14 days, the percentage of roots that formed an ROL barrier ranged from 73 to 87%, values which were significantly higher than those in aerated conditions ($P < 0.05$, **Figure 1**), with the exception

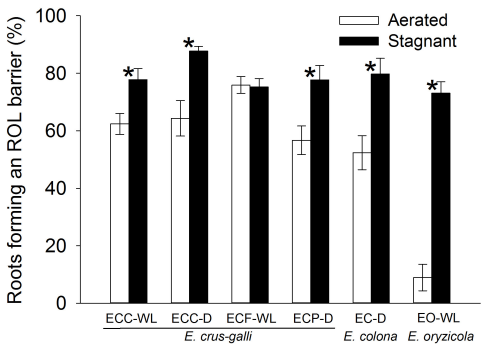

FIGURE 1 | Percentages of the roots that formed an ROL barrier in *Echinochloa* accessions grown under aerated or stagnant conditions for 14 days. Methylene blue was used to evaluate the formation of ROL barrier in roots. Means ± SE. $n = 5$ or 6. Asterisks denote a significant difference between aerated and stagnant conditions ($P < 0.05$, Fisher's exact test). Plants were grown in aerated nutrient solution for 10 days, and then transferred to deoxygenated stagnant 0.1% agar solution or continued in aerated nutrient solution for 14 days. Abbreviations (collected from): ECC-WL, *E. crus-galli* var. *crus-galli* (waterlogged field); ECC-D, *E. crus-galli* var. *crus-galli* (well-drained field); ECF-WL, *E. crus-galli* var. *formosensis* (waterlogged field); ECP-D, *E. crus-galli* var. *praticola* (well-drained field); EO-WL, *E. oryzicola* (waterlogged field); EC-D, *E. colona* (well-drained field).

of ECC-WL. To clarify the difference between *E. oryzicola* and the other accessions, we evaluated the distributions of root lengths of adventitious roots with an ROL barrier formation under aerated conditions (**Figure 2**). In *E. colona* and all three varieties of *E. crus-galli*, most of the adventitious roots over 51 mm-length formed an ROL barrier (**Figure 2**) and none of their basal parts stained blue (**Figures 3A–E** and **Supplementary Figures 1A–E**). However, blue-stained spots were occasionally observed at the root surface where lateral roots were predicted to emerge (**Supplementary Figures 1A–D**).

On the other hand, in *E. oryzicola* grown under aerated conditions, roots shorter than 150 mm-length rarely formed an ROL barrier (**Figure 2**, EO-WL). Interestingly, slit-like stained spots were observed along the basal part of the roots (**Figure 3F** and **Supplementary Figure 1F**). These roots were frequently shorter than 150 mm (**Supplementary Figure 2**, EO-WL). When *E. oryzicola* was grown in stagnant solutions for 14 days, the adventitious roots did not stain blue (**Supplementary Figure 3F**) and none were observed with slit-like stained spots. This staining pattern was similar to the other *Echinochloa* accessions under aerated (**Figures 3A–E**) and stagnant conditions (**Supplementary Figures 3A–E**). Over 40% of the roots, even those shorter than 50 mm, formed an ROL barrier (**Supplementary Figure 4**, EO-WL).

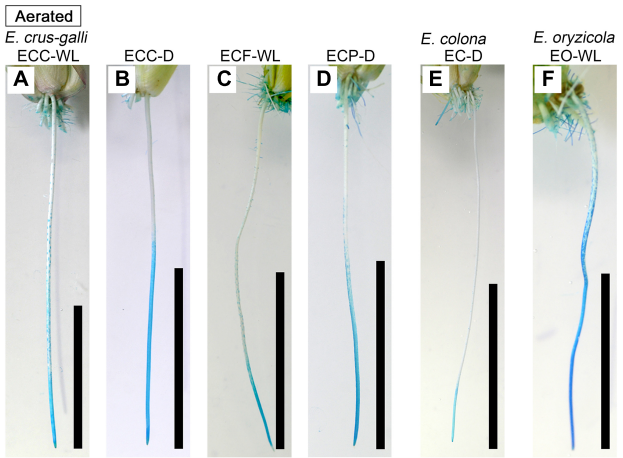

FIGURE 3 | Patterns of oxygen leakage from adventitious roots in *Echinochloa* accessions under aerated conditions. **(A–D)** *E. crus-galli*. **(E)** *E. colona*. **(F)** *E. oryzicola*. Oxygen leakage from adventitious roots (100–120 mm length) was visualized with methylene blue. When the roots formed an ROL barrier, the basal part of roots was colorless. Blue color indicates that the methylene blue is oxidized by oxygen leaking from adventitious root. Plants were grown in aerated nutrient solution for 10 days, and then continued in aerated solution for 14 days. Scale bars: 50 mm.

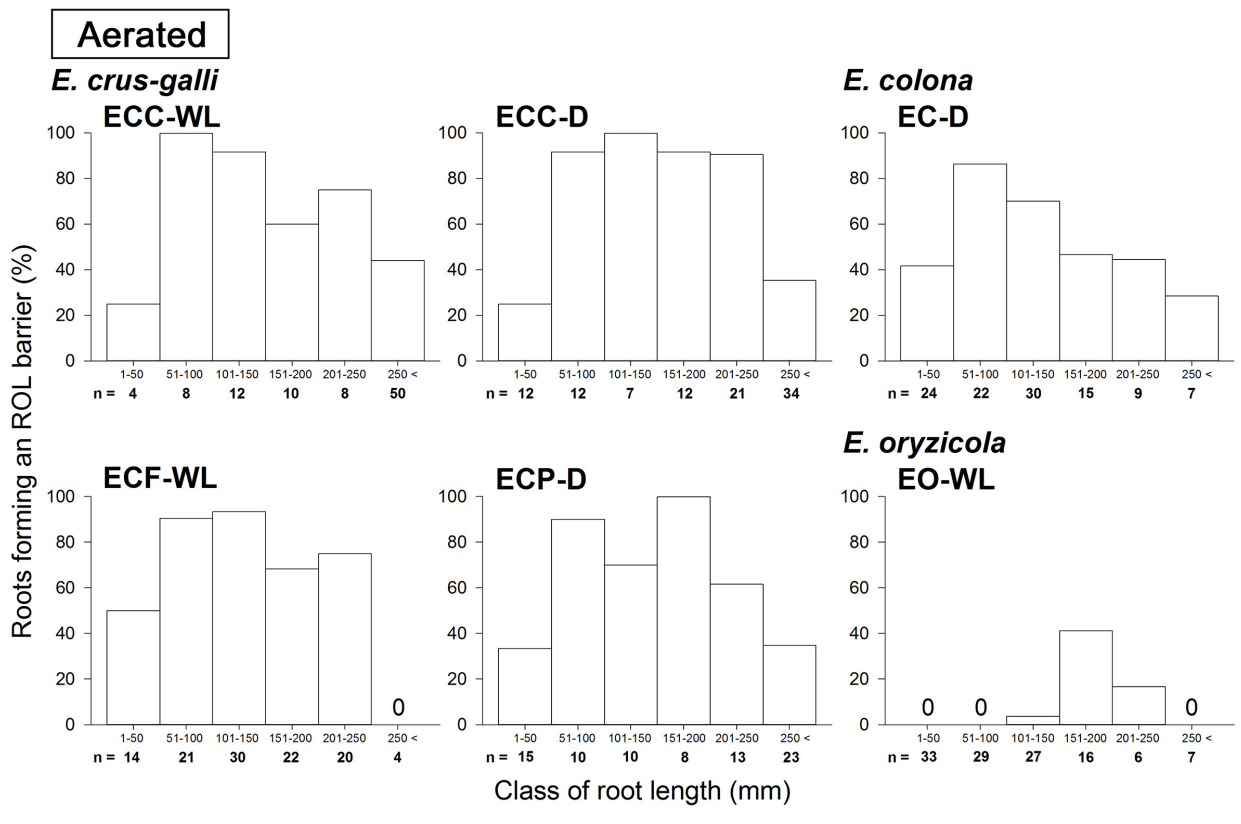

FIGURE 2 | Distributions of root length of adventitious roots with an ROL barrier in *Echinochloa* accessions under aerated conditions. The data in this figure are replotted from the data in **Figure 1** based on root length. All roots in five or six plants were used for each accession. Methylene blue was used to evaluate the formation of an ROL barrier in roots. Plants were grown in aerated nutrient solution for 10 days, and continued in aerated nutrient solution for 14 days.

To confirm the methylene blue results, oxygen leakage along 100–120 mm-long adventitious roots was also measured with an oxygen electrode. Under aerated conditions, *E. colona* and all three varieties of *E. crus-galli* constitutively formed a barrier to ROL along their adventitious roots (**Figure 4**). Both ecotypes of *E. crus-galli* var. *crus-galli* (ECC-WL and ECC-D) had a barrier to ROL along their adventitious roots. In each of the above accessions, ROL was substantially lower in the basal regions than in the more apical positions, consistent with the formation of an ROL barrier (**Figure 4**). The rate of ROL at the basal regions at 80 mm behind the root apex was extremely low (3.4–9.7 nmol O_2 m^{-2} s^{-1}). Interestingly, the adventitious roots in *E. oryzicola* (EO-WL) did not have an ROL barrier. The oxygen flux from the basal part to the root tips remained high (**Figure 4**). Moreover, the rate of ROL was 41.4 ± 3.9 nmol O_2 m^{-2} s^{-1} at 80 mm behind the root apex, which was still higher than the rates in the other wild *Echinochloa* accessions. The higher ROL from the basal part of roots agreed with the visualized oxygen leakage pattern in *E. oryzicola* (**Figure 3F** and **Supplementary Figure 1F**). Under stagnant conditions, these *Echinochloa* accessions including *E. oryzicola* formed a barrier to ROL along their adventitious roots (**Figure 4**). Even in *E. oryzicola*, the rate of ROL at the basal regions at 60–80 mm from the root apex was extremely low (0–1.8 nmol O_2 m^{-2} s^{-1}). Both the methylene blue and oxygen electrode results showed that *E. colona* and all three varieties of *E. crus-galli* constitutively formed a constitutive ROL barrier under aerated conditions, but *E. oryzicola*, whose main habitat is waterlogged rice paddies, did not. The ability to form a constitutive ROL barrier was different among these accessions, but it was not related to the habitat (waterlogged or well-drained field).

In each of the *Echinochloa* accessions, the root porosity was high (over 10%) under aerated nutrient solutions (**Table 2**). The root porosity of the waterlogged ecotype *E. crus-galli* var. *crus-galli* (ECC-WL) was slightly higher than that of the well-drained ecotype (ECC-D), but the difference was not significant ($P > 0.05$). The porosity was slightly lower in the accessions from waterlogged fields [i.e., *E. crus-galli* var. *formosensis* (ECF-WL) and *E. oryzicola* (EO-WL)], than in the other accessions, but the difference was not significant. Although these accessions constitutively formed air spaces in their roots under aerated conditions, root porosity did not seem to be related to their habitat. For most of the accessions, both total root number and root porosity were greater under stagnant conditions than under aerated conditions (**Table 2**). In addition, root DW increased dramatically (2.5- to 6.5-fold) under stagnant conditions (**Table 2**). The longest root lengths in the accessions from well-drained fields (ECC-D, ECP-D, and EC-D) were reduced under the stagnant conditions, but those of the accessions from waterlogged fields (ECF-WL and EO-WL) were not reduced significantly ($P > 0.05$), except for ECC-WL. Other parameters (leaf age, shoot length and shoot DW) in almost all of the accessions were not significantly suppressed under stagnant conditions. The percent control values (stagnant/aerated) of both shoot DW and root DW in the accession from a waterlogged field (ECC-WL) were significantly higher than those in the accession from a well-drained field (ECC-D) (**Table 2**). However, root porosity, total root number, longest root length, shoot length and leaf age were not significantly different between the two ecotypes.

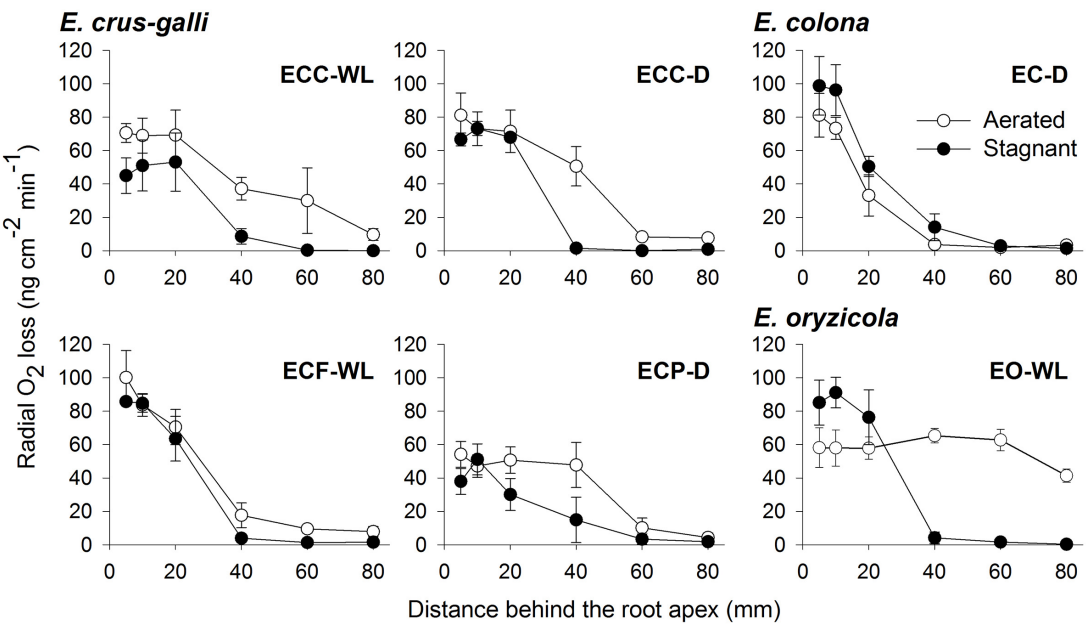

FIGURE 4 | Rates of radial oxygen loss (ROL) along adventitious roots in *Echinochloa* accessions under aerated or stagnant conditions. ROL along adventitious roots (100–120 mm length) was measured by Pt cylindrical electrode. Means ± SE. n = 3 or 4. Plants were grown in aerated nutrient solution for 10 days, and then transferred to deoxygenated stagnant 0.1% agar solution or continued in aerated solution for 13–15 days.

TABLE 2 | Plant growth and root porosity in *Echinochloa* accessions under aerated or stagnant conditions.

Accessions	Aerated	Stagnant	*t*-test	% control (stagnant/aerated) [§]
Leaf age				
ECC-WL	6.5 ± 0.1^{bc}	6.8 ± 0.2^{bc}	n.s.	103 ± 3^{ab}
ECC-D	4.5 ± 0.2^{d}	5.7 ± 0.5^{c}	n.s.	126 ± 11^{a}
ECF-WL	9.3 ± 0.2^{a}	8.6 ± 0.3^{a}	n.s.	92 ± 3^{b}
ECP-D	7.0 ± 0.3^{b}	7.2 ± 0.2^{b}	n.s.	103 ± 3^{ab}
EC-D	5.7 ± 0.3^{c}	5.9 ± 0.2^{c}	n.s.	103 ± 3^{ab}
EO-WL	7.0 ± 0.2^{b}	6.4 ± 0.0^{bc}	n.s.	92 ± 0^{b}
Shoot length (cm)				
ECC-WL	41.6 ± 0.8^{bc}	43.5 ± 0.6^{b}	n.s.	105 ± 2^{ab}
ECC-D	39.5 ± 3.4^{bc}	46.0 ± 0.9^{ab}	n.s.	116 ± 2^{a}
ECF-WL	59.5 ± 3.1^{a}	52.9 ± 1.6^{a}	n.s.	89 ± 3^{b}
ECP-D	47.3 ± 6.5^{ab}	47.0 ± 1.9^{ab}	n.s.	99 ± 4^{ab}
EC-D	30.5 ± 2.8^{c}	27.4 ± 2.5^{c}	n.s.	90 ± 8^{b}
EO-WL	44.3 ± 1.0^{abc}	41.5 ± 1.0^{b}	n.s.	94 ± 2^{b}
Longest root length (cm)				
ECC-WL	43.5 ± 1.8^{a}	24.0 ± 1.3^{a}	*	55 ± 3^{c}
ECC-D	45.5 ± 2.9^{a}	24.0 ± 0.4^{a}	*	53 ± 1^{c}
ECF-WL	22.8 ± 2.3^{c}	27.1 ± 0.9^{a}	n.s.	119 ± 4^{a}
ECP-D	34.6 ± 3.7^{ab}	24.6 ± 0.9^{a}	*	71 ± 3^{c}
EC-D	26.3 ± 2.5^{bc}	14.9 ± 2.1^{b}	*	57 ± 8^{c}
EO-WL	28.5 ± 1.4^{bc}	26.1 ± 1.4^{a}	n.s.	92 ± 5^{b}
Total root number				
ECC-WL	17 ± 1^{b}	37 ± 5^{bc}	*	216 ± 30^{a}
ECC-D	24 ± 2^{b}	33 ± 2^{bc}	*	138 ± 8^{ab}
ECF-WL	44 ± 6^{a}	63 ± 2^{a}	*	143 ± 5^{ab}
ECP-D	21 ± 1^{b}	36 ± 4^{bc}	*	176 ± 16^{ab}
EC-D	19 ± 3^{b}	25 ± 6^{c}	n.s.	135 ± 31^{ab}
EO-WL	42 ± 4^{a}	44 ± 2^{b}	n.s.	105 ± 4^{b}
Shoot DW (g)				
ECC-WL	0.37 ± 0.02^{bc}	0.97 ± 0.08^{ab}	*	266 ± 22^{a}
ECC-D	0.63 ± 0.11^{abc}	0.84 ± 0.04^{b}	n.s.	134 ± 7^{b}
ECF-WL	1.19 ± 0.26^{a}	1.21 ± 0.06^{a}	n.s.	101 ± 5^{b}
ECP-D	0.80 ± 0.17^{ab}	0.98 ± 0.05^{ab}	n.s.	123 ± 6^{b}
EC-D	0.13 ± 0.03^{c}	0.23 ± 0.07^{c}	n.s.	178 ± 56^{ab}
EO-WL	0.75 ± 0.04^{ab}	0.78 ± 0.05^{b}	n.s.	103 ± 7^{b}
Root DW (g)				
ECC-WL	0.08 ± 0.01^{bc}	0.54 ± 0.02^{a}	*	650 ± 29^{a}
ECC-D	0.13 ± 0.03^{abc}	0.44 ± 0.04^{a}	*	337 ± 31^{b}
ECF-WL	0.21 ± 0.05^{a}	0.63 ± 0.02^{a}	*	301 ± 11^{b}
ECP-D	0.13 ± 0.02^{abc}	0.52 ± 0.07^{a}	*	388 ± 49^{ab}
EC-D	0.04 ± 0.01^{c}	0.11 ± 0.05^{b}	n.s.	302 ± 124^{b}
EO-WL	0.17 ± 0.01^{ab}	0.43 ± 0.06^{a}	*	251 ± 34^{b}
Root porosity (%)				
ECC-WL	22.7 ± 1.8^{a}	30.8 ± 0.6^{a}	*	135 ± 3^{b}
ECC-D	18.9 ± 0.9^{ab}	24.1 ± 0.4^{a}	*	127 ± 2^{b}
ECF-WL	12.4 ± 1.7^{c}	30.6 ± 0.9^{a}	*	246 ± 7^{a}
ECP-D	15.8 ± 0.6^{bc}	29.6 ± 1.2^{a}	*	188 ± 7^{ab}
EC-D	17.2 ± 2.2^{abc}	28.1 ± 6.2^{a}	n.s.	164 ± 36^{b}
EO-WL	11.9 ± 0.4^{c}	28.9 ± 0.6^{a}	*	244 ± 5^{a}

The aerated and stagnant growth experiments were conducted simultaneously. Mean ± SE. n = 3 or 4. Different lower-case letters denote significant differences among wild Echinochloa accessions ($P < 0.05$, one-way ANOVA and then Tukey HSD for multiple comparisons). Asterisks indicate significant differences between means of aerated and stagnant conditions ($P < 0.05$, two-sample t-test) n.s., not significant. [§] % controls for each growth parameter were calculated as: [(value under stagnant conditions)/(average value under aerated conditions)] × 100. Plants were grown in aerated nutrient solution for 10 days, and then transferred to deoxygenated stagnant 0.1% agar solution or continued in aerated solution for 14 days.

Suberized Exodermis Was Found in the Roots Forming a Constitutive ROL Barrier

In *E. colona* and all three varieties of *E. crus-galli* that formed a constitutive ROL barrier under aerated conditions, the basal parts (15–25 mm below root–shoot junction) of the adventitious roots (100–120 mm length) were clearly surrounded by well suberized exodermis, as shown by the yellowish-green fluorescence (**Figures 5A–E**). Over 85% of their exodermal cells clearly developed suberin lamellae (**Figure 5Y**). However, part of the exodermis of *E. oryzicola* (a species that does not form a constitutive ROL barrier) lacked the yellowish-green fluorescence of suberin lamellae (**Figure 5F**). Passage cells, which are a type of exodermal cell that lacks suberin lamellae, were observed frequently (**Figure 5F**), so that the ratio of cells with suberin lamellae (45%) was significantly lower than the ratios of the other accessions (**Figure 5Y**, $P < 0.05$). On the other hand, orange/red (from staining of lignin) at the sclerenchyma was observed at the basal part of roots in *E. oryzicola* (**Figure 5R**); 87% of the sclerenchyma cells developed lignin deposits (**Figure 5Z**). Three of four accessions in *E. crus-galli* (ECC-D, ECF-WL and ECP-D) had well lignified sclerenchyma (**Figures 5N–P,Z**). Lignin deposits were not observed at the sclerenchyma in *E. crus-galli* var. *crus-galli* (ECC-WL) or *E. colona* (EC-D) (**Figures 5M,Q,Z**), although both accessions constitutively formed an ROL barrier. Not all the accessions that formed an ROL barrier had well-lignified sclerenchyma, but development of a constitutive ROL barrier was associated with the presence of suberized exodermis surrounding the roots.

Under stagnant conditions, the basal parts of the adventitious roots of in all wild *Echinochloa* accessions including *E. oryzicola*, were clearly surrounded by well suberized exodermis (**Figures 5G–L**). *E. oryzicola*, which inducibly formed an ROL barrier under stagnant conditions, had hardly any passage cells (**Figure 5L**) and over 97% of their exodermal cells clearly developed suberin lamellae (**Figure 5Y**). Lignin deposits at the sclerenchyma were also observed in all of the *Echinochloa* accessions (**Figures 5S–X**). In both *E. crus-galli* var. *crus-galli* (ECC-WL) and *E. colona* (EC-D), over 96% of the sclerenchyma cells developed lignin deposits (**Figure 5Z**). Development of an inducible ROL barrier in *E. oryzicola* was also associated with lignification at the exodermis.

Association of an Apoplastic Barrier With a Constitutive ROL Barrier

Because suberin lamellae help to form an apoplastic transport barrier that separates plant tissue from the surrounding conditions, we evaluated the ability of an apoplastic tracer (periodic acid) to penetrate the basal parts (15–25 mm below root–shoot junction) of 100–120 mm-long adventitious roots. In *E. colona* and all three varieties of *E. crus-galli* under aerated and stagnant conditions, the purple color of periodic acid was detected only in the epidermal cells (**Figures 6A–E,G–K**). Penetration of the tracer was blocked at the outside of the exodermis. In *E. oryzicola*, penetration of the tracer was also blocked at the outside of the exodermis under stagnant conditions (**Figure 6L**), but not under aerated conditions (**Figure 6F**). Thus, in all accessions, the basal part of roots that formed an ROL barrier developed an apoplastic barrier at the exodermis.

Casparian strips as well as suberin lamellae inhibit apoplastic transport at the exodermis. Like the suberin lamellae, Casparian strips were well developed in *E. colona* and all three varieties of *E. crus-galli* under aerated conditions (**Figures 7A–E** and **Supplementary Figures 5A–E**), but they were only patchy in *E. oryzicola* (**Figure 7F** and **Supplementary Figure 5F**). The number of cells that formed Casparian strips at the exodermis was also drastically lower in *E. oryzicola* than in the other *Echinochloa* accessions ($P < 0.05$) (**Figure 7M** and **Supplementary Figure 5M**). Under stagnant conditions, Casparian strips were clearly visible at the exodermis in *E. oryzicola* (**Figure 7L** and **Supplementary Figure 5L**) as well as the other *Echinochloa* accessions (**Figures 7G–K** and **Supplementary Figures 5G–K**). The number of cells that formed Casparian strips had risen to over 95% in *E. oryzicola* (**Figure 7M** and **Supplementary Figure 5M**). The development of Casparian strips at the exodermis was closely associated with the development of three structures: suberin lamellae, an apoplastic barrier against penetration of periodic acid and a constitutive ROL barrier.

DISCUSSION

A constitutive ROL barrier has been found in a limited number of wetland plants including one species of *Echinochloa* (*E. crus-galli* var. *mitis*) (McDonald et al., 2001, 2002). Here, by investigating all known annual wild *Echinochloa* species, we showed that *E. crus-galli* and *E. colona* had a constitutive ROL barrier under aerated conditions, but *E. oryzicola* did not (**Figures 1**, **4**). Although *E. crus-galli* has several varieties and ecotypes, each of these varieties and ecotypes, including those previously investigated by McDonald et al. (2001, 2002), formed a constitutive ROL barrier. Under aerated conditions, *E. colona* and all accessions of *E. crus-galli* developed suberin lamellae (**Figures 5A–E,Y**) and Casparian strips (**Figures 7A–E,M** and **Supplementary Figures 5A–E,M**) at the exodermis, but *E. crus-galli* var. *crus-galli* (ECC-WL in **Figure 5M**) and *E. colona* (EC-D in **Figure 5Q**) did not develop lignified sclerenchyma. These results are consistent with the reductions of ROL from the basal part of roots (40–80 mm from the root apex) (**Figure 4**). Previous studies of the inducible ROL barrier in rice suggest that exodermal suberization is important for formation of an ROL barrier because genes and metabolites associated with suberin biosynthesis are strongly upregulated under ROL barrier induction, whereas genes associated with lignin biosynthesis were not (Kulichikhin et al., 2014; Shiono et al., 2014b). A *Zea nicaraguensis* chromosome segment introgression line in maize (IL#468) that formed an inducible ROL barrier also developed a well suberized exodermis along the basal parts of adventitious roots (Watanabe et al., 2017). However, a lignified epidermis was not observed (Watanabe et al., 2017). Accumulation of suberin at the exodermis was closely associated with a reduction of oxygen leakage at the basal parts of roots in *Tabernaemontana juruana*, an Amazonian tree species (De Simone et al., 2003) and *Phragmites australis* (Soukup et al., 2007), although it is not

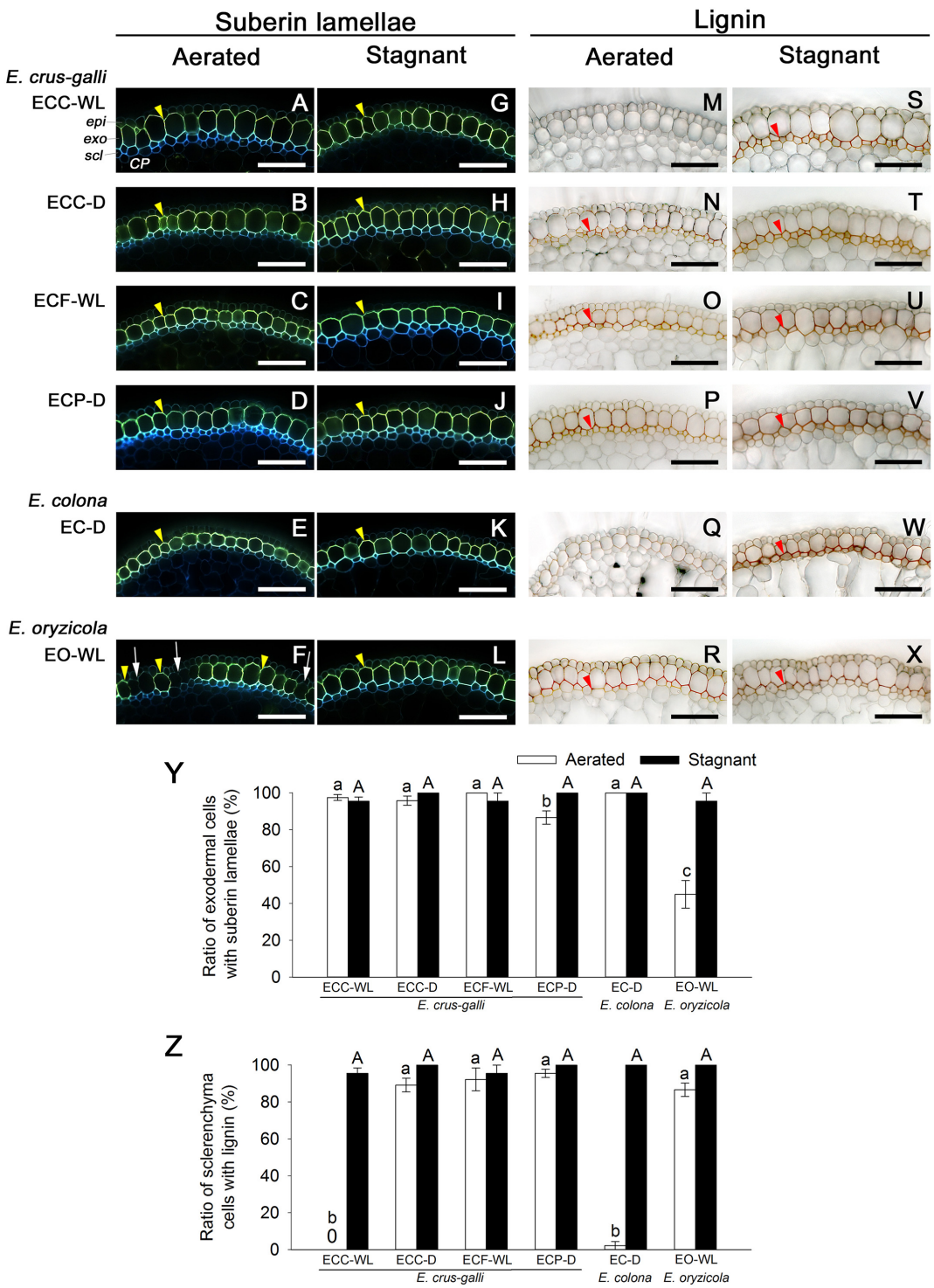

FIGURE 5 | Suberization and lignification in the outer part of roots in *Echinochloa* accessions under aerated or stagnant conditions. Suberin lamellae and lignin deposits were observed in the basal parts (15–25 mm below root–shoot junction) of adventitious roots of 100–120 mm length. **(A–L)** Suberin lamellae at the exodermis. Suberin lamellae are indicated as yellow-green fluorescence with Fluorol Yellow 088 (yellow arrowhead). White arrows denote the site of exodermis/hypodermis without suberin lamellae. Blue fluorescence indicates autofluorescence. **(M–X)** Lignin deposits at the sclerenchyma. Lignin is indicated as orange/red with phloroglucinol-HCl (red arrowhead). *CP*, cortical parenchyma; *epi*, epidermis; *exo*, exodermis; *scl*, sclerenchyma. Scale bars: 100 μm. **(Y)** Ratios of cell numbers observed suberin lamellae. **(Z)** Ratios of cell numbers observed lignin. Means ± SE. $n = 4$. Different lower-case letters denote significant differences among *Echinochloa* accessions ($P < 0.05$, Fisher's exact test for multiple comparisons). Plants were grown in aerated nutrient solution for 10 days, and then transferred to deoxygenated stagnant 0.1% agar solution or continued in aerated solution for 14 days.

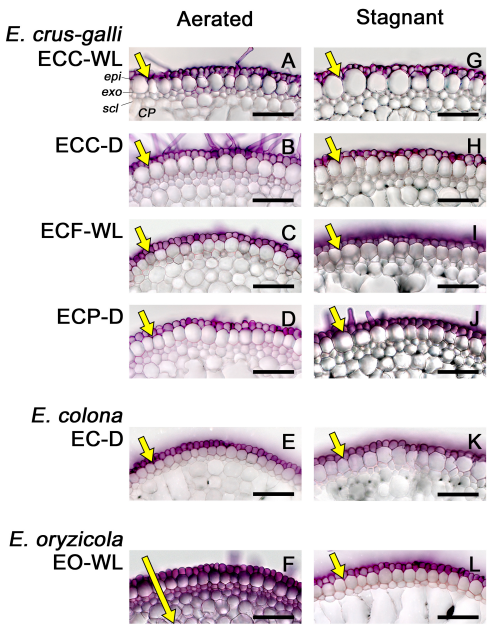

FIGURE 6 | Permeability of the exodermis to an apoplastic tracer (periodic acid) in *Echinochloa* accessions under aerated or stagnant conditions. **(A–F)** Aerated conditions. **(G–L)** Stagnant conditions. The permeability of the exodermis was evaluated at the basal parts (17.5–22.5 mm below root–shoot junction) of adventitious roots of 100–120 mm length. Purple color indicates that periodic acid penetrated into root tissues. The length of yellow arrows indicates the extent of penetration. Plants were grown in aerated nutrient solution for 10 days, and then transferred to deoxygenated stagnant 0.1% agar solution or continued in aerated solution for 14 days. *CP*, cortical parenchyma; *epi*, epidermis; *exo*, exodermis; *scl*, sclerenchyma. Scale bars: 100 μm.

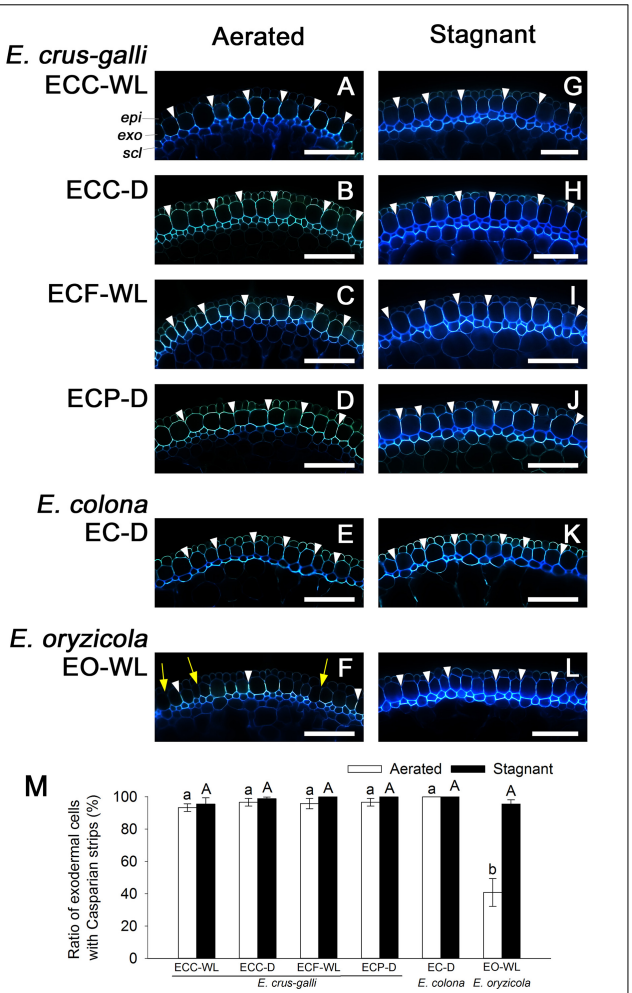

FIGURE 7 | Casparian strips at the exodermis in *Echinochloa* accessions that were grown under aerated or stagnant conditions. Casparian strips (stained by berberine-aniline blue) were observed in the basal parts (15–25 mm below root–shoot junction) of adventitious roots of 100–120 mm length. **(A–L)** Casparian strips at the exodermis. Casparian strips are indicated as a bright white fluorescence with berberine-aniline blue. Representative Casparian strips are shown with white arrowheads. Yellow arrows denote the region of exodermis/hypodermis without Casparian strips. Blue fluorescence indicates autofluorescence. *CP*, cortical parenchyma; *epi*, epidermis; *exo*, exodermis; *scl*, sclerenchyma. Scale bars: 100 μm. **(M)** Ratios of cell numbers observed Casparian strips. Means ± SE. $n = 4$. Different lower-case letters denote significant differences among *Echinochloa* accessions ($P < 0.05$, Fisher's exact test for multiple comparisons). Plants were grown in aerated nutrient solution for 10 days, and then transferred to deoxygenated stagnant 0.1% agar solution or continued in aerated solution for 14 days.

known whether these species form inducible or constitutive ROL barriers. *E. oryzicola* developed lignified sclerenchyma under aerated conditions (**Figures 5R,Z**) although this did not reduce oxygen leakage from basal part of roots (40–80 mm from the root apex) (EO-WL in **Figure 4**) and did not block the infiltration of an apoplastic tracer (**Figure 6F**). Although lignified sclerenchyma was not observed in *E. crus-galli* var. *crus-galli* and *E. colona* (**Figures 5M,Q,Z**), oxygen leakage from the basal part of the roots was impeded (ECC-WL and EC-D in **Figure 4**) and infiltration of the apoplastic tracer was blocked (**Figures 6A,E**). Additionally, when *E. oryzicola* formed an inducible ROL barrier under stagnant conditions (**Figures 1**, **4**), its exodermis also had well suberized cells (**Figures 5L,Y**) and Casparian strips (**Figures 7L,M** and **Supplementary Figures 5L,M**). The *E. oryzicola* exodermis blocked the infiltration of the apoplastic tracer (**Figure 6L**). Lignin has roles in providing mechanical support and plant defense due to its resistance to degradation (Campbell and Sederoff, 1996; Schreiber et al., 1999; Barros et al., 2015). Some of the observed lignification at the sclerenchyma might provide mechanical support and plant defense, but the lignification does not appear to contribute to an ROL barrier. Like previous findings on inducible ROL barriers, our results suggest that suberin, but not lignin, is an important component of a constitutive ROL barriers.

Oxygen Leakage Through Areas of Passage Cells (Windows)

Passage cells in the outer part of roots, which lack suberin lamellae, are found in some roots that are leaky to oxygen (Armstrong et al., 2000; Abiko et al., 2012). Areas of passage cells where oxygen leaks and lateral roots emerge have been called "windows" (Armstrong et al., 2000). Under aerated conditions, *E. oryzicola* does not develop an ROL barrier, as the basal part

of its roots lost a substantial amount of oxygen (**Figure 4**). In addition, oxygen was found to leak from narrow slits in the basal part of roots (**Figure 3F** and **Supplementary Figure 1**). In *E. oryzicola* under aerated conditions, in agreement with its weak ROL barrier (**Figure 4**), most (55%) of its exodermal cells at the basal parts of roots were passage cells lacking suberin lamellae (**Figures 5F,Y**). Although the basal part of roots of maize species (including inbred line Mi29) grown in stagnant conditions have a suberized exodermis, they lose a substantial amount of oxygen, apparently because 4–15% of the exodermal cells are passage cells that lack suberin lamellae (Abiko et al., 2012). The *E. oryzicola* grown in aerated conditions had 4–14 times more passage cells than did Mi29, which appears to be the reason for the leakiness of its roots. Some of the other accessions with a constitutive barrier (i.e., with low ROL) also showed a few spots of methylene blue staining along the adventitious roots (**Figures 3A–D** and **Supplementary Figure 1**). These spots seemed to be the sites where lateral roots emerged (**Supplementary Figure 1**). Similarly, in *Phragmites australis*, oxygen was found to leak from areas of passage cells where the lateral root emerges (Armstrong et al., 2000). In agreement with the observations of Armstrong et al. (2000), the sites of lateral root emergence in *E. crus-galli* var. *crus-galli* (ECC-WL and ECC-D) and *E. crus-galli* var. *praticola* (ECP-D) under aerated conditions lacked suberin lamellae at the exodermis (**Supplementary Figure 6**). These observations support the idea that suberin lamellae impede the leakage of oxygen from the roots.

Distribution of *Echinochloa* Species With an ROL Barrier

The ability to form a constitutive or inducible barrier is considered an adaptation to waterlogging (Colmer, 2003b). Two of the *E. crus-galli* accessions that came from waterlogged fields (ECC-WL and ECF-WL) formed an ROL barrier under aerated conditions (**Figures 1**, **4**). However, *E. oryzicola* whose main habitat is waterlogged rice paddies (Yabuno, 1984; Yamasue, 2001), did not have a constitutive ROL barrier under aerated conditions (**Figures 1**, **4**). When *E. oryzicola* was grown in stagnant conditions for 7 days, 40% of the roots formed an ROL barrier (EO-WL in **Supplementary Figure 7**). At 14 days after stagnant treatment, 73% of the roots formed an ROL barrier (EO-WL in **Figure 1**). Like rice, *E. oryzicola* had an inducible ROL barrier under stagnant conditions (EO-WL in **Figures 1**, **4** and **Supplementary Figure 7**). This might help *E. oryzicola* to adapt to waterlogged rice paddy fields.

So far, ROL barriers have been found only in wetland species (McDonald et al., 2002; Colmer, 2003b). However, some of the accessions from well-drained fields [two of *E. crus-galli* (ECC-D and ECP-D) and *E. colona* (EC-D)] constitutively formed an ROL barrier (**Figures 1**, **4**). Moreover, these accessions had well developed apoplastic barriers at the exodermis (**Figures 6B,D,E**) with suberin (**Figures 5B,D,E**) and Casparian strips (**Figures 7B,D,E** and **Supplementary Figures 5B,D,E**). Our previous finding that a rice mutant (*reduced culm number1*) that lacks both suberin lamellae and Casparian strips did not block the infiltration of apoplastic tracers (periodic acid and berberine) (Shiono et al., 2014a), suggests that exodermal suberization and Casparian strips act as an apoplastic barrier. The apoplastic barrier at the exodermis serves to protect the plant from various environmental stresses, such as mycorrhizal infections (Damus et al., 1997), water loss to dry soil (Aloni et al., 1998) and penetration of ions (e.g., Na^+) (Enstone et al., 2003; Ranathunge et al., 2011). The constitutive apoplastic barriers in these *Echinochloa* accessions collected from well-drained fields might help to adapt to waterlogging and other environmental stresses because they prepare the plants for environmental changes.

In most annual wild *Echinochloa* that form a constitutive ROL barrier, formation of the barrier was closely associated with exodermal suberization. A phylogenic analysis suggests that *E. crus-galli* (hexaploid) was derived from *E. oryzicola* (tetraploid) (Aoki and Yamaguchi, 2008, 2009). *E. oryzicola* is limited to waterlogged paddies, while *E. crus-galli* has several varieties that are adapted to wet and dry areas (Yamasue, 2001; Rao et al., 2007; Tanesaka et al., 2010). *E. crus-galli* may have diversified its habitat by acquiring a constitutive apoplastic barrier at the exodermis. Although it appears likely that a constitutive apoplastic barrier helps a plant to adapt to environmental stresses such as drought, high salinity and waterlogging, further studies using a larger number of wild accessions are needed to confirm this. *Echinochloa* appears to be well-suited for such studies because of its wide variety of species adapted to different environmental conditions. Such studies will lead to a better understanding of *Echinochloa*'s high adaptability to various environmental conditions and thus to develop better measures for their control.

AUTHOR CONTRIBUTIONS

ME and KS designed the experiments and wrote the draft of article. KS wrote the article and supervised the experiments. ME performed the most of the experiments and analyses.

FUNDING

This work was partly supported by JSPS KAKENHI (JP16KK0173 and JP17K15211 to KS).

ACKNOWLEDGMENTS

Prof. Toshihito Yoshioka (Fukui Prefectural University) and Dr. Yuichiro Nakayama (Osaka Prefecture University) are thanked for providing seeds of *Echinochloa* accessions for the experiments. Ms. Sumiyo Yamada is thanked for her technical support with the experiments.

SUPPLEMENTARY MATERIAL

The Supplementary Material for this article can be found online at: https://www.frontiersin.org/articles/10.3389/fpls.2019.00254/full#supplementary-material

REFERENCES

Abiko, T., Kotula, L., Shiono, K., Malik, A. I., Colmer, T. D., and Nakazono, M. (2012). Enhanced formation of aerenchyma and induction of a barrier to radial oxygen loss in adventitious roots of *Zea nicaraguensis* contribute to its waterlogging tolerance as compared with maize (*Zea mays* ssp. *mays*). *Plant Cell Environ.* 35, 1618–1630. doi: 10.1111/j.1365-3040.2012.02513.x

Aloni, R., Enstone, D. E., and Peterson, C. A. (1998). Indirect evidence for bulk water flow in root cortical cell walls of three dicotyledonous species. *Planta* 207, 1–7. doi: 10.1007/s004250050449

Aoki, D., and Yamaguchi, H. (2008). Genetic relationship between *Echinochloa crus-galli* and *Echinochloa oryzicola* accessions inferred from internal transcribed spacer and chloroplast DNA sequences. *Weed Biol. Manag.* 8, 233–242. doi: 10.1111/j.1445-6664.2008.00303.x

Aoki, D., and Yamaguchi, H. (2009). Oryza *sh4* gene homologue represents homoeologous genomic copies in polyploid *Echinochloa*. *Weed Biol. Manag.* 9, 225–233. doi: 10.1111/j.1445-6664.2009.00343.x

Armstrong, J., and Armstrong, W. (2005). Rice: sulfide-induced barriers to root radial oxygen loss, Fe^{2+} and water uptake, and lateral root emergence. *Ann. Bot.* 96, 625–638. doi: 10.1093/aob/mci215

Armstrong, W. (1979). Aeration in higher plants. *Adv. Bot. Res.* 7, 225–332. doi: 10.1016/S0065-2296(08)60089-0

Armstrong, W. (1994). Polarographic oxygen electrodes and their use in plant aeration studies. *Proc. R. Soc. Edinb. Sec. B. Biol. Sci.* 102, 511–527. doi: 10.1017/S0269727000014548

Armstrong, W., Cousins, D., Armstrong, J., Turner, D. W., and Beckett, P. M. (2000). Oxygen distribution in wetland plant roots and permeability barriers to gas-exchange with the rhizosphere: a microelectrode and modelling study with *Phragmites australis*. *Ann. Bot.* 86, 687–703. doi: 10.1006/anbo.2000.1236

Armstrong, W., and Wright, E. J. (1975). Radial oxygen loss from roots: the theoretical basis for the manipulation of flux data obtained by the cylindrical platinum electrode technique. *Physiol. Plant.* 35, 21–26. doi: 10.1111/j.1399-3054.1975.tb03861.x

Barrett, S. C. H. (1983). Crop mimicry in weeds. *Econ. Bot.* 37, 255–282. doi: 10.1007/BF02858881

Barros, J., Serk, H., Granlund, I., and Pesquet, E. (2015). The cell biology of lignification in higher plants. *Ann. Bot.* 115, 1053–1074. doi: 10.1093/aob/mcv046

Brundrett, M. C., Enstone, D. E., and Peterson, C. A. (1988). A berberine-aniline blue fluorescent staining procedure for suberin, lignin, and callose in plant tissue. *Protoplasma* 146, 133–142. doi: 10.1007/BF01405922

Brundrett, M. C., Kendrick, B., and Peterson, C. A. (1991). Efficient lipid staining in plant material with sudan red 7B or fluoral yellow 088 in polyethylene glycol-glycerol. *Biotech. Histochem.* 66, 111–116. doi: 10.3109/10520299109110562

Campbell, M. M., and Sederoff, R. R. (1996). Variation in lignin content and composition: mechanisms of control and implications for the genetic improvement of plants. *Plant Physiol.* 110, 3–13. doi: 10.1104/pp.110.1.3

Cheng, H., Chen, D.-T., Tam, N. F.-Y., Chen, G.-Z., Li, S.-Y., and Ye, Z.-H. (2012). Interactions among Fe^{2+}, S^{2-}, and Zn^{2+} tolerance, root anatomy, and radial oxygen loss in mangrove plants. *J. Exp. Bot.* 63, 2619–2630. doi: 10.1093/jxb/err440

Colmer, T. D. (2003a). Aerenchyma and an inducible barrier to radial oxygen loss facilitate root aeration in upland, paddy and deep-water rice (*Oryza sativa* L.). *Ann. Bot.* 91, 301–309. doi: 10.1093/aob/mcf114

Colmer, T. D. (2003b). Long-distance transport of gases in plants: a perspective on internal aeration and radial oxygen loss from roots. *Plant Cell Environ.* 26, 17–36. doi: 10.1046/j.1365-3040.2003.00846.x

Colmer, T. D., Cox, M. C. H., and Voesenek, L. A. C. J. (2006). Root aeration in rice (*Oryza sativa*): evaluation of oxygen, carbon dioxide, and ethylene as possible regulators of root acclimatizations. *New Phytol.* 170, 767–778. doi: 10.1111/j.1469-8137.2006.01725.x

Colmer, T. D., Gibberd, M. R., Wiengweera, A., and Tinh, T. K. (1998). The barrier to radial oxygen loss from roots of rice (*Oryza sativa* L.) is induced by growth in stagnant solution. *J. Exp. Bot.* 49, 1431–1436. doi: 10.1093/jxb/49.325.1431

Damus, M., Peterson, R. L., Enstone, D. E., and Peterson, C. A. (1997). Modifications of cortical cell walls in roots of seedless vascular plants. *Bot. Acta* 110, 190–195. doi: 10.1111/j.1438-8677.1997.tb00628.x

De Simone, O., Haase, K., Müller, E., Junk, W. J., Hartmann, K., Schreiber, L., et al. (2003). Apoplasmic barriers and oxygen transport properties of hypodermal cell walls in roots from four Amazonian tree species. *Plant Physiol.* 132, 206–217. doi: 10.1104/pp.102.014902

Enstone, D. E., Peterson, C. A., and Ma, F. (2003). Root endodermis and exodermis: structure, function, and responses to the environment. *J. Plant Growth Regul.* 21, 335–351. doi: 10.1007/s00344-003-0002-2

Ernst, W. H. O. (1990). Ecophysiology of plants in waterlogged and flooded environments. *Aquat. Bot.* 38, 73–90. doi: 10.1016/0304-3770(90)90099-7

Garthwaite, A. J., von Bothmer, R., and Colmer, T. D. (2003). Diversity in root aeration traits associated with waterlogging tolerance in the genus *Hordeum*. *Funct. Plant Biol.* 30, 875–889. doi: 10.1071/FP03058

Graça, J. (2015). Suberin: the biopolyester at the frontier of plants. *Front. Chem.* 3:62. doi: 10.3389/fchem.2015.00062

Jackson, M. B., Fenning, T. M., Drew, M. C., and Saker, L. R. (1985). Stimulation of ethylene production and gas-space (aerenchyma) formation in adventitious roots of *Zea mays* L. by small partial pressures of oxygen. *Planta* 165, 486–492. doi: 10.1007/BF00398093

Jensen, W. A. (1962). *Botanical Histochemistry: Principles and Practice*. San Francisco, CA: WH Freeman and Co.

Katayama, T. (1961). Studies on the intercellular spaces in rice. I. *Jpn. J. Crop Sci.* 29, 229–233. doi: 10.1626/jcs.29.229

Kawai, M., Samarajeewa, P. K., Barrero, R. A., Nishiguchi, M., and Uchimiya, H. (1998). Cellular dissection of the degradation pattern of cortical cell death during aerenchyma formation of rice roots. *Planta* 204, 277–287. doi: 10.1007/s004250050257

Kraehmer, H., Jabran, K., Mennan, H., and Chauhan, B. S. (2016). Global distribution of rice weeds – a review. *Crop Prot.* 80, 73–86. doi: 10.1016/j.cropro.2015.10.027

Kreuzwieser, J., Papadopoulou, E., and Rennenberg, H. (2004). Interaction of flooding with carbon metabolism of forest trees. *Plant Biol.* 6, 299–306. doi: 10.1055/s-2004-817882

Kulichikhin, K., Yamauchi, T., Watanabe, K., and Nakazono, M. (2014). Biochemical and molecular characterization of rice (*Oryza sativa* L.) roots forming a barrier to radial oxygen loss. *Plant Cell Environ.* 37, 2406–2420. doi: 10.1111/pce.12294

Laanbroek, H. J. (1990). Bacterial cycling of minerals that affect plant growth in waterlogged soils: a review. *Aquat. Bot.* 38, 109–125. doi: 10.1016/0304-3770(90)90101-P

Lamers, L. P. M., Tomassen, H. B. M., and Roelofs, J. G. M. (1998). Sulfate-induced entrophication and phytotoxicity in freshwater wetlands. *Environ. Sci. Technol.* 32, 199–205. doi: 10.1021/es970362f

Lux, A., Morita, S., Abe, J., and Ito, K. (2005). An improved method for clearing and staining free-hand sections and whole-mount samples. *Ann. Bot.* 96, 989–996. doi: 10.1093/aob/mci266

Mano, Y., Omori, F., Takamizo, T., Kindiger, B., Bird, R. M., and Loaisiga, C. H. (2006). Variation for root aerenchyma formation in flooded and non-flooded maize and teosinte seedlings. *Plant Soil* 281, 269–279. doi: 10.1007/s11104-005-4268-y

Manzur, M. E., Grimoldi, A. A., Insausti, P., and Striker, G. G. (2015). Radial oxygen loss and physical barriers in relation to root tissue age in species with different types of aerenchyma. *Funct. Plant Biol.* 42, 9–17. doi: 10.1071/FP14078

McDonald, M. P., Galwey, N. W., and Colmer, T. D. (2001). Waterlogging tolerance in the tribe Triticeae: the adventitious roots of *Critesion marinum* have a relatively high porosity and a barrier to radial oxygen loss. *Plant Cell Environ.* 24, 585–596. doi: 10.1046/j.0016-8025.2001.00707.x

McDonald, M. P., Galwey, N. W., and Colmer, T. D. (2002). Similarity and diversity in adventitious root anatomy as related to root aeration among a range of wetland and dryland grass species. *Plant Cell Environ.* 25, 441–451. doi: 10.1046/j.0016-8025.2001.00817.x

Naseer, S., Lee, Y., Lapierre, C., Franke, R., Nawrath, C., and Geldner, N. (2012). Casparian strip diffusion barrier in *Arabidopsis* is made of a lignin polymer without suberin. *Proc. Natl. Acad. Sci. U.S.A.* 109, 10101–10106. doi: 10.1073/pnas.1205726109

Nishiuchi, S., Yamauchi, T., Takahashi, H., Kotula, L., and Nakazono, M. (2012). Mechanisms for coping with submergence and waterlogging in rice. *Rice* 5:2. doi: 10.1186/1939-8433-5-2

Pecková, E., Tylová, E., and Soukup, A. (2016). Tracing root permeability: comparison of tracer methods. *Biol. Plant.* 60, 695–705. doi: 10.1007/s10535-016-0634-2

Ponnamperuma, F. N. (1984). "Effects of flooding on soils," in *Flooding and Plant Growth*, ed. T. T. Kozlowski (New York, NY: Academic press), 9–45. doi: 10.1016/B978-0-12-424120-6.50007-9

R Core Team (2018). *R: A Language and Environment for Statistical Computing*. Vienna: R Foundation for Statistical Computing.

Ranathunge, K., Lin, J., Steudle, E., and Schreiber, L. (2011). Stagnant deoxygenated growth enhances root suberization and lignifications, but differentially affects water and NaCl permeabilities in rice (*Oryza sativa* L.) roots. *Plant Cell Environ.* 34, 1223–1240. doi: 10.1111/j.1365-3040.2011.02318.x

Rao, A. N., Johnson, D. E., Sivaprasad, B., Ladha, J. K., and Mortimer, A. M. (2007). Weed management in direct-seeded rice. *Adv. Agron.* 93, 153–255. doi: 10.1016/s0065-2113(06)93004-1

Raskin, I. (1983). A method for measuring leaf volume, density, thickness, and internal gas volume. *HortScience* 18, 698–699.

Schreiber, L., and Franke, R. B. (2011). "Endodermis and exodermis in roots," in *eLS* (Chichester: John Wiley & Sons Ltd.). doi: 10.1002/9780470015902.a0002086.pub2

Schreiber, L., Hartmann, K., Skrabs, M., and Zeier, J. (1999). Apoplastic barriers in roots: chemical composition of endodermal and hypodermal cell walls. *J. Exp. Bot.* 50, 1267–1280. doi: 10.1093/jxb/50.337.1267

Shiono, K., Ando, M., Nishiuchi, S., Takahashi, H., Watanabe, K., Nakamura, M., et al. (2014a). RCN1/OsABCG5, an ATP-binding cassette (ABC) transporter, is required for hypodermal suberization of roots in rice (*Oryza sativa*). *Plant J.* 80, 40–51. doi: 10.1111/tpj.12614

Shiono, K., Yamauchi, T., Yamazaki, S., Mohanty, B., Malik, A. I., Nagamura, Y., et al. (2014b). Microarray analysis of laser-microdissected tissues indicates the biosynthesis of suberin in the outer part of roots during formation of a barrier to radial oxygen loss in rice (*Oryza sativa*). *J. Exp. Bot.* 65, 4795–4806. doi: 10.1093/jxb/eru235

Shiono, K., Ogawa, S., Yamazaki, S., Isoda, H., Fujimura, T., Nakazono, M., et al. (2011). Contrasting dynamics of radial O_2-loss barrier induction and aerenchyma formation in rice roots of two lengths. *Ann. Bot.* 107, 89–99. doi: 10.1093/aob/mcq221

Soukup, A., Armstrong, W., Schreiber, L., Franke, R., and Votrubová, O. (2007). Apoplastic barriers to radial oxygen loss and solute penetration: a chemical and functional comparison of the exodermis of two wetland species, *Phragmites australis* and *Glyceria maxima*. *New Phytol.* 173, 264–278. doi: 10.1111/j.1469-8137.2006.01907.x

Soukup, A., Votrubová, O., and Čížková, H. (2002). Development of anatomical structure of roots of *Phragmites australis*. *New Phytol.* 153, 277–287. doi: 10.1046/j.0028-646X.2001.00317.x

Tanesaka, E., Ohno, T., and Yamaguchi, H. (2010). Species diversity of the genus *Echinochloa* (Poaceae), native to eastern Australia: a focus on their habitat and the threat of exotic species. *J. Crop Res.* 55, 13–17. doi: 10.18964/jcr.55.0_13

Thomson, C. J., Armstrong, W., Waters, I., and Greenway, H. (1990). Aerenchyma formation and associated oxygen movement in seminal and nodal roots of wheat. *Plant Cell Environ.* 13, 395–403. doi: 10.1111/j.1365-3040.1990.tb02144.x

Visser, E. J. W., Colmer, T. D., Blom, C. W. P. M., and Voesenek, L. A. C. J. (2000). Changes in growth, porosity, and radial oxygen loss from adventitious roots of selected mono- and dicotyledonous wetland species with contrasting types of aerenchyma. *Plant Cell Environ.* 23, 1237–1245. doi: 10.1046/j.1365-3040.2000.00628.x

Watanabe, K., Nishiuchi, S., Kulichikhin, K., and Nakazono, M. (2013). Does suberin accumulation in plant roots contribute to waterlogging tolerance? *Front. Plant Sci.* 4:178. doi: 10.3389/fpls.2013.00178

Watanabe, K., Takahashi, H., Sato, S., Nishiuchi, S., Omori, F., Malik, A. I., et al. (2017). A major locus involved in the formation of the radial oxygen loss barrier in adventitious roots of teosinte *Zea nicaraguensis* is located on the short-arm of chromosome 3. *Plant Cell Environ.* 40, 304–316. doi: 10.1111/pce.12849

Wiengweera, A., Greenway, H., and Thomson, C. J. (1997). The use of agar nutrient solution to simulate lack of convection in waterlogged soils. *Ann. Bot.* 80, 115–123. doi: 10.1006/anbo.1996.0405

Yabuno, T. (1962). Cytotaxonomic studies on the two cultivated species and the wild relatives in the genus *Echinochloa*. *Cytologia* 27, 296–305. doi: 10.1508/cytologia.27.296

Yabuno, T. (1984). A biosystematic study on *Echinochloa oryzoides* (Ard.) Fritsch. *Cytologia* 49, 673–678. doi: 10.1508/cytologia.49.673

Yamasue, Y. (2001). Strategy of *Echinochloa oryzicola* Vasing. for survival in flooded rice. *Weed Biol. Manag.* 1, 28–36. doi: 10.1046/j.1445-6664.2001.00008.x

Zeier, J., Ruel, K., Ryser, U., and Schreiber, L. (1999). Chemical analysis and immunolocalisation of lignin and suberin in endodermal and hypodermal/rhizodermal cell walls of developing maize (*Zea mays* L.) primary roots. *Planta* 209, 1–12. doi: 10.1007/s004250050601

Conflict of Interest Statement: The authors declare that the research was conducted in the absence of any commercial or financial relationships that could be construed as a potential conflict of interest.

frontiers in Plant Science

ORIGINAL RESEARCH
published: 26 March 2019
doi: 10.3389/fpls.2019.00339

Flooding Responses on Grapevine: A Physiological, Transcriptional, and Metabolic Perspective

*Benedetto Ruperti[1,2,3], Alessandro Botton[1,2,3], Francesca Populin[1], Giulia Eccher[1], Matteo Brilli[4], Silvia Quaggiotti[1,3], Sara Trevisan[1], Nadia Cainelli[1], Paola Guarracino[5], Elisabetta Schievano[5] and Franco Meggio[1,2]**

[1] Department of Agronomy, Food, Natural Resources, Animals and Environment, University of Padova, Legnaro, Italy, [2] Interdepartmental Research Centre for Viticulture and Enology, University of Padova, Conegliano, Italy, [3] CRIBI Biotechnology Centre, University of Padova, Padova, Italy, [4] Department of Biosciences, University of Milan, Milan, Italy, [5] Department of Chemical Sciences, University of Padova, Padova, Italy

OPEN ACCESS

Edited by:
Iduna Arduini,
University of Pisa, Italy

Reviewed by:
Chiara Pucciariello,
Sant'Anna School of Advanced Studies, Italy
Francesco Licausi,
University of Pisa, Italy
Li Song,
Yangzhou University, China

***Correspondence:**
Franco Meggio
franco.meggio@unipd.it

Specialty section:
This article was submitted to Plant Abiotic Stress, a section of the journal Frontiers in Plant Science

Received: 03 December 2018
Accepted: 05 March 2019
Published: 26 March 2019

Citation:
Ruperti B, Botton A, Populin F, Eccher G, Brilli M, Quaggiotti S, Trevisan S, Cainelli N, Guarracino P, Schievano E and Meggio F (2019) Flooding Responses on Grapevine: A Physiological, Transcriptional, and Metabolic Perspective. Front. Plant Sci. 10:339. doi: 10.3389/fpls.2019.00339

Studies on model plants have shown that temporary soil flooding exposes roots to a significant hypoxic stress resulting in metabolic re-programming, accumulation of toxic metabolites and hormonal imbalance. To date, physiological and transcriptional responses to flooding in grapevine are poorly characterized. To fill this gap, we aimed to gain insights into the transcriptional and metabolic changes induced by flooding on grapevine roots (K5BB rootstocks), on which cv Sauvignon blanc (*Vitis vinifera* L.) plants were grafted. A preliminary experiment under hydroponic conditions enabled the identification of transiently and steadily regulated hypoxia-responsive marker genes and drafting a model for response to oxygen deprivation in grapevine roots. Afterward, over two consecutive vegetative seasons, flooding was imposed to potted vines during the late dormancy period, to mimick the most frequent waterlogging events occurring in the field. Untargeted transcriptomic and metabolic profiling approaches were applied to investigate early responses of grapevine roots during exposure to hypoxia and subsequent recovery after stress removal. The initial hypoxic response was marked by a significant increase of the hypoxia-inducible metabolites ethanol, GABA, succinic acid and alanine which remained high also 1 week after recovery from flooding with the exception of ethanol that leveled off. Transcriptomic data supported the metabolic changes by indicating a substantial rearrangement of primary metabolic pathways through enhancement of the glycolytic and fermentative enzymes and of a subset of enzymes involved in the TCA cycle. GO and KEGG pathway analyses of differentially expressed genes showed a general down-regulation of brassinosteroid, auxin and gibberellin biosynthesis in waterlogged plants, suggesting a general inhibition of root growth and lateral expansion. During recovery, transcriptional activation of gibberellin biosynthetic genes and down-regulation of the metabolic ones may support a role for gibberellins in signaling grapevine rootstocks waterlogging metabolic and hormonal changes to the above ground plant. The significant internode elongation measured upon budbreak during recovery in plants that had experienced flooding supported this

hypothesis. Overall integration of these data enabled us to draft a first comprehensive view of the molecular and metabolic pathways involved in grapevine's root responses highlighting a deep metabolic and transcriptomic reprogramming during and after exposure to waterlogging.

Keywords: waterlogging, hypoxia, root, transcriptome, gene expression, *Vitis*

INTRODUCTION

During the past decade unprecedented high-impact climate extremes including droughts, heat waves and floods have occurred in all parts of the world (IPCC, 2012, 2013). The frequency of floodings, causing globally more climate-related disasters than any other extreme climate event, increased of about 65% over the last 25 years (FAO et al., 2018). Heavy rainfall events have become on average more intense and more frequent in Europe (Westra et al., 2014). The extent of flooding damage is hardly predictable due to the complex nature of its occurrence, which may significantly vary depending on the amount, intensity, duration and spatial distribution of precipitations, thus making many ecosystems worldwide vulnerable (Bailey-Serres et al., 2012; Shabala, 2012). Furthermore, at least one-tenth (about 12 million ha) of irrigated cropland in the developing world, has lost its productivity due to flooding events (Mancuso and Shabala, 2010; Olesen et al., 2011; Bailey-Serres et al., 2012; Shabala, 2012).

Flooding drastically reduces O_2 availability for plants' root respiration and survival (Shabala, 2012), adversely affecting crop production and wild species distribution in natural ecosystems (Bailey-Serres and Voesenek, 2008, 2010). Furthermore, hypoxic conditions exacerbate the competition for oxygen between root and soil microorganisms, thus affecting also the nitrate availability as a consequence of a lower extent of microbiological nitrification (Mancuso and Shabala, 2010).

Deficiency or lack of oxygen in the soil (hypoxia or anoxia, respectively) as well as the overall reducing soil conditions that are generated by anaerobic microorganisms, lead to the accumulation of toxic metabolites (including H_2S, N_2, Mn^{+2}, Fe^{+2}) and ROS (see the list of abbreviations and notations) (Ponnamperuma, 1972), and affect the synthesis of stress hormones (i.e., abscisic acid and ethylene) in roots (Bailey-Serres and Chang, 2005; Miller et al., 2008; Van Breusegem et al., 2008; Lee et al., 2011; Bailey-Serres et al., 2012; Sauter, 2013; Carvalho et al., 2015; Loreti et al., 2016).

Plant adaptation responses to flooding can be classified into two main strategies: the LOQS and the LOES, which hinge on a number of different biochemical and developmental adjustments deeply discussed by Colmer and Voesenek (2009) and Voesenek and Bailey-Serres (2015). A major feature of the LOQS is the reduction of shoot growth, to conserve substrate availability until the water recedes, whereas plants displaying LOES exhibit fast growth of shoot to reach the water surface thus re-enabling gas exchange (Colmer and Voesenek, 2009; Voesenek and Bailey-Serres, 2015). While the LOQS has only been described in lowland tolerant rice varieties, the promotion of shoot elongation by submergence (LOES) is known to occur in wetland and amphibious species over a wide taxonomic range, and in general, in those plants that have adapted to environments prone to temporary shallow floods (e.g., *Rumex palustris*, *Ranunculus sceleratus*, *Nymphoides peltata*, *Potamogeton pectinatus,* and *P. distinctus*) (Ishizawa et al., 1999; Summers et al., 2000; Sato et al., 2002; Voesenek et al., 2004; Mommer et al., 2005).

Grapevine is one of the most widely cultivated plant species worldwide, and in Europe it represents a crop of major economic interest (Anderson and Nelgen, 2011) and is integral to the cultural heritage and landscape (Terral et al., 2010).

The most famous wine-growing regions are located in a narrow geographical area where the best expression of *terroir*, i.e., the optimal combination of environmental and human factors (van Leeuwen et al., 2004), has been tuned through millenary experience. The high specificity of these climatic niches exposes viticulture to the effect of climate change (Kenny and Harrison, 1992; Schultz, 2000; Duchêne and Schneider, 2005; Jones et al., 2005; Santos et al., 2011). The present climate scenario poses new unexpected and urgent challenges to traditional viticulture, that is already threatened and will increasingly face more intense and frequent extreme weather events (Frei et al., 2000; Prosdocimi et al., 2016; Leolini et al., 2018).

Abbreviations: ^{1}H-NMR, proton nuclear magnetic resonance spectroscopy; ABA-GT, ABA glycosyltransferase; ACC, Aminocyclopropane-1-carboxylic acid; ACS, Aminocyclopropane-1-carboxylic acid synthase (ACC synthase); ACX, Acetyl-coenzyme A oxidase; AGR, absolute growth rate; AHP, Histidine-containing phosphotransmitters; AO3, aldehyde oxidase; AP2/ERF, APETALA2/Ethylene-Responsive Factor; ARFs, Auxin Response Factors; ARR factors, transcription factors; ATP, adenosine triphosphate; C, control treatment; cDNA, complementary DNA; D_2O, Deuterium oxide; DEGs, differentially expressed genes; DNase, deoxyribonuclease; DOY, day of the year; EBF 1/2, F-box proteins; ERF, ethylene responsive factor; ETR, ethylene response; F, flooding treatment; FDR, false discovery rate; FID, free induction decay; GABA, gamma amino butyric acid; GO, Gene Ontology; IPT, isopentenyltransferase; JAZ, jasmonate-zim-domain protein; K5BB, Kober 5BB; KEGG, Kyoto Encyclopedia of Genes and Genomes; LOES, Low Oxygen Escape Syndrome; LOQS, Low Oxygen Quiescence Syndrome; MeOH, methanol; MeOH-d_4, deuterated methanol; MFP2, Peroxisomal fatty acid beta-oxidation multifunctional protein; n.d., not detectable; NADH, Nicotinamide adenine dinucleotide hydride; NCED, 9-*cis*-epoxycarotenoid oxidases; NMR, Nuclear Magnetic Resonance; NOESY, nuclear overhauser effect spectroscopy; OPCL, Peptidoglycan-associated protein; OPLS-DA, supervised partial least squares discriminant analysis; PCA, principal component analysis; PDC, pyruvate decarboxylase; PIN, PIN-formed; PPi, inorganic pyrophosphate; RNA-seq, RNA sequencing; ROS, reactive oxygen species; RPKM, reads per kilobase million; RT-qPCR, real time quantitative polymerase chain reaction; SAUR, Small Auxin Up RNA; SDH, succinate dehydrogenase; T1, 1 day after stress application; T2, 2 days after stress application; T3, 8 days after stress application; T4, 16 days after stress application; T5, 21 days after stress application; T6, 7 days after stress removal; TCA cycle, tricarboxylic acid cycle; *VvACO2*, *VvACO1*, *Vitis vinifera* genes encoding for 1-aminocyclopropane-1-carboxylic acid oxidases; *VvADH1*, *Vitis vinifera* genes encoding for alcohol dehydrogenase; *VvSUS4*, *Vitis vinifera* genes encoding for sucrose synthase; *VvUBC28*, *Vitis vinifera* genes encoding for ubiquitin C.

Only few studies have been conducted to characterize the effects of flooding events on grapevine's cultivation. Initial efforts aimed at describing morphological and physiological aspects of grapevine adaptation to waterlogging stress pointed out an overall reduction in stomatal conductance, photosynthetic rate and plant height, as well as premature senescence and disturbances to yield components (Striegler et al., 1993; Stevens and Prior, 1994; Stevens and Harvey, 1995; Kawai et al., 1996; Stevens et al., 1999; Mancuso and Boselli, 2002; de Herralde et al., 2005; Mancuso and Marras, 2006; Mugnai et al., 2011).

In the present study, we aimed to gain insights into the transcriptional and metabolic changes induced by flooding in grapevine roots. A preliminary experiment under controlled hydroponic conditions was aimed at developing a model for the root grapevine response to O_2 deprivation. Results enabled the identification of transiently and steadily regulated candidate hypoxia-responsive marker genes. Afterward, over two consecutive vegetative seasons, flooding was imposed to vines during the late dormancy period, the most susceptible to high-frequency precipitations events (Crawford, 2003). Transcriptomic and metabolic profiling untargeted approaches were applied on roots to investigate their early molecular and metabolic responses to both the hypoxia and the subsequent recovery after stress removal. Internode elongation was taken as a proxy for low oxygen adaptive responses to hypoxic stress in grapevine and overall data integration enabled drafting a first comprehensive view of the molecular pathways involved in a deep metabolic and transcriptomic reprogramming of grapevine response to waterlogging.

MATERIALS AND METHODS

Plant Material and Treatments

Two experimental set-ups were adopted to study hypoxic responses of grapevine plants using, *Vitis vinifera* L., cultivar Sauvignon blanc (clone 108) grafted on Kober 5 BB (K5BB) (*V. berlandieri* x *V. riparia*) rootstock as experimental material. The first experimental set-up was performed in hydroponics under strictly controlled conditions in a growth chamber while the second one was performed in pots, reproducing a situation similar to that found in the field, in semi-controlled conditions under a tunnel located at the Experimental Farm of the University of Padova "L. Toniolo" in Legnaro, north-east of Italy. K5BB was chosen as a rootstock in all the experiments, since it is one of the most widely distributed rootstocks across european viticulture and it is known to display a moderate tolerance to flooding stress.

Hydroponic Experiment

Preliminary experiments were conducted to identify potential grapevine hypoxia-responsive genes. To this end, six vines were grown in 5 L pots in hydroponic solution (modified Hoagland medium) and arranged under two experimental conditions: three control plants were maintained in a constantly oxygenated solution and three plants were maintained in a solution without oxygenation and isolated from ambient air by adding a vaseline layer in order to prevent oxygen diffusion into the solution and enable progressive oxygen depletion by root respiration.

O_2 concentration (mg/L) was monitored in the solution using a portable multiparametric probe (HQ40d HACH, Loveland, CO, United States) and roots were sampled after 12, 24, and 96 h after stress imposition, during an experimental period of 6 days.

Pot Experiments

Pot experiments were carried out over two consecutive years (2016 and 2017) to achieve extensive transcriptome and metabolic profilings to characterize grape response to flooding. Three years-old plants were grown in 10 L pots filled with a sand–pumice-peat mixture (2:2:6 in volume). Sixty plants were selected each year based upon homogeneous developmental characteristics (i.e., length of the cane and number of buds), pruned before bud burst by retaining three or four latent buds per plant, and arranged under the following two experimental conditions at the phenological stage BBCH05 ("Wool stage" according to Lorenz et al., 1995): (i) control (C), plants that were maintained at 80% of soil field capacity, and (ii) flooded (F), plants that were flooded by inserting the pots in wider containers filled with tap water, so that the water level was maintained 5 cm above soil surface. During an experimental period of 21 days, measurements of dissolved O_2 concentration (mg/L) and flooding water temperature were conducted using a portable AquaPlus (Aquaread water monitoring instruments) (**Supplementary Figure S1**). Sampling of plant material was carried out in both years at 2 (T2), 8 (T3), 16 (T4), and 21 (T5) days after stress application. In 2017, an additional sample was collected at 1 day (T1) after flooding application to pinpoint early responses to flooding. After the last sampling, the water was withdrawn from the pots and after 7 days (28 days after stress application, T6) an additional sampling of material was performed (**Supplementary Figure S1**). For each time point and sampling, the roots of five plants for both control (C) and stress (F) conditions were gently washed with water to remove soil and the young roots were immediately dissected, frozen in liquid nitrogen and stored at −80°C for following analyses. The roots of each plant were kept separate representing a single biological replicate, for a total of five independent biological replicates for each experimental condition and time-point.

Samples and biological replicates for RNA-Seq analyses of both years were selected on the basis of the time-course and on the relative level of expression of the hypoxia marker genes *VvACO1*, *VvSUS4,* and *VvADH1*, identified as described below.

RNA Extraction, cDNA Synthesis, and RT-qPCR

Total RNA was extracted from 80 mg of young roots using the "Spectrum^{TM} Plant total RNA Kit" (Sigma, St. Louis, MO, United States) according to manufacturer's instructions. DNase treatment was performed using the On-Colum Dnase I Digest set (DNASE70, Sigma, St. Louis, MO, United States) during the RNA purification. Total RNA was quantified with the NanoDrop 2000c (Thermo Scientific, Waltham, MA,

United States) and its integrity was checked by running 200 ng in a 1% agarose gel stained with SYBER® Safe (Life Technologies, Carlsbad, CA, United States). cDNA was synthesized with the SuperScript® VILO™ cDNA Synthesis Kit (Life Technologies, Carlsbad, CA, United States) from 500 ng of DNA-free total RNA in a final volume of 20 μl, according to the instruction provided by the manufacturer. RT-qPCR was performed using StepOne Real-Time PCR System (Applied Biosystems, Monza, Italy) as described by Nonis et al. (2008) and Eccher et al. (2015), using SYBR Green reagent (Applied Biosystems, Monza, Italy). The analysis was performed on three independent biological replicates for each treatment by using specific primers listed in **Supplementary Table S1**. Gene expression levels were calculated using the automated Excel spreadsheet Q-Gene designed by Simon (2003), using the modification of the ΔCt method suggested by Pfaffl (2001). Gene expression values were normalized with *V. vinifera* genes encoding for *VvUBC28* published by Castellarin et al. (2007) and reported as arbitrary unit of Mean Normalized Expression.

Vitis vinifera genes encoding two 1-ACC oxidases (*VvACO2* and *VvACO1*), an *VvADH1* and a *VvSuS4* were identified (Jaillon et al., 2007; Vitulo et al., 2014) as candidate hypoxic marker genes, on the base of the general involvement of their homologs from model plants in plants' responses to hypoxia and anoxia (Licausi et al., 2011; Bailey-Serres et al., 2012). Their low-oxygen-dependent expression in grapevine was confirmed by comparing RNAs obtained from control and O_2-deprived roots from the hydroponic experiment.

RNA-Seq Analyses

Genome and Annotation

The revised version of the Grape genome available at http://genomes.cribi.unipd.it/DATA/ and the corresponding gff file were used as a reference in all the experiments. The genome is based on the 12X Genoscope Pinot Noir genome (Jaillon et al., 2007), while the annotation has been later on revised by extensive use of RNA-seq data (Vitulo et al., 2014). GO functional annotation was also downloaded from the same location and used for all enrichment analyses as described below.

RNA-Seq 2016

Total RNA was sent to the center Genomix4life (University of Salerno, Salerno, Italy) for quality check, libraries preparation, and sequencing. Libraries were sequenced by using an Illumina NextSeq 500 platform (Illumina, San Diego, CA, United States) obtaining ∼33 millions of stranded single-end reads of 50 base pairs per sample.

RNA-seq reads were checked for quality using FastQC (Brabaham Bioinformatics, Cambridge, United Kingdom), resulting of average very high quality. Adapter content was negligible and the reads were not trimmed before mapping. Sequence duplication levels were moderate, and since for single-end reads the removal of duplicates can give problems (Klepikova et al., 2017), the entire set of reads was mapped. Spliced alignments were performed with TopHat (Trapnell et al., 2009) and only uniquely mapping reads (identified by the flag NH:i:1 in the bam alignment file) were used for transcript abundance quantification. Quantification was performed by using the Bedtools coverage program (Quinlan and Hall, 2010) and the gff file.

RNA-Seq 2017

Samples from 2017 were sequenced with a different protocol called mRNA QuantSeq FWD by Lexogen (Lexogen GmbH, Vienna, Austria) and therefore were also analyzed differently, as in this case there is an accumulation of reads at the end of the transcripts. Libraries were sequenced by using an Illumina NextSeq 500 platform (Illumina, San Diego, CA, United States) allowing to obtain ∼20 millions of stranded single-end reads of 75 base pairs per sample. More in detail, QuantSeq FWD reads were trimmed by following the instructions given by the manufacturer[1] and mapped with TopHat. Transcript abundance was quantified as explained above.

The raw sequence reads data files of both years were uploaded to the SRA database with BioProject ID PRJNA521303.

Differential Expression Analysis

Genes undergoing differential expression in treated Vs untreated samples were identified by using the DESeq2 package (Love et al., 2014). Lowly expressed genes were filtered in a homogeneous way for all libraries, by first normalizing the counts into RPKM, and then all transcripts with an average expression below 1 RPKM were removed from the counts matrix to be used for differential expression analysis. In this way, the number of tests performed by DESeq2 to detect differential expression prior to *p*-value adjustment was reduced. Significantly changing transcripts were defined at an alpha of 1E-04 and having at least a doubling/halving of their expression level in the two contrasted conditions. The FDR was fixed at 5E-05. The FDR threshold was kept very stringent, as the *p*-value correction is made on a per contrast basis, but the analyses were performed on a high number of different samples (**Supplementary Tables S2, S3**).

Enrichment Analysis

Functional enrichment of GO categories was obtained by exploiting the available GO annotation of the Grapevine genome. For this objective, the GOStats package (Falcon and Gentleman, 2007) was used in R (R Core Team, 2018). Enrichments of Biological Processes were calculated separately for the up and down regulated genes identified as differentially expressed, at a FDR level of 0.05.

Metabolites

Sample Preparation

Five independent biological replicates of each treatment (from control or flooded roots, season 2017) and time point (T1, T2, and T6) were used for ^{1}H-NMR analysis. Metabolites were extracted from 30 mg of freeze-dried powder of young roots using a 1:1 (v/v) mixture of D_2O (in 400 mM phosphate buffer, pH = 6.00) and Methanol-*d4*, >= 99.8

[1] https://www.lexogen.com/quantseq-data-analysis/

atom % D (Sigma-Aldrich) in a final volume of 1 ml, and mixed briefly by vortexing for 15 s. Samples were sonicated for 30 min at 20°C and then centrifuged at 9000 rpm for 5 min.

A solution of 15 mM Calcium formiate ($Ca(HCOO)_2$ (Sigma-Aldrich TraceCERT, product no. 03826) was prepared in D_2O to be used as internal standard for the quantification of metabolites. For each sample, 593 µl of the supernatant were transferred to a NMR tube and 7 µl of the standard solution were added, leading to a 0.18 mM concentration of internal standard in the tubes.

NMR Parameters

A Bruker DMX 600 spectrometer, operating at a proton frequency of 599.90 MHz, was used for the ^{1}H-NMR experiments. The magnetic field was locked to the MeOH-d_4 resonance. The spectra were recorded using NOESY pulse sequence with a water presaturation (noesy1dpr in Bruker notation), 256 transients of 32 K points, spectral width of 14 ppm, relaxation time of 2 s, acquisition time 25 min, at 298 K.

To provide quantitative data, a reference sample has been acquired with an additional relaxation time of 60 s to ensure complete spin relaxation of the nuclei in all metabolites. In this way the metabolites concentration of this sample was determined. A relaxation time (T_1) correction factor was calculated by comparing the signal absolute value of each metabolite in the reference spectra acquired with 2 and 60 s of relaxation delay, respectively. The concentration of the metabolites in all the other extracts was obtained by using this correction factor.

The ACDlab v.12.5 software was used to process FIDs and spectra. The FIDs were multiplied by an exponential window function with 0.5 Hz line broadening and zero-filled to 64K points. The spectra resulting from Fourier transformation were manually phased and baseline-corrected. The MeOH-d_4 signal was used to calibrate the frequency.

Data Pre-processing and Statistical Analysis

Each ^{1}H spectrum was bucketed and integrated using intelligent bucketing of intervals of 0.035 ppm. The spectra were normalized to the total sum of integral covering the interval 9–0.5 ppm (excluding the solvent signal regions). Pareto scaling and mean centering were applied before multivariate data analysis. The obtained data set resulted to be composed of 240 variables.

The data matrix was analyzed using the pattern recognition methods in the SIMCA software (version 14.0, Umetrics, 2015) including unsupervised PCA and OPLS-DA. The quality of the discriminant models was evaluated by the goodness of fit score (R^2Y) and the goodness of prediction score (Q^2Y). The S-plot (Wiklund et al., 2008) was used to identify the characteristic resonances (significant based on both the *t*-test for the means and of the Mann-Whitney test for the medians, $p < 0.001$) responsible for classes distinction.

Biometrical Measurements

Once bud-break occurred, internode elongation rate was measured on ten primary shoots per treatment from the lower side of one node to the lower side of the node above it using a graduated ruler on a weekly basis throughout all the vegetative season.

Internode extension in grapevine shoot has been described being sigmoidal over time in four stages (Lebon et al., 2004; Louarn et al., 2007). These are: Stage I, during which elongation is exponential; Stage II, which is short and during which the extension rate increases rapidly; Stage III, during which the extension rate is essentially constant and internode length increases linearly; and Stage IV, during which the extension rate decreases as the internode approaches its final length. Internodes have been arranged in 6 classes starting from the basal to the apical ones: 1–2 (class I), 3–5 (class II), 6–10 (class III), 11–15 (class IV), 16–20 (class V), and 21–25 (class VI). For each class, final internode length, internode elongation duration and maximum internode elongation rate were estimated by non-linear least square regression of the change in internode length on a DOY basis, using a three-parameter Gompertz sigmoidal model as follow:

$$Internode\ length = a \cdot e^{-e^{-\left(\frac{x-x_0}{b}\right)}} \quad (1)$$

where a is the asymptote corresponding to final internode length, x_0 is the x-value at the inflection point corresponding to the midway point in the duration of internode expansion, and b is the maximal slope at the inflection point, corresponding to maximal internode elongation rate. The values and confidence intervals of these parameters were estimated with Sigmaplot software. No R^2 was lower than 0.98 and no standard error of estimate was higher than 0.15 (data reported in **Supplementary Table S4**). For each internode class, the first derivative from the sigmoidal growth functions, representing the AGR were computed in order to assess the duration of growth and their rates in term of cm per day. At the '5 separated leaves' stage (stage 15 according to the extended BBCH scale; Lorenz et al., 1995), the plants were thinned to two branches and were trained vertically.

RESULTS

Identification and Validation of Low Oxygen Stress Markers in Grapevine Roots

Due to the absence of published studies on hypoxic responses in grapevine roots, putative candidate low oxygen responsive marker genes for grapevine were initially identified on the base of similarity searches, leading to the selection of genes encoding two ACC oxidases (*VvACO1* and *VvACO2*), one *VvSuS4* and one *VvADH1*, respectively known to mark hypoxic responses in a wide range of species of both model and crop plants (Licausi et al., 2011; Bailey-Serres et al., 2012). A preliminary experiment was carried out to correlate the oxygen levels in the solution and the expression of hypoxia responsive marker genes in roots of grapevine plants grown in hydroponics. Significant differences in terms of dissolved O_2 concentration could be detected between control and

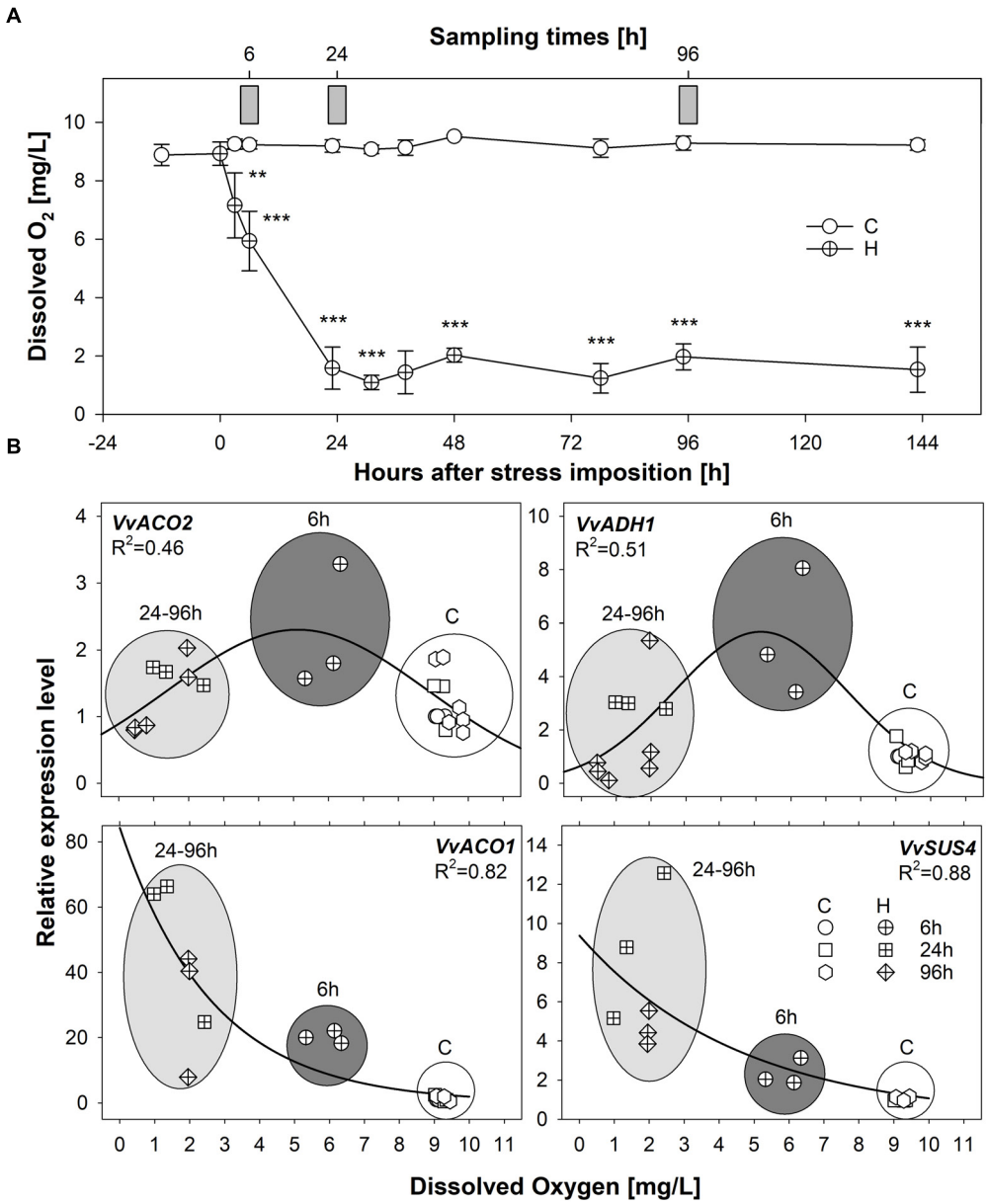

FIGURE 1 | (A) Levels of dissolved oxygen (mg/L) in hydroponic solution, measured in the vicinity of roots during a time-course experiment of 6 days in 5 L beakers constantly oxygenated (control plants; empty circles) or not oxygenated and isolated from oxygen (plants exposed to hypoxia; crossed circles); values represent mean ± SE and asterisks denote mean values that are statistically different at $^{**}p < 0.01$, $^{***}p < 0.005$; gray bars indicate sampling points for gene expression analyses of hypoxia-responsive marker genes shown in panel **B**. **(B)** Scatter plot of the expression of the candidate hypoxia-responsive markers *VvACO1* and *VvACO2*, *VvADH1* and *VvSuS4* plotted against levels of dissolved oxygen in hydroponic solution under well oxygeneted (empty symbols) and progressive hypoxic conditions (crossed symbols). Gray-shaded ellipses/circles indicate the expression levels measured at 6 h (dark gray) and 24–96 h /light gray); indicate the expression levels measured at successive time-points; white circles group the expression levels measured in roots of control plants at all time-points. Solid lines indicate three-parameter Gaussian and hyperbola decay best fit curves for (*VvACO2*, *VvADH1*) and (*VvACO1, VvSuS4)*, respectively. **Supplementary Figure S2** enables the statistical identification of significant differences among the samples under the different Control and Flooded treatments.

hypoxic conditions already after 6 h from stress imposition (**Figure 1A**). The concentration of dissolved O_2 dropped to less than 2 mg/L after 24 h from the start of application of stress and remained very low throughout the experiment. The transcriptional profiles observed for the selected genes (*VvACO1* and *VvACO2*, *VvADH1* and *VvSuS4*) showed an induction in response to oxygen levels lower than 8 mg/L thus confirming their hypoxia-dependent regulation (**Figure 1B**). More in detail, *VvACO2* and *VvADH1* were transiently induced after 6 h followed by a subsequent down-regulation after 24 and 96 h of O_2-deprivation, while *VvACO1* and *VvSuS4* showed a progressive trend of increase of transcription along the duration of stress

condition, with a maximum accumulation of transcripts after 96 h (**Supplementary Figure S2**).

Transcriptional Responses of Flooded Grapevines

VvACO1, *VvSuS4,* and *VvADH1* genes were used as markers to select reproducible and representative biological replicates for further RNA-Seq (both in 2016 and 2017) and metabolic analyses (in 2017). Their expression was higher in flooded roots than in roots of control plants in all the four independent biological replicates considered (**Supplementary Figure S3**). Differently from roots of plants grown in hydroponics, all genes displayed a transient induction at T1 that leveled off at later time-points in both years. Measurements of the oxygen levels dissolved in the free solution of pots confirmed that flooded plants experienced a drop in oxygen availability that roughly halved at day 1 (T1) from stress imposition in comparison to control plants, reaching 4.6 mg/L and 5.7 mg/L in 2016 and 2017, respectively. Already at day 2 (T2), flooded plants experienced a drop in oxygen availability that reached values of 2.9 mg/L and 4.4 mg/L in 2016 and 2017, respectively. A further drop in oxygen availability was observed at day 16 (T4) with values around 2 mg/L that settled until the end of the flooding (day 21) for both years analyzed (**Supplementary Figure S1**). Based on the kinetics of both oxygen levels and marker gene expression, three out of four independent replicates were selected for further untargeted molecular analyses among the samples collected in both 2016 and 2017 at T2 (hypoxia) and T6 (1 week of recovery to normal conditions). An additional time point at day 1 (T1, early hypoxia) was also included in 2017 analyses to gain more insight into the early molecular responses to low oxygen.

The RNA-Seq transcriptomic profiles observed for flooded and control roots evidenced very similar and nearly overlapping transcriptional signatures for the different biological replicates and for both the years analyzed (**Supplementary Figure S4**).

Our results overall pointed out that the same groups of genes were consistently up- or down-regulated in both years (**Supplementary Figure S5**) even though with slightly different dynamics especially for the up-regulated ones. A clearly identifiable group of genes appeared to be collectively up-regulated in flooded plants at T2 in 2016 (**Supplementary Figure S6A**), while appeared to undergo a two step regulation in 2017 with some of them showing a maximum induction either at T1 or T2 (**Supplementary Figure S6B**). In addition, the expression of such genes appeared to return to levels comparable to those of control plants at T6 (**Supplementary Figure S6**).

Overall, RNA-Seq analyses led to the *bona fide* identification of groups of genes that are reliably and consistently regulated as a consequence of exposure to flooding and, therefore, to a low oxygen stress in grapevine roots (K5BB).

GO Enrichment and KEGG Pathway Analyses of Hypoxia-Regulated DEGs in Grapevine Roots

Analyses of enriched GO terms (biological process) for genes that were up- or down-regulated in response to flooding showed large similarities with results previously achieved in other species in response to low oxygen availability (Blokhina et al., 2003; Mustroph et al., 2010). Several GO terms resulted to be significantly enriched in both seasons analyzed and are listed in **Table 1** with their statistics for both T1 and T2 of year 2017. GO terms enriched in up-regulated genes included categories related to oxygen depletion and oxidative stress such as "response to hypoxia" and "response to oxygen levels", "oxygen transport", "regulation of hydrogen peroxide", and "ROS metabolic process", as well as the GO categories related to carbon and nitrogen metabolism such as "carbon utilization", "gluconeogenesis", and "nitrate assimilation" (**Table 1**). A different time-course of transcriptional regulation could be observed among the GO functional groups, with some of them being significantly enriched at both time points, while others at either T1 or T2.

Among GO categories enriched in down-regulated genes in response to hypoxia, those related to hormone biosynthesis and, in particular, to "sterol", "steroid", and "brassinosteroid biosynthetic process" and those related to "isoprenoid" and "diterpenoid metabolic process" as well as "carotene biosynthetic process" and "regulation of hormone levels" appeared to be significant in both years. GO functional categories involved in catabolic and growth processes, such as "regulation of meristem growth" and "cell wall, chitin and amino sugar catabolic processes", resulted to be enriched as well.

Primary Metabolism: Glycolysis and TCA Cycle

Based on the assignment of the identified DEGs on KEGGs Maps several transcriptional changes could be assigned to well-defined metabolic pathways, among which primary metabolism appeared remarkably impacted. Considering the higher temporal resolution of the 2017 RNA-Seq analysis, due to the inclusion of an additional time-point at day 1 (T1) from the start of flooding, and the overall comparability between the transcriptomic profiles in the two seasons, for simplicity further in depth data elaboration has been focused on the 2017 season only.

Hypoxia is known to determine a complete rearrangement of primary metabolism to ensure cell survival in oxygen shortage, by hijacking sugar metabolism from the tricarboxylic acid (TCA) cycle, which is inhibited and reversed, toward an increased glycolytic flux. In hypoxic grapevine roots the induction of the genes responsible for the conversion of citrate to oxaloacetate (citrate synthase [EC:2.3.3.1], of malate to fumarate (fumarate hydratase, class I [EC:4.2.1.2]) and, to a minor extent, of fumarate to succinic acid (SDH, [EC:1.3.5.1]) and of the ATP citrate-lyase [EC:2.3.3.8]), are coherent with the above described reversion of the reactions of the Citrate Cycle, which results in the accumulation of succinate in response to hypoxia (Bailey-Serres et al., 2012). Succinic acid formation appeared to be further sustained through the activation of the gene encoding the alpha subunit of succinyl-CoA synthetase [EC:6.2.1.5] (**Figure 2**).

Consistently with the inhibition of the TCA cycle, leading to acetyl-CoA shortage in hypoxic cells, fatty acids biosynthesis and elongation appeared overall inhibited (data not shown). Regarding glycolysis, the transcriptomic data from

TABLE 1 | GO terms, for the "biological process" dictionary, that were enriched ($p < 0.001$; FDR < 0.05) at either T1 or T2 (or both) in 2017, in up- (red block) and down- (blue block) regulated genes.

	GO id	GO term	T1		T2	
			P-value	FDR	*P*-value	FDR
	GO:0001666	Response to hypoxia	1.06E-15	8.90E-13	1.41E-10	1.28E-07
	GO:0070482	Response to oxygen levels	1.47E-15	8.90E-13	1.87E-10	1.28E-07
	GO:0009862	Systemic acquired resistance, salicylic acid mediated signaling pathway	3.38E-07	1.37E-04	3.05E-04	2.32E-02
	GO:0010310	Regulation of hydrogen peroxide metabolic process	8.01E-07	2.43E-04	ns	ns
	GO:0072593	ROS metabolic process	4.02E-06	9.76E-04	ns	ns
	GO:0019530	Taurine metabolic process	4.01E-05	6.78E-03	2.60E-05	5.08E-03
	GO:0051707	Response to other organism	4.47E-05	6.78E-03	5.30E-05	9.07E-03
	GO:0015671	Oxygen transport	5.56E-05	7.50E-03	3.45E-04	2.33E-02
	GO:0046364	Monosaccharide biosynthetic process	1.68E-04	1.85E-02	3.53E-07	1.58E-04
	GO:0006094	Gluconeogenesis	2.85E-04	2.59E-02	4.63E-07	1.58E-04
	GO:0015976	Carbon utilization	2.99E-04	2.59E-02	2.27E-04	1.95E-02
	GO:0042128	Nitrate assimilation	4.66E-04	3.77E-02	ns	ns
	GO:0002229	Defense response to oomycetes	ns	ns	2.77E-06	7.59E-04
	GO:0006165	Nucleoside diphosphate phosphorylation	ns	ns	1.26E-04	1.84E-02
	GO:0009185	Ribonucleoside diphosphate metabolic process	ns	ns	2.01E-04	1.84E-02
	GO:0009135	Purine nucleoside diphosphate metabolic process	ns	ns	2.01E-04	1.84E-02
	GO:0006096	Glycolytic process	ns	ns	2.01E-04	1.84E-02
	GO:0046031	ADP metabolic process	ns	ns	2.01E-04	1.84E-02
	GO:0046034	ATP metabolic process	ns	ns	2.69E-04	2.16E-02
	GO:0009750	Response to fructose	ns	ns	3.81E-04	2.37E-02
	GO:0043086	Negative regulation of catalytic activity	7.37E-07	7.47E-04	5.84E-09	1.01E-05
	GO:0042538	Hyperosmotic salinity response	1.60E-06	8.10E-04	ns	ns
	GO:0006801	Superoxide metabolic process	5.93E-06	2.00E-03	2.19E-04	1.27E-02
	GO:0009759	Indole glucosinolate biosynthetic process	1.94E-05	3.32E-03	ns	ns
	GO:0052544	Defense response by callose deposition in cell wall	3.15E-05	3.99E-03	ns	ns
	GO:0016101	Diterpenoid metabolic process	1.33E-04	1.34E-02	2.22E-05	4.19E-03
	GO:0033037	Polysaccharide localization	1.70E-04	1.51E-02	ns	ns
	GO:0070301	Cellular response to hydrogen peroxide	2.00E-04	1.51E-02	ns	ns
	GO:0080167	Response to karrikin	2.33E-04	1.51E-02	5.67E-04	2.40E-02
	GO:0006066	Alcohol metabolic process	3.56E-04	2.12E-02	3.99E-04	1.87E-02
	GO:0071475	Cellular hyperosmotic salinity response	7.88E-04	3.99E-02	ns	ns
	GO:0010075	Regulation of meristem growth	ns	ns	2.24E-07	1.95E-04
	GO:0016998	Cell wall macromolecule catabolic process	ns	ns	4.89E-07	2.29E-04
	GO:0009813	Flavonoid biosynthetic process	ns	ns	5.29E-07	2.29E-04
	GO:0006857	Oligopeptide transport	ns	ns	3.14E-06	1.09E-03
	GO:0016126	Sterol biosynthetic process	ns	ns	5.35E-06	1.55E-03
	GO:0007169	Transmembrane receptor protein tyrosine kinase signaling pathway	ns	ns	4.81E-05	5.72E-03
	GO:0071705	Nitrogen compound transport	ns	ns	4.94E-05	5.72E-03
	GO:0016132	Brassinosteroid biosynthetic process	ns	ns	1.50E-04	1.00E-02
	GO:0006720	Isoprenoid metabolic process	ns	ns	1.71E-04	1.06E-02
	GO:0006022	Aminoglycan metabolic process	ns	ns	3.42E-04	1.74E-02
	GO:0006032	Chitin catabolic process	ns	ns	3.50E-04	1.74E-02
	GO:0046348	Amino sugar catabolic process	ns	ns	3.50E-04	1.74E-02
	GO:0006687	Glycosphingolipid metabolic process	ns	ns	3.62E-04	1.74E-02
	GO:0005975	Carbohydrate metabolic process	ns	ns	4.17E-04	1.90E-02
	GO:0006694	Steroid biosynthetic process	ns	ns	4.69E-04	2.09E-02
	GO:1901071	Glucosamine-containing compound metabolic process	ns	ns	5.34E-04	2.32E-02
	GO:0016120	Carotene biosynthetic process	ns	ns	5.94E-04	2.45E-02
	GO:0010817	Regulation of hormone levels	ns	ns	8.56E-04	3.23E-02

Only the terms enriched also in 2016 are shown.

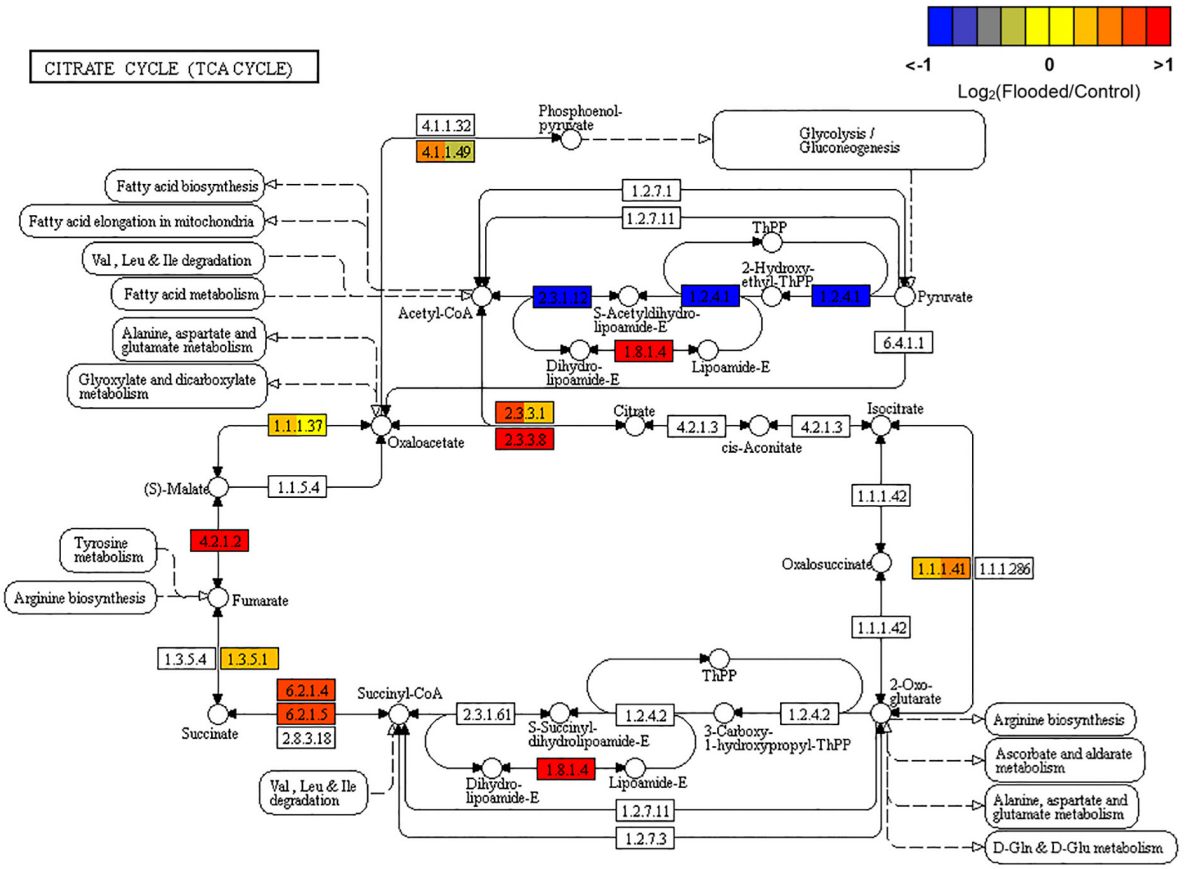

FIGURE 2 | KEGG map of the Citrate Cycle (TCA cycle; map00020) pathway, rendered by Pathview (Luo et al., 2017). Each box is divided in three sub-boxes and represents a specific enzymatic step with the relative expression of the corresponding genes in Flooded versus Control roots, calculated as log2-ratio at T1, T2, and T6 (from left to right).

flooded grapevine roots indicated that phosphoglucomutase [EC:5.4.2.2] was down regulated, probably to reduce flux through gluconeogenesis, while all genes encoding enzymes involved in the glycolytic and fermentative pathways were induced. These genes included hexokinase [EC:2.7.1.1] as well as glucose-6-phosphate 1-epimerase [EC:5.1.3.15], the latter involved in the conversion of beta-D-glucose 6-phosphate into alpha-D-glucose 6-phosphate, thus enhancing the channeling of glucose-6P into glycolysis. The stable induction of diphosphate-dependent phosphofructokinase [EC:2.7.1.90] in the absence of changes in the transcripts encoding the ATP dependent 6-phosphofructokinase 1 [EC:2.7.1.11], both responsible for the glycolytic flux maintenance through the conversion of D-fructose 6-phosphate to D-fructose 1,6-bisphosphate, is a hallmark of the typical metabolic shift taking place in response to low oxygen, by the stimulation of PPi-dependent rather than ATP-dependent processes as an energy saving mechanism. Interestingly, a gene encoding fructose-1,6-bisphosphatase I [EC:3.1.3.11], leading to regeneration of D-fructose 6-phosphate and phosphate was also induced. Further flooding/hypoxia-induced genes in grapevine roots controlling key steps in glycolysis included phosphoglycerate kinase [EC:2.7.2.3], 2,3-bisphosphoglycerate-dependent and -independent phosphoglycerate mutase [EC:5.4.2.12 and EC:5.4.2.12, respectively] and enolase [EC:4.2.1.11], overall leading to increased later formation of pyruvate, a central hub for the alcoholic fermentation pathway. This latter pathway, appeared consistently up-regulated by the co-ordinated transcriptional activation of PDC [EC:4.1.1.1] and *VvADH1* [EC:1.1.1.1], controlling the formation of acetaldehyde and ethanol, respectively (**Figure 3**).

Overall these data confirm previous reports showing consistently an augmented flux through glycolysis as the preferential pathway to provide metabolic energy while ensuring recycling of reduced NADH, through PPi-dependent and ATP-independent pathways and through the activation of the ethanolic fermentation in which PDC and ADH play a key role. In parallel to the induction of the fermentative pathway, a number of genes involved in amino acid metabolism (Reggiani, 1999) evidenced an overexpression during low oxygen exposure of grapevine roots: alanine aminotransferase (alanine transaminase [EC:2.6.1.2]), responsible for the conversion of pyruvate to alanine, glutamate dehydrogenase [EC:1.4.1.3], converting glutamic acid to 2-oxoglutarate, and glutamate

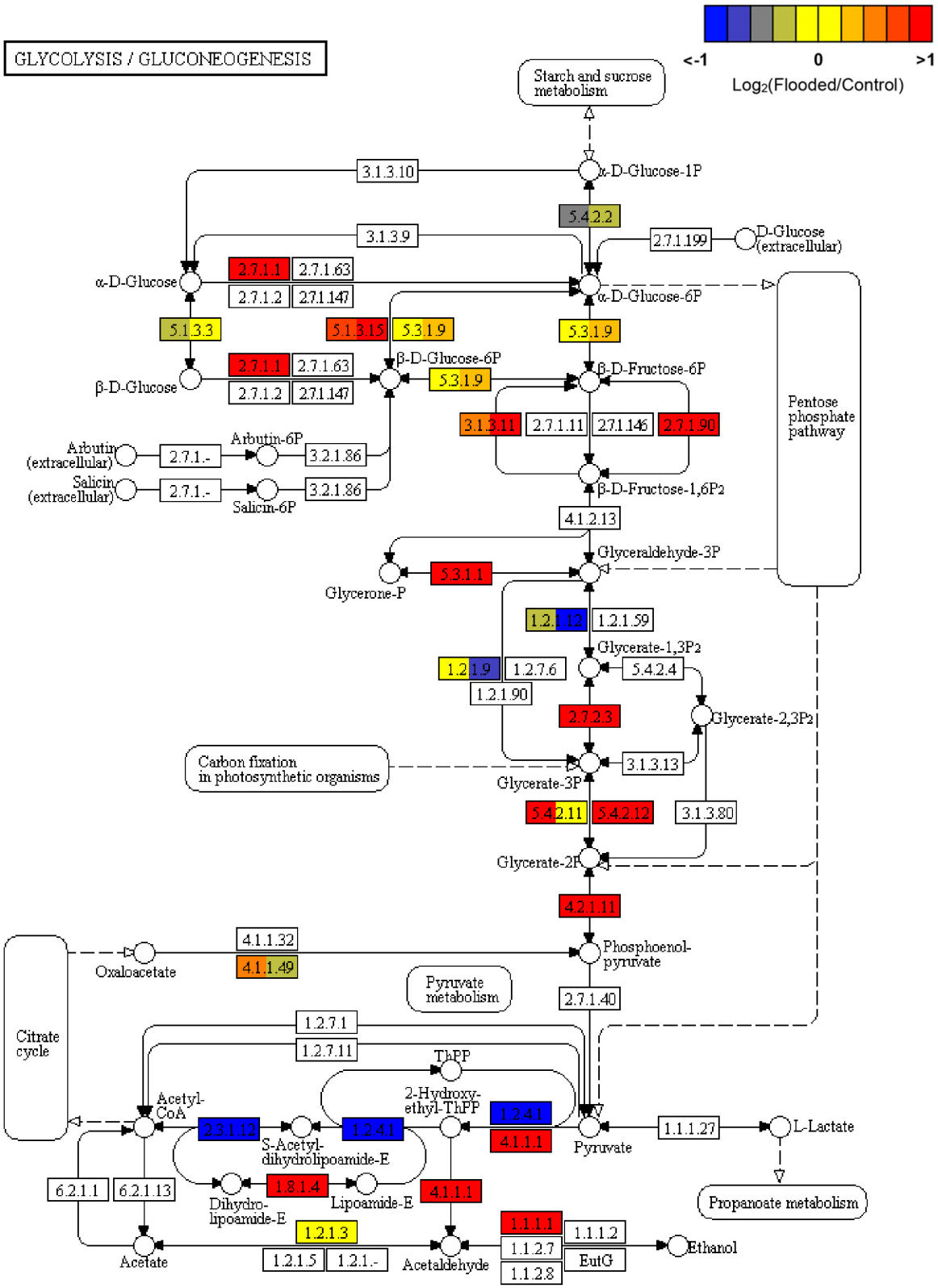

FIGURE 3 | KEGG map of Glycolysis and Gluconeogenesis (map00010) pathway, rendered by Pathview (Luo et al., 2017). Each box is divided in three sub-boxes and represents a specific enzymatic step with the relative expression of the corresponding genes in Flooded versus Control roots, calculated as log2-ratio at T1, T2, and T6 (from left to right).

synthase [EC:1.4.1.13 and EC:1.4.1.14], re-converting 2-oxoglutarate into glutamate, the latter further metabolized to glutamine by the induction of glutamine synthetase [EC:6.3.1.2]. The steps involved in the synthesis and metabolism of GABA shunt (glutamate decarboxylase [EC:4.1.1.15] and 4-aminobutyrate-pyruvate transaminase [EC:2.6.1.96], respectively) appeared to be down-regulated (**Figure 4**).

Quantification of Key Primary Metabolites Confirmed the Transcriptomic Analyses

^{1}H-NMR data clearly showed the effects of time and treatment on the metabolic profile of the roots as it can be observed in the score scatter plots of the OLPS-DA model reported in **Figure 5**. The x axis (t[1]) enabled a clear separation of flooded roots from control ones (**Figure 5**), underlying a prevailing effect of the hypoxic response (exemplified by the segregation of all flooded samples with respect to the control into the positive and negative sides of the *x* axis of **Figure 5**, respectively). The effect of time/development (described by the distribution of samples at different time-points along the *y* axis, to[1]rpm) on the overall NMR-detectable metabolic profile appeared similar in both control and flooded roots. Some differences could be shown at T6, when flooded samples resulted to be more similar to their T1 and T2 counterparts while T6 control samples evidenced a wider distribution (**Figure 5**).

The prevalent metabolic shift appeared specifically associated with the hypoxic stress, responsible for the separation of flooded samples is highlighted by the OPLS-DA models performed

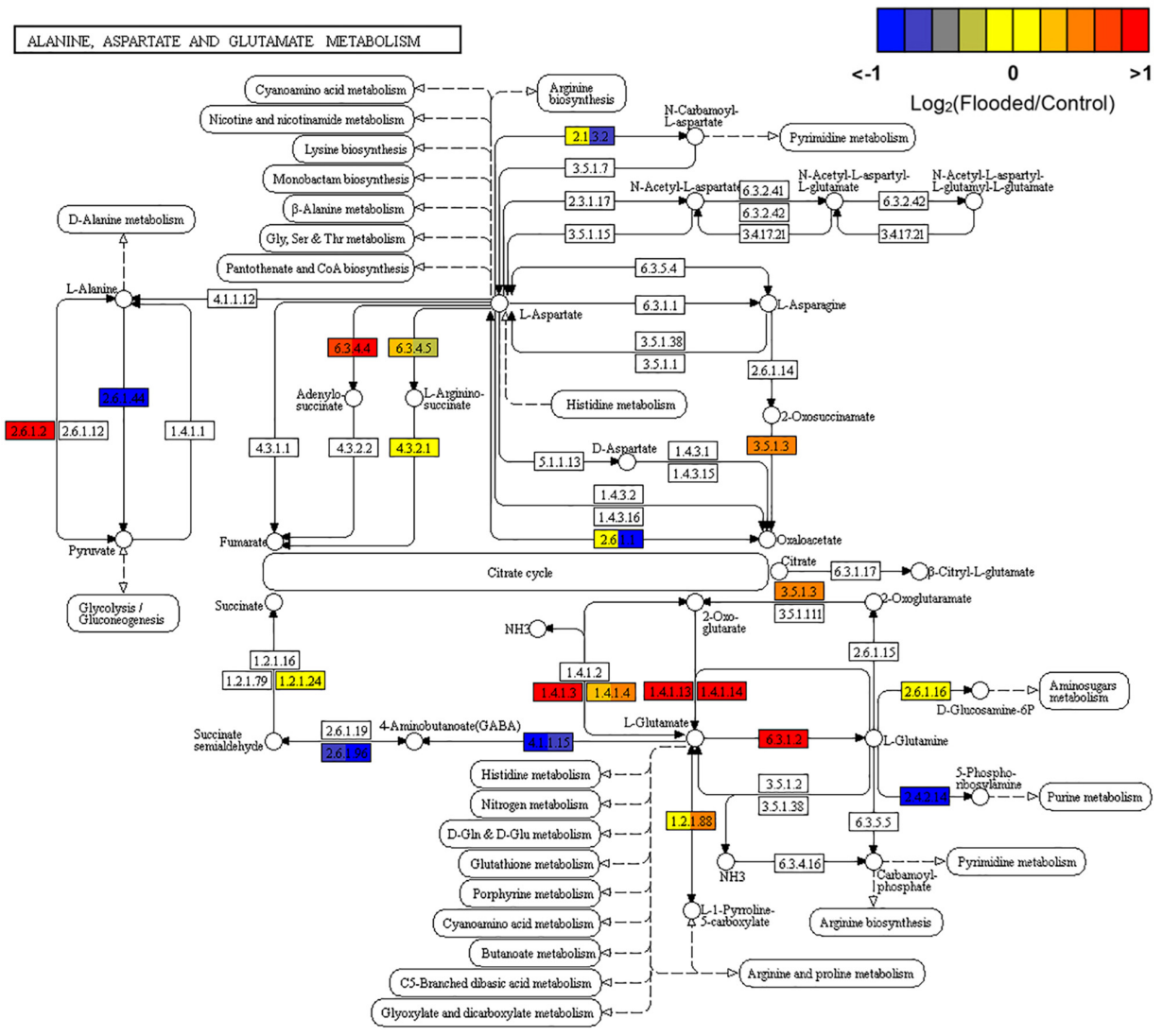

FIGURE 4 | KEGG map of Alanine, Aspartate and Glutamate metabolism (map00250) pathway rendered by Pathview (Luo et al., 2017). Each box is divided in three sub-boxes and represents a specific enzymatic step with the relative expression of the corresponding genes in Flooded versus Control roots, calculated as log2-ratio at T1, T2, and T6 (from left to right).

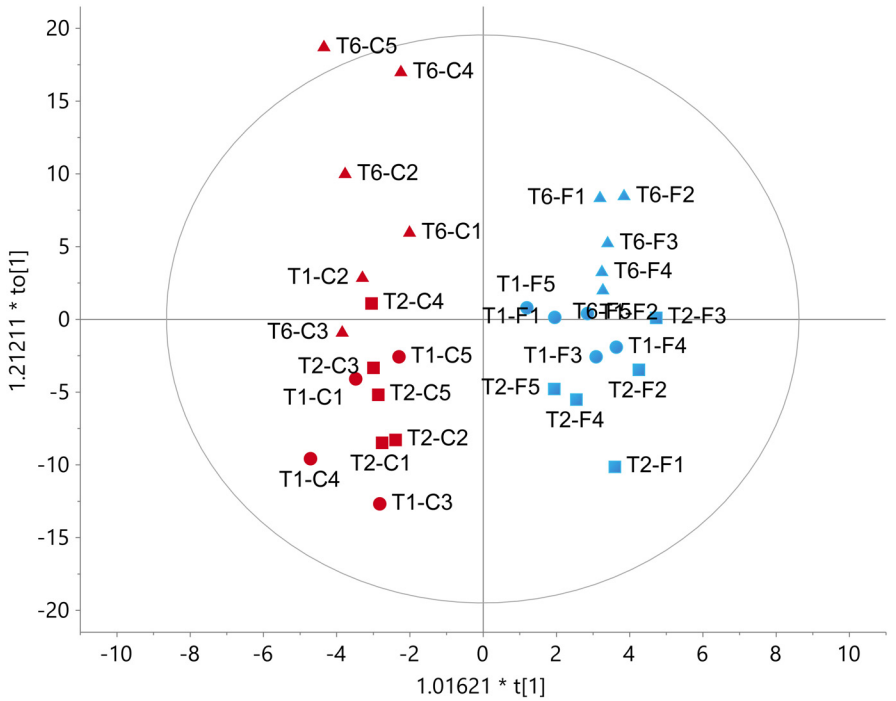

FIGURE 5 | Score scatter plot for the OPLS-DA model on ^{1}H-NMR spectra for D_2O/ MeOH-d_4 roots extracts of flooded (F, blue symbols) and control (C, red symbols) plants in five biological replicates (C1 to C5 and F1 to F5) at the three time points considered ($R^2Y = 0.93$, $Q^2Y = 0.27$). Solid cicles (●): T1; Squares (■): T2; Triangles (▲): T6.

on the T2 (**Figures 6A,C**) and T6 (**Figures 6B,D**) replicates, respectively. The insets of the S-plots in **Figures 6C,D** show the characterizing resonances of flooded samples together with the metabolite assignment of some of them. The profiles of these metabolites in control and flooded roots over the time are reported in **Figure 7**. The concentration levels of known hypoxia inducible metabolites, such as ethanol, succinic acid, alanine and gamma-aminobutyric acid (GABA) increased in flooded samples (Rocha et al., 2010; Bailey-Serres et al., 2012; António et al., 2016; **Figure 6**). These differences were particularly evident at T2 (**Figure 6A**) and leveled off 1 week after the recovery from flooding (T6) for some metabolites, including ethanol which became undetectable (**Figures 6B**, **7**). On the contrary, GABA, succinic acid, alanine and valine levels remained significantly higher at T6 in samples that had previously experienced flooding with respect to control ones (**Figures 6B**, **7**).

Rearrangement of Hormonal Homeostasis and Action as a Response to Flooding

GO analysis of RNA-Seq data pointed out a significant enrichment of the "regulation of hormone levels" category, suggesting a significant rearrangement of hormonal homeostasis of grapevine roots in response to flooding and during recovery thereafter. Specific assignment of DEGs to the respective KEGG hormone biosynthesis and signal transduction maps pinpointed an overall down-regulation of ethylene and ABA biosynthesis during waterlogging (T1 and T2) through a lower accumulation of transcripts encoding the enzymes involved in the respective rate limiting steps: ACC synthase (ACS or ACC synthase) for ethylene (Ju and Chang, 2015; **Figure 8C**) and NCED and AO3 for ABA (Schwartz et al., 2003; **Figure 8E**). For the latter hormone, this effect was also paralleled by an increased conjugative and degradative metabolism, witnessed by higher transcript levels of genes controlling ABA glycosylation (ABA-GT) and hydroxylation (CYP707A) steps. A partial re-activation of ABA biosynthesis and metabolism was evident during the recovery phase (T6). As far as the signaling pathways of these two hormones are concerned, an overall negative regulation of ethylene signaling was evidenced by the co-ordinated up-regulation of genes encoding ethylene receptors (ETR) and EBF 1/2 factors (Binder et al., 2007), both exerting an inhibitory action on downstream responses of the canonical ethylene signal transduction pathway (Ju and Chang, 2015). On the other hand, analysis of the grapevine genes encoding ERF ARR factors enabled the identification of three group IX, two group III and one group VII ERF encoding genes that were up-regulated during waterlogging (T1 and T2) and later down-regulated during recovery (T6) (**Figure 8C**, bottom right inset). An overall down-regulation of genes encoding key biosynthetic limiting steps was evident for brassinosteroids (CYP92A6 encoding genes), gibberellins (ent-kaurene oxidase encoding genes) and auxins (YUCCA and indole-3-acetaldehyde oxidase encoding genes) during waterlogging. The down-regulation of auxin biosynthesis was paralleled by the transcriptional repression of

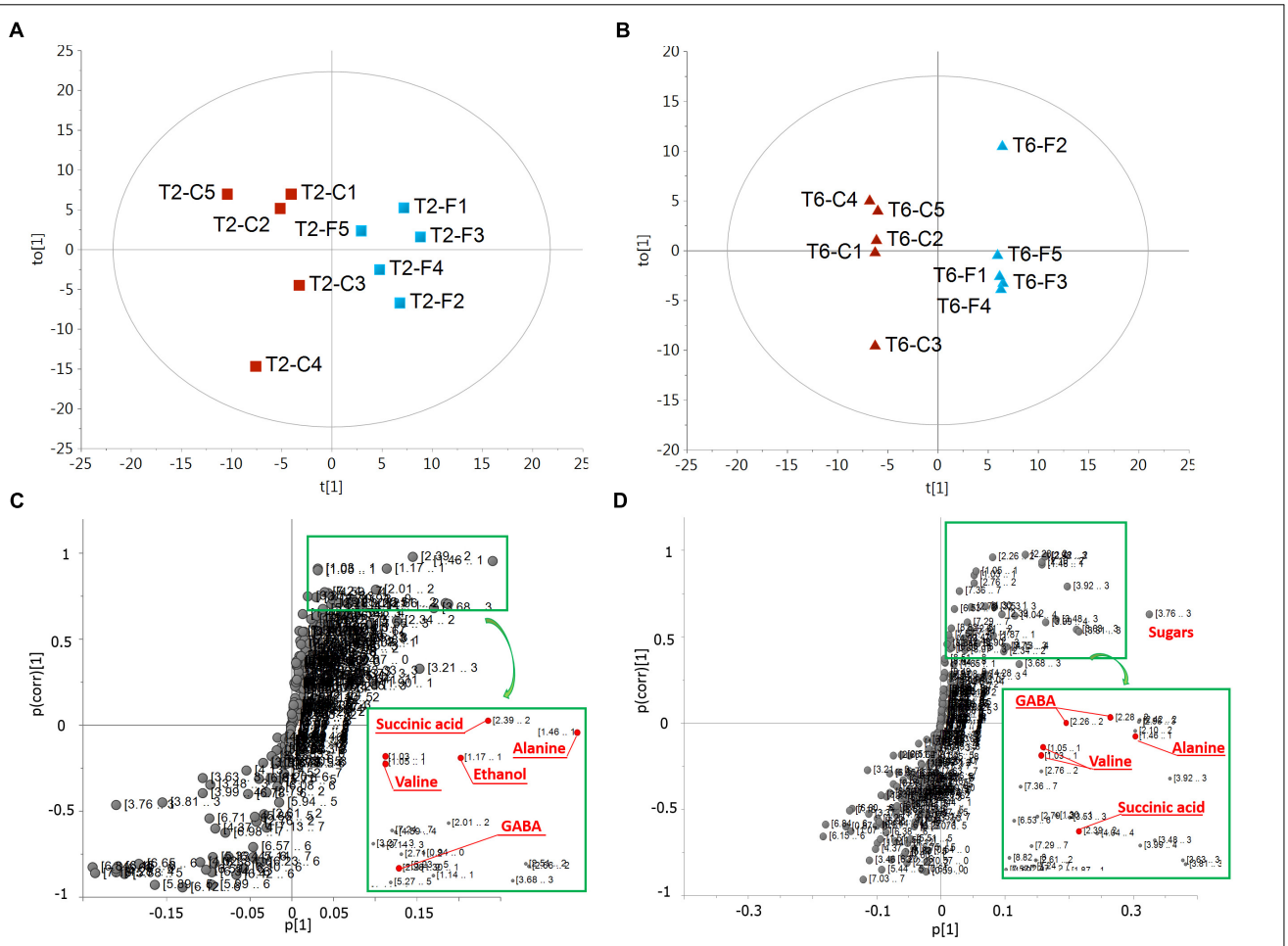

FIGURE 6 | Scores **(A,B)** and corresponding S-plot **(C,D)** of orthogonal partial least-squares-discriminant analysis (OPLS-DA) on ^{1}H-NMR spectra for extracts of control **(C)** and flooded **(F)** samples at the T2 (**A**,**C**, $R^2Y = 0.87$, $Q^2Y = 0.77$) and T6 (**B**,**D**, $R^2Y = 0.99$, $Q^2Y = 0.89$) time point, respectively. Square insets in the S-plots on the bottom right highlight the metabolites mainly contributing to the separation of flooded samples.

genes encoding both influx (AUX1) and efflux (PINs) carrier proteins (**Figure 8D**) and GH3 proteins, while ARFs and SAUR encoding genes were up-regulated. Remarkably the down-regulation of GA biosynthesis was accompanied by a parallel up-regulation of degradative metabolic hydroxylation (GA2ox encoding genes) during waterlogging (T1 and T2) while both these effects were reversed during recovery (T6) (**Figure 8B**) suggesting a reappraisal of biosynthesis and a reduction of metabolism during this latter phase. As far as cytokinins are concerned, an up-regulation of biosynthetic genes (IPT) was present, while general negative regulators of signaling (type A ARR factors) (To et al., 2004) appeared up-regulated and positive regulators (AHP and type B ARR factors) (Mason et al., 2005) appeared up-regulated during flooding, an effect that was reversed during recovery (**Figure 8F**). Finally, an up-regulation of genes involved in key steps of jasmonic acid synthesis (OPCL1; ACX; MFP2) was evident at all time points, while a clear up-regulation at T1 and T2, followed by down-regulation at T6, was found for the negative regulators of jasmonic acid responses (JAZ) transcriptional repressors (Chini et al., 2016; **Figure 8G**).

Differential Effects of Flooding on Grafted Shoot Elongation in Relation to Internode Position Along the Plant Axis

Shoot length varied significantly as a result of internode extension kinetics under C and F conditions in season 2017 (**Figure 9**). The same pattern and significant differences among treatments were present in season 2016 (**Supplementary Figure S15**). In both seasons, bud-break occurred during the last days of flooding, leading to a significant initial reduction of shoot length in flooded plants. This inhibitory effect lasted about 20 days after stress removal. After that, a marked recovery on shoot elongation of F plants was observed leading initially, to a similar shoot length among treatments (after 2 months from the end of the stress), and to significantly longer shoots in F plants compared to C at the end of the season, with average shoot length of about 170 cm and 130 cm for F and C plants, respectively (**Figure 9A**). For a deeper understanding of these growth dynamics, the growth of single internodes was measured throughout the season (**Figure 9B**). To do so,

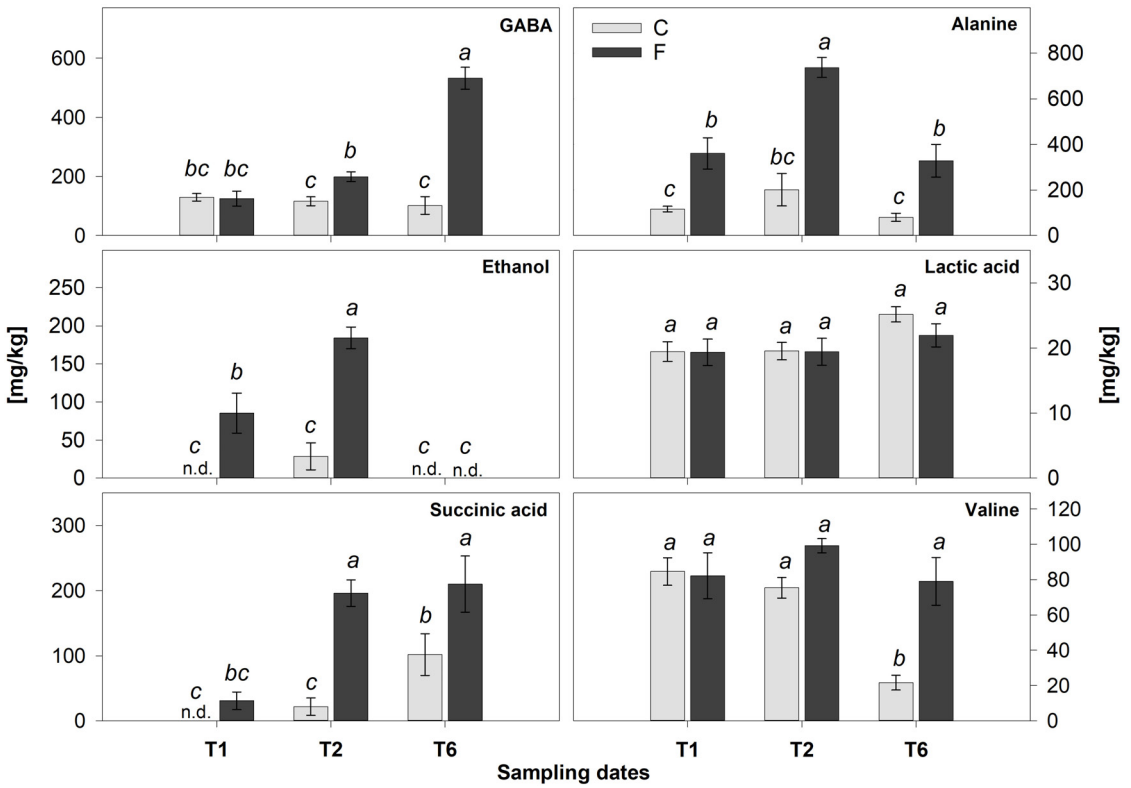

FIGURE 7 | Quantification of the main metabolites identified by ^{1}H-NMR in flooded (F) and control (C) samples at T1, T2, and T6. Values are mean ± SE (n = 5). Significant differences (Duncan's test, $p < 0.05$) are marked by different letters, n.d., not detectable.

internodes have been arranged in 6 classes of internodes starting from the basal to the apical ones: 1–2 (class I), 3–5 (class II), 6–10 (class III), 11–15 (class IV), 16–20 (class V), and 21–25 (class VI) and their elongation dynamics were computed during both seasons (**Figure 9B**, season 2017; season 2016, **Supplementary Figure S15**). Upon recovery, the mean length of F internodes resulted significantly shorter of about 23 and 33%, and maximum growth rates were lower of about 42 and 34%, than C ones for class I and II, respectively. The growth dynamics of class III internodes resulted to be similar both in timing of development, maximum length and elongation rates. On the contrary, median to apical F internode classes IV, V and VI (11–15, 16–20, and 21–25 nodes) resulted longer (19.6, 15, and 18%), with higher (17.4, 49.3, and 23.1%) and earlier (1.1, 4.4, and 4.2 days) elongation rates compared to C ones (**Figure 9B**).

DISCUSSION

The past decade has seen an astonishing run of record-breaking storms, forest fires, droughts, heat waves, and floods around the world with just 1.0°C of global warming (IPCC, 2018). More frequent flooding events due to heavier precipitations are expected worldwide in the context of climate change posing new challenges to traditional viticulture.

The most important constraint that plants have to deal with during flooding is O_2 deficiency. The drastic reduction of O_2 availability consequent to waterlogging impacts plant metabolism and, in turn, crop growth and productivity. In depth studies have shed light on the low oxygen adaptive responses in different models, both crop and wild plants (Licausi and Perata, 2009; Bailey-Serres et al., 2012; Loreti et al., 2016). The information on grapevine (*Vitis spp*) responses to waterlogging is scattered and basic information on molecular and metabolic responses of grapevine roots to hypoxia is lacking. Such studies are further complicated by the fact that cultivated grapevines are hybrid plants resulting from different rootstock x scion combinations thus making it necessary to take into account complex interactions between different genotypes and the environment. Clarifying how the metabolic events taking place in the below ground organs (rootstock) may co-ordinate or influence the development of above ground organs (scion), during and after waterlogging stress, must necessarily consider different genotypic combinations. Pioneering studies have reported various degrees of tolerance to flooding for some grapevine rootstock genotypes obtained by inter-specific crosses of American varieties: 'K5BB' and '420A' (*V. berlandieri* x *V. riparia*), '3309C' (*V. riparia* x *V. rupestris*) and '1616C' (*V. longii x V. riparia*) have been reported as moderate flooding tolerant compared to more sensitive ones such as '41B', '110 R', '140Ru', and '1103 P' (*V. berlandieri* x *V. rupestris*)

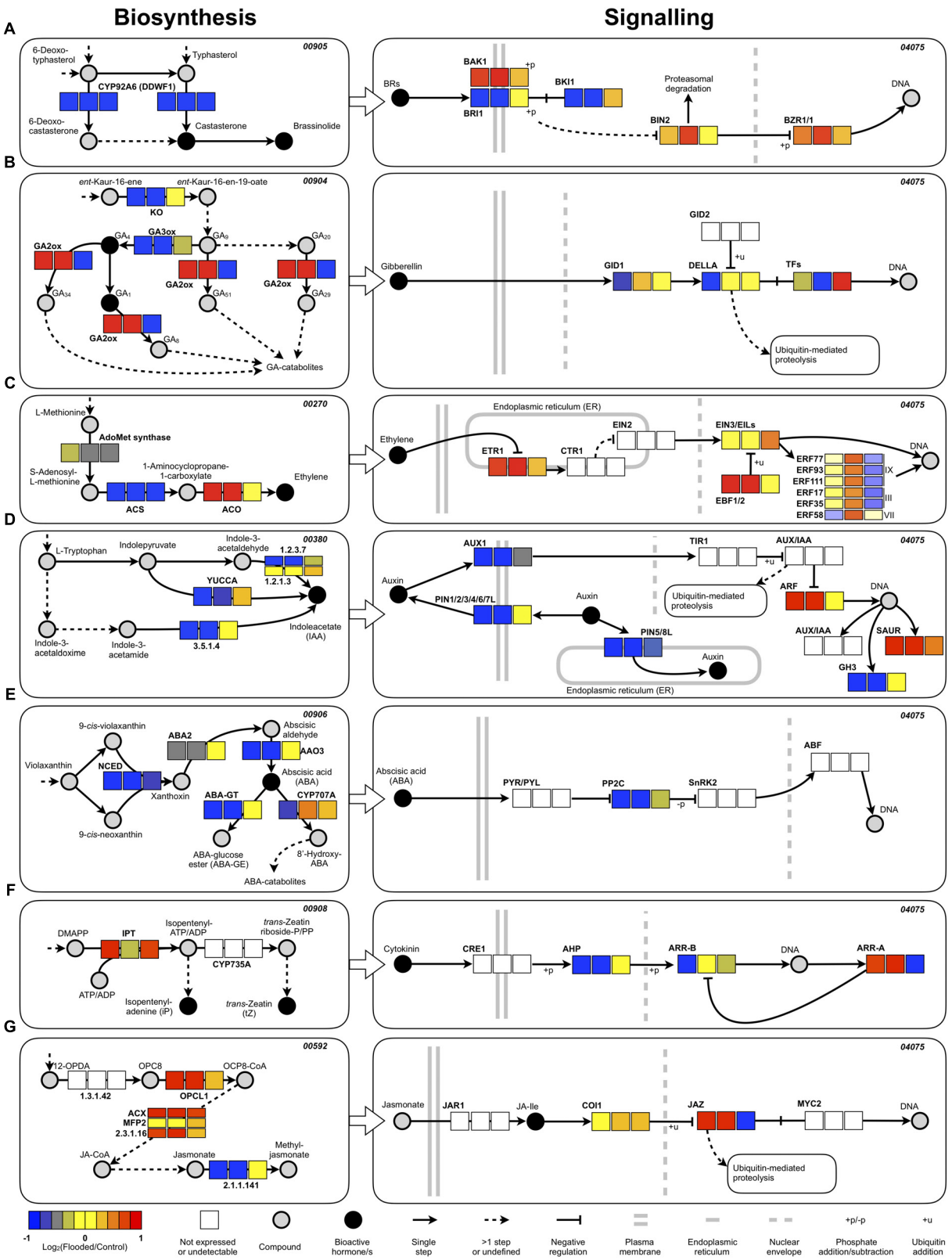

FIGURE 8 | Expression patterns of the most relevant genes related to hormone biosynthesis/homeostasis, perception, and signal transduction plotted within the correspondent KEGG maps (the pathway code is also indicated at the top-right of eachmap). Only the most relevant part of the pathways of brassinosteroids **(A)**, (*Continued*)

FIGURE 8 | Continued
gibberellins **(B)**, ethylene **(C)**, auxin **(D)**, abscisic acid **(E)**, cytokinins **(F)**, and jasmonate **(G)** were extracted (the whole maps are available as **Supplementary Figures S7–S14**) and represented according to the standard KEGG visualization, with the same colors rendered by Pathview (Luo et al., 2017) and some slight variations (an additional legend is provided): the names of the compounds and the key enzymes/proteins are reported with regular and bold fonts, respectively. Concerning the ERFs, only those with consistent expression patterns in both years are reported along with their nomenclature (Licausi et al., 2011) and classification. The differential expression level was calculated as log2-ratio (Flooded versus Control), scale-centered for each time point, and color-coded as displayed in the legend (blue: <–1; red: >+1). Each box, representing a specific enzymatic or regulatory step, is divided in three sub-boxes representing the different time points: from left to right T1, T2, and T6.

(Striegler et al., 1993; Kawai et al., 1996; de Herralde et al., 2005; Mugnai et al., 2011). Such differences may be at least in part ascribed to the different adaptive behavior to hypoxia and/or anoxia of the parental genotypes *V. riparia* (originating from riverbanks and thus tolerant to short term flooding) and *V. rupestris* (originating from arid areas and flooding sensitive). *V. riparia*'s higher tolerance has been functionally connected to its better ability to maintain ion homeostasis (sustaining K^+ uptake) during prolonged hypoxia and to preserve enough O_2 for the respiratory needs in the root apical meristem (Mancuso and Boselli, 2002; Mancuso and Marras, 2006; Mugnai et al., 2011). As far as the coordinated development of the below and above ground organs is concerned, previous studies reported that root flooding occurring in coincidence with the onset of budbreak did not suppress budbreak but rather inhibited shoot and later root growth (Striegler et al., 1993; Stevens and Prior, 1994; Kawai et al., 1996; Mancuso and Boselli, 2002; Mancuso and Marras, 2006; Mugnai et al., 2011). So far, short term (up to 2 weeks) single or repeated cycles of waterlogging have been shown to cause growth reductions in grapevine, in terms of shoot elongation, leaf growth, altered nutrient composition and leaf gas exchange (Striegler et al., 1993; Stevens and Prior, 1994; Stevens and Harvey, 1995; Stevens et al., 1999; de Herralde et al., 2005).

In the present study, we aimed at obtaining the first molecular and metabolic characterization of the low oxygen responses of the moderate flooding tolerant K5BB rootstock on which *V. vinifera* cv. Sauvignon blanc vines had been grafted. Over two consecutive vegetative seasons, a long term flooding stress was imposed for 21-days to vines at the late dormancy period preceding budbreak. The rate of internode elongation was measured as a proxy for rootstock to scion signaling during the 95 days following the end of the flooding stress. This experimental set-up is peculiar in that the flooding stress was imposed in a period preceding budbreak when grapevine roots had started to be metabolically active but plants did not have shoots and leaves to compensate for oxygen deficiency in roots. This choice was made in order to mimic exactly the timing at which the most frequent flooding events occur in the field (IPCC, 2012, 2013). Genome-scale RNA-Seq transcriptomic analyses have been integrated with ^{1}H-NMR metabolic profiling to pinpoint molecular and metabolic changes taking place at the root level in time-course experiments at 1 day (T1) and 2 days (T2) of flooding as well as after 1 week from the recovery from flooding (T6, 28 days) (**Supplementary Figure S1**).

Indeed, transcriptomic data consistently pointed out a significant primary metabolic reprogramming of K5BB grapevine roots in response to flooding already after 1 (T1) and 2 (T2) days from the onset of stress, showing the up-regulation of a set of genes involved in the enhancement of the glycolytic and ethanolic fermentative pathways, the partial reversal of the TCA cycle and a substantial change in amino acid metabolism (**Figures 2–4**). These gene expression changes were supported by metabolic data showing significantly increased accumulation of ethanol (but not of lactic acid), succinic acid, alanine and GABA, respectively, in flooded roots in comparison to control ones (**Figure 7**). These data are in agreement with a metabolic adjustment typical of a low oxygen quiescent strategy (LOQS). LOQS is typical of plants experiencing long periods of exposure to flooding or submergence for which a higher survival rate is ensured by energy saving strategies based on substantial metabolic reprogramming (Bailey-Serres et al., 2012). This consists in a shift toward fermentative metabolism coupled with an increase in the glycolytic flux and with changes in amino acid metabolism. In LOQS, the accumulation of metabolites such as lactate, ethanol, succinate, and even malate witnesses the rewiring of plant cell primary metabolism and the activation of hypoxia-inducible metabolic pathways (van Dongen and Licausi, 2015; Paul et al., 2016). Increased levels of alanine and GABA are specific landmarks of low oxygen conditions (Ricard et al., 1994; Reggiani, 1999) and underlie the substantial change in metabolism of amino acids in response to anoxia, for which a central role is played by glutamate, the common precursor of both alanine and GABA (Branco-Price et al., 2008). Indeed, a recent work by António et al. (2016), implementing an earlier work by Rocha et al. (2010), has provided evidence showing that the increase in GABA, alanine and succinic acid in response to hypoxia is manly a consequence of the activation of the GABA shunt and of the inhibition of the conversion of succinate to fumarate by SDH. Our metabolic and transcriptomic data are in agreement with such findings. Our data, besides confirming such metabolic shifts in response to hypoxia also pointed out that in K5BB grapevine roots the accumulation of GABA and succinic acid, differently from that of ethanol that can diffuse out of the roots, tends to persist also after 1 week of recovery.

The mechanisms involved in the low oxygen sensing and transduction, underpinning the LOQS metabolic shifts, have been largely clarified (Gibbs et al., 2011; Licausi et al., 2011) and sets of specific genes up- or down-regulated in plants in response to flooding and low oxygen have been identified (Loreti et al., 2016).

A prominent role in oxygen sensing and signal transduction in plants has been attributed to the ERF ARR factors belonging to group VII, which behave as master regulators of at least a subset of low oxygen responses (Gibbs et al., 2011; Licausi et al., 2011).

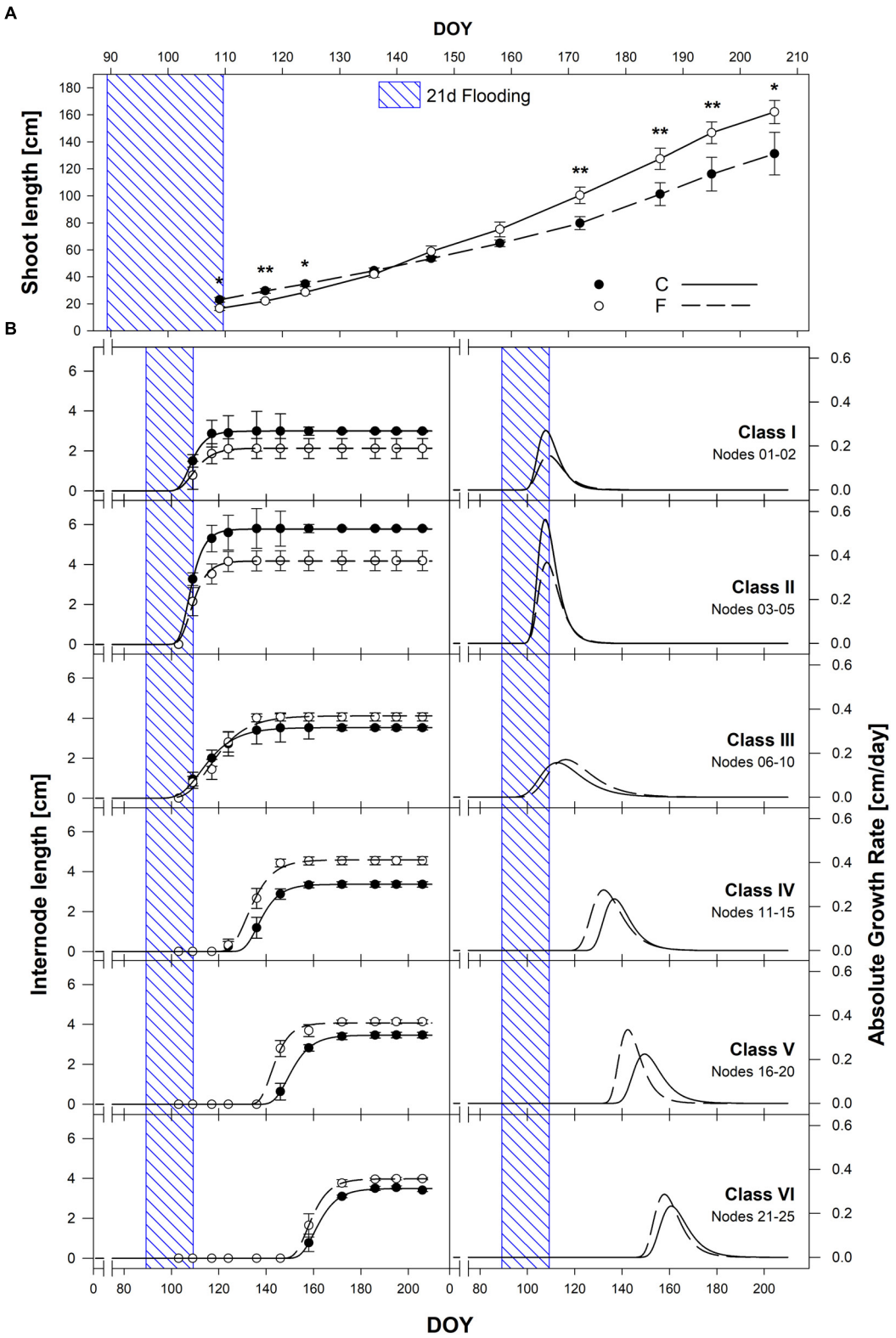

FIGURE 9 | (A) Shoot length growth dynamics among (C, black circles) and flooded (F, white circles) treatments throughout the 2017 season. **(B)** Mean internode classes elongation dynamics: 1–2 (class I), 3–5 (class II), 6–10 (class III), 11–15 (class IV), 16–20 (class V), and 21–25 (class VI). Sigmoidal curves represent best fitting curves through non-linear regression for C (solid line) and F (dotted line) treatments enabling AGR dynamics computation for each internode class. Asterisks denote mean values that are statistically different at $*p < 0.05$, $**p < 0.01$.

The proteins encoded by these genes are subject to a finely tuned post-translational regulation, being degraded in the presence and stabilized in the absence of oxygen, thus leading to their migration into the nucleus and to the activation of the transcription of the LOQS adaptive genes. Our transcriptomic and metabolic data show that K5BB grapevine roots, possibly due to the parental contribution of *V. riparia*, undergo the typical metabolic changes that represent a hallmark of a quiescent metabolic state. These data may support the hypothesis that K5BB or, more in general, grapevine rootstocks with a moderate tolerance to flooding events (e.g., those including *V. riparia* as a parent) (Striegler et al., 1993; Kawai et al., 1996; de Herralde et al., 2005; Mugnai et al., 2011) may base their low oxygen adaptation strategy on a quiescent (LOQS) rather than on an escape behavior (LOES). Among the known grapevine AP2/ERF ARR factors family (Licausi et al., 2010) expressed in K5BB roots we could identify a single gene encoding a *bona fide* group VII ERF protein that appeared to be transcriptionally up-regulated during hypoxia (T2) and later down-regulated during recovery (T6). Whether this gene may be the one ERF responsible for part of the adaptive metabolic responses evidenced in this work on hypoxic K5BB roots will need to be further investigated.

Ethylene plays a primary role in the regulation of hypoxic responses (reviewed by Sasidharan et al., 2018) also through the regulation of AP2/ERF genes. However, the transcriptomic profiling of flooded K5BB roots pointed out substantial transcriptional changes connecting several hormonal biosynthetic and signal transduction pathways and suggesting that an entire rearrangement of the hormonal balance takes place in response to hypoxia as a consequence of reciprocally dependent cross-talks (**Figure 8**). A general down-regulation of brassinosteroids, auxin and gibberellin biosynthesis appeared evident during waterlogging (T1 and T2). These changes may pinpoint decreased auxin levels in hypoxic K5BB roots, also associated with the down-regulation of both influx (AUX1) and efflux (PINs) auxin carriers, known to be connected with the intracellular auxin content and involved in the determination of its flux (Band et al., 2014). On the other hand, an up-regulation of transcription of ARF genes, positive regulators of auxin responses, was also seen in the absence of regulation of AUX/IAAs. Even though an univocal conclusion on the regulation of auxin responses cannot be drawn, these data may complement those recently reported by Eysholdt-Derzsó and Sauter (2017) showing the hypoxia-induced and ethylene- and RAP2.12-dependent down-regulation of auxin transport through a decreased protein abundance of the auxin efflux carrier PIN2, leading to increased auxin responses in hypoxic *Arabidopsis* roots. These evidences taken together strongly suggest a cross-talk between ethylene and auxin under hypoxic conditions, in which ethylene exerts a regulation on auxin levels/transport and on root growth and gravitropic responses through the control of the group VII ERF protein RAP2-12, a major regulator of low oxygen responses (Gibbs et al., 2011; Licausi et al., 2011; Eysholdt-Derzsó and Sauter, 2017). In parallel to the overall down-regulation of auxin, brassinosteroids and gibberellins biosynthesis, the biosynthesis of cytokinin and jasmonate appeared transcriptionally induced during waterlogging, suggesting that the latter two hormones may exert a further control over root growth (Wasternack and Hause, 2013). These changes, taken as a whole, suggest a highly co-ordinated reprogramming of the root hormonal profile which may fine-tune root growth and lateral root initiation in the presence of different oxygen availability. The significant enrichment of down-regulated DEGs in the GO category "regulation of meristem growth" may support an overall inhibition of root growth processes and lend further evidence to the hypothesis of a LOQS response taking place in K5BB roots exposed to low oxygen.

At 1 week after removal of the flooding stress (T6), most of these pathways resulted to be fully recovered at the transcriptional level, indicating a prompt readjustment of hormonal responses during the recovery phase. This was particularly evident for gibberellin biosynthetic genes that appeared down-regulated during flooding (T1 and T2) while those involved in metabolism were up-regulated. This effects appeared to be reversed as soon as the waterlogging ceased, indicating also a highly modulated control on gibberellin levels in relation to oxygen. The latter hormonal changes may be connected with the response of the upper, above ground, aerial plant. The inhibition of internode elongation soon after stress exposure (at the onset of budbreak) and the significant stimulation of internode elongation during later recovery time-points in plants that had experienced flooding in comparison to control ones are consistent with the timing of inactivation and reactivation of GA biosynthesis and action (**Figure 9**).

These findings are also in agreement with those reported by Stevens and Prior (1994) in potted Sultana vines during initial growth stages after budbreak with an initial shoot elongation rate of about 30% during the first 4 weeks after stress removal. Also the recovery of shoot elongation rates resulted in agreement with data available in the literature (Stevens and Prior, 1994; Stevens et al., 1999) reporting that the vines took more than 11 days to overcome flooding stress. In the present experiment, the inhibitory effect on shoot elongation lasted about 20 days after stress removal. Interestingly, budbreak in flooded plants appeared slightly but significantly slower than in non-flooded control ones. This early effect may also be related to the substantial hormonal changes leading to a likely abundance of ethylene in hypoxic roots immediately (within 1–2 days) followed by a likely accumulation of ACC, which could not be any more converted to the active hormone due to the lack of oxygen.

Additional experimental evidence will be needed to show how the main parental grapevine rootstock genotypes *V. riparia*, *V. rupestris* and *V. berlandieri* are affected by waterlogging in the short and long term to further clarify the role of the metabolic and transcriptomic reprogramming described in this work and to elucidate which processes are decisive in regulating flooding tolerance in grapevine. A comparison between a resistant and a sensitive genotype to waterlogging would thus enable to identify genotype-specific responses and to define key markers for tolerance to flooding that could be used to improve selection of waterlogging tolerant rootstocks. Furthermore, serious attention should be paid on that the effects of the hormonal rearrangement

taking place in the roots, shown in this study, may differ significantly between different rootstocks genotypes. This may happen both during waterlogging or during the recovery phase, the latter one being an equally essential step defining plants adaptation and survival to flooding (Yeung et al., 2018), and may result in a range of phenological effects on the above ground plant, with varied viticultural implications.

DATA AVAILABILITY

The datasets generated for this study can be found in NCBI BioProject database, PRJNA521303.

AUTHOR CONTRIBUTIONS

FM, BR, AB, and SQ developed the concept of the manuscript and wrote the manuscript. MB and AB performed the whole transcriptome and bioinformatic analyses. GE, FP, ST, and NC carried out qRT-PCR analyses and sample preparation. ES and PG carried out NMR metabolic profiling and FM collected and analyzed biometrical data. All authors discussed and commented on the manuscript.

FUNDING

This work was supported by Italian Ministry of Research and University (MIUR) in the frame of SIR 2014, project GrapeXtreme, cod. RBSI14H5R0.

SUPPLEMENTARY MATERIAL

The Supplementary Material for this article can be found online at: https://www.frontiersin.org/articles/10.3389/fpls.2019.00339/full#supplementary-material

REFERENCES

Anderson, K., and Nelgen, S. (2011). *Global Wine Markets, 1961 to 2009: A Statistical Compendium*. Adelaide: University of Adelaide Press. doi: 10.1104/pp.15.00266

António, C., Päpke, C., Rocha, M., Diab, H., Limami, A. M., Obata, T., et al. (2016). Regulation of primary metabolism in response to low oxygen availability as revealed by carbon and nitrogen isotope redistribution. *Plant Physiol.* 170, 43–56. doi: 10.1104/pp.15.00266

Bailey-Serres, J., and Chang, R. (2005). Sensing and signalling in response to oxygen deprivation in plants and other organisms. *Ann. Bot.* 96, 507–518. doi: 10.1104/pp.112.208173

Bailey-Serres, J., Lee, S. C., and Brinton, E. (2012). Waterproofing crops: effective flooding survival strategies. *Plant Physiol.* 160, 1698–1709. doi: 10.1146/annurev.arplant.59.032607.092752

Bailey-Serres, J., and Voesenek, L. A. (2008). Flooding stress: acclimations and genetic diversity. *Annu. Rev. Plant Biol.* 59, 313–339. doi: 10.1146/annurev.arplant.59.032607.092752

Bailey-Serres, J., and Voesenek, L. A. (2010). Life in the balance: a signaling network controlling survival of flooding. *Curr. Opin. Plant Biol.* 13, 489–494. doi: 10.1016/j.pbi.2010.08.002

Band, L. R., Wells, D. M., Fozard, J. A., Ghetiu, T., French, A. P., Pound, M. P., et al. (2014). Systems analysis of auxin transport in the *Arabidopsis* root apex. *Plant Cell* 26, 862–875. doi: 10.1105/tpc.113.119495

Binder, B. M., Walker, J. M., Gagne, J. M., Emborg, T. J., Hemmann, G., Bleecker, A. B., et al. (2007). The Arabidopsis EIN3 binding F-Box proteins EBF1 and EBF2 have distinct but overlapping roles in ethylene signaling. *Plant Cell* 19, 509–523. doi: 10.1093/aob/mcf118

Blokhina, O., Virolainen, E., and Fagerstedt, K. V. (2003). Antioxidants, oxidative damage and oxygen deprivation stress: a review. *Ann. Bot.* 91, 179–194. doi: 10.1111/j.1365-313X.2008.03642.x

Branco-Price, C., Kaiser, K. A., Jang, C. J. H., Larive, C. K., and Bailey-Serres, J. (2008). Selective mRNA translation coordinates energetic and metabolic adjustments to cellular oxygen deprivation and reoxygenation in *Arabidopsis thaliana*. *Plant J.* 56, 743–755. doi: 10.1111/j.1365-313X.2008.03642.x

Carvalho, L. C., Vidigal, P., and Amâncio, S. (2015). Oxidative stress homeostasis in grapevine (*Vitis vinifera* L.). *Front. Environ. Sci.* 3:20. doi: 10.3389/fenvs.2015.00020

Castellarin, S. D., Pfeiffer, A., Sivilotti, P., Degan, M., Peterlunger, E., and Di Gaspero, G. (2007). Transcriptional regulation of anthocyanin biosynthesis in ripening fruits of grapevine under seasonal water deficit. *Plant Cell Environ.* 30, 1381–1399. doi: 10.1016/j.pbi.2016.07.005

Chini, A., Gimenez-Ibanez, S., Goossens, A., and Solano, R. (2016). Redundancy and specificity in jasmonate signalling. *Curr. Opin. Plant Biol.* 33, 147–156. doi: 10.1016/j.pbi.2016.07.005

Colmer, T. D., and Voesenek, L. A. C. J. (2009). Flooding tolerance: suites of plant traits in variable environments. *Funct. Plant Biol.* 36, 665–681. doi: 10.1111/j.1755-0238.1995.tb00086.x

Crawford, R. M. M. (2003). Seasonal differences in plant responses to flooding and anoxia. *Can. J. Bot.* 81, 1224–1246. doi: 10.1139/b03-127

de Herralde, F., Savé, R., and Biel, C. (2005). Ecophysiological response to flood of seven grapevine cultivars. *Acta Hortic.* 689, 137–144. doi: 10.17660/ActaHortic.2005.689.13

Duchêne, E., and Schneider, C. (2005). Grapevine and climatic changes: a glance at the situation in Alsace. *Agron. Sustain. Dev.* 25, 93–99. doi: 10.1051/agro:2004057

Eccher, G., Begheldo, M., Boschetti, A., Ruperti, B., and Botton, A. (2015). Roles of ethylene production and ethylene receptor expression in regulating apple fruitlet abscission. *Plant Physiol.* 169, 125–137. doi: 10.1104/pp.15.00358

Eysholdt-Derzsó, E., and Sauter, M. (2017). Root bending is antagonistically affected by hypoxia and ERF-mediated transcription via Auxin signaling. *Plant Physiol.* 175, 412–423. doi: 10.1104/pp.17.00555

Falcon, S., and Gentleman, R. (2007). Using GOstats to test gene lists for GO term association. *Bioinformatics* 23, 257–258. doi: 10.1093/bioinformatics/btl567

FAO, IFAD, UNICEF, WFP, and WHO (2018). *The State of Food Security and Nutrition in the World 2018. Building Climate Resilience for Food Security and Nutrition*. Rome: FAO.

Frei, C., Davies, H. C., Gurtz, J., and Schär, C. (2000). Climate dynamics and extreme precipitation and flood events in Central Europe. *Integr. Assess.* 1, 281–300. doi: 10.1023/A:1018983226334

Gibbs, D. J., Lee, S. C., Md Isa, N., Gramuglia, S., Fukao, T., Bassel, G. W., et al. (2011). Homeostatic response to hypoxia is regulated by the N-end rule pathway in plants. *Nature* 479, 415–418. doi: 10.1038/nature10534

IPCC (2012). *Managing the Risks of Extreme Events and Disasters to Advance Climate Change Adaptation. A Special Report of Working Groups I and II of the Intergovernmental Panel On Climate Change,* [Field, C. B., V. Barros, T. F. Stocker, D. Qin, D. J. Dokken, K. L. Ebi, M. D. Mastrandrea, et al. (Cambridge: Cambridge University Press), 582.

IPCC (2013). *Climate Change 2013: The Physical Science Basis. Contribution of Working Group I to the Fifth Assessment Report of the Intergovernmental Panel on Climate Change*, [eds T. F. Stocker, D. Qin, G.-K. Plattner, M. Tignor, S. K. Allen, J. Boschung, et al. (Cambridge: Cambridge University Press), 1535.

IPCC (2018). *Global warming of 1.5°C. An IPCC Special Report on the Impacts of Global Warming of 1.5°C Above Pre-Industrial Levels and Related Global*

Greenhouse Gas Emission Pathways, in the Context Of Strengthening the Global Response to the Threat of Climate Change, Sustainable Development, and Efforts to Eradicate Poverty, eds V. Masson-Delmotte, P. Zhai, H. O. Pörtner, D. Roberts, J. Skea, P. R. Shukla, et al. (Cambridge: Cambridge University Press).

Ishizawa, K., Murakami, S., Kawakami, Y., and Kuramochi, H. (1999). Growth and energy status of arrowhead tubers, pondweed turions and rice seedlings under anoxic conditions. *Plant Cell Environ.* 22, 505–514. doi: 10.1046/j.1365-3040.1999.00439.x

Jaillon, O., Aury, J. M., Noel, B., Policriti, A., Clepet, C., Casagrande, A., et al. (2007). The grapevine genome sequence suggests ancestral hexaploidization in major angiosperm phyla. *Nature* 449, 463–467. doi: 10.1038/nature06148

Jones, G. V., White, M. A., Cooper, O. R., and Storchmann, K. (2005). Climate change and global wine quality. *Clim. Change* 73, 319–343. doi: 10.1007/s10584-005-4704-2

Ju, C., and Chang, C. (2015). Mechanistic insights in ethylene perception and signal transduction. *Plant Physiol.* 169, 85–95. doi: 10.1104/pp.15.00845

Kawai, Y., Benz, J., and Kliewer, W. M. (1996). Effect of flooding on shoot and root growth of rooted cuttings of four grape rootstocks. *J. Jpn. Soc. Hortic. Sci.* 65, 455–461. doi: 10.2503/jjshs.65.455

Kenny, G. J., and Harrison, P. A. (1992). The effects of climate variability and change on grape suitability in Europe. *J. Wine Res.* 3, 163–183. doi: 10.1080/09571269208717931

Klepikova, A. V., Kasianov, A. S., Chesnokov, M. S., Lazarevich, N. L., Penin, A. A., and Logacheva, M. (2017). Effect of method of deduplication on estimation of differential gene expression using RNA-seq. *PeerJ* 5:e3091. doi: 10.7717/peerj.3091

Lebon, E., Pellegrino, A., Tardieu, F., and Lecoeur, J. (2004). Shoot development in grapevine (*Vitis vinifera*) is affected by the modular branching pattern of the stem and intra- and inter-shoot trophic competition. *Ann. Bot.* 93, 263–274. doi: 10.1093/aob/mch038

Lee, S. C., Mustroph, A., Sasidharan, R., Vashisht, D., Pedersen, O., Oosumi, T., et al. (2011). Molecular characterization of the submergence response of the *Arabidopsis thaliana* ecotype Columbia. *New Phytol.* 190, 457–471. doi: 10.1111/j.1469-8137.2010.03590.x

Leolini, L., Moriondo, M., Fila, G., Costafreda-Aumedes, S., Ferrise, R., and Bindi, M. (2018). Late spring frost impacts on future grapevine distribution in Europe. *Field Crops Res.* 222, 197–208. doi: 10.1016/j.fcr.2017.11.018

Licausi, F., Giorgi, F. M., Zenoni, S., Osti, F., Pezzotti, M., and Perata, P. (2010). Genomic and transcriptomic analysis of the AP2/ERF superfamily in *Vitis vinifera*. *BMC Genomics* 11:719. doi: 10.1186/1471-2164-11-719

Licausi, F., and Perata, P. (2009). Low oxygen signaling and tolerance in plants. *Adv. Bot. Res.* 50, 139–198. doi: 10.1016/S0065-2296(08)00804-5

Licausi, F., Weits, D. A., Pant, B. D., Scheible, W. R., Geigenberger, P., and van Dongen, J. T. (2011). Hypoxia responsive gene expression is mediated by various subsets of transcription factors and miRNAs that are determined by the actual oxygen availability. *New Phytol.* 190, 442–456. doi: 10.1111/j.1469-8137.2010.03451.x

Lorenz, D. H., Eichhorn, K. W., Bleiholder, H., Klose, R., Meier, U., and Weber, E. (1995). Growth Stages of the Grapevine: Phenological growth stages of the grapevine (*Vitis vinifera* L. ssp. *vinifera*)-Codes and descriptions according to the extended BBCH scale. *Aust. J. Grape Wine Res.* 1, 100–103. doi: 10.1111/j.1755-0238.1995.tb00085.x

Loreti, E., van Veen, H., and Perata, P. (2016). Plant responses to flooding stress. *Curr. Opin. Plant Biol.* 33, 64–71. doi: 10.1016/j.pbi.2016.06.005

Louarn, G., Guedon, Y., Lecoeur, J., and Lebon, E. (2007). Quantitative analysis of the phenotypic variability of shoot architecture in two grapevine (*Vitis vinifera*) cultivars. *Ann. Bot.* 99, 425–437. doi: 10.1093/aob/mcl276

Love, M. I., Huber, W., and Anders, S. (2014). Moderated estimation of fold change and dispersion for RNA-seq data with DESeq2. *Genome Biol.* 15:550. doi: 10.1186/s13059-014-0550-8

Luo, W., Pant, G., Bhavnasi, Y. K., Blanchard, S. G., and Brouwer, C. (2017). Pathview Web: user friendly pathway visualization and data integration. *Nucleic Acids Res.* 45, W501–W508. doi: 10.1093/nar/gkx372

Mancuso, S., and Boselli, M. (2002). Characterisation of the oxygen fluxes in the division, elongation and mature zones of Vitis roots: influence of oxygen availability. *Planta* 214, 767–774. doi: 10.1007/s004250100670

Mancuso, S., and Marras, A. M. (2006). Adaptative response of Vitis root to anoxia. *Plant Cell Physiol.* 47, 401–409. doi: 10.1093/pcp/pcj007

Mancuso, S., and Shabala, S. (eds) (2010). *Waterlogging Signalling and Tolerance in Plants*. Heidelberg: Springer. doi: 10.1007/978-3-642-10305-6

Mason, M. G., Mathews, D. E., Argyros, D. A., Maxwell, B. B., Kieber, J. J., Alonso, J. M., et al. (2005). Multiple type-B response regulators mediate cytokinin signal transduction in Arabidopsis. *Plant Cell* 17, 3007–3018. doi: 10.1105/tpc.105.035451

Miller, G., Shulaev, V., and Mittler, R. (2008). Reactive oxygen signaling and abiotic stress. *Physiol. Plant* 133, 481–489. doi: 10.1111/j.1399-3054.2008.01090.x

Mommer, L., De Kroon, H., Pierik, R., Bögemann, G. M., and Visser, E. J. W. (2005). A functional comparison of acclimation to shade and submergence in two terrestrial plant species. *New Phytol.* 167, 197–206. doi: 10.1111/j.1469-8137.2005.01404.x

Mugnai, S., Marras, A. M., and Mancuso, S. (2011). Effect of hypoxic acclimation on anoxia tolerance in Vitis roots: response of metabolic activity and K+ fluxes. *Plant Cell Physiol.* 52, 1107–1116. doi: 10.1093/pcp/pcr061

Mustroph, A., Lee, S. C., Oosumi, T., Zanetti, M. E., Yang, H., Ma, K., et al. (2010). Cross-kingdom comparison of transcriptomic adjustments to low-oxygen stress highlights conserved and plant-specific responses. *Plant Physiol.* 152, 1484–1500. doi: 10.1104/pp.109.151845

Nonis, A., Ruperti, B., Pierasco, A., Canaguier, A., Adam-Blondon, A-F, Di Gaspero, G., et al. (2008). Neutral invertases in grapevine and comparative analysis with *Arabidopsis*, poplar and rice. *Planta* 229, 129–142. doi: 10.1007/s00425-008-0815-0

Olesen, J. E., Trnka, M., Kersebaum, K. C., Skjelvåg, A. O., Seguin, B., Peltonen-Sainio, P., et al. (2011). Impacts and adaptation of European crop production systems to climate change. *Eur. J. Agron.* 34, 96–112. doi: 10.1016/j.eja.2010.11.003

Paul, M. V., Iyer, S., Amerhauser, C., Lehmann, M., van Dongen, J. T., and Geigenberger, P. (2016). Oxygen sensing via the ethylene response transcription factor RAP2.12 affects plant metabolism and performance under both normoxia and hypoxia. *Plant Physiol.* 172, 141–153. doi: 10.1104/pp.16.00460

Pfaffl, M. W. (2001). A new mathematical model for relative quantification in real-time RT-PCR. *Nucleic Acids Res.* 29:e45. doi: 10.1093/nar/29.9.e45

Ponnamperuma, F. N. (1972). The chemistry of submerged soil. *Adv. Agron.* 24, 29–96. doi: 10.1016/S0065-2113(08)60633-1

Prosdocimi, M., Cerdà, A., and Tarolli, P. (2016). Soil water erosion on Mediterranean vineyards: a review. *Catena* 141, 1–21. doi: 10.1016/j.catena.2016.02.010

Quinlan, A. R., and Hall, I. M. (2010). BEDTools: a flexible suite of utilities for comparing genomic features. *Bioinformatics* 26, 841–842. doi: 10.1093/bioinformatics/btq033

R Core Team (2018). *R: A Language and Environment for Statistical Computing*. Vienna: R Foundation for Statistical Computing. Available at: https://www.R-project.org

Reggiani, R. (1999). Amino acid metabolism under oxygen deficiency. *Curr. Top. Phytochem.* 2, 171–174.

Ricard, B., Couée, I., Raymond, P., Saglio, P. H., Saint-Ges, V., and Pradet, A. (1994). Plant metabolism under hypoxia and anoxia. *Plant Physiol. Biochem.* 32, 1–10.

Rocha, M., Licausi, F., Araújo, W. L., Nunes-Nesi, A., Sodek, L., Fernie, A. R., et al. (2010). Glycolysis and the tricarboxylic acid cycle are linked by alanine aminotransferase during hypoxia induced by waterlogging of Lotus japonicus. *Plant Physiol.* 152, 1501–1513. doi: 10.1104/pp.109.150045

Santos, J. A., Malheiro, A. C., Karremann, M. K., and Pinto, J. G. (2011). Statistical modelling of grapevine yield in the Port Wine region under present and future climate conditions. *Int. J. Biometeorol.* 55, 119–131. doi: 10.1007/s00484-010-0318-0

Sasidharan, R., Hartman, S., Liu, Z., Martopawiro, S., Sajeev, N., van Veen, H., et al. (2018). Signal dynamics and interactions during flooding stress. *Plant Physiol.* 176, 1106–1117. doi: 10.1104/pp.17.01232

Sato, T., Harada, T., and Ishizawa, K. (2002). Stimulation of glycolysis in anaerobic elongation of pondweed (*Potamogeton distinctus*) turions. *J. Exp. Bot.* 53, 1847–1856. doi: 10.1093/jxb/erf036

Sauter, M. (2013). Root responses to flooding. *Curr. Opin. Plant Biol.* 16, 282–286. doi: 10.1016/j.pbi.2013.03.013

Schultz, H. (2000). Climate change and viticulture: a European perspective on climatology, carbon dioxide and UV-B effects. *Aust. J. Grape Wine Res.* 6, 2–12. doi: 10.1111/j.1755-0238.2000.tb00156.x

Schwartz, S. H., Qin, X., and Zeevaart, J. A. D. (2003). Elucidation of the indirect pathway of abscisic acid biosynthesis by mutants, genes, and enzymes. *Plant Physiol.* 131, 1591–1601. doi: 10.1104/pp.102.017921

Shabala, S. (ed.) (2012). *Plant Stress Physiology*. Wallingford: CAB International, 1–318. doi: 10.1079/9781845939953.0000

Simon, P. (2003). Q-Gene: processing quantitative real-time RT-PCR data. *Bioinformatics* 19, 1439–1440. doi: 10.1093/bioinformatics/btg157

Stevens, R., and Harvey, G. (1995). Effects of waterlogging, rootstock and salinity on Na, Cl and K concentrations of the leaf and root, and shoot growth of sultana grapevines. *Aust. J. Agric. Res.* 46, 541–551. doi: 10.1071/AR9950541

Stevens, R. M., Harvey, G., and Johns, R. E. (1999). Waterlogging reduces shoot growth and bud fruitfulness in pot-grown grapevines with a split-root system. *Aust. J. Grape Wine Res.* 5, 99–103. doi: 10.1111/j.1755-0238.1999.tb00293.x

Stevens, R. M., and Prior, L. D. (1994). The effect of transient waterlogging on the growth, leaf gas exchange, and mineral composition of potted sultana grapevines. *Am. J. Enol. Vitic.* 45, 285–290.

Striegler, R. K., Howell, G. S., and Flore, J. A. (1993). Influence of rootstock on the response of seyval grapevines to flooding stress. *Am. J. Enol. Vitic.* 44, 313–319.

Summers, J. E., Ratcliffe, R. G., and Jackson, M. B. (2000). Anoxia tolerance in the aquatic monocot *Potamogeton pectinatus*: absence of oxygen stimulates elongation in association with an unusually large pasteur effect. *J. Exp. Bot.* 51, 1413–1422. doi: 10.1093/jexbot/51.349.1413

Terral, J. F., Tabard, E., Bouby, L., Ivorra, S., Pastor, T., Figueiral, I., et al. (2010). Evolution and history of grapevine (Vitis vinifera) under domestication: new morphometric perspectives to understand seed domestication syndrome and reveal origins of ancient European cultivars. *Ann. Bot.* 105, 443–455. doi: 10.1093/aob/mcp298

To, J. P. C., Haberer, G., Ferreira, F. J., Deruère, J., Mason, M. G., Schaller, G. E., et al. (2004). Type-A Arabidopsis response regulators are partially redundant negative regulators of cytokinin signaling. *Plant Cell* 16, 658–671. doi: 10.1105/tpc.018978

Trapnell, C., Pachter, L., and Salzberg, S. L. (2009). TopHat: Discovering splice junctions with RNA-Seq. *Bioinformatics* 25, 1105–1111. doi: 10.1093/bioinformatics/btp120

Umetrics (2015). *SIMCA-P+ (Version 14.0.0)*. Umeå: Umetrics Inc. Available at: http://umetrics.com/products/simca

Van Breusegem, F., Bailey-Serres, J., and Mittler, R. (2008). Unraveling the tapestry of networks involving reactive oxygen species in plants. *Plant Physiol.* 147, 978–984. doi: 10.1104/pp.108.122325

van Dongen, J. T., and Licausi, F. (2015). Oxygen sensing and signaling. *Annu. Rev. Plant Biol.* 66, 345–367. doi: 10.1146/annurev-arplant-043014-114813

van Leeuwen, C., Friant, P., Choné, X., Tregoat, O., Koundouras, S., and Dubourdieu, D. (2004). Influence of Climate, Soil, and Cultivar on Terroir. *Am. J. Enol. Vitic.* 55, 207–217.

Vitulo, N., Forcato, C., Carpinelli, E. C., Telatin, A., Campagna, D., D'Angelo, M., et al. (2014). A deep survey of alternative splicing in grape reveals changes in the splicing machinery related to tissue, stress condition and genotype. *BMC Plant Biol.* 14:99. doi: 10.1186/1471-2229-14-99

Voesenek, L. A., and Bailey-Serres, J. (2015). Flood adaptive traits and processes: an overview. *New Phytol.* 206, 57–73. doi: 10.1111/nph.13209

Voesenek, L. A. C. J., Rijnders, J. H. G. M., Peeters, A. J. M., van de Steeg, H. M., and de Kroon, H. (2004). Plant hormones regulate fast shoot elongation under water: from genes to communities. *Ecology* 85, 16–27. doi: 10.1890/02-740

Wasternack, C., and Hause, B. (2013). Jasmonates: biosynthesis, perception, signal transduction and action in plant stress response, growth and development. An update to the 2007 review in Annals of Botany. *Ann. Bot.* 111, 1021–1058. doi: 10.1093/aob/mct067

Westra, S., Fowler, H. J., Evans, J. P., Alexander, L. V., Berg, P., Johnson, F., et al. (2014). Future changes to the intensity and frequency of short-duration extreme rainfall. *Rev. Geophys.* 52, 522–555. doi: 10.1002/2014RG000464

Wiklund, S., Johansson, E., Sjóström, L., Mellerowicz, E. J., Edlund, U., Shockcor, J. P., et al. (2008). Visualization of GC/TOF-MS-based metabolomics data for identificationof biochemically interesting compounds using OPLS classmodels. *Anal. Chem.* 80, 115–122. doi: 10.1021/ac0713510

Yeung, E., van Veen, H., Vashisht, D., Sobral Paiva, A. L., Hummel, M., Rankenberg, T., et al. (2018). A stress recovery signaling network for enhanced flooding tolerance in *Arabidopsis thaliana*. *Proc. Natl. Acad. Sci. U.S.A.* 115, E6085–E6094. doi: 10.1073/pnas.1803841115

Conflict of Interest Statement: The authors declare that the research was conducted in the absence of any commercial or financial relationships that could be construed as a potential conflict of interest.

frontiers in Plant Science

ORIGINAL RESEARCH
published: 29 March 2019
doi: 10.3389/fpls.2019.00259

Root Cortex Provides a Venue for Gas-Space Formation and Is Essential for Plant Adaptation to Waterlogging

Takaki Yamauchi[1,2], Fumitaka Abe[3], Nobuhiro Tsutsumi[2] and Mikio Nakazono[4,5]*

[1]Japan Science and Technology Agency, PRESTO, Kawaguchi, Japan, [2]Graduate School of Agricultural and Life Sciences, University of Tokyo, Tokyo, Japan, [3]Institute of Crop Science, NARO, Tsukuba, Japan, [4]Graduate School of Bioagricultural Sciences, Nagoya University, Nagoya, Japan, [5]UWA School of Agriculture and Environment, The University of Western Australia, Crawley, WA, Australia

Lysigenous aerenchyma, which develops by death and subsequent lysis of the cortical cells in roots, is essential for internal long-distance oxygen transport from shoot base to root tips of plants in waterlogged soil. Although many studies focus on the amounts of aerenchyma in roots, significance of the size of the root cortex in which aerenchyma forms has received less research attention. In the present study, we evaluated the cross-sectional area of each root tissue in adventitious roots of upland crops, wheat (*Triticum aestivum*) and maize (*Zea mays* ssp. *mays*), and the wetland crop, rice (*Oryza sativa*) under aerated or stagnant deoxygenated conditions; the latter can mimic the changes in gas composition in waterlogged soils. Our analyses revealed that the areas of whole root and cortex of the three species increased under stagnant conditions. In rice roots, cortex to stele ratio (CSR) and aerenchyma to cortex ratio (ACR), which is associated with the areas of gas spaces, were much higher than those in wheat and maize roots, suggesting that these anatomical features are essential for a high capacity for oxygen transport along roots. To test this hypothesis, rates of radial oxygen loss (ROL), which is the diffusive flux of oxygen from within a root to the external medium, from thick and thin adventitious roots of rice were measured using a cylindrical (root-sleeving) oxygen electrode, for plants with shoots in air and roots in an oxygen-free medium. As expected, the rate of ROL from thick roots, which have larger cortex and aerenchyma areas, was higher than that of thin roots. The rate of ROL was highest at the apical part of rice roots, where aerenchyma was hardly detected, but at which cuboidal cell arrangement in the cortex provides tissue porosity. We conclude that high CSR in combination with large root diameter is a feature which promotes oxygen transport from shoot base to root tips of plants. Moreover, we propose that CSR should be a useful quantitative index for the evaluation and improvement of root traits contributing to tolerance of crops to soil waterlogging.

Keywords: aerenchyma, cereal crops, cortex to stele ratio, intercellular spaces, longitudinal oxygen transport, radial oxygen loss, waterlogging

OPEN ACCESS

Edited by:
Francesco Licausi, University of Pisa, Italy

Reviewed by:
Gustavo Gabriel Striker, CONICET Instituto de Investigaciones Fisiológicas y Ecologicas Vinculadas a la Agricultura (IFEVA), Argentina
María Laura Vidoz, Instituto de Botánica del Nordeste (IBONE-CONICET), Argentina

****Correspondence:***
Takaki Yamauchi
atkyama@mail.ecc.u-tokyo.ac.jp

Specialty section:
This article was submitted to Plant Abiotic Stress, a section of the journal Frontiers in Plant Science

Received: *29 October 2018*
Accepted: *18 February 2019*
Published: *29 March 2019*

Citation:
Yamauchi T, Abe F, Tsutsumi N and Nakazono M (2019) Root Cortex Provides a Venue for Gas-Space Formation and Is Essential for Plant Adaptation to Waterlogging. Front. Plant Sci. 10:259. doi: 10.3389/fpls.2019.00259

INTRODUCTION

Roots are mainly composed of four concentric cell layers: from the outside to inside, these cell layers are the epidermis, cortex, endodermis, and stele (Scheres et al., 2002). The stele contains xylem vessels and phloem tissue which are essential for the transport of water, inorganic ions, and organic compounds (Nissen, 1974; Petricka et al., 2012), as well as a pith in the case of monocots (Watt et al., 2008). The primary root of *Arabidopsis* (*Arabidopsis thaliana*) has a single cortex cell layer which is produced by the asymmetric cell division of cortex/endodermis initial cell (Dolan et al., 1993; Laurenzio et al., 1996). By contrast, roots of rice (*Oryza sativa*) have several cortex cell layers produced by the sequential cell divisions of the endodermal cells (Kamiya et al., 2003). Unlike *Arabidopsis*, many plant species including the family Poaceae, members of which include important crops, have several cortex cell layers (Armstrong, 1979; Justin and Armstrong, 1987).

The principal cause of damage to plants grown in waterlogged soil is inadequate supply of oxygen to submerged roots (Armstrong, 1979; Colmer and Voesenek, 2009). Therefore, internal oxygen transport from shoot base to root tips is crucial for the survival of plants under waterlogged conditions (Armstrong, 1979; Colmer, 2003b). Diffusivity of oxygen in water is approximately 10,000-fold slower than in air (Armstrong and Drew, 2002). Because plants have no active oxygen transport mechanisms, oxygen movement from shoot to submerged tissues is dominated by diffusion (Armstrong and Armstrong, 2014). Aerenchyma consists of longitudinally connected gas spaces which enhances the diffusion of oxygen within plants (Armstrong, 1979; Colmer, 2003b). Lysigenous aerenchyma in roots is formed by the creation of gas spaces as a result of death and the subsequent lysis of cortical cells (Evans, 2003). Plants in the family Poaceae, such as wheat (*Triticum aestivum*), maize (*Zea mays* ssp. *mays*), and rice form lysigenous aerenchyma in the roots (Yamauchi et al., 2018). Under aerobic conditions, roots of wheat and maize typically form small amounts of aerenchyma, but the amount of aerenchyma nevertheless increases under oxygen-deficient conditions (Abiko et al., 2012; Mano and Omori, 2013; Yamauchi et al., 2014b). Rice forms aerenchyma constitutively, and its formation further increases under oxygen-deficient conditions (Colmer et al., 2006; Shiono et al., 2011; Yamauchi et al., 2016, 2017). Oxygen within aerenchyma will be consumed by the cells in adjacent tissues and/or diffuse radially to the rhizosphere (Armstrong, 1979; Colmer, 2003b). In addition to the large amount of aerenchyma, rice roots form a barrier impermeable to radial oxygen loss (ROL), and this further enhances longitudinal oxygen diffusion from shoot base to the root tip (Armstrong, 1979; Colmer et al., 1998; Kotula et al., 2009; Shiono et al., 2011). In contrast to the many wetland species, none of the upland crops have ROL barrier in the roots, and thus its formation is an important mechanism for plants to adapt to waterlogging (Colmer, 2003b).

The amount of longitudinal oxygen diffusion along submerged organs is determined by anatomical, morphological, and physiological characteristics (Colmer, 2003b). Root thickness is a morphological feature which associates with the porosities (i.e., gas volumes) within roots (Colmer, 2003b). Root porosities under oxygen-deficient conditions are higher in the wetland species having thicker root diameters when compared with the dryland species with thinner root diameters (Visser et al., 2000a,b). From the anatomical aspects, thick root diameter is associated with large cortex and aerenchyma areas. Indeed, thicker roots of wheat seedlings that emerge under oxygen-deficient conditions have a larger aerenchyma area than thinner roots that emerge under aerobic conditions (Yamauchi et al., 2014a). On the other hand, mathematical modelings showed that large stele in which porosity is lower than in the cortex has a disadvantage in terms of oxygen diffusion within the root (Armstrong and Beckett, 1987; Armstrong et al., 1994, 2000). Indeed, the proportion of the stele area within roots is smaller in the wetland species than that in dryland species (McDonald et al., 2002). These studies suggest that not only aerenchyma, but also root thickness and ratio of cortex-to-stele within roots are essential to consider the plant adaptability to waterlogging.

The aim of this study was to understand the significance of higher CSR, which is associated with larger cortex area, for the adaptation of plants to waterlogging. Specifically, we addressed the following questions. (1) How is CSR related with plant adaptation to waterlogging? (2) Does CSR affect the amount of gas space in root? (3) What is the adaptive value of high CSR in terms of root aeration? To this end, we evaluated growth of wheat, maize, and rice seedlings under aerated or stagnant deoxygenated conditions, which can mimic the changes in gas composition in waterlogged soils. Moreover, we measured areas of stele, cortex, and aerenchyma in cross sections of adventitious roots and calculated the ratio of each tissue. To further evaluate the advantage of larger cortex to enhance internal oxygen movement within roots, we measured rates of ROL from thick and thin adventitious roots of rice seedlings by a cylindrical oxygen electrode, when in an oxygen-free root zone. We also measured elongation of the two types of adventitious roots under stagnant conditions. Based upon these results, here we discuss the adaptive consequence of high CSR to waterlogging and the potential application of CSR to improve tolerance of crops to waterlogging.

MATERIALS AND METHODS

Plant Materials and Growth Conditions

Seeds of wheat (cv. Bobwhite), maize (inbred line B73), and rice (cv. Nipponbare) were sterilized with 0.5% (v/v) sodium hypochlorite for 30 min and then rinsed thoroughly with deionized water. Seeds of maize and wheat were germinated on filter paper in Petri dishes with deionized water. Each species was in a different growth chamber; maize was at 28°C in light [photosynthetically active radiation (PAR), 200–250 μmol m^{-2} s^{-1}] for 16 h and 25°C in dark for 8 h, and wheat at 23°C under continuous light conditions (PAR, 200–250 μmol m^{-2} s^{-1}), respectively. Seeds of rice were germinated in Petri dishes with deionized water in growth chamber at 28°C under dark conditions. After 2 days, maize seedlings were placed on a mesh-float with an aerated half-strength nutrient solution [28°C in light (PAR, 200–250 μmol m^{-2} s^{-1}) for 16 h and 25°C in dark for 8 h]. Wheat and rice seedlings were each placed on each different

mesh-floats with an aerated quarter-strength nutrient solution [23°C (wheat) or 28°C (rice) continuous light conditions; PAR, 200–250 μmol m^{-2} s^{-1}]. Composition of the nutrient solution for maize was as described by Watanabe et al. (2017), and that of the nutrient solution for wheat and rice was as described by Colmer et al. (2006). After 7 days (9 days old), wheat, maize, and rice seedlings were transferred to 2-L pots (2 plants per pot, 250 mm height × 80 mm length × 110 mm width) containing aerated full-strength nutrient solution (aerated conditions) or stagnant deoxygenated solution (stagnant conditions) and grown for 7 days, and 16-day-old seedlings were used for each experiment. For maize, $FeSO_4$ (final concentration of 1 μM) was added to aerated nutrient solution every day on days 9–15. For 14 days of treatment of rice seedlings, stagnant deoxygenated solution was renewed at 7 days after the start of treatment (16 days old), and 23-day-old seedlings were used for each experiment. Stagnant deoxygenated solution contained 0.1% (w/v) dissolved agar and was deoxygenated (dissolved oxygen, <0.5 mg L^{-1}) prior to use by flushing with nitrogen gas (Wiengweera et al., 1997).

Measurements of Growth and Leaf Chlorophyll Content

Wheat, maize, and rice seedlings were harvested at 7 days (16 days old) after the transfer to aerated or stagnant conditions. Lengths of shoots, longest seminal roots, and longest adventitious roots were measured using a ruler, and number of emerged leaves, adventitious roots, and tillers were counted. Chlorophyll content of leaves was measured three times at the middle part of leaves using a Soil Plant Analysis Development (SPAD) meter (SPAD-502, Konica Minolta), and the average value was used as the SPAD value of each individual. Wheat, maize, and rice seedlings were divided into shoots and roots and dried at 50°C for 7 days, and shoot and root dry weights were measured.

Anatomical Analysis of Root Cross Sections

Root segments at 10, 20, 30, 40, and 50 mm (±2 mm) from the tips were prepared from 80- to 100-mm-long adventitious roots of wheat, maize, and rice seedlings grown under aerated or stagnant conditions for 7 days (16 days old). For the comparison between the thick and thin adventitious roots, root segments at 5, 10, 20, 30, 40, and 50 mm (±2 mm) from the tips were prepared from 110- to 130-mm-long adventitious roots of rice seedlings grown under stagnant conditions for 14 days (23 days old). Root cross sections were prepared by hand sectioning with a razor blade. Each section was photographed using an optical microscope (BX60, OLYMPUS) with a CCD camera (DP70, OLYMPUS). Areas of each root tissue were measured using ImageJ software (Ver. 1.43u, US National Institutes of Health), and the ratio (proportion) of each root tissue was calculated using the cross-sectional areas.

Detection of Oxygen Loss From Roots by Redox Indicator Dyes

Methylene blue is a redox indicator dye which enables qualitative assessments of spatial ROL from roots (Armstrong and Armstrong, 1988). Crystal violet was applied as an alternative redox indicator dye. The reduced forms of methylene blue and crystal violet are colorless, but when they react with oxygen this results in blue and purple colors, respectively. Methylene blue and crystal violet were added to a deoxygenated solution containing 0.1% (w/v) agar at final concentration of 30 and 10 μM, respectively. Subsequently, sodium dithionite ($Na_2S_2O_3$) was added at a final concentration of 300 μM to reduce the indicator dyes. One each of thick and thin adventitious roots (110–130 mm long) were selected from rice seedlings grown under stagnant conditions for 14 days (23 days old), and all of the other roots were trimmed off immediately before the start of staining. The shoot base with the adventitious root was immersed in a transparent acrylic pot (350 mm height × 250 mm length × 15 mm width) containing the reduced methylene blue or crystal violet solution. The shoot-root junction was 20 mm below the surface of the solution. The staining patterns of methylene blue and crystal violet on the adventitious roots were evaluated every 30 min for a period of 2 h, and photographs were taken at 2 h (methylene blue) and 1 h (crystal violet) after the start of the staining experiments.

Measurement of Oxygen Loss From Roots by a Cylindrical Electrode

One each of thick and thin adventitious roots (110–130 mm long) were selected from rice seedlings grown under stagnant conditions for 14 days (23 days old). Oxygen loss from the adventitious roots of intact rice seedlings was measured by using a cylindrical oxygen electrode in accordance with the method of Armstrong and Wright (1975). The adventitious roots were immersed in a transparent acrylic pot (250 mm height × 80 mm length × 110 mm width) containing a deoxygenated solution of 5 mM KCl, 0.5 mM $CaSO_4$, and 0.1% (w/v) dissolved agar (Colmer, 2003a), and placed in a growth chamber [28°C, light conditions; PAR, 200–250 μmol m^{-2} s^{-1}]. The shoot-root junction was immersed 20 mm below the surface of the deoxygenated solution. One adventitious root was inserted through the cylindrical electrode (inner diameter: 2.25 mm; height: 5 mm), and the oxygen loss from the root surface was measured at 5, 10, 20, 30, 40, 50, and 60 mm (±2.5 mm) from the tips of adventitious roots. After the measurements, root cross sections were prepared as described above. The rates of total oxygen loss (ng min^{-1}) within the range of cylindrical electrode was calculated by [$-4.974 \times I$], and the rates of ROL (ng cm^{-2} min^{-1}) were calculated by [$-4.974 \times I/A_1$] as described by Armstrong and Wright (1975), where I = diffusion current (μA) with the adventitious roots in the cylindrical electrode, and the A_1 = surface area of adventitious roots within the electrode (m^{-2}). After the calculations, the units of the rates of total oxygen loss and ROL were converted into nmol s^{-1} and nmol m^{-2} s^{-1}, respectively.

Measurement of Root Elongation

One each of thick and thin adventitious roots (10–40 mm long) were selected from rice seedlings grown under stagnant conditions for 7 days (16 days old). The selected roots were

marked by threads, and their lengths were measured every day on days 16–26. Stagnant deoxygenated solution was renewed at day 16, when the measurement started.

Statistical Analyses

Statistical differences between means were calculated using two-sample *t*-test. For multiple comparisons, data were analyzed by one-way ANOVA and *post hoc* Tukey's test using SPSS Statistics Version 19 (IBM Software).

RESULTS

Growth of Wheat, Maize, and Rice Seedlings Under Aerated and Stagnant Conditions

To evaluate the effect of stagnant conditions on growth of wheat, maize, and rice, 9-day-old aerobically grown seedlings were further grown under aerated or stagnant conditions for 7 days (**Figures 1A–F**). Stagnant conditions significantly decreased the shoot lengths of wheat and maize, and also reduced leaf and tiller numbers of maize and wheat, respectively (**Table 1**). Shoot dry weights of wheat and maize decreased by 11 and 13%, respectively (**Table 1**). In rice, stagnant conditions did not affect shoot length, leaf, and tiller numbers, and thus shoot dry weight was similar under aerated and stagnant conditions (**Table 1**). The chlorophyll content (SPAD value) of second and third leaves of wheat and maize significantly decreased under stagnant conditions (**Table 1**). In rice, the chlorophyll content of the second leaf was not affected, and that of the third leaf rather increased when plants were growing under stagnant conditions (**Table 1**).

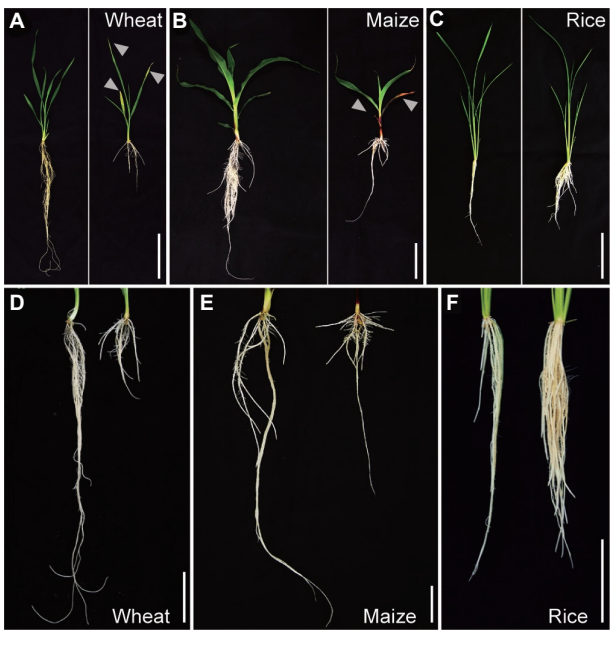

FIGURE 1 | Growth of wheat, maize, and rice under aerated or stagnant conditions. Pictures of seedlings of wheat **(A)**, maize **(B)**, and rice **(C)** and roots of wheat **(D)**, maize **(E)**, and rice **(F)** under aerated conditions (left) or stagnant conditions (right). Nine-day-old wheat, maize, and rice seedlings were further grown under aerated or stagnant conditions for 7 days. Yellowing or brownish parts of leaves are indicated by arrowheads. Bars = 10 cm.

Root dry weights of wheat and maize respectively decreased by 70 and 27% under stagnant conditions, whereas that of rice increased by 132% (**Table 1**). The lengths of longest adventitious roots decreased by 43, 67, and 21% in wheat, maize, and rice under stagnant conditions, respectively (**Table 1**). Stagnant conditions increased the numbers of adventitious roots in wheat and rice by 14 and 29%, respectively (**Table 1**). By contrast, the number of adventitious roots in maize was not affected (**Table 1**). Seminal roots strongly contribute to the root dry weights of wheat and maize under aerated conditions, but most of those roots died during the growth under stagnant conditions (**Figures 1D,E**; **Table 1**). These results clearly show that rice is more adaptive to stagnant conditions (which mimic waterlogging) than wheat and maize.

Size of Each Root Tissue of Wheat, Maize, and Rice Under Aerated and Stagnant Conditions

Root cross sections at 10, 20, 30, 40, and 50 mm from the tips of 80- to 100-mm-long adventitious roots were prepared from wheat, maize, and rice seedlings grown under aerated or stagnant conditions, and the size of each root tissue was measured (at 50 mm; **Figures 2A–C**). Areas of whole root, stele, and cortex at 50 mm from the tips of wheat, maize, and rice roots, except for stele area of wheat roots, significantly increased under stagnant conditions (**Figures 2D–F**). Stele areas in maize and rice roots increased by 72 and 40%, respectively (**Figure 2E**). In wheat, maize, and rice, areas of cortex respectively increased by 49, 164, and 88% under stagnant conditions (**Figure 2F**). These results indicate that the increases of the cortex areas are greater than those of stele areas under stagnant conditions. Similar results were obtained at 10, 20, 30, and 40 mm from the tips of adventitious roots of wheat, maize, and rice seedlings (**Supplementary Figures S1A–C, S2A–C, S3A–C**).

Although aerenchyma formation was minor in wheat and maize roots under aerated conditions, aerenchyma formation gradually increased toward basal parts of the roots under stagnant conditions (**Supplementary Figures S1D, S2D**). In rice roots, aerenchyma formation was first detected at 20 mm from the tips both under aerated and stagnant conditions, and its formation gradually increased toward basal parts of the roots (**Supplementary Figure S3D**). Areas of aerenchyma at 50 mm from the root tips significantly increased in wheat, maize, and rice roots under stagnant conditions (**Figure 2G**).

Because the area of whole roots in maize strongly increased under stagnant conditions (**Figure 2D**), areas of living cortex (cortex minus aerenchyma; 77%) and living root cells (whole roots minus aerenchyma; 92%) also strongly increased (**Figures 2H,I**). In wheat roots, areas of living cortex and living root cells were comparable between aerated and stagnant conditions (**Figures 2H,I**). In rice roots, areas of living cortex were comparable between aerated and stagnant conditions, and

TABLE 1 | Growth of wheat, maize, and rice under aerated or stagnant conditions.

Conditions	Length (mm)				Number		Dry weight (mg)		SPAD	
	Shoot	Longest seminal root	Longest adventitious root	Leaf	Adventitious root	Tiller	Shoot	Root	Second leaf	Third leaf
Wheat (*Triticum aestivum*) cv. Bobwhite										
Aerated	277.7 ± 19.1	370.1 ± 32.7	155.3 ± 23.2	4.0 ± 0.0	5.7 ± 1.0	2.3 ± 0.6	193.5 ± 22.2	74.7 ± 10.0	52.6 ± 2.8	49.0 ± 3.3
Stagnant	233.5 ± 19.1**	n.d.	88.3 ± 10.3**	4.0 ± 0.0	6.5 ± 0.6*	1.3 ± 0.5**	172.1 ± 15.7*	22.5 ± 5.1**	24.3 ± 12.7**	37.1 ± 5.6**
% of control[a]	16	–	43	(0)	14	44	11	70	54	24
Maize (*Zea mays*) inbred line B73										
Aerated	353.4 ± 22.9	501.0 ± 53.9	282.9 ± 35.1	6.0 ± 0.4	8.1 ± 1.6	0.0 ± 0.0	431.4 ± 77.8	151.4 ± 26.7	43.0 ± 6.0	47.4 ± 6.1
Stagnant	303.3 ± 22.8**	n.d.	93.7 ± 9.5**	5.2 ± 0.4**	8.1 ± 1.1	0.0 ± 0.0	374.9 ± 35.3*	109.9 ± 12.4**	6.3 ± 4.0**	31.7 ± 5.4**
% of control[a]	14	–	67	13	(1)	–	13	27	85	33
Rice (*Oryza sativa*) cv. Nipponbare										
Aerated	309.7 ± 28.5	n.d.	168.2 ± 13.4	5.0 ± 0.0	19.7 ± 2.3	1.8 ± 0.6	122.5 ± 17.5	24.1 ± 4.0	39.2 ± 1.4	30.5 ± 3.8
Stagnant	324.7 ± 20.8	n.d.	133.7 ± 16.4**	5.0 ± 0.0	25.5 ± 2.5**	1.8 ± 0.4	126.9 ± 19.9	55.9 ± 15.4**	40.0 ± 2.4	41.4 ± 1.8**
% of control[a]	(5)	–	21	(0)	29	(0)	(4)	132	(2)	36

Nine-day-old rice, wheat, and maize seedlings were grown under aerated or stagnant conditions for 7 days, and all growth parameters were measured immediately after the treatments.

Values are means ± SD (n = 15). Significant differences between aerated and stagnant conditions at $^{**}p < 0.01$ and $^{*}p < 0.05$ (two-sample t-test).

Numbers within parentheses indicate that the percentage increase or decrease is not significant. [a]Percentage of increase (red font) or decrease (blue font) in growth parameters under stagnant conditions in comparison with those under aerated conditions.

the area of living root cells increased by 32% under stagnant conditions (**Figures 2H,I**). Areas of living cortex gradually decreased toward basal parts of the roots in maize and rice, but not in wheat, under stagnant conditions (**Supplementary Figures S1E, S2E, S3E**). Area of living root cells in rice also gradually decreased toward the basal part of the roots, whereas those of living root cells did not significantly change along wheat and maize roots (**Supplementary Figures S1F, S2F, S3F**).

Ratio of Each Root Tissue Size of Wheat, Maize, and Rice Under Aerated and Stagnant Conditions

To compare the root anatomical features of wheat, maize, and rice, the ratio of each root tissue was calculated (**Figure 3**; **Supplementary Figures S4–S6**). Stagnant conditions significantly increased aerenchyma to cortex ratio (ACR) and cortex to stele ratio (CSR) at 50 mm from the tips of adventitious roots in wheat, maize, and rice (**Figures 3A,B**). ACR and CSR in rice roots were much higher than those in wheat and maize roots both under aerated and stagnant conditions (**Figures 3A,B**). ACR in rice roots under stagnant conditions was respectively 1.8-fold and 1.5-fold higher than that in wheat and maize roots (**Figure 3A**), and CSR in rice roots under stagnant conditions was respectively 2.8-fold and 3.5-fold higher than that in wheat and maize roots (**Figure 3B**). These results indicate that rice roots have more aerenchyma within cortex when compared with wheat and maize roots, and suggest that higher CSR in rice roots further amplifies the ratio of aerenchyma within whole root. Indeed, aerenchyma to whole root ratio in rice roots under stagnant conditions was respectively 2.0-fold and 1.6-fold higher than that in wheat and maize roots (**Figure 3C**), and the proportion of difference between rice roots and wheat or maize roots was larger than ACR (**Figures 3A,C**). Moreover, ratio of living cells to whole root in rice roots under stagnant conditions was 1.3-fold lower than that in wheat and maize roots under stagnant conditions (**Figure 3D**), and ratio of aerenchyma to living cells in rice roots was respectively 2.7-fold and 2.2-fold higher than that in wheat and maize roots under stagnant conditions (**Figure 3E**). These results indicate that rice has larger area of aerenchyma and smaller area of living cells within roots when compared with wheat and maize. In other words, rice roots suppress oxygen demands of living cells and enhance oxygen diffusion rates through aerenchyma to adapt to waterlogging.

Anatomy of Thick and Thin Rice Roots Under Stagnant Conditions

Analysis of root anatomical features in wheat, maize, and rice revealed that the ratio of cortex area within roots in rice is higher than that in wheat and maize roots (**Figure 3B**). To demonstrate the advantages of high CSR in rice roots for oxygen transport from shoot to root, one each of thick and thin adventitious roots (110- to 130-mm long) were selected from each rice seedling grown under stagnant conditions for 14 days, and anatomical features of those roots were evaluated (**Figures 4A,B**). Whole root areas at 10, 20, 30, 40, and 50 mm from the tips of thick roots were 1.9- to 2.1-fold larger than those of thin roots

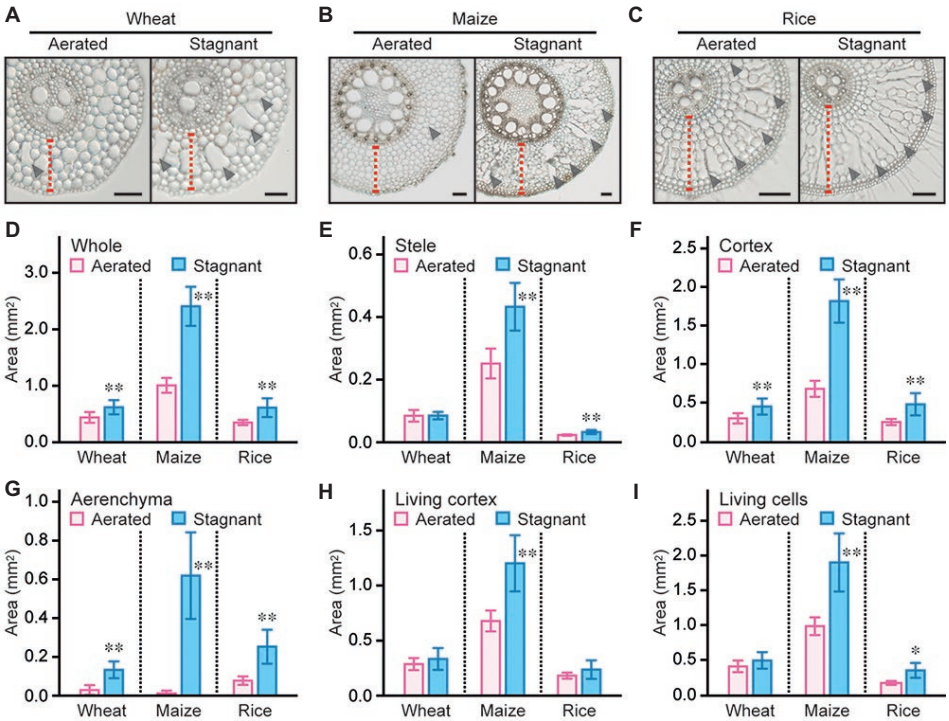

FIGURE 2 | Area of each tissue in adventitious roots of wheat, maize, and rice. Cross sections at 50 mm from the tips of adventitious roots of wheat **(A)**, maize **(B)**, and rice **(C)** under aerated or stagnant conditions. Cortex cell layers and lysigenous aerenchyma are indicated by red dashed lines and black arrowheads, respectively. Bars = 100 μm. Areas of whole root **(D)**, stele **(E)**, cortex **(F)**, aerenchyma **(G)**, living cortex (cortex minus aerenchyma) **(H)**, and living cells (whole root minus aerenchyma) **(I)** at 50 mm from the tips of adventitious roots of wheat, maize, and rice seedlings under aerated or stagnant conditions. Nine-day-old wheat, maize, and rice seedlings were further grown under aerated or stagnant conditions for 7 days. Significant differences between aerated and stagnant conditions at $p < 0.01$ and $p < 0.05$ (two-sample *t*-test) are denoted by ∗∗ and ∗, respectively. Values are means ± SD ($n = 9$).

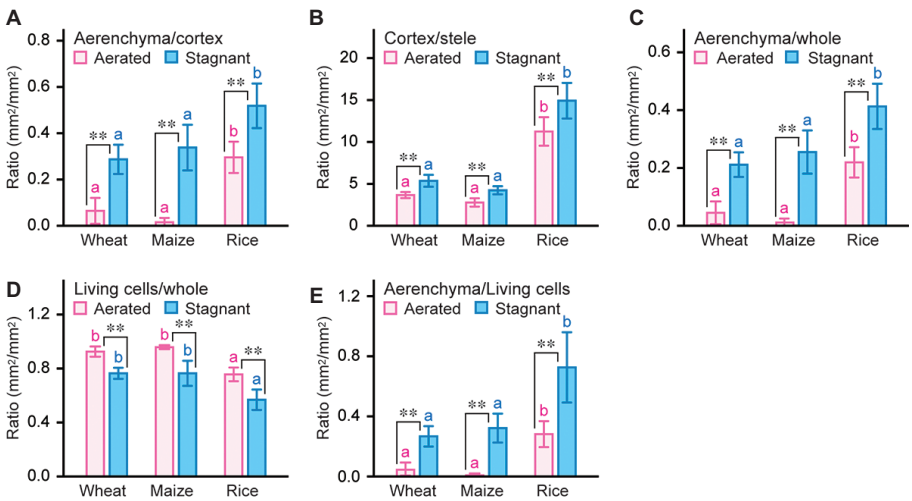

FIGURE 3 | Ratio of each tissue size in adventitious roots of wheat, maize, and rice. Ratio of aerenchyma to cortex **(A)**, cortex to stele **(B)**, aerenchyma to whole root **(C)**, living cells to whole root **(D)**, and aerenchyma to living cells **(E)** at 50 mm from the tips of adventitious roots of wheat, maize, and rice under aerated or stagnant conditions. Nine-day-old wheat, maize, and rice seedlings were further grown under aerated or stagnant conditions for 7 days. Significant differences between aerated and stagnant conditions at $p < 0.01$ (two-sample *t*-test) are denoted by ∗∗. Different lowercase letters denote significant differences among different species ($p < 0.05$, one-way ANOVA and then Tukey's test for multiple comparisons). Values are means ± SD ($n = 9$).

(**Supplementary Figure S7A**). Although stele and cortex areas of thick roots were respectively 1.8- to 1.9-fold and 2.0- to 2.2-fold larger than those of thin roots (**Figures 4C,D**), CSR was not significantly different between the two types of roots (**Supplementary Figure S7B**). Areas of aerenchyma at 10 and 20 mm of thick and thin roots were comparable with each other, whereas those at 30–50 mm were 1.8- to 2.0-fold larger in thick roots (**Figure 4E**). Areas of living cells of thick roots were 1.9- to 2.2-fold larger than those of thin roots (**Figure 4F**). Interestingly, the longitudinal gradients of areas of aerenchyma and living cells were more prominent in thick roots than those in thin roots (**Figures 4E,F**). Aerenchyma to whole root ratio, living cells to whole root ratio, and aerenchyma to living cells ratio were not significantly different between thick and thin roots (**Supplementary Figures S7C–E**). These results suggest that thick roots have larger oxygen demands at the apical part due to having more living cells, and that thick roots have larger amounts of aerenchyma at the basal part when compared with thin roots. Taken together, these features could synergistically enhance oxygen diffusion from shoot base to the tips of thick roots.

Oxygen Loss From Thick and Thin Rice Roots Under Stagnant Conditions

To evaluate the contribution of cortex to the oxygen transport from shoot base to the root tips, oxygen loss from the thick and thin adventitious roots of rice seedlings were detected by redox indicator dyes, methylene blue, and crystal violet, under the deoxygenated solution. We found that thick roots with larger cortex and aerenchyma areas showed more dense and broad staining patterns (**Figures 5A,B**). Subsequently, rates of oxygen loss within a cylindrical oxygen electrode (total oxygen loss) from thick and thin adventitious roots were measured at 5, 10, 20, 30, 40, 50, and 60 mm (±2.5 mm) in deoxygenated solution (**Figure 5C**). The total oxygen loss was hardly detectable at 30–60 mm from the tips of thick and thin roots, indicating that the both types of roots had formed a strong barrier to ROL in our experimental conditions (**Figure 5C**). Although the patterns of total oxygen loss along roots were similar between both types of roots, the rates of total oxygen loss at 5 and 10 mm of thick roots were 1.8- and 2.2-fold higher than those in thin roots, respectively (**Figure 5C**). Root diameters of thick roots at 5–60 mm from the tips were 1.3- to 1.5-fold higher than those in thin roots (**Figure 5D**). Nevertheless, the rates of ROL (total oxygen loss/root surface area) at 5 and 10 mm of thick roots were 1.4- and 1.6-fold higher than those of thin roots (**Figure 5E**). These results indicate that large cortex and aerenchyma areas strongly contribute to the efficient oxygen transport within rice roots.

Intercellular Space of Thick and Thin Rice Roots Under Stagnant Conditions

High rates of oxygen loss were detected at 5 mm from the tips of thick and thin adventitious roots of rice seedlings (**Figure 5E**), even though aerenchyma formation was hardly detectable (at 10 mm; see **Figure 4E**). Although thick roots have larger cortex area (**Figure 4D**), areas of aerenchyma at 10 and 20 mm

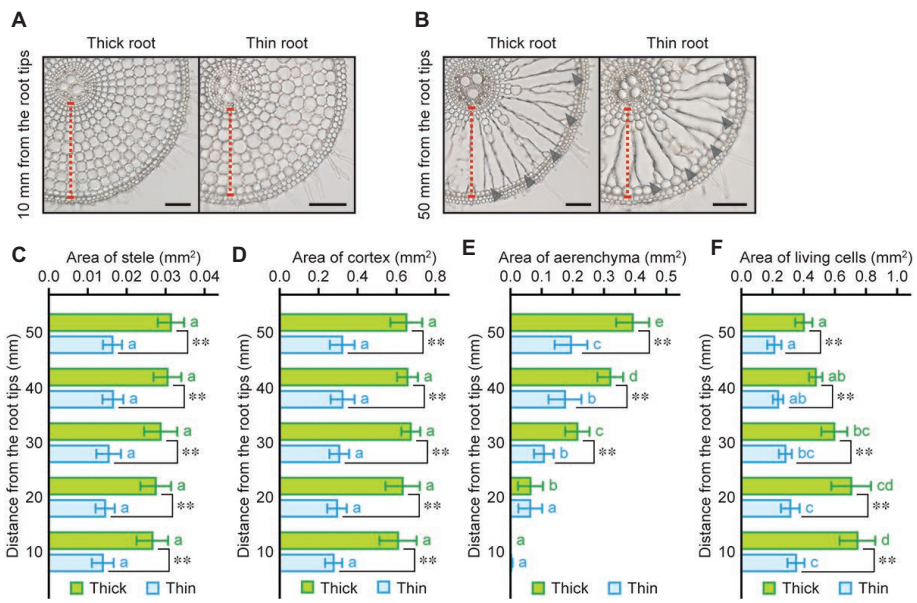

FIGURE 4 | Size of each tissue in thick and thin adventitious roots of rice. Cross sections at 10 mm **(A)** and 50 mm **(B)** from the tips of thick and thin adventitious roots of rice under stagnant conditions. Cortex cell layers and lysigenous aerenchyma are indicated by red dashed lines and black arrowheads, respectively. Bars = 100 μm. Area of stele **(C)**, cortex **(D)**, aerenchyma **(E)**, and living cells **(F)** at 10, 20, 30, 40, and 50 mm from the tips of thick and thin adventitious roots of rice seedlings under stagnant conditions. Nine-day-old rice seedlings were further grown under stagnant conditions for 14 days. Significant differences between thick and thin roots at $p < 0.01$ (two-sample *t*-test) are denoted by **. Different lowercase letters denote significant differences among different positions of roots ($p < 0.05$, one-way ANOVA and then Tukey's test for multiple comparisons). Values are means ± SD ($n = 8$).

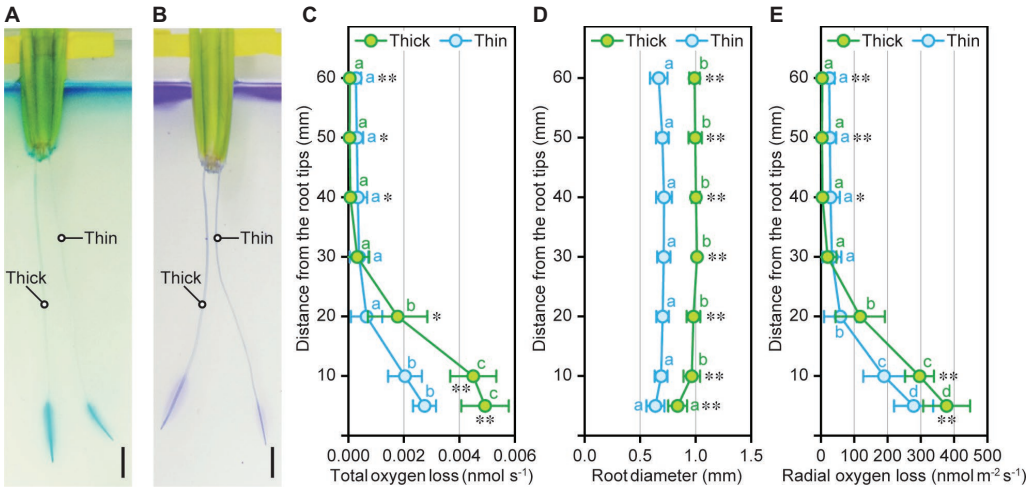

FIGURE 5 | Oxygen movement in thick and thin adventitious roots of rice. Methylene blue staining **(A)** and crystal violet staining **(B)** of thick and thin adventitious roots of rice seedlings under stagnant conditions. Bars = 10 mm. Total oxygen loss from adventitious roots **(C)**, adventitious root diameter **(D)**, and radial oxygen loss (ROL) from adventitious roots **(E)** at 5, 10, 20, 30, 40, 50, and 60 mm from the tips of thick and thin adventitious roots of rice seedlings under stagnant conditions. Nine-day-old rice seedlings were further grown under stagnant conditions for 14 days. Significant differences between thick and thin roots at $p < 0.01$ and $p < 0.05$ (two-sample *t*-test) are denoted by ∗∗ and ∗, respectively. Different lowercase letters denote significant differences among different positions of roots ($p < 0.05$, one-way ANOVA and then Tukey's test for multiple comparisons). Values are means ± SD ($n = 8$).

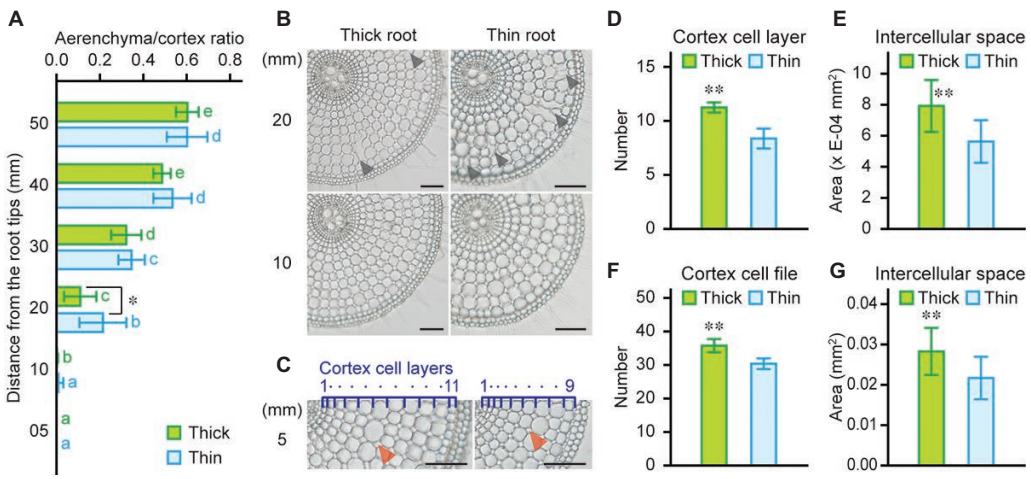

FIGURE 6 | Intercellular spaces of thick and thin adventitious roots of rice. **(A)** Ratio of aerenchyma to cortex at 5, 10, 20, 30, 40, and 50 mm from the tips of thick and thin adventitious roots of rice under stagnant conditions. **(B)** Cross-sections at 10 and 20 mm from the tips of thick and thin adventitious roots under stagnant conditions. Lysigenous aerenchyma is indicated by black arrowheads. Bars = 100 μm. **(C)** Cross-sections at 5 mm from the tips of thick and thin adventitious roots under stagnant conditions. Cortex cell layers are indicated by dark blue numbers and dots. Intercellular spaces are indicated by red arrowheads. Bars = 100 μm. Number of cortex cell layers **(D)**, area of intercellular spaces (per two cortical cell files) **(E)**, number of cortex cell files at the middle part of cortex cell layers **(F)**, and area of total intercellular spaces **(G)** at 5 mm from the tips of thick and thin adventitious roots under stagnant conditions. Nine-day-old rice seedlings were further grown under stagnant conditions for 14 days. **(A,D–G)** Significant differences between thick and thin adventitious roots at $p < 0.01$ and $p < 0.05$ (two-sample *t*-test) are denoted by ∗∗ and ∗, respectively. **(A)** Different lowercase letters denote significant differences among different positions of roots ($p < 0.05$, one-way ANOVA and then Tukey's test for multiple comparisons). Values are means ± SD ($n = 8$).

of thick roots were comparable with those of thin roots (**Figure 4E**). Moreover, ACR at 20 mm was smaller in thick roots than that in thin roots (**Figures 6A,B**). To further evaluate the contribution of large cortex area to the efficient oxygen transport within roots, areas of intercellular spaces at 5 mm of thick and thin roots were measured. Because number of cortex cell layers of thick roots was larger than that in thin roots (**Figures 6C,D**), area of intercellular spaces per two cortical cell files was significantly larger in thick roots (1.4-fold; **Figure 6E**). Moreover, thick roots have more cortical cell files (**Figure 6F**), and thus they have greater total intercellular spaces in the cortex than those in thin roots (1.7-fold; **Figure 6G**). Interestingly, area of intercellular

spaces at 5 mm of thick roots was almost equal to half of aerenchyma area at 20 mm of thick roots (**Figures 4E, 6G**). These results indicate that larger cortex contributes to form larger gas spaces, which are comprised of not only aerenchyma but also intercellular spaces, and thus, it is essential for efficient internal oxygen transport from shoot base to the root tips of rice.

Elongation of Thick and Thin Rice Roots Under Stagnant Conditions

To further evaluate the advantage of larger gas spaces in thick rice roots on the growth under stagnant conditions, lengths of thick and thin adventitious roots were measured every day up to 10 days (on days 16–26) under stagnant conditions (**Figure 7A**). Root lengths were comparable between thick and thin roots until 4 days after the start of treatment (**Figure 7A**). Elongation rate of thin roots became slower than that of thick roots at day 4, and it almost stopped on days 9–10 (**Figure 7B**). By contrast, the elongation rate of thick roots did not change until day 10 (**Figure 7B**), and thus differences in lengths of thick and thin roots gradually increased between days 5 and 10 (**Figure 7A**). These results further support that thick roots with larger cortex and gas spaces are better adapted to waterlogged conditions than thin roots.

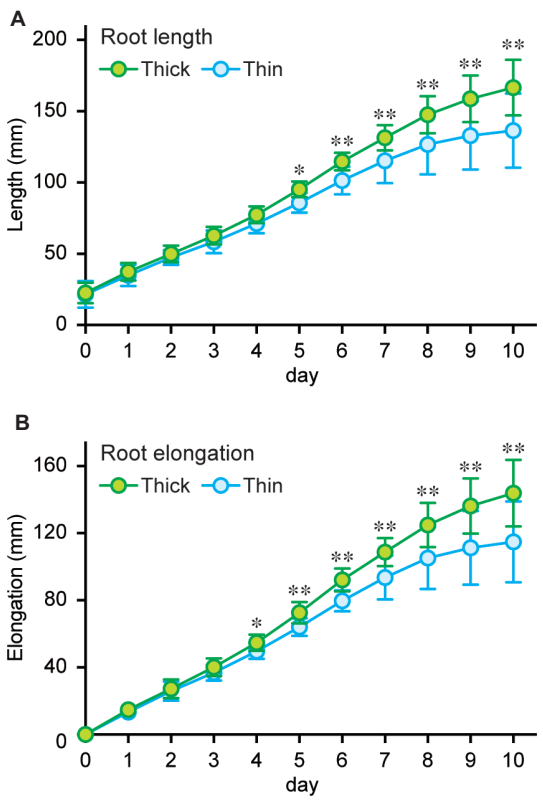

FIGURE 7 | Elongation of thick and thin adventitious roots of rice. Lengths **(A)** and elongation **(B)** of thick and thin adventitious roots of rice under stagnant conditions. Nine-day-old rice seedlings were further grown under stagnant conditions for 7 days, and lengths of thick and thin adventitious roots were measured every day on days 16–26 under stagnant conditions. Significant differences between thick and thin adventitious roots at $p < 0.01$ and $p < 0.05$ (two-sample *t*-test) are denoted by ∗∗ and ∗, respectively. Values are means ± SD ($n = 12$).

DISCUSSION

Growth of rice under stagnant conditions, which mimic the changes in gas composition in waterlogged soil, was greater than for upland crops, wheat and maize (**Figure 1; Table 1**). Roots of rice, which is generally cultivated in waterlogged paddy fields, have higher ratio of aerenchyma within roots (i.e., ACR) and higher ratio of cortex to stele (i.e., CSR) than those of wheat and maize both under aerated and stagnant conditions (**Figures 3A,B**). Because the cortex is the tissue in which aerenchyma formation occurs, large CSR in rice roots amplifies the aerenchyma to whole root ratio (**Figure 3C**), and this also results in rice roots maintaining a smaller amount of living cells (**Figure 3D**). On the other hand, whole root areas increased in wheat, maize, and rice under stagnant conditions (**Figure 2D**), and this led to the increases in cortex areas of the three species (**Figure 2F**). These results suggest that increase in root diameter is a common trait for wetland and upland species in response to waterlogging. While aerenchyma is essential for the efficient internal oxygen transport within roots (Colmer, 2003b; Yamauchi et al., 2018), the cortical cell death (i.e., aerenchyma formation) also contributes to reduce the respiratory costs of roots under oxygen-deficient conditions (Drew, 1997). Indeed, larger CSR in rice roots (**Figure 3B**), which was associated with higher aerenchyma to whole root ratio and less living cells to whole root ratio (**Figures 3C,D**), was associated with the better growth of rice under stagnant conditions when compared with wheat and maize having smaller CSRs in the roots (**Figure 3B; Table 1**). Stele contains xylem vessels and which are essential for water and nutrient transports within roots (Petricka et al., 2012). In maize and barley (*Hordeum vulgare*), anoxia (no oxygen) or hypoxia (low oxygen) in the stelar cells severely restricted the loading of essential ions into the xylem (Gibbs et al., 1998; Colmer and Greenway, 2011; Kotula et al., 2015). Because the proportion of the stele area within roots is smaller in the wetland species than that in dryland species (McDonald et al., 2002), smaller stele which is associated with larger cortex and aerenchyma areas, could be more adaptive to waterlogged conditions.

Shoot and root dry weights of maize seedlings were much greater than those of wheat and rice seedlings both under aerated and stagnant conditions (**Table 1**), and the stele area of maize roots was also much larger than those of wheat and rice roots (**Figure 2E**). A study of 19 grass species showed that plant height at maturity stages correlated positively with the root cross-sectional areas of stele (Pearson correlation coefficient, $r = 0.52$, $p < 0.05$) and total xylems ($r = 0.63$, $p < 0.01$; Wahl and Ryser, 2000), suggesting that smaller capacities of water and nutrient transports (i.e., smaller stele and xylem vessels) is a disadvantage for the growth of plants. One way to resolve this problem would be to increase the number of roots to compensate less effective water and nutrient transports caused by the smaller stele and xylem

sizes. Indeed, adventitious root number of the wetland species *Rumex palustris* is much larger than that of the non-wetland species *Rumex thyrsiflorus* both under aerated and stagnant conditions (Visser et al., 1995, 1996). In our experimental conditions, CSR in rice roots was much higher than that in wheat and maize roots, and rice also has a much larger number of roots than wheat and maize (**Figure 3B; Table 1**). Interestingly, both CSR and root numbers in wheat and rice significantly increased under stagnant conditions (**Figure 3B; Table 1**). By contrast, root number in maize was not significantly different between aerated and stagnant conditions (**Table 1**). Previous study showed that root number of another maize inbred line Mi29 is comparable between under aerated and stagnant conditions, whereas the soil waterlogging significantly increases root number when compared with that under drained soil conditions (Abiko et al., 2012). Although further studies are required to demonstrate the correlation between CSR and root number of plants under waterlogging, having high cortex ratio is essential to express the efficient oxygen transport from shoot base to root tips. On the other hand, rice (and other wetland species) may require a large number of roots to compensate for the less efficient water and nutrient uptakes due to the smaller stele ratio than upland species (**Figure 3B**).

From the results of anatomical analyses along the adventitious roots, we found that the patterns of areas of living cells along roots were different among wheat, maize, and rice (**Supplementary Figures S1F, S2F, S3F**). In wheat and maize under stagnant conditions, the areas of living cells at apical parts of the roots were not much changed when compared with those at basal parts of the roots (**Supplementary Figures S1F, S2F**), even though areas of aerenchyma gradually increased toward basal part of the roots (**Supplementary Figures S1D, S2D**). By contrast, the areas of living cells at apical part of rice roots was much larger than those at basal part of the roots (**Supplementary Figure S3F**), and the areas of aerenchyma and living cells gradually increased and decreased toward basal part of the roots, respectively (**Supplementary Figures S3D,F**). Longitudinal oxygen gradient along the root axis is essential for the oxygen diffusion longitudinally from shoot base to root tip (Colmer, 2003b). Oxygen within gas spaces in roots not only diffuses but also is consumed by the root cells, and thus, the death of cells in the root cortex reduces not only the physical resistance of oxygen diffusion but also the respiratory consumption within roots. (Armstrong, 1979; Drew, 1997; Colmer, 2003b). Taking these into account, longitudinal gradient of respiratory activity along roots is particularly important for the efficient oxygen transport from shoot base to root tips. In rice, basal part of the roots has more aerenchyma and less living cells than apical part of the roots (**Supplementary Figures S3D,F**). If the apical part of rice roots has higher oxygen demands due to larger respiratory activity of living cells, rice roots may have more prominent longitudinal oxygen gradient than wheat and maize roots, although the steepness of the gradient is also influenced by the resistance along the path.

Many wetland species, including rice, form a barrier to ROL at basal parts of the roots, and this further enhances longitudinal oxygen diffusion from shoot base to the root tips (Armstrong, 1979; Colmer, 2003b). Therefore, a barrier to ROL is one of the most important mechanisms for the roots of wetland species to adapt to waterlogging (Colmer 2003b). Profiles of the rates of ROL along thick and thin adventitious roots of rice revealed that thick roots can transport greater amounts of oxygen from shoot base to the root tips than thin roots, even though both types of roots form a barrier to ROL under stagnant conditions (**Figure 5C**). The rate of ROL, which is expressed on a surface area basis of root to derive the rate, in thick roots was still higher than that in the thin roots (**Figure 5E**), thereby demonstrating that thick roots have an ability to sustain greater internal oxygen movement than thin roots. The longitudinal gradients of the areas of aerenchyma and living cells along the roots were more prominent in thick roots than those in thin roots (**Figures 4E**,**F**), suggesting that the respiratory activity at the apical part of the roots, which results in an oxygen concentration gradient that is the driving force of oxygen diffusion (Colmer, 2003b), is higher in the thick roots than that in the thin roots, and that respiratory consumption at the basal part of roots, which in turn reduces longitudinal oxygen diffusion (Colmer, 2003b), is relatively low in thick roots. Indeed, thick roots elongated more than thin roots under stagnant conditions (**Figures 7A**,**B**), further indicating that large cortex and aerenchyma areas within thick roots contribute to efficient oxygen transport from shoot base to the root tips. Although rates of oxygen loss from roots to the external medium depend not only on the amounts of gas spaces but also on root respiration and the tightness of barriers to ROL (Colmer, 2003b), the total flux of oxygen from just behind the root tip was substantially greater for the thicker than the thinner roots (**Figure 5C**), which supports that these thicker roots have more internal oxygen movement. Further analysis is needed to reveal the entire pictures of all resistances and respiratory consumption along the diffusion path for internal aeration in thick and thin adventitious roots of rice, and also for the roots of wheat and maize.

Interestingly, ROL at the apical part of rice roots, where little aerenchyma formation was detected (**Figure 4E**), was very high under stagnant conditions (**Figure 5E**). Further anatomical analysis revealed that intercellular spaces in the cortex strongly contribute to constitute gas spaces in rice roots (**Figure 6G**), as noted also by Armstrong (1971). Moreover, area of intercellular spaces was larger in thick roots having much cortex cell layers and the cell files than that in thin roots (**Figure 6G**). Arrangement of the cortical cells can be divided into two types, one is cuboidal and another is hexagonal packing (Colmer, 2003b). The root porosity was much higher at the apical parts of roots with cuboidal packing of cortex cells than those with hexagonal packing of cortical cells (Armstrong, 1971; Justin and Armstrong, 1987). Interestingly, rice roots have cortex cells with cuboidal packing and wheat roots have those with hexagonal packing, and maize roots have cortex cells with mixtures of both types (**Figures 2A–C; Supplementary Figures S8A–C**). These results suggest that the

different arrangements of cortical cells among wheat, maize, and rice roots are also associated with their adaptabilities to waterlogging. It should be noted that the amount of intercellular spaces in cortex is amplified in roots with high CSR as is the case with the amount of aerenchyma in cortex.

From the detailed anatomical analyses and ROL measurements, we suggest that high CSR with large root diameter contributes to the efficient oxygen transport from shoot base to root tips of plants, and thus, it is essential for plant adaptation to waterlogging. Soil waterlogging negatively impacts agricultural yields of upland crops all over the world (Bailey-Serres et al., 2012; Pucciariello et al., 2014; Voesenek and Bailey-Serres, 2015; Herzog et al., 2016), so that the development of waterlogging-tolerant crops by introgression of quantitative trait loci (QTL) associated with root aeration into elite cultivars is urgent (Yamauchi et al., 2018). QTLs for root aerenchyma formation in cereal crops were identified using mapping populations of barley (Zhang et al., 2016) and hybridization of a wetland wild relative *Zea nicaraguensis* with a maize inbred line (Mano et al., 2016). Here, we showed that CSR is a reliable quantitative index, which likely contributes to waterlogging tolerance and is available for consideration in future QTL analysis of cereal crops. Moreover, CSR might synergistically enhance the root aeration with aerenchyma formation. It is attractive to identify major QTL for CSR using mapping populations of cereal crops and to improve waterlogging tolerance of cereal crops in the future.

DATA AVAILABILITY

All datasets generated for this study are included in the manuscript and/or the **Supplementary Files**.

AUTHOR CONTRIBUTIONS

TY designed the research plans, performed the experiments, and wrote the article. MN provided important advice on the research plans, and read the article and gave suggestions. FA and NT provided advice on the research plans, and read the article and gave suggestions.

FUNDING

This work was supported by PRESTO from Japan Science and Technology Agency (JST) to TY.

ACKNOWLEDGMENTS

We thank the International Maize and Wheat Improvement Center (CIMMYT), Mexico, for providing the seeds of wheat cv. Bobwhite. We also thank Dr. Yoshiro Mano for kindly providing the seeds of maize cv. B73, reading manuscript, and stimulating discussion, and Drs. Timothy D. Colmer and Ole Pedersen for reading manuscript and stimulating discussion. We also thank Yusaku Uga, Al Imran Marik, Hirokazu Takahashi, Kohtaro Watanabe, Masaru Fujimoto, and Hideki Takanashi for stimulating discussion.

SUPPLEMENTARY MATERIAL

The Supplementary Material for this article can be found online at: https://www.frontiersin.org/articles/10.3389/fpls.2019.00259/full#supplementary-material

REFERENCES

Abiko, T., Kotula, L., Shiono, K., Malik, A. I., Colmer, T. D., and Nakazono, M. (2012). Enhanced formation of aerenchyma and induction of a barrier to radial oxygen loss in adventitious roots of *Zea nicaraguensis* contribute to its waterlogging tolerance as compared with maize (*Zea mays* ssp. *mays*). *Plant Cell Environ.* 35, 1618–1630. doi: 10.1111/j.1365-3040.2012.02513.x

Armstrong, W. (1971). Radial oxygen losses from intact rice roots as affected by distance from the apex, respiration and waterlogging. *Physiol. Plant.* 25, 192–197. doi: 10.1111/j.1399-3054.1971.tb01427.x

Armstrong, W. (1979). Aeration in higher plants. *Adv. Bot. Res.* 7, 225–332.

Armstrong, W., and Armstrong, J. (1988). *Phragmites australis* – a preliminary study of soil-oxidizing sites and internal gas transport pathways. *New Phytol.* 108, 373–382. doi: 10.1111/j.1469-8137.1988.tb04177.x

Armstrong, W., and Armstrong, J. (2014). Plant internal oxygen transport (diffusion and convection) and measuring and modeling oxygen gradients. *Plant Cell Monographs* 21, 267–297. doi: 10.1007/978-3-7091-1254-0_14

Armstrong, W., and Beckett, P. M. (1987). Internal aeration and the development of stelar anoxia in submerged roots: a multishelled mathematical model combining axial diffusion of oxygen in the cortex with radial losses to the stele, the wall layers and the rhizosphere. *New Phytol.* 105, 221–245. doi: 10.1111/j.1469-8137.1987.tb00860.x

Armstrong, W., Cousins, D., Armstrong, J., Turner, D. W., and Beckett, P. M. (2000). Oxygen distribution in wetland plant roots and permeability barriers to gas-exchange with the rhizosphere: a microelectrode and modelling study with *Phragmites australis*. *Ann. Bot.* 86, 687–703. doi: 10.1006/anbo.2000.1236

Armstrong, W., and Drew, M. C. (2002). "Root growth and metabolism under oxygen deficiency" in *Plant roots: the hidden half.* 3rd edn. eds. Y. Waisel, A. Eshel, and U. Kafkafi (New York and Basel: Marcel Dekker), 729–761.

Armstrong, W., Strange, M. E., Cringle, S., and Beckett, P. M. (1994). Microelectrode and modelling study of oxygen distribution in roots. *Ann. Bot.* 74, 287–299. doi: 10.1006/anbo.1994.1120

Armstrong, W., and Wright, E. J. (1975). Radial oxygen loss from roots: the theoretical basis for the manipulation of flux data obtained by the cylindrical platinum electrode technique. *Physiol. Plant.* 35, 21–26. doi: 10.1111/j.1399-3054.1975.tb03861.x

Bailey-Serres, J., Lee, S. C., and Brinton, E. (2012). Waterproofing crops: effective flooding survival strategies. *Plant Physiol.* 160, 1698–1709. doi: 10.1104/pp.112.208173

Colmer, T. D. (2003a). Aerenchyma and an inducible barrier to radial oxygen loss facilitate root aeration in upland, paddy and deep-water rice (*Oryza sativa* L.). *Ann. Bot.* 91, 301–309. doi: 10.1093/aob/mcf114

Colmer, T. D. (2003b). Long-distance transport of gases in plants: a perspective on internal aeration and radial oxygen loss from roots. *Plant Cell Environ.* 26, 17–36. doi: 10.1046/j.1365-3040.2003.00846.x

Colmer, T. D., Cox, M. C. H., and Voesenek, L. A. C. J. (2006). Root aeration in rice (*Oryza sativa*): evaluation of oxygen, carbon dioxide, and ethylene as possible regulators of root acclimatizations. *New Phytol.* 170, 767–778. doi: 10.1111/j.1469-8137.2006.01725.x

Colmer, T. D., Gibberd, M. R., Wiengweera, A., and Tinh, T. K. (1998). The barrier to radial oxygen loss from roots of rice (*Oryza sativa* L.) is induced by growth in stagnant solution. *J. Exp. Bot.* 49, 1431–1436. doi: 10.1093/jxb/49.325.1431

Colmer, T. D., and Voesenek, L. A. C. J. (2009). Flooding tolerance: suites of plant traits in variable environments. *Funct. Plant Biol.* 36, 665–681. doi: 10.1071/FP09144

Colmer, T. D., and Greenway, H. (2011). Ion transport in seminal and adventitious roots of cereals during O2 deficiency. *J. Exp. Bot.* 62, 39–57. doi: 10.1093/jxb/erq271

Dolan, L., Janmaat, K., Willemsen, V., Linstead, P., Poethig, S., Roberts, K., et al. (1993). Cellular organization of the *Arabidopsis thaliana* root. *Development* 119, 71–84.

Drew, M. C. (1997). Oxygen deficiency and root metabolism: injury and acclimation under hypoxia and anoxia. *Annu. Rev. Plant Physiol. Plant Mol. Biol.* 48, 223–250. doi: 10.1146/annurev.arplant.48.1.223

Evans, D. E. (2003). Aerenchyma formation. *New Phytol.* 161, 35–49. doi: 10.1046/j.1469-8137.2003.00907.x

Gibbs, J., Turner, D. W., Armstrong, W., Darwent, M. J., and Greenway, H. (1998). Response to oxygen deficiency in primary maize roots. I. Development of oxygen deficiency in the stele reduces radial solute transport to the xylem. *Aust. J. Plant Physiol.* 25, 745–758.

Herzog, M., Striker, G. G., Colmer, T. D., and Pedersen, O. (2016). Mechanisms of waterlogging tolerance in wheat - a review of root and shoot physiology. *Plant Cell Environ.* 39, 1068–1086. doi: 10.1111/pce.12676

Justin, S. H. F. W., and Armstrong, W. (1987). The anatomical characteristics of roots and plant response to soil flooding. *New Phytol.* 106, 465–495. doi: 10.1111/j.1469-8137.1987.tb00153.x

Kamiya, N., Ito, J.-I., Morikami, A., Nagato, Y., and Matsuoka, M. (2003). The SCARECROW gene's role in asymmetric cell divisions in rice plants. *Plant J.* 36, 45–54. doi: 10.1046/j.1365-313X.2003.01856.x

Kotula, L., Clode, P. L., Striker, G. G., Pedersen, O., Läuchli, A., Shabala, S., et al. (2015). Oxygen deficiency and salinity affect cell-specific ion concentrations in adventitious roots of barley (*Hordeum vulgare*). *New Phytol.* 208, 1114–1125. doi: 10.1111/nph.13535

Kotula, L., Ranathunge, K., Schreiber, L., and Steudle, E. (2009). Functional and chemical comparison of apoplastic barriers to radial oxygen loss in roots of rice (*Oryza sativa* L.) grown in aerated or deoxygenated solution. *J. Exp. Bot.* 60, 2155–2167. doi: 10.1093/jxb/erp089

Laurenzio, L. D., Wysocka-Diller, J., Malamy, J. E., Pysh, L., Helariutta, Y., Freshour, G., et al. (1996). The *SCARECROW* gene regulates an asymmetric cell division that is essential for generating the radial organization of the *Arabidopsis* root. *Cell* 86, 423–433. doi: 10.1016/S0092-8674(00)80115-4

Mano, Y., and Omori, F. (2013). Flooding tolerance in interspecific introgression lines containing chromosome segments from teosinte (*Zea nicaraguensis*) in maize (*Zea mays* subsp. *mays*). *Ann. Bot.* 112, 1125–1139. doi: 10.1093/aob/mct160

Mano, Y., Omori, F., Tamaki, H., Mitsuhashi, S., and Takahashi, W. (2016). DNA marker-assisted selection approach for developing flooding-tolerant maize. *Jpn. Agric. Res. Q.* 50, 175–182. doi: 10.6090/jarq.50.175

McDonald, M. P., Galwey, N. W., and Colmer, T. D. (2002). Similarity and diversity in adventitious root anatomy as related to root aeration among a range of wetland and dryland grass species. *Plant Cell Environ.* 25, 441–451. doi: 10.1046/j.0016-8025.2001.00817.x

Nissen, P. (1974). Uptake mechanisms: inorganic and organic. *Annu. Rev. Plant Physiol.* 25, 25–53. doi: 10.1146/annurev.pp.25.060174.000413

Petricka, J. J., Winter, C. M., and Benfey, P. N. (2012). Control of *Arabidopsis* root development. *Annu. Rev. Plant Biol.* 63, 563–590. doi: 10.1146/annurev-arplant-042811-105501

Pucciariello, C., Voesenek, L. A. C. J., Perata, P., and Sasidharan, R. (2014). Plant responses to flooding. *Front. Plant Sci.* 5:226. doi: 10.3389/fpls.2014.00226

Scheres, B., Benfey, P., and Dolan, L. (2002). Root development. *Arabidopsis Book* 1:e0101. doi: 10.1199/tab.0101

Shiono, K., Ogawa, S., Yamazaki, S., Isoda, H., Fujimura, T., Nakazono, M., et al. (2011). Contrasting dynamics of radial O_2-loss barrier induction and aerenchyma formation in rice roots of two lengths. *Ann. Bot.* 107, 89–99. doi: 10.1093/aob/mcq221

Visser, E. J. W., Bögemann, G. M., Blom, C. W. P. M., and Voesenek, L. A. C. J. (1996). Ethylene accumulation in waterlogged *Rumex* plants promotes formation of adventitious roots. *J. Exp. Bot.* 47, 403–410. doi: 10.1093/jxb/47.3.403

Visser, E. J. W., Bögemann, G. M., Van de Steeg, H. M., Pierik, R., and Blom, C. W. P. M. (2000a). Flooding tolerance of *Carex* species in relation to field distribution and aerenchyma formation. *New Phytol.* 148, 93–103. doi: 10.1046/j.1469-8137.2000.00742.x

Visser, E. J. W., Colmer, T. D., Blom, C. W. P. M., and Voesenek, L. A. C. J. (2000b). Changes in growth, porosity, and radial oxygen loss from adventitious roots of selected mono- and dicotyledonous wetland species with contrasting types of aerenchyma. *Plant Cell Environ.* 23, 1237–1245. doi: 10.1046/j.1365-3040.2000.00628.x

Visser, E. J. W., Heijink, C. J., van Hout, K. J. G. M., and Voesenek, L. A. C. J. (1995). Regulatory role of auxin in adventitious root formation in two species of *Rumex*, differing in their sensitivity to waterlogging. *Physiol. Plant.* 93, 116–122. doi: 10.1034/j.1399-3054.1995.930117.x

Voesenek, L. A. C. J., and Bailey-Serres, J. (2015). Flood adaptive traits and processes: an overview. *New Phytol.* 206, 57–73. doi: 10.1111/nph.13209

Wahl, S., and Ryser, P. (2000). Root tissue structure is linked to ecological strategies of grasses. *New Phytol.* 148, 459–471. doi: 10.1046/j.1469-8137.2000.00775.x

Watanabe, K., Takahashi, H., Sato, S., Nishiuchi, S., Omori, F., Malik, A. I., et al. (2017). A major locus involved in the formation of the radial oxygen loss barrier in adventitious roots of teosinte *Zea nicaraguensis* is located on the short-arm of chromosome 3. *Plant Cell Environ.* 40, 304–316. doi: 10.1111/pce.12849

Watt, M., Magee, L. J., and McCully, M. E. (2008). Types, structure and potential for axial water flow in the deepest roots of field-grown cereals. *New Phytol.* 178, 135–146. doi: 10.1111/j.1469-8137.2007.02358.x

Wiengweera, A., Greenway, H., and Thomson, C. J. (1997). The use of agar nutrient solution to simulate lack of convection in waterlogged soils. *Ann. Bot.* 80, 115–123. doi: 10.1006/anbo.1996.0405

Yamauchi, T., Abe, F., Kawaguchi, K., Oyanagi, A., and Nakazono, M. (2014a). Adventitious roots of wheat seedlings that emerge in oxygen-deficient conditions have increased root diameters with highly developed lysigenous aerenchyma. *Plant Signal. Behav.* 9:e28506. doi: 10.4161/psb.28506

Yamauchi, T., Colmer, T. D., Pedersen, O., and Nakazono, M. (2018). Regulation of root traits for internal aeration and tolerance to soil waterlogging-flooding stress. *Plant Physiol.* 176, 1118–1130. doi: 10.1104/pp.17.01157

Yamauchi, T., Tanaka, A., Mori, H., Takamure, I., Kato, K., and Nakazono, M. (2016). Ethylene-dependent aerenchyma formation in adventitious roots is regulated differently in rice and maize. *Plant Cell Environ.* 39, 2145–2157. doi: 10.1111/pce.12766

Yamauchi, T., Watanabe, K., Fukazawa, A., Mori, H., Abe, F., Kawaguchi, K., et al. (2014b). Ethylene and reactive oxygen species are involved in root aerenchyma formation and adaptation of wheat seedlings to oxygen-deficient conditions. *J. Exp. Bot.* 65, 261–273. doi: 10.1093/jxb/ert371

Yamauchi, T., Yoshioka, M., Fukazawa, A., Mori, H., Nishizawa, N. K., Tsutsumi, N., et al. (2017). An NADPH oxidase RBOH functions in rice roots during lysigenous aerenchyma formation under oxygen-deficient conditions. *Plant Cell* 29, 775–790. doi: 10.1105/tpc.16.00976

Zhang, X., Zhou, G., Shabala, S., Koutoulis, A., Shabala, L., Johnson, P., et al. (2016). Identification of aerenchyma formation-related QTL in barley that can be effective in breeding for waterlogging tolerance. *Theor. Appl. Genet.* 129, 1167–1177. doi: 10.1007/s00122-016-2693-3

Conflict of Interest Statement: The authors declare that the research was conducted in the absence of any commercial or financial relationships that could be construed as a potential conflict of interest.

frontiers in Plant Science

ORIGINAL RESEARCH
published: 05 April 2019
doi: 10.3389/fpls.2019.00408

Photosynthetic and Growth Responses of *Arundo donax* L. Plantlets Under Different Oxygen Deficiency Stresses and Reoxygenation

Antonio Pompeiano[1,2], Thais Huarancca Reyes[3], Tommaso M. Moles[3], Lorenzo Guglielminetti[3] and Andrea Scartazza[4]*

[1]International Clinical Research Center, St. Anne's University Hospital, Brno, Czechia, [2]Central European Institute of Technology, Brno University of Technology, Brno, Czechia, [3]Department of Agriculture, Food and Environment, University of Pisa, Pisa, Italy, [4]Institute of Research on Terrestrial Ecosystems, National Research Council, Pisa, Italy

Promotion of nonfood species production to marginal, degraded lands abandoned by mainstream agriculture is affected by extremes of water availability (droughts and floods), which have increased in frequency and intensity and account for severe yield reduction. *Arundo donax* L., known as giant cane or giant reed, spontaneously grows in different kinds of environments with limitation to low temperature and is thus widespread in temperate and hot areas around the world. Moreover, this perennial rhizomatous grass has been recognized as a leading candidate crop in the Mediterranean for lignocellulosic feedstock due to its high C_3 photosynthetic capacity, positive energy balance and low agroecological management demand. In this study, the photosynthetic performance and growth response of *A. donax* to waterlogging and submergence stress following a time course as well as their respective re-oxygenation were analyzed under reproducible and controlled environment conditions. Results of growth response showed that biomass production was strongly conditioned by the availability of oxygen. In fact, only waterlogged plants showed similar growth capacity to those under control conditions, while plants under submergence resulted in a dramatic reduction of this trait. The simultaneous measurements of both gas exchanges and chlorophyll fluorescence highlighted an alteration of both stomatal and non-stomatal photosynthetic behaviors during a short/medium period of oxygen deprivation and re-oxygenation. Photosynthetic CO_2 uptake was strictly related to a combination of stomatal and mesophyll diffusional constrains, depending on the severity of the treatment and exposure time. Conditions of waterlogging and hypoxia revealed a slight growth plasticity of the species in response to prolonged stress conditions, followed by a fast recovery upon reoxygenation. Moreover, the rapid restoration of physiological functions after O_2 deprivation testifies to the environmental plasticity of this species, although prolonged O_2 shortage proved detrimental to *A. donax* by hampering growth and photosynthetic CO_2 uptake.

Keywords: anaerobiosis, chlorophyll fluorescence, giant reed, leaf gas exchange, stomatal conductance, mesophyll conductance

OPEN ACCESS

Edited by:
Guangcheng Shao, Hohai University, China

Reviewed by:
Héctor Abel Busilacchi, National University of Rosario, Argentina
Roberto Pilu, University of Milan, Italy

****Correspondence:***
Lorenzo Guglielminetti
lorenzo.guglielminetti@unipi.it

Specialty section:
This article was submitted to Plant Abiotic Stress, a section of the journal Frontiers in Plant Science

Received: *29 October 2018*
Accepted: *18 March 2019*
Published: *05 April 2019*

Citation:
Pompeiano A, Huarancca Reyes T, Moles TM, Guglielminetti L and Scartazza A (2019) Photosynthetic and Growth Responses of Arundo donax L. Plantlets Under Different Oxygen Deficiency Stresses and Reoxygenation. Front. Plant Sci. 10:408. doi: 10.3389/fpls.2019.00408

INTRODUCTION

The use of marginal lands has gained attention as a sustainable strategy for bioenergy decreasing not only conflicts within food and fuel, but also negative environmental impacts due to indirect land-use change (Gopalakrishnan et al., 2011). To accomplish this goal, it is essential to develop and adopt germplasms that are better able to tolerate abiotic threats, selecting non-food species based on their performance under less than favorable conditions. Perennial rhizomatous grasses are the best candidates as lignocellulosic energy crops because of their high biomass yield and quality, their broad adaptation and tolerance to adverse environmental conditions (Lewandowski et al., 2003).

Hypoxia has recently shown to be a relevant environmental component, thus globally impacting on plant biodiversity and crop production (Pucciariello and Perata, 2017). Events such as strong and frequent precipitation, poor soil quality, slow drainage after over-irrigation, or winter ice encasement limit the oxygen (O_2) in plants. Such adverse conditions can be intensified by environmental issues, such as flooding, which have dramatically increased in terms of severity and frequency over the past decades (Voesenek and Bailey-Serres, 2015). Limitation of O_2 occurs normally in plant developmental processes, especially in densely packed and metabolically active tissues such as meristems, seeds, fruits, tubers, and stems (Licausi and Perata, 2009). However, prolonged low O_2 conditions are harmful for most terrestrial plants, disturbing their growth and resulting in premature death and consequent reduction in yields. In addition, some grass species grown in waterlogged soils or poorly drained areas are susceptible to pests such as *Pythium* spp., *Colletotrichum graminicola* (Ces.) Wils., or *Gaeumannomyces graminis* var. *graminis*, which can develop perfectly under these environmental conditions (Pompeiano et al., 2017a).

Reduced diffusion of gases in floodwaters (-10^4 fold approximately) limits the availability of O_2 for aerobic respiration and carbon dioxide (CO_2) for photosynthesis (Bailey-Serres et al., 2012), being accomplished with diminished light availability for photosynthesis and functional changes in the photosynthetic machinery. The increase in stomatal closure is one dramatic response in plants grown under low O_2 conditions (e.g. during prolonged waterlogging) (Ahmed et al., 2002). Prolonged or severe stress negatively affects photosynthesis, leading to the accumulation of excess excitation energy *via* light absorption, and thus altering the redox balance and inducing oxidative damage to the photosynthetic apparatus. Since plant growth depends on the supply of carbohydrate and energy from photosynthesis, post-submergence growth recovery may require an efficient acclimation of the photosynthetic apparatus to increased O_2 and irradiance in order to reduce photo-oxidative damage (Luo et al., 2009).

Arundo donax L., also known as giant reed, is a perennial rhizomatous grass of the subfamily *Arundinoideae*. It is well adapted to broad ecological conditions and is dispersed from the Mediterranean basin to subtropical wetlands. This species is mainly riparian, forming robust monospecific stands. *A. donax* has been recently recognized as a leading candidate crop for lignocellulosic feedstock (for the production of energy, fuels and chemicals) due to its high biomass yield and quality, positive energy balance and low ecological/agronomical requirements for its management (Lewandowski et al., 2003; Angelini et al., 2005). Additionally, the levels of nitrogen and water inputs do not affect its above-ground biomass quality composition when used as lignocellulosic feedstock for bioprocessing into fuels (Pompeiano et al., 2013). The species has been characterized by its efficient C_3 pathway, with high photosynthetic rates resulted from a high capacity for both maximum Rubisco and ribulose-1,5-bisphosphate limited carboxylation rate under light-saturated conditions (Webster et al., 2016). Its ability to fully reinstate photosynthesis after controlled drought stress was observed upon its rewatering, with a rapid restoration of all the key physiological functions (Pompeiano et al., 2017c). Also, during a short/medium period of salt stress, *A. donax* is able to grow without effects on its photosynthetic apparatus, testifying to the environmental plasticity of this species (Pompeiano et al., 2017b).

Recently, a metabolic analysis of *A. donax* exposed to anoxic and hypoxic conditions was performed in a time-course experiment. The species under low O_2 stress showed a reduction of its absolute growth and alterations in the derived physiological traits in a time-dependent manner (Pompeiano et al., 2015), confirming its ability to cope under the aforementioned stress conditions. Although the responses of giant reed to anoxic and hypoxic treatments showed a similar energy crisis related to the anaerobic metabolism, they differ in the activity of alcohol dehydrogenase and related genes. Overall, the strategy of giant reed under low O_2 conditions suggested a mechanism where cellular metabolism and growth are restricted and thus plants are able to avoid the stress and endure deep floods.

Along with the abilities to cope with limited O_2, CO_2 and energy availability during hypoxia, the capacity to quickly resume normal physiological and metabolic activities upon reoxygenation is an important trait to evaluate stress tolerance (Gibbs and Greenway, 2003). Therefore, to better define the photosynthetic persistence under limited O_2 conditions and subsequent capacity of recovery of giant reed, our aim was to characterize the short-term dynamic of the post-submergence recovery of growth and photosynthetic performance in plants subjected to waterlogging and hypoxia.

MATERIALS AND METHODS

Plant Material and Growth Conditions

Arundo donax L. micropropagated plants of an Italian natural accession (Pisa, IT) were used in the present study. Healthy 10-week-old plantlets were transplanted into 160-hole seed trays (single cell volume 5 cm^3), filled with a peat-based mix, and then kept in growth chambers for 8 weeks under controlled conditions (22 ± 1°C, 12-h photoperiod, and 800 μmol m^{-2} s^{-1} of light intensity). Plants were daily watered and fertilized weekly with a half-strength Hoagland's solution (pH 6.50 ± 0.05, EC 1.1 dS m^{-1}). Two different treatments were conducted:

(1) Waterlogging or soil flooding treatment was carried out flooding the plants with water 2 cm above soil surface; (2) hypoxic or submergence treatment was performed throughout the experiment time using giant reed plants subjected to complete submergence. All treatments were carried out up to 10 days at 22 ± 1°C, 12-h light photoperiod (light intensity: 800 μmol m^{-2} s^{-1}). Comparative growth behavior and physiological characterization were performed in three independent, replicated experiments for each experimental condition. For each treatment, nine plants were removed at each time point (4, 7, and 10 days of treatment, DOT) and transferred to the growth chambers. Recovery after oxygen deprivation was evaluated by monitoring the ability of the treated plants to resume growth after returning to control conditions for 10 days [above-ground fresh weight (FW) and dry matter for each plant], and to recover photosynthetic activity after 72 h of reoxygenation. Control plants were kept in the growth chamber during the time course (22 ± 1°C, 12-h photoperiod, 800 μmol m^{-2} s^{-1}).

Chlorophyll *a* Fluorescence and Leaf Gas Exchange Measurements

Gas exchange and chlorophyll fluorescence were measured simultaneously by means of a LI-6400-40 portable photosynthesis system equipped with an integrated fluorescence chamber head (Li-Cor, Lincoln, NE). Measurements were performed on fully expanded leaves after waterlogging and submergence treatment at each time point (4, 7, and 10 DOT) and after 3, 6, 24, and 72 h of recovery. Six individual plants for each treatment and control were selected. Instantaneous measurements of steady state photosynthetic CO_2 assimilation rate (A), stomatal conductance (g_s), intercellular CO_2 concentration (C_i), transpiration rate (E), and actual photon yield of PSII photochemistry (Φ_{PSII}) were recorded at a photosynthetic photon flux density (PPFD) of 800 μmol m^{-2} s^{-1}, CO_2 concentration of 400 μmol mol^{-1}, relative humidity of about 45–55% and leaf temperature of 22°C. Measurements were taken at steady-state when gas exchange and fluorescence parameters were stable (about 3–5 min). The values of Φ_{PSII} in the light were determined as $\Phi_{PSII} = (F'_m - F')/F'_m$ at steady-state, where F'_m is the maximum fluorescence yield with all PSII reaction centers in the reduced state obtained by superimposing a saturating light flash during exposition to actinic light, and F' is the fluorescence at the actual state of PSII reaction centers during actinic illumination. The actual reduction state of PSII reaction centers, which gives an estimate of the excitation pressure on PSII, was calculated as $1 - q_p = (F_t - F'_0)/(F'_m - F'_0)$, where q_p is the photochemical quenching, F_t the transient fluorescence and F'_0 the minimal fluorescence, with all reaction centers open in the presence of quenching. The potential efficiency of PSII photochemistry was calculated on dark-adapted leaves as described in Fiorini et al. (2016) as $F_v/F_m = (F_m - F_o)/F_m$, where F_v, F_o, and F_m are the variable fluorescence in the dark, the minimum fluorescence yield in the dark and the maximum fluorescence yield in the dark after application of a saturation flash, respectively. The non-photochemical quenching (NPQ) was determined according to the Stern-Volmer equation as $NPQ = F_m / F'_m - 1$.

The mesophyll conductance (g_m) was estimated using the variable J method (Loreto et al., 1992) based on the comparison of the electron transport rate (J_f) calculated by both gas exchange and fluorescence measurements. The J_f was estimated by fluorescence measurements multiplying Φ_{PSII} by the incident light intensity and then correcting for the actual fraction of absorbed light (α) and the distribution of light between the two photosystems (β), as described in Scartazza et al. (2017). The gas exchange algorithm used in the variable J method is dependent on the CO_2 compensation point between photosynthesis and photorespiration (Γ^*) and respiration in the light (R_l). Rubisco specific factor estimated for annual herbs was used to calculate Γ^* as described by Galmés et al. (2005), while dark respiration, which was taken as a proxy for R_l (Centritto et al., 2009), was measured on leaves maintained in darkness for at least 10 min. The value of total conductance to CO_2 (g_{tot}) was calculated as $g_{tot} = (g_s \times g_m)/(g_s + g_m)$.

Statistical Analysis

After performing the Shapiro-Wilk test for normality assumption diagnostics, linear mixed-effects models were used to control the effects of experimental runs and blocks (i.e. random variables) while testing the effects of treatment, exposure and recovery time, as well as their interactions, on all response variables. To this end, the lmer function implemented in the *lme4* R package (Bates et al., 2015) was used. The package *lmerTest* was used to estimate the p for each of the factors in the model, which apply the Satterthwaite approximation for the denominator degrees of freedom or the F-statistic (Kuznetsova et al., 2017). Statistically different means in the other response variables were identified by Tukey's HSD using the *multcomp* package (Hothorn et al., 2008), and probability levels lower than 0.05 were considered as significant.

To identify relationships among the experimental conditions based on data obtained from post-hypoxia chlorophyll *a* fluorescence and leaf gas exchange data, multiple factorial analysis (MFA) was used, implemented in the R package *FactoMineR* (Lê et al., 2008). MFA was performed in two steps. Firstly, a principal component analysis (PCA) was computed on each data set, which was then "normalized" by dividing all its elements by the square root of the first eigenvalue obtained from of its PCA. Then, the normalized data sets were merged to form a single matrix and a global PCA was performed on this matrix. The individual data sets were then projected onto the global analysis to analyze communalities and discrepancies. Each experimental condition had two partial points corresponding to the trait classes (fluorescence and gas exchange). Traits that significantly contributed to MFA dimensions were used to explain differences among genotypes ($\alpha = 0.05$). The length and the direction of the vectors were directly correlated to their significance within each genotype. All computations were performed with R 3.5.1 (R Core Team, 2018), and the R package *ggplot2* (Wickham, 2009) was used for data visualization.

RESULTS

Analysis of all the biometric and physiological traits revealed a significant ($p < 0.05$) treatment × exposure time × recovery time interaction. Following that, subsequent data were presented for clarity within each exposure time.

Growth and Biomass Characterization

Under oxygen deficiency, giant reed exhibited increasing susceptibility in terms of above-ground FW as exposure time was prolonged, although the differences were less pronounced for prolonged exposure times, and no significant differences were detected among the two low O_2 treatments (**Figure 1**). On the other hand, marked differences in their recovery performance upon reoxygenation were observed compared to normoxic control. Although waterlogging affected above-ground FW, we observed a comparable dynamic of recovery with control plants regardless of exposure time (i.e. after 10 days of recovery, we recorded a 2.1-fold increase on average over 0 days versus 2.2 observed in the normoxia). Also, at 4 days of treatment (DOT), waterlogged plants exhibited rapid regrowth and gradually increased above-ground FW starting from 1 day of recovery. For longer exposure times, as well as for plants fully submerged, giant reed showed no significant increase in above-ground FW until 10 days of recovery.

Under normoxia, dry matter remained very constant throughout the experiment time at ~13%, whereas significant increases occurred under the other conditions (**Figure 1**). Under waterlogging, plants subjected to 4 and 7 days of stress gradually increased the epigeal dry matter (from control levels to ~19%), whereas for prolonged exposure time a significant increase was observed immediately after returning to control conditions, reaching 21% at the end of the recovery time. A different pattern was observed under submergence, with a slight increase of dry matter compared to normoxic control plants, following which the dry matter remained constantly high for the remainder of the recovery experiment.

Chlorophyll *a* Fluorescence

The maximum quantum yield of photosystem II (PSII), as estimated by F_v/F_m values in dark-acclimated leaves, declined sharply in response to prolonged exposure and more severe scarcity of O_2 (**Figure 2A**). Although no significant reduction was observed in 4 days waterlogged plants, a slight decline was detected after prolonged exposure. For instance, at seven DOT, F_v/F_m significantly declined although a complete and full recovery in F_v/F_m was visible upon 72 h of reoxygenation. Prolonged exposure caused greater decline, and no recovery was recorded. Submerged plants showed a slight but significant decline starting from four DOT. The species suffered with higher exposure time, although at seven DOT showed a rapid—but not complete—recovery of F_v/F_m after stress ceased. At the longer exposure level, the plant greatly suffered, especially after 6 h of recovery, and exhibited significantly lower F_v/F_m levels compared to normoxic controls at the end of the recovery time.

Dynamics of Φ_{PSII} recorded during the recovery showed a similar trend as observed in the F_v/F_m, although a greater sensitivity occurred under stress conditions (**Figure 2B**). A slight decrease in Φ_{PSII} was visible from the start of waterlogging treatment. At seven DOT marked differences were observed, although the species showed a remarkable ability to restore the PSII photochemistry during recovery. Moreover, a partial

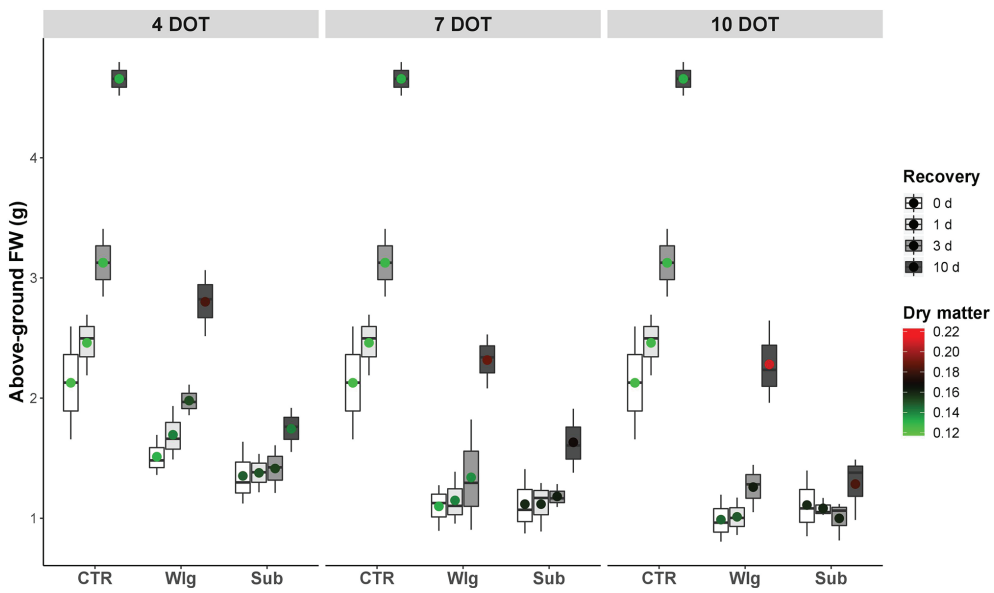

FIGURE 1 | Giant reed (*Arundo donax* L.) biometric traits evaluated as regrowth (above ground FW and dry matter) in a growth chamber up to 10 days at 22 ± 1°C, with a 12-h light photoperiod (light intensity: 800 μmol m^{-2} s^{-1}). The dot in the box and whiskers plot indicates the arithmetic mean of the aboveground FW, the color the changes in dry matter.

recovery was recorded after prolonged oxygen deprivation. Under submergence, the species exhibited an increasing susceptibility to Φ_{PSII} as exposure time was prolonged, and a full recovery was observed only after four DOT. Also, exposure to 10 days submergence treatment exhibited a remarkable ability to partly recovery, which was similar to waterlogged plants.

Observing the dynamics of excitation pressure to PSII, estimated through the $1 - q_p$ index, it exhibited increasing susceptibility according to the severity of the treatment and prolonged exposure time (**Figure 2C**). A complete and full recovery was reached in all plants exposed to prolonged low O_2 stress, with the exception of the most severe condition. The prolonged exposure until 10 DOT did seemingly affect this parameter, although exposure to submergence treatment resulted in a 10% increase over normoxic levels at the end of the recovery period.

Contrasting variations in NPQ have been observed over time (**Figure 2D**). At the beginning of the recovery, NPQ showed lower values compared to normoxia under waterlogging and submergence conditions at seven DOT and prolonged exposure times. Moreover, during the recovery we observed a progressive increase in NPQ, reaching higher values compared to normoxia under 7 days of waterlogging and 4–7 days of submergence. For instance, after 10 DOT, NPQ declined by 19 and 40% under submergence and waterlogging, respectively, both presented as the percentage compared to the normoxic control plants after 72 h of recovery. On the other hand, a partial NPQ recovery was detected following both stress treatments after 10 DOT.

Leaf Gas Exchange Measurements

Changes in leaf gas exchange were recorded at chosen intervals during the time-course experiment. For all the parameters, no significant changes were recorded after waterlogging exposure in the range of 4–7 DOT compared to the control (**Figures 3, 4A,B**). Furthermore, *A. donax* was able to reach a complete and full recovery after 4 days of submergence treatment for most parameters, with the exception of a partial recovery of C_i only (**Figure 3C**). Under waterlogging, a significant reduction in *A* was observed only after 10 DOT, showing a strong but not full recovery in the first 72 h (**Figure 3A**). Overall, a partial recovery in *A* was recorded in the range of 7–10 days of submergence. Immediately after 3 h of recovery, 10 days-submerged plants exhibited a sharper decline of *A* (−68% compared with the control), whereas observing the dynamics of recovery, it showed a steeper slope in the range of 3–72 h.

Overall, the reduction observed in *A* has been related to a concomitant reduction recorded in g_s and *E* (**Figures 3B,D**). Also, we recorded a full recovery in the aforementioned parameters except under the most severe experimental condition,

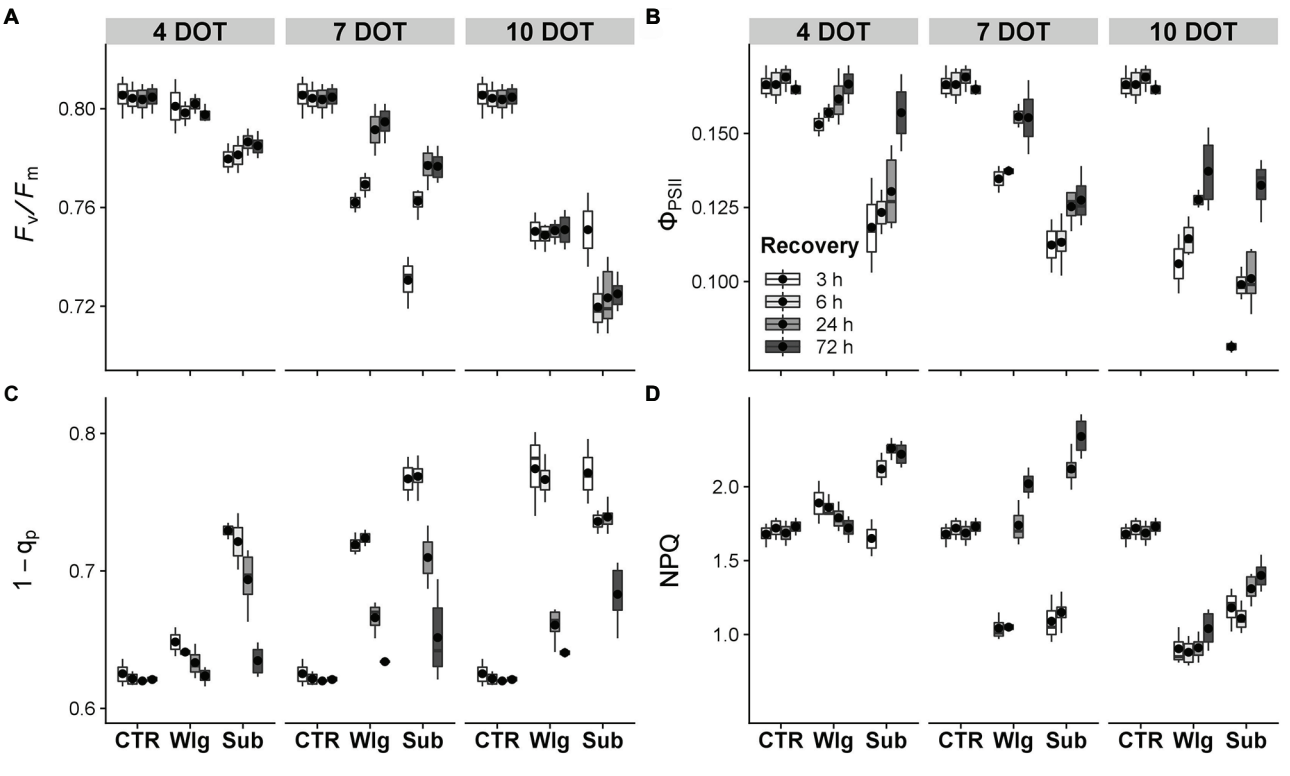

FIGURE 2 | Fluorescence of chlorophyll *a* in giant reed (*Arundo donax* L.) after waterlogging (Wlg) and submergence (Sub) treatment at each time point (4, 7, and 10 DOT) and after 3, 6, 24, and 72 h of recovery for each treatment and control (CTR). **(A)** Potential efficiency of PSII photochemistry (F_v/F_m); **(B)** actual photon yield of PSII photochemistry (Φ_{PSII}); **(C)** actual reduction state of PSII reaction centers ($1 - q_p$); **(D)** non-photochemical quenching (NPQ). The dot in the box and whiskers plot indicates the arithmetic mean of six replicates.

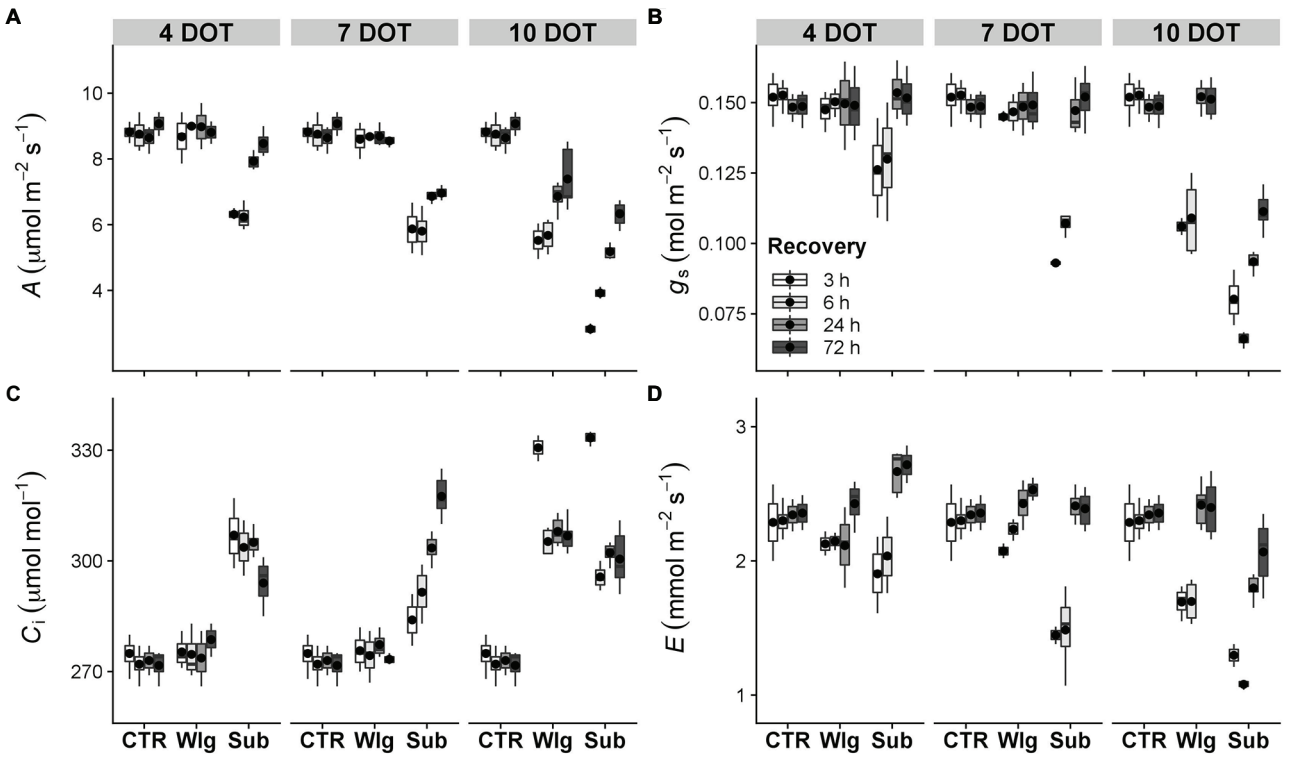

FIGURE 3 | Gas exchanges in giant reed (*Arundo donax* L.) after waterlogging (Wlg) and submergence (Sub) treatment at each time point (4, 7, and 10 DOT) and after 3, 6, 24, and 72 h of recovery for each treatment and control (CTR) were recorded at a photosynthetic photon flux density (PPFD) of 800 μmol m^{-2} s^{-1}. **(A)** Photosynthetic CO_2 assimilation rate (*A*); **(B)** stomatal conductance (g_s); **(C)** intercellular CO_2 concentration (C_i); **(D)** transpiration rate (*E*). The dot in the box and whiskers plot indicates the arithmetic mean of six replicates.

where only partial and significantly lower values compared to control levels were reached at the end of the recovery time.

Significant increases in C_i were visible from only after 10 days of waterlogging treatment, with more pronounced changes in plants exposed to submergence starting from 4 days of treatment (**Figure 3C**). After 7 days of submergence, a progressive increase in C_i was observed in correspondence with an increase of g_s. Under both stress conditions, 10 days of treatments strongly enhanced C_i followed by a partial recovery.

As expected, g_m and g_{tot} showed an analogous pattern, with significant reductions detected as the stress became more severe (**Figures 4A,B**). Under waterlogging, significant changes were observed only after 10 DOT, although starting after 4 days under submergence. Marked differences among treatments were observed in kinetic recovery for the aforementioned parameters. A complete recovery was observed for 4 days-submerged plants; meanwhile, prolonged stress conditions caused only a partial recovery. Additionally, under 10 days of waterlogging we recorded only a slight recovery of both parameters after 72 h of re-exposure to O_2, although reaching higher levels compared with the submerged plants.

Photosynthetic rates of the species were largely determined by conductance to CO_2 (**Figure 4C**). Under control conditions, *A. donax* generally exhibited the highest levels of g_s, g_m, and g_{tot}, while as the stress became more severe the lowest levels were displayed. Assessing the significant relationships between *A* and conductance to CO_2 from g_s and g_m to the combined g_{tot} led to an increase in the Pearson correlation coefficient (from 0.83 to 0.95).

Multiple Factorial Analysis

MFA revealed the canonical relationship between the experimental condition's fingerprints (seven entries including two treatments under three exposure times, plus the control) obtained from chlorophyll *a* fluorescence and leaf gas exchange analyses recorded at the beginning (3 h) and end (72 h) of recovery (**Figure 5**). The coordinates of the two groups of variables were displayed and used to create a map of the groups (data not shown). The coordinates were calculated using the first two dimensions of the MFA (Dim 1 and 2 on the diagram), which resumed 92.7 and 86.1% of the total inertia at 3 and 72 h of recovery, respectively.

The representation of the entries provided by MFA can be read as in a usual PCA (**Figures 5A,B**; Individuals—3 and 72 h). The coordinates of the descriptors correspond to the correlation coefficients between these variables (chlorophyll *a* fluorescence and leaf gas exchange traits) and the factors (entries). The length and the direction of the vectors are directly correlated to their significance within each experimental condition. The hierarchical clustering provided by each MFA highlighted the

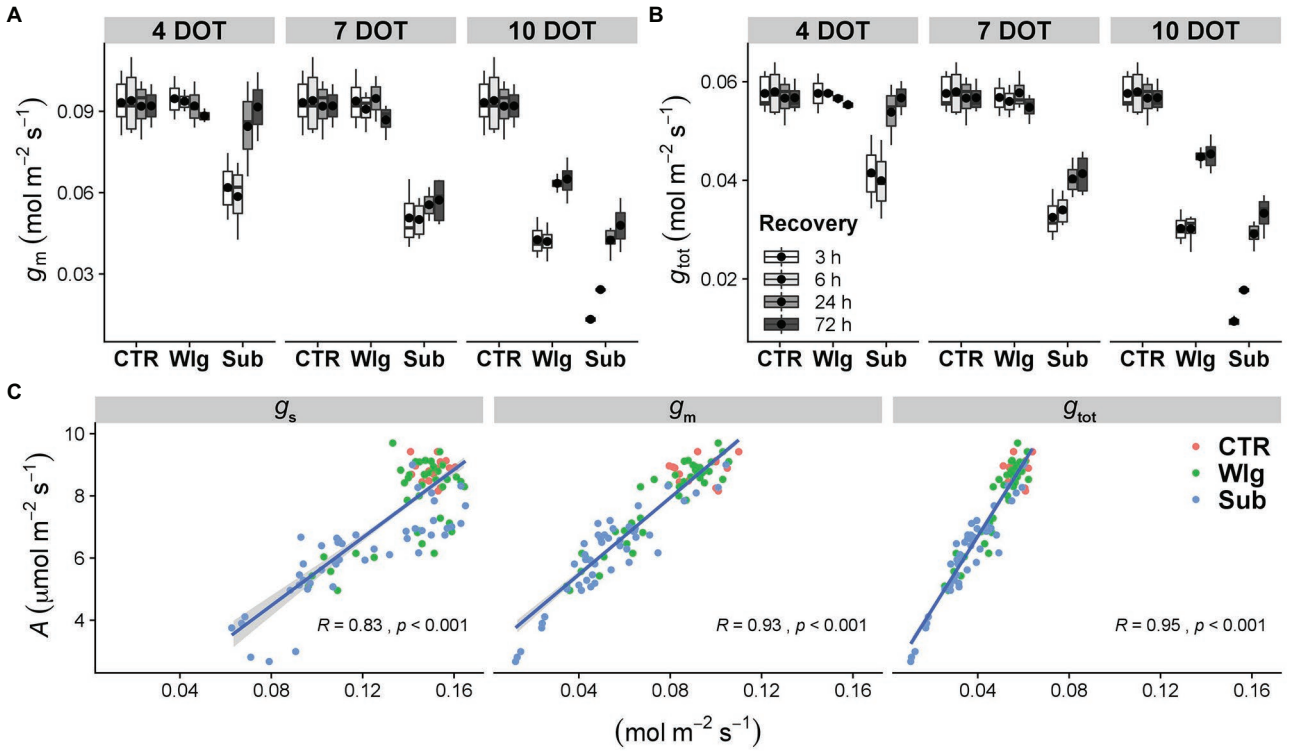

FIGURE 4 | (A) Mesophyll (g_m) and **(B)** total (g_{tot}) conductance to CO_2 in giant reed (*Arundo donax* L.) after waterlogging (Wlg) and submergence (Sub) treatment at each time point (4, 7, and 10 DOT) and after 3, 6, 24, and 72 h of recovery for each treatment and control (CTR). The dot in the box and whiskers plot indicates the arithmetic mean of six replicates. **(C)** Relationships of CO_2 assimilation rate (A) with stomatal (g_s), mesophyll (g_m), and total (g_{tot}) conductance. Pearson correlation coefficients (R) and significance level (p) of the linear regressions are shown.

overall performance of the entries obtained through the single analysis of the chlorophyll *a* fluorescence and leaf gas exchange data (**Figures 5C,D**; Cluster dendogram—3 and 72 h). At both recovery times, factorial axis 1 (80.9 and 71.9% of the variance at 3 and 72 h of recovery, respectively) clearly separated the main clusters obtained. At the beginning of the recovery time, the four phylogenetic trees showed that 4 and 7 days-waterlogged plants share more similarity to the control and that 4 days-submerged plants cannot be separated from 10 days-waterlogged plants, while 7 and 10 days-submerged plants are clearly differentiated from the other analyzed treatments (**Figure 5C**). A different pattern was observed at the end of the recovery time, with the 4 days-submerged plants sharing more similarity to the control group while 10 days-waterlogged plants could not be separated from 7 days submerged plants, and the most extreme treatment (10 days submerged plants) was clearly differentiated from the others on the basis of their chlorophyll *a* fluorescence and leaf gas exchange traits (**Figure 5D**).

DISCUSSION

In the present study, biometric alterations and time-dependent alterations in the photosynthetic performance were observed in response to reduced O_2 availability. As expected, the degree of oxygen deficiency (waterlogging vs. submergence) affected the biometric and physiological response. Overall, our biometric data highlight the ability of *A. donax* to cope with severe hypoxic stress, as well as a rapid recovery upon the cessation of stress under waterlogging conditions, maintaining mostly unaltered regrowth response following treatments lasting up to 10 DOT. Although the present data are not directly comparable to the work performed by Pompeiano et al. (2015) on how the anoxic and hypoxic stress response of the species cause marked differences in ecotype and length of the time-course experiment, previous ecological characterization of the species conducted in riparian habitat confirm the aforementioned perspective (Else, 1996; Bell, 1997).

Reoxygenation stress also triggers a significant drop in hydraulic conductivity in shoots, causing leaf desiccation even in the presence of sufficient soil water (Tamang and Fukao, 2015). Any decrease in hydraulic conductivity in the roots might be due to the regulation of aquaporins in the roots, which occurs when roots are suddenly exposed to hypoxia or anoxia (Setter et al., 2010). Mechanisms regulating shoot dehydration upon recovery also remain to be elucidated. In rice (*Oryza sativa* L.), the flooding tolerance-associated *SUB1A* gene also confers drought and oxidative stress tolerance during reoxygenation through increased ROS scavenging and enhanced abscisic acid (ABA) responsiveness. Following

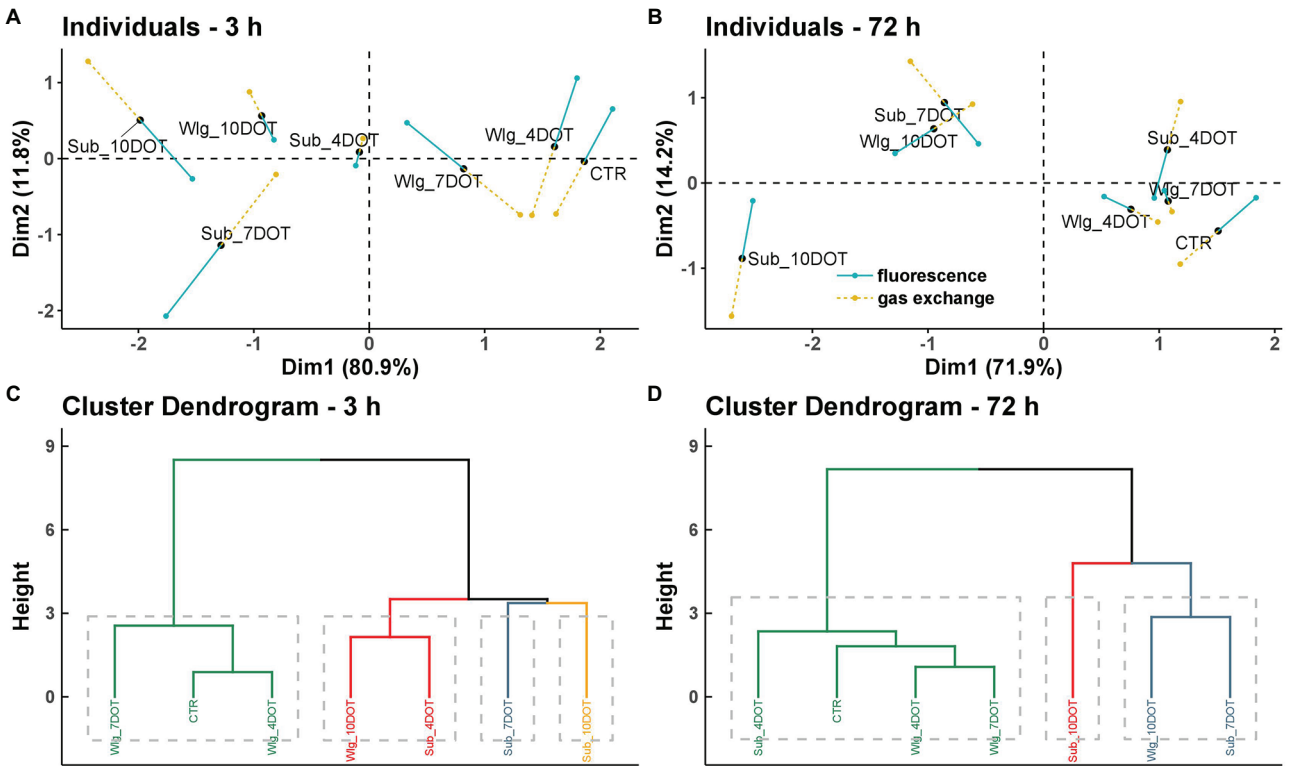

FIGURE 5 | Multiple factor analysis (MFA) of post-anoxia chlorophyll *a* fluorescence and leaf gas exchange data in *Arundo donax* L. plants as affected by incremental oxygen deficiency stress under three exposure times: submergence (Sub), waterlogging (Wlg), and control (CTR). **(A)** Score plot describing the experimental conditions and groups of variables of the two-first principal components recorded at the beginning and **(B)** end of our recovery time. Key: blue "fluorescence", F_v/F_m, Φ_{PSII}, $1 - q_p$, and NPQ; yellow gold "gas exchange", g_s, g_m, A, C_i, and E. **(C)** Hierarchical clustering of entries based on their traits recorded at the beginning and **(D)** end of recovery time.

de-submergence, dehydration caused by reduced root function and reoxygenation generates the submergence recovery signals ROS, ABA and ethylene that elicit downstream signaling pathways regulating various aspects of recovery (Yeung et al., 2018).

Chlorophyll fluorescence represents a powerful indicator of stress-induced damage to PSII (Guidi and Calatayud, 2014). A decrease of F_v/F_m under O_2 shortage conditions has previously been observed in warm- and cool-season perennial grasses (Pompeiano et al., 2017a). Mauchamp and Méthy (2004) showed that PSII photochemistry in *Phragmites australis* (Cav.) Trin. ex Steudel, a closely related and ecologically similar species to *A. donax*, was affected by submergence and exhibited a different recovery behavior depending on duration and degree of submergence, with completely submerged leaves that did not recover after 1 week. Moreover, the determination of Φ_{PSII} has an advantage with respect to F_v/F_m, since it is more sensitive to a large number of stressors including flooding (Ren et al., 2016). The analysis of post-anoxia recovery of the fluorescence indices F_v/F_m and Φ_{PSII} has been previously used for selecting species and cultivars of grasses more able to acclimate their photosynthetic apparatus to oxygen deprivation (Pompeiano et al., 2017a). Overall, these results highlight the sensitivity of the photosynthetic apparatus and PSII photochemical processes to O_2 deficiency and suggest the use of fluorescence techniques as a fast and reliable tool for studying the photosynthetic responses under waterlogging and submergence conditions and recovery. Accordingly, our results showed that waterlogging and submergence caused a change of both F_v/F_m and Φ_{PSII} in giant reed during the recovery period, depending on the treatment (waterlogging or submergence) and its duration. In particular, post-submergence and -waterlogging treatments were characterized by a decreased PSII photochemistry followed by a progressive recovery (Luo et al., 2009). The lower Φ_{PSII} in waterlogged and submerged plants during the first hours of recovery can be explained by a rapid enhancement of the reduction state of the PSII primary acceptors (Q_A pool), as indicated by the concomitant increased $1 - q_p$ values. This parameter is a proxy of the excess excitation pressure at PSII (Scartazza et al., 2016), which needs to be dissipated as heat to avoid photodamage to the photosynthetic apparatus. Hence, the reduced Φ_{PSII} in waterlogged and submerged plants during the first hours of recovery, associated with enhanced $1 - q_p$, highlights a decreased efficiency of excitation energy capture by open PSII reaction centers in the light-acclimated state (Roháček and Barták, 1999). It has been suggested that a reduced electron transport capacity during the first hours of recovery after submergence could be beneficial for the plants, preventing irreversible damage due to electron leakage and ROS formation through interaction with oxygen.

Subsequently, an increase of photochemistry activity associated with a decreased reduction state of the PSII reaction centers was observed from 24 to 72 h of recovery, depending on the treatment and duration. Indeed, at the end of the recovery period, both F_v/F_m and Φ_{PSII} values remained lower than the control starting from 7 to 10 days of submergence and waterlogging, respectively. A significant drop in dark-adapted F_v/F_m and Φ_{PSII} was previously observed in rice leaves immediately following de-submergence and was attributed to light-mediated inhibition of PSII performance in the submergence-sensitive cultivar (Alpuerto et al., 2016), although these authors observed a full recovery of PSII photochemistry within 24 h after de-submergence.

In order to avoid possible damage to the photosynthetic apparatus, excess light energy must be safely dissipated in thermal energy processes, estimated by means of NPQ. Our data showed a decreased NPQ in the first hours after de-submergence followed by a progressive increase of both Φ_{PSII} and NPQ within 72 h of recovery associated with a reduced $1 - q_P$. This suggests a restoration of the ability to dissipate the radiative energy as both photochemical and non-photochemical processes following the waterlogging and submergence treatments. In agreement with these results, Alpuerto et al. (2016) reported a decline of NPQ immediately after de-submergence followed by a rapid recovery in rice and highlighted that a greater capability for NPQ-mediated photoprotection may be crucial for a faster recovery of photosynthetic performance. However, our data indicate that this ability was partly compromised after 10 days of submergence and waterlogging, when both Φ_{PSII} and NPQ showed only a partial recovery and remained lower than control after 72 h of re-oxygenation, possibly leading to excess energy at PSII and, consequently, to photodamage in the reaction centers. This hypothesis is supported by the significant reduction, although slight, of F_v/F_m in both waterlogged and submergence plants compared to normoxic control, indicating a sustained quenching and, possibly, chronic photoinhibition of PSII. This negative effect on PSII photochemistry was evident starting from 7 days of submergence, when both the maximum and the effective quantum yields of PSII photochemistry were partially impaired after 72 h of recovery. These results, also remarked by the multivariate analysis, suggest that after a relatively long period of submergence or waterlogging (a threshold of 7 DOT for submergence and 10 DOT for waterlogging), plants showed a sustained decrease in photochemistry capacity without a compensatory increase of non-radiative energy dissipation ability, leading to PSII photodamage. This is in agreement with previous works on trees of a tropical seasonally flooded forest (Rengifo et al., 2005) and on off-season flooding *Distylium chinense* (Fr.) Diels (Liu et al., 2014), showing a decreased maximum quantum efficiency of PSII without a compensatory increase in NPQ. Hence, our data suggest that giant reed showed an impairment of the photosynthetic capacity that was due to both stomatal and non-stomatal factors, depending on the treatment (waterlogging or submergence) and its duration.

The appearance of both stomatal and non-stomatal detrimental effects on CO_2 photosynthetic uptake in *A. donax* was confirmed by the gas exchange analysis. The limited leaf gas exchanges induced a reduction in photosynthetic CO_2 uptake during the first hours of recovery following submergence (4, 7, and 10 DOT) or waterlogging (10 DOT) treatments, with only a partial recovery to control values after 7 and 10 days of submergence and 10 days of waterlogging. In agreement with our results, Alpuerto et al. (2016) found that the net CO_2 assimilation rate was reduced by submergence in rice and partially recovered within 24 h after treatment, but it did not recover completely in the more submergence-sensitive rice genotype. The root system may be impaired from waterlogging or submergence, leading to a reduced hydraulic conductance of the roots and inability to take up water from the soil (Shahzad et al., 2016). As a consequence, plants recovering from submergence generally show drought-like symptoms and tend to close stomata in order to reduce water loss through transpiration (Fukao et al., 2011; Alpuerto et al., 2016). Although stomatal closure is the most common response in plants growing under O_2 deficiency (Ahmed et al., 2002), the reduction of the CO_2 assimilation rate can also be attributed to non-stomatal factors (Herrera et al., 2008). Our data showed a decrease of g_s associated with reduced A and E and increased C_i during the first hours of recovery. This was evident in submerged plants starting from four DOT, while in waterlogged plants an increase of C_i with respect to the control was observed after only 10 DOT. According to Farquhar and Sharkey (1982), an increase of C_i in response to changes in A and decrease of g_s indicates a strong contribution of non-stomatal limitation to carbon photosynthetic uptake. These results are in agreement with Liu et al. (2014), who observed a gradual increase in C_i with increasing flooding duration in *D. chinense*, and with Yordanova and Popova (2007) who showed that C_i increased in all the flooded maize plants without significant changes in g_s. The C_i trend during the recovery period in giant reed was dependent on the coordinated variations of A and g_s. For example, after 7 days of submergence, plants showed a full recovery of g_s from 3 to 72 h of re-oxygenation associated with only a partial recovery of A, leading to a progressive increase of C_i after de-submergence. Non-stomatal constrains to photosynthetic CO_2 uptake can be due to ROS formation following the over-reduction of PSII reaction centers. Indeed, it has been shown that plants growing under waterlogging or submergence conditions face oxidative damage due to ROS production, which alters membrane integrity and induces damage to the photosynthetic apparatus (Blokhina et al., 2003). Our data showed that negative effects on the photosynthetic apparatus were more pronounced in submerged plants after only four DOT than in waterlogged ones. It has been suggested that injuries in plant tissues and organs developed underwater can be amplified upon de-submergence, because of the sudden increase in O_2 and light intensity that could exacerbate ROS production (Blokhina et al., 2003). Accordingly, Fernández (2006), studying the fluorescence responses to flooding in leaves of *Pouteria orinocoensis* (Aubr.)

Penn. Ined., showed that submerged leaves exhibited chronic photoinhibition, whereas the fluorescence analysis on emerged leaves revealed the occurrence of dynamic, rather than chronic, photoinhibition.

The reduced g_s in waterlogged plants has been associated with an enhanced leaf ABA content (Jackson and Hall, 1987), although stomatal behavior may also be affected by the impairment of root hydraulic conductivity and permeability due to low O_2 levels (Else et al., 2001, 2009). Rodríguez-Gamir et al. (2011) observed that ABA concentration in leaves only started to increase after 3 weeks of flooding in citrus seedlings, suggesting that stomatal closure occurs in the absence of a rise in leaf ABA content. The modulation of stomatal closure was attributed to downregulation of the expression of PIP aquaporins. Other than stomatal closure, it has been proposed that plants growing in waterlogged soil may reduce the CO_2 transfer from the substomatal cavities to the carboxylation sites within the chloroplasts (i.e. the mesophyll conductance to CO_2 or g_m), leading to a reduction in photosynthetic CO_2 uptake (Gaur and Sharma, 2013). A negative effect of flooding on g_m was observed by Moldau (1973) in *Phaseolus vulgaris* (L.). Moreover, Black et al. (2005) showed an alteration of both g_s and g_m in waterlogged seedlings of *Picea sitchensis* [Bong. (Carr.)] grown under exposed and shaded conditions. It has been reported that photosynthetic CO_2 uptake is dependent on a tight mutual regulation between stomatal and mesophyll conductance (Chaves et al., 2002; Scartazza et al., 2017) and that the improvement of mesophyll behavior may be an important criterion to enhance the flood resistance of greengram cultivars (Araki et al., 2014). According to the previous findings, our data showed that both g_s and g_m regulate simultaneously A as a function of the total conductance to CO_2 (Sorrentino et al., 2016; Santaniello et al., 2017; Scartazza et al., 2017). Herrera et al. (2008) reported that leaves of *Campsiandra laurifolia* Benth. developed under full flood exhibited a thicker mesophyll compared to leaves developed after falling water, possibly leading to a reduced g_m due to a longer diffusion path for CO_2. Ren et al. (2016) showed that waterlogging negatively affects leaf mesophyll ultrastructure and photosynthetic characteristics in summer maize, suggesting an impact of waterlogging on membrane integrity leading to chloroplast, mitochondria and membrane deterioration that increased with increasing waterlogging duration. These alterations could affect CO_2 diffusion through cell and chloroplastic membranes, thus reducing the mesophyll conductance (Flexas et al., 2008).

The ability to recover the photosynthetic performance after submergence or waterlogging treatment is a valuable trait in order to select the most tolerant species and genotypes to reduced O_2 availability. In the present work, only 10 days of waterlogging treatment showed sustained reduced photosynthetic activity after 72 h of recovery, while submergence induced a reduction in photosynthesis after just seven DOT. It is worth noting that notwithstanding the full recovery of photosynthetic parameters, plant biomass remained reduced compared to the control depending on treatment and duration. Accordingly, in a previous work of Smethurst et al. (2005) on *Medicago sativa* L., PSII photochemistry, which was impaired due to waterlogging, recovered almost completely after draining alongside the concentrations of several nutrients, although growth remained suppressed. These authors attributed the reduced growth to both the smaller CO_2 assimilation during waterlogging, due to nutrient deficiency and associated inhibition of PSII photochemistry, and the plant's need to redirect available nutrient and assimilate pools to repair the damage to the photosynthetic apparatus and roots. In addition, the reduction in leaf area in plants subjected to waterlogging could also substantially contribute to a decrease of the photosynthetic area and hence plant biomass (Malik et al., 2001).

MFA enabled the set of observations based on chlorophyll *a* fluorescence and leaf gas exchange data to be analyzed within the same framework, thus giving an integrated picture of the observations and the relationships between the variables recorded at the beginning and end of the time-course recovery experiment. The analysis led to the gradual separation of the entries as affected by incremental O_2 deficiency conditions with respect to the performance obtained. Moreover, the use of the multicanonical analysis highlighted the presence of specific thresholds (7 and 10 DOT, respectively, for submergence and waterlogging), which implied a treatment tolerance to the discrimination of the treatments.

CONCLUSION

In the present study, *A. donax* confirmed its ability and a distinct response strategy that allowed the species to cope with harsh stress conditions. Plants subjected to waterlogging showed similar growth capacity to those under normoxia, while plants fully submerged showed a dramatic reduction of this trait. Conditions of waterlogging and submergence revealed a slight growth plasticity of the species in response to prolonged stress conditions, followed by fast plant recovery upon reoxygenation. Moreover, the rapid restoration of physiological functions during the recovery period after O_2 deprivation testifies to the environmental plasticity of this species, although prolonged scarcity of O_2 proved detrimental to giant reed by hampering growth and photosynthetic CO_2 uptake. Those responses are today biologically and ecologically relevant for a species that has been promoted to marginal, degraded lands, and should be selected based on their performance under less than favorable conditions.

AUTHOR CONTRIBUTIONS

AP, AS, and LG conceived and designed the experiments. AP, AS, THR, and TM performed the experiments. AP, AS, and LG analyzed the data. AP, AS, LG, and THR wrote the paper.

FUNDING

AP was supported by the project no. LQ1605 from the National Program of Sustainability II (MEYS CR).

ACKNOWLEDGMENTS

The authors wish to express their sincere gratitude to Prof. Stefano Morini for providing plant material.

REFERENCES

Ahmed, S., Nawata, E., Hosokawa, M., Domae, Y., and Sakuratani, T. (2002). Alterations in photosynthesis and some antioxidant enzymatic activities of mungbean subjected to waterlogging. *Plant Sci.* 163, 117–123. doi: 10.1016/S0168-9452(02)00080-8

Alpuerto, J. B., Hussain, R. M. F., and Fukao, T. (2016). The key regulator of submergence tolerance, SUB1A, promotes photosynthetic and metabolic recovery from submergence damage in rice leaves. *Plant Cell Environ.* 39, 672–684. doi: 10.1111/pce.12661

Angelini, L. G., Ceccarini, L., and Bonari, E. (2005). Biomass yield and energy balance of giant reed (*Arundo donax* L.) cropped in Central Italy as related to different management practices. *Eur. J. Agron.* 22, 375–389. doi: 10.1016/j.eja.2004.05.004

Araki, T., Oo, T. T., and Kubota, F. (2014). Effects of flooding treatments on photosynthetic activity of different greengram (*Vigna radiata* (L.) Wilczek) cultivars. *Environ. Control Biol.* 52, 1–5. doi: 10.2525/ecb.52.1

Bailey-Serres, J., Lee, S. C., and Brinton, E. (2012). Waterproofing crops: effective flooding survival strategies. *Plant Physiol.* 160, 1698–1709. doi: 10.1104/pp.112.208173

Bates, D., Mächler, M., Bolker, B., and Walker, S. (2015). Fitting linear mixed-effects models using *lme4*. *J. Stat. Softw.* 67, 1–48. doi: 10.18637/jss.v067.i01

Bell, G. P. (1997). "Ecology and management of *Arundo donax*, and approaches to riparian habitat restoration in Southern California" in *Plant invasions: Studies from North America and Europe*. eds. J. H. Brock, M. Wade, P. Pysek, and D. Green (Leiden, The Netherlands: Backhuys Publishers), 103–113.

Black, K., Davis, P., Grath, J. M., Doherty, P., and Osborne, B. (2005). Interactive effects of irradiance and water availability on the photosynthetic performance of *Picea sitchensis* seedlings: implications for seedling establishment under different management practices. *Ann. Forest Sci.* 62, 413–422. doi: 10.1051/forest:2005037

Blokhina, O., Virolainen, E., and Fagerstedt, K. V. (2003). Antioxidants, oxidative damage and oxygen deprivation stress: a review. *Ann. Bot.* 91, 179–194. doi: 10.1093/aob/mcf118

Centritto, M., Lauteri, M., Monteverdi, M. C., and Serraj, R. (2009). Leaf gas exchange, carbon isotope discrimination, and grain yield in contrasting rice genotypes subjected to water deficits during the reproductive stage. *J. Exp. Bot.* 60, 2325–2339. doi: 10.1093/jxb/erp123

Chaves, M. M., Pereira, J. S., Maroco, J., Rodrigues, M. L., Ricardo, C. P. P., Osóirio, M. L., et al. (2002). How plants cope with water stress in the field? Photosynthesis and growth. *Ann. Bot.* 89, 907–916. doi: 10.1093/aob/mcf105

Else, J. A. (1996). *Post-flood establishment of native woody species and an exotic, Arundo donax, in a southern Californian riparian system*. San Diego State University. http://books.google.com.br/books?id=Tc5HtwAACAAJ

Else, M. A., Coupland, D., Dutton, L., and Jackson, M. B. (2001). Decreased root hydraulic conductivity reduces leaf water potential, initiates stomatal closure and slows leaf expansion in flooded plants of castor oil (*Ricinus communis*) despite diminished delivery of ABA from the roots to shoots in xylem sap. *Physiol. Plant.* 111, 46–54. doi: 10.1034/j.1399-3054.2001.1110107.x

Else, M. A., Janowiak, F., Atkinson, C. J., and Jackson, M. B. (2009). Root signals and stomatal closure in relation to photosynthesis, chlorophyll *a* fluorescence and adventitious rooting of flooded tomato plants. *Ann. Bot.* 103, 313–323. doi: 10.1093/aob/mcn208

Farquhar, G. D., and Sharkey, T. D. (1982). Stomatal conductance and photosynthesis. *Annu. Rev. Plant Physiol.* 33, 317–345. doi: 10.1146/annurev.pp.33.060182.001533

Fernández, M. D. (2006). Changes in photosynthesis and fluorescence in response to flooding in emerged and submerged leaves of *Pouteria orinocoensis*. *Photosynthetica* 44, 32–38. doi: 10.1007/s11099-005-0155-2

Fiorini, L., Guglielminetti, L., Mariotti, L., Curadi, M., Picciarelli, P., Scartazza, A., et al. (2016). *Trichoderma harzianum* T6776 modulates a complex metabolic network to stimulate tomato *cv.* Micro-tom growth. *Plant Soil* 400, 351–366. doi: 10.1007/s11104-015-2736-6

Flexas, J., Ribas-Carbó, M., Diaz-Espejo, A., Galmés, J., and Medrano, H. (2008). Mesophyll conductance to CO_2: current knowledge and future prospects. *Plant Cell Environ.* 31, 602–621. doi: 10.1111/j.1365-3040.2007.01757.x

Fukao, T., Yeung, E., and Bailey-Serres, J. (2011). The submergence tolerance regulator SUB1A mediates crosstalk between submergence and drought tolerance in rice. *Plant Cell* 23, 412–427. doi: 10.1105/tpc.110.080325

Galmés, J., Flexas, J., Keys, A. J., Cifre, J., Mitchell, R. A. C., Madgwick, P. J., et al. (2005). Rubisco specificity factor tends to be larger in plant species from drier habitats and in species with persistent leaves. *Plant Cell Environ.* 28, 571–579. doi: 10.1111/j.1365-3040.2005.01300.x

Gaur, R. K., and Sharma, P. K. (2013). *Molecular approaches in plant abiotic stress*. (Boca Raton, FL: CRC Press).

Gibbs, J., and Greenway, H. (2003). Review: mechanisms of anoxia tolerance in plants. I. Growth, survival and anaerobic catabolism. *Funct. Plant Biol.* 30:353. doi: 10.1071/PP98095_ER

Gopalakrishnan, G., Cristina Negri, M., and Snyder, S. W. (2011). A novel framework to classify marginal land for sustainable biomass feedstock production. *J. Environ. Qual.* 40, 1593–1600. doi: 10.2134/jeq2010.0539

Guidi, L., and Calatayud, A. (2014). Non-invasive tools to estimate stress-induced changes in photosynthetic performance in plants inhabiting Mediterranean areas. *Environ. Exp. Bot.* 103, 42–52. doi: 10.1016/j.envexpbot.2013.12.007

Herrera, A., Tezara, W., Marín, O., and Rengifo, E. (2008). Stomatal and non-stomatal limitations of photosynthesis in trees of a tropical seasonally flooded forest. *Physiol. Plant.* 134, 41–48. doi: 10.1111/j.1399-3054.2008.01099.x

Hothorn, T., Bretz, F., and Westfall, P. (2008). Simultaneous inference in general parametric models. *Biom. J.* 50, 346–363. doi: 10.1002/bimj.200810425

Jackson, M. B., and Hall, K. C. (1987). Early stomatal closure in waterlogged pea plants is mediated by abscisic acid in the absence of foliar water deficits. *Plant Cell Environ.* 10, 121–130. doi: 10.1111/1365-3040.ep11602085

Kuznetsova, A., Brockhoff, P. B., and Christensen, R. H. B. (2017). lmerTest package: tests in linear mixed effects models. *J. Stat. Softw.* 82, 1–26. doi: 10.18637/jss.v082.i13

Lê, S., Josse, J., and Husson, F. (2008). FactoMineR: an R package for multivariate analysis. *J. Stat. Softw.* 25, 1–18. doi: 10.18637/jss.v025.i01

Lewandowski, I., Scurlock, J. M. O., Lindvall, E., and Christou, M. (2003). The development and current status of perennial rhizomatous grasses as energy crops in the US and Europe. *Biomass Bioenergy* 25, 335–361. doi: 10.1016/S0961-9534(03)00030-8

Licausi, F., and Perata, P. (2009). Low oxygen signaling and tolerance in plants. *Adv. Bot. Res.* 50, 139–198.

Liu, Z., Cheng, R., Xiao, W., Guo, Q., and Wang, N. (2014). Effect of off-season flooding on growth, photosynthesis, carbohydrate partitioning, and nutrient uptake in *Distylium chinense*. *PLoS One* 9:e107636. doi: 10.1371/journal.pone.0107636

Loreto, F., Harley, P. C., Di Marco, G., and Sharkey, T. D. (1992). Estimation of mesophyll conductance to CO_2 flux by three different methods. *Plant Physiol.* 98, 1437–1443. doi: 10.1104/pp.98.4.1437

Luo, F.-L., Nagel, K. A., Zeng, B., Schurr, U., and Matsubara, S. (2009). Photosynthetic acclimation is important for post-submergence recovery of photosynthesis and growth in two riparian species. *Ann. Bot.* 104, 1435–1444. doi: 10.1093/aob/mcp257

Malik, A. I., Colmer, T. D., Lambers, H., and Schortemeyer, M. (2001). Changes in physiological and morphological traits of roots and shoots of wheat in

response to different depths of waterlogging. *Funct. Plant Biol.* 28, 1121–1131. doi: 10.1071/PP01089

Mauchamp, A., and Méthy, M. (2004). Submergence-induced damage of photosynthetic apparatus in *Phragmites australis*. *Environ. Exp. Bot.* 51, 227–235. doi: 10.1016/j.envexpbot.2003.11.002

Moldau, H. (1973). Effects of various water regimes on stomatal and mesophyll conductances of bean leaves. *Photosynthetica* 7, 1–7.

Pompeiano, A., Guglielminetti, L., Bargiacchi, E., and Miele, S. (2013). Responses in chemical traits and biomass allocation of *Arundo donax* L. to deficit resources in the establishment year. *Chil. J. Agric. Res.* 73, 377–384. doi: 10.4067/S0718-58392013000400008

Pompeiano, A., Huarancca Reyes, T., Moles, T. M., Villani, M., Volterrani, M., Guglielminetti, L., et al. (2017a). Inter- and intraspecific variability in physiological traits and post-anoxia recovery of photosynthetic efficiency in grasses under oxygen deprivation. *Physiol. Plant.* 161, 385–399. doi: 10.1111/ppl.12608

Pompeiano, A., Landi, M., Meloni, G., Vita, F., Guglielminetti, L., and Guidi, L. (2017b). Allocation pattern, ion partitioning, and chlorophyll *a* fluorescence in *Arundo donax* L. in responses to salinity stress. *Plant Biosyst.* 151, 613–622. doi: 10.1080/11263504.2016.1187680

Pompeiano, A., Remorini, D., Vita, F., Guglielminetti, L., Miele, S., and Morini, S. (2017c). Growth and physiological response of *Arundo donax* L. to controlled drought stress and recovery. *Plant Biosyst.* 151, 906–914. doi: 10.1080/11263504.2016.1249427

Pompeiano, A., Vita, F., Alpi, A., and Guglielminetti, L. (2015). *Arundo donax* L. response to low oxygen stress. *Environ. Exp. Bot.* 111, 147–154. doi: 10.1016/j.envexpbot.2014.11.003

Pucciariello, C., and Perata, P. (2017). New insights into reactive oxygen species and nitric oxide signalling under low oxygen in plants. *Plant Cell Environ.* 40, 473–482. doi: 10.1111/pce.12715

R Core Team (2018). *R: A language and environment for statistical computing*. 3.5.1 edn. (Vienna, Austria: R Foundation for Statistical Computing).

Ren, B., Zhang, J., Dong, S., Liu, P., and Zhao, B. (2016). Effects of duration of waterlogging at different growth stages on grain growth of summer maize (*Zea mays* L.) under field conditions. *J. Agron. Crop Sci.* 202, 564–575. doi: 10.1111/jac.12183

Rengifo, E., Tezara, W., and Herrera, A. (2005). Water relations, chlorophyll *a* fluorescence, and contents of saccharides in tree species of a tropical forest in response to flood. *Photosynthetica* 43, 203–210. doi: 10.1007/s11099-005-0034-x

Rodríguez-Gamir, J., Ancillo, G., González-Mas, M. C., Primo-Millo, E., Iglesias, D. J., and Forner-Giner, M. A. (2011). Root signalling and modulation of stomatal closure in flooded citrus seedlings. *Plant Physiol. Biochem.* 49, 636–645. doi: 10.1016/j.plaphy.2011.03.003

Roháček, K., and Barták, M. (1999). Technique of the modulated chlorophyll fluorescence: basic concepts, useful parameters, and some applications. *Photosynthetica* 37, 339–363. doi: 10.1023/A:1007172424619

Santaniello, A., Scartazza, A., Gresta, F., Loreti, E., Biasone, A., Di Tommaso, D., et al. (2017). *Ascophyllum nodosum* seaweed extract alleviates drought stress in *Arabidopsis* by affecting photosynthetic performance and related gene expression. *Front. Plant Sci.* 8:1362. doi: 10.3389/fpls.2017.01362

Scartazza, A., Di Baccio, D., Bertolotto, P., Gavrichkova, O., and Matteucci, G. (2016). Investigating the European beech (*Fagus sylvatica* L.) leaf characteristics along the vertical canopy profile: leaf structure, photosynthetic capacity, light energy dissipation and photoprotection mechanisms. *Tree Physiol.* 36, 1060–1076. doi: 10.1093/treephys/tpw038

Scartazza, A., Picciarelli, P., Mariotti, L., Curadi, M., Barsanti, L., and Gualtieri, P. (2017). The role of *Euglena gracilis* paramylon in modulating xylem hormone levels, photosynthesis and water-use efficiency in *Solanum lycopersicum* L. *Physiol. Plant.* 161, 486–501. doi: 10.1111/ppl.12611

Setter, T. L., Bhekasut, P., and Greenway, H. (2010). Desiccation of leaves after de-submergence is one cause for intolerance to complete submergence of the rice cultivar IR 42. *Funct. Plant Biol.* 37, 1096–1104. doi: 10.1071/FP10025

Shahzad, Z., Canut, M., Tournaire-Roux, C., Martinière, A., Boursiac, Y., Loudet, O., et al. (2016). A potassium-dependent oxygen sensing pathway regulates plant root hydraulics. *Cell* 167, 87.e14–98.e14. doi: 10.1016/j.cell.2016.08.068

Smethurst, C. F., Garnett, T., and Shabala, S. (2005). Nutritional and chlorophyll fluorescence responses of lucerne (*Medicago sativa*) to waterlogging and subsequent recovery. *Plant Soil* 270, 31–45. doi: 10.1007/s11104-004-1082-x

Sorrentino, G., Haworth, M., Wahbi, S., Mahmood, T., Zuomin, S., and Centritto, M. (2016). Abscisic acid induces rapid reductions in mesophyll conductance to carbon dioxide. *PLoS One* 11:e0148554. doi: 10.1371/journal.pone.0148554

Tamang, B., and Fukao, T. (2015). Plant adaptation to multiple stresses during submergence and following desubmergence. *Int. J. Mol. Sci.* 16, 30164–30180. doi: 10.3390/ijms161226226

Voesenek, L. A. C. J., and Bailey-Serres, J. (2015). Flood adaptive traits and processes: an overview. *New Phytol.* 206, 57–73. doi: 10.1111/nph.13209

Webster, R. J., Driever, S. M., Kromdijk, J., McGrath, J., Leakey, A. D. B., Siebke, K., et al. (2016). High C3 photosynthetic capacity and high intrinsic water use efficiency underlies the high productivity of the bioenergy grass *Arundo donax*. *Sci. Rep.* 6:20694. doi: 10.1038/srep20694

Wickham, H. (2009). *ggplot2: Elegant graphics for data analysis*. (New York: Springer).

Yeung, E., van Veen, H., Vashisht, D., Sobral Paiva, A. L., Hummel, M., Rankenberg, T., et al. (2018). A stress recovery signaling network for enhanced flooding tolerance in *Arabidopsis thaliana*. *Proc. Natl. Acad. Sci. USA*. 115, 6085–6094. doi: 10.1073/pnas.1803841115

Yordanova, R. Y., and Popova, L. P. (2007). Flooding-induced changes in photosynthesis and oxidative status in maize plants. *Acta Physiol. Plant.* 29, 535–541. doi: 10.1007/s11738-007-0064-z

Conflict of Interest Statement: The authors declare that the research was conducted in the absence of any commercial or financial relationships that could be construed as a potential conflict of interest.

frontiers in Plant Science

ORIGINAL RESEARCH
published: 09 April 2019
doi: 10.3389/fpls.2019.00444

Polar Auxin Transport Determines Adventitious Root Emergence and Growth in Rice

*Chen Lin and Margret Sauter**

Plant Developmental Biology and Physiology, University of Kiel, Kiel, Germany

Flooding is a severe limitation for crop production worldwide. Unlike other crop plants, rice (*Oryza sativa* L.) is well adapted to partial submergence rendering it a suitable crop plant to understand flooding tolerance. Formation of adventitious roots (ARs), that support or replace the main root system, is a characteristic response to flooding. In rice, AR emergence is induced by ethylene and in the dark where roots grow upward. We used the synthetic auxins 2,4-D and α-NAA, and the auxin transport inhibitor naphthylphtalamic acid (NPA) to study emergence, growth rate and growth angle of ARs. While α-NAA had no effect, NPA and 2,4-D reduced the root elongation rate and the angle with a stronger effect on root angle in the dark than in the light. Furthermore, NPA delayed emergence of AR primordia suggesting that efflux carrier-mediated auxin transport is required for all aspects of directed AR growth. Expression analysis using *OsPIN:GUS* reporter lines revealed that *OsPIN1b* and *OsPIN1c* promoters were active in the stele and root cap in accord with their predicted role in acropetal auxin transport. *OsPIN2* was expressed at the root tip and was reduced in the presence of NPA. Auxin activity, detected with *DR5:VENUS,* increased in primordia following growth induction. By contrast, auxin activity was high in epidermal cells above primordia and declined following growth induction suggesting that auxin levels are antagonistically regulated in AR primordia and in epidermal cells above AR primordia suggesting that auxin signaling contributes to the coordinated processes of epidermal cell death and AR emergence.

Keywords: adventitious roots, polar auxin transport, auxin efflux carrier, root angle, root emergence, rice, flooding

OPEN ACCESS

Edited by:
Iduna Arduini,
University of Pisa, Italy

Reviewed by:
Laurent Gutierrez,
University of Picardie Jules Verne, France
Philip B. Brewer,
The University of Adelaide, Australia
Randy Ortiz-Castro,
National Council of Science and Technology (CONACYT), Mexico

***Correspondence:**
Margret Sauter
msauter@bot.uni-kiel.de

Specialty section:
This article was submitted to Plant Abiotic Stress, a section of the journal Frontiers in Plant Science

Received: *16 January 2019*
Accepted: *25 March 2019*
Published: *09 April 2019*

Citation:
Lin C and Sauter M (2019) Polar Auxin Transport Determines Adventitious Root Emergence and Growth in Rice. Front. Plant Sci. 10:444. doi: 10.3389/fpls.2019.00444

INTRODUCTION

Rice is semi-aquatic showing remarkable tolerance to partial submergence. Adventitious root (AR) primordia form at each node during normal development that emerge during submergence to replace the original dysfunctional root system (Sauter, 2013). AR formation is regarded as a characteristic response to flooding not only in rice but also in other flooding tolerant and flooding-intolerant plants such as tomato (*Lycopersicon esculentum*) (Vidoz et al., 2010) and pecan tree (*Catya illinoinensis*) (Smith and Ager, 1988). ARs are located closer to the shoot than the original root system thereby facilitating oxygen supply. Furthermore, ARs take up oxygen from flood waters further improving their oxygen status. Recent work on rice revealed that ARs grow upward in the dark such that roots get closer to the oxygen-rich water surface (Lin and Sauter, 2018). The hormones and molecular mechanisms that control AR growth direction need yet to be elucidated. This study sets out with the mechanistic analysis by studying the role of auxin transport and

signaling in AR growth. In the past decades, the number of flooding events has increased worldwide causing increasing crop losses (Voesenek and Bailey-Serres, 2015). It is hence rather timely to decipher in more depth the molecular mechanisms that control AR growth in flooded crop plants.

In rice and *Solanum dulcamara*, the gaseous hormone ethylene that accumulates in submerged tissues due to a reduced diffusion rate in water, promotes AR growth (Drew and Sisworo, 1979; Lorbiecke and Sauter, 1999; Dawood et al., 2016). Both, ethylene-induced AR emergence and AR growth rate are enhanced by gibberellic acid and inhibited by abscisic acid (Steffens and Sauter, 2005; Steffens et al., 2006).

Unlike growth of nodal ARs, growth of crown roots in rice seedlings is inhibited by ethylene. Inhibition of root growth by ethylene and auxin has been reported for Arabidopsis where ethylene and auxin pathways interact (Stepanova et al., 2007; Swarup et al., 2007). A recent study in rice seedlings revealed that auxin signaling downstream of ethylene is required for root growth inhibition by ethylene (Chen et al., 2018) suggesting similar hormonal crosstalk in monocots and dicots. Auxin signal transduction through $SCF^{TIR1/AFBs}$-Aux/IAAs has been well studied (Salehin et al., 2015). The E3 ubiquitin ligase $SCF^{TIR1/AFB}$ recognizes Aux/IAA proteins as a target upon binding of auxin to the F-Box subunit TIR1/AFB resulting in their ubiquitination and proteasome-dependent degradation. Canonical Aux/IAA proteins act as transcriptional repressors of auxin response factors (ARFs). Their degradation allows transcription of ARFs which regulate auxin-responsive genes including most Aux/IAA genes, hence providing a negative feedback loop (Salehin et al., 2015). In rice seedlings, ethylene signaling induces *OsIAA26* expression whereby the OsIAA26 protein stability is controlled by the auxin-dependent E3 ubiquitin ligase Soil-surface Rooting 1 (SOR1). This study hence revealed a molecular link between ethylene and auxin signaling in rice root development.

A widely used tool to monitor auxin distribution *in planta* is DR5-based auxin-inducible reporters. The DR5 promoter contains several ARF binding sites resulting in reporter gene induction in the presence of auxin (Ulmasov et al., 1997). A more recently developed auxin reporter uses the destabilizing DII-domain of an Aux/IAA protein that is fused to the fluorescent VENUS protein. An increase in auxin results in degradation of DII-VENUS as an immediate response to $SCF^{TIR1/AFB}$ activation through auxin binding (Brunoud et al., 2012). Local auxin accumulation due to synthesis or polar auxin transport can be tracked with these reporters (Brumos et al., 2018) which aids in deciphering the contribution of an auxin gradient to a development process. Chemiosmosis is widely accepted as mechanism of polar auxin transport (Rubery and Sheldrake, 1974; Raven, 1975; Adamowski and Friml, 2015). While auxin diffuses passively into the cell through the membrane or by way of facilitated diffusion through AUX1/LAX influx carriers, the efflux of the IAA anion requires auxin efflux carriers of the PIN-FORMED (PIN) protein family or ATP-Binding Cassette family B (ABCB) transporters. PIN and ABCB activity is a target of the auxin transport inhibitor 1-naphthylphtalamic acid (NPA) and of flavonoids that interfere with the interaction of ABCB and its partner TWISTED DWARF 1 (TWD1) (Bailly et al., 2008). The direction of auxin flux and the establishment of an auxin gradient are achieved by the polar distribution of PINs in the plasma membrane (Tanaka et al., 2006). For Arabidopsis, seven PIN genes and for rice, twelve PIN genes were reported (Wang et al., 2009). In Arabidopsis roots, auxin moves acropetally in the central cylinder driven by AtPIN1 activity. Auxin is laterally deflected in the root cap mediated by AtPIN3, AtPIN4 and AtPIN7 activity and moves basipetally in the peripheral cell layers due to AtPIN2 localized in the apical part of the plasma membrane (Vanneste and Friml, 2009). The PIN1 clade has diversified into four members in rice, OsPIN1a-d. OsPIN10a and OsPIN10b are most closely related to AtPIN3, AtPIN4 and AtPIN7, whereas the PIN2 clade is represented by a single member in Arabidopsis and rice (**Supplementary Figure S1**).

In rice, little is known about the role of auxin and polar auxin transport in the development of ARs. A number of genes related to crown root formation and growth have been identified (Liu et al., 2005; Zhao et al., 2009, 2015). *Crown-rootless 4 (crl4)* and *OsGNOM1* show reduced crown root initiation and delayed lateral root differentiation (Kitomi et al., 2008; Wang et al., 2011). OsGNOM1 controls PIN1 trafficking within the cell, and thus alters polar auxin transport that is required for the formation of an auxin gradient which triggers the asymmetrical division of parenchyma cells that develop into crown roots (Richter et al., 2010). Interestingly, an RNAi-knockdown line for the *OsPIN1b* gene displays a reduced AR penetration rate at the seedling stage (Xu et al., 2005).

In this study, we investigated auxin activity and *OsPIN* gene promoter activities with high spatial resolution during AR emergence and growth. Our results indicate that local auxin gradients determine AR penetration, growth rate and growth direction and thereby have a deep impact on the overall architecture of the AR system.

RESULTS

Inhibition of Auxin Transport Inhibits AR Penetration and Growth and Reduces the Root Growth Angle

To study the role of auxin on AR growth in rice, we employed the auxin transport inhibitor naphthylphtalamic acid (NPA) and two auxin analogs, 2,4-dichlorophenoxyacetic acid (2,4-D) and 1-naphthalene acetic acid (α-NAA). Rice stem sections were treated with NPA, 2,4-D or α-NAA in the dark (**Figure 1**). Darkness induced AR emergence with an upward direction of AR growth as described previously (Lin and Sauter, 2018). The root penetration rate, i.e., the number of AR primordia that emerged from the node in relation to the total number of AR primordia, given as percentage, was not significantly altered by 2,4-D or α-NAA at concentrations of 0.3 to 5 μM whereas inhibition of auxin efflux at 5 μM NPA significantly reduced AR penetration (**Figure 1B**). The length of penetrated ARs was reduced by NPA and 2,4-D in a dose-dependent manner, with an average of 0.3 cm at 5 μM 2,4-D compared to 1.9 cm in the absence of 2,4-D. By contrast, α-NAA did not inhibit AR elongation revealing a functional similarity

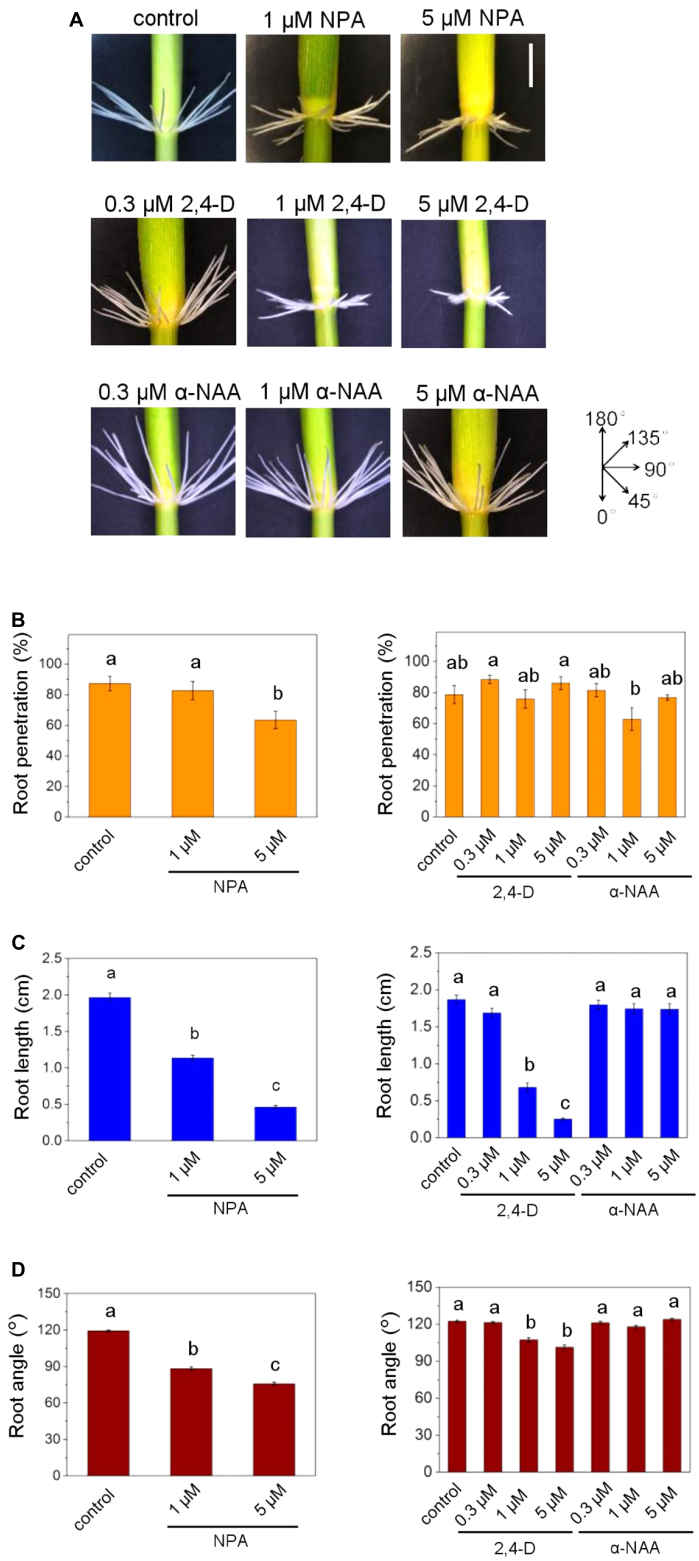

FIGURE 1 | Auxin transport inhibition alters emergence, growth rate and angle of adventitious roots (ARs) in rice. **(A)** ARs were analyzed at the third node using stem sections kept in the dark for 3 days in the presence of NPA, 2,4-D or α-NAA at the concentrations indicated. Phenotypes of ARs exposed to the auxins 2,4-D or α-NAA or to the auxin transporter inhibitor NPA; bar=1 cm. **(B)** Percentage of penetrated ARs. **(C)** Average lengths of penetrated ARs. **(D)** Mean growth angles of ARs. Bars in **B–D** indicate means (±SE) of ARs measured from nine stems per treatment in three independent experiments. Different letters indicate statistically significant differences ($P < 0.05$; ANOVA with Tukey test).

between auxin efflux inhibition by NPA and 2,4-D activity and a functional difference between the two synthetic auxins 2,4-D and α-NAA (**Figure 1C**). Similarly, the AR angle decreased in the presence of 2,4-D and NPA but not after exposure to α-NAA (**Figure 1D**). Taken together, our data suggested that increased intracellular auxin levels induced by chemical inhibition of auxin efflux through NPA or by supplying 2,4-D, that is taken up by cells but not actively secreted by auxin efflux carriers, reduced AR elongation and growth angle whereas the auxin analog α-NAA that is actively exported from the cell through efflux carriers (Delbarre et al., 1996; Simon et al., 2013) did not.

Adventitious root emergence is facilitated by programmed death of epidermal cells covering root primordia (Mergemann and Sauter, 2000). To study a possible involvement of auxin in epidermal cell death, we employed a *DR5:VENUS* auxin reporter line (**Figures 2A,B**). Fluorescence microscopy revealed auxin activity in epidermal cells above root primordia and/or the primordia but not in other epidermal cells indicating a specific function of auxin.

For better spatial resolution, we peeled off the epidermis above a root primordium and isolated root primordia (**Figure 3**). Interestingly, when AR growth was induced by transfer to the dark, auxin activity appeared to decline within 6 h in epidermal cells covering a primordium (**Figure 3A**). At the same time, auxin activity increased in AR primordia following growth induction (**Figure 3B**). A time course analysis of epidermal cell death (**Figure 4A**) and root penetration (**Figure 4B**) showed that 5 μM NPA delayed both and resulted in reduced auxin activity at the AR apex (**Figure 4C**). These findings suggest that auxin activity coordinates epidermal cell death and AR emergence. The data further indicated that polar auxin transport through efflux carriers controls auxin levels.

OsPIN Genes Are Differentially Expressed in ARs and in Epidermal Cells Above ARs

PINs are carrier proteins that facilitate auxin efflux from plant cells and are responsible for directed auxin flux in plant organs.

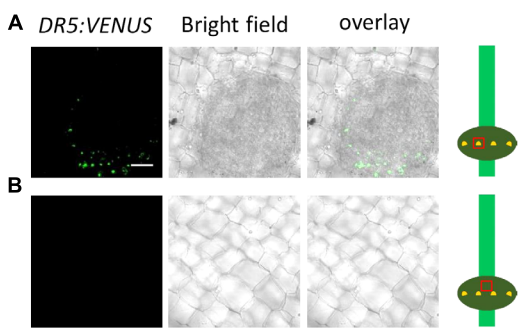

FIGURE 2 | Auxin activity is detected in cells above root primordia but not in other cells. **(A)** Top view on the epidermis and an underlying root primordium at the third node of a *DR5:VENUS* reporter line. Bar (=25 (um. Green channel: VENUS. **(B)** Top view on the epidermis not covering a root primordium.

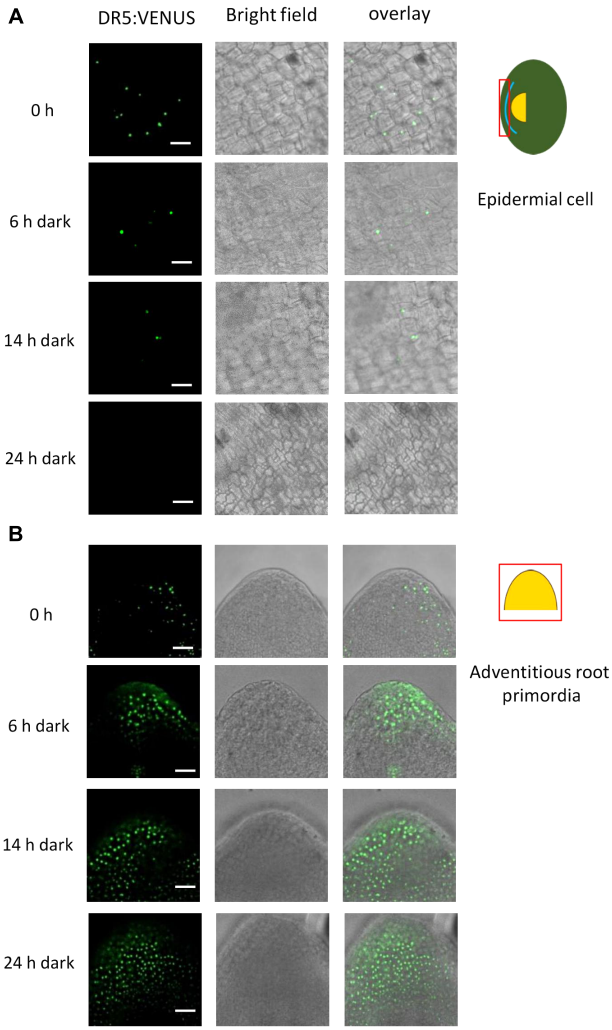

FIGURE 3 | Auxin activity decreases in the epidermis above primordia and increases in AR primordia after induction of AR growth in the dark. Bar (=25 μm. **(A)** Epidermal peels above a root primordium. Auxin activity was detected by CLSM using the *DR5:VENUS* reporter. **(B)** Isolated AR primordia from the *DR5:VENUS* reporter line.

PINs are encoded by gene families with 7 members in Arabidopsis and 12 members in rice (**Supplementary Figure S1**) and have mostly been studied in Arabidopsis (Křeček et al., 2009). In Arabidopsis roots, PIN1 drives acropetal auxin transport in the central cylinder, PIN3, 4, and 7 redirect the auxin flux in the root tip to the outer cell layers and PIN2 drives basipetal auxin flow in the outer root cell layers. To find out whether homologous transporters in rice might be involved in generating auxin gradients in ARs and at the site of AR emergence, we obtained GUS reporter lines for the Arabidopsis *PIN1* orthologs *OsPIN1b* and *OsPIN1c*, for the *PIN2* ortholog *OsPIN2* and for *OsPIN10a* which is phylogenetically most closely related to PINs 3, 4 and 7 (**Supplementary Figure S1**).

OsPIN1b:GUS and *OsPIN1c:GUS* was expressed in AR primordia and penetrated ARs (**Figure 5A** and

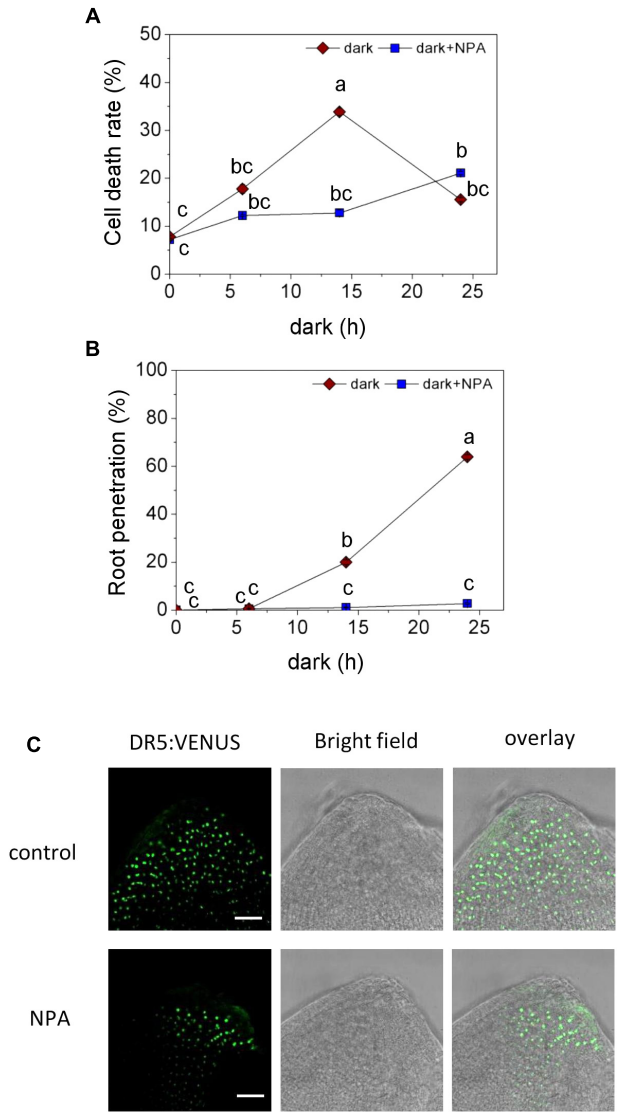

FIGURE 4 | Effect of auxin transport inhibition on programmed cell death (PCD) and AR emergence. **(A)** Cell death of epidermal cells above AR primordia, analyzed with Evans Blue at the third node of stem sections kept in the dark for 6 h, 14 h or 24 h with or without 5 μM NPA. **(B)** Percentage of penetrated ARs. Bars in **A, B** indicate means (± SE) of ARs from 9 stems per treatment measured in 3 independent experiments. Different letters indicate statistically significant differences ($P < 0.05$; ANOVA with Tukey test). **(C)** Auxin activity detected with *DR5:VENUS* in AR primordia with or without 5 μM NPA for 1 day; Bar=25 μm.

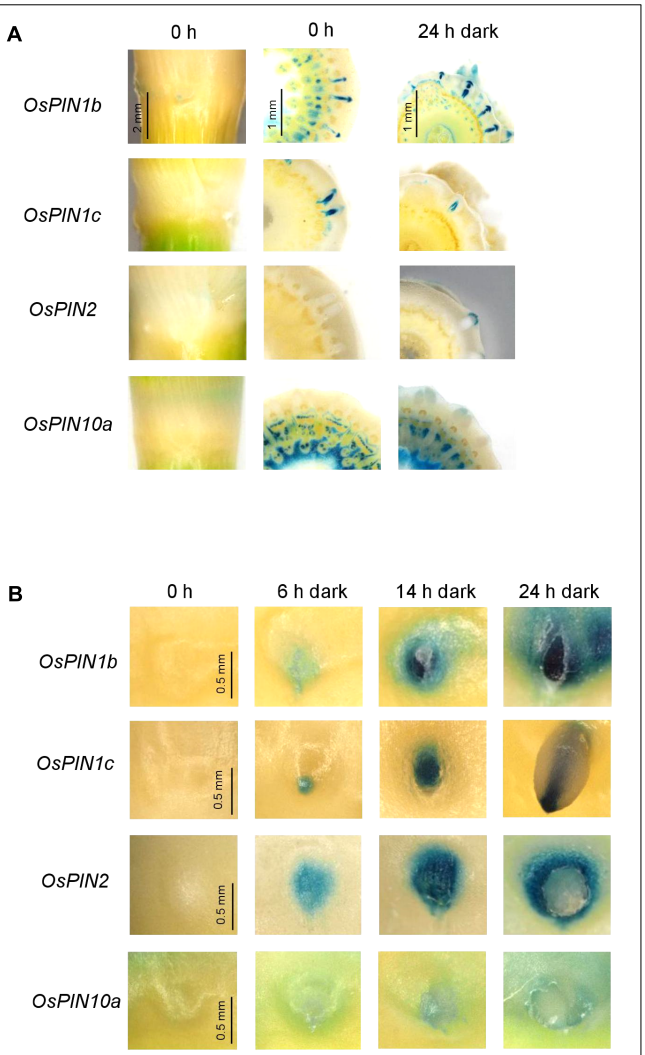

FIGURE 5 | *OsPIN2* expression is induced in epidermal cells above AR primordia after AR growth induction in the dark. **(A)** Expression of *OsPIN1b:GUS*, *OsPIN1c:GUS*, *OsPIN2:GUS*, and *OsPIN10a:GUS* was visualized in nodal cross sections following dark exposure for the times indicated. **(B)** Top view on emerging ARs in *OsPIN1b:GUS*, *OsPIN1c:GUS*, *OsPIN2:GUS*, and *OsPIN10a:GUS* reporter lines reveals induction of *OsPIN2* expression in the epidermis.

Supplementary Figure S2A). *OsPIN2:GUS* expression was not detected in uninduced nodes and appeared in epidermal cells above AR primordia within 6 h after transferring to the dark to trigger AR emergence (**Figures 5A,B**). *OsPIN2:GUS* was also active at the apex of emerged ARs in what appeared to be the root cap (**Supplementary Figure S2**). *OsPIN10a:GUS* expression was observed at AR tips within 24 h after transfer to the dark and was maintained during subsequent AR elongation (**Figure 5A** and **Supplementary Figure S2A**). Overall, the results revealed regulation of *OsPIN* gene expression following growth-inducing dark treatment. Interestingly, *OsPIN2* expression was induced specifically in epidermal cells above AR primordia following growth induction coincident with reduced auxin activity in these cells (**Figure 3A**). These findings suggest that OsPIN2-mediated auxin depletion in the epidermis promotes epidermal cell death and root penetration.

Auxin Transport Is Required for AR Growth Promotion by Ethylene

Adventitious roots emerge in the dark but not in the light (**Figures 6A,B**). Emergence in the dark was related to dark-induced ethylene synthesis (Fukao et al., 2012) which is in

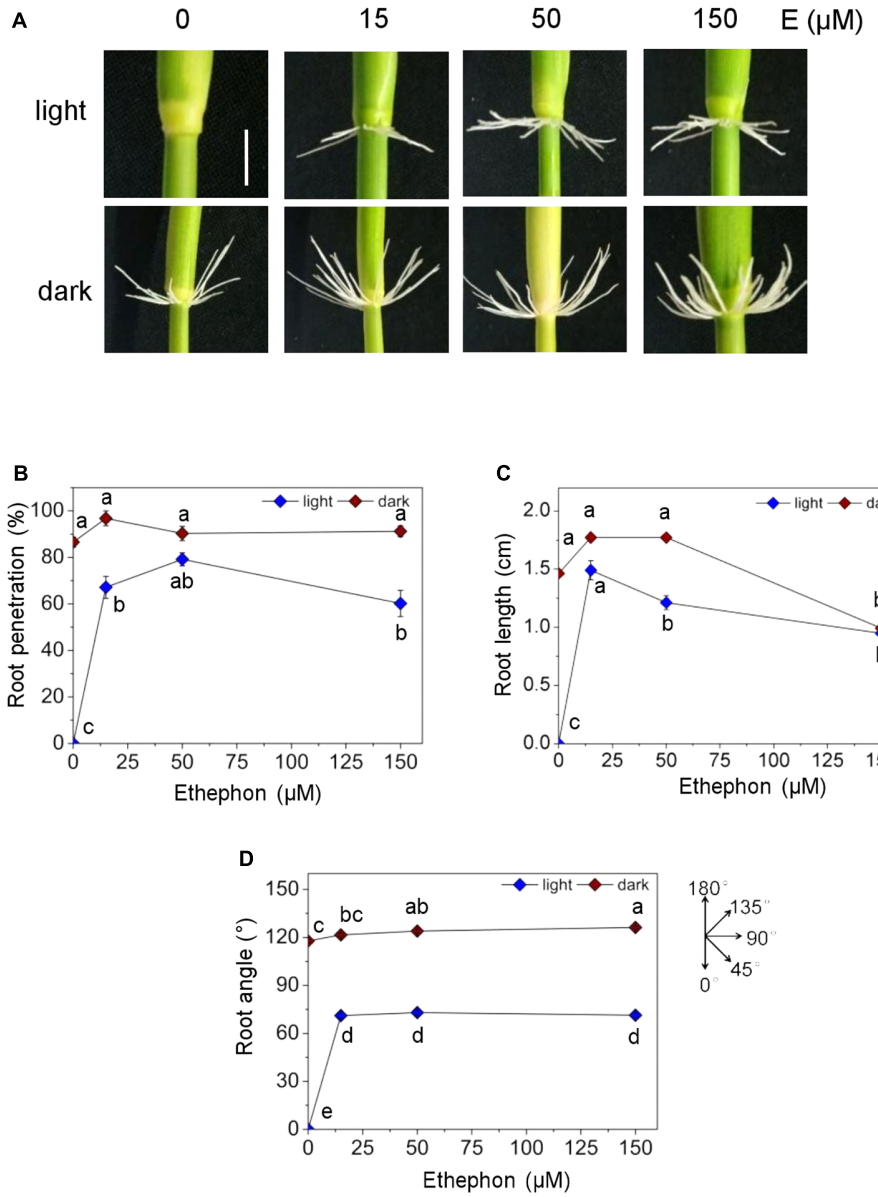

FIGURE 6 | Effect of ethephon on penetration, growth and angle of ARs in the dark. Rice stem sections including the third node were exposed to white light (WL) or kept in the dark for 3 days in the presence of different concentrations of ethephon. **(A)** Phenotypes of AR growth in the dark and in light (bar=1 cm). **(B)** Percentage of root penetration determined with Evans Blue staining. **(C)** Average length of AR. **(D)** Angle of AR growth. Bars in **B–D** indicate means (±SE) from nine stem sections analyzed per treatment in three independent experiments. Different letters indicate statistically significant differences (P <0.05; ANOVA with Tukey test).

accord with the observation that ethylene promotes emergence and growth of ARs in the light (**Figures 6A,B**; Mergemann and Sauter, 2000). A dose-response analysis of AR growth revealed that root emergence was elevated to 67.1% at 15 μM ethephon, an ethylene-releasing compound, and remained at this level at higher concentrations while the emergence rate in the dark was close to 100% (**Figure 6B**). AR elongation was similar in the light and in the dark at 15 and 150 μM ethephon and was lower in the light than in the dark at 50 μM ethephon possibly indicating different responsiveness to ethylene (**Figure 6C**). ARs grew upward in the dark and downward in the light as described previously (**Figures 6A,D**; Lin and Sauter, 2018). While the growth angle in the light was independent of ethephon, the growth angle in the dark increased slightly but significantly from 117.8 to 126.2° with increasing ethephon concentration.

In order to investigate a possible cross-talk between auxin and ethylene in AR growth, we exposed stem sections to ethephon together with NPA, 2,4-D or α-NAA for 3 days (**Figure 7**). Neither 2,4-D or α-NAA nor auxin transport inhibition by NPA altered AR penetration in the light in the long term (**Figure 7B**) whereas root length was significantly elevated from 1 to 1.4 cm at 1 μM NPA and reduced to 0.2 cm at 5 μM NPA revealing

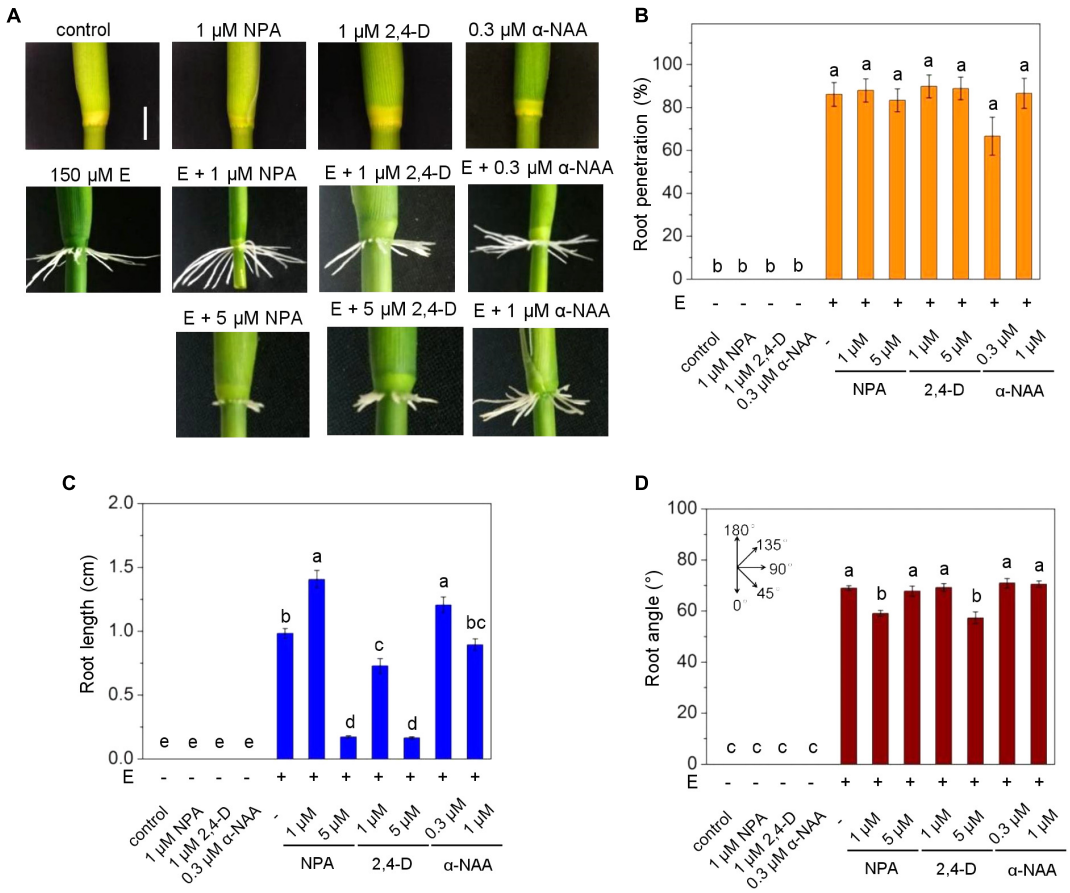

FIGURE 7 | Auxin controls ethylene-induced AR elongation in the light. ARs were analyzed at the third node of stems treated with or without 150 ethephon and NPA, 2,4-D or α-NAA for 3 days in the light as indicated. **(A)** AR growth phenotypes (bar=1 cm). **(B)** Percentage of penetrated ARs. **(C)** Average lengths of penetrated ARs. **(D)** Average growth angle of ARs. Means (±SE) in **B–D** were determined from nine stems analyzed per treatment in three independent experiments. Different letters indicate statistically significant differences (P <0.05; ANOVA with Tukey test).

a dose-dependent opposite response. Root elongation was also promoted by low (0.3 µM) α-NAA and was inhibited by 1 and 5 µM 2,4-D in a dose-dependent manner suggesting that the native auxin activity is at a suboptimal level in ethephon-induced ARs (**Figure 7C**). The growth angle was slightly reduced at 1 µM NPA and 5 µM 2,4-D and was unaffected by α-NAA (**Figure 7D**). These findings support the idea that ethylene overrides the inhibitory effect of NPA on AR emergence in the long run whereas control of AR elongation and, to a lesser degree, growth angle by auxin is not. Since NPA and 2,4-D reduced the growth angle in the dark and, to a minor degree, in the light, we next investigated a possible contribution of auxin in redirecting AR growth.

Time Course Analysis of AR Redirection

To study the mechanisms underlying redirection of AR growth, we established a time course of AR bending induced by light (**Figure 8**). Stem sections were exposed to darkness for 2 days to induce AR growth at an upward angle as visualized by toluidine-stained cross sections (**Figure 8A**). In the dark, emerged ARs were bending upward after 24 h. The upward angle of growth was fully established after 48 h. After 3 days in the dark, stems were exposed to white light (WL) and the root angle was monitored. Roots grew at an angle of 117.8° in the dark (**Figures 8B,C**). A significant change in growth direction to 111.4° was measured after 30 min. Within 15 h, the growth angle reached 68.3° which is about the angle at which ARs grow in the light (**Figure 6D**).

Gravitropic root growth is initiated by starch-containing statoliths in root cap statocytes. To exclude a possible role of statoliths in light-induced redirection of AR growth, statoliths were visualized at the root tip as brown precipitate from Lugols starch staining (**Supplementary Figure S3**). Neither exposure of stems to darkness in an upright or inverse orientation, nor a shift from dark to light for 1, 3 or 6 h altered the detectable pattern of starch staining.

OsPIN Expression and Auxin Distribution in ARs That Change Their Growth Direction

To test whether a change in growth direction of ARs is accompanied by altered expression of *OsPIN* genes, we

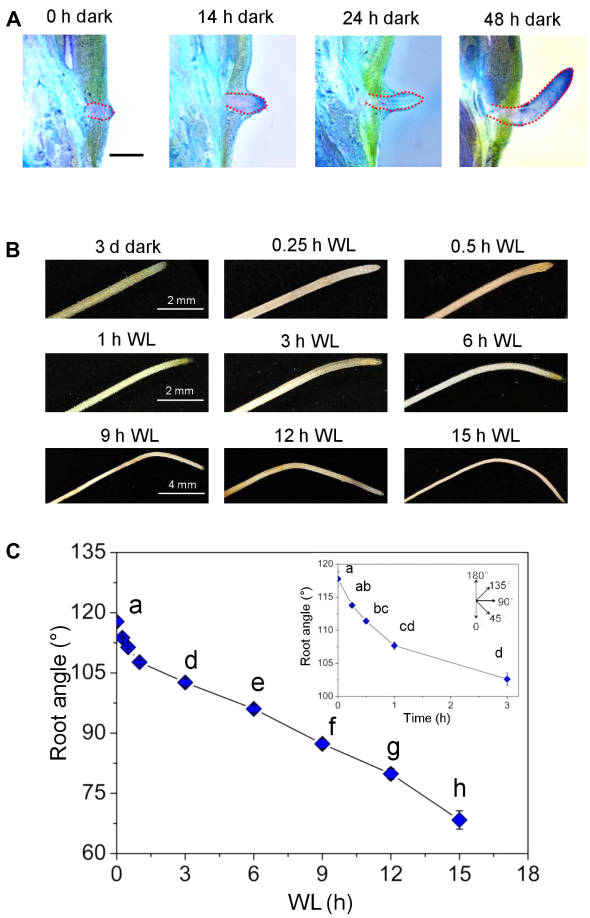

FIGURE 8 | Light changes the growth angle within 30 min. **(A)** Stems sections including the third node were kept in the dark for up to 3 days. Longitudinal sections were obtained and stained with toluidine after 0, 14, 24, and 48 h to visualize AR growth (bar=2 mm). **(B)** Growth phenotype of ARs that were grown for 3 days in the dark and subsequently exposed to WL for the times indicated. **(C)** Changes in AR angle after exposure to light. Bars indicate means (±SE) from nine stem sections for per treatment analyzed in three independent experiments. Different letters indicate statistically significant differences ($P < 0.05$; ANOVA with Tukey test).

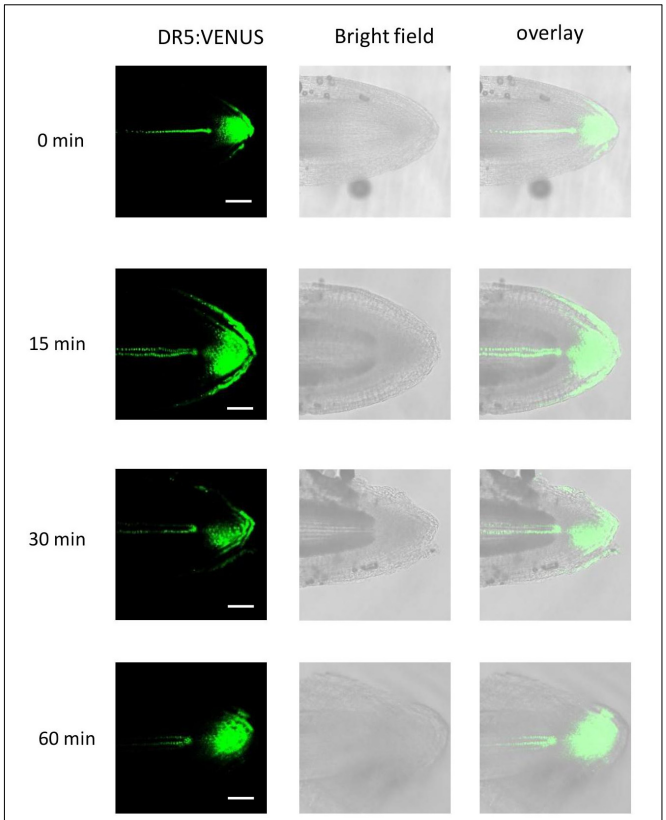

FIGURE 9 | Light exposure triggers higher auxin activity at the lower side of AR tips. Stem section of the *DR5:VENUS* reporter line were kept in the dark for 5 days and subsequently transferred to the light for 15, 30, and 60 min. Auxin activity was detected by CLSM (bar=100 μm).

transferred rice stems that were kept in the dark for 3 days to induce AR growth at an upward angle, to the light for 0.5, 1, or 3 h (**Supplementary Figure S2A**). *OsPIN1b:GUS* expression was detected in the stele and in the root cap. Expression in the root cap was intensified within 3 h of exposure to light. A similar expression pattern was observed when ARs were exposed to ethephon in the light indicating that *OsPIN1b* expression is under light control (**Supplementary Figure S2B**). *OsPIN1c:GUS* was active at the root apex, xylem and stele tissues but not in lateral root cap cells. Neither transfer from dark to light (**Supplementary Figure S2A**) nor growth in the light with ethephon changed *OsPIN1c:GUS* expression (**Supplementary Figure S2B**). *OsPIN2:GUS* and *OsPIN10a:GUS* displayed a patchy expression pattern at AR tips in what appeared to be root cap cells that appeared to become stronger within 3 h after transfer to the light and weaker in the presence of NPA (**Supplementary Figure S2C**). Overall, the expression patterns were in accord with OsPIN1b and OsPIN1c-driven auxin transport in the stele, redistribution of auxin at the root tip and auxin transport in root cap cells by OsPIN2 and OsPIN10a. Altered expression of *OsPIN1b* and *OsPIN2* suggested an altered auxin distribution in response to the dark-to-light switch.

To test if altered *OsPIN* gene expression affects auxin distribution, we employed the DR5:VENUS reporter (**Figure 9**). AR growth was induced in the dark. After 5 days in the dark, the stems were transferred to the light and auxin distribution was visualized at the root tip for up to 1 h. Auxin appeared to accumulate at the lower side within 30 min suggesting that elevated auxin inhibits growth at this side resulting in downward bending of the root (**Figure 8C**). In summary, polar auxin transport likely regulates the angle at which ARs grow indicating that auxin plays a key role in shaping the AR system architecture in rice.

DISCUSSION

Plant root systems mainly consist of secondary roots that develop postembryonically from the primary root as lateral

roots or from the shoot as ARs. Auxin is a key hormone that regulates secondary root formation and growth (Olatunji et al., 2017). In tomato, induction of ARs during flooding is mediated by ethylene that promotes auxin flux toward the submerged stem thereby increasing local auxin activity (Liu et al., 2009; Vidoz et al., 2010). In rice, the Lateral Organ Boundaries Domain (LBD) transcription factor Crown Rootless1/Adventitious Rootless1 (CRL1/ARL1) acts downstream of ARFs to control the formation of ARs (Inukai et al., 2005; Liu et al., 2005). Consequently, *arl1* mutants have fewer ARs at their stem nodes. While auxin is well known to promote formation of secondary roots including formation of ARs, the role of auxin in AR emergence and growth is less well studied. In rice, AR formation is developmentally programmed whereas emergence and growth are induced by environmental cues, rendering rice highly suitable to study these aspects. Flooding promotes AR emergence through ethylene signaling. The AR growth-promoting activity of ethylene is enhanced by gibberellic acid and repressed by abscisic acid (Steffens et al., 2006).

Our current study supported a role for polar auxin transport in shaping the AR system since inhibition of polar auxin transport by NPA reduced AR emergence, AR elongation growth and the angle at which roots grew in the dark. A similar phenotype was observed after treatment with the synthetic auxin 2,4-D. PIN proteins facilitate auxin efflux of the natural auxin IAA and of the synthetic auxin α-NAA but not of 2,4-D supporting the conclusion that high levels of 2,4-D accumulate in plant cells and thereby mimic inhibition of efflux carriers by NPA (Delbarre et al., 1996). By contrast, α-NAA did not similarly, alter AR growth, presumably because local auxin activity did not increase. Interestingly, when ARs were induced by ethylene to grow in the light, the growth rate was strongly repressed by NPA and 2,4-D whereas emergence and growth angle were not or only marginally affected suggesting that responsiveness to auxin differs in the light and in the dark. A previous study on rice showed that repression of the auxin efflux carrier gene *OsPIN1* repressed AR emergence supporting the conclusion that locally altered auxin activity controls AR development (Xu et al., 2005).

Analysis of defined *PIN* genes revealed differential expression patterns in ARs and epidermal cells above ARs. Expression patterns were in accord with their predicted functions based on protein similarity to Arabidopsis homologs. *PIN1b* and *PIN1c* were predominately expressed in the central cylinder as is *AtPIN1* which facilitates acropetal auxin movement. *PIN1b* and *PIN1c* were further expressed in the root cap where expression was enhanced when roots were exposed to light possibly indicating that *PIN1b* contributes to control of AR growth direction. Expression of *OsPIN1c* in AR primordia agrees with the observation that auxin levels are high at the primordia apex. High auxin activity at the root apex has also been shown for Arabidopsis (Petersson et al., 2009).

An unexpected and previously not reported finding was the accumulation of auxin specifically in epidermal cells covering root primordia but not in other epidermal cells. Programmed cell death (PCD) of epidermal cells was suggested to facilitate AR emergence (Mergemann and Sauter, 2000). Epidermal cells covering AR primordia were shown to have a unique molecular identity that allows them to undergo PCD in response to a specific trigger (Steffens and Sauter, 2009). Induction of PCD requires the hormonal signal ethylene and in addition a mechanical signal that provides spatial resolution and thereby limits PCD to the site where an AR emerges (Steffens et al., 2012). Ethylene signaling sets the stage in two ways, for one by promoting AR growth and, secondly, by activating the cell death program that, however, is executed only in cells that perceive mechanical force exerted by the growing AR primordium. Auxin that accumulates in epidermal cells could be synthesized locally in the epidermis itself or in the root tip from where it is transported to epidermal cells above it. However, auxin activity was low in AR primordia. Alternatively, efflux carrier-mediated auxin transport in epidermal cells could generate an auxin maximum in these cells. However, none of the efflux carrier genes analyzed was expressed at detectable levels in epidermal cells. Finally, it is possible, that local auxin synthesis is responsible for elevated auxin activity in these cells. The decline in auxin activity in epidermal cells above AR primordia upon growth induction of ARs in the dark occurs in parallel, and possibly as a consequence of, elevated *OsPIN2* expression in these epidermal cells and suggests a role of polar auxin transport in epidermal cells during AR emergence. Inhibition of polar auxin transport by NPA delayed epidermal cell death and reduced the rate of AR emergence. Taken together, our findings indicate that controlled local auxin activities through polar auxin transport contribute to rapid weakening of the epidermis as a physical barrier. At the same time, auxin activity in the root meristem increases likely promoting cell division activity.

The growth angle contributes substantially to AR system architecture. It is controlled by red and blue light signaling (Lin and Sauter, 2018). Upward AR growth in the dark is reverted to a downward angle in the light. The change in growth angle occurs within 30 min. Polar auxin transport is required to maintain an upward growth angle in the dark. It seems reasonable to assume that directed auxin flux is altered to change AR growth direction after exposure to light. Fluorescence auxin reporter data indicate that auxin accumulates at the lower side within 30 min. Auxin is known to inhibit root growth already at low concentrations. It is hence conceivable that growth is slowed down at this side resulting in downward bending of the AR tip. Whether differential expression of auxin carrier genes or regulation at the protein level alters efflux carrier activity remains to be resolved. In Arabidopsis, the growth direction of the primary root changes in response to hypoxic conditions such that the primary root no longer grows downward (Eysholdt-Derzso and Sauter, 2017). While auxin activity was asymmetrically distributed between epidermal cells of either side of the primary root, AtPIN2 protein, responsible for auxin transport in this cell layer, was symmetrically distributed. AtPIN2 distribution in the plasma membrane is regulated via phosphorylation/dephosphorylation (Santner and Watson, 2006; Michniewicz et al., 2007; Adamowski

and Friml, 2015) pointing to multiple levels of auxin transport regulation in plants.

CONCLUSION

Adventitious root emergence is controlled by polar auxin transport likely through activation of the auxin efflux carrier gene *OsPIN2* in epidermal cells above AR primordia and subsequent depletion of auxin in these cells. Polar auxin transport furthermore controls AR elongation and determines growth direction. Taken together, local auxin activities controlled by polar auxin transport through OsPIN efflux carriers is a major determinant of AR system architecture in rice.

MATERIALS AND METHODS

Growth Conditions and Treatments

The seeds of the deepwater rice variety PG56 (*Oryza sativa* L., Pin Gaew 56) were originally obtained from the International Rice Research Institute (Philippines). The *OsPIN:GUS* lines in the rice *japonica* cultivar Nipponbare were generously donated by Prof. Chuanzao Mao (Zhejiang University, China). The *DR5:VENUS* line of the japonica rice cultivar 9522 was generously provided by Prof. Zheng Yuan (Shanghai Jiao Tong University, China). The VENUS protein is directed to the nucleus for better detection and resolution (Yang et al., 2017). Seeds were germinated in a 12.5 × 12.5 cm Petri dish with a surface-moist Whatman filter paper at 27°C in the dark for 4 days. Seedlings were transferred to 1.7-liter pots with a soil mixture consisting of two thirds of soil and one third of volcanic soil. Plants were grown in a growth chamber with 16 h light (362.3 μmol $m^{-2}s^{-1}$) at 27°C and 8 h dark at 19°C with 70% relative humidity for 12–14 weeks (Sauter, 1997). Stems were excised 2 cm below the third youngest node with a total length of 20 cm (Mergemann and Sauter, 2000). Stem sections were incubated in 150 ml beakers with 20 ml aqueous solution with or without different concentrations of ethephon, 2,4-D or α-NAA or NPA. Plastic cylinders covered the beakers to ensure high humidity. To investigate the effect of light on the growth angle of ARs, stem sections were either kept in the dark for 3 days to induce roots to emerge and subsequently exposed to WL (43 μmol $m^{-2}s^{-1}$) for the times indicated or exposed to light in the presence of the ethylene-releasing compound ethephon.

To determine the root angle, each AR was photographed (Canon SX 220 HS) and the angle measured with ImageJ (Fiji). Subsequently, roots were excised to determine the root length with a ruler.

Evans Blue and Lugol Staining

Evans Blue staining was used for epidermal cell death determination and to better visualize AR penetration at the rice stem. Five mm of the node were cut and stained in a 2% (w/v) Evans Blue solution for 3 min followed by two washing steps in tap water. Root penetration was determined using a light microscope (Olympus SZ61, Japan) and the percentage was calculated based on the total number of AR initials that was taken as 100%. For Lugols staining, 1 cm of the root tip was isolated and stained with Lugols' solution for 1 min. Subsequently, the samples were washed once in distilled water. The starch-containing statoliths were visualized and photographed using a binocular (Nikon H600L, Japan).

Histochemical GUS Analysis

Histochemical β-glucuronidase (GUS) staining was performed according to Blázquez et al. (1997) with minor modifications. Rice stem sections were kept in the dark or exposed to WL for the duration indicated with or without 150 μM ethephon or 5 μM NPA. Isolated ARs or nodes were rapidly transferred to 90% pre-cooled acetone for 20 min and subsequently washed twice with 50 mM sodium-phosphate buffer (pH 7.2) for 5 min on a shaker. After removing the washing solution, 1 ml staining buffer (50 mM sodium phosphate, 0.2% [v/v] Triton X(-100, 2 mM $K_4[Fe(CN)_6]$, 2 mM $K_3[Fe(CN)_6]$, and 2 mM 5-bromo-4-chloro-3-indolyl-β-D-glucuronide [Duchefa], pH 7.5) was added to each sample. Samples were kept in a vacuum chamber for 10 min followed by shaking at 37°C in the dark (*OsPIN1b:GUS* and *OsPIN1c:GUS* for 1 h, *OsPIN2:GUS* and *OsPIN10a:GUS* overnight). The staining buffer was removed and samples were incubated in 70% ethanol to remove chlorophyll. GUS staining was visualized using a binocular (Nikon H600L, Japan).

Confocal Laser Scanning Microscopy

Fluorescence images of *DR5:VENUS* samples were taken with a Leica SP5 confocal laser scanning microscope (CLSM). For an overview, a 5 mm segment containing an AR primordium and the surrounding nodal tissue was excised from the node. Root primordia and the epidermis were isolated and prepared on a slide with a drop of 10% (w/v) glycerol for imaging. Imaging of VENUS was done at 510–550 nm and bright field was regarded as a control. ARs that were transferred from dark to light were marked on the upper and lower sides to allow for proper orientation of the root in CLSM.

Statistical Analysis

Statistical analysis was performed using Minitab. The *P*-value was set to $P < 0.05$. Comparison of means was analyzed for statistical difference with an analysis of variance (ANOVA) (Tukey test) or a two sample *t*-test.

AUTHOR CONTRIBUTIONS

CL and MS designed the project. CL performed the experiments. MS wrote the manuscript with contributions from CL.

FUNDING

This work was supported by the CSC through a grant to CL.

ACKNOWLEDGMENTS

The authors would like to thank Prof. Chuanzao Mao (Zhejiang University, China) for generously providing *OsPIN:GUS* lines and Prof. Zheng Yuan (Shanghai Jiao Tong University, China) for generously providing the *DR5:VENUS* line.

SUPPLEMENTARY MATERIAL

The Supplementary Material for this article can be found online at: https://www.frontiersin.org/articles/10.3389/fpls.2019.00444/full#supplementary-material

REFERENCES

Adamowski, M., and Friml, J. (2015). PIN-dependent auxin transport: action, regulation, and evolution. *Plant Cell* 27, 20–32. doi: 10.1105/tpc.114.134874

Bailly, A., Sovero, V., Vincenzetti, V., Santelia, D., Bartnik, D., Koenig, B. W., et al. (2008). Modulation of P-glycoproteins by auxin transport inhibitors is mediated by interaction with immunophilins. *J. Biol. Chem.* 283, 21817–21826. doi: 10.1074/jbc.M709655200

Blázquez, M. A., Soowal, L. N., Lee, I., and Weigel, D. (1997). LEAFY expression and flower initiation in Arabidopsis. *Development* 124, 3835–3844.

Brumos, J., Robles, L. M., Yun, J., Vu, T. C., Jackson, S., Alonso, J. M., et al. (2018). Local auxin biosynthesis is a key regulator of plant development. *Dev. cell* 47:306-318.e5. doi: 10.1016/j.devcel.2018.09.022

Brunoud, G., Wells, D. M., Oliva, M., Larrieu, A., Mirabet, V., Burrow, A. H., et al. (2012). A novel sensor to map auxin response and distribution at high spatio-temporal resolution. *Nature* 482, 103–106. doi: 10.1038/nature10791

Chen, H., Ma, B., Zhou, Y., He, S. J., Tang, S. Y., Lu, X., et al. (2018). E3 ubiquitin ligase SOR1 regulates ethylene response in rice root by modulating stability of Aux/IAA protein. *Proc. Natl. Acad. Sci. U.S.A.* 115, 4513–4518. doi: 10.1073/pnas.1719387115

Dawood, T., Yang, X., Visser, E. J., Te Beek, T. A., Kensche, P. R., Cristescu, S. M., et al. (2016). A co-opted hormonal cascade activates dormant adventitious root primordia upon flooding in *Solanum dulcamara*. *Plant Physiol.* 170, 2351–2364. doi: 10.1104/pp.15.00773

Delbarre, A., Muller, P., Imhoff, V., and Guern, J. (1996). Comparison of mechanisms controlling uptake and accumulation of 2, 4-dichlorophenoxy acetic acid, naphthalene-1-acetic acid, and indole-3-acetic acid in suspension-cultured tobacco cells. *Planta* 198, 532–541. doi: 10.1007/BF00262639

Drew, M., and Sisworo, E. (1979). The development of waterlogging damage in young barley plants in relation to plant nutrient status and changes in soil properties. *New Phytol.* 82, 301–314. doi: 10.1111/j.1469-8137.1979.tb02656.x

Eysholdt-Derzso, E., and Sauter, M. (2017). Root bending is antagonistically affected by hypoxia and ERF-mediated transcription via auxin signaling. *Plant Physiol.* 175, 412–423. doi: 10.1104/pp.17.00555

Fukao, T., Yeung, E., and Bailey-Serres, J. (2012). The submergence tolerance gene, SUB1A, delays leaf senescence under prolonged darkness through hormonal regulation in rice. *Plant Physiol.* 160, 1795–1807. doi: 10.1104/pp.112.207738

Inukai, Y., Sakamoto, T., Ueguchi-Tanaka, M., Shibata, Y., Gomi, K., Umemura, I., et al. (2005). Crown rootless1, which is essential for crown root formation in rice, is a target of an AUXIN RESPONSE FACTOR in auxin signaling. *Plant Cell* 17, 1387–1396. doi: 10.1105/tpc.105.030981

Kitomi, Y., Ogawa, A., Kitano, H., and Inukai, Y. (2008). CRL4 regulates crown root formation through auxin transport in rice. *Plant Root* 2, 19–28. doi: 10.3117/plantroot.2.19

Křeček, P., Skùpa, P., Libus, J., Naramoto, S., Tejos, R., Friml, J., et al. (2009). The PIN-FORMED (PIN) protein family of auxin transporters. *Genome Biol.* 10:249. doi: 10.1186/gb-2009-10-12-249

Lin, C., and Sauter, M. (2018). Control of adventitious root architecture in rice by darkness, light, and gravity. *Plant Physiol.* 176, 1352–1364. doi: 10.1104/pp.17.01540

Liu, H., Wang, S., Yu, X., Yu, J., He, X., Zhang, S., et al. (2005). ARL1, a LOB-domain protein required for adventitious root formation in rice. *Plant J.* 43, 47–56. doi: 10.1111/j.1365-313X.2005.02434.x

Liu, S., Wang, J., Wang, L., Wang, X., Xue, Y., Wu, P., et al. (2009). Adventitious root formation in rice requires OsGNOM1 and is mediated by the OsPINs family. *Cell Res.* 19, 1110–1119. doi: 10.1038/cr.2009.70

Lorbiecke, R., and Sauter, M. (1999). Adventitious root growth and cell-cycle induction in deepwater rice. *Plant Physiol.* 119, 21–30. doi: 10.1104/pp.119.1.21

Mergemann, H., and Sauter, M. (2000). Ethylene induces epidermal cell death at the site of adventitious root emergence in rice. *Plant Physiol.* 124, 609–614. doi: 10.1104/pp.124.2.609

Michniewicz, M., Zago, M. K., Abas, L., Weijers, D., Schweighofer, A., Meskiene, I., et al. (2007). Antagonistic regulation of PIN phosphorylation by PP2A and PINOID directs auxin flux. *Cell* 130, 1044–1056. doi: 10.1016/j.cell.2007.07.033

Olatunji, D., Geelen, D., and Verstraeten, I. (2017). Control of endogenous auxin levels in plant root development. *Int. J. Mol. Sci.* 18:E2587. doi: 10.3390/ijms18122587

Petersson, S. V., Johansson, A. I., Kowalczyk, M., Makoveychuk, A., Wang, J. Y., Moritz, T., et al. (2009). An auxin gradient and maximum in the Arabidopsis root apex shown by high-resolution cell-specific analysis of IAA distribution and synthesis. *Plant Cell* 21, 1659–1668. doi: 10.1105/tpc.109.066480

Raven, J. (1975). Transport of indoleacetic acid in plant cells in relation to pH and electrical potential gradients, and its significance for polar IAA transport. *New Phytol.* 74, 163–172. doi: 10.1111/j.1469-8137.1975.tb02602.x

Richter, S., Anders, N., Wolters, H., Beckmann, H., Thomann, A., Heinrich, R., et al. (2010). Role of the GNOM gene in *Arabidopsis* apical-basal patterning–From mutant phenotype to cellular mechanism of protein action. *Eur. J. Cell Biol.* 89, 138–144. doi: 10.1016/j.ejcb.2009.11.020

Rubery, P., and Sheldrake, A. (1974). Carrier-mediated auxin transport. *Planta* 118, 101–121. doi: 10.1007/BF00388387

Salehin, M., Bagchi, R., and Estelle, M. (2015). SCFTIR1/AFB-based auxin perception: mechanism and role in plant growth and development. *Plant Cell* 27, 9–19. doi: 10.1105/tpc.114.133744

Santner, A. A., and Watson, J. C. (2006). The WAG1 and WAG2 protein kinases negatively regulate root waving in Arabidopsis. *Plant J.* 45, 752–764. doi: 10.1111/j.1365-313X.2005.02641.x

Sauter, M. (1997). Differential expression of a CAK (cdc2-activating kinase)-like protein kinase, cyclins and cdc2 genes from rice during the cell cycle and in response to gibberellin. *Plant J.* 11, 181–190. doi: 10.1046/j.1365-313X.1997.11020181.x

Sauter, M. (2013). Root responses to flooding. *Curr. Opin. Plant Biol.* 16, 282–286. doi: 10.1016/j.pbi.2013.03.013

Simon, S., Kubeš, M., Baster, P., Robert, S., Dobrev, P. I., Friml, J., et al. (2013). Defining the selectivity of processes along the auxin response chain: a study using auxin analogues. *New Phytol.* 200, 1034–1048. doi: 10.1111/nph.12437

Smith, M., and Ager, P. (1988). Effects of soil flooding on leaf gas exchange of seedling pecan trees. *HortScience* 23, 370–372.

Steffens, B., Kovalev, A., Gorb, S. N., and Sauter, M. (2012). Emerging roots alter epidermal cell fate through mechanical and reactive oxygen species signaling. *Plant Cell* 24, 3296–3306. doi: 10.1105/tpc.112.101790

Steffens, B., and Sauter, M. (2005). Epidermal cell death in rice is regulated by ethylene, gibberellin, and abscisic acid. *Plant Physiol.* 139, 713–721. doi: 10.1104/pp.105.064469

Steffens, B., and Sauter, M. (2009). Epidermal cell death in rice is confined to cells with a distinct molecular identity and is mediated by ethylene and H2O2 through an autoamplified signal pathway. *Plant Cell* 21, 184–196. doi: 10.1105/tpc.108.061887

Steffens, B., Wang, J., and Sauter, M. (2006). Interactions between ethylene, gibberellin and abscisic acid regulate emergence and growth rate of adventitious roots in deepwater rice. *Planta* 223, 604–612. doi: 10.1007/s00425-005-0111-1

Stepanova, A. N., Yun, J., Likhacheva, A. V., and Alonso, J. M. (2007). Multilevel interactions between ethylene and auxin in Arabidopsis roots. *Plant Cell* 19, 2169–2185. doi: 10.1105/tpc.107.052068

Swarup, R., Perry, P., Hagenbeek, D., Van Der Straeten, D., Beemster, G. T., Sandberg, G., et al. (2007). Ethylene upregulates auxin biosynthesis in *Arabidopsis* seedlings to enhance inhibition of root cell elongation. *Plant Cell* 19, 2186–2196. doi: 10.1105/tpc.107.052100

Tanaka, H., Dhonukshe, P., Brewer, P. B., and Friml, J. (2006). Spatiotemporal asymmetric auxin distribution: a means to coordinate plant development. *Cell Mol. Life Sci.* 63, 2738–2754. doi: 10.1007/s00018-006-6116-5

Ulmasov, T., Murfett, J., Hagen, G., and Guilfoyle, T. J. (1997). Aux/IAA proteins repress expression of reporter genes containing natural and highly active synthetic auxin response elements. *Plant Cell* 9, 1963–1971. doi: 10.1105/tpc.9.11.1963

Vanneste, S., and Friml, J. (2009). Auxin: a trigger for change in plant development. *Cell* 136, 1005–1016. doi: 10.1016/j.cell.2009.03.001

Vidoz, M. L., Loreti, E., Mensuali, A., Alpi, A., and Perata, P. (2010). Hormonal interplay during adventitious root formation in flooded tomato plants. *Plant J.* 63, 551–562. doi: 10.1111/j.1365-313X.2010.04262.x

Voesenek, L. A., and Bailey-Serres, J. (2015). Flood adaptive traits and processes: an overview. *New Phytol.* 206, 57–73. doi: 10.1111/nph.13209

Wang, J. R., Hu, H., Wang, G. H., Li, J., Chen, J. Y., and Wu, P. (2009). Expression of PIN genes in rice (Oryza sativa L.): tissue specificity and regulation by hormones. *Mol. Plant* 2, 823–831. doi: 10.1093/mp/ssp023

Wang, X. F., He, F. F., Ma, X. X., Mao, C. Z., Hodgman, C., Lu, C. G., et al. (2011). OsCAND1 is required for crown root emergence in rice. *Mol. Plant* 4, 289–299. doi: 10.1093/mp/ssq068

Xu, M., Zhu, L., Shou, H., and Wu, P. (2005). A PIN1 family gene, OsPIN1, involved in auxin-dependent adventitious root emergence and tillering in rice. *Plant Cell Physiol.* 46, 1674–1681. doi: 10.1093/pcp/pci183

Yang, J., Yuan, Z., Meng, Q., Huang, G., Périn, C., Bureau, C., et al. (2017). Dynamic regulation of auxin response during rice development revealed by newly established hormone biosensor markers. *Front. Plant Sci.* 8:256. doi: 10.3389/fpls.2017.00256

Zhao, Y., Cheng, S., Song, Y., Huang, Y., Zhou, S., Liu, X., et al. (2015). The interaction between rice ERF3 and WOX11 promotes crown root development by regulating gene expression involved in cytokinin signaling. *Plant Cell* 27, 2469–2483. doi: 10.1105/tpc.15.00227

Zhao, Y., Hu, Y., Dai, M., Huang, L., and Zhou, D. X. (2009). The WUSCHEL-related homeobox gene WOX11 is required to activate shoot-borne crown root development in rice. *Plant Cell* 21, 736–748. doi: 10.1105/tpc.108.061655

Conflict of Interest Statement: The authors declare that the research was conducted in the absence of any commercial or financial relationships that could be construed as a potential conflict of interest.

frontiers in Plant Science

ORIGINAL RESEARCH
published: 03 May 2019
doi: 10.3389/fpls.2019.00546

Day-Length Is Involved in Flooding Tolerance Response in Wild Type and Variant Genotypes of Rootstock *Prunus cerasifera* L.

*Calogero Iacona[1†], Laura Pistelli[1†], Marco Cirilli[2,3], Lorenzo Gatti[2], Roberto Mancinelli[2], Maria Nicolina Ripa[2] and Rosario Muleo[2,4]**

[1] Department of Agriculture, Food and Environment, University of Pisa, Pisa, Italy, [2] Laboratory of Molecular Ecophysiology of Woody Plant, Department of Agricultural and Forestry Sciences, University of Tuscia, Viterbo, Italy, [3] Department of Agricultural and Environmental Sciences, University of Milan, Milan, Italy, [4] Tree and Timber Institute, National Research Council of Italy, Sesto Fiorentino, Italy

OPEN ACCESS

Edited by:
Guangcheng Shao,
Hohai University, China

Reviewed by:
Petronia Carillo,
Università degli Studi della Campania Luigi Vanvitelli Caserta, Italy
Keisuke Nagai,
Nagoya University, Japan

***Correspondence:**
Rosario Muleo
muleo@unitus.it

[†] These authors have contributed equally to this work as first authors

Specialty section:
This article was submitted to Plant Abiotic Stress, a section of the journal Frontiers in Plant Science

Received: 03 January 2019
Accepted: 10 April 2019
Published: 03 May 2019

Citation:
Iacona C, Pistelli L, Cirilli M, Gatti L, Mancinelli R, Ripa MN and Muleo R (2019) Day-Length Is Involved in Flooding Tolerance Response in Wild Type and Variant Genotypes of Rootstock Prunus cerasifera L. Front. Plant Sci. 10:546. doi: 10.3389/fpls.2019.00546

Current and predicted climate changes scenarios require crops with an improved adaptability to mutable environmental features, such as, hypoxia for the root system. In order to overcome the reduction of oxygen, plants activate coping mechanisms and strategies. *Prunus* spp. are hypoxia-sensitive woody species and although many information has been gathered over the last decades, many physiological mechanisms remain unclear. To verify whether anoxic plant responses are also regulated by photoperiod, plants of Mr.S.2/5-*WT* plum, and its variant genotypes *S.4* tolerant (plus) and *S.1* sensitive (minus) to flooding, were grown in a greenhouse and were submitted to natural photoperiod (NP) and to constant photoperiod (CP) from mid-July until the first 10 days of October. From mid-September plants from each genotype, grown under the two photoperiods, were divided into two groups, and one of them underwent long-term flooding. Gas exchange parameters, energetic and biochemical activities, leaf chlorophyll contents, and stress symptoms were measured at different times, whereas soluble sugars were quantified in leaves and roots 14 days after flooding, when stress symptoms in *WT* and *S.1* became prominent. Seasonal changes in the photoperiod played a role in the adaptability to anoxia, although flooding stress response differed among the three genotypes. Anoxia affected leaf gas exchange and *S.4* flooded-leaves retained higher ACO_2 under conditions of NP and CP. Leaf soluble sugar concentration differed among genotypes. Regardless the photoperiod, *S.4* anoxic-leaf sugar concentration was the lowest, except for sorbitol. *S.4* anoxic-roots under CP accumulated the highest levels of sucrose and sorbitol. Influences of the photoperiod were observed in *WT* and *S.1* anoxic-leaves, whereas *S.1* anoxic roots accumulated the lowest concentration of sugars, regardless of photoperiod. Leaf and root respiratory activity in flooded-plants was highest in *S.4*, and ADH activity increased in all flooded

plants under CP but the highest activity was observed only in *S.1* under NP during flooding. Results are consistent with the hypothesis that the *S.4* genotype has a plastic adaptability to flooding stress, escaping from the photoperiod regulatory cross-talk system, and can better cope with the new scenarios generated by climate changes.

Keywords: anoxia, off-season flooding, photoperiod, physiological plasticity, plum, seasonal changes, waterlogging adaptation

INTRODUCTION

Climate change are causing seasonal changes in air temperatures and local rainfall distribution, and more frequent extreme precipitations events can occur (IPCC, 2014). These events are mainly concentrated in spring and late summer and they damage the ecosystem conservation and agricultural production, affected by soil waterlogging (Alpert et al., 2002; McFarlane and Williamson, 2002; Kijne, 2006). The gas emission from the soil due to water excess, coupled with the low availability of oxygen (hypoxia) and/or complete O_2 depletion in the rhizosphere, generate inhospitable condition of flooding, and cause the reduction in growth and crop productivity for a wide range of plants (Wang and Jiang, 2007; Arbona et al., 2008; Voesenek and Bailey-Serres, 2013). Without oxygen, plants shift in few hours from aerobic to anaerobic respiration undergoing ethanol fermentation, it regenerates NAD^+ via alcohol dehydrogenase (ADH), meanwhile the ATP yield is strongly reduced (Bailey-Serres and Voesenek, 2008). Under anaerobic respiration the anoxic cell could increase its rate of glycolysis to equate the energy levels of aerobic cells (Greenway and Gibbs, 2003). Flooding stress, a few days after its onset, is frequently accompanied by a reduction and/or complete blockage of photosynthesis and gas exchanges, thus reducing carbohydrate-availability to roots or other storage plant organs (Núñez-Elisea et al., 1999; García-Sánchez et al., 2007). Long-term exposure to flooding also induces a decline in leaf and stem water content causing accumulation of leaf carbohydrate, epinasty, leaf desiccation with premature senescence and abscission (Kozlowski, 1997; McLeod et al., 1999; Pezeshki, 2001). These events are preceded by chlorophyll damage due to the impairment of Photosystem II (PSII) and light harvesting complexes (LHCII), with the consequent formation of oxidant compounds, which in turn damage cellular components, lipids and proteins, resulting in a decrease in ATP and NADPH production especially in the chloroplast, necessary for carbon fixation reactions (Cai and Xu, 2002; Mauchamp and Méthy, 2004).

Plants perceive the flooding stress differently, showing intensity, timing and duration peculiar for each species; tolerance involves the activation of physiological complexes, metabolic pathways and molecular networks (Bailey-Serres and Voesenek, 2008; Pucciariello et al., 2014; Rubio-Cabetas et al., 2018; Zhu et al., 2018). The set of various morphological and physiological adaptations confers flood tolerance to woody plants. Major adaptations include the induction of adventitious roots to compensate the decay of portions of the original root system, the formation of lenticels and aerenchyma tissues in roots and stems to facilitate O_2 and CO_2 movement (Kozlowski and Pallardy, 2002).

Temperate trees subject to flood are simultaneously exposed to other environmental conditions, such as the seasonal variation of temperature and photoperiod. Trees enter a state of dormancy during the process of vernalization and this allows them to overcome the adverse winter condition, through adaptive mechanisms that protect flower buds (Preston and Sandve, 2013). Therefore, besides being an important trait for plant adaptation, vernalization has also a great agronomical importance (Iqbal et al., 2007). Dormancy or quiescence in perennial plants is controlled by temperature and daylength (photoperiod) seasonal changes (Campoy et al., 2011). Although the photoperiod is a reliable and predictable environmental cue at middle and higher latitudes, however, its role in the onset of dormancy in some Rosaceae species is strongly debated (Heide and Prestrud, 2005; Cooke et al., 2012). For *Prunus* species, vernalization starts from mid-July and lasts throughout the summer; it is stimulated by day-shortening, frequently coupled with the first reduction of temperatures, that trigger to arrest the aerial plant growth, and to set terminal bud as well as wintering cold acclimation processes (Looney and Jackson, 2011). In recent years, researchers highlighted some molecular mechanisms regulating the wintering processes, suggesting that photoperiod enables plants to program for periodic future events (Bouché et al., 2017). Photoperiod, through the circadian rhythm depending on an internal clock system, synchronizes the internal rhythm with the environment, a crucial aspect for plant adaption to adverse conditions (Seo and Más, 2015). Investigations have been undertaken to understand the cross talk between the circadian clock and abiotic stresses (e.g., drought, cold, heat, osmotic) in the *Arabidopsis* model plant (Grundy et al., 2015) and in trees, and on the relationship existing between circadian clock and bud dormancy induced by cold (Artlip et al., 2013; Lloret et al., 2018). However, there are no known reports on the relationship with prolonged submergence during off-season waterlogging. Through dormancy, woody plants become tolerant to the adverse environmental conditions of autumn and winter, like waterlogging due to rainfalls. So far, literature is scarce on cross-talk between the regulatory signaling of photoperiod and plant flooding response; the accepted results deal with plant-water relationship and stomatal conductance as influenced by flooding stress imposed at the beginning and at the end of the photoperiod (Dell'Amico et al., 2001; Else et al., 2009).

Abbreviations: A_{CO2}, net CO_2 assimilation rate; Ci, intercellular CO_2 concentration; CP constant photoperiod; E, leaf transpiration rate; *gs*, stomatal conductance; LWUE, leaf water-use efficiency; NP, natural photoperiod.

Prunus species are reported to be intolerant to flooded conditions and it has been observed that they decline or die under excessive waterlogging (Ranney, 1994; Rubio-Cabetas et al., 2011; Amador et al., 2012; Pistelli et al., 2012; Almada et al., 2013; Rubio-Cabetas et al., 2018). This research aims to establish whether the adaptive response to long-term flooding is linked to a photoperiodic regulatory system of plant phenology in the wild type (*WT*) of rootstock Mr.S. 2/5 of *P. cerasifera* and in two variants, with divergent tolerance (Pistelli et al., 2012). In other words, whether the different adaption behaviors observed among the genotypes should be also associated to mutations in the photoperiodic responses of plants generating circadian entrainment to the natural light-dark cycle across seasons.

MATERIALS AND METHODS

Plant Materials and Experimental Stress Conditions

Five months old plantlets of the Mr.S.2/5 *WT* (*P. cerasifera* Ehrh), *S.1* (minus variant) and *S.4* (plus variant) genotypes (Muleo et al., 2006) were acclimatized in a greenhouse to *extra-vitro* conditions at University of Tuscia (DAFNE-department, at the latitude of 42° 42′N), and cultured in pots containing 1 L of soil composed of 45% clay, 45% sand and 10% silt.

To evaluate photoperiod-mediated response to flooding, 20 days after the summer solstice, the plants (approximately 15 cm long) were randomly divided into two groups: 40 plants of each clone were grown under Natural Photoperiod condition (NP) and other 40 potted plants of each clone were grown under Constant Photoperiod condition (CP), and maintained until October, after the soil waterlogging experiments. The trials were repeated in 2015 and 2016 for 2 years consecutive tests. CP was obtained by keeping the time of lighting similar to summer solstice (16:8 h light:dark). It was provided by fluorescent lamps (TLD18W/33 cool-white fluorescent tubes), emitting 6 μmol m^{-2} s^{-1} measured just above the height of the plants, and turned on before dusk. During the summer, the plants were exposed to a maximum PAR (LI-170; LICOR Inc., Lincoln, NE) of 1500 μmol m^2 s^{-1}. Average day/night temperature was 26°/18,6°C, and the daily cycle of relative humidity ranged between 35 and 95% during the summer period. Plants were regularly ferti-irrigated three times a week with 100 mL of half-strength Hoagland's solution.

In mid-September, the 40 plants of each genotype grown under each photoperiod were randomly divided into two groups. Twenty uniform plants were exposed to complete soil submersion for 28 days by placing them in large plastic containers (90 cm × 60 cm × 25cm) in a randomized pattern, filled 3 cm above the soil surface with tap water. The other 20 plants were kept under well-drained soil (normoxic plants) and watered every day. The flooding stress experiment was performed in 2 years consecutive tests. The experimental pattern was a 3 × 2 × 2 factorial of plant genotypes (3) × photoperiod (2) × stress (2, control and flooding), with 16 replicate plants completely randomized in each treatment. The flooding experiments were carried out in a greenhouse at a daily cycle of relative humidity between 40 and 100%, at the day/night average temperature of 22.1°/17.6°C and daily vapor pressure deficit of 4–10.2 kPa and at a maximum photosynthetic active radiation of 1240 μmol m^{-2} s^{-1}. During the experiment, oxygen depletion measurements were periodically recorded with a portable dissolved oxygen meter (Hanna Instruments, Lansing, MI, United States) inserted into the soil at 5 cm depth. The diffusion of O_2 in the soil of non-flooded plants was always constant (903.3 ± 40.4 ppm).

Plant Growth and Morphological Adaptation

In all the trials, the plants height, from the soil surface to the top of the apical bud, and the amount of phytomers, were measured the day before the soil submersion treatments (Day 0) and at the end of the photoperiod treatment and flooding test (28th day). Abscised and/or dried leaves were evaluated on Days 0, 7, 14, 21, 28 of the soil waterlogging experiments. Leaf and root morphology, and hydration status were also monitored at the end of the test. The dry weight of leaf and root samples was obtained by oven-drying plant material at 70°C to a constant weight.

Leaf Gas Exchange

Gas exchange parameters were measured in the 1st and 4th healthy, full expanded mature leaves, when available, during the 2016 test period. Measurements were conducted at the 7th and 14th day, because the *S.1*- and *WT*-plants up to that period retained the physiological activity on most of the surface of leaf lamina. Leaf measurements of net CO_2 assimilation (A_{CO2}, μmol m^{-2} s^{-1}), stomatal conductance (*gs*, mmol H_2O m^{-2} s^{-1}), intercellular CO_2 concentration (C_i, μmol m^{-2} s^{-1}) and transpiration rate (E, mmol H_2O m^{-2} s^{-1}), were performed at the end of the experiment using a portable infrared gas analyzer with a leaf chamber (LI-6400XT, LI-COR Inc., United States), with a 0.25 l cuvette. The LICOR-6200 was equipped with an external light source (Model QB1205LI-670, Quantum Devices Inc. Barneveld, WI, United States) to maintain a constant PAR of 600 μmol m^{-2} s^{-1} during measurements. All measurements were carried out in the morning from 8 to 10 a.m. to avoid high temperatures, on five plants per clone and per treatment. During all measurements, leaf temperature was 26 ± 1°C and leaf-to-leaf-to-air vapor pressure difference was 2.4 ± 0.4 kPa within the cuvette.

Chlorophyll Determination

Chlorophylls were determined in leaves of each genotype at the end of trials (28th day) from two diameter leaf discs (Ø 0.6 cm), sampled from the mid-lamina area of the intervene zone. Chlorophyll *a* and *b* were extracted and quantified according to Moran (1982).

TTC Reactivity Test

The triphenyltetrazolium chloride (TTC) reactivity test was used to measure tissue vitality and respiratory activity of leaves and roots. Analyses were carried out on 100 mg of

fresh tissues, using the same protocol as described in Pistelli et al. (2012). The reactivity of the samples with TTC was measured as absorption of triphenyl formazan per g dry mass (A_{520} g D.W.$^{-1}$).

Soluble Sugars Analysis

Extraction and quantification of soluble sugars (sorbitol, sucrose, glucose, and fructose) were performed by sampling fully expanded leaves and roots of plants from all genotypes. Measurements have been conducted at 14th day in control and flooded-plants. The amounts of glucose, fructose and sucrose were then determined using a coupled enzymatic assay method (Pistelli et al., 2012). The efficiency of the methods was tested using known amounts of carbohydrate (glucose) as standards. Sorbitol determination was carried out using spectrophotometric analysis using La Roche Kit, monitoring the formazan formation at 492 nm (Bergmeyer et al., 1974). Carbohydrate concentrations were expressed in units of mg g^{-1} DW.

ADH Determination and Total Protein Determination

Root samples (at 0, 21st, and 28th day of treatment) were gently washed in water, and the main root apex (the last 3 cm from the tip) was cut with a razor blade and rapidly frozen in liquid nitrogen. Protein extraction and ADH activity were carried out as already described (Pistelli et al., 2012). Total protein contents were determined according to the method of Bradford (1976) by using bovine serum albumin (BSA) as standard.

Statistical Analysis

The data were subject to variance analysis by using a three-way ANOVA test, performed by the SigmaStat 3.1 package (SYSTAT software Inc., Chicago, IL, United States). Effects of clones, photoperiod and stress treatment on leaf gas exchange, chlorophyll amount and TTC activity were evaluated. When treatment interaction terms were significant ($P < 0.05$), treatment means were separated using Tukey's multiple range test. The statistical samples for leaf gas exchange, chlorophyll amount and TTC activity included five plants, while for the other biochemical parameters three biological independent repeats were used. Percentage data before the ANOVA test were transformed in arcsin values before analysis in order to homogenize the variance and the data shown in the results were back-transformed. Differences were accepted as statistically significant when $P < 0.05$. PCA (principal component analysis) and MDA (Multigroup Discriminant Analysis) factorial discriminant analysis were carried out on morpho-physiological traits and carbohydrates accumulation. MDA and PCA allowed us to discriminate among genotypes under anoxia and photoperiod the changes of the morpho-biochemical traits in response to the stress. All analyses were performed in JMP 4.0 statistical software package (SAS Institute Inc., Cary, NC, United States).

RESULTS

Anoxic Status

The hypoxic condition during the flooding treatment has been determined by the diffusion of O_2 in the soil. In the soil of normoxic exposed plants, the values were always constant (932.4 $\pm$ 50.3 ppm), while in the waterlogged soil the O_2 decreased rapidly. After 3 days the values ranged from 236.7 to 264.8 ppm and after the sixth day in the waterlogged soil anoxic conditions the O_2 level in the waterlogging soil was maintained in the range of 10.5–29 ppm.

Plant Growth and Morphological Response

Plants kept under natural photoperiod (NP) have ceased to grow and set the terminal bud immediately after the middle of July; meanwhile, the plants kept under CP exhibited stem elongation (**Figures 1A,B**, **2A**) and development of new phytomers (**Figures 1C,D**, **2A**), in the 2 years consecutive tests that were performed. When exposed to prolonged waterlogging, from 10th of September, plants blocked their growth, except for the plants of *S.4* (**Figure 1**). This genotype lost the basal leaves but developed sprouts and suckers from the lateral buds and root systems (**Figure 2M**).

At the end of the flooding period, the leaves of *S.1*-stressed plants were almost lost and/or had a visible loss of vitality (**Figures 2B,C**). The most important effect under prolonged flooding stress is the typically induction of an intense leaf epinasty, that became particularly evident after the second week of stress in *WT* plants, and in *S.1* plants since the first week of stress under CP. Extending the stress, the browning increased in the leaf area and the whole organ dried (**Figures 2E,F**). As a consequence, a higher percentage of epinasty in the leaves with or without consequent dropping of foliage, occurred in these plants at the end of flooding treatment (**Figure 3**). *WT*-plants showed a reduced response compared to that of *S.1*-plants, i.e., yellowing of the leaves after the initial days of stress treatment (**Figures 2G–I**, 3). Apical leaves of *WT* and *S.1* genotypes did not grow properly and at 14th day, they appeared greatly stressed with a dried large region in *S.1* (**Figure 2D**) or partially browning of the leaf edge in *WT* (**Figure 2G**).

The effect of photoperiod and its interaction with the genotype become particularly evident when comparing the percentages of dropped and dried leaves during flooding period under CP and NP conditions. CP-plants of *S.1* showed an early stress damage, with withered leaves and strong epinasty since 7th day of stress (**Figure 3**). At 14th day of flooding NP-plants of both *WT* and S.1 genotypes had a lower percentage of dropped leaves compared to CP-plants (40 vs. 70 and 20 vs. 40%, respectively). On the other hand, at 28 days of flooding, *S.4*-plants showed a better fitness under stress (**Figures 2J–L**), with absence of epinasty, lack of yellowing and browning and reduced dieback and dropping leaves (**Figure 3**). Although S.4-plantsunder CP showed an increment of percentage of abscised leaves compared to that under NP (35 vs. 10%, respectively), the percentage of abscised leaves was lower than *WT* and *S.1*-plants (85 and 100%,

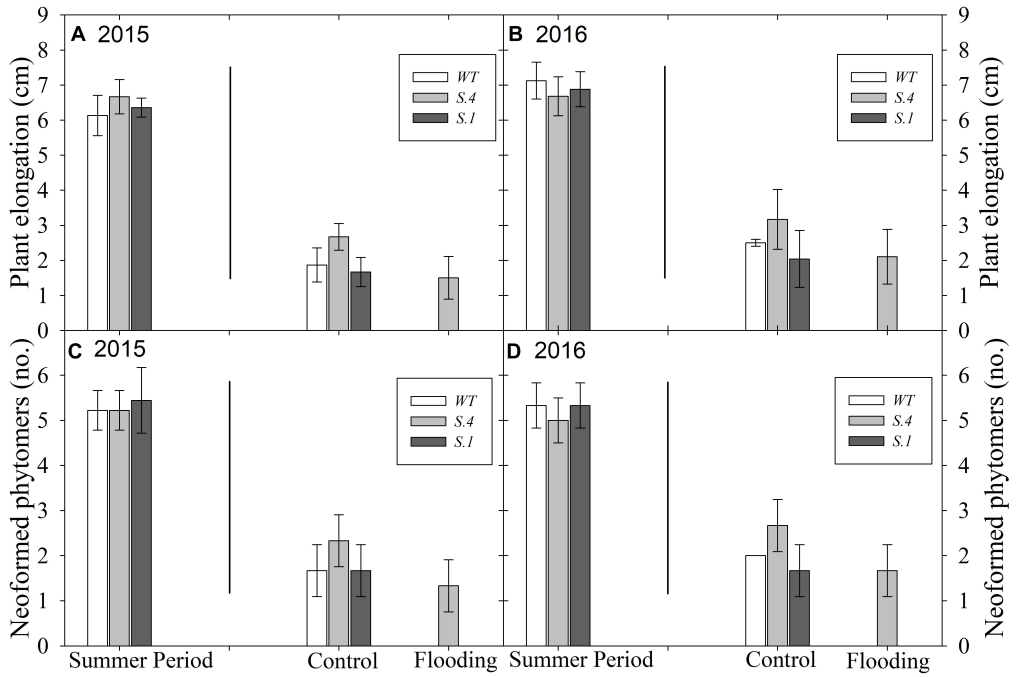

FIGURE 1 | Plant growth and development under Constant Photoperiod (CP) performed in 2 years consecutive tests. In **(A,B)** is shown the plant growth detected as stem elongation; in **(C,D)** is shown the development of new laterals buds (phytomers). Lines inside the graphics separate, on the left, the plant behavior under CP starting from 10th day of July until the beginning of flooding treatment, and on the right, the plant behavior under flooding treatment starting from the 10th day of September. All data were detected at the end of waterlogging treatment (n = 5 biological replicate samples, ± SD).

respectively). Adventitious roots only developed from the flooded *S.4*-plants under a condition of CP, and an average of 3.2 roots per plant was detected (data not shown).

Chlorophyll Content

The chlorophyll content was detected in adult expanded leaves located near the apex (**Figure 4**). The amount of total chlorophyll (per cm^2 of leaf area) was lower in all the genotypes under CP for the 2 years tests, even if it wasn't statistically different from NP (**Figure 4** and **Table 1**). A similar trend has been identified during flooding conditions, although only the genotype per flooding interaction was significant (e.g., under flooding the total chlorophyll content differed among genotypes) (**Figure 4**). The amount of total chlorophylls was lower in *WT* and *S.1*-plants in both experimental years regardless of the photoperiod. This change was due to the reduction in the synthesis and accumulation of chlorophyll *a*, since the chlorophyll *b* was only slightly reduced in *WT* and *S.1*-plants, but it was increased in *S.4*-plants, independently of the photoperiodic regime (**Table 1**). Therefore, the *a*/*b* chlorophyll ratio tends to decrease under flooding conditions but the observed decrease due to the photoperiod was not significant.

Energetic Adaptation, ADH and Respiratory Activity

The ADH activity of the roots was similar among the three genotypes under NP conditions, after 21 days of flooding (**Figure 5A**). At the CP where the photoperiod regime was like mid-July, ADH activity differed among genotypes: the roots of *WT* and *S.4* plants showed a higher ADH activity than those of *S.1* plants after 21 days of flooding (**Figure 5B**). These values were higher than the ones detected on the same day under NP, except for those of the *S.1* plants. On day 28, regardless of the photoperiod, ADH activity increased significantly in the roots of *S.1* plants, reaching 16-fold higher values than those detected on day 21 under NP (**Figure 5A**). Also, ADH activity increased more than twofold in the roots of *S.4*-plants under NP, while it remained constant or slightly decreased in *WT*-plants (**Figure 5A**). At the 28th day under CP conditions, *WT* and *S.4* plants retained a similar or slightly decreased of ADH activity than that determined at 21 days of root waterlogging, unlike the *S.1* genotype where it increased by 4.5-fold (**Figure 5B**).

The TTC (triphenyltetraziolum chloride) test was used to establish the respiratory activity in leaves and roots during flooding under the two photoperiods. The photoperiod regime did not affect the respiratory activity and any statistical difference has resulted from the ANOVA analysis in the 2 years consecutive tests, and analogous reproducible results have also been detected. In the leaves of flood-stressed plants, TTC activity decreased in all clones (**Figures 6A,B**). In the *S.4* plants, the decline in activity of 31% was less substantial, compared to that of the plants of the other two genotypes, where the decline was of around 56 and 60% in *WT* and *S.1* plants, respectively, for both photoperiods (**Figures 6A,B**). The total decrease in TTC activity detected in the roots was lower than leaves, and the decline

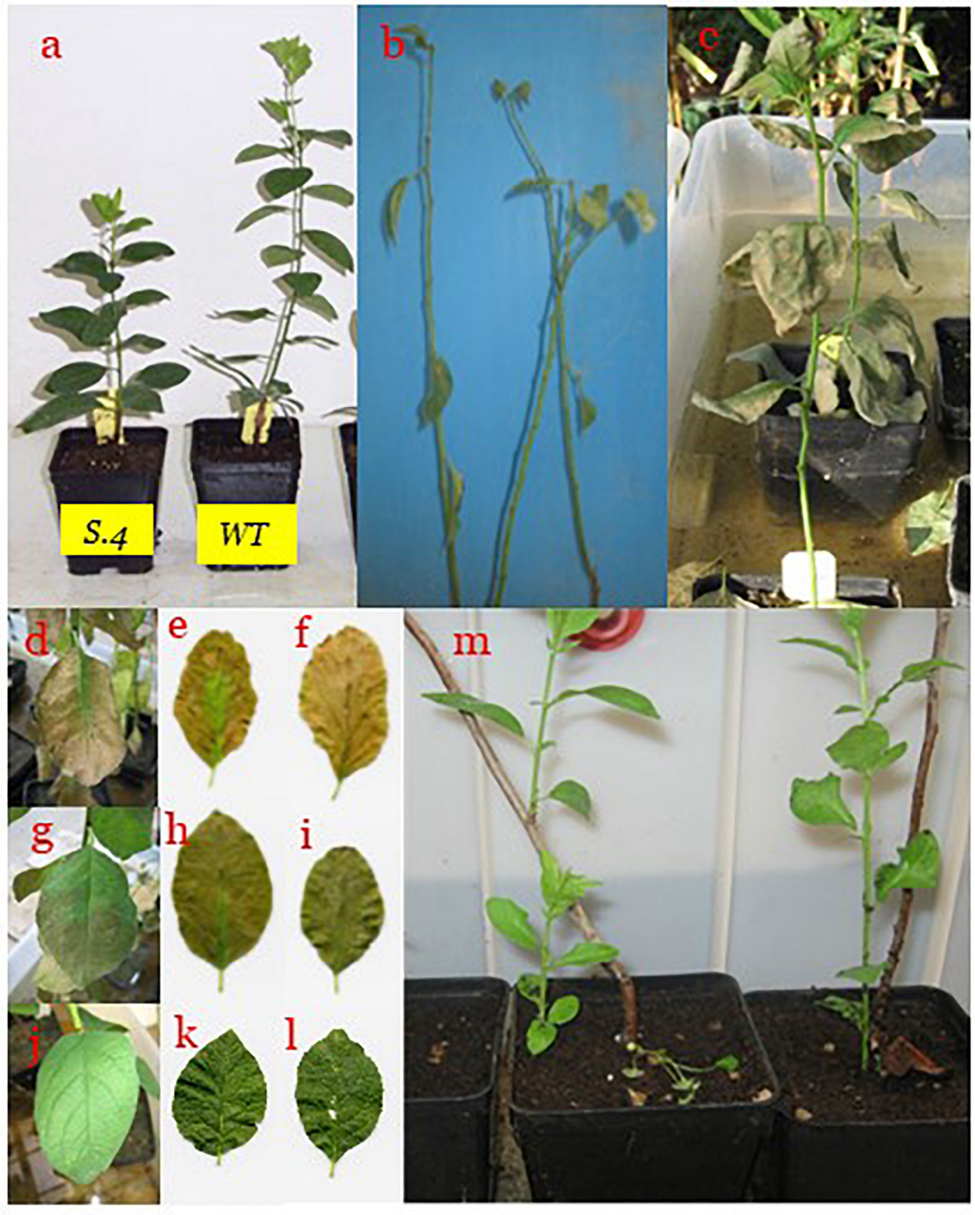

FIGURE 2 | Plant behavior during treatments. Re-growth of apical bud **(A)** in *S.4* and *WT* plants exposed to the constant photoperiod (CP) since the mid-July under normoxic conditions. *S.1*-plants behaviors at the end of flooding period (28 days) exposed to CP **(B)** and to NP **(C)**. State of leaf detected during flooding (14th, 21st, 28th day) in *S.1* **(D–F)**, *WT* **(G–I),** and *S.4* **(J–L),** respectively. *S.4*-stressed plants exposed to CP showed loss of basal leaves, development of sprouts and suckers from lateral buds and root systems **(M),** respectively.

was more significant in the *WT* and *S.1* plants, regardless of the exposure to a photoperiod regime (**Figures 6C,D**). The *S.4* genotype confirmed the better ability to withstand the electron transport chain compared to the other clones.

Gas Exchange Parameters

Gas exchange parameters were detected on the 1st apical fully expanded leaves from the stem apex, throughout the flooding experiments. While the 4th healthy fully expanded leaves, of both the *S.1* and *WT* genotypes were completely dried or were greatly damaged after the 14th day of flooding (**Figures 2D,G**), therefore, from that moment onwards, gas exchange detection was only carried out on the 1st leaf of each genotype, and on the 4th leaf only in *S.4* plants. Variance-analysis between photoperiod, genotype and time of flooding showed no significant interaction for all the parameters of gas exchange, as detected in the 1st leaf (**Table 2**).

During flooding, photosynthesis (A_{CO2}) detected in the 1st leaf significantly decreased on the 14 day in *WT* and *S.1* plants, in contrast to *S.4* plants (**Table 2** and **Supplementary Figure S1**),

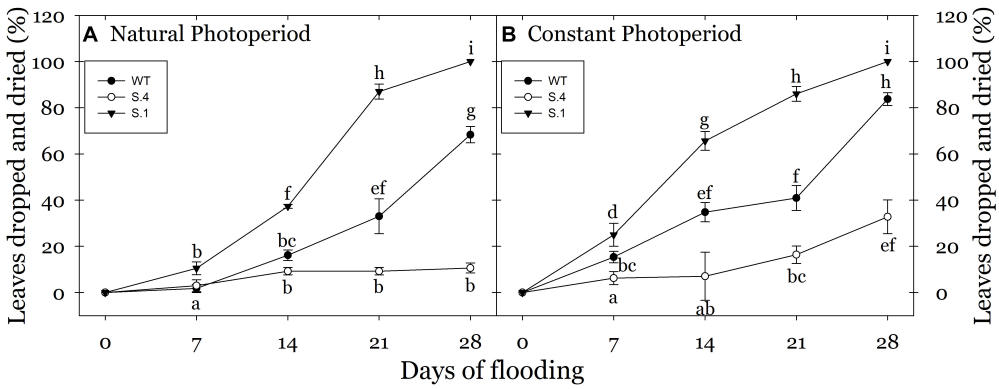

FIGURE 3 | Percentage of leaves (dried or dropped) detected in plant during the flooding stress grown under NP **(A)** and CP **(B).** No abscission events have been detected in plant grown under normoxic condition (n = 5 biological replicate samples, ± SD). Different letters indicate statistical significance for $P < 0.001$. In the case of low value of SD, the bar is covered by the symbol.

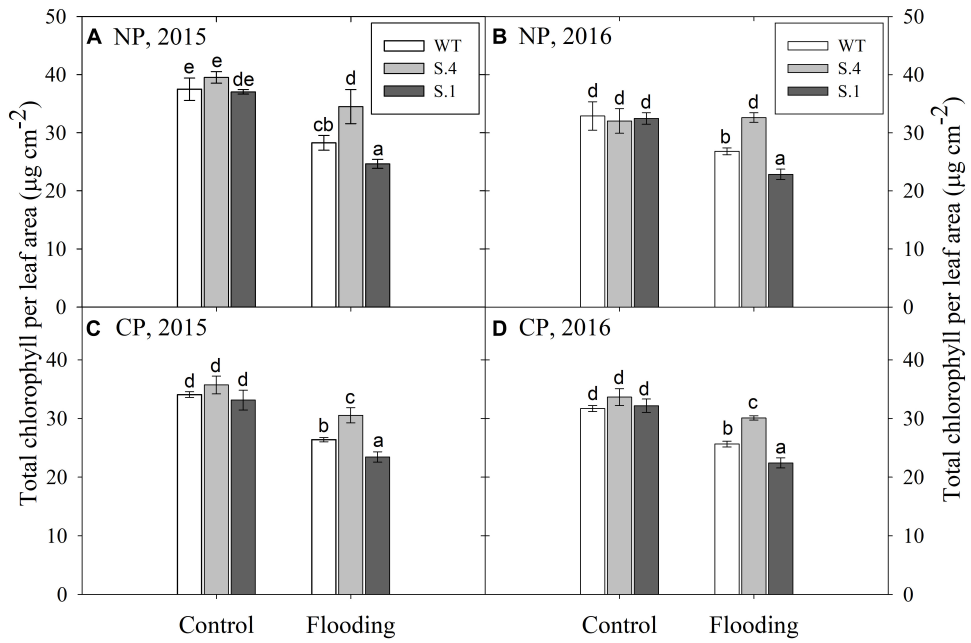

FIGURE 4 | Total chlorophyll content detected on adult expanded leaves at the end of flooding experiments (28th) in plant grown under NP **(A,B)** and CP **(C,D)**, for 2 years consecutive tests. Histograms represent the average of five biological replication and the bars ± S.D. Different letters within the same year indicate statistical significance for $P < 0.001$.

irrespective of photoperiod. The A_{CO2} values had a 40–50% drop in the *S.1* and *WT* 1st leaf and at the 14th days of flooding, irrespective of photoperiod, whereas in *S.4* the reduction was around 14–16%. The photosynthetic capacity was also related to leaf position, resulting higher in the 4th leaf of *S.4* than in the other two genotypes at the 14th days of flooding, and was fairly constant throughout the stress, albeit the observation of a partial reduction (**Table 2** and **Supplementary Figure S1**). Stomatal conductance (*gs*) in plants undergoing the flooding stress, detected in the leaves of both *S.1* and *WT* plants was higher in NP than CP (**Table 2** and **Supplementary Figure S2**). In *S.4* plants, on the other hand, *gs* values, overall, resulted generally higher for those under CP. However, the values were lower than those detected in leaves of the other two genotypes, thus indicating a partial closure of the stomata (**Table 2**). Only the interaction between Genotype and Photoperiod was statistically significant (**Table 2** and **Supplementary Materials**). Sub-stomatal CO_2 concentration (Ci), measured in the 1st leaf under flooding stress, increased at the 14th day irrespective of genotype (**Table 2** and **Supplementary Figure S3**), whereas it decreased under CP reaching its lowest value in *S.4*-plants. A significant interaction between Genotype and Photoperiod resulted from the ANOVA test (**Table 2**), pointing out that under CP Ci was lower in *WT* and *S.1* plants than under

TABLE 1 | Level (μg cm^{-2}) of chlorophyll *a*, *b,* and *a/b* ratio in control, flooded-stressed Mr.S. 2/5-*WT*, and *S.1* and *S.4* plants at the end of the flooding experiment.

Main factors		Chlorophyll *a*	Chlorophyll *b*	a/b ratio
Genotype	*WT*	20.50 b	8.75 a	2.36 b
	S.4	21.29 c	10.80 b	2.01 a
	S.1	18.50 a	8.98 a	2.06 a
Photoperiod	NP	20.55 b	9.38	2.22
	CP	19.64 a	9.63	2.07
Treatment	Control	22.75 b	9.72	2.38 b
	Flooding	17.44 a	9.29	1.90 a
Interaction				
	WT × NP × Control	23.69 de	9.18	2.66
	NP × Flooding	18.21 b	8.60	2.12
	CP × Control	22.66 cde	9.03	2.52
	CP × Flooding	17.46 b	8.18	2.14
	S.4 × NP × Control	22.40 cd	9.63	2.36
	NP × Flooding	21.81 c	10.79	2.03
	CP × Control	22.47 cd	11.16	2.04
	CP × Flooding	18.48 b	11.61	1.60
	S.1 × NP × Control	22.33 cd	10.13	2.23
	NP × Flooding	14.87 a	7.97	1.90
	CP × Control	22.97 de	9.20	2.50
	CP × Flooding	13.83 a	8.59	1.62
Genotype (1)		***	***	**
Photoperiod (2)		***	ns	ns
Treatment (3)		***	ns	***
	1 × 2	*	ns	ns
	1 × 3	***	ns	ns
	2 × 3	***	ns	ns
	1 × 2 × 3	**	ns	ns

*To simplify, only the results of 2016 are reported, since a similar trend in the 2-years tests was observed. Within each column, means followed by the same letters are not significantly different at P < 0.05. *P < 0.05; **P < 0.01; ***P < 0.001.*

NP (**Supplementary Figure S3**). The 4th leaves of the *S.1* and *WT* plants showed a similar behavior to Ci, i.e., it slightly increased during flooding, while in the *S.4* leaves it retained similar values on both photoperiodic conditions and during the flooding (**Supplementary Figure S3**). The leaf transpiration rate (E) decreased under flooding stress, and although photoperiod was not significant, the lowest values were detected in *S.1* plants under CP (**Table 2**). ANOVA highlighted an interaction between Genotype and Photoperiod significantly higher (**Table 2** and **Supplementary Figure S4**) in *S.1* and *WT* plants and was like LWUE which, during flooding stress, decreased more under NP than under CP, whereas it kept generally stable in *S.4* plants (**Table 2** and **Supplementary Figure S5**). The *S.4* 4th leaves behaved like the one of the other genotypes, while the 1st leaves maintained a significant value of LWUE. This can be explained by an active metabolism still working during stress.

Soluble Sugars

There was a statistically significant interaction between the main factors (Genotype, Photoperiod, and Flooding) for glucose, fructose, and sucrose detected in the leaves, whereas no significant interaction was shown for the accumulation of sorbitol (**Table 3A**). The behavior of each genotype was similar when exposed to the two photoperiodic regimes under normoxic condition, the highest amount of sugars was detected in leaves of plants grown under NP, except for sucrose and sorbitol detected in the leaves of *WT*-plants. In contrast, the photoperiod regime has a not negligible effects in plants exposed to flooding stress (**Table 3A**).

Irrespective of the genotype, the quantity of the carbohydrates analyzed was basically higher in leaves of CP plants subjected to flooding (**Table 3**). Noteworthy, the amount of glucose and fructose in the *S.1* leaves, under normoxic conditions, was higher in NP than CP, and this sugars accumulation behavior during the exposure to flooding stress was increased (**Table 3A**). An analogous trend was observed for the quantity of carbohydrates detected in *WT* leaves, except for sucrose and sorbitol; in fact, in flooded plants exposed to CP the amount of the sugars decreased (**Table 3A**). In the leaves of *S.4* plants, the amount of glucose, fructose, and sorbitol did not statistically differed, instead, irrespective of the photoperiod regime the amount of sorbitol increased under flooding stress (**Table 3A**).

The factorial analysis shows a statistically significant interaction between the main factors (Genotype, Photoperiod, and Flooding) for the accumulation of sucrose and sorbitol in root tissues, while no significant interaction resulted from glucose and fructose accumulation (**Table 3B**). In the *S.4*-roots a major accumulation of all analyzed carbohydrates was detected, differently from the other genotypes (**Table 3B**). Under normoxic conditions, the accumulation of carbohydrates was highest in the *S.4*-root grown under NP; conversely, under anoxic conditions the accumulation of carbohydrates resulted highest in CP roots, except for glucose. Even in *WT* roots, under normoxic conditions, the accumulation of carbohydrates resulted highest in the roots of plant grown under NP, except for sucrose (although not significant) (**Table 3B**). In the roots of flooded-plants the accumulation of carbohydrates was markedly reduced in CP plants, where the values were halved, except for sorbitol. In the *S.1*-roots there were detected the lowest values of carbohydrate-accumulation, irrespective of photoperiodic and stress conditions (**Table 3B**).

Principal Component Analysis

Principal component analysis carried out on the data for all the analyzed set of parameters identified two synthetic variables, that explain 64.2% of the variability, with component1 (PC1) accounting for 51.0%, and component2 (PC2) for 13.2%. The PCA scatter-plot split the samples into three main groups. The position of the samples summarizes the phenotypic variability of *Prunus* genotypes in the response to Flooding stress, which is the main factor that affect the separation on PC1 (**Supplementary Figure S6A**). The separation induced by this factor didn't occur at the same extent inside of each genotype. All *S.4*-plant samples were grouped in the lower right quadrant, characterized by the improved tolerance, photosynthetic performance even at the 4th leaf, and high energy activity in leaf and root. Inside the other two genotypes the PC1 synthetic variable contributed to a strong clustering of the normoxic plants from the anoxic

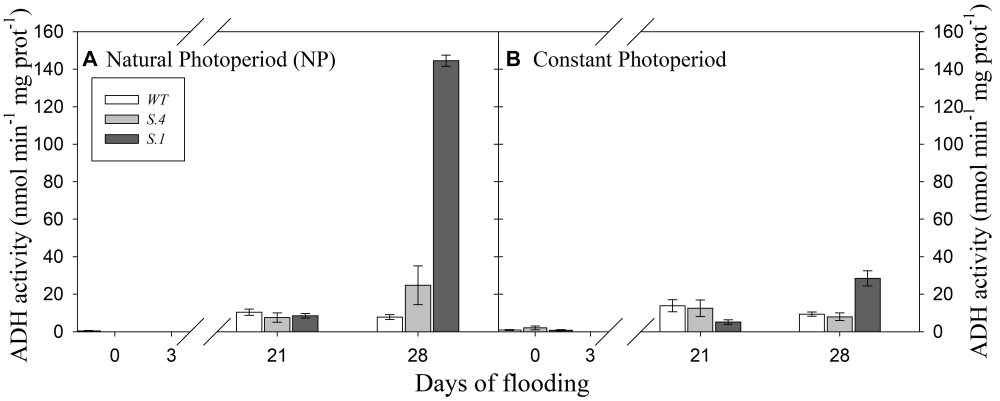

FIGURE 5 | Alcohol dehydrogenase (ADH) activity detected in the roots of the genotypes during flooding under NP **(A)** and CP **(B).** Activity was determined as nmol min^{-1} mg $protein^{-1}$. Histograms represent the mean of three biological repeats ($N = 3$), ± SD. Differences were accepted as statistically significant when $P < 0.05$.

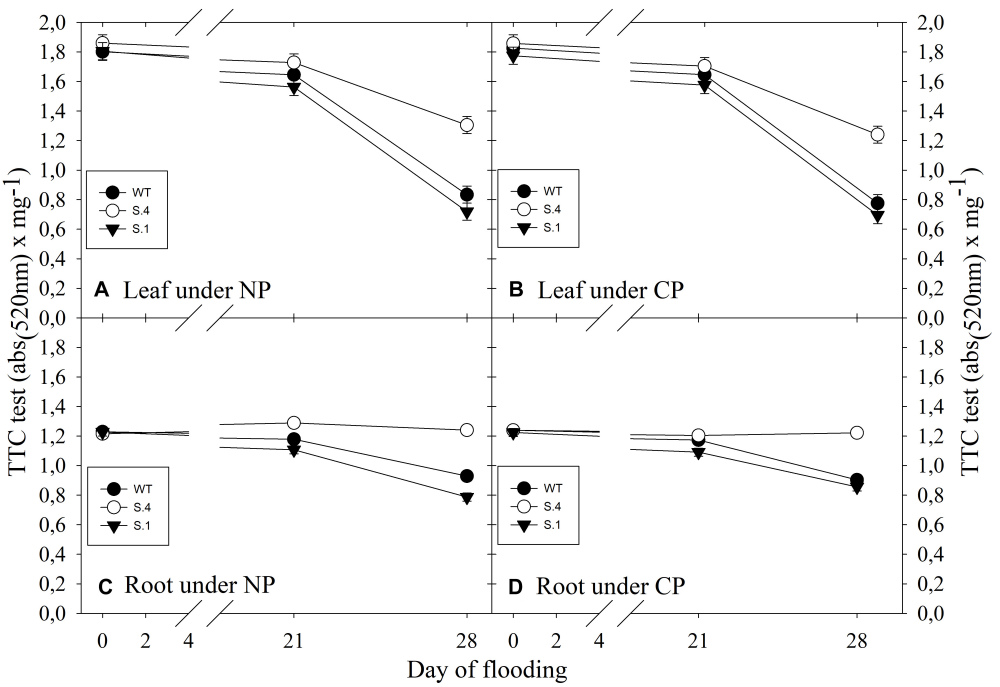

FIGURE 6 | Respiratory activity (as TTC reactivity) detected in the leaf **(A,B)** and in the root **(C,D)** during flooding trials. Symbols represent the average of five biological replicate samples and bars represent ± SD. In the case of very low value of SD the bar is covered by the symbol.

plants. The photoperiod factor contributed to separation on PC2 (**Supplementary Figure S6A**), with different extent among the genotypes, high pronounced in *S.1* genotype, less pronounced in *WT* genotype and almost absent in *S.4* genotype.

An exhaustive view of the morphological, physiological and carbohydrates accumulation and partitioning in leaf and root of plants of the three genotypes in response to flooding stress under photoperiodic conditioning was obtained through principal component analysis (PCA), as reported in **Supplementary Figure 6B**. PC1 was positively correlated to CHLA, CHL-tot, FW, and DW leaf area, TTC leaf and Root, Drop-leaf, and many of the photosynthetic parameters of the 1st and the 4th leaf. PC1 was also negatively correlated to glucose (GL) and fructose (FR) accumulation in the leaf. PC2 was positively correlated to GL-Root, SU-leaf, GL-leaf, and FR-leaf, CHL-ratio, gs-leaf1, Ci-leaf1, and E-leaf1. Moreover, PC2 was negatively correlated with WUE-leaf1. The most informative variables (loadings $> | 0.3|$) were leaf gas exchange parameters, followed by drop leaf, TTC activity and chlorophylls content. Among the carbohydrates glucose and fructose resulted informative, suggesting that the gas exchange, energy activity and glucose and fructose accumulations are more involved in adaption to a

TABLE 2 | Gas exchange parameters measured at 0, 7th, and 14th days from the beginning of flooding stress for plant of the three genotypes grown under NP and CP, detected during the 2016 test.

		First fully expanded leaf				
Main factors		**A**	***gs***	**Ci**	**E**	**LWUE**
Genotype	*WT*	4.55 a	0.121 b	269.0 b	2.406 b	1.898
	S.4	5.49 b	0.099 a	239.5 a	2.076 ab	2.742
	S.1	4.44 a	0.098 a	249.8 ab	1.988 a	2.420
Photoperiod	NP	4.77	0.112 b	261.4 b	2.259	2.225
	CP	4.89	0.096 a	244.1 a	2.051	2.482
Flooding Time	0	5.64 c	0.107	238.0 a	2.303 b	2.561
	7	4.96 b	0.110	252.7 ab	2.234 b	2.297
	14	3.89 a	0.102	267.6 b	1.919 a	2.203
Interaction						
	WT × NP × 0	5.60	0.140	266.7	2.803	1.998
	NP × 7	4.88	0.150	274.7	2.820	1.778
	NP × 14	3.30	0.126	297.0	2.213	1.490
	CP × 0	5.69	0.107	241.7	2.513	2.282
	CP × 7	4.92	0.102	241.7	2.870	2.165
	CP × 14	2.93	0.102	292.3	1.800	1.677
	S.4 × NP × 0	5.64	0.082	222.0	1.750	3.230
	NP × 7	5.27	0.105	254.3	2.113	2.508
	NP × 14	4.86	0.085	230.3	1.677	3.091
	CP × 0	6.28	0.125	242.7	2.650	2.465
	CP × 7	5.60	0.097	236.7	2.250	2.497
	CP × 14	5.27	0.102	251.0	1.990	2.662
	S.1 × NP × 0	5.06	0.120	262.0	2.423	2.160
	NP × 7	4.60	0.115	258.7	2.247	2.062
	NP × 14	3.74	0.124	287.3	2.287	1.708
	CP × 0	5.56	0.068	193.0	1.737	3.29
	CP × 7	4.49	0.091	250.3	1.690	2.771
	CP × 14	3.21	0.073	247.3	1.547	2.588
Genotype (1)		***	**	**	*	***
Photoperiod (2)		ns	***	*	ns	ns
Flooding Time (3)		***	ns	**	*	ns
	1 × 2	ns	***	*	***	**
	1 × 3	**	ns	ns	ns	ns
	2 × 3	ns	ns	ns	ns	ns
	1 × 2 × 3	ns	ns	ns	ns	ns

*The factorial analysis was run on Net photosynthesis (A_{CO2}), stomatal conductance (gs), sub-stomatal CO_2 concentration (Ci), transpiration rate (E), and Leaf Water Use Efficiency (LWUE, A_{CO2}/gs). Within each column, means followed by the same letters are not significantly different at $P < 0.05$. *$P < 0.05$; **$P < 0.01$; ***$P < 0.001$.*

waterlogged environment of the *S.4* genotypes (**Supplementary Figure 6B**).

DISCUSSION

Investigation on rainfall variations has been carried out several times in both Northern and Southern hemispheres, focusing on the Mediterranean environments, and considering different parameters such as total precipitations, intensity, temporal repetition, etc. (Alpert et al., 2002; Homar et al., 2010; Trenberth, 2011; Arnone et al., 2013; IPCC, 2014). The extent and the variation of extreme environmental changes affect the functioning of agroecosystems. Crop production, food security and stability depend on the impact of these changes on the previous conditions and on the plasticity of crop plants to adapt to new environmental scenarios. Therefore, the central goal of the agricultural industry is to reach the security and stability of food available for human-consumption (Dhankher and Foyer, 2018).

In temperate and higher latitude countries, persistent flooding usually occurs in autumn, concomitantly with the physiological and biochemical events triggered by vernalization process which could also have evolved for plant survival against anoxic soil condition. To cope with the seasonal change of environmental conditions, perennial woody plants have evolved a "memory" to keep themselves synchronized and activating appropriate adaptive strategies. Photoperiod is one of the main seasonal cues perceived by plant that indicate the change of seasons

TABLE 3 | (A) Carbohydrates detected in leaves of *S.1*, *S.4,* and *WT* plants, exposed to natural photoperiod (NP) and constant photoperiod (CP) after 14 days of flooding.

Main factors		Leaves			
		Glucose	**Fructose**	**Sucrose**	**Sorbitol**
Genotype	*WT*	0.919 b	0.445 b	2.201 b	2.329 a
	S.4	0.215 a	0.144 a	1.527 ab	2.076 a
	S.1	1.131 c	0.862 c	1.114 a	3.673 b
Photoperiod	NP	1.077 b	0.685 b	1.874	3.080 b
	CP	0.433 a	0.282 a	1.354	2.306 a
Treatment	Control	0.580 a	0.345 a	1.513	2.607
	Flooding	0.930 b	0.622 b	1.716	2.779
Interaction					
WT × NP × Control		0.901 bc	0.339 b	1.338 a	2.226
NP × Flooding		1.653 d	0.985 d	3.301 c	2.401
CP × Control		0.354 ab	0.195 ab	2.869 c	2.523
CP × Flooding		0.768 b	0.262 ab	1.298 a	2.167
S.4 × NP × Control		0.314 a	0.174 ab	1.667 b	1.975
NP × Flooding		0.194 a	0.169 ab	1.436 ab	2.470
CP × Control		0.192 a	0.099 a	1.479 ab	1.802
CP × Flooding		0.161 a	0.135 a	1.527 ab	2.058
S.1 × NP × Control		1.123 c	0.692 c	1.156 a	4.303
NP × Flooding		2.277 e	1.755 e	2.349 bc	5.107
CP × Control		0.597 b	0.574 c	0.567 a	2.813
CP × Flooding		0.528 ab	0.427 bc	0.384 a	2.472
Genotype (1)		***	***	*	***
Photoperiod (2)		***	***	Ns	***
Treatment (3)		***	***	Ns	ns
1 × 2		***	***	Ns	***
1 × 3		***	***	Ns	ns
2 x3		***	***	**	ns
1 × 2 x3		***	***	*	ns

*Values represent the average of each carbohydrate, expressed as mg for gram of dry weight, as detected in three biological samples. Different letters indicate statistically difference among the column of each factor and interaction. Within each column, means followed by the same letters are not significantly different at $P < 0.05$. *$P < 0.05$; **$P < 0.01$; ***$P < 0.001$.*

in each location. Photoperiodic signals regulate the synchrony or asynchrony of plant phenology and the adaptation to the functionally related environmental cues (Kobayashi and Weigel, 2007; Hänninen and Tanino, 2011).

In this study, the possible connections between the photoperiodic signal perceived by plants and the adaptive response to flooding stress have been explored in somaclonal variants of *P. cerasifera* with divergent ability to tolerate waterlogging. *Prunus* are considered a flood-sensitive species (Domingo et al., 2002; Amador et al., 2012; Almada et al., 2013; Rubio-Cabetas et al., 2018) because few days of hypoxia and/or anoxia lead to a strong reduction in the growth and production, compromising plant survival under prolonged exposure. Other than *WT* genotype, two previously characterized somaclonal mutants were included in the experimental design: *S.1* and *S.4* having a lower and higher tolerance compared to *WT*, respectively (Pistelli et al., 2012; Iacona et al., 2013).

The extension of daylight hours number (constant photoperiod, CP) was able to block the signal induced by the seasonal changes, allowing to extend the growth period in late summer and autumn, when *Prunus* spp. usually arrest aerial growth. As ascertained by gas exchanges measures, light intensity was below the compensation point but efficient to maintain long day photoperiodic signal. Under CP conditions, plants of the three clones escape growth cessation and continued to differentiate new phytomers compared to those exposed to normal photoperiod (NP). The longer the waterlogging period, the higher the sensitivity to anoxic conditions in the *WT* and *S.1* genotypes grown in CP, as supported by the higher percentage of leaves abscission and desiccation. In contrast, the photoperiod modification only slightly affects the flooding-tolerant *S.4* clone, which showed an increase of leaves abscission only after a prolonged period of exposure to waterlogging conditions. Flooded *S.4* plants continued to grow, developing new shoots and suckers as well as roots from stems, that increased root conductivity, as it was previously reported (Pistelli et al., 2012). These features indicated that the *S.4* genotype has acquired a tolerance to flooding stress regardless of the photoperiod. In previous experiments performed during July, whole plants generated from a graft combination between cv Suncrest peach

TABLE 3 | (B) Carbohydrates detected in roots (b) of *S.1*, *S.4,* and *WT* plants, exposed to natural photoperiod (NP) and constant photoperiod (CP) after 14 days of flooding.

Main factors		Roots			
		Glucose	Fructose	Sucrose	Sorbitol
Genotype	*WT*	6.920 b	4.173 b	6.586 b	6.033 b
	S.4	7.097 b	5.590 a	10.020 c	7.170 c
	S.1	1.430 a	1.538 b	1.829 a	2.007 a
Photoperiod	NP	6.249 b	4.122 b	6.048	5.410 b
	CP	4.049 a	3.412 a	6.243	4.730 a
Treatment	Control	6.245 b	4.346 b	6.367	5.708 b
	Flooding	4.053 a	3.188 a	5.924	4.432 a
Interaction					
WT × NP × Control		10.610	5.659	5.823 bc	7.680 f
NP × Flooding		8.336	4.661	8.562 d	5.47 cd
CP × Control		5.720	4.036	7.539 cd	7.205 ef
CP × Flooding		3.017	2.335	4.420 b	4.199 c
S.4 × NP × Control		10.300	6.626	12.050 e	8.937 g
NP × Flooding		5.320	4.671	6.098 c	6.363 e
CP × Control		8.055	6.031	8.409 d	5.518 de
CP × Flooding		4.175	5.032	13.530 f	7.864 fg
S.1 × NP × Control		1.639	1.984	2.363*a*	2.724 b
NP × Flooding		1.293	1.130	1.398 a	1.709 g
CP × Control		1.149	1.740	2.024 a	2.187 fg
CP × Flooding		1.641	1.299	1.531 a	1.408 g
Genotype (1)		***	***	***	***
Photoperiod (2)		***	**	ns	**
Treatment (3)		***	***	ns	***
1 × 2		***	**	***	ns
1 × 3		***	ns	ns	****
2 × 3		ns	ns	**	**
1 × 2 × 3		ns	ns	***	***

*Values represent the average of each carbohydrate, expressed as mg for gram of dry weight, as detected in three biological samples. Different letters indicate statistically difference among the column of each factor and interaction. *P < 0.05; **P < 0.01; ***P < 0.001.*

and *S.4* (rootstock) underwent 21 days of flooding, and strong tolerance to anoxia resulted compared to the *WT* and minus variant genotype *S.1* (Iacona et al., 2013). In our study, *WT* and *S.1* plants under NP showed symptoms of stress later than the plants under CP, as flooding persisted. Essentially, leaves undergo edge necrosis, wilt and abscission very rapidly under CP, i.e., plants were not able to activate any efficient strategy to counteract anoxia. Conversely, plants were somehow able to oppose the damages induced by anoxia under NP. These results may suggest a decreasing plants ability of adapting to stress occurring in an asynchronous period (e.g., during summer), while they are potentially capable of responding to stress during a synchronous period (late summer and/or fall) (Pistelli et al., 2012; Iacona et al., 2013).

Apart from morphological evidences, other metabolic and physiological parameters were analyzed, in order to collect more information about adaptation mechanisms and photoperiod effects. A_{CO2} of leaves was not affected by the photoperiod, although the interaction between genotypes and time of waterlogging resulted significant. The decline in A_{CO2} of flooded-leaves was observed in both sensitive and tolerant genotypes and was clearly associated with the increase in Ci in both the *S.1* and *WT* genotype. The increase in Ci due to the reduction in A_{CO2} causes stomatal closure, with a consequent decrease in gs, in agreement with previous reports (Pérez-Jiménez et al., 2017, 2018). The increase of Ci concomitant with a decrease in chlorophyll in *S.1* and *WT* plants compared to normoxic plants, indicates that non-stomatal factors may play a prevalent role in the limitation of A_{CO2} compared to stomatal conductance. In citrus, the limitation of A_{CO2} in flood-stressed plants was not associated to non-stomatal factors, such as chlorophyll degradation and chlorophyll fluorescence, that were more determinant than stomatal limitation on A_{CO2} (García-Sánchez et al., 2007). The leaves of the *S.4* flooded-plants retained their functions under stress conditions, indicating that this genotype allowed an active metabolism with a good photosynthetic activity. The observed slight reduction in A_{CO2} detected in flooded-leaves was not accompanied by any significant variation in Ci, and *gs* remained largely constant. Moreover, no difference in gas exchange parameters was detected under the two photoperiods.

Total chlorophylls content resulted lower in all genotypes under CP. The decrease of chlorophyll *a* in *S.4* plants is less prominent than in the other genotypes, especially under NP. Moreover, a significant interaction was detected for its content among photoperiod, genotype and flooding. Instead, chlorophyll *b* increased in *S.4* flooded leaves and decreased in the corresponding leaves of *WT* and *S.1*. These data indicate that the photosystems were better preserved in *S.4* genotype as it is reported for tolerant species, counteracting the decrease in the efficiency of the harvested light energy generated by the damage in the photosystems (Mauchamp and Méthy, 2004; Gururani et al., 2015). This justifies the higher capability of the *S.4* leaves to retain a photosynthetic activity even in the 4th leaf (**Supplementary Material**) under a condition of anoxia, regardless of photoperiod. Essentially, under anoxic flooding stress the inhibition of photosynthesis can take place by either a reduction in the photosynthetic activity due to protective mechanisms, or by photoinhibition (Mauchamp and Méthy, 2004; Fernández, 2006).

The *S.4* plants under anoxic conditions, despite photoperiod, kept a sufficiently efficient metabolism throughout the flooding period, and although it may be reduced after 28 days of stress, they produced energy and maintained a higher respiratory activity than the other two genotypes both in the leaves and in the roots. Although carbohydrate-availability in the leaves and in the roots of the *S.4* flooded-plants was reduced, the total chlorophyll content underwent a slight reduction, however, the TTC activity never dropped below 60% of the initial value. The high TTC levels observed in the roots can be attributed to the slight loss in the oxygen supply, since active metabolism might still have occurred.

An efficient use of carbohydrates and their accumulation within plant organs especially to the root tissues is indeed a crucial factor for preserving cell functionality during flooding stress (Parent et al., 2008). The maintenance of carbohydrate reserves and capacity to metabolize them to sustain ATP levels at anoxic conditions is preserved in flood-tolerant tree, along with the avoidance of toxic compounds accumulation that could damage the membrane integrity (Kozlowski and Pallardy, 2002; Parent et al., 2008). The sugar content showed a significant difference among the genotypes. Independently from photoperiod, *S.4* showed a functional leaf with a preserved photosynthetic activity, and the lower levels of sugars, except for sorbitol, are probably linked to the capacity to translocate the sugars from the leaves to the roots (Noiraud et al., 2001; Centritto, 2005). The higher content of sorbitol detected in leaves of flooding-exposed plants could be associated to the double role of sorbitol, as main load transported sugar, e.g., in the roots, and as an agent for the osmoregulation of the leaf under abiotic stress (Lo Bianco et al., 2000; Centritto, 2005). In a previous work, a high level of expression of sorbitol transporter-1 gene (*SOT1*) had been detected in both leaf and root tissues in plants subjected to anoxia (Pistelli et al., 2012), indicating an active role in translocation of this sugar to counteract the stress. It is recognized that plants under prolonged flooding are subjected to starvation and that the leaves retain non-structural carbohydrates to hinder the progress of oxidative stress, therefore they are accumulated in the tissues and not translocated (Tamang and Fukao, 2015). The sugar-content in the leaves of the *WT* and *S.1* genotypes confirm this scenario in flooded-plants under NP. Under CP, higher amounts of sugars in the anoxic-leaves were found only in the *WT*-genotype, while in the anoxic-leaves of the *S.1*-genotype, the amount was equal to or lower than normoxic leaves, even for sorbitol. These results confirm once again that the *S.1* genotype is very anoxic-sensitive, and this behavior is worsened by an extended photoperiod. The reduced amount of sugars found in the anoxic-roots of the *S.1* genotype compared to that of the other two genotypes, indicates that under prolonged flooding conditions the *S.1* roots undergo to degeneration of the tissues, as it was previously reported (Pistelli et al., 2012).

It is understood that the anaerobic condition of roots alters plant growth and respiration, and ADH activity plays a key role in producing ATP (Geigenberger, 2003; Kreuzwieser et al., 2004). ADH activity in *WT* and *S.4* genotypes showed a similar behavior with perpetuated flooding under both NP and CP, confirming the previous study performed during early summer (Pistelli et al., 2012). If during the summer period (and/or CP) this increase can be linked to a tolerance, already expressed at the beginning of flooding (Toro et al., 2018), under NP this behavior could be attributed to the seasonal change linked to the process of vernalization, i.e., plants subject to vernalization could acquire a tolerance to flooding. On the other hand, *S.1* plants showed different and very high level of ADH with the prolonged flooding, more prominent in NP rather than in CP. This big increase could be due to the leakage in the roots, and great fermentation processes, and it is supported by the recent observation on other root respiration components of the *Prunus* rootstock (Toro et al., 2018), where long term flooding tolerance depends on the responses induced in the short term hypoxia: *S.1* is always sensitive to flooding, confirming its minus variant status (Pistelli et al., 2012).

In this paper we have focused our attention on carbohydrates, although other compounds play a role in the regulation of abiotic stress and can be involved in the flooding stress. Protective molecules as proline, but also glycine-betaine, can be produced and accumulated for the osmotic adjustment during salinity and/or drought stress, as well as GABA shunt can contribute to the dissipation of energy excess and CO_2 release, and support the electron transport chain where ROS could increase (Carillo, 2018; Annunziata et al., 2019). Further research on the involvement of these compounds in the flooding tolerance could lead to an improvement of the knowledge of this mechanism. Furthermore, the redox state is also important to maintain a balance between energy production and consumption, and during several abiotic stress this equilibrium is affected by the production of oxidative compounds (Suzuki et al., 2012). Reactive oxygen species (ROS) are common compounds of several abiotic stress, leading to damage of membrane integrity and alteration of chloroplast electron chain (Suzuki et al., 2012). The production of secondary metabolites, as antioxidant compounds (polyphenols and others) are considered good scavenging products to remove ROS. In our previous paper (Pistelli et al., 2012) these secondary metabolites were determined, and their contribution of flooding tolerance has been already discussed.

Recent studies (Alfieri et al., 2015) aimed at evaluating climate projections using the EURO CORDEX RCP8.5 scenarios, show a positive trend for the maximum daily precipitations in most European countries by the end of the century. Furthermore, a significant increase in the frequency of extreme events larger than 100% is predicted for the period 2006-2035 in 21 out of 37 European countries with a worsening in the following period until 2095. Changes in intensity and persistence of flooding and drought occur significantly during the summer all over the European region, with Central Mediterranean and Central/Western Europe particularly vulnerable to these phenomenon (Pal et al., 2004). The moisture holding capacity of the atmosphere due to the climate change, in fact, can increase the strength of the precipitation and the occurrence of flood events (Trenberth et al., 2003).

Phenotypical plasticity is required to counteract the new occurring scenario where extreme daily rainfall will become frequent. Therefore, rather than resistant crop plants the new agronomic contest require plants with an evolved plasticity that shift from submergence to the de-submergence without undergoing physiological stress. This happens only if plants will be not constrained by the regulatory cross-talk related with daily-length seasonal change (photoperiod).

To our knowledge, this is the first report addressing the relationship between photoperiod (seasonal changes) and adaptive plant response to flooding. Results indicate that *S.4* genotype is tolerant to flooding regardless of photoperiodic regime, while *S.1* and *WT* genotypes are less sensitive or tolerant under NP respect to CP, when natural daylight becomes shorter (September-October) and vernalization process has been already started. Although an interaction with photoperiod appear evident at morphological level, metabolic and physiological analyses does not depict a clear framework. The molecular and physiological cross-talk that may exist between these two plant biological processes should not be considered unreal, since recent papers have shown that photoperiod and circadian rhythm play a key role in the adaptive responses to stresses in *Arabidopsis* and in some trees (Artlip et al., 2013; Grundy et al., 2015; Lloret et al., 2018). This cross-talk must be completely explored, and the *S.4* and *S.1* genotypes studied, that share an identical genetic background with the *WT*, provide an interesting study material to contribute for deciphering the signaling elements of the regulatory networks governing the dialogue itself. The *S.4* genotype has an increased tolerance that appears possibly to be independent from photoperiod, while the *S.1* genotype has an increased susceptibility to anoxia. A comprehensive understanding on how adaptive responses to flooding stress are linked to photoperiod is pre-requisite for the development of adapted genotypes to the environmental anoxic fluctuations. Furthermore, understanding the regulation of the adaptation to extreme flooding conditions under the climate changes may suggest cultural practices to ameliorate their negative impact.

AUTHOR CONTRIBUTIONS

RMu, CI, and LP developed the concept and with RMa and MR wrote the manuscript. CI, MC, and LG performed eco-physiological analysis, collected, and analyzed meteorological data. LP performed sugar and ADH analysis and quantification. RMa and MR discussed climate changes. LG, MC, and RMa performed statistical analyses. All authors discussed and commented on the manuscript.

FUNDING

This study was supported by the grant from "Fondazione Anna Maria Catalano – ONLUS," Italy, and by MIUR (Minister for Education, University and Research, Law 232/2016, Department of Excellence). The funders had no role in study design, data collection and analysis, decision to publish, or preparation of the manuscript.

ACKNOWLEDGMENTS

We wish to thank Dr. Giuliano Dradi, Dr. Romano Roncasaglia, and Dr. Paolo Laghi of Battistini Vivai srl for the accurate propagation of the plants of the rootstock Mr.S 2/5 wild type and its variant genotypes *S.4* and *S.1*.

SUPPLEMENTARY MATERIAL

The Supplementary Material for this article can be found online at: https://www.frontiersin.org/articles/10.3389/fpls.2019.00546/full#supplementary-material

REFERENCES

Alfieri, L., Forzieri, G., and Burek, P. A. (2015). Global warming increases the frequency of river floods in Europe. *Hydrol. Earth Syst. Sci. Discuss.* 19, 2247–2260. doi: 10.5194/hessd-12-1119-2015

Almada, R., Arismendi, M. J., Pimentel, P., Rojas, P., Hinrichsen, P., Pinto, M., et al. (2013). Class 1 non-symbiotic and class 3 truncated hemoglobin-like genes are differentially expressed in stone fruit rootstocks (*Prunus* L.) with different degrees of tolerance to root hypoxia. *Tree Genet. Genomes* 9, 1051–1063. doi: 10.1007/s11295-013-0618-8

Alpert, P., Ben-gai, T., Baharad, A., Benjamini, Y., Yekutieli, D., Colacino, M., et al. (2002). The paradoxical increase of mediterranean extreme daily rainfall in spite of decrease in total values. *Geophys. Res. Lett.* 29:11. doi: 10.1029/2001GL013554

Amador, M. L., Sancho, S., Bielsa, B., Gomez-Aparisi, J., and Rubio-Cabetas, M. J. (2012). Physiological and biochemical parameters controlling waterlogging stress tolerance in *Prunus* before and after drainage. *Physiol. Plant.* 144, 357–368. doi: 10.1111/j.1399-3054.2012.01568.x

Annunziata, M. G., Ciarmiello, L. F., Woodrow, P., Dell'Aversana, E., and Carillo, P. (2019). Spatial and temporal profile of glycine betaine accumulation in plants under abiotic stresses. *Front. Plant Sci.* 10:230. doi: 10.3389/fpls.2019.00230

Arbona, V., Hossain, Z., López-Climent, M. F., Pérez-Clemente, R. M., and Gómez-Cadenas, A. (2008). Antioxidant enzymatic activity is linked to waterlogging stress tolerance in citrus. *Physiol. Plant.* 132, 452–466. doi: 10.1111/j.1399-3054.2007.01029.x

Arnone, E., Pumo, D., Viola, F., Noto, L. V., and La Loggia, G. (2013). Rainfall statistics changes in sicily. *Hydrol. Earth Syst. Sci.* 17, 2449–2458. doi: 10.5194/hess-17-2449-2013

Artlip, T. S., Wisniewski, M. E., Bassett, C. L., and Norelli, J. L. (2013). CBF gene expression in peach leaf and bark tissues is gated by a circadian clock. *Tree Physiol.* 33, 866–877. doi: 10.1093/treephys/tpt056

Bailey-Serres, J., and Voesenek, L. A. (2008). Flooding stress: acclimations and genetic diversity. *Ann. Rev. Plant Biol.* 59, 313–339. doi: 10.1146/annurev.arplant.59.032607.092752

Bergmeyer, H. U., Gruber, W., and Gutmann, I. (1974). "Methoden der enzymatischen Analyse," in *Methods of Enzymatic Analysis*, Vol. 3, ed. H. U. Bergmeyer (New York, NY: Academic Press, Inc), 1323–1330.

Bouché, F., Woods, D. P., and Amasino, R. M. (2017). Winter memory throughout the plant kingdom: different paths to flowering1. *Plant Physiol.* 173, 27–35. doi: 10.1104/pp.16.01322

Bradford, M. M. (1976). A rapid and sensitive method for the quantitation of microgram quantities of protein utilizing the principle of protein-dye binding. *Anal. Biochem.* 72, 248–254. doi: 10.1006/abio.1976.9999

Cai, S. Q., and Xu, D. Q. (2002). Light intensity-dependent reversible downregulation and irreversible damage of PSII in soybean leaves. *Plant Sci.* 163, 847–853. doi: 10.1016/S0168-9452(02)00234-0

Campoy, J. A., Ruiz, D., and Egea, J. (2011). Dormancy in temperate fruit trees in a global warming context: a review. *Sci. Hortic.* 130, 357–372. doi: 10.1016/j.scienta.2011.07.011

Carillo, P. (2018). GABA shunt in durum wheat. *Front. Plant Sci.* 9:100. doi: 10.3389/fpls.2018.00100

Centritto, M. (2005). Photosynthetic limitations and carbon partitioning in cherry in response to water deficit and elevated [CO2]. *Agric. Ecosyst. Environ.* 106, 233–242. doi: 10.1016/j.agee.2004.10.011

Cooke, J. E. K., Eriksson, M. E., and Junttilam, O. (2012). The dynamic nature of bud dormancy in trees: environmental control and molecular mechanisms. *Plant Cell Environ.* 35, 1707–1728. doi: 10.1111/j.1365-3040.2012.02552.x

Dell'Amico, J., Torrecillas, A., Rodríguez, P., Morales, D., and Sánchez-Blanco, M. J. (2001). Differences in the effects of flooding the soil early and late in the photoperiod on the water relations of pot-grown tomato plants. *Plant Sci.* 160, 481–487. doi: 10.1016/s0168-9452(00)00409-x

Dhankher, O. M., and Foyer, C. H. (2018). Climate resilient crops for improving global food security and safety. *Plant Cell Environ.* 41, 877–884. doi: 10.1111/pce.13207

Domingo, R., Pérez-Pastor, A., and Ruiz-Sánchez, M. C. (2002). Physiological responses of apricot plants grafted on two different rootstocks to flooding conditions. *J. Plant Physiol.* 159, 725–732. doi: 10.1078/0176-1617-0670

Else, M. A., Janowiak, F., Atkinson, C. J., and Jackson, M. B. (2009). Root signals and stomatal closure in relation to photosynthesis, chlorophyll a fluorescence and adventitious rooting of flooded tomato plants. *Ann. Bot.* 103, 313–323. doi: 10.1093/aob/mcn208

Fernández, M. D. (2006). Changes in photosynthesis and fluorescence in response to flooding in emerged and submerged leaves of *Pouteria orinocoensis*. *Photosynthetica* 44, 32–38. doi: 10.1007/s11099-005-0155-2

García-Sánchez, F., Syvertsen, J. P., Gimeno, V., Botía, P., and Perez-Perez, J. G. (2007). Responses to flooding and drought stress by two citrus rootstock seedlings with different water-use efficiency. *Physiol. Plant.* 130, 532–542. doi: 10.1111/j.1399-3054.2007.00925.x

Geigenberger, P. (2003). Response of plant metabolism to too little oxygen. *Curr. Opin. Plant Biol.* 6, 223–250.

Greenway, H., and Gibbs, J. (2003). Mechanisms of anoxia tolerance in plants. I. growth, survival and anaerobic catabolism. *Funct. Plant Biol.* 30, 1–47. doi: 10.1071/PP98095_ER

Grundy, J., Stoker, C., and Carré, I. A. (2015). Circadian regulation of abiotic stress tolerance in plants. *Front. Plant Sci.* 6:648. doi: 10.3389/fpls.2015.00648

Gururani, M. A., Venkatesh, J., and Tran, L.-S. P. (2015). Regulation of photosynthesis during abiotic stress induced photoinhibition. *Mol. Plant.* 8, 1304–1320. doi: 10.1016/j.molp.2015.05.005

Hänninen, H., and Tanino, K. (2011). Tree seasonality in a warming climate. *Trends Plant Sci.* 16, 412–416. doi: 10.1016/j.tplants.2011.05.001

Heide, O. M., and Prestrud, A. K. (2005). Low temperature, but not photoperiod, controls growth cessation and dormancy induction and release in apple and pear. *Tree Physiol.* 25, 109–114. doi: 10.1093/treephys/25.1.109

Homar, V., Ramis, C., Romero, R., and Alonso, S. (2010). Recent trends in temperature and precipitation over the Balearic Islands (Spain). *Clim. Change* 98, 199–211. doi: 10.1007/s10584-009-9664-5

Iacona, C., Cirilli, M., Zega, A., Frioni, E., Silvestri, C., and Muleo, R. (2013). A somaclonal myrobalan rootstock increases waterlogging tolerance to peach cultivar in controlled conditions. *Sci. Hortic.* 156, 1–8. doi: 10.1016/j.scienta.2013.03.014

IPCC (2014). *Climate Change 2014: Synthesis Report. Contribution of Working Groups I, II and III to the Fifth Assessment Report of the Intergovernmental Panel on Climate Change*, eds R. K. Pachauri and L. A. Meyer (Geneva: IPCC), 151.

Iqbal, M., Navabi, A., Yang, R.-C., Salmon, D. F., and Spaner, D. (2007). The effect of vernalization genes on earliness and related agronomic traits of spring wheat in northern growing regions. *Crop Sci.* 47, 1031–1039. doi: 10.2135/cropsci2006.09.0618

Kijne, J. W. (2006). Abiotic stress and water scarcity: identifying and resolving conflicts from plant level to global level. *Field Crops Res.* 97, 3–18. doi: 10.1016/j.fcr.2005.08.011

Kobayashi, Y., and Weigel, D. (2007). Move on up, it's time for change - mobile signals controlling photoperiod-dependent flowering. *Genes Dev.* 21, 2371–2384. doi: 10.1101/gad.1589007

Kozlowski, T. T. (1997). *Responses of Woody Plants to Flooding and Salinity. Tree Physiology Monograph No. 1*. Victoria: Heron Publishing.

Kozlowski, T. T., and Pallardy, S. G. (2002). Acclimation and adaptive responses of woody plants to environmental stresses. *Bot. Rev.* 68, 270–334. doi: 10.1663/0006-8101(2002)068%5B0270:aaarow%5D2.0.co;2

Kreuzwieser, J., Papadopoulou, E., and Rennenberg, H. (2004). Interaction of flooding with carbon metabolism of forest trees. *Plant Biol.* 6, 299–306. doi: 10.1055/s-2004-817882

Lloret, A., Badenes, M. L., and Ríos, G. (2018). Modulation of dormancy and growth responses in reproductive buds of temperate trees. *Front. Plant Sci.* 9:1368. doi: 10.3389/fpls.2018.01368

Lo Bianco, R., Rieger, M., and Sung, S.-J. S. (2000). Effect of drought on sorbitol and sucrose metabolism in sinks and sources of peach. *Physiol. Plant.* 108, 71–78. doi: 10.1034/j.1399-3054.2000.108001071.x

Looney, N., and Jackson, D. (2011). "Stone Fruit," in *Temperature and Subtropical Fruit Production*, 3rd Edn, eds D. Jackson, N. E. Looney, and M. Morley-Bunker (Cambridge MA: CABI), 161–180.

Mauchamp, A., and Méthy, M. (2004). Submergence-induced damage of photosynthetic apparatus in *Phragmites australis*. *Environ. Exp. Bot.* 51, 227–235. doi: 10.1016/j.envexpbot.2003.11.002

McFarlane, D. J., and Williamson, D. R. (2002). An overview of waterlogging and salinity in southwestern Australia as related to the "Ucarro" experimental catchment. *Agric. Water Manage.* 53, 5–29. doi: 10.1016/S0378-3774(01)00153-6

McLeod, K. W., McCarron, J. K., and Conner, W. H. (1999). Photosynthesis and water relations of four oak species: impact of flooding and salinity. *Trees* 13, 178–187.

Moran, R. (1982). Formulae for determination of chlorophyllous pigments extracted with N. N-dimethylformamide. *Plant Physiol.* 9, 1376–1381. doi: 10.1104/pp.69.6.1376

Muleo, R., Iacona, C., Pistelli, L., and Loreti, F. (2006). A novel Mr.S.2/5 peach rootstock clone tolerant to flooding stress. *Adv. Hortic. Sci.* 20, 208–214.

Noiraud, N., Maurousset, L., and Lemoine, R. (2001). Transport of polyols in higher plants. *Plant Physiol. Biochem.* 39, 717–728. doi: 10.1016/S0981-9428(01)01292-X

Núñez-Elisea, R., Schaffer, B., Fisher, J. B., Colls, A. M., and Crane, J. H. (1999). Influence of flooding on net CO2 assimilation, growth and stem anatomy of *Annona* species. *Ann. Bot. London* 84, 771–780. doi: 10.1006/anbo.1999.0977

Pal, J. S., Giorgi, F., and Bi, X. (2004). Consistency of recent European summer precipitation trends and extremes with future regional climate projections. *Geophys. Res. Lett.* 31:L13202.

Parent, C., Capelli, N., Berger, A., Crèvecoeur, M., and Dat, J. F. (2008). An overview of plant responses to soil waterlogging. *Plant Stress* 2, 20–27.

Pérez-Jiménez, M., Hernández-Munuera, M., Carmen Piñero, M., López-Ortega, G., and del Amor, F. M. (2018). Are commercial sweet cherry rootstocks adapted to climate change? Short-term waterlogging and CO2 effects on sweet cherry cv. 'Burlat'. *Plant Cell Environ.* 41, 908–918. doi: 10.1111/pce.12920

Pérez-Jiménez, M., Hernández-Munuera, M., Piñero Zapata, M. C., López-Ortega, G., and del Amor, F. M. (2017). Two minuses can make a plus: waterlogging and elevated CO2 interactions in sweet cherry (*Prunus avium*) cultivars. *Physiol. Plant.* 161, 257–272. doi: 10.1111/ppl.12590

Pezeshki, S. R. (2001). Wetland plant responses to soil flooding. *Environ. Exp. Bot.* 46, 299–312. doi: 10.1016/S0098-8472(01)00107-1

Pistelli, L., Iacona, C., Miano, D., Cirilli, M., Colao, M. C., Mensuali-Sodi, A., et al. (2012). Novel Prunus rootstock somaclonal variants with divergent ability to tolerate waterlogging. *Tree Physiol.* 32, 355–368. doi: 10.1093/treephys/tpr135

Preston, J. C., and Sandve, S. R. (2013). Adaptation to seasonality and the winter freeze. *Front. Plant Sci.* 4:167. doi: 10.3389/fpls.2013.00167

Pucciariello, C., Voesenek, L. A. C. J., Perata, P., and Sasidharan, R. (2014). Plant responses to flooding. *Front. Plant Sci.* 5:226. doi: 10.3389/fpls.2014.00226

Ranney, T. G. (1994). Differential tolerance of eleven Prunus taxa to root zone flooding. *J. Environ. Hortic.* 12, 138–141.

Rubio-Cabetas, M. J., Amador, M. L., Gómez-Aparisi, J., Jaime, J., and Sancho, S. (2011). Physiological and biochemical parameters involved in waterlogging stress in *Prunus*. *Acta Hortic.* 903, 1215–1224.

Rubio-Cabetas, M. J., Pons, C., Bielsa, B., Amador, M. L., Marti, C., and Granell, A. (2018). Preformed and induced mechanisms underlie the differential responses of *Prunus* rootstock to hypoxia. *J. Plant Physiol.* 228, 134–149. doi: 10.1016/j.jplph.2018.06.004

Seo, P. J., and Más, P. (2015). STRESSing the role of the plant circadian clock. *Trends Plant Sci.* 20, 230–237. doi: 10.1016/j.tplants.2015.01.001

Suzuki, N., Koussevitzky, S. H., Mittler, R. O. N., and Miller, G. A. D. (2012). ROS and redox signalling in the response of plants to abiotic stress. *Plant Cell Environ.* 35, 259–270. doi: 10.1111/j.1365-3040.2011.02336.x

Tamang, G., and Fukao, T. (2015). Plant adaptation to multiple stresses during submergence and following desubmergence. *Int. J. Mol. Sci.* 16, 30164–30180. doi: 10.3390/ijms161226226

Toro, G., Pinto, M., and Pimentel, P. (2018). Root respiratory components of *Prunus* spp. rootstocks under low oxygen: Regulation of growth, maintenance, and ion uptake respiration. *Sci. Hortic.* 239, 259–268. doi: 10.1016/j.scienta.2018.05.040

Trenberth, K. E. (2011). Changes in precipitation with climate change. *Clim. Res.* 47, 123–138. doi: 10.3354/cr00953

Trenberth, K. E., Dai, A., Rasmussen, R. M., and Parsons, D. B. (2003). The changing character of precipitation. *Bull. Am. Meteorol. Soc.* 84, 1205–1217.

Voesenek, L. A. C. J., and Bailey-Serres, J. (2013). Flooding tolerance: O2 sensing and survival strategies. *Curr. Opin. Plant Biol.* 16, 647–653. doi: 10.1016/j.pbi.2013.06.008

Wang, K., and Jiang, Y. (2007). Waterlogging tolerance of Kentucky bluegrass cultivars. *HortScience* 42, 386–390. doi: 10.21273/hortsci.42.2.386

Zhu, X., Li, X., Jiu, S., Zhang, K., Wang, C., and Fang, J. (2018). Analysis of the regulation networks in grapevine reveals response to waterlogging stress and candidate gene-marker selection for damage severity. *R. Soc. Open Sci.* 5:172253. doi: 10.1098/rsos.172253

Conflict of Interest Statement: The authors declare that the research was conducted in the absence of any commercial or financial relationships that could be construed as a potential conflict of interest.

frontiers in Plant Science

MINI REVIEW
published: 08 May 2019
doi: 10.3389/fpls.2019.00578

Exploring Legume-Rhizobia Symbiotic Models for Waterlogging Tolerance

Chiara Pucciariello[1], Alexandre Boscari[2], Andrea Tagliani[1], Renaud Brouquisse[2] and Pierdomenico Perata[1]*

[1] PlantLab, Institute of Life Sciences, Sant'Anna School of Advanced Studies, Pisa, Italy, [2] Institut Sophia Agrobiotech, Centre National de la Recherche Scientifique, Institut National de la Recherche Agronomique, Université Côte d'Azur, Nice, France

Unexpected and increasingly frequent extreme precipitation events result in soil flooding or waterlogging. Legumes have the capacity to establish a symbiotic relationship with endosymbiotic atmospheric dinitrogen-fixing rhizobia, thus contributing to natural nitrogen soil enrichment and reducing the need for chemical fertilization. The impact of waterlogging on nitrogen fixation and legume productivity needs to be considered for crop improvement. This review focuses on the legumes-rhizobia symbiotic models. We aim to summarize the mechanisms underlying symbiosis establishment, nodule development and functioning under waterlogging. The mechanisms of oxygen sensing of the host plant and symbiotic partner are considered in view of recent scientific advances.

Keywords: hypoxia, legumes, nitric oxide, oxygen sensing, symbiosis, waterlogging

OPEN ACCESS

Edited by:
Iduna Arduini, University of Pisa, Italy

Reviewed by:
Reinhard Turetschek, Independent Researcher, Getzersdorf, Austria
Daniel Roberts, The University of Tennessee, Knoxville, United States

****Correspondence:***
Chiara Pucciariello
chiara.pucciariello@santannapisa.it;
c.pucciariello@sssup.it

Specialty section:
This article was submitted to Plant Abiotic Stress, a section of the journal Frontiers in Plant Science

Received: *03 December 2018*
Accepted: *18 April 2019*
Published: *08 May 2019*

Citation:
Pucciariello C, Boscari A, Tagliani A, Brouquisse R and Perata P (2019) Exploring Legume-Rhizobia Symbiotic Models for Waterlogging Tolerance. Front. Plant Sci. 10:578. doi: 10.3389/fpls.2019.00578

INTRODUCTION

Global population is expected to reach around 9.6 billion in 2050 (Gerland et al., 2014), leading to a rise in the demand for food. Food issues are also aggravated by unexpected and increasingly frequent extreme weather events connected to climate change such as soil flooding or waterlogging, occurring especially in areas close to watercourses, characterized by poor soil drainage or exposure to monsoons.

In agriculture, the conversion to alternative, more ecologically sustainable sources is moving toward productive systems that reduce the input of fertilizers. Nitrogen (N) is one of the most important nutrients for crops and today a reduction in crop dependence on chemical N fertilization is essential. This is due to the cascade of environmental changes resulted from the huge increase of ammonia (NH_3) production in the last century, such as water and soil pollution (Erisman et al., 2008). Legumes are well known for their agronomical and food properties, thanks to their capacity to establish a symbiotic relationship with endosymbiotic atmospheric dinitrogen (N_2)-fixing rhizobia, thus contributing to natural N soil enrichment and reduced need for chemical fertilization. These crops are also a key protein resource for human and animal foods.

In legume plant roots, the interaction with rhizobia leads to the development of the nodule organ, where the nitrogenase enzyme reduces atmospheric N_2 to NH_3 which is afterward transferred to and assimilated by the plant. In parallel, the plant provides steady carbon source to the symbiont and a suitable microenvironment for development (Markmann and Parniske, 2009).

When selecting stress-tolerant legume crops, the impact of soil flooding and waterlogging on N_2 fixation and legume productivity need to be considered. This is particularly important in areas where forage and grain legumes are cultivated on wetlands or temporarily flooded areas. Legume species differ markedly in adaptation to flood-prone areas (Striker and Colmer, 2017). Tolerant legume species are generally able to sustain the oxygen (O_2) diffusion path under waterlogging via physiological adaptation. An increased aerenchyma network in the root and nodule cortex, the presence of a barrier to radial O_2 loss in the outer root tissues and an increased permeability of the nodule O_2 diffusion barrier (ODB) can facilitate tolerance (Striker and Colmer, 2017). Metabolic acclimation and the presence of alternative nodulation strategies are additional adaptation responses to waterlogging (Roberts et al., 2010).

The aim of this mini review is to explore the mechanisms underlying legume plant adaptation, symbiosis development and nodule functioning under waterlogging.

WATERLOGGING EFFECTS ON PLANT-BACTERIA INTERACTION

Effects of Hypoxia on Nodulation

Successful symbiosis involves an initial cross-talk between plants and bacteria, with the coordinated expression of genes from both partners to induce molecular re-programming, which leads to the development of a nodule (Oldroyd and Downie, 2008). Bacteria sense the plant-derived flavonoids of the root exudates and produce nodulation factors (named Nod factors), lipochito-oligosaccharide molecules that participate in bacterial infection and, when perceived by the plant, trigger the nodule's specific developmental program (Dénarié and Cullimore, 1993).

Several studies have considered the waterlogging effect on nodulation capacity. Hypoxia-sensitive legumes, such as pea (Minchin and Pate, 1975), alfalfa (Arrese-Igor et al., 1993), and soybean (Sung, 1993) exhibit reduced nodule weight when grown under hypoxic conditions. *Medicago truncatula* nodulation shows a 45% decrease under 0.1 % O_2 but is not affected by 4.5% O_2 treatment, and the nodule fresh weight per plant is not dampened by 4 weeks of hypoxia (El Msehli et al., 2016). Two studies analyzing nodulation ratings of 21 species of annual pasture legumes and 13 species of perennial legumes (Nichols et al., 2008a,b) report that most legume, including waterlogging sensitive species such as *Melilotus albus* and *Medicago sativa*, showed effective nodulation after several weeks of inundation. In this context, it is unclear whether the nature of nodule types may support different mechanisms of dealing with the stress, considering that indeterminate nodules (*Medicago* spp., *Pisum* spp., and *Melilotus* spp.) are characterized by a persistent meristem and a continuous growth, while determinate nodules (*Glycine* spp, *Vigna* spp, and *Lotus* spp.) are characterized by a not persistent meristem and a limited growth potential.

In flood-tolerant legume species, the nodulation process shows some morphological and physiological adaptations. In *Melilotus siculus*, nodules formed during waterlogging stress have been observed above all on adventitious roots (Konnerup et al., 2018). Under flooding, *Sesbania rostrata*, a tropical legume that grows in temporary flooded habitats (Capoen et al., 2010), switches from a typical root hair curling (RHC) mechanism of nodulation to a lateral root based (LRB) one (D'Haeze et al., 2000; Goormachtig et al., 2004). When grown in aerated soils, *S. rostrata* nodulation occurs through the mechanism of RHC, where bacterial colony is entrapped in growing root hairs that start to curl. When LRB infection occurs, bacteria enter at the base of the adventitious or lateral roots where they form an infection pocket prior to bacteria release into the nodule primordium.

Interestingly, *S. rostrata* LRB nodulation requires ethylene (Goormachtig et al., 2004), whose production is stimulated in plants by flooding and accumulates under water due to a slow diffusion. Ethylene inhibitors blocks *S. rostrata* initiation of nodulation, since bacterial invasion, infection pocket formation and nodule primordia were not observed in hydroponic roots (D'Haeze et al., 2003). Moreover, ethylene is likely involved together with ROS in inducing the programmed cell death of cortical cells, which is necessary for the formation of the infection pocket occurring during crack invasion (D'Haeze et al., 2003).

On the other hand, ethylene accumulation inhibits the RHC invasion of *S. rostrata* (Goormachtig et al., 2004). The application of ethylene biosynthesis inhibitors resulted in an increased RHC nodulation, while the opposite was observed adding ethylene precursors (Goormachtig et al., 2004). Indeed, ethylene inhibits nodulation in several legumes, such as *M. truncatula* (Penmetsa and Cook, 1997) and *Pisum sativum* (Guinel and Sloetjes, 2000).

Effects of Oxygen Availability on Nodule Functioning

Once inside the forming nodule, bacteria differentiate into bacteroids, which can fix N_2 via the activity of nitrogenase enzyme, representing the fundamental reaction of the symbiosis (Roberts et al., 2010). Nitrogenase is inactivated by free O_2, thus N_2 fixation is made possible thanks to the microoxic conditions predominant in the nodules. Furthermore, bacterial genes for nitrogenase assembly are expressed at low O_2 concentration (Soupène et al., 1995). Nodules have evolved adaptations to maintain an inner low O_2 environment, among which the presence of the ODB and by expressing O_2-carrying symbiotic plant hemoglobins (Appleby, 1992; Berger et al., 2018). Thus, the developing nodule shifts from a normoxic state during the formation of the symbiosis to a microoxic one in mature nodules (Witty and Minchin, 1990). As a consequence, nodules are naturally microoxic organs that maintain a low O_2 level, while preserving an active energy production.

The presence of a flexible ODB that regulates the O_2 influx into the infected zone of the nodule was questioned over years. The ODB is likely composed by cortical boundary layers, matrix glycoproteins and endodermis modifications, which depend on the nature of the legume-rhizobia association (Minchin et al., 2008). Early studies on nodule structure identified the absence of a physical barrier in the soybean nodules cortex and the presence of continuous air pathways (Bergersen and Goodchild, 1972; Sprent, 1972). Subsequently, studies on pea and lupine nodules

identified few intercellular spaces in the cortical cell layers and the absence of intercellular space connections within the nodule infected areas (Dixon et al., 1981). Indeed, occlusion in intercellular spaces were observed in the inner cortex of soybean nodule exposed to high O_2 level, suggesting the presence of a flexible mechanism of morphological and structural adaptation (Serraj et al., 1995).

As underground organs, nodules can be exposed to flooding. The adaptation of functioning nodules to waterlogging includes structural and metabolic changes. Several adaptive processes have been described in nodules, including the tight regulation of the ODB flexibility, the development of aerenchyma and the setup of a specific ATP regenerating metabolism under low O_2 level. Hypoxia-tolerant *Lotus uliginosus* nodules under flooding showed a lower concentration of matrix glycoproteins within intercellular spaces of the cortex in comparison with the sensitive species *L. corniculatus* (James and Crawford, 1998). This suggests a hypoxia-dependent mechanism capable to decrease the occlusions under low O_2 availability and finalized to open air pathways when necessary. Recently, nodules of *M. truncatula* exposed to high O_2 concentration showed a tightening of the ODB (Avenhaus et al., 2016). As consequence, the modulation of the O_2 supply to the infected zone may be a key factor of nodule activity regulation. Under high O_2 concentration, after a transient nitrogenase inhibition, the recovery of nitrogenase was observed and attributed to flexible ODB (Hunt et al., 1989; del Castillo et al., 1992; Avenhaus et al., 2016).

A crucial trait for plant survival under waterlogging is the possibility to develop aerenchyma, in order to provide a path for O_2 diffusion along the roots from the aerated organs above (Colmer and Voesenek, 2009). The fact that some forage legumes are sensitive to waterlogging has been attributed to the limited possibility of O_2 flux through aerenchyma to the root nodules (Arrese-Igor et al., 1993; Pugh et al., 1995; Konnerup et al., 2018). Some tolerant legumes have developed an extensive network of aerenchyma tissues, as indicated by the tolerant species phenotype identified in **Table 1**.

Given that N_2 fixation is sensitive to low O_2 condition occurring under flooding, soybean nodules have shown an impaired N_2 fixation activity when transferred to a hydroponic solution (Justino and Sodek, 2013; Souza et al., 2016). Under these conditions, a change in N metabolism (Souza et al., 2016) and in the export of N_2 fixation products in the xylem have been observed (Amarante and Sodek, 2006). In soybean nodules under flooding, a reduction in asparagine an accumulation of γ-aminobutyric acid (GABA) has been detected, which have been suggested to have a temporary storage role (Souza et al., 2016). These changes were reversible during recovery. Under hypoxia, the activation of the alanine metabolism was observed in waterlogging tolerant *L. japonicus* root and nodules, independently of the N status of the plant (Rocha et al., 2010b). Alanine accumulation was also observed in soybean roots under waterlogging (Rocha et al., 2010a). Alanine metabolism may be crucial to prevent pyruvate accumulation in order to facilitate glycolysis during waterlogging (Rocha et al., 2010b).

A further adaptive mechanism is related to the presence of hemoglobin-like proteins in the nodules, recently renamed phytoglobins (Hill et al., 2016). Three types of phytoglobins (phytoglobin1, leghemoglobin, and phytoglobin3) have been characterized in legume nodules (Bustos-Sanmamed et al., 2011; Berger et al., 2018). They are known to buffer O_2 concentration and to scavenge nitric oxide (NO). Hypoxia generates NO in plants, likely with the presence of a cyclic respiration that improves the plant's capacity to tolerate hypoxic stress by maintaining the cell energy status (Igamberdiev and Hill, 2009; Gupta and Igamberdiev, 2011). This phytoglobin-NO respiration (PNR) involves the following phases: nitrate to nitrite reduction via the activity of nitrate reductase; nitrite translocation from the cytosol into the mitochondria; production of NO through the reduction of nitrite at both the cytochrome C oxidase and the alternative oxidase sites of the mitochondrial electron transport chain, which allows ATP regeneration; NO movement from the mitochondrial matrix to the cytosol; and NO oxidation to nitrate by phytoglobins.

Interestingly, functional nodules of *M. truncatula* (Baudouin et al., 2006), *Glycine max* (Meakin et al., 2007), and *L. japonicus* (Shimoda et al., 2009), have been shown to produce NO, and flooding conditions significantly increases NO production in soybean (Meakin et al., 2007; Sánchez et al., 2010), and *M. truncatula* hypoxic nodules (Horchani et al., 2011). In *M. truncatula* nodules, energy status appears to be dependent on the PNR cycle partly under normoxia and totally under hypoxia (Horchani et al., 2011). Thus, the functioning of PNR in microoxic nodules enables the plant to oxidize NADH and to sustain ATP synthesis also under O_2 shortage.

OXYGEN SIGNALING IN PLANT AND BACTERIAL PARTNERS

Oxygen Sensing in the Plant Partner

The Ethylene Responsive Factor group VII family (ERF-VII) guides the response to O_2 level variations to ensure plant survival (Gibbs et al., 2011; Licausi et al., 2011). In *Arabidopsis*, this family is composed of five transcription factors which all possess an N-terminal amino acid (N-degron) and Cys residue in the second position of the protein. ERF-VII proteins are degraded via the N-end rule-dependent proteasome pathway triggered by Plant Cysteine Oxidases (PCOs) in an O_2-dependent manner (Weits et al., 2014; White et al., 2017; **Figure 1A**).

Together with O_2, NO destabilizes ERF-VIIs, and a reduction in the availability of either gasses is sufficient to stabilize them (Gibbs et al., 2014). The discovery of this O_2/NO sensing mechanism has opened up new possibilities for better understanding the plant adaptation to low O_2 and for improving flooding tolerance in crops.

An interesting link has been found between *Arabidopsis* ERF-VIIs and microorganisms. Infection by the obligate biotroph *Plasmodiophora brassicae*, which causes clubroot development (Gravot et al., 2016), was found to involve ERF-VIIs control. Subsequent to the identification of fermentation-related genes induced in infected root galls, the authors suggested that N-end rule-driven hypoxia responses are a general trait of pathogen-induced gall growth (Gravot et al., 2016). In the context of

TABLE 1 | Waterlogging tolerant and sensitive legumes.

Species	Treatment	Phenotype	References
Cicer arietinum, *Vicia faba* (sensitive)	Deoxygenated stagnant solution (7 days)	Death of root tips	Munir et al., 2019
Melilotus siculus accessions (tolerant)	Deoxygenated stagnant solution (7 days)	Root phellem abundance	Striker et al., 2019
Lotus tenuis, *L. tenuis* × *L. corniculatus* (tolerant)	Partial submergence stress (55 days)	Aerenchyma and adventitious root formation	Antonelli et al., 2018
Melilotus siculus (tolerant)	Waterlogging (21 days)	Aerenchymatous phellem in hypocotyl, roots and the outer tissue layers of nodules	Konnerup et al., 2018
Pisum sativum (tolerant accessions)	Waterlogging (4, 8 days)	Successful germination	Zaman et al., 2018
Phaseolus vulgaris (sensitive and tolerant accessions)	Flooding conditions (1, 10 days)	Root weight and germination rate traits associated to flooding tolerance	Soltani et al., 2017
Lens culinaris (sensitive and tolerant genotypes)	Waterlogging (6 days)	Successful germination	Wiraguna et al., 2017
Vicia faba (tolerant), *Pisum sativum* (sensitive), *Lupinus albus* (sensitive)	Waterlogging at flowering (0, 5, 10, 15, 20 days)	Better seed yield and biomass of shoots, roots and nodules in tolerant genotypes	Pampana et al., 2016
Phaseolus coccineus (tolerant)	Flooding (24, 48 hours)	Vascular cavity formation	Takahashi et al., 2016
Pisum sativum, *Lens culinaris* and *Lathyrus sativus* (sensitive and tolerant genotypes)	Waterlogging (14 days)	High root porosity and unaffected shoot nitrogen content in tolerant genotypes	Malik et al., 2015
Melilotus siculus accessions (tolerant)	Hypoxic saline condition (21 days)	Plant ability to regulate ions	Striker et al., 2015
Aeschynomene americana (tolerant)	Waterlogging (30–40 days)	High nitrogenase activity and growth	Tobisa et al., 2014
Lotus japonicus recombinant inbred lines (tolerant)	Waterlogging (21 days)	Aerenchyma formation and high stomatal conductance	Striker et al., 2014
Melilotus siculus (tolerant accessions), *Trifolium michelianum* (sensitive), and *Medicago polymorpha* (sensitive)	Waterlogging combined to salinity (5 days)	High root porosity in tolerant genotypes	Teakle et al., 2012
Melilotus siculus (tolerant)	Stagnant solution (21 days)	Aerenchymatous phellem development	Teakle et al., 2011
Lotus tenuis (tolerant)	Waterlogging (30 days)	Shoot elongation	Manzur et al., 2009
Vigna radiata (tolerant and sensitive genotypes)	Waterlogging (4, 8 days)	Availability of root sugar reserves in tolerant genotypes	Sairam et al., 2009
Lotus spp (tolerant and sensitive genotypes)	Waterlogging (19 weeks)	Aerenchyma and adventitious roots formation in tolerant genotypes	Real et al., 2008
Faba bean, yellow lupin, grass pea, narrow-leafed lupin, chickpea, lentil, field pea (tolerant and sensitive genotypes)	Waterlogging (7 days)	Adventitious root and aerenchyma formation in tolerant genotypes	Solaiman et al., 2007
Lupinus luteus (tolerant), *L. angustifolius* (sensitive) reciprocal- and self-grafted combinations	Waterlogging (14 days)	Tolerance influenced by the root genotype	Davies et al., 2000
Trifolium tomentosum (tolerant) and *T. glomeratum* (sensitive)	Hypoxic solution (7–21 days)	High root porosity in the tolerant genotype	Gibberd et al., 1999

pathogenesis, the resistance to the hemibiotrophic pathogen, *Pseudomonas syringae* pv tomato has been shown to involve ERF-VIIs substrates to regulate pathogen-induced stomatal closure in Arabidopsis (Vicente et al., 2018).

To date, no data are available on the ERF-VIIs role in N_2-fixing symbioses in legumes. In fact, the genome of *M. truncatula* (version Mt4.0[1]) harbors four genes that belong to the ERF-VIIs group (Boscari et al. (2013), personal communication), and phylogenetic analysis revealed the presence of ERF-VIIs in the *G. max* genome (Licausi et al., 2011). These ERF-VIIs harbor the conserved N-terminal degron, which suggests their control by O_2 levels. A previous RNA-Seq analysis of *M. truncatula* during the symbiotic interaction with *Sinorhizobium meliloti* showed that *ERF-VII* genes are expressed in both roots and nodules (Boscari et al., 2013), where they may be crucial under microoxic conditions. ERF-VIIs might be an excellent candidate for deciphering O_2 perception and NO signaling in N_2-fixing symbioses. Indeed, interesting aspects are related to the possible targets of ERF-VIIs in nodule, which may be involved in morphological and metabolic adaptations in the microoxic nodule niche and under environmental hypoxia. In particular, speculation can be done on the possible role of ERF-VIIs on the metabolic modification in order to supply ATP under O_2 scarcity and on the regulation of the ODB flexibility to different O_2

[1]http://www.medicagogenome.org/home

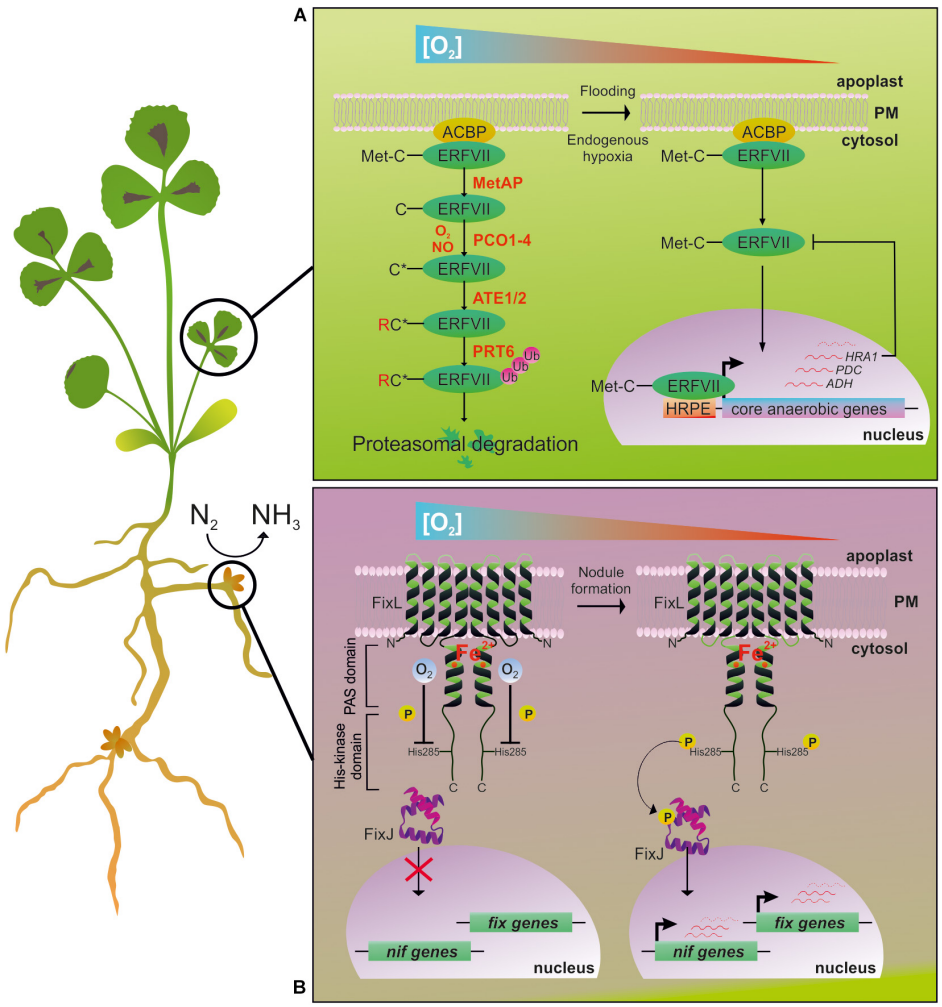

FIGURE 1 | The main O_2-sensing pathways described in plants (identified in *Arabidopsis* and hypothesized to be present in *M. truncatula*) and *S. meliloti* N_2-fixing bacteria. **(A)** In *Arabidopsis*, the Cys branch of the N-end rule pathway for protein degradation allows the O_2-dependent regulation of gene expression (Licausi et al., 2013). ERF-VIIs are a class of transcription factors characterized by a conserved N-termini (N-degron) in which Cys_2 determines the protein's fate in response to O_2 level inside the cell. In aerobic conditions (**left**), ERF-VIIs are unable to activate the transcription of anaerobic genes. In these conditions, Met Aminopeptidase (MetAP) removes the N-terminal Met, and PCOs oxidize the resulting exposed Cys (C*) (Weits et al., 2014; White et al., 2017). After arginylation by Arginyl Transferases (ATE1-2), an Ubiquitin Ligase (PRT6) identifies the proteins as a degradation substrate for the 26S proteasome. Under O_2 deficient conditions (**right**), the efficiency of ERF-VIIs oxidation is dampened, allowing the stabilization and translocation into the nucleus to finally induce a set of anaerobic genes (Kosmacz et al., 2015), with Arabidopsis RAP2.2 and RAP2.12 playing a major role in comparison to the other ERF-VIIs (Bui et al., 2015). This also happens through fine regulation controlled by the Hypoxia Response Attenuator (HRA1), which antagonizes RAP2.12 through a feedback mechanism that enables a flexible response to different levels of O_2 availability (Giuntoli et al., 2014, 2017). The *cis*-regulatory element Hypoxia Responsive Promoter Element (HRPE) has been identified as being enriched in some hypoxia-responsive genes (Gasch et al., 2016). **(B)** FixL-FixJ two-component regulatory system in *S. meliloti* symbiotic bacteria regulates the expression of *nif* and *fix* gene clusters in an O_2-dependent way. In free-living bacteria (**left**), FixL is inhibited by the binding of O_2 to the heme moiety inside the PAS domain. By establishing symbiosis with the plant, nodule formation gives rise to a microoxic environment surrounding the microbial cells (**right**). In turn, FixL is activated by auto-phosphorylation and transfers the phosphoryl group to the FixJ transcriptional activator, thus regulating *nif* and *fix* genes expression.

level. Furthermore, it would be of interest to understand whether ERF-VIIs nodule targets may be involved in plant interaction with bacteria during the infection and the N fixation process.

The FixL-FixJ Bacterial Two Component System

In N_2-fixing rhizobia, the nitrogenase expression needs to be tightly regulated in response to changing O_2 concentrations, due to the fact that O_2 irreversibly inhibits the enzyme activity (Poole and Hill, 1997). The fine-tuning of nitrogenase related genes expression and the compartmentalization of the enzyme inside the nodule are thus prerequisites for an efficient N_2 fixation (Soupène et al., 1995).

The induction of the N_2-fixing gene cluster in *S. meliloti* and other symbiotic bacteria is regulated by a two-component system composed of the O_2-sensing histidine kinase FixL and the response transcriptional regulator FixJ (**Figure 1B**;

De Philip et al., 1990; Bobik et al., 2006). In *S. meliloti*, FixL is a protein composed of four transmembrane helices and a cytoplasmic region comprising a heme-containing Per Arnt Sim (PAS) domain and a C-terminal histidine kinase domain (Monson et al., 1992). The O_2 sensing relies on the PAS domain (Gilles-Gonzalez, 2001), which is a widespread sequence found in bacterial (Green and Paget, 2004), animal (Adaixo et al., 2013), and plant (Christie et al., 2002) proteins. Oxygen exerts a negative regulation on FixL through interaction with the PAS domain.

The formation of a microoxic environment hampers the inhibitions that O_2 exerts on FixL, and activates the reversible autophosphorylation of a His residue in the FixL kinase domain. Phosphorylated FixL transfers the phosphoryl group to the signal transducer, FixJ, whose phosphorylation status induces the transcription of the *nif* and *fix* gene clusters involved in nitrogen fixation and respiration (Reyrat et al., 1993; Bobik et al., 2006), via the activation of two intermediary regulatory genes, *nifA* and *fixK*. Interestingly, in *S. meliloti*, Meilhoc et al. (2010) identified about 100 genes up-regulated by NO, among which 70% have been described to be induced by microoxia (Bobik et al., 2006) and regulated through the FixL-FixJ system. NO present in nodules could serve as a signal to activate the FixL-FixJ system (Meilhoc et al., 2010).

CONCLUDING REMARKS

The study of symbiotic models in response to waterlogging can help in deciphering the mechanism that may be crucial for the isolation of tolerant legume crop species and varieties in the field. The steps in signal exchange for the mutual recognition, nodule organogenesis and efficient N_2 fixation under waterlogging are crucial aspects of the symbiosis. It would thus be of interest to decipher whether the sensing of O_2 shortage in plant can (i) modify the perception of the partner during the symbiotic establishment, (ii) influence the nodule development, and (iii) affect the functioning of the nitrogenase enzyme in the bacteroid. These aspects may be further influenced by the high level of NO encountered in the nodule organ, which is involved, together with O_2, in ERF-VIIs degradation. At the same time, the PNR cycle may offer an alternative way to produce energy under O_2 shortage. A detailed analysis of these steps would help in finding interesting solutions for marginal land cultivation with waterlogging tolerant legumes capable of fixing N_2 where limited O_2 is available.

AUTHOR CONTRIBUTIONS

CP and AB conceived the idea of the review. All the authors were involved in the manuscript writing.

FUNDING

We would like to thank Campus France and the Franco Italian University for funding and supporting the scientific exchange under the Partnership Hubert Curien (PHC) Galilee Project 34602QF, G15-11. CP, AT, and PP acknowledge funding by Scuola Superiore Sant'Anna. AB and RB are supported by the French Institut National de la Recherche Agronomique (INRA) and by the Partnership Hubert Curien (PHC) Utique Project 17G0904.

REFERENCES

Adaixo, R., Harley, C. A., Castro-Rodrigues, A. F., and Morais-Cabral, J. H. (2013). Structural properties of PAS domains from the KCNH potassium channels. *PLoS One* 8:e59265. doi: 10.1371/journal.pone.0059265

Amarante, L., and Sodek, L. (2006). Waterlogging effect on xylem sap glutamine of nodulated soybean. *Biol. Plant.* 50, 405–410. doi: 10.1007/s10535-006-0057-6

Antonelli, C. J., Calzadilla, P. I., Vilas, J. M., Campestre, M. P., Escaray, F. J., and Ruiz, O. A. (2018). Physiological and anatomical traits associated with tolerance to long-term partial submergence stress in the Lotus genus: responses of forage species, a model and an interspecific hybrid. *J. Agron. Crop Sci.* 205, 65–76. doi: 10.1111/jac.12303

Appleby, C. A. (1992). The origin and functions of haemoglobin in plants. *Sci. Prog.* 76, 365–398. doi: 10.2307/43421309

Arrese-Igor, C., Royuela, M., de Lorenzo, C., de Felipe, M. R., and Aparicio-Tejo, P. M. (1993). Effect of low rhizosphere oxygen on growth, nitrogen fixation and nodule morphology in lucerne. *Physiol. Plant.* 89, 55–63. doi: 10.1111/j.1399-3054.1993.tb01786.x

Avenhaus, U., Cabeza, R. A., Liese, R., Lingner, A., Dittert, K., Salinas-Riester, G., et al. (2016). Short-term molecular acclimation processes of legume nodules to increased external oxygen concentration. *Front. Plant Sci.* 6:1133. doi: 10.3389/fpls.2015.01133

Baudouin, E., Pieuchot, L., Engler, G., Pauly, N., and Puppo, A. (2006). Nitric oxide is formed in *Medicago truncatula-Sinorhizobium meliloti* functional nodules. *Mol. Plant Microbe Interact.* 19, 970–975. doi: 10.1094/MPMI-19-0970

Berger, A., Brouquisse, R., Pathak, P. K., Hichri, I., Singh, I., Bhatia, S., et al. (2018). Pathways of nitric oxide metabolism and operation of phytoglobins in legume nodules: missing links and future directions. *Plant. Cell Environ.* 41, 2057–2068. doi: 10.1111/pce.13151

Bergersen, F. J., and Goodchild, D. J. (1972). Aeration pathways in soybean root nodules. *Aust. J. Biol. Sci.* 26, 729–740. doi: 10.1071/BI9730729

Bobik, C., Meilhoc, E., and Batut, J. (2006). FixJ: a major regulator of the oxygen limitation response and late symbiotic functions of *Sinorhizobium meliloti*. *J. Bacteriol.* 188, 4890–4902.

Boscari, A., Del Giudice, J., Ferrarini, A., Venturini, L., Zaffini, A. L., Delledonne, M., et al. (2013). Expression dynamics of the *Medicago truncatula* transcriptome during the symbiotic interaction with *Sinorhizobium meliloti*: which role for nitric oxide? *Plant Physiol.* 161, 425–439. doi: 10.1104/pp.112.208538

Bui, L. T., Giuntoli, B., Kosmacz, M., Parlanti, S., and Licausi, F. (2015). Constitutively expressed ERF-VII transcription factors redundantly activate the core anaerobic response in *Arabidopsis thaliana*. *Plant Sci.* 236, 37–43. doi: 10.1016/j.plantsci.2015.03.008

Bustos-Sanmamed, P., Tovar-Méndez, A., Crespi, M., Sato, S., Tabata, S., and Becana, M. (2011). Regulation of nonsymbiotic and truncated hemoglobin genes of *Lotus japonicus* in plant organs and in response to nitric oxide and hormones. *New Phytol.* 189, 765–776. doi: 10.1111/j.1469-8137.2010.03527.x

Capoen, W., Goormachtig, S., and Holsters, M. (2010). Water-tolerant legume nodulation. *J. Exp. Bot.* 61, 1251–1255. doi: 10.1093/jxb/erp326

Christie, J. M., Swartz, T. E., Bogomolni, R. A., and Briggs, W. R. (2002). Phototropin LOV domains exhibit distinct roles in regulating

photoreceptor function. *Plant J.* 32, 205–219. doi: 10.1046/j.1365-313X.2002.01415.x

Colmer, T. D., and Voesenek, L. A. C. J. (2009). Flooding tolerance: suites of plant traits in variable environments. *Funct. Plant Biol.* 36, 665–681. doi: 10.1071/FP09144

Davies, C. L., Turner, D. W., and Dracup, M. (2000). Yellow lupin (*Lupinus luteus*) tolerates waterlogging better than narrow-leafed lupin (*L. angustifolius*): II. Leaf gas exchange, plant water status, and nitrogen accumulation. *Aust. J. Agric. Res.* 51, 711–719. doi: 10.1071/AR99074

De Philip, P., Batut, J., and Boistard, P. (1990). Rhizobium meliloti FixL is an oxygen sensor and regulates *R. meliloti* nifA and fixK genes differently in *Escherichia coli*. *J. Bacteriol.* 172, 4255–4262. doi: 10.1128/jb.172.8.4255-4262.1990

del Castillo, L. D. D., Hunt, S., and Layzell, D. B. (1992). O2 regulation and O2-limitation of nitrogenase activity in root nodules of pea and lupin. *Physiol. Plant.* 86, 269–278. doi: 10.1034/j.1399-3054.1992.860212.x

Dénarié, J., and Cullimore, J. (1993). Lipo-oligosaccharide nodulation factors: a new class of signaling molecules mediating recognition and morphogenesis. *Cell* 74, 951–954. doi: 10.1016/0092-8674(93)90717-5

D'Haeze, W., De Rycke, R., Mathis, R., Goormachtig, S., Pagnotta, S., Verplancke, C., et al. (2003). Reactive oxygen species and ethylene play a positive role in lateral root base nodulation of a semiaquatic legume. *Proc. Natl. Acad. Sci. U.S.A.* 100, 11789–11794. doi: 10.1073/pnas.1333899100

D'Haeze, W., Mergaert, P., Promé, J. C., and Holsters, M. (2000). Nod factor requirements for efficient stem and root nodulation of the tropical legume *Sesbania rostrata*. *J. Biol. Chem.* 275, 15676–15684. doi: 10.1074/jbc.275.21.15676

Dixon, R. O. D., Blunden, E. A. G., and Searl, J. W. (1981). Intercellular space and hydrogen diffusion in pea and lupin root nodules. *Plant Sci. Lett.* 23, 109–116.

El Msehli, S., Rima, N., Sghaier, H., Aschi-Smiti, S., and Brouquisse, R. (2016). Impact of hypoxia on nodulation and growth of the legume plant *Medicago truncatula* in symbiosis with *Sinorhizobium meliloti*. *Int. J. Curr. Res. Biosci. Plant Biol.* 3, 53–60.

Erisman, J. W., Sutton, M. A., Galloway, J., Klimont, Z., and Winiwarter, W. (2008). How a century of ammonia synthesis changed the world. *Nat. Geosci.* 1:636. doi: 10.1038/ngeo325

Gasch, P., Fundinger, M., Müller, J., Lee, T., Bailey-Serres, J., and Mustroph, A. (2016). Redundant ERF-VII transcription factors bind to an evolutionarily conserved cis-motif to regulate hypoxia-responsive gene expression in *Arabidopsis*. *Plant Cell* 28, 160–180. doi: 10.1105/tpc.15.00866

Gerland, P., Raftery, A. E., Ševčíková, H., Li, N., Gu, D., and Spoorenberg, T. (2014). World population stabilization unlikely this century. *Science* 346, 234–237. doi: 10.1126/science.1257469

Gibberd, M. R., Colmer, T. D., and Cocks, P. S. (1999). Root porosity and oxygen movement in waterlogging-tolerant *Trifolium tomentosum* and -intolerant *Trifolium glomeratum*. *Plant Cell Environ.* 22, 1161–1168. doi: 10.1046/j.1365-3040.1999.00472.x

Gibbs, D. J., Lee, S. C., Md Isa, N., Gramuglia, S., Fukao, T., Bassel, G. W., et al. (2011). Homeostatic response to hypoxia is regulated by the N-end rule pathway in plants. *Nature* 479, 415–418. doi: 10.1038/nature10534

Gibbs, D. J., Mdisa, N., Movahedi, M., Lozano-Juste, J., Mendiondo, G. M., Berckhan, S., et al. (2014). Nitric oxide sensing in plants is mediated by proteolytic control of group VII ERF transcription factors. *Mol. Cell.* 53, 369–379. doi: 10.1016/j.molcel.2013.12.020

Gilles-Gonzalez, M. A. (2001). Oxygen signal transduction. *IUBMB Life* 51, 165–173. doi: 10.1080/152165401753544232

Giuntoli, B., Lee, S. C., Licausi, F., Kosmacz, M., Oosumi, T., van Dongen, J. T., et al. (2014). A trihelix DNA binding protein counterbalances hypoxia-responsive transcriptional activation in *Arabidopsis*. *PLoS Biol.* 12:e1001950. doi: 10.1371/journal.pbio.1001950

Giuntoli, B., Licausi, F., van Veen, H., and Perata, P. (2017). Functional balancing of the hypoxia regulators RAP2.12 and HRA1 takes place in vivo in *Arabidopsis thaliana* plants. *Front. Plant Sci.* 8:591. doi: 10.3389/fpls.2017.00591

Goormachtig, S., Capoen, W., and Holsters, M. (2004). Rhizobium infection: lessons from the versatile nodulation behaviour of water-tolerant legumes. *Trends Plant Sci.* 9, 518–522. doi: 10.1016/j.tplants.2004.09.005

Gravot, A., Richard, G., Lime, T., Lemarié, S., Jubault, M., Lariagon, C., et al. (2016). Hypoxia response in *Arabidopsis* roots infected by *Plasmodiophora brassicae* supports the development of clubroot. *BMC Plant Biol.* 16:251. doi: 10.1186/s12870-016-0941-y

Green, J., and Paget, M. S. (2004). Bacterial redox sensors. *Nat. Rev. Microbiol.* 2, 954–966. doi: 10.1038/nrmicro1022

Guinel, F. C., and Sloetjes, L. L. (2000). Ethylene is involved in the nodulation phenotype of *Pisum sativum* R50 (sym 16), a pleiotropic mutant that nodulates poorly and has pale green leaves. *J. Exp. Bot.* 51, 885–894. doi: 10.1093/jexbot/51.346.885

Gupta, K. J., and Igamberdiev, A. U. (2011). The anoxic plant mitochondrion as a nitrite: NO reductase. *Mitochondrion* 11, 537–543. doi: 10.1016/j.mito.2011.03.005

Hill, R., Hargrove, M., and Arredondo-Peter, R. (2016). Phytoglobin: a novel nomenclature for plant globins accepted by the globin community at the 2014 XVIII conference on oxygen-binding and sensing proteins. *F1000Res.* 5:212. doi: 10.12688/f1000research.8133.1

Horchani, F., Prévot, M., Boscari, A., Evangelisti, E., Meilhoc, E., Bruand, C., et al. (2011). Both plant and bacterial nitrate reductases contribute to nitric oxide production in *Medicago truncatula* nitrogen-fixing nodules. *Plant Physiol.* 155, 1023–1036. doi: 10.1104/pp.110.166140

Hunt, S., King, B. J., and Layzell, D. B. (1989). Effects of gradual increases in O2 concentration on nodule activity in soybean. *Plant Physiol.* 91, 315–321. doi: 10.1104/pp.91.1.31

Igamberdiev, A. U., and Hill, R. D. (2009). Plant mitochondrial function during anaerobiosis. *Ann. Bot.* 103, 259–268. doi: 10.1093/aob/mcn100

James, E. K., and Crawford, R. M. M. (1998). Effect of oxygen availability on nitrogen fixation by two *Lotus* species under flooded conditions. *J. Exp. Bot.* 49, 599–609. doi: 10.1093/jxb/49.320.599

Justino, G. C., and Sodek, L. (2013). Recovery of nitrogen fixation after short-term flooding of the nodulated root system of soybean. *J. Plant Physiol.* 170, 235–241. doi: 10.1016/j.jplph.2012.10.006

Konnerup, D., Toro, G., Pedersen, O., and Colmer, T. D. (2018). Waterlogging tolerance, tissue nitrogen and oxygen transport in the forage legume *Melilotus siculus*: a comparison of nodulated and nitrate-fed plants. *Ann. Bot.* 121, 699–709. doi: 10.1093/aob/mcx202

Kosmacz, M., Parlanti, S., Schwarzländer, M., Kragler, F., Licausi, F., and Van Dongen, J. T. (2015). The stability and nuclear localization of the transcription factor RAP2.12 are dynamically regulated by oxygen concentration. *Plant Cell Environ.* 38, 1094–1103. doi: 10.1111/pce.12493

Licausi, F., Kosmacz, M., Weits, D. A., Giuntoli, B., Giorgi, F. M., Voesenek, L. A. C. J., et al. (2011). Oxygen sensing in plants is mediated by an N-end rule pathway for protein destabilization. *Nature* 479, 419–422. doi: 10.1038/nature10536

Licausi, F., Pucciariello, C., and Perata, P. (2013). New role for an old rule: N-end rule-mediated degradation of ethylene responsive factor proteins governs low oxygen response in plants. *J. Integr. Plant Biol.* 55, 31–39. doi: 10.1111/jipb.12011

Malik, A. I., Ailewe, T. I., and Erskine, W. (2015). Tolerance of three grain legume species to transient waterlogging. *AoB Plants* 7:lv041. doi: 10.1093/aobpla/plv041

Manzur, M. E., Grimoldi, A. A., Insausti, P., and Striker, G. G. (2009). Escape from water or remain quiescent? *Lotus tenuis* changes its strategy depending on depth of submergence. *Ann. Bot.* 104, 1163–1169. doi: 10.1093/aob/mcp203

Markmann, K., and Parniske, M. (2009). Evolution of root endosymbiosis with bacteria: how novel are nodules? *Trends Plant Sci.* 14, 77–86. doi: 10.1016/j.tplants.2008.11.009

Meakin, G. E., Bueno, E., Jepson, B., Bedmar, E. J., Richardson, D. J., and Delgado, M. J. (2007). The contribution of bacteroidal nitrate and nitrite reduction to the formation of nitrosylleghaemoglobin complexes in soybean root nodules. *Microbiology* 153, 411–419. doi: 10.1099/mic.0.2006/000059-0

Meilhoc, E., Cam, Y., Skapski, A., and Bruand, C. (2010). The response to nitric oxide of the nitrogen-fixing symbiont *Sinorhizobium meliloti*. *Mol. Plant Microbe Interact.* 23, 748–759. doi: 10.1094/MPMI-23-6-0748

Minchin, F. R., James, E. K., and Becana, M. (2008). "Oxygen diffusion, production of reactive oxygen and nitrogen species, and antioxidants in legume nodules," in *Nitrogen-Fixing Leguminous Symbioses. Nitrogen Fixation: Origins, Applications, and Research Progress*, eds M. J. Dilworth, E. K. James, J. I. Sprent, and W. E. Newton (Dordrecht: Springer), 321–362. doi: 10.1007/978-1-4020-3548-7_11

Minchin, F. R., and Pate, J. S. (1975). Effects of water, aeration, and salt regime on nitrogen fixation in a nodulated legume-definition of an optimum root environment. *J. Exp. Bot.* 26, 60–69.doi: 10.1093/jxb/26.1.60

Monson, E. K., Weinstein, M., Ditta, G. S., and Helinski, D. R. (1992). The FixL protein of *Rhizobium meliloti* can be separated into a heme-binding oxygen-sensing domain and a functional C-terminal kinase domain. *Proc. Natl. Acad. Sci. U.S.A.* 89, 4280–4284. doi: 10.1073/pnas.89.10.4280

Munir, R., Konnerup, D., Khan, H. A., Siddique, K. H. M., and Colmer, T. D. (2019). Sensitivity of chickpea and faba bean to root-zone hypoxia, elevated ethylene, and carbon dioxide. *Plant Cell Environ.* 42, 85–97. doi: 10.1111/pce.13173

Nichols, P. G. H., Craig, A. D., Rogers, M. E., Albertsen, T. O., Miller, S. M., McClements, D. R., et al. (2008a). Production and persistence of annual pasture legumes at five saline sites in southern Australia. *Aust. J. Exp. Agric.* 48, 518–535. doi: 10.1071/EA07167

Nichols, P. G. H., Rogers, M. E., Craig, A. D., Albertsen, T. O., Miller, S. M., McClements, D. R., et al. (2008b). Production and persistence of temperate perennial grasses and legumes at five saline sites in southern Australia. *Aust. J. Exp. Agric.* 48, 536–552. doi: 10.1071/EA07168

Oldroyd, G. E. D., and Downie, J. A. (2008). Coordinating nodule morphogenesis with rhizobial infection in legumes. *Annu. Rev. Plant Biol.* 59, 519–546. doi: 10.1146/annurev.arplant.59.032607.092839

Pampana, S., Masoni, A., and Arduini, I. (2016). Response of cool-season grain legumes to waterlogging at flowering. *Can. J. Plant Sci.* 96, 597–603. doi: 10.1139/cjps-2015-0268

Penmetsa, R. V., and Cook, D. R. (1997). A legume ethylene-insensitive mutant hyperinfected by its rhizobial symbiont. *Science* 275, 527–530. doi: 10.1126/science.275.5299.527

Poole, R. K., and Hill, S. (1997). Respiratory protection of nitrogenase activity in *Azotobacter vinelandii*—roles of the terminal oxidases. *Biosci. Rep.* 17, 303–317.

Pugh, R., Witty, J. F., Mytton, L. R., and Minchin, F. R. (1995). The effect of waterlogging on nitrogen fixation and nodule morphology in soil-grown white clover (*Trifolium repens* L.). *J. Exp. Bot.* 46, 285–290. doi: 10.1093/jxb/46.3.285

Real, D., Warden, J., Sandral, G. A., and Colmer, T. D. (2008). Waterlogging tolerance and recovery of 10 Lotus species. *Anim. Prod. Sci.* 48, 480–487. doi: 10.1071/EA07110

Reyrat, J. M., David, M., Blonski, C., Boistard, P., and Batut, J. (1993). Oxygen-regulated in vitro transcription of *Rhizobium meliloti nifA* and *fixK* genes. *J. Bacteriol.* 175, 6867–6872. doi: 10.1128/JB.00251-06

Roberts, D. M., Choi, W. G., and Hwang, J. H. (2010). "Strategies for adaptation to waterlogging and hypoxia in nitrogen fixing nodules of legumes," in *Waterlogging Signaling and Tolerance in Plants*, eds S. Mancuso and S. Shabala (Berlin: Springer), 37–59. doi: 10.1007/978-3-642-10305-6_3

Rocha, M., Licausi, F., Araujo, W. L., Nunes-Nesi, A., Sodek, L., Fernie, A. R., et al. (2010a). Glycolysis and the tricarboxylic acid cycle are linked by alanine aminotransferase during hypoxia induced by waterlogging of *Lotus japonicus*. *Plant Physiol.* 152, 1501–1513. doi: 10.1104/pp.109.150045

Rocha, M., Sodek, L., Licausi, F., Hameed, M. W., Dornelas, M. C., and Van Dongen, J. T. (2010b). Analysis of alanine aminotransferase in various organs of soybean (*Glycine max*) and in dependence of different nitrogen fertilisers during hypoxic stress. *Amino Acids.* 39, 1043–1053. doi: 10.1007/s00726-010-0596-1

Sairam, R. K., Dharmar, K., Chinnusamy, V., and Meena, R. C. (2009). Waterlogging-induced increase in sugar mobilization, fermentation, and related gene expression in the roots of mung bean (*Vigna radiata*). *J. Plant Physiol.* 166, 602–616. doi: 10.1016/j.jplph.2008.09.005

Sánchez, C., Gates, A. J., Meakin, G. E., Uchiumi, T., Girard, L., Richardson, D. J., et al. (2010). Production of nitric oxide and nitrosylleghemoglobin complexes in soybean nodules in response to flooding. *Mol. Plant. Microbe Interact.* 23, 702–711. doi: 10.1094/MPMI-23-5-0702

Serraj, R., Fleurat-Lessard, P., Jaillard, B., and Drevon, J. J. (1995). Structural changes in the inner-cortex cells of soybean root-nodules are induced by short-term exposure to high salt or oxygen concentrations. *Plant Cell Environ.* 18, 455–462. doi: 10.1111/j.1365-3040.1995.tb00380.x

Shimoda, Y., Shimoda-Sasakura, F., Kucho, K., Kanamori, N., Nagata, M., Suzuki, A., et al. (2009). Overexpression of class 1 plant hemoglobin genes enhances symbiotic nitrogen fixation activity between *Mesorhizobium loti* and *Lotus japonicus*. *Plant J.* 57, 254–263. doi: 10.1111/j.1365-313X.2008.03689.x

Solaiman, Z., Colmer, T. D., Loss, S. P., Thomson, B. D., and Siddique, K. H. M. (2007). Growth responses of cool-season grain legumes to transient waterlogging. *Aust. J. Agric. Res.* 58, 406–412. doi: 10.1071/AR06330

Soltani, A., MafiMoghaddam, S., Walter, K., Restrepo-Montoya, D., Mamidi, S., Schroder, S., et al. (2017). Genetic architecture of flooding tolerance in the dry bean middle-american diversity panel. *Front. Plant Sci.* 8:1183. doi: 10.3389/fpls.2017.01183

Soupène, E., Foussard, M., Boistard, P., Truchet, G., and Batut, J. (1995). Oxygen as a key developmental regulator of *Rhizobium meliloti* N2-fixation gene expression within the alfalfa root nodule. *Proc. Natl. Acad. Sci. U.S.A.* 92, 3759–3763.

Souza, S. C. R., Mazzafera, P., and Sodek, L. (2016). Flooding of the root system in soybean: biochemical and molecular aspects of N metabolism in the nodule during stress and recovery. *Amino Acids* 48, 1285–1295. doi: 10.1007/s00726-016-2179-2

Sprent, J. I. (1972). The effects of water stress on nitrogen-fixing root nodules. *New Phytol.* 71, 443–450. doi: 10.1111/j.1469-8137.1972.tb01944.x

Striker, G. G., Casas, C., Manzur, M. E., Ploschuk, R. A., and Casal, J. J. (2014). Phenomic networks reveal largely independent root and shoot adjustment in waterlogged plants of *Lotus japonicus*. *Plant Cell Environ.* 37, 2278–2293. doi: 10.1111/pce.12268

Striker, G. G., and Colmer, T. D. (2017). Flooding tolerance of forage legumes. *J. Exp. Bot.* 68, 1851–1872. doi: 10.1093/jxb/erw239

Striker, G. G., Kotula, L., and Colmer, T. D. (2019). Tolerance to partial and complete submergence in the forage legume *Melilotus siculus*: an evaluation of 15 accessions for petiole hyponastic response and gas-filled spaces, leaf hydrophobicity and gas films, and root phellem. *Ann. Bot.* 123, 1–12. doi: 10.1093/aob/mcy153

Striker, G. G., Teakle, N. L., Colmer, T. D., and Barrett-Lennard, E. G. (2015). Growth responses of *Melilotus siculus* accessions to combined salinity and root-zone hypoxia are correlated with differences in tissue ion concentrations and not differences in root aeration. *Environ. Exp. Bot.* 109, 89–98. doi: 10.1016/j.envexpbot.2014.08.006

Sung, F. J. M. (1993). Waterlogging effect on nodule nitrogenase and leaf nitrate reductase activities in soybean. *F. Crop. Res.* 35, 183–189. doi: 10.1016/0378-4290(93)90152-D

Takahashi, M., Niki, T., Deem, K. D., and Gladish, D. K. (2016). Vascular cavity formation enhances oxygen availability during flooding in root tips of *Phaseolus coccineus* L. primary roots. *Int. J. Plant Sci.* 177, 277–286. doi: 10.1086/684524

Teakle, N. L., Armstrong, J., Barrett-Lennard, E. G., and Colmer, T. D. (2011). Aerenchymatous phellem in hypocotyl and roots enables O2 transport in *Melilotus siculus*. *New Phytol.* 190, 340–350. doi: 10.1111/j.1469-8137.2011.03655.x

Teakle, N. L., Bowman, S., Barrett-Lennard, E. G., Real, D., and Colmer, T. D. (2012). Comparisons of annual pasture legumes in growth, ion regulation and root porosity demonstrate that *Melilotus siculus* has exceptional tolerance to combinations of salinity and waterlogging. *Environ. Exp. Bot.* 77, 175–184. doi: 10.1016/j.envexpbot.2011.11.020

Tobisa, M., Shimojo, M., and Masuda, Y. (2014). Root distribution and nitrogen fixation activity of tropical forage legume american jointvetch (*Aeschynomene americana* L.) Cv. glenn under waterlogging conditions. *Int. J. Agron.* 2014:507405. doi: 10.1155/2014/507405

Vicente, J., Mendiondo, G. M., Pauwels, J., Pastor, V., Izquierdo, Y., Naumann, C., et al. (2018). Distinct branches of the N-end rule pathway modulate the plant immune response. *New Phytol.* 221, 988–1000. doi: 10.1111/nph.15387

Weits, D. A., Giuntoli, B., Kosmacz, M., Parlanti, S., Hubberten, H. M., Riegler, H., et al. (2014). Plant cysteine oxidases control the oxygen-dependent branch of the N-end-rule pathway. *Nat. Commun.* 5, 1–10. doi: 10.1038/ncomms4425

White, M. D., Klecker, M., Hopkinson, R. J., Weits, D. A., Mueller, C., Naumann, C., et al. (2017). Plant cysteine oxidases are dioxygenases that directly enable

arginyl transferase-catalysed arginylation of N-end rule targets. *Nat. Commun.* 8:14690. doi: 10.1038/ncomms14690

Wiraguna, E., Malik, A. I., and Erskine, W. (2017). Waterlogging tolerance in lentil (*Lens culinaris* Medik. subsp. culinaris) germplasm associated with geographic origin. *Genet. Resour. Crop Evol.* 64, 579–586. doi: 10.1007/s10722-016-0385-0

Witty, J. F., and Minchin, F. R. (1990). Oxygen diffusion in the legume root nodule. *Nitrogen. Fixat. Achiev. Object.* 2, 285–292. doi: 10.1007/978-1-4684-6432-0_29

Zaman, M. S., Malik, A. I., Kaur, P., and Erskine, W. (2018). Waterlogging tolerance of pea at germination. *J. Agron. Crop Sci.* 204, 155–164. doi: 10.1111/jac.12230

Conflict of Interest Statement: The authors declare that the research was conducted in the absence of any commercial or financial relationships that could be construed as a potential conflict of interest.

frontiers in Plant Science

ORIGINAL RESEARCH
published: 12 September 2019
doi: 10.3389/fpls.2019.01087

Reduced Growth and Nitrogen Uptake During Waterlogging at Tillering Permanently Affect Yield Components in Late Sown Oats

Iduna Arduini, Marco Baldanzi and Silvia Pampana*

Department of Agriculture, Food and Environment, University of Pisa, Pisa, Italy

OPEN ACCESS

Edited by:
Jairo A. Palta, Commonwealth Scientific and Industrial Research Organisation (CSIRO), Australia

Reviewed by:
Rocio Antonella Ploschuk, CONICET Instituto de Investigaciones Fisiológicas y Ecologicas Vinculadas a la Agricultura (IFEVA), Argentina
Romina Paola De San Celedonio, Universidad de Buenos Aires, Argentina

***Correspondence:**
Iduna Arduini
iduna.arduini@unipi.it

Specialty section:
This article was submitted to Plant Abiotic Stress, a section of the journal Frontiers in Plant Science

Received: *01 March 2019*
Accepted: *09 August 2019*
Published: *12 September 2019*

Citation:
Arduini I, Baldanzi M and Pampana S (2019) Reduced Growth and Nitrogen Uptake During Waterlogging at Tillering Permanently Affect Yield Components in Late Sown Oats. Front. Plant Sci. 10:1087. doi: 10.3389/fpls.2019.01087

In Mediterranean Europe, winter cereals can experience soil waterlogging starting from crop establishment up to stem elongation and, in late sowings, this stress is combined with temperatures favorable to plant metabolism. Oats response to waterlogging has been rarely investigated, but these species seems to recover better than other cereals. In a 2-year experiment, *Avena sativa* and *Avena byzantina* were sown at the end of winter in pots placed outdoors. At the two-tiller stage, plants were exposed to waterlogging for periods ranging from 0 to 35 days. The dry weight and the N-concentration of shoots and roots were determined on waterlogged plants and drained controls at the start and the end of each waterlogging period, and at maturity. At maturity, the grain yield and its components were determined. To relate oat response to its specific morphological and developmental traits, results were compared to the published results in wheat and barley. Both oat species suffered severe damage during waterlogging: the uptake of nitrogen and the N-concentration of shoots were reduced after 7 days, tiller initiation and root growth after 14 days, and shoot growth after 21 days. All plants survived waterlogging, and the relative growth rates of roots and shoots and the net uptake rate of nitrogen were resumed during recovery. Nevertheless, at maturity, the straw and root biomass were markedly lower with all waterlogging durations, and grain yield decreased by 42% up to approximately 81% following an asymptotic equation. The most affected yield components were the number of panicles per plant and the number of kernels per panicle, but their relative sensitivity changed according to waterlogging duration. The slight increase in tiller fertility in response to short waterlogging and the small and irregular decrease in the number of kernels per spikelet suggest that the two oats could recover the initiation and size of inflorescences better than other winter cereals. Despite this, waterlogging in spring was highly detrimental to these oats because of severe damage under waterlogging and because of the inability to initiate new tillers and adequately resume root growth during recovery, once plants had achieved the phase of stem elongation.

Keywords: ***Avena byzantina***, ***Avena sativa***, **grain-yield-components, N-status, recovery, roots, tillers, waterlogging**

INTRODUCTION

Soil is considered waterlogged when excess water saturates the soil pores, with either no layer or a very fine layer of water on the soil surface, so that the gas exchange of roots with the atmosphere is inhibited (Sasidharan et al., 2017). Waterlogging is a major abiotic constraint on the growth and development of agricultural crops and occurs in many regions worldwide because of poor drainage and/or excessive rainfall. Crop losses due to waterlogging are expected to increase as a consequence of increased extreme precipitation events associated with climate change (Herzog et al., 2016).

Waterlogging is a compound stress that severely changes the soil environment, first by reducing oxygen availability. It is commonly accepted that anaerobiosis takes place within a few hours after the soil has been saturated and that the rate of depletion is greatly affected by soil depth and temperature (Belford et al., 1985; Cannell et al., 1985). Additional negative conditions caused by waterlogging in soil are the accumulation of CO2, ethylene, and biochemically reduced compounds in the root environment, generally combined with nutrient deficiency (Pang et al., 2007; Herzog et al., 2016). In particular, lower soil nitrogen has been reported as a consequence of denitrification and N leaching (Bronson and Fillery, 1998; Nguyen et al., 2018).

High oxygen-consuming tissues, such as actively dividing root meristems and those involved in mineral uptake, are the first targets of depleted oxygen, and their cells enter an "energy crisis" within a short time (Setter and Waters, 2003; Loreti et al., 2016). Brisson et al. (2002) observed the first effects of waterlogging on the growth of wheat roots after 48 h. Plants cope differently with occasional waterlogging toward which they display a variety of tolerance mechanisms such as the formation of aerenchyma in roots and the down-regulation of energy requirements (Herzog et al., 2016; Ploschuk et al., 2018).

Crop tolerance to waterlogging has been variously defined in the literature. Physiological tolerance takes into account the survival or the maintenance of growth rates similar to drained conditions under waterlogging, whereas agronomic tolerance is based on the maintenance of relatively high grain yields, despite waterlogging exposure during the growth cycle (Setter and Waters, 2003). Thus, the agronomic tolerance takes into account total plant behavior during and after the stress and is, therefore, the result of the direct effects of waterlogging on plant growth and the recovery ability after the waterlogging ceases.

Recovery upon drainage is particularly important for winter cereals grown in Mediterranean regions, where rainfall concentrates in the period November–April and drought can occur during the late reproductive phase. In these conditions, rapid growth of deep roots following drainage is required to obtain sufficient water to flower effectively and to complete seed ripening (Colmer and Greenway, 2011). In this area, winter cereals are traditionally sown from autumn to the end of winter and are, therefore, likely to experience waterlogging at different growth stages. In dependence on sowing time, the stress can be combined with either winter or spring temperatures, which can affect both the severity of damages and the time to recover. The sensitivity to waterlogging stress and the subsequent effects on grain yield is reported to depend on the development stage during waterlogging, on the duration of the event, and on the external conditions, primarily soil parameters and temperature (Setter and Waters, 2003; Arduini et al., 2016a; Ploschuk et al., 2018). Plant sensitivity to waterlogging was reported to be higher with higher temperatures, because of faster oxygen depletion from the soil (Belford et al., 1985; Setter and Waters, 2003) and because higher temperatures enhance transpiration and favor plant metabolism, thus increasing both energy consumption (de San Celedonio et al., 2014; Herzog et al., 2016; Loreti et al., 2016) and damages to growing points (Malik et al., 2002). According to de San Celedonio et al. (2014), losses in wheat and barley yield were higher with delayed sowings and when waterlogging occurred around anthesis compared to tillering, whereas according to Ghobadi and Ghobadi (2010), the susceptibility of wheat decreased with plant development from the first-leaf stage until stem elongation.

Most studies on waterlogging have focused on wheat and barley, while oat species have rarely been investigated (Mustroph, 2018). Nevertheless, oats rank sixth in global cereal production statistics, and in addition of being an important component of livestock feed, their cultivation has increased due to the demand for cosmetic uses and human nutrition, which is driven by their nutraceutical properties (Mahadevan et al., 2016; Finnan and Spink, 2017). In wheat and barley, damages caused by soil waterlogging include chlorosis and premature leaf senescence, reduced root growth, tillering, dry matter accumulation, number and weight of kernels, and increased floral sterility (Marti et al., 2015; Masoni et al., 2016; Arduini et al., 2016a; de San Celedonio et al., 2018; Ploschuk et al., 2018; Sundgren et al., 2018). Research of Watson et al. (1976) and Cannell et al. (1985) has suggested that oats recover better than other winter cereals from waterlogging stress, maybe because of the higher maintenance of green leaves during waterlogging and the higher tiller fertility at maturity (Setter and Waters, 2003).

Vegetative traits are similar in the three cereals, but differences are reported in the initial growth rate, which is slower in oats compared to wheat and especially to barley, and in the longer persistence of seminal roots in oats (Bonnett, 1961). The three species are highly responsive to nitrogen, and, in all of them, N supply during recovery was found to compensate, though only partially, for the waterlogging damage (Watson et al., 1976; Robertson et al., 2009; Rasaei et al., 2012). Conversely, oats differ from wheat and barley in the architecture of the inflorescence, in the timing of yield component determination and in the plasticity of them (Bonnett, 1966; Mahadevan et al., 2016).

The oat inflorescence is a panicle consisting of several branches grouped in clusters at the nodes of the main axis (Bonnett, 1966). Due to this morphology, oats have the potential to produce other spikelets after the initiation of a terminal spikelet at the end of each branch and, thus, after the start of stem elongation (Sonego et al., 2000; Browne et al., 2006). In contrast, the inflorescences of wheat and barley are spikes, in which spikelets are initiated only at the end of the main axis. Their final number is largely determined at the start of stem elongation, either because of the formation of a terminal spikelet (wheat) or because later initiated primordia will abort (barley) (Arduini et al., 2010). In addition, oats have the ability to either abort or fill additional kernels per spikelet in response to assimilate availability later in the crop cycle compared to the other cereals (Finnan and Spink, 2017). All above differences delay to approximately the start of grain filling the determination of the final

number of kernels per plant in oats, whereas this character has been definitively fixed earlier in the other cereals: around anthesis in barley and at early post-flowering in wheat (Finnan and Spink, 2017). In all cereals, kernel number per plant is a crucial yield determinant, as it is the yield component which is most strongly related to grain yield and also more variable in response to environmental and stress conditions (Mahadevan et al., 2016). It is a complex trait resulting from the number of fertile tillers per plant and the number of kernels per inflorescence, which in turn results from the product of the number of spikelets and the number of kernels per spikelet. According to Mahadevan et al. (2016), in oats, the variations of the number of kernels per plant in response to stress conditions were primarily driven by variations of the number of kernels per panicle, whereas in wheat by the number of spikes per plant.

Starting from this, we hypothesized that the better ability of oats to recover from waterlogging imposed at tillering compared to wheat and barley (Watson et al., 1976; Cannell et al., 1985; Setter and Waters, 2003) could largely rely on the later determination and higher plasticity of its inflorescence, which allowed plants to adjust panicle components to compensate for the lower tillering and spikelet initiation during the waterlogging stress.

For the present research, we choose *Avena sativa* L. (common oat) and *Avena byzantina* C. Koch (red oat) that are the two most cultivated oat species in Italy. The two crops cover approximately equivalent surfaces, the former in northern regions and the latter in southern regions. Both crops are traditionally sown in autumn, but high autumn rainfall often prevents sowing at optimal times, so spring sowings are also frequent. To the best of our knowledge, no research has been conducted on the waterlogging tolerance of *A. byzantina*. However, because of the different geographic distribution of the two crops, it is to be expected that it could be less tolerant to waterlogging than *A. sativa*.

Aiming to fill the lack of knowledge about the response of oats to waterlogging, and to give insight into both the direct effects of waterlogging on plant growth parameters and the ability to resume them during recovery, we exposed plants of *A. sativa* and *A. byzantina* sown at the end of winter to different waterlogging durations. In specific, our research aimed to: (i) assess the immediate damage of waterlogging on root and shoot growth, and on nitrogen uptake of the two oat species; (ii) evaluate their ability to recover biomass production and N-uptake from the end of waterlogging up to maturity; and (iii) assess the delayed effects of waterlogging on the vegetative biomass and the grain yield and its components, at maturity. To give a better understanding of oats response to waterlogging and to relate this to the oat-specific plasticity of yield components, our results were discussed in comparison to published results on wheat and barley.

MATERIALS AND METHODS

Experimental Location and Weather Conditions

The research was carried out in 2015 (11 February–2 July) and 2016 (8 February–4 July) at the Research Centre of the Department of Agriculture, Food and Environment of the University of Pisa, Italy, which is located approximately 5 km from the sea (43° 40′ N, 10° 19′ E) and 1 m above sea level. The climate of the area is hot-summer Mediterranean (Csa) with mean annual maximum and minimum daily air temperatures of 20.2 and 9.5°C respectively, and a mean rainfall of 971 mm per year. Daily air minimum and maximum temperatures and rainfall were recorded throughout the entire period of the research by an automatic meteorological station located close to the experimental site.

Between the two growth seasons, no differences in mean temperature were recorded during the entire vegetative phase of oats (14.3 and 14.4°C in 2015 and 2016, respectively), while the mean temperature during the waterlogging treatment was 18.6°C in 2015 and 20.0°C in 2016 (**Figure 1**). During the reproductive phase, however, the mean temperature was higher in 2015 (19.9°C) than in 2016 (18.4°C). In 2015, minimum temperatures were lower and maximum temperatures higher than in 2016, but the range was lower than 1°C. Rainfall varied considerably between years, with the growing season wetter in 2016 (509 mm) than in 2015 (only 257 mm).

Experimental Design, Equipment, and Crop Management

The experimental design consisted of two oat species that were exposed to six waterlogging durations (0, 7, 14, 21, 28, and 35 days)

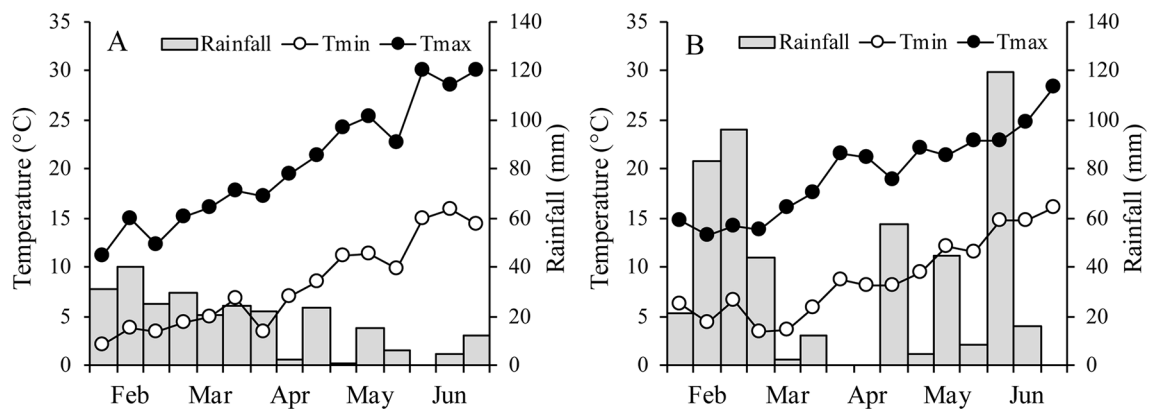

FIGURE 1 | Air minimum and maximum temperatures and rainfall over the growing season of the two oats in 2015 **(A)** and 2016 **(B)**.

at the tillering stage. We used the commercial cultivars Genziana for *A. sativa* L. (common oat) and Argentina for *A. byzantina* C. Koch (red oat), which are standard cultivars in Europe (Murariu et al., 2013). Both have medium-early growth cycles, medium-height, and a good resistance to lodging. In previous experiments carried out on wheat, durum wheat, and barley sown in autumn, we found that plants showed grain yield reductions when exposed to waterlogging at the tillering stage for more than 16 days (barley) and 20 days (wheat and durum wheat) (Masoni et al., 2016; Pampana et al., 2016; Arduini et al., 2016a). In the present study, we expected that the higher temperatures during waterlogging, imposed by the later sowing, would increase plant sensitivity at tillering. For this reason, we chose 35 days as the longest exposure time.

Plants were grown in 16-L pots made from polyvinyl chloride (PVC) tubes (80 cm long and 16 cm in diameter) fitted with a PVC base. A 30-mm diameter hole was drilled in the bottom of each pot, which was fitted with a 0.9-mm mesh to contain roots and substrate loss. In both years, pots were filled with a sandy-loam soil collected from a field previously cultivated with rapeseed. Differences in soil properties for the 2 years were negligible, and the average soil properties were 54.7% sand (2–0.05 mm), 33.4% silt (0.05–0.002 mm), 11.9% clay (< 0.002 mm), 7.6 pH, 0.7 g kg^{-1} total nitrogen (Kjeldahl method), 4.6 mg kg^{-1} available P (Olsen method), and 68.6 mg kg^{-1} available K (BaCl2-TEA method).

Oat species were sown on 11 February in 2015 and 8 February in 2016 (**Table 1**), which correspond to early spring sowings in the Mediterranean conditions. After emergence, the seedlings were thinned to five plants per pot, to mimic a field density of 250 plants m^{-2}. Phosphorus and potassium were applied pre-planting as triple mineral phosphate and potassium sulfate, at the rates of 150 kg ha^{-1} of P2O5 and K2O. At sowing, all pots also received 30 kg N ha^{-1}, as ammonium sulfate. As nitrogen application was found to reduce the detrimental effects of waterlogging on grain yield, in experiment 2, an additional 120 kg N ha^{-1} was applied as urea at the start of the recovery period.

During the entire growth cycle, the timings of the principal growth stages were recorded following the BBCH scale for cereals (Meier, 2001); weed control was conducted by hand hoeing, and weekly checks were conducted for the occurrence of diseases.

In both years, we filled and sowed 68 pots per species. Pots were placed outdoors and kept under drained conditions until plants reached the two-tiller stage (20 March 2015 and 24 March 2016). At these dates, four pots were harvested (T0), 24 pots were maintained in drained conditions, and 40 pots were exposed to waterlogging by placing them into containers (2 m x 1 m x 1 m) filled with water. A layer of 1 cm of free water was maintained above the soil surface throughout the period of waterlogging, to ensure that the soil was completely saturated by water. Accordingly, the treatment consisted of a stagnant soil waterlogging (Sasidharan et al., 2017).

To assess the extent to which *A. sativa* and *A. byzantina* are able to both resist and recover from waterlogging stress, the 68 pots per species were used for two combined experiments that were conducted in parallel.

TABLE 1 | Timing of principal growth stages of *A. sativa* and *A. byzantina* in the two growing seasons.

Growth stage	BBCH Code	Growing Season	Species	
			Avena sativa	*Avena byzantina*
Sowing	00	2015	11 February	11 February
		2016	8 February	8 February
Emergence	09	2015	25 February	25 February
		2016	22 February	22 February
Beginning of tillering	21	2015	15 March	13 March
		2016	21 March	18 March
Two tillers detectable	22	2015	20 March	19 March
		2016	24 March	23 March
First node detectable	31	2015	3 April	4 April
		2016	6 April	7 April
Full flowering	65	2015	7 May	11 May
		2016	11 May	13 May
Maturity	89	2015	2 July	2 July
		2016	4 July	4 July

Experiment 1

Experiment 1 was aimed at assessing the effects of waterlogging on the growth and N uptake of plants harvested immediately after the end of exposure. Each year, the experimental design consisted of two species (*A. sativa* and *A. byzantina*), two growth conditions (drained control—C and waterlogged—WL) and six waterlogging durations (T0, T7, T14, T21, T28, T35). Four replicate pots were used for all combinations of treatments.

For this experiment, each year, 44 pots per species were harvested as follows: four pots before the WL treatment was imposed (T0) and, then, four pots kept under water (WL) and four drained pots (C) at week intervals (T7, T14, T21, T28, T35).

Experiment 2

Experiment 2 was aimed at assessing if damage caused by the waterlogging imposed at tillering affected oat performance at maturity. Each year, the experimental design consisted of two species (*A. sativa* and *A. byzantina*) and six waterlogging durations (T0, T7, T14, T21, T28, T35). Four replicate pots were used for all combinations of treatments.

For this experiment, four pots per species were moved from the container filled with water to drained conditions at week intervals starting 1 week after waterlogging was imposed (T7, T14, T21, T28, T35). Then, pots were supplied with 120 kg N ha^{-1} and kept in drained conditions until plants reached maturity. For each species, T0 consisted of four pots that were kept in well-drained conditions throughout the entire growth cycle. These pots received N at the same time of the WL pots that were drained at T7. All pots, 24 per species at a whole, were harvested at maturity.

Recovery From Waterlogging

The ability of the oat plants to recover from waterlogging stress was assessed by determining growth and nitrogen uptake between the end of waterlogging and maturity.

For each combination of treatments, the recovery of growth parameters and N uptake was calculated as the difference of the values recorded at maturity in experiment 2 and those of the correspondent combination of treatments recorded at the end of waterlogging in experiment 1.

Plant Measurements

At all harvests, plants were manually cut at ground level, and roots were separated from the soil by gently washing to minimize loss or damage. In experiment 1, the number of culms per plant was recorded. In experiment 2, shoots were partitioned into culms+leaves, chaff, and grain. The number of culms and panicles per plant, and the number of spikelets per panicle were recorded. The mean kernel weight was determined, and the number of kernels per plant and kernels per spikelet were calculated. The harvest index was calculated as the ratio between grain yield and total aboveground biomass.

For the dry weight determination of roots and aerial parts, the samples were oven dried at 65°C to a constant weight. All plant parts were analyzed for nitrogen concentration using the micro-Kjeldahl standard method (AOAC, Association of Official Analytical Chemists, 2005). Nitrogen content was obtained by multiplying N concentrations by dry matter.

To determine the effect of waterlogging on the growth and nitrogen uptake of oats during and after waterlogging, the following indexes were calculated for each waterlogging duration and for the periods of recovery.

The absolute growth rates (AGR) of shoots and roots was calculated following Hunt (1990) as:

$$AGR = \frac{W_2 - W_1}{t_2 - t_1}$$

where W is the dry biomass at the beginning (W_1) and at the end (W_2) of each period, and t_2–t_1 is the duration of the period. In experiment 1, t_1 and t_2 are two consecutive harvests, whereas in experiment 2, t_1 corresponds to the end of each WL duration and t_2 to maturity.

The relative growth rates (RGR) of shoots and roots was calculated following Hunt (1990) as:

$$RGR = \frac{lnW_2 - lnW_1}{t_2 - t_1}$$

where W is the dry biomass of shoots or roots at the beginning (W_1) and at the end (W_2) of each period, and t_2–t_1 is the duration of the period. As for AGR, in experiment 1, t_1 and t_2 are two consecutive harvests, whereas in experiment 2, t_1 corresponds to the end of each WL duration and t_2 to maturity.

The net uptake rates (NUR) of nitrogen were calculated following Engels (1993) as:

$$NUR = \frac{N_2 - N_1}{t_2 - t_1} \times \frac{ln\left(R_2 / R_1\right)}{R_2 - R_1}$$

where N is the nitrogen content of the entire plant, R is the dry weight of the roots at the beginning (1) and at the end (2) of each period, and t_2–t_1 is the duration of the period. As for AGR, in experiment 1, t_1 and t_2 are two consecutive harvests, whereas in experiment 2, t_1 corresponds to the end of each WL duration and t_2 to maturity.

Statistical Analyses

All results were subjected to analysis of variance separately for *A. sativa* and *A. byzantina*. To evaluate the damage of waterlogging on plant growth and nitrogen uptake just after the end of waterlogging, data from experiment 1 were arranged in a split-split-plot design with years allocated as main plots, growth conditions (drained control—C and waterlogged—WL) as subplots, and waterlogging durations (T0, T7, T14, T21, T28, and T35) as sub-subplots. Four replicates were used.

To evaluate the permanent damage of waterlogging on plant growth, grain yield, grain yield components, and nitrogen uptake, data from experiment 2 were arranged in a split-plot design with years allocated as main plots and waterlogging durations as subplots. Four replicates were used.

To analyze plant growth and nitrogen uptake during recovery, data from experiments 1 and 2 were arranged, for each species, in a split-split-plot design with years allocated as main plots, growth conditions (C and WL) as subplots, and waterlogging durations (T0, T7, T14, T21, T28, and T35) as sub-subplots, with four replicates.

In all analyses, treatments were considered fixed. Significantly different means were separated at the 0.05 probability level using the Tukey test (Steel et al., 1997).

RESULTS

Analyses of variance for experiments 1 and 2 and for recovery revealed for both *A. sativa* and *A. byzantina* a significant interaction growth condition x waterlogging duration for most of the measured parameters. Conversely, the year mean effect and the interactions with year were not significant for all variables measured, probably because differences in temperature between the years 2015 and 2016 were small (**Figure 1**), and crops were irrigated when necessary. Accordingly, all data are presented averaged over years.

Plant Phenology

The variety Argentina of *A. byzantina* started tillering 2–3 days earlier than the variety Genziana of *A. sativa* but reached flowering approximately 3 days later (**Table 1**). The achievement of the other growth stages differed between species by maximum 1 day.

Waterlogging did not slow plant development and the first-node-detectable stage was achieved in both species, and all treatments approximately 2 weeks after waterlogging was imposed (**Table 1**). Similarly, the plants reached flowering and maturity at the same time in both waterlogged and control conditions.

Visual observations detected chlorosis and early senescence of leaves with waterlogging durations longer than 21 days in both species, while plants remained almost disease-free during and after the treatment.

Experiment 1

Plant Growth Under Waterlogging

In the drained C plants, the number of culms per plant increased significantly between T0 and T14 but no more after then, whereas in the waterlogged plants, it increased only up to T7 (**Figures 2A**, **B**). At T35, control plants had approximately five culms in *A. sativa* and nine in *A. byzantina*, whereas WL plants had three and five culms, respectively. These results indicate that tillering ceased around the first-node-detectable stage in C plants and was severely inhibited under waterlogging. Treatments longer than 14 days also reduced tiller growth and stopped it after 28 days (**Figures 2C**, **D**). Thus, the dry matter accumulation in the shoots of both species was similar in C and WL conditions up to T14, after which it increased linearly in drained conditions and almost stopped under waterlogging (**Figures 3A**, **B**).

Root growth was more severely affected than shoot growth and was significantly lower in WL than in C plants from T14 on (**Figures 3C**, **D**). After 35 days, the dry weight of shoots of the drained plants had increased by 57 times either the species, whereas that of roots by 37 and 44 times, respectively, in *A. sativa* and *A. byzantina*. Conversely, WL plants of both species increased by only approximately 13 times in shoots and 5 times in roots. The higher and prompter sensitivity of roots to waterlogging caused the root:shoot ratio to be lower in WL than C plants (**Figures 3E**, **F**).

The RGR of shoots and roots decreased progressively in both control and waterlogged plants as plant development proceeded, but values were lower in WL (Figure 4). In shoots, the RGR was approximately halved during the third week of waterlogging (**Figures 4A**, **B**), whereas in roots, this had occurred during the first week (**Figures 4C**, **D**). After 28 days of WL, the roots of *A. sativa* showed a negative RGR suggesting that some died roots were detached.

Nitrogen Uptake Under Waterlogging

The nitrogen concentration progressively decreased both in shoots and in roots of the two oats from T0 to T35, independent of the growth conditions (**Table 2**). Compared to the drained controls, WL plants showed lower N concentration in shoots. However, in *A. sativa*, the decrease was significant after 7-, 14-, and 21-day waterlogging, but not for longer exposures, while in *A. byzantina*, values differed significantly only for T14 and T21. Conversely, the N concentration of roots was never significantly affected by waterlogging. The N content of WL plants was always lower than that of controls, with differences that became significant in shoots at T14 in both species, whereas in roots at T7 in *A. sativa* and T14 in *A. byzantina* (**Table 2**).

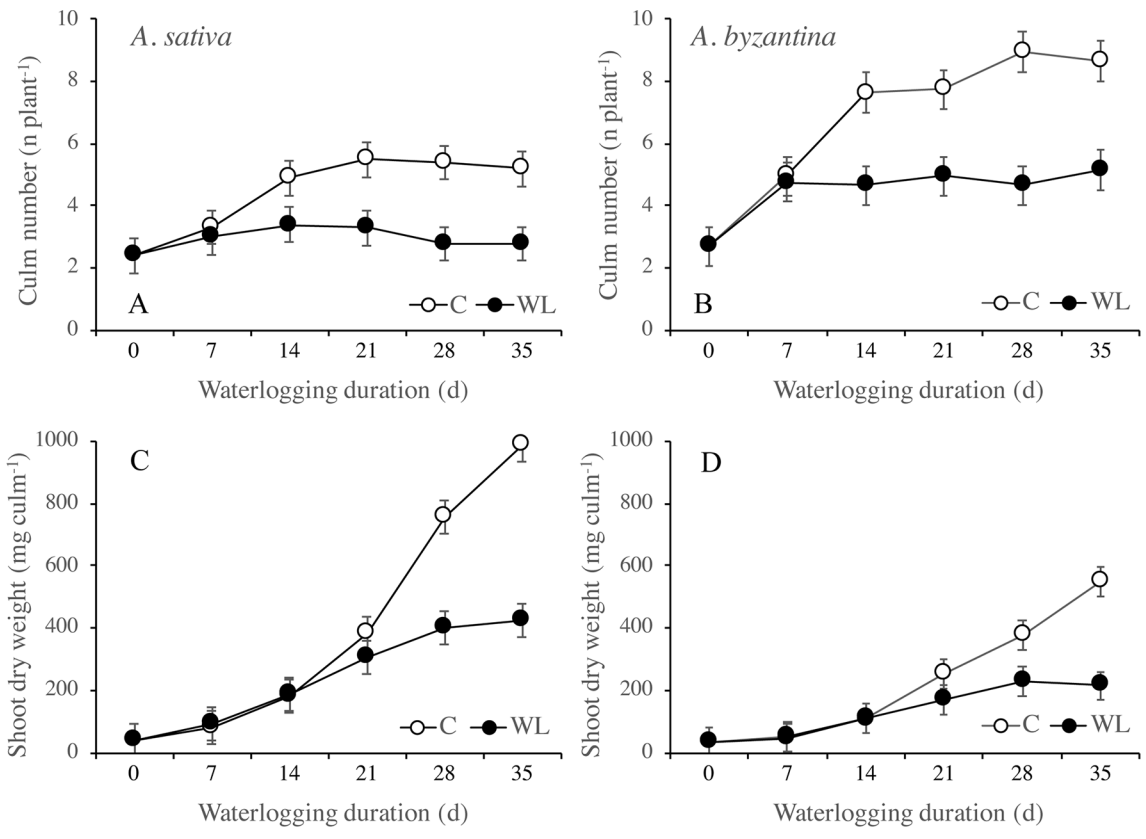

FIGURE 2 | Number of culms **(A**, **B)** and shoot dry weight per culm **(C**, **D)** of *A. sativa* (left column) and *A. byzantina* (right column), as affected by the growth condition x waterlogging duration interaction. Values are means of 2 years and four replicates. Vertical bars represent HSD at $P < 0.05$.

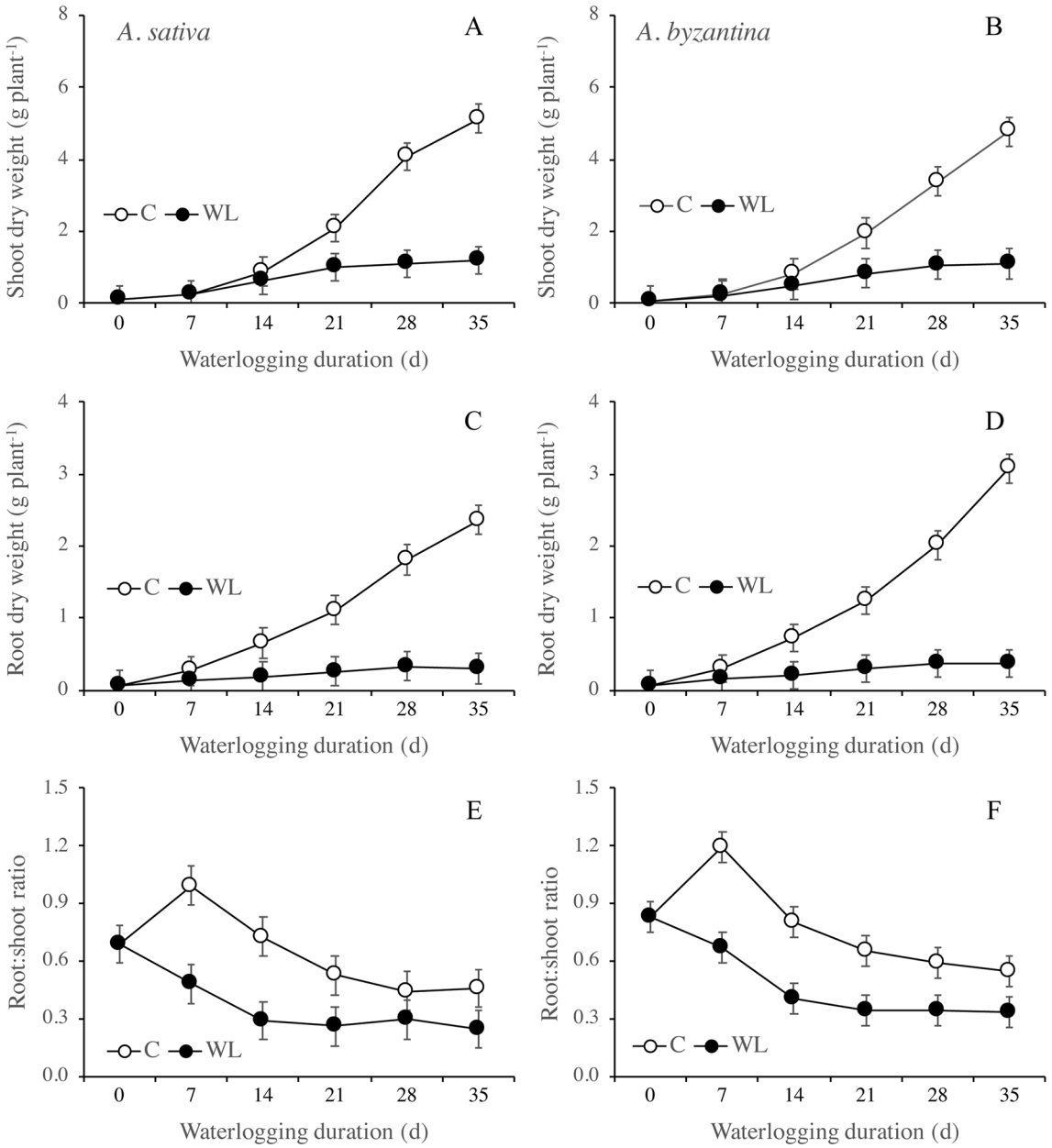

FIGURE 3 | Dry weight of shoots **(A**, **B)** and roots **(C**, **D)**, and root to shoot ratio **(E**, **F)** of *A. sativa* (left column) and *A. byzantina* (right column), as affected by the growth condition x waterlogging duration interaction. Values are means of 2 years and four replicates. Vertical bars represent HSD at $P < 0.05$.

In the two oats, the amount of N taken up by the whole plant in the first 7 days of waterlogging was approximately half that of the controls and it then decreased sharply (**Figures 5A**, **B**). A loss of N occurred in plants waterlogged for more than 21 days, which could be due to both N leakage from damaged root tissues or to the death and consequent detachment of roots and leaves. The amount of N taken up by plants depends on the development of the root system and the rate at which it absorbs N. The latter parameter, estimated by the NUR, decreased in both waterlogged and drained plants during the period of treatment (**Figures 5C**, **D**). In waterlogged plants, however, it was dramatically lower than in the controls from the second week of waterlogging on, and it became negative after 3 weeks.

Experiment 2 and Recovery

Growth Rate and Nitrogen Uptake After Waterlogging

As both species reached maturity on the same date in all treatments, the recovery time decreased from 102 to 67 days with an increase of WL duration from 0 to 35 days. Thus, plants that suffered waterlogging for a shorter period had also a longer time and, therefore, better chances of recovery. To eliminate these differences in the length of time from the end of waterlogging up to maturity,

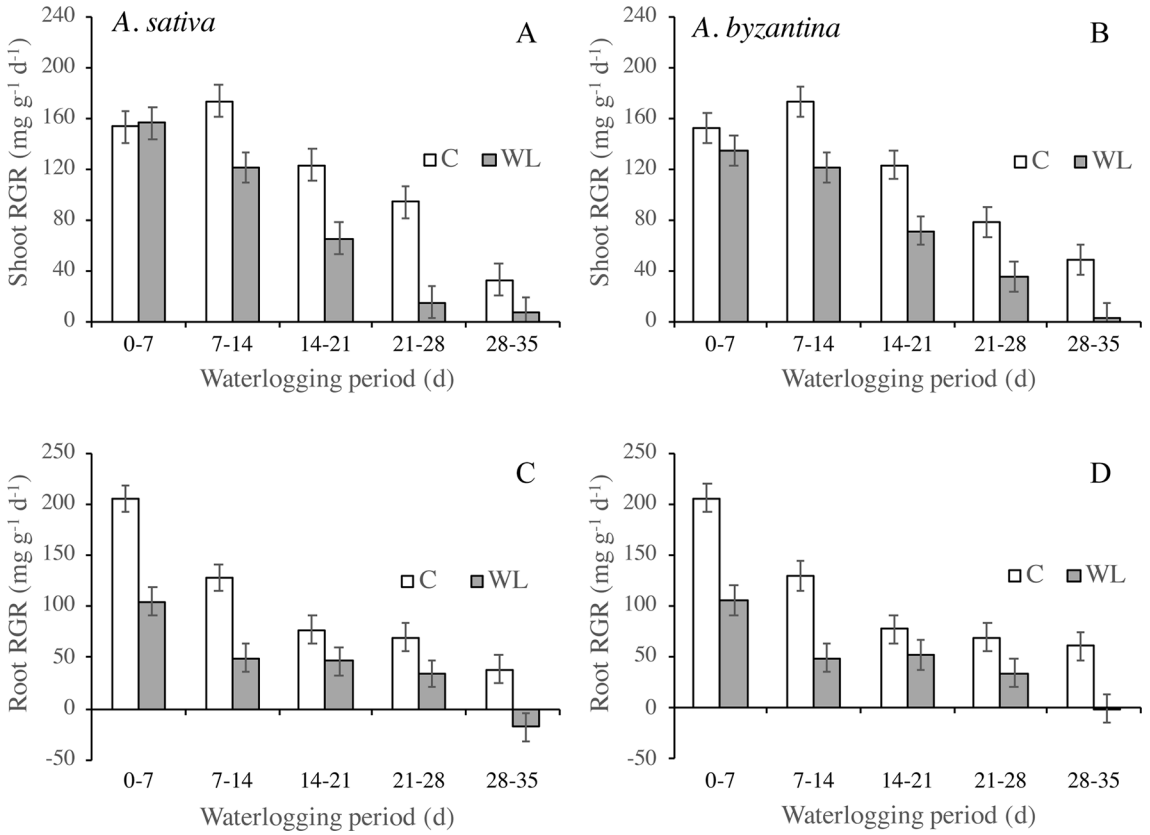

FIGURE 4 | Relative growth rate (RGR) of shoots **(A**, **B)** and roots **(C**, **D)** of drained controls and waterlogged plants of *A. sativa* (left column) and *A. byzantina* (right column) during the waterlogging treatment. Values are means of 2 years and four replicates. Vertical bars represent HSD at $P < 0.05$.

the dry matter and N accumulations during recovery were expressed as daily absolute and RGR.

Between the end of waterlogging and maturity, the AGR of the shoot was markedly lower in WL plants than in the controls, with very similar trends in the two species (**Figures 6A**, **B**). The AGR of control shoots was quite constant throughout the period, while in WL plants, it tended to decrease with increasing duration of exposure, demonstrating a lower AGR after longer WL. Accordingly, the difference from the controls increased from 38% (T7) to 72% in *A. sativa* and to 76% in *A. byzantina* (T35). The AGR of the roots was much lower than that of the shoot and showed a decreasing trend in both C and WL plants (**Figures 6C**, **D**). In controls, values decreased sharply after T21, thus suggesting that, approximately 2 weeks after the first node became detectable (T14), either root growth ceased, or it was nullified by a consistent remobilization of reserves from roots to panicles. The decrease in root growth was more pronounced in *A. byzantina*, in which root AGR became negative toward the end of the growth cycle. In the WL plants of both species, root growth was very low with all WL durations exceeding 7 days, which demonstrates that root recovery was greatly impaired after the start of stem elongation. The RGR of both shoots and roots decreased as the development proceeded, with trends that did not differ between control and waterlogged plants and were similar in the two organs (**Figures 6E**, **F**). No appreciable differences between species were observed in the RGR of shoots, while that of roots was always lower in *A. byzantina*.

Nitrogen uptake from the end of waterlogging to maturity was approximately 50% lower in previous WL plants of *A. sativa* compared to drained controls, with small differences in response to the duration of treatment (Figure 7A). In *A. byzantina*, the N uptake progressively decreased with the proceeding of the growth cycle in control plants, so that differences between WL and C plants were lower than in the other oat species (**Figure 7B**). The NUR for nitrogen was by 22% higher in *A. byzantina* than in *A. sativa* at T0 (**Figures 7C**, **D**). In the controls of both species, it showed a decreasing trend indicating that the N-uptake efficiency of roots declined with plant development. In contrast, in plants that had recovered from waterlogging, it remained relatively constant, and higher than in the controls, independently of the duration of waterlogging and/or the length of the recovery period. These results suggest that, in waterlogged oats, the smaller root systems were compensated by a higher level of uptake efficiency in the root units.

Waterlogging Effects on Dry Matter and Grain and Nitrogen Yields at Maturity

In the drained conditions, the straw (culms+leaves+chaff) dry weight at maturity was slightly higher in *A. byzantina*, whereas that of roots was by 22% higher in *A. sativa* (**Table 3**). In addition, grain yield was by 16% higher in *A. sativa* (**Figures 8A**, **B**).

TABLE 2 | Nitrogen concentration and content of shoots and roots of *A. sativa* and *A. byzantina*, as affected by growth condition x waterlogging duration interaction.

Growth conditions	Waterlogging duration (d)	Nitrogen concentration (%)		Nitrogen content (mg plant^{-1})	
		Shoot	Roots	Shoot	Roots
		Avena sativa			
Control	0	3.0 ab	2.4 a	2.7 f	1.5 f
	7	3.4 a	1.7 bc	8.9 de	4.4 e
	14	2.9 ab	1.5 cde	25.9 c	9.9 d
	21	1.8 c	1.1 def	38.5 b	11.8 c
	28	1.1 de	0.8 f	46.7 a	15.1 b
	35	1.0 de	0.8 f	49.5 a	18.9 a
Waterlogged	0	3.0 ab	2.4 a	2.7 f	1.5 f
	7	2.6 b	2.1 ab	7.1 de	2.7 f
	14	1.4 cd	1.6 bcd	9.2 de	2.9 ef
	21	1.1 de	1.1 def	10.8 d	2.7 f
	28	0.6 e	1.0 ef	7.2 de	3.1 ef
	35	0.6 e	0.9 ef	6.6 e	2.5 f
		Avena byzantina			
Control	0	3.1 a	2.3 a	2.6 e	1.6 f
	7	3.6 a	1.6 bc	8.7 d	4.6 e
	14	3.0 a	1.2 cde	24.9 c	8.4 d
	21	2.0 b	1.0 de	38.3 b	12.5 c
	28	1.2 cd	1.0 de	41.8 b	20.7 b
	35	1.0 cd	0.7 e	47.3 a	22.7 a
Waterlogged	0	3.1 a	2.3 a	2.6 e	1.6 f
	7	2.9 a	1.9 ab	6.3 d	2.8 ef
	14	1.6 bc	1.5 bcd	8.1 d	3.1 ef
	21	1.2 cd	1.0 de	9.7 d	3.0 ef
	28	0.7 d	0.9 e	7.7 d	3.4 ef
	35	0.6 d	0.8 e	6.6 d	3.1 ef

Values are mean of 2 years and four replicates. For each species, means followed by the same letter within a column are not significantly different at $P < 0.05$, using the Tukey test.

Accordingly, *A. sativa* accounted for a higher root:shoot ratio and harvest index compared to *A. byzantina* (**Table 3**). In both species, the exposure to waterlogging at tillering significantly reduced the dry matter recorded at maturity, and straw and root biomass were approximately 35% lower after only 7 days of waterlogging in both species (**Table 3**). In straw, the decrease progressively reached 70% in *A. sativa* and 73% in *A. byzantina*, whereas in roots, it was approximately 84% in both oats. As a consequence, the straw biomass of plants waterlogged for 35 days was similar in the two species, while that of roots was by 29% higher in *A. sativa*. Patterns of decrease were similar in leaves, culms, and chaff and were associated with a significant decrease in the number of culms, which were 4.1 and 5.8 per plant in the controls of *A. sativa* and *A. byzantina*, respectively, and approximately 3 in the former and 4 in the latter in WL plants, without differences among waterlogging durations (data not shown). In both species, the root:shoot ratio was similar in controls and 7-day waterlogged plants, but markedly lower in longer treatments (**Table 3**).

Grain yield significantly decreased with the increase of waterlogging duration, following a negative asymptotic relationship in both species (**Figures 8A**, **B**). Specifically, a 35-day waterlogging decreased grain yield by 79% in *A. sativa* and by 83% in *A. byzantina*, but approximately 42% of this yield was lost after only 7 days of waterlogging in both species. With the increase in waterlogging duration, the harvest index decreased progressively by 8 percent points in *A. sativa* and by 10 percent points in *A. byzantina*, highlighting that the decrease in grain yield was higher than that of straw in both species (**Table 3**).

The nitrogen concentration of all plant parts at maturity was not significantly modified by the duration of waterlogging in both species so that the differences in N content revealed those in biomass (data not reported). The N content was significantly lowered after 7-day WL duration in straw and grain, and after 14-day duration in roots, without appreciable differences between species (**Table 3**). With longer durations, the N content did not change in the roots but decreased further in straw and grain, with significant differences between T28 and T35. Overall, the plants of either *A. sativa* and *A. byzantina* subjected to the longest period of waterlogging (T35) demonstrated N content in straw, roots, and grain, of approximately 57, 75, and 79% lower than the controls, respectively.

Waterlogging Effects on Grain Yield Components at Maturity

The principal components of grain yield, which are the number of panicles per plant, the number of kernels per panicle, and the mean kernel weight, were all decreased by waterlogging but differed in the rate of decrease in response to increasing WL duration (**Figures 8** and **9**). The number of panicles per plant was 3.1 and 3.8, respectively, in the controls of *A. sativa* and *A. byzantina*, and in both species, it decreased following a negative asymptotic relationship with the increase of WL duration (**Figures 8C**, **D**). Similar to grain yield (**Figures 8A**, **B**), also the number of panicles per plant decreased markedly with the 7-day WL, but then only slightly with longer durations, so that it accounted for approximately 2 and 2.3 panicles per plant in *A. sativa* and *A. byzantina* waterlogged for more than 1 week (**Figures 8C**, **D**). In contrast, both the number of kernels per panicle (**Figures 8E**, **F**) and the mean kernel weight (**Figures 8G**, **H**) decreased progressively with the increase of WL duration, thus following a negative linear relationship. In drained controls, the number of kernels per panicle and the mean kernel weight were both higher in *A. sativa*, by 34% the former and by 10% the latter. With the increase in WL duration, the number of kernels per panicle decreased slightly more in *A. byzantina*, so that, at T35, this parameter equaled 22.8 in *A. sativa* and 14.5 in *A. byzantina*. Conversely, the mean kernel weight decreased with similar rates in the two species.

The number of kernels per panicle can be further split into the sub-components number of spikelets per panicle and number of kernels per spikelet. In drained conditions, *A. sativa* had approximately five more spikelets per panicle (**Figures 9A**, **B**), whereas the number of kernels per spikelet equaled in the two species (**Figures 9C**, **D**). Both parameters were negatively affected by waterlogging imposed at tillering, but the patterns of decrease in response to WL duration were different: the number of spikelets per panicle followed a negative linear relationship, whereas an irregular decreasing trend was observed for the number of kernels per spikelet without appreciable differences between species.

The different patterns of decrease in response to longer WL revealed that the relative sensitivity of yield components and sub-components changed according to WL duration. With the shortest WL treatment (T7), the percentage decreases to controls ranked

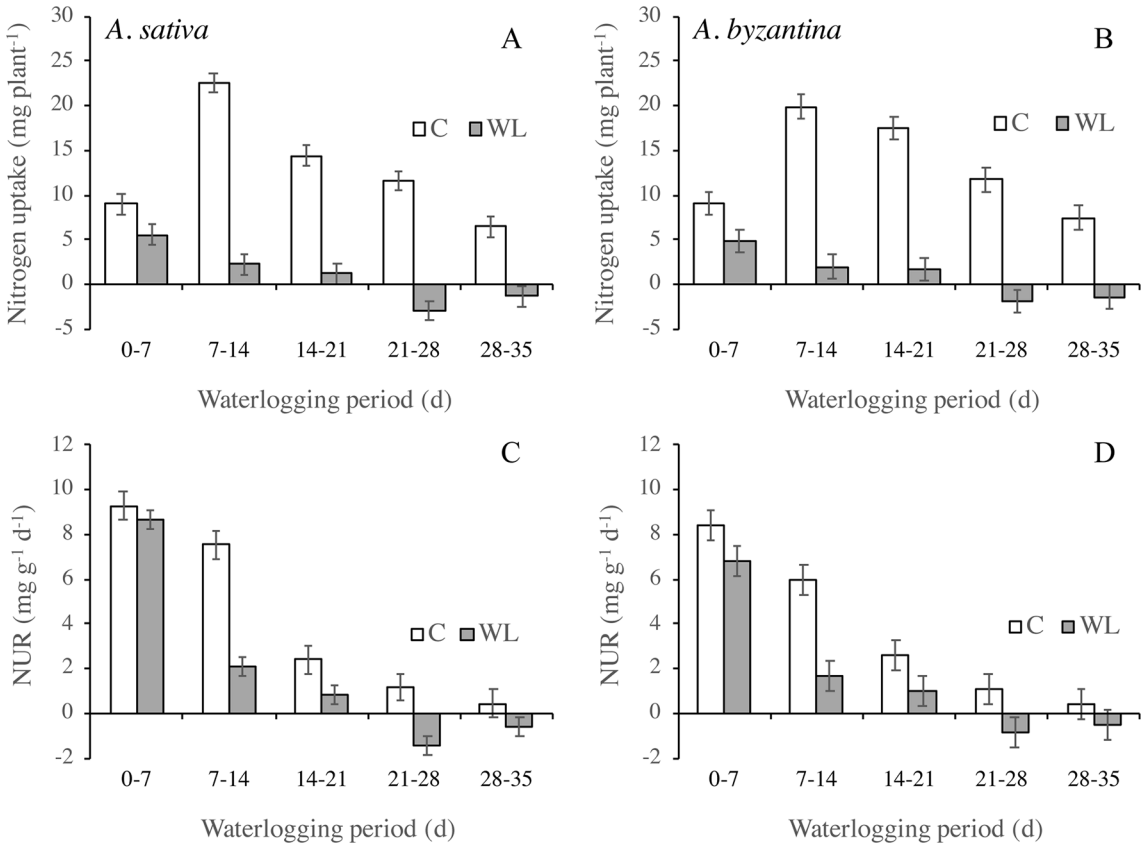

FIGURE 5 | Nitrogen uptake **(A**, **B)** and net uptake rate (NUR) of nitrogen **(C**, **D)** of drained controls and waterlogged plants of *A. sativa* (left column) and *A. byzantina* (right column) during the waterlogging treatment. Values are means of 2 years and four replicates. Vertical bars represent HSD at $P < 0.05$.

in the descending order: number of panicles (26%), number of kernels per panicle (21%), number of spikelets per panicle (15.7% in *A. sativa* and 18.6% in *A. byzantina*), number of kernels per spikelet (5.3% in *A. sativa* and 2.6% in *A. byzantina*), and mean kernel weight (1.3% in *A. sativa* and 2.6% in *A. byzantina*). With the longest WL treatment (T35), the decrease to controls was: kernels per panicle (60% in *A. sativa* and 62% in *A. byzantina*), panicles per plant (44% in *A. sativa* and 47% in *A. byzantina*), spikelets per panicle (44%), kernels per spikelet (29% in *A. sativa* and 32% in *A. byzantina*), and mean kernel weight (6.5%). Above figures demonstrate that waterlogging at tillering affected yield components similarly in the two oat species. However, short waterlogging decreased the number of spikelets per panicle slightly more in *A. byzantina*, which was compensated by a lower decrease in the number of kernels per spikelet. With the longest WL duration, conversely, both the number of panicles per plant and the number of spikelets per panicle were slightly more reduced in *A. byzantina*, which was responsible of the 4-percent-point higher loss in grain yield recorded in this species.

DISCUSSION

In this study, the physiological and agronomic tolerance of *A. sativa* and *A. byzantina* exposed to stagnant soil waterlogging at tillering was assessed by determining growth parameters and N uptake immediately after the end of waterlogging and at maturity, which occurred 2–3 months later. In order to relate the waterlogging response of oats to their specific morphological and phenological traits, our results are discussed in comparison to published results in wheat and barley, which responses to waterlogging have been investigated more deeply.

In drained conditions, *A. sativa* displayed a higher grain yield and root:shoot ratio than *A. byzantina*, but this did not influence their response to waterlogging, which similarly reduced the biomass and N uptake of the two species both during waterlogging and at maturity. Thus, in these standard European oat genotypes (Murariu et al., 2013), we did not find a diverse waterlogging tolerance, such that reported among Brazilian and Australian oat genotypes by Lemons e Silva et al. (2003) and by Setter and Waters (2003).

Plant Growth Under Waterlogging

Plants of both species survived all of the waterlogging durations, but they suffered a strong growth reduction from exposures exceeding 7 days.

Growth was more hindered in roots than in shoots under waterlogging and ceased almost completely after 14 days in the former and after 21 days in the latter. The RGR of roots became negative after 28 days of waterlogging, which could be a

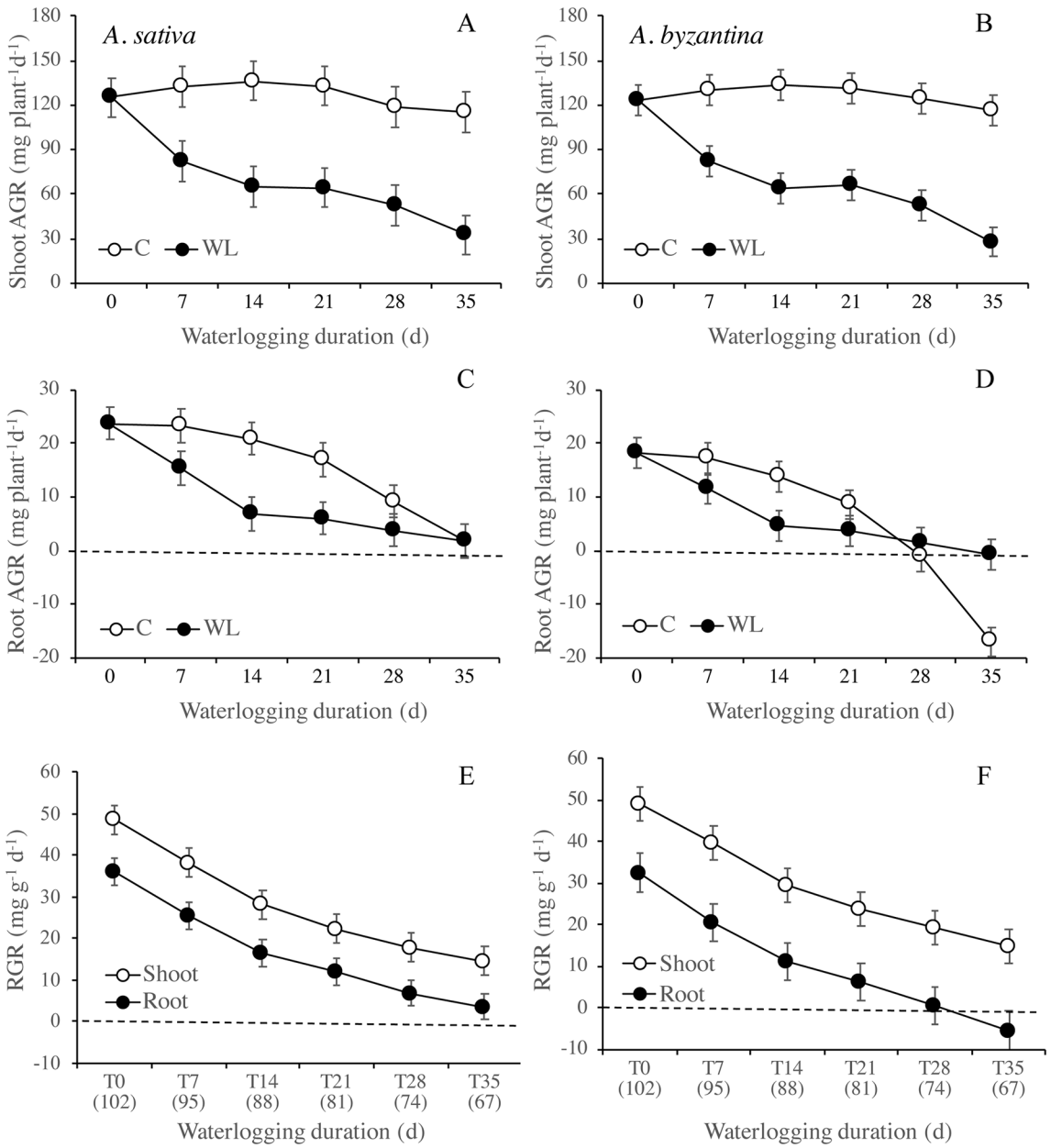

FIGURE 6 | Absolute growth rate (AGR) of shoots **(A**, **B)** and roots **(C**, **D)** of *A. sativa* (left column) and *A. byzantina* (right column) during recovery, as affected by the growth condition x waterlogging duration interaction, and relative growth rates (RGR) of shoots and roots **(E**, **F)** as affected by waterlogging duration. Values of AGR are means of 2 years and four replicates. Values of RGR are means of 2 years, two growth conditions, and four replicates. Vertical bars represent HSD at $P < 0.05$. In brackets, the duration of recovery, in days.

consequence of the detachment of dead root fragments (Brisson et al., 2002; Ploschuk et al., 2018), which was more pronounced in *A. sativa*. Accordingly, at the end of the treatment, the WL plants had a lower root:shoot ratio compared to the drained controls and started recovery not only with a smaller shoot biomass, but also with a proportionally smaller root system supporting the growth of shoots and panicles. A higher waterlogging sensitivity of roots is generally interpreted as a direct consequence of oxygen depletion or other detrimental changes in the root environment (Herzog et al., 2016; de San Celedonio et al., 2017). However, as this different sensitivity of shoots and roots was also observed in germinating wheat seedlings that were completely submerged (Arduini et al., 2016b), we suggest that it may also be because cell division, which is much more energy demanding than cell elongation, contributes more to root growth than to shoot growth (Malik et al., 2002; Loreti et al., 2016). In our research, waterlogging reduced markedly both root and shoot RGRs in the two oats. Conversely, wheat and barley exposed to waterlogging for 14–15 days at a comparable growth stage showed only reduced root RGR, while that of shoots was similar to drained controls (de San Celedonio et al., 2017;

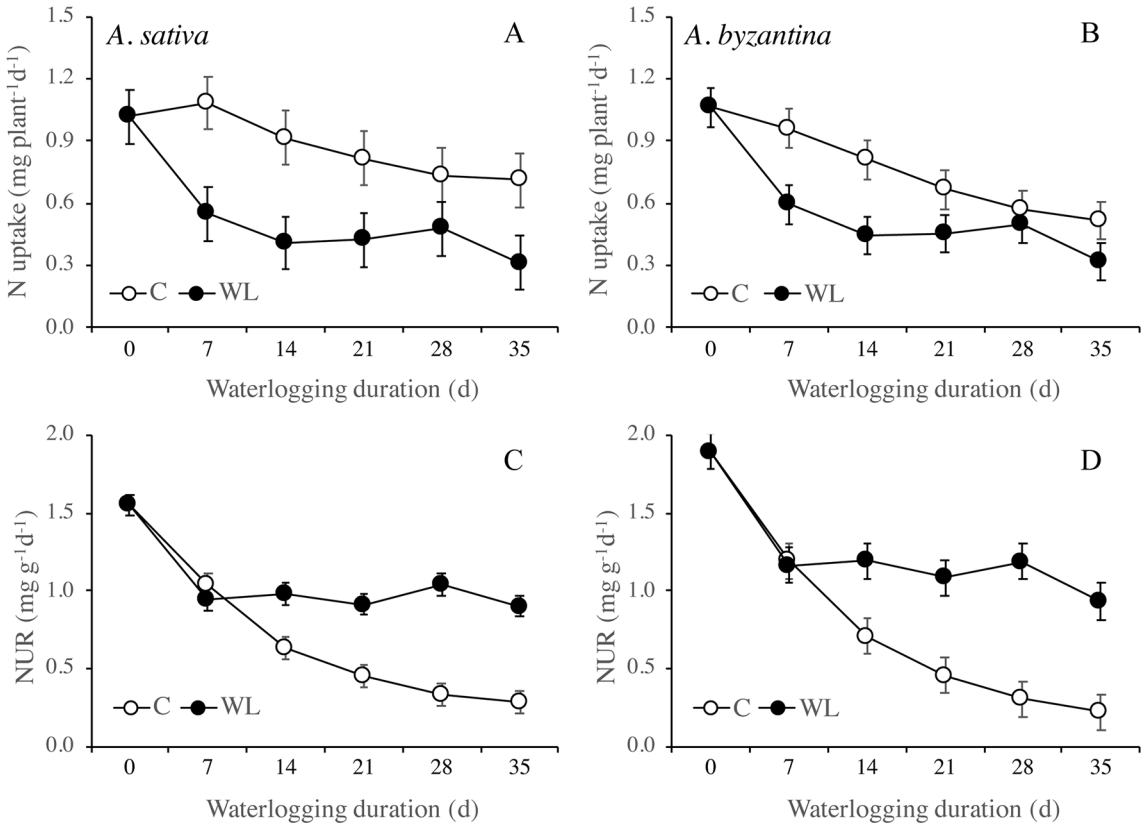

FIGURE 7 | Nitrogen uptake **(A**, **B)** and net uptake rate (NUR) of nitrogen **(C**, **D)** of *A. sativa* (left column) and *A. byzantina* (right column) during recovery, as affected by the growth condition x waterlogging duration interaction. Values are means of 2 years and four replicates. Vertical bars represent HSD at $P < 0.05$. In brackets, the duration of recovery, in days.

Ploschuk et al., 2018). The detrimental effect of waterlogging on shoot growth rate observed in *A. sativa* and *A. byzantina* could be due, at least in part, to a lower ability to activate fermentative metabolism (Gibbs and Greenway, 2003). On the short period, indeed, fermentation could enable roots to withstand the energy shortage induced by anaerobiosis, thus maintaining water and mineral supply to the shoot. We found that shoot growth reduction resulted first from less tillering and second from reduced biomass accumulation per unit culm. Similar to what we hypothesized for root growing points, the inhibition of tiller production probably depended on the negative effect of anaerobiosis on the cell division of submerged tiller buds. In support, Watson et al. (1976) found that the inhibition of tiller initiation under waterlogging was more pronounced in oat than in wheat and barley.

Despite the higher growth reduction in roots compared to shoots, Malik et al. (2001) and Robertson et al. (2009) found that, in wheat, waterlogging reduced the number of adventitious roots per plant proportionally less than the number of tillers, so that the number of adventitious roots per tiller increased. According to Herzog et al. (2016), this is a strategy to overcome the reduced root efficiency caused by waterlogging. In our research, the root dry weight per culm increased from 26 to 71 and 105 mg, respectively, in *A. byzantina* and *A. sativa*, but, in contrast to the findings of Malik et al. (2001), this increment was much higher in drained controls, suggesting a lack of ability of oat roots to react to waterlogging stress. A reason of this could be that seminal roots, which are more sensitive than nodal roots, play a more prominent role during vegetative growth in oats than in wheat and barley (Bonnett, 1961; Malik et al., 2002).

Nitrogen Uptake Under Waterlogging

Reduced shoot growth under waterlogging has been associated with lower photosynthetic CO2 assimilation rate (Pang et al., 2004), but this, however, is more likely a consequence of reduced water and mineral uptake by damaged roots, rather than a direct effect on leaf efficiency (Colmer and Greenway, 2011; de San Celedonio et al., 2017). In specific, the reduced growth of the main culm and of tillers during waterlogging was often associated with the reduced N supply to the shoot, which, in turn, leads to a lower chlorophyll content in leaves (Malik et al., 2002; Masoni et al., 2016; Arduini et al., 2016a). The insufficient nitrogen status of waterlogged plants is due to one or more of the following effects: the depletion of N in soil (Belford et al., 1985; Nguyen et al., 2018), the reduced root growth (Brisson et al., 2002; Ploschuk et al., 2018), or the "energy crisis" caused by anaerobiosis in the root environment, which impairs the active transport of nitrate against its electrochemical gradient (Gibbs and Greenway, 2003; Pang et al., 2007). Thus, it is not easy to

TABLE 3 | Vegetative biomass, root to shoot ratio, harvest index, and N content of grain, straw, and roots of *A. sativa* and *A. byzantina* at maturity, as affected by the waterlogging duration treatment at the tillering stage.

Waterlogging duration (d)	Dry matter (g plant^{-1})		Root: shoot	Harvest index (%)	Nitrogen content (mg plant^{-1})		
	Straw	Roots			Grain	Straw	Roots
				Avena sativa			
0	7.6 a	2.5 a	0.19 a	41.1 a	66.7 a	29.6 a	11.9 a
7	5.0 b	1.6 b	0.19 a	38.8 ab	33.3 b	19.3 b	9.4 a
14	3.9 bc	0.8 c	0.13 b	37.4 ab	26.0 c	16.8 b	5.2 b
21	4.0 bc	0.7 c	0.12 b	34.5 b	25.0 c	18.2 b	4.2 b
28	3.3 cd	0.6 c	0.12 b	33.8 b	23.0 c	19.6 b	3.1 b
35	2.2 d	0.4 c	0.12 b	33.2 b	14.3 d	12.8 c	3.0 b
				Avena byzantina			
0	8.2 a	1.9 a	0.15 a	35.2 a	65.7 a	32.6 a	14.2 a
7	5.4 b	1.2 b	0.16 a	31.5 ab	33.0 b	21.5 b	11.1 a
14	4.2 b	0.6 c	0.10 b	31.8 ab	26.1 c	18.2 b	5.8 b
21	4.4 b	0.6 c	0.09 b	29.1 b	24.6 c	20.1 b	4.9 b
28	3.6 bc	0.5 c	0.10 b	28.5 b	22.6 c	21.2 b	4.0 b
35	2.2 c	0.3 c	0.11 b	25.4 b	13.5 d	14.1 c	3.5 b

Values are mean of 2 years and four replicates. For each species, means followed by the same letter within a column are not significantly different at $P < 0.05$, using the Tukey test.

discern whether the lower N availability to roots and/or the lower N translocation to the shoot are the cause of reduced root and shoot growth, or vice versa; it depends on the lower demand.

In both *A. sativa* and *A. byzantina*, shoot N concentration was the first parameter to be significantly reduced by waterlogging, along with root RGR. As root N concentration never differed significantly for waterlogged and control plants, while NUR was markedly decreased, we argue that waterlogging affected primary root growth and N translocation to the shoot, rather than N availability in the soil. The negative values of root RGR, plant N accumulation, and NUR recorded with the longer waterlogging durations also suggest that consistent N leakage from root tissues started after 21 days of continuous waterlogging, which was followed 1 week later by the loss of root fragments (Malik et al., 2002).

In the present research, N concentration in shoots was progressively lower than that of controls, with an increasing waterlogging duration of up to 21 days. A similar N dilution in shoot tissues has been reported in waterlogged wheat and barley, and it is probably due to the decreased N supply by the roots coupled to the maintenance of shoot growth (de San Celedonio et al., 2017; Ploschuk et al., 2018). In such a case, shoot growth can be sustained by the mobilization of nitrogen from older leaves to both younger leaves and the reproductive apex (Colmer and Greenway, 2011). According to Belford et al. (1985), the resulting lower N concentration of older leaves is primarily responsible for restricted tiller production in waterlogged wheat, and thus leaf chlorosis and reduced tillering are closely related (de San Celedonio et al., 2016; Sundgren et al., 2018). In the present research, however, reduced N concentration was associated with reduced tillering but not with leaf chlorosis, which became visible in both species only with WL treatments that completely stopped shoot growth (T21).

Recovery From Waterlogging

From an agronomic point of view, the waterlogging tolerance of crops relies on their ability to recover at the end of the stress period, and thus achieve an acceptable yield. In winter cereals, the survival of root apices and lateral root initials under waterlogging, and the restoration of tillering upon drainage, are considered crucial plant traits to ensuring recovery (Cannell et al., 1985; Robertson et al., 2009; Hayashi et al., 2013; de San Celedonio et al., 2016; Herzog et al., 2016). The former allows plants to rapidly resume root growth to supply the shoot with adequate nutrients, and the latter is essential to replace tillers that have died or developed minor inflorescence under waterlogging.

In the present research, plants of both oat species reached maturity and produced grain with all the waterlogging durations. However, the root, straw, and grain biomass recorded at maturity were significantly lower than in the controls even with the shortest exposure, thus demonstrating that plants of *A. sativa* and *A. byzantina* were permanently damaged when they experienced a 7-day or longer waterlogging at tillering combined with spring temperatures. The current data contrast with our previous findings on barley and wheat, which showed reduced biomass and grain yield only after 16 and 20 days of waterlogging (Masoni et al., 2016; Pampana et al., 2016; Arduini et al., 2016a), and with those of Cannell et al. (1985) and Watson et al. (1976), who found that oats waterlogged at tillering recovered better than other cereals. In all these studies, waterlogging was imposed at the same growth stage as in our study, i.e., tillering, but the sowing was performed in autumn, while in the present study, it was performed in early spring conditions. Thus, we suggest that the higher temperatures during waterlogging and the shorter time to recover could, at least in part, be responsible of the higher sensitivity found in oats. The mean temperatures experienced by oats throughout the 35 days of waterlogging were, in this experiment, close to 20°C, whereas they were only approximately 6°C in our previous research into wheat (Arduini et al., 2016a). Higher temperatures increase metabolic activities and speed up plant development, so that oat plants sown in February reached the stage first-node-detectable approximately 14 days after the beginning of the waterlogging treatment (T14), whereas autumn sown barley and wheat plants reached this stage long after the end of waterlogging (Masoni et al., 2016; Arduini et al., 2016a). This may be because plants did not resume tillering during recovery,

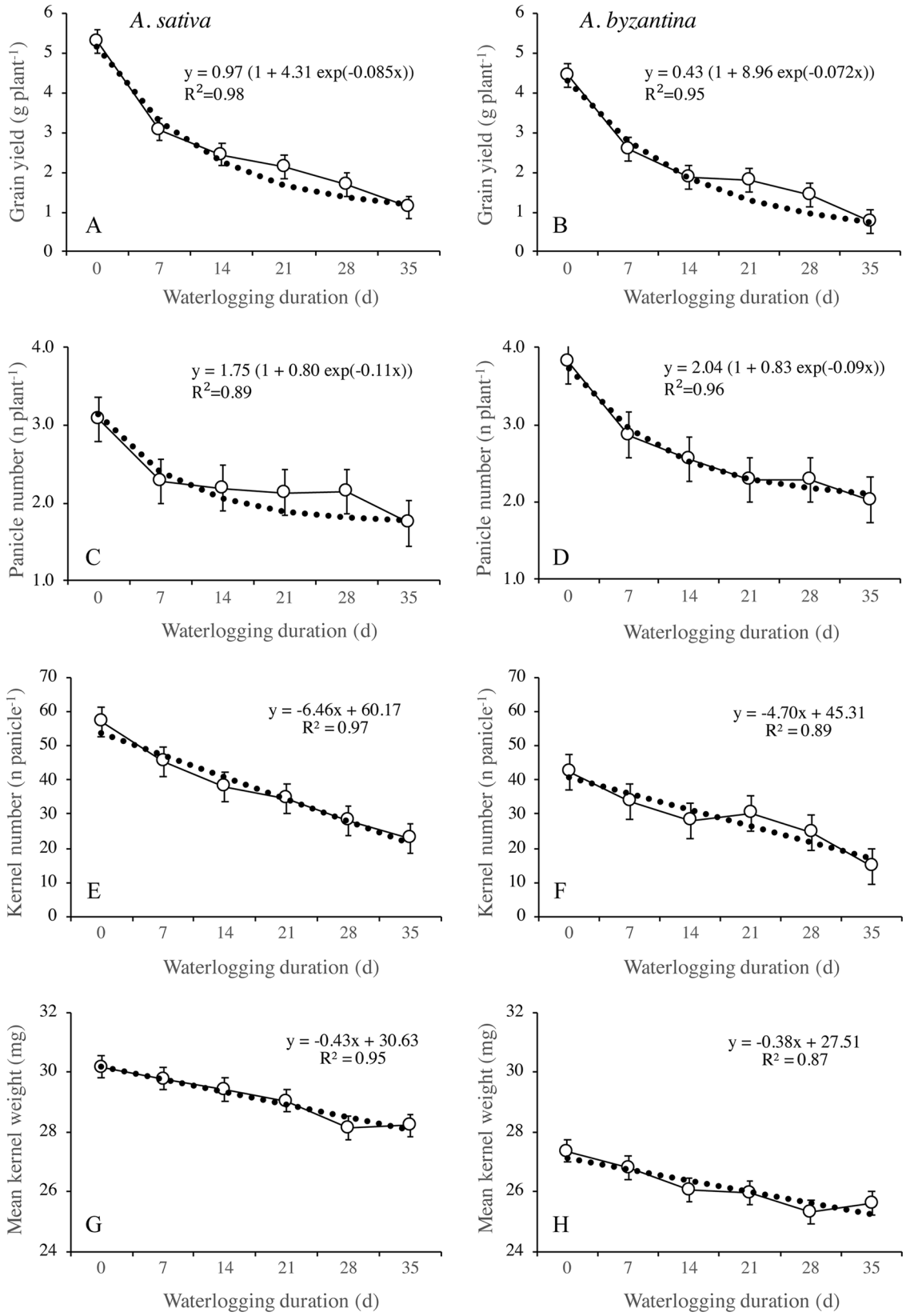

FIGURE 8 | Grain yield **(A**, **B)**, number of panicles per plant **(C**, **D)**, number of kernels per panicle **(E**, **F)**, and mean kernel weight **(G**, **H)** of *A. sativa* (left column) and *A. byzantina* (right column), as affected by waterlogging duration at tillering. Values are means of 2 years and four replicates. Vertical bars represent HSD at $P < 0.05$.

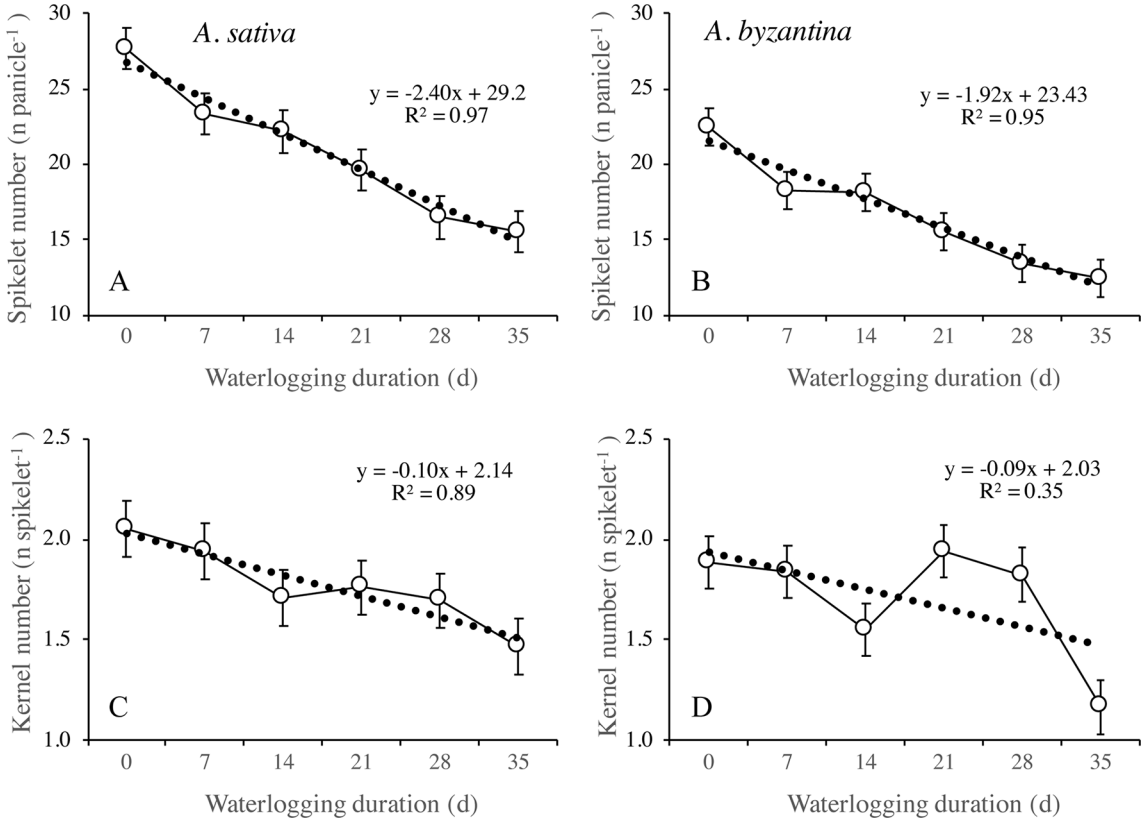

FIGURE 9 | Number of spikelets per panicle **(A**, **B)** and number of kernels per spikelet **(C**, **D)** of *A. sativa* (left column) and *A. byzantina* (right column), as affected by waterlogging duration at tillering. Values are means of 2 years and four replicates. Vertical bars represent HSD at $P < 0.05$.

as reported by Cannell et al. (1985) and by de San Celedonio et al. (2016), and also because N application was ineffective. In support of our hypothesis, after the stage, first-node-detectable tiller production also almost ceased in the controls of both species, and the newly formed tillers did not produce panicles. Moreover, our research highlighted that despite *A. sativa* and *A. byzantina* showed different tiller production in control conditions, this trait was reduced with similar rates by waterlogging.

As root growth is generally more affected by waterlogging than shoot growth, effective recovery would involve a preferential allocation of carbon to roots to re-establish the root:shoot ratio typical of plants in drained soil (Malik et al., 2002; Robertson et al., 2009). In wheat and barley, Ploschuk et al. (2018) found that root RGR was higher in waterlogged plants than in controls just after drainage. Conversely, we found in both oats that the RGR measured over the entire recovery period equaled in WL and control plants, which induce to exclude that root growth rate was faster after waterlogging. Accordingly, the root:shoot ratio reached control values only in plants waterlogged for 7 days. In addition, through visual observations, we could not detect a higher development of crown roots in previously waterlogged plants compared to the controls. In wheat and barley seedlings, in contrast, the recovery of root mass was sustained by the vigorous initiation and elongation of nodal roots and by the proliferation of laterals on these roots (Malik et al., 2002; Pang et al., 2004). In the present research, the inability of *A. sativa* and *A. byzantina* to resume root growth after waterlogging could also depend on the advanced growth stage during recovery. Trends of AGR showed, indeed, that the allocation of resources to roots declined both in controls and waterlogged plants after the start of stem elongation, and, according to Araki et al. (2012), cereals cease to initiate new nodal roots when they approach the reproductive stage. However, while in *A. sativa*, the AGR of roots was always equal or higher in controls than in WL treatments; in *A. byzantina* control, values were markedly lower at T35, which could suggest a higher remobilization of assimilates from the roots of this species.

Poor recovery after waterlogging has often been attributed to nitrogen deficiency in soil (Robertson et al., 2009; Nguyen et al., 2018), but this was not the case in our study, as nitrogen was supplied when pots were drained. Even though the timing of N application differed according to the duration of waterlogging, the nitrogen concentration of all plant parts did not differ among treatments at maturity, suggesting that neither WL nor the time of supply affected the N status of plants during the reproductive phase. In addition, the RGR of shoots and roots were similar during recovery in previously waterlogged plants and in controls, which allows to infer that the physiological processes involved in biomass accumulation were not impaired. Thus, the lower N uptake during recovery of waterlogged plants compared to controls was more reliable, as a consequence of the smaller root system and/or the

reduced request by the smaller shoots, rather than as a consequence of lower N availability in soil or lower root efficiency. The NUR for nitrogen was even higher in the waterlogged plants than in the controls, demonstrating a higher N uptake per unit root. The values were slightly higher in *A. byzantina*, which thus compensated the smaller root system with a higher uptake efficiency of roots.

The above results clearly demonstrate that the plants of *A. sativa* and *A. byzantina* did not recover from the waterlogging experienced at tillering, as they accumulated less biomass and nitrogen after the end of treatment, and consequently, at maturity, they were smaller and yielded less grain compared to the drained plants. This was essentially the consequence of the reduced growth and the damage suffered during WL exposure, as the rates of biomass accumulation and nutrient uptake proceeded similar to controls during recovery, thus suggesting that physiological processes were resumed. We argue that the more advanced growth stage at the end of waterlogging was an important reason for the scarce recovery observed in *A. sativa* and *A. byzantina* sown at the end of winter, and our hypothesis is in agreement with de San Celedonio et al. (2014), who found that delayed sowings increased the negative response of wheat to waterlogging. In addition, Peltonen-Sainio and Peltonen (1995) reported that wheat, but not oat, formed new tillers even close to anthesis in response to late N application. These findings suggest that the ability of oat plants to recover vegetative growth after waterlogging is greatly impaired when they have achieved the stem elongation phase.

Waterlogging Impact on Grain Yield Components

Although tillering is defined as a vegetative growth phase, during this period, oats and all cereals determine the number of tillers and also the size of inflorescences (Arduini et al., 2010). Accordingly, stress conditions during tillering can strongly affect the final yield and are of crucial agronomic interest. The lower harvest index recorded in *A. sativa* and *A. byzantina* with all waterlogging durations demonstrated that grain yield was even more affected than the accumulation of vegetative biomass, which was also found in wheat (de San Celedonio et al., 2014; Pampana et al., 2016; Arduini et al., 2016a), whereas in barley, vegetative biomass and grain yield were reduced at the same rate (Masoni et al., 2016).

When wheat and barley plants were exposed to waterlogging at tillering, the most affected yield components were spike number, because of either reduced tillering (barley) or tiller fertility (wheat), and the number of kernels per spike (Amri et al., 2014; de San Celedonio et al., 2018; Sundgren et al., 2018). Due to the different architecture of wheat and barley spikes, however, the lower spike yield was related to lower spikelet fertility in the former, and to lower spikelet number in the latter (Masoni et al., 2016; Arduini et al., 2016a). Differently from in wheat and barley, oat plants exposed to WL at tillering showed higher tiller fertility, which largely compensated for the lower tiller initiation (Watson et al., 1976; Cannell et al., 1985). The lack of synchronization of the development stages of tillers with the stages of the main shoot or with each other is a specific trait of oats allowing the transition of the apical meristem of tillers from vegetative to reproductive also during main stem elongation (Bonnett, 1966). In our research, however, tiller fertility increased only in plants waterlogged for 7 and 14 days, and only by approximately 5 percent points compared to controls in both species, which we imputed to the late sowing, which caused the shortening of all growth phases, thus reducing the time for the initiation of additional panicles.

All yield components were negatively affected by waterlogging, but the relative sensitivity of those that underwent the greatest reduction, i.e., numbers of panicles per plant and kernels per panicle, varied with increasing WL duration following the former an asymptotic relationship and the latter a linear relationship.

The asymptotic trend observed in both species demonstrates that all WL durations almost equally reduced the number of panicles per plant, which could be because this component was fully established around T14, when stem elongation started. As a consequence, this trait could not recover upon drainage, as it was found by Cannell et al. (1985) in oat, and by de San Celedonio et al. (2016) in wheat and barley. Conversely, the linear decrease of the number of grains per panicle suggests that this number was not definitively fixed at the end of waterlogging, which allowed oats to resume panicle development during recovery. The number of kernels per spikelet was the panicle component that displayed the highest stability, as it achieved values close to controls even with 21- and 28-day long waterlogging. In contrast, this trait proved to be the most sensitive to waterlogging in wheat (Ghobadi et al., 2011; Marti et al., 2015; Masoni et al., 2016; Arduini et al., 2016a; de San Celedonio et al., 2018), which supports the hypothesis of Mahadevan et al. (2016) of an inverted hierarchy of plasticities in the components of grain number in wheat compared to oat. In oat, floret differentiation begins during tillering as in all cereals, but the final number of florets is established later than in wheat and barley, close to the start of grain filling. Thus, when adverse conditions during vegetative growth are followed by favorable nutrient supplies, oat plants have the capacity to compensate for the smaller panicles by filling all fertilized florets within a spikelet (Finnan and Spink, 2017). Starting from our findings and from literature, we infer that the N supply to plants waterlogged at tillering differently affects the yield components of winter cereals; in that, it sustains floret differentiation in oats, whereas it promotes tillering in wheat (Watson et al., 1976; Peltonen-Sainio and Peltonen, 1995; Robertson et al., 2009). Grain yield per plant was slightly higher in *A. sativa* than in *A. byzantina*, primarily due to the higher number of spikelets per panicle and mean kernel weight. Despite these differences, patterns of decrease in response to waterlogging followed similar trends, and after 7-day waterlogging, they both lost 42% of grain yield. The further decrease of grain yield with increasing WL durations was slightly higher in *A. byzantina* causing a 4-percent-point higher yield loss, which, however, we do not consider to be enough to suggest a higher tolerance to waterlogging of *A. sativa*.

Mean kernel weight is the last determined yield component in cereals, and it was not affected by waterlogging at tillering in oat, wheat, and barley (Cannell et al., 1985; Robertson et al., 2009; Masoni et al., 2016; Pampana et al., 2016), probably because plants adjusted kernel size to compensate for the lower number. In contrast, this parameter was found to be sensitive to waterlogging imposed later in the growth cycle, primarily because of reduced ovary growth (Watson et al., 1976; Araki et al., 2012; de San Celedonio et al., 2014;

Marti et al., 2015). In our research, the slight decrease in mean kernel weight recorded in both oat species was probably due to reduced grain filling, driven by either the lower assimilation during recovery or the smaller amount of pre-anthesis resources to be remobilized (Li et al., 2011).

CONCLUSION

A. sativa and *A. byzantina* sown at the end of winter and exposed to stagnant waterlogging for 7 to 35 days from the two-tiller stage onwards, showed markedly reduced grain yield starting from the shortest exposure, primary due to the severe damages suffered under waterlogging.

In both species, the first parameters that decreased under waterlogging were the RGR of roots and the N concentration of shoots, followed by the number of tillers per plant, which suggests that root growing points and tiller buds were the first targets of waterlogging stress. During recovery, the RGR and the N NUR either achieved control values or were even higher, highlighting that the physiological processes involved in dry matter accumulation and mineral uptake were resumed upon drainage. In contrast, damage to growing points appeared to be permanent and plants were unable to initiate new roots and new tillers, probably because of their advanced growth stage during recovery.

The sensitivity of grain yield components changed according to waterlogging duration, so that grain yield loss was primarily due to reduced tiller and panicle initiation with short waterlogging, whereas to reduced panicle number and also panicle size with longer durations. These results demonstrate that oat plants partially compensated the lower number of tillers with higher tiller and spikelet fertilities after short waterlogging. This is to impute to the asynchronous and longer phase of panicle differentiation and to the determination of the number of kernels per panicle close to grain filling, which is a specific trait of oat compared to other winter cereals that produce spikes, such as wheat and barley.

In the present research, we did not screen for waterlogging tolerance among *A. sativa* and *A. byzantina* genotypes, but we chose standard cultivars that are widely used in our environment because of stabile yields, which probably also includes the ability to cope with occasional soil waterlogging. The two species responded with similar patterns to increasing waterlogging duration. Thus, our results demonstrated that late sown oats were not able to produce acceptable yield, primarily because they did not resume tillering after the end of waterlogging, and the plasticity of panicle components was not able to compensate for the reduced panicle number.

This study contributes to the understanding of oat response to waterlogging through the detailed analysis of the morphological traits and the nitrogen uptake and distribution patterns which are more or less affected under waterlogging and are more or less able to recover after the stress. The comparison with published results in wheat and barley allows to highlight oat-specific traits in response to waterlogging.

DATA AVAILABILITY

The raw data supporting the conclusions of this manuscript will be made available by the authors, without undue reservation, to any qualified researcher.

AUTHOR CONTRIBUTIONS

All authors contributed equally in planning and conducting the experiment, so as in the elaboration of data and in the preparation of the manuscript.

REFERENCES

Amri, M., El Ouni, M. H., and Salem, M. B. (2014). Waterlogging affect the development, yield and components, chlorophyll content and chlorophyll fluorescence of six bread wheat genotypes (*Triticum aestivum* L.). *Bulg. J. Agric. Sci.* 20 (3), 647–657.

AOAC, Association of Official Analytical Chemists (2005). *Official methods of analysis*. 17th ed. Gaithersburg, MD: AOAC International.

Araki, H., Hossain, M. A., and Takahashi, T. (2012). Waterlogging and hypoxia have permanent effects on wheat root growth and respiration. *J. Agron. Crop Sci.* 198, 264–275. doi: 10.1111/j.1439-037X.2012.00510.x

Arduini, I., Ercoli, L., Mariotti, M., and Masoni, A. (2010). Coordination between plant and apex development in Hordeum vulgare spp. distichum. *C. R. Biol.* 333, 454–460. doi: 10.1016/j.crvi.2010.01.003

Arduini, I., Orlandi, C., Pampana, S., and Masoni, A. (2016a). Waterlogging at tillering affects spike and spikelet formation in wheat. *Crop Pasture Sci.* 67, 703–711. doi: 10.1071/CP15417

Arduini, I., Orlandi, C., Ercoli, L., and Masoni, A. (2016b). Submergence sensitivity of durum wheat, bread wheat and barley at the germination stage. *Ital. J. Agron.* 11 (706), 100–106. doi: 10.4081/ija.2016.706

Belford, R. K., Cannell, R. Q., and Thomson, R. J. (1985). Effects of single and multiple waterloggings on the growth and yield of winter wheat on a clay soil. *J. Sci. Food Agric.* 36, 142–156. doi: 10.5539/ijb.v1n2p87

Bonnett, O. T. (1961). *The oat plant: its histology and development. Bulletin 672*. Urbana, IL: University of Illinois Agricultural Experiment Station, 7–112. Available at: http://hdl.handle.net/2142/8676.

Bonnett, O. T. (1966). *Inflorescences of maize, wheat, rye, barley, and oats: their initiation and development. Bulletin 721*. Urbana, IL: University of Illinois Agricultural Experiment Station, 92–102. Available at: http://www.ideals.illinois.edu/bitstream/handle/2142/27945/inflorescencesof721bonn.pdf?sequence=1

Brisson, N., Rebière, B., Zimmer, D., and Renault, P. (2002). Response of the root system of a winter wheat crop to waterlogging. *Plant Soil* 243, 43–55. doi: 10.1023/A:1019947903041

Bronson, K. F., and Fillery, I. R. P. (1998). Fate on nitrogen-15-labelled urea applied to wheat on a waterlogged texture-contrast soil. *Nutr. Cycl. Agroecosys.* 51, 175–183. doi: 10.1023/A:1009725900571

Browne, R. A., White, E. M., and Burke, J. I. (2006). Responses of developmental yield formation processes in oats to variety, nitrogen, seed rate and plant growth regulator and their relationship to quality. *J. Agric. Sci.* 144, 533–545. doi: 10.1017/S0021859606006538

Cannell, R. Q., Belford, R. K., Blackwell, P. S., Govi, G., and Thomson, R. J. (1985). Effects of waterlogging on soil aeration and on root and shoot growth and yield of winter oats (*Avena sativa* L.). *Plant Soil* 85, 361–373. doi: 10.1007/BF02220191

Colmer, T. D., and Greenway, H. (2011). Ion transport in seminal and adventitious roots of cereals during O_2. deficiency. *J. Exp. Bot.* 62, 39–57. doi: 10.1093/jxb/erq271

de San Celedonio, R. P., Abeledo, L. G., and Miralles, D. J. (2014). Identifying the critical period for waterlogging on yield and its components in wheat and barley. *Plant Soil* 378, 265–277. doi: 10.1007/s11104-014-2028-6

de San Celedonio, R. P., Abeledo, L. G., Brihet, J. M., and Miralles, D. J. (2016). Waterlogging affects leaf and tillering dynamics in wheat and barley. *J. Agron. Crop Sci.* 202, 409–420. doi: 10.1111/jac.12151

de San Celedonio, R. P., Abeledo, L. G., Mantese, A. I., and Miralles, D. J. (2017). Differential root and shoot biomass recovery in wheat and barley with transient waterlogging during preflowering. *Plant Soil* 417, 481–498. doi: 10.1007/s11104-017-3274-1

de San Celedonio, R. P., Abeledo, L. G., and Miralles, D. J. (2018). Physiological traits associated with reductions in grain number in wheat and barley under waterlogging. *Plant Soil* 429, 469–481. doi: 10.1007/s11104-018-3708-4

Engels, C. (1993). Differences between maize and wheat in growth-related nutrient demand and uptake of potassium and phosphorus at suboptimal root zone temperatures. *Plant Soil* 150, 129–138. doi: 10.1007/BF00779183

Finnan, J. M., and Spink, J. (2017). Identification of yield limiting phenological phases of oats to improve crop management. *J. Agric. Sci.* 155, 1–17. doi: 10.1017/S0021859616000071

Ghobadi, M. E., and Ghobadi, M. (2010). Effect of anoxia on root growth and grain yield of wheat cultivars. *World Acad. Sci. Eng. Technol.* 70, 85–88.

Ghobadi, M. E., Ghobadi, M., and Zebarjadi, A. (2011). The response of winter wheat to flooding. *World Acad. Sci. Eng.Technol.* 78, 440–442.

Gibbs, J., and Greenway, H. (2003). Mechanisms of anoxia tolerance in plants. I. Growth, survival and anaerobic catabolism. *Funct. Plant Biol.* 30, 1–47. doi: 10.1071/PP98095

Hayashi, T., Yoshida, T., Fujii, K., Mitsuya, S., Tsuji, T., Okada, Y., et al. (2013). Maintained root length density contributes to the waterlogging tolerance in common wheat (*Triticum aestivum* L.). *Field Crops Res.* 152, 27–35. doi: 10.1016/j.fcr.2013.03.020

Herzog, M., Striker, G. G., Colmer, T. D., and Pedersen, O. (2016). Mechanisms of waterlogging tolerance in wheat–a review of root and shoot physiology. *Plant Cell Environ.* 39, 1068–1086. doi: 10.1111/pce.12676

Hunt, R. (1990). *Basic growth analysis: plant growth analysis for beginners*. London: Unwin Hyman. doi: 10.1007/978-94-010-9117-6

Lemons e Silva, C. F., de Mattos, L. A. T., de Oliveira, A. C., de Carvalho, F. I. F., de Freitas, F. A., and dos Anjos e Silva, S. D. (2003). Flooding tolerance in oats. *J. New Seeds* 54, 29–42. doi: 10.1300/J153v05n04_03

Li, C., Dong, J., Wollenweber, B., Li, Y., Dai, T., and Cao, W. (2011). Waterlogging pretreatment during vegetative growth improves tolerance to waterlogging after anthesis in wheat. *Plant Sci.* 180, 672–678. doi: 10.1016/j.plantsci.2011.01.009

Loreti, E., van Veen, H., and Perata, P. (2016). Plant responses to flooding stress. *Curr. Opin. Plant Biol.* 33, 64–71. doi: 10.1016/j.pbi.2016.06.005

Mahadevan, M., Calderini, D. F., Zwer, P. K., and Sadras, V. O. (2016). The critical period for yield determination in oat (*Avena sativa* L.). *Field Crops Res.* 199, 109–116. doi: 10.1016/j.fcr.2016.09.021

Malik, A. I., Colmer, T. D., Lambers, H., and Schortemeyer, M. (2001). Changes in physiological and morphological traits of roots and shoots of wheat in response to different depths of waterlogging. *Aust. J. Plant Physiol.* 28, 1121–1131. doi: 10.1071/PP01089

Malik, A. I., Colmer, T. D., Lambers, H., Setter, T. L., and Schortemeyer, M. (2002). Short-term waterlogging has long-term effects on the growth and physiology of wheat. *New Phytol.* 153, 225–236. doi: 10.1046/j.0028-646X.2001.00318.x

Marti, J., Savin, R., and Slafer, G. A. (2015). Wheat yield as affected by length of exposure to waterlogging during stem elongation. *J. Agron. Crop Sci.* 201, 473–486. doi: 10.1111/jac.12118

Masoni, A., Pampana, S., and Arduini, I. (2016). Barley response to waterlogging duration at tillering. *Crop Sci.* 56, 2722–2730. doi: 10.2135/cropsci2016.02.0106

Meier, U. (2001). *Growth stages of mono and dicotyledonous plants. BBCH*. Monograph. Berlin and Braunschweig: Federal Biological Research Centre for Agriculture and Forestry.

Murariu, D., Placinta, D. D., Germeier, C. U., Annamaa, K., Antonomova, N., Bulinska-Radomska, Z., et al. (2013). Quality characteristics of European Avena genetic resources collections. *Rom. Agric. Res.* 30, 45–55.

Mustroph, A. (2018). Improving flooding tolerance of crop plants. *Agronomy* 8, 160. doi: 10.3390/agronomy8090160

Nguyen, L. T. T., Osanai, Y., Anderson, I. C., Bange, M. P., Braunack, M., Tissue, D. T., et al. (2018). Impacts of waterlogging on soil nitrification and ammonia-oxidizing communities in farming system. *Plant Soil* 426, 299–311. doi: 10.1007/s11104-018-3584-y

Pampana, S., Masoni, A., and Arduini, I. (2016). Grain yield of durum wheat as affected by waterlogging at tillering. *Cereal Res. Commun.* 44, 706–716. doi: 10.1556/0806.44.2016.026

Pang, J., Zhou, M., Mendham, N., and Shabala, S. (2004). Growth and physiological responses of six barley genotypes to waterlogging and subsequent recovery. *Aust. J. Agr. Res.* 55, 895–906. doi: 10.1071/AR03097

Pang, J., Ross, J., Zhou, M., Mendham, N., and Shabala, S. (2007). Amelioration of detrimental effects of waterlogging by foliar nutrient sprays in barley. *Funct. Plant Biol.* 34, 221–227. doi: 10.1071/FP06158

Peltonen-Sainio, P., and Peltonen, J. (1995). Floret set and abortion in oat and wheat under high and low nitrogen regimes. *Eur. J. Agron.* 4, 253–262. doi: 10.1016/S1161-0301(14)80052-X

Ploschuk, R. A., Miralles., D. J., Colmer, T. D., Ploschuk, E. L., and Striker, G. G. (2018). Waterlogging of winter crops at early and late stages: impacts on leaf physiology, growth and yield. *Front. Plant Sci.* 9, 1863. doi: 10.3389/fpls.2018.01863

Rasaei, A., Ghobadi, M. E., Jalali-Honarmand, S., Ghobadi, M., and Saeidi, M. (2012). Impacts of waterlogging on shoot apex development and recovery effects of nitrogen on grain yield of wheat. *Eur. J. Exp Biol.* 2 (4), 1000–1007. www.pelagiaresearchlibrary.com.

Robertson, D., Zhang, H., Palta, J. A., Colmer, T., and Turner, N. C. (2009). Waterlogging affects the growth, development of tillers, and yield of wheat through a severe, but transient, N deficiency. *Crop Pasture Sci.* 60, 578–586. doi: 10.1071/CP08440

Sasidharan, R., Bailey-Serres, J., Ashikari, M., Atwell, B. J., Colmer, T. D., Fagerstedt, K., et al. (2017). Community recommendations on terminology and procedures used in flooding and low oxygen stress research. *New Phytol.* 214, 1403–1407. doi: 10.1111/nph.14519

Setter, T. L., and Waters, I. (2003). Review of prospects for germ plasm improvement for waterlogging tolerance in wheat, barley and oats. *Plant Soil* 253, 1–34. doi: 10.1023/A:1024573305997

Sonego, M., Moot, D. J., Jamieson, P. D., Martin, R. J., and Scott, W. R. (2000). Apical development in oats predicted by the leaf stage. *Field Crops Res.* 65, 79–86. doi: 10.1016/S0378-4290(99)00073-8

Steel, R. G. D., Torrie, J. H., and Dickey, D. A. (1997). *Principles and procedure of statistics: a biometrical approach*. New York: McGraw-Hill.

Sundgren, T. K., Uhlen, A. K., Waalen, W., and Lillemo, M. (2018). Field screening of waterlogging tolerance in spring wheat and spring barley. *Agronomy* 8, 38. doi: 10.3390/agronomy8040038

Watson, E. R., Lapins, P., and Barron, R. J. W. (1976). Effect of waterlogging on the growth, grain and straw yield of wheat, barley and oats. *Aus. J. Exp. Agr.* 16, 114–122. doi: 10.1071/EA9760114

Conflict of Interest Statement: The authors declare that the research was conducted in the absence of any commercial or financial relationships that could be construed as a potential conflict of interest.

Advantages of publishing in Frontiers

OPEN ACCESS
Articles are free to read for greatest visibility and readership

FAST PUBLICATION
Around 90 days from submission to decision

HIGH QUALITY PEER-REVIEW
Rigorous, collaborative, and constructive peer-review

TRANSPARENT PEER-REVIEW
Editors and reviewers acknowledged by name on published articles

Frontiers
Avenue du Tribunal-Fédéral 34
1005 Lausanne | Switzerland

Visit us: www.frontiersin.org
Contact us: info@frontiersin.org | +41 21 510 17 00

REPRODUCIBILITY OF RESEARCH
Support open data and methods to enhance research reproducibility

DIGITAL PUBLISHING
Articles designed for optimal readership across devices

FOLLOW US
@frontiersin

IMPACT METRICS
Advanced article metrics track visibility across digital media

EXTENSIVE PROMOTION
Marketing and promotion of impactful research

LOOP RESEARCH NETWORK
Our network increases your article's readership